Sterno-Clavicular Kinematics – A New Measurement System

Sandro Scattareggia Marchese

This thesis is submitted in fulfilment of the requirements for the Degree of Doctor of Philosophy

Centre for Rehabilitation and Engineering Studies
Department of Mechanical, Materials and Manufacturing Engineering
University of Newcastle Upon Tyne

July 2000

NEWCASTLE UNIVERSITY LIBRARY
200 13988 5
Thesis L6852

Declaration

This Thesis describes work carried out by the author in the Department of Mechanical, Material and Manufacturing Engineering of the University of Newcastle upon Tyne, UK and in the offices of Signo Motus srl, Messina, Italy from October 1995 to October 1999, under the supervision of Professor G. R. Johnson and of Prof. Massimo Bergamasco as an external advisor.

This thesis describes original work, which has not submitted for a higher degree at any other University and is the work solely of the undersigned author, except where acknowledged in the text.

Sandro Scattareggia Marchese

Copyright © 2000 by Sandro Scattareggia Marchese

The copyright of this thesis rests with the author. No quotation from it should be published without prior written consent and any information derived from it should be acknowledged.

"ciò che non si vede o non si comprende desta da sempre neil'uomo un occhio vigile e attento... passo necessario per la ricerca ed il progresso"

a Carmelina, Adriana e Simone

ACKNOWLEDGEMENTS

A work evolving for 5 years has had contributions from a number of people to whom I wish to express my deep thanks.

I thank the European Union which has permitted the development of this work in the framework of the Project "Tremor" and the Company Signo Motus srl, Messina, Italy in whose offices the main part of the systems have been developed.

If Prof. G. R. Johnson is the person who has introduced me in the world of rehabilitation technology particularly from the clinical point of view, Prof. Massimo Bergamasco has deeply contributed to my professional education. To both of them are directed my sincere thanks. Another person I would like to thank, although he was not directly involved in this 9work, is dr R. Platts who has let me meditate on the real meaning of the words "disabled people".

Finally a particular thanks goes to my colleagues at CREST and particularly to Stefano Donato, for the interesting discussions on the kinematics of the arm and particularly because without his help in setting of the tests and in the preparation of the software I may have not finished this work at all.

I thank my wife for the contributions given in the preparation of the photographs and particularly for her support during the writing of this work.

INDEX

1 INTRODUCTION 8

1.1 OBJECTIVES 10

1.2 LAYOUT OF THE THESIS 11

2 ANATOMY OF THE ARM 13

2.1 SKELETAL APPARATUS OF THE ARM 14

2.1.1 Clavicle 15

2.1.2 Scapula (shoulder blade) 17

2.1.3 Humerus 19

2.1.4 Radius and Ulna 19

2.2 UPPER LIMB JOINTS 20

2.3 MUSCULAR APPARATUS OF THE ARM 22

2.3.1 Shoulder Muscles 23

2.3.2 Elbow Joint Muscles 28

3 FORWARD KINEMATICS: BASIC RULES, DEFINITIONS AND TERMINOLOGY 30

3.1 FORMALISM AND NOTATIONS USED FOR SPATIAL DESCRIPTION 31

3.1.1 Description of a Position (Cartesian frame) 31

3.1.2 Description of a Rotation 32

3.1.3 Description of objects 33

3.1.4 Transformations 34

3.2 KINEMATICS OF A MULTI-DEGREE-OF-FREEDOM SYSTEM 37

3.2.1 Forward kinematics 37

3.2.2 Inverse Kinematics 37

3.3 KINEMATIC MODELLING 38

3.3.1 The Denavit-Hartenberg Notation 39

3.3.2 Kinematic Relationship 41

3.3.3 Kinematic Equations *43*
3.3.4 Exception to the Denavit-Hartenberg notation rule *45*
3.4 ON THE WORKSPACE OF THE HUMAN ARM 48
4 TECHNIQUES USED TO MONITOR JOINT ROTATION 53
4.1 ELECTROMAGNETIC MEASUREMENT SYSTEMS 56
4.2 CAMERA-BASED SYSTEMS 56
4.3 THE SHOULDER COMPLEX 58
4.4 SUMMARY OF THE RELEVANT FINDINGS 82
5 MATERIALS AND METHODS 84
5.1 PRELIMINARY DESIGN STEPS 84
5.2 SENSOR DEVELOPMENT 88
5.3 DESIGN PHASE 89
5.4 SENSOR MODELLING 92
5.5 MECHANICAL DESIGN OF A ROTATING DEVICE 95
5.5.1 Concluding remarks *98*
5.6 THE MODEL FOR STERNO-CLAVICULAR MOVEMENTS 98
5.7 DESIGN OF THE DETECTOR OF STERNO-CLAVICULAR MOVEMENTS 102
5.8 GLOBAL AND LOCAL COORDINATE SYSTEMS 105
6 VALIDATION STUDIES 107
6.1 APPLICABILITY OF A STATISTICAL MODEL 109
6.2 VALIDATION OF THE ALGORITHM 110
6.2.1 Concluding remarks *116*
6.3 SENSITIVITY OF THE ALGORITHM TO THE VARIATION OF THE PARAMETERS L/R .. 116
6.4 MISALIGNMENT ERRORS 121
6.5 SENSITIVITY OF THE SYSTEM TO OPERATOR (INTER-INTRA OPERATOR ERRORS) .. 123
6.6 CONCLUSIONS 137
7 MODELLING OF CLAVICLE KINEMATICS 138
7.1 DEVELOPMENT OF A MATHEMATICAL MODEL 138

7.2 DATA COLLECTION 141

8 DISCUSSION 144

8.1 THESIS LEITMOTIV 144

8.2 MATHEMATICAL MODELLING 147

8.3 CLAVICLE MOTION 148

8.4 COMPARISON WITH DATA OF LITERATURE 152

9 CONCLUSIONS AND RECOMMENDATIONS FOR FUTURE WORK 162

9.1 RESULTS 163

9.2 TECHNICAL DEVELOPMENT 164

9.3 RECOMMENDATIONS FOR FUTURE WORK 165

9.3.1 Increased workspace 165

9.3.2 Arm kinematics 165

10 REFERENCES 168

11 APPENDIX A 179

12 APPENDIX B - RAW DATA OF THE TESTS 201

13 APPENDIX C – MATHCAD CODE 232

14 APPENDIX D – RESEARCH PUBLICATION 235

1 Introduction

The experimental and theoretical study of any complex system requires the cooperation of many disciplines such as biology, medicine, physics, chemistry, engineering and others. Thus it becomes necessary for scientists to look across the fence of their disciplines in order to allow a true cooperation and a consequent real progress. This Thesis is precisely written in this spirit giving ample space to verbal and pictorial description of the different topics treated in order to allow a more fluid reading.

The study of the human motion as a discipline is ancient almost like the man. Early theories and observations on these topics can be found in Hyppocrates' and Galeno's work. More recently Duchenne de Boulogne (1867), Marey (1885), Braune and Fisher (1888), Sherrington (1933), Luria and finally Haken (1996) applied new techniques to the study of movement trying to understand and localise also the main areas of the brain involved during motion.

Despite the richness of the literature produced, "man in motion" still represents a fascinating and partially unknown theme to deal with, particularly in the dynamic behaviour of the arms during the execution of specific tasks. Such movement, indeed individual expression of the complex interaction of biological subsystems (brain, muscles, skeleton, etc.) against the surrounding environment, hides nowadays its features and very few data are available on its kinematic and dynamic response.

This gap is largely due to the lack of knowledge on the dynamic movement of the "shoulder complex" and of the related muscles involved during motion. In fact, the large number of degrees of freedom to be measured and the high deformability of skin and soft tissues prevent the direct measurement of skeletal movements and contribute to increment the above described indetermination. Against this complex background, the rehabilitationist faces the pragmatic difficulties to decide which joints require attention as a priority or, in the case of biological damage, to assess the degree of impairment and subsequent recovery. As a result, clinical assessment is performed by the use of relatively elementary test tasks, which can be monitored either by timing or by some indirect measurement of the success of the execution.

The aim of the present research is then to provide new means of measurements to be used for gaining objective information on the motion particularly of "non visible" joints like the shoulder complex in order to characterise properly their motion and, in turn, the workspace of the arm.

1.1 Objectives

The main objectives of the research are to demonstrate, through an extensive review, the lack of knowledge in the field of clavicle kinematics, which, in turn, affects the knowledge of motion of the entire arm. The inadequacy of state-of-the-art techniques in providing accurate information on the kinematics of the clavicle is shown and, therefore, a new measurement system able to measure accurately clavicle kinematics proposed.

Such objectives will be pursued experimentally through the design and development of a new system of measurement as the necessary pre-requisite for the investigation on the nature of motion of a hidden joint. The logical steps carried out to pursue such objectives can be summarized as follows:

- To develop a technique able to provide information on the motion of the clavicle on "in vivo subjects";
- To develop a new miniaturized device to be located in close proximity of the joint under investigation able to monitor the angular motion of the limb;
- To carry out a thorough validation of the new measuring technique quantifying all the sources of errors during the execution of the tests;
- To investigate the motion of the clavicle in a subset of the allowable workspace as a function of scapular and humeral movements;
- To investigate the subject variability of clavicle kinematics with view to develop a statistical model of the clavicle behaviour in humans.

1.2 Layout of the Thesis

Chapter 2 deals with the anatomy of the upper limb describing the skeletal and muscular apparatuses and the concept of joint.

Chapter 3 is an introduction to the formalism and notations used to describe the position and orientation of an object with respect to a fixed frame. The Denavit-Hartenberg notation widely accepted in robotics as a systematic method to extract information on a chain mechanism is here extensively described. The last section of the Chapter deals with the concept of workspace and of the attempts followed to measure the workspace of the arm. Also in this field sterno-clavicular kinematics has been poorly treated.

Chapter 4 reviews literature concerning the techniques used in order to monitor the joint rotations. Advantages and drawbacks of each technique are extensively treated and the inadequacy of the methods proposed for the correct monitoring of "non-visible joints" like the sterno-clavicular one is demonstrated. From the conclusions of this chapter clearly emerges the need to have accurate information on the motion of non-visible joints in order to predict correctly the behaviour of the arm during motion.

Chapter 5 deals with the development of a new measurement system for the monitoring of each joint of the body. The "core" device is a miniaturized sensor exploiting the Hall effect that can be arranged conveniently in order to provide information on spherical joints. This section treats the mechanical development of the device, of its upgrading necessary to improve its performance and with the tests carried out in order to determine its precision, accuracy and repeatability. Based on this device, a detector of sterno-clavicular movements has been developed as a new technique for the monitoring of clavicle kinematics. It is demonstrated how, by exploiting the geometry of the joint, it is possible to design and develop an external kinematic chain able to monitor the 3 rotations of the clavicle.

Chapter 6 deals with the extensive battery of trials carried out in order to validate the results. The modelling and development phases of the devices are shown and the accuracy of the method determined through an extensive battery of validation tests.

Chapter 7 describes the development of a mathematical model based on the analysis of a set of experimental data taken on a sample of 10 subjects able to provide information on the 3D clavicle motion in the investigated workspace.

Chapter 8 presents the discussion of the findings compared with the existing knowledge.

Chapter 9 deals with the conclusion of the research including recommendations for future work.

Appendix A contains the graphs of the tests performed on subjects.

Appendix B contains the raw data obtained by the tests performed.

Appendix C contains the Mathcad code used to generate the model.

Appendix D contains a research publication written during the work undertaken within the thesis

2 Anatomy of the Arm

This chapter deals with the anatomy of the arm from a skeletal and muscular point of view as a pre-requirement necessary for the correct understanding of its kinematics. The systematic organization of joints and links together with the literature attempts to highlight its behaviour are given.

Before the advent of photography in 1839 (Thomas 1964), all the anatomy studies referred to the upper limb have been carried out by means of artists and professionals' drawings. Indeed, early studies on anatomic dissection are very rare; the first reliable is due to Erasistrato and Erofilo of the Ptolemaic Medical School of Alessandria in II Century B.C. Nevertheless, the best results have been obtained during the Renaissance, when the human body was the object of intense researches and enthusiasm. Inside the numerous reports of anatomic studies, surely the most important is linked to the name of Leonardo da Vinci in his Secret Writings on the examination of more than ten human cadavers.
Another fascinating aspect has dealt with human body proportions. The first researchers on divine proportions of the human body are the Egyptians while the clearest example of the relationship between art and mathematics is represented again by the deduction of Leonardo in his famous anatomic studies.

Regarding the human arm, its study can only be carried with an "a priori" deep understanding of the organisation of the skeletal and muscular apparatuses and their relationship. For this reason, in the following a brief overview of the skeletal and muscular apparatuses involved in the arm movement is given.

2.1 Skeletal Apparatus of the Arm

The upper limb articulates with the trunk at the level of the shoulder. From a skeletal point of view, by proceeding from the sternum to the humerus, the shoulder is basically formed by:

- clavicle;
- scapula;
- humerus.

The bones anatomical position can be seen in the assembly drawing shown in figure 2.1.

Figure 2.1 *Skeletal organization of clavicle, scapula and humerus*

In order to give a more comprehensible overview of the skeletal apparatus, a brief description of each bone is given before to deal with their functionalities proceeding from the sternum to the humerus.

2.1.1 Clavicle

The clavicle (see figure 2.2) takes its origin from the manubrium of the sternum (breast bone). The other extremity articulates with the acromion of the scapula. The superior surface of the clavicle is very close to the skin surface. In general, it has two curvatures: a medial anteriorly directed convexity, and a lateral, posteriorly directed convexity, both of which vary, depending upon the muscular and ligamentous attachments to the bone. A great part of the loads acting on the upper limb, are transmitted to the thorax through the clavicle.

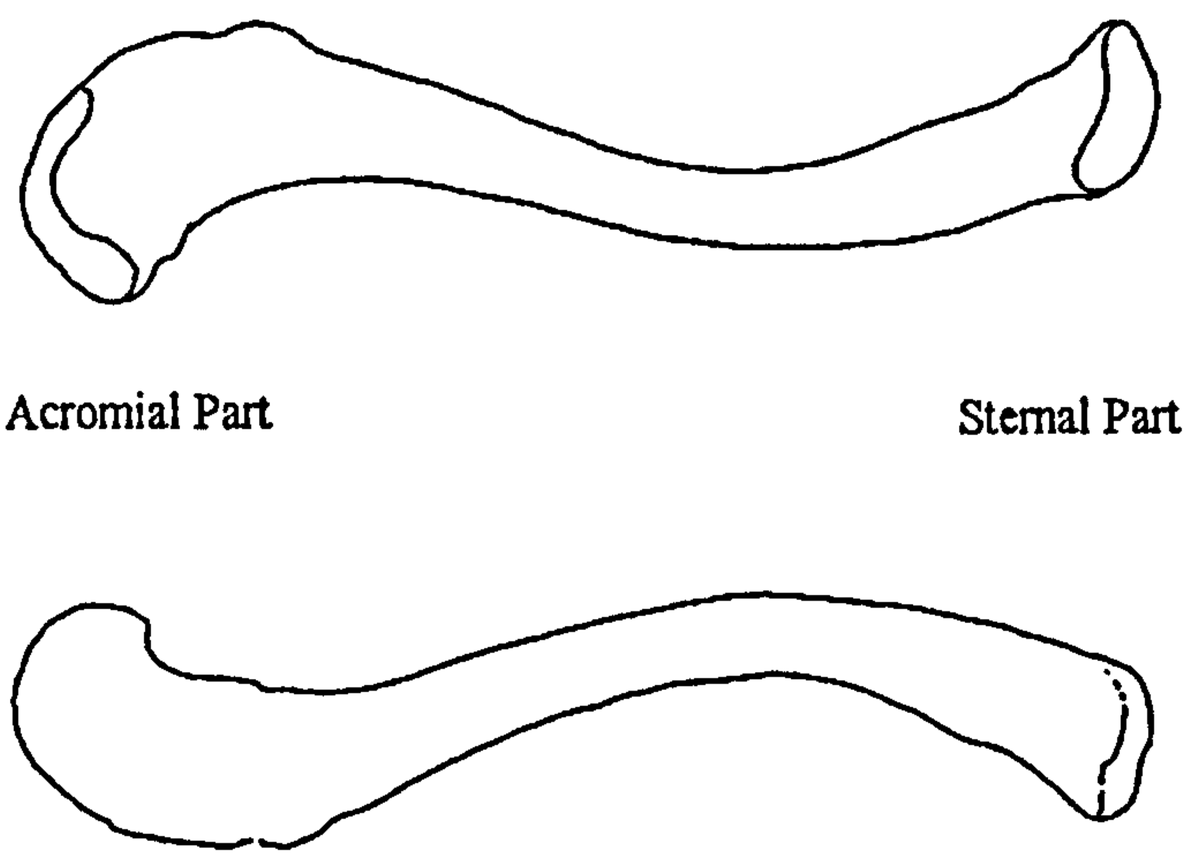

Figure 2.2: *Clavicle: frontal and dorsal views*

This fact combined with its superficial location, helps to make the clavicle the most commonly fractured bone in the human body (Harrington et al, 1993). Despite this fact, very little is known about its biomechanical function. Since it projects laterally and articulates with the scapula, the clavicle holds the shoulder out in a position that allows for

free swinging of the arms. It is worth mentioning that feline animals possessing a high dexterity and ability in using the anterior legs do not possess the clavicle. Functionally it serves as a strut for the upper extremity and the thorax. The mechanical behaviour of the clavicle is dependent upon the bone's material and geometric properties. By examining these variables, Harrington et al (1993) studied the biomechanical response of the clavicle to trauma and used the results to evaluate mechanisms of injury. In order to better understand its dynamic behaviour, in the following, a brief review is given of the ligamentous structure of the bone, with view to highlight the interaction with the other shoulder joints.

As shown in figure 2.3 and demonstrated by Bearn (1967), the costo-clavicular ligament, disposed as an inverted, truncated cone, acts as the limiting factor in elevation of the lateral end of the clavicle; as elevation proceeds, some researchers believe that the tension in the costo-clavicular ligament establishes a fulcrum and the further terminal elevation can occur only by a translation of the clavicular head in the inferior direction which is ended by tension in the superior fibres of the sterno-clavicular (SC) joint capsule. Although there is an impressive lack of data about the rotations occurring at the SC joint, most investigators assume that the point of intersection of the three rotation axes is positioned close to the clavicular attachment to such ligament.

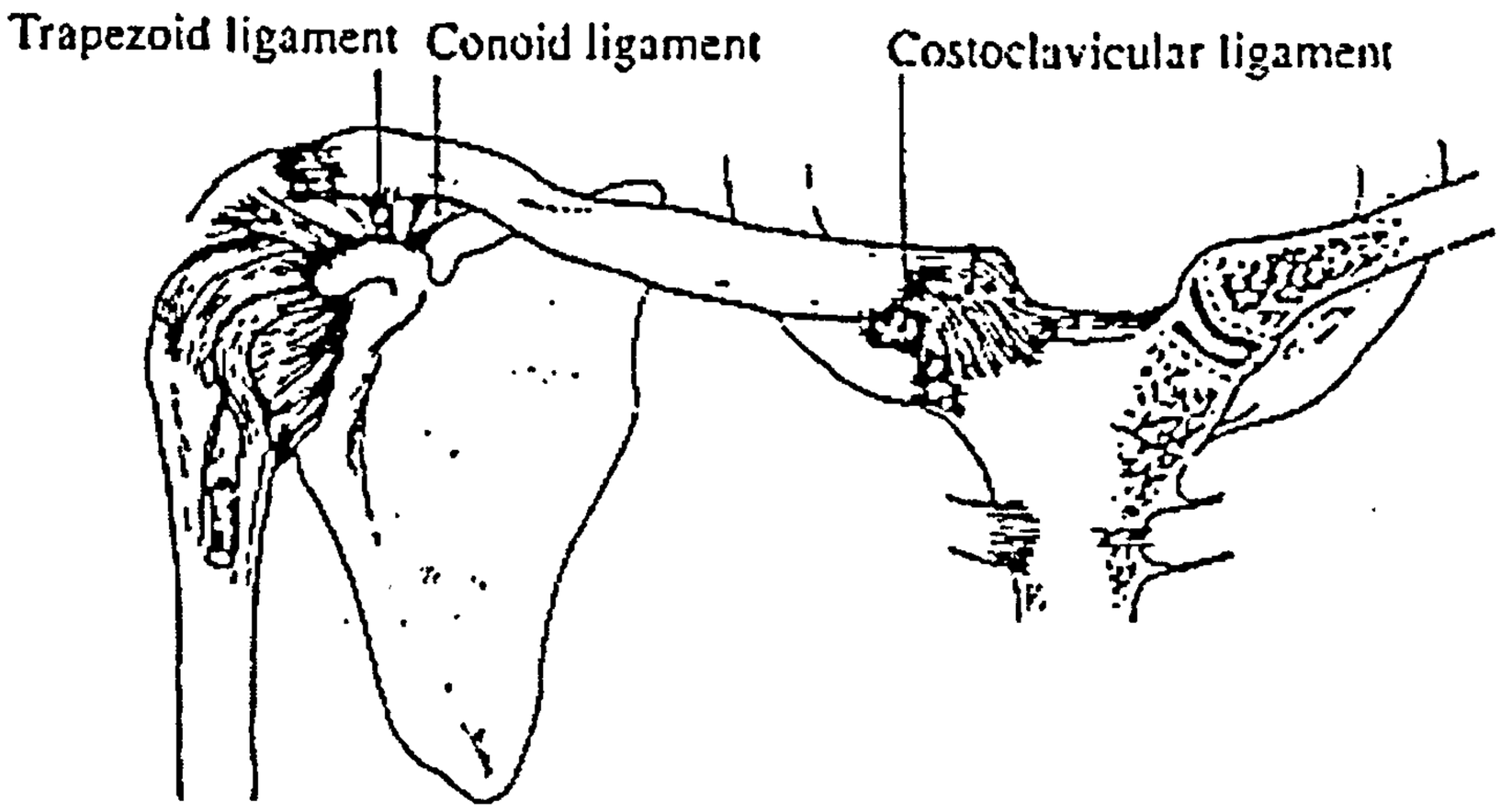

Figure 2.3 *Clavicle: main ligamentous structures*

The clavicle is highly variable in shape, and exhibits variations in both curvature and cross-sectional geometry along its length. In general the sternal portion of the clavicle is circular or ellipsoid in cross section, and the acromial portion is flatter on its superior and inferior surfaces.

The movements of clavicle and scapula determine the position of the shoulder joint. Once the shoulder joint has been positioned, the relevant muscles involved help to move the entire upper limb.

2.1.2 Scapula (shoulder blade)

The scapula is suspended in space by the muscles acting upon it and it is therefore not surprising that this bone reflects more clearly than any other the changes, during evolution, which have been brought about by more specialised functional demands.

The most striking and obvious modifications are those, which have occurred, in scapular shape. Those alterations, as shown by Inman et al (1944), can best be expressed by an index known as the scapular index, indicating the relationships of length to breadth of the bone. This index is extremely high in the pronograde, where the scapula is long and narrow, but due to increasing breadth, it progressively falls as we approach the orthograde, such as man, in which the forelimb has been completely freed. With reference to figure 2.4, another relevant feature is represented by the extension of the infraspinous fossa altering the relationship of the angle of action of its attached muscles, thereby establishing a feature of great importance in shoulder mechanism. The extension of the infraspinous fossa is undoubtedly related to the change of functional requirements of the attached muscles and, in addition, emphasizes the extraordinary significance of the infraspinal musculature in the attainment of a shoulder joint with the great range of motion of that found in man.

In figure 2.4 the anatomy of the scapula is shown. The anterior face of the scapula forms a triangle whose sides are called:

- superior side;
- medial side;
- lateral side.

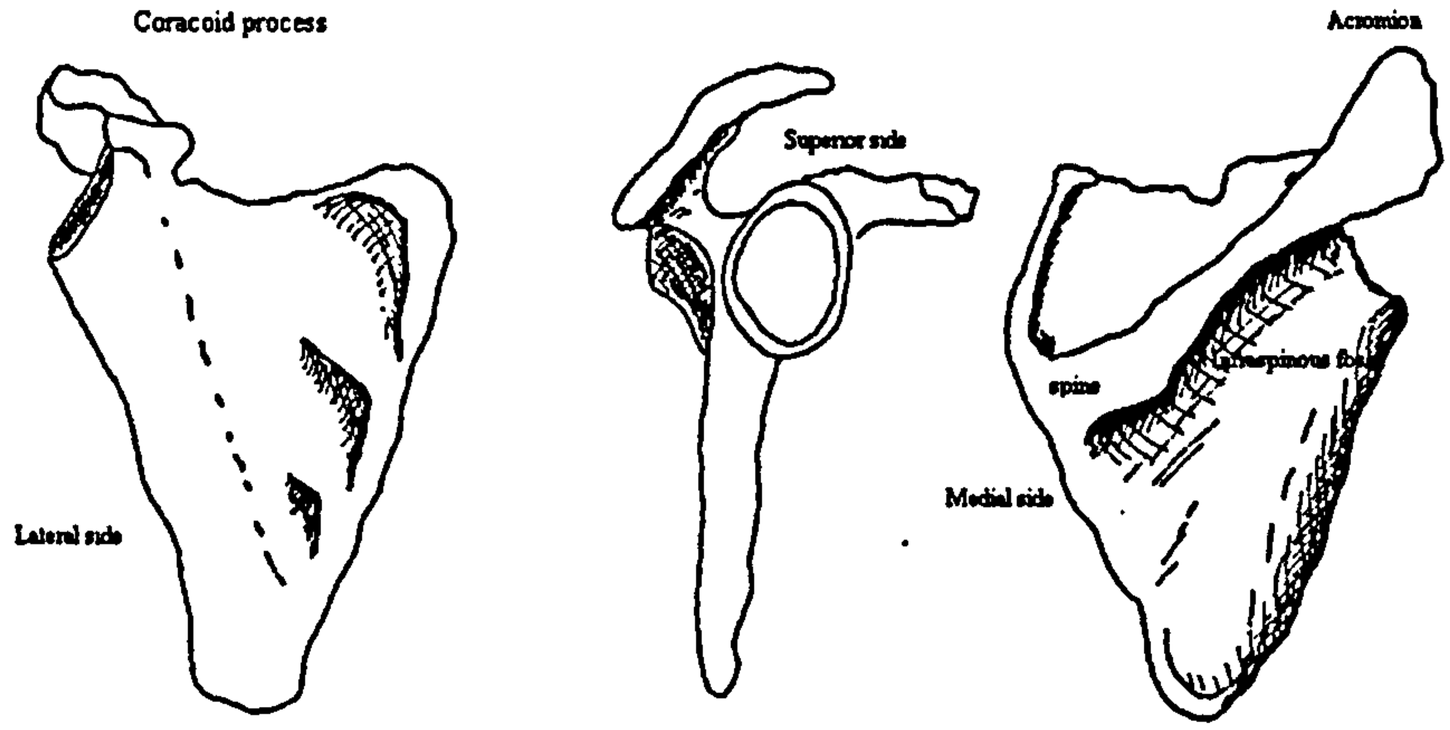

Figure 2.4: *Scapula: frontal, lateral and dorsal views* *

The muscles determining the spatial position of the scapula are inserted in these sides. At the level of the glenoid cavity, the scapula articulates with the extremity of the humerus. The lateral view (see figure 2.4) shows two different processes: the anterior one is called the coracoid process; the posterior is called the acromion. The acromion articulates with the clavicle (collar bone) at the acromio-clavicular (AC) joint. The acromion is a part of the spine of the scapula, which divides the back surface of the scapula into two regions, which are the insertion surfaces of the Supraspinatus and Infraspinatus muscles.

* The drawings from figure 2.4 to figure 2.13 have been made by the author

2.1.3 Humerus

In figure 2.5 the anatomy of the humerus is shown. Close to the humerus head two tuberosities can be distinguished:

- greater tuberosity;
- lesser tuberosity.

Both of them are areas for important muscle attachment. On the opposite side, the articulation with the ulna is obtained by means of the trochlea.

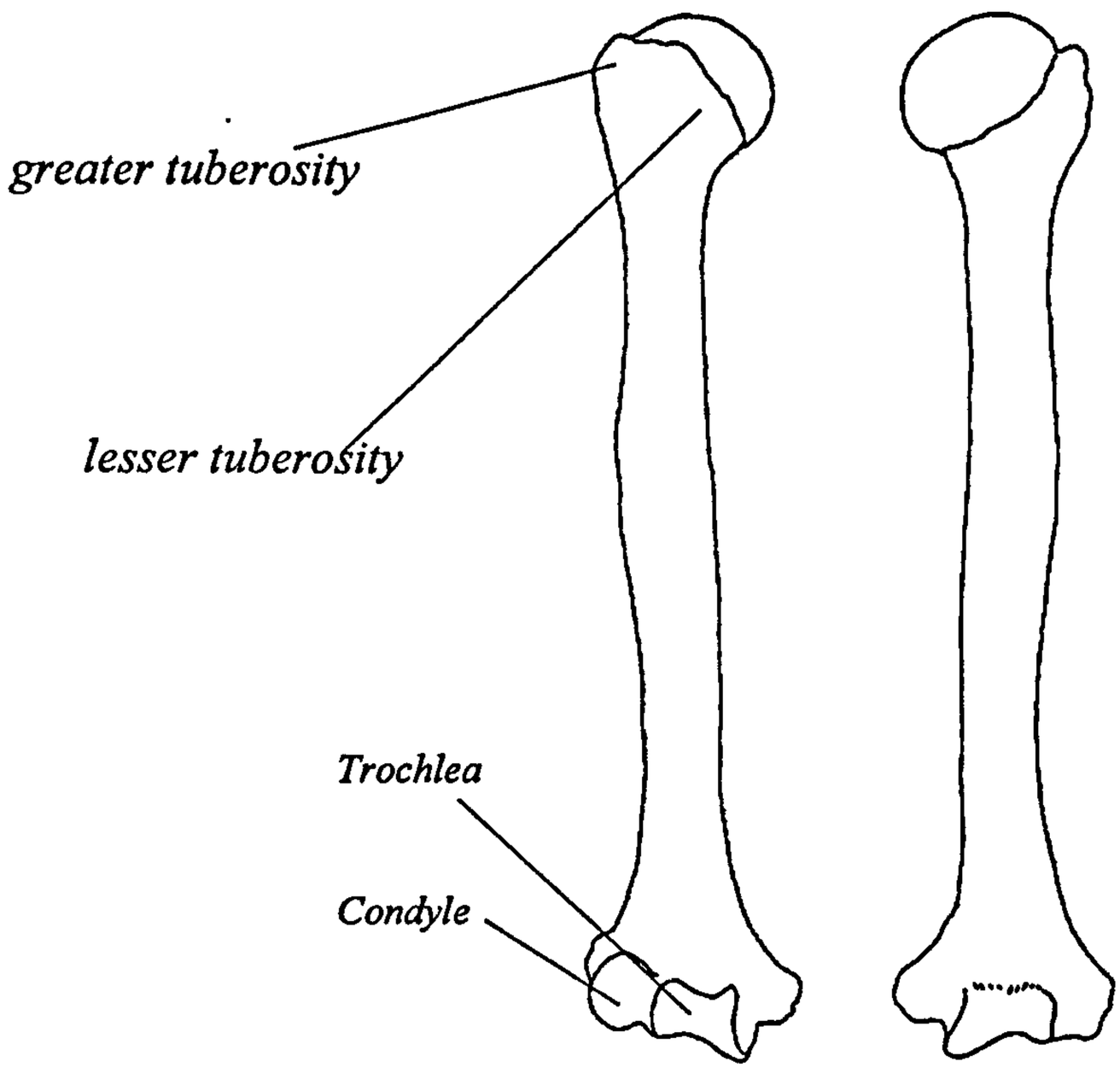

Figure 2.5: *Humerus: frontal and dorsal view*

2.1.4 Radius and Ulna

The Radius and Ulna are the bones of forearm. Ulna represents the sustaining structure for the elbow and articulates with the radius. In figure 2.6 the two bones are shown.

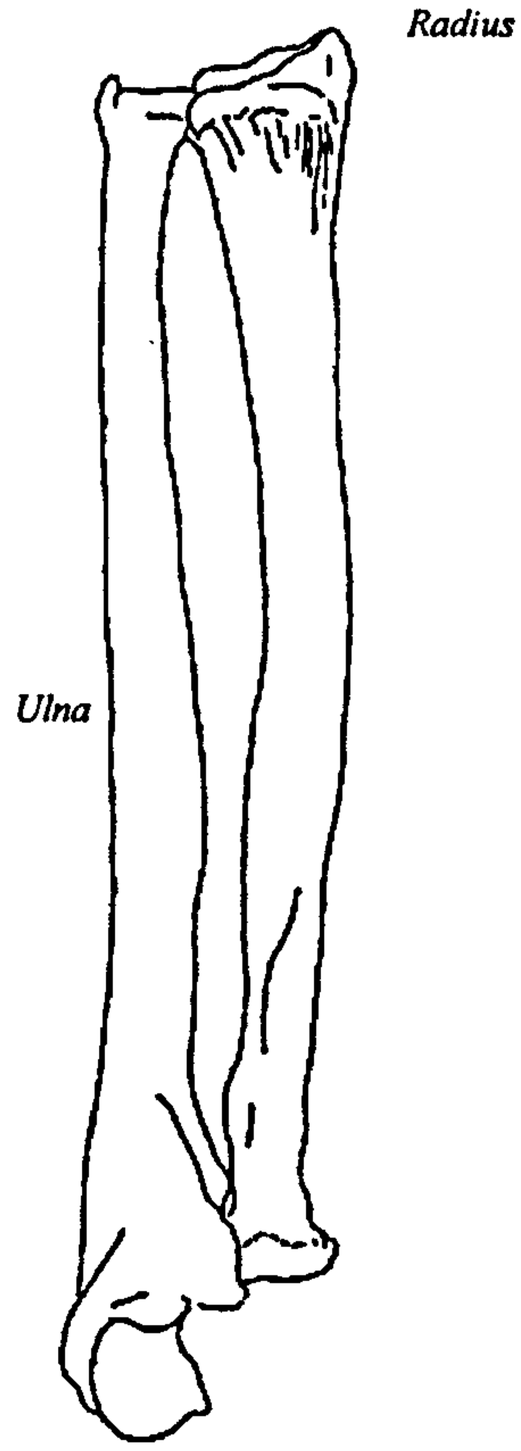

Figure 2.6: *Ulna and radius: frontal and dorsal view*

2.2 Upper Limb Joints

The different parts of the skeleton are connected either by attachments such as membranes or by joints. The function of joints is usually described with the aid of mechanical models; however, there is not always a close resemblance between mechanical models and actual joints of the human body.

As pointed out by Panjabi et al (1982) and Abdel-Rahman and Hefzy M.S. (1993), the articular surfaces are usually geometrically complex and somewhat compliant so that all joints are in reality six-degree-of-freedom joints. A deep investigation on the real behaviour of the real joints of the upper limb, very interesting from the modelling point of view, drops outside the purpose of the present research. In fact a good approximation of the arm structure can be obtained by considering it as a serial structure of links connected through joints. Nevertheless since during the past century a large number of papers and books have

appeared on anatomical joint motion both in terms of joint models and methods for describing the resulting motion, in the following a description of the real joint and some mechanical models proposed by different authors is given. Among the models proposed, the most often used have been described by Kinzel and Gutkowski (1982) who have shown the following 4 models:

1. one-degree-of-freedom hinge or revolute joint;
2. three-degrees-of-freedom planar joint;
3. three-degrees-of-freedom spherical or ball and socket joint;
4. six-degrees-of-freedom spatial joint.

Let us analyse in depth each of the four types presented:

1. Revolute Joint

It is used to describe the motion of the human elbow and wrist. The motion of the moving member is characterised by a single rotation axis embedded in the fixed member. Assuming that the location of the rotation axis is known, motion can be defined by the relative rotation between two reference lines intersecting in the rotation centre. The revolute joint is simple and it is commonly use in prosthetics and orthotics.

2. Planar Joint

The three degrees of freedom planar joint is often used as a model for the human knee. In a planar joint the relative motion between the fixed and moving member takes place in parallel planes; their relative position can be established by X, Y coordinates of two points in the moving member defined with respect to some arbitrary coordinate system in the fixed member. Although displacement can be defined in a large number of ways, the most used two dimensional procedure implies the concept of an instant centre of rotation. Let us assume F as the fixed member and M the moving one; if member F is taken as the reference member and the motion of M is defined into a series of discrete but infinitesimal displacements, the resulting instant centres of rotation become instant centres of velocity and form a curve in member F called the centrode of M with respect to F. Or, if M is taken

as the reference member and F is allowed to move, the resulting instant centres of rotation trace another curve in M called the moving centrode. As member M moves with respect to F, the moving centrode appears to roll on the fixed centrode and the relative displacement can be defined by the geometries of the fixed and moving centrodes. The centrodes are unique properties of the motion and are independent of the measurement method used to define them.

3. Three-degrees-of-freedom spherical Joint

The three-degrees-of-freedom spherical model is frequently used for the human hip and shoulder. The motion is characterized by all points of the moving member travelling on concentric spheres. In this model the moving member, such as the humerus, femur, or tibia, usually has a fairly well defined longitudinal axis.

4. Six-degrees-of-freedom Joint

The general six degrees of freedom joint does not assume any limitations on the number of degrees of freedom between the moving and fixed members. Six independent coordinates are necessary to identify the motion of the moving member.

The above-mentioned joint models can be applied to all the joints of the upper limb obtaining a well-defined kinematic model of the arm. In the following, before reviewing the techniques used to monitor the motion of the arm, a classical description of the muscular apparatus is given.

2.3 Muscular Apparatus of the Arm

Many muscles control the movements of the arm. From a mechanical point of view the muscular system is the "*actuator network*" responsible for movement and stabilisation of the arm. In order to give an overview of the upper limb, the muscular apparatus of each joint is presented.

2.3.1 Shoulder Muscles

Many authors have studied the muscular apparatus. In the present work, because of the relative focus given to shoulder dynamics, a classical description of the shoulder muscles is used. The adopted definitions take into account that the muscles can be grouped according to a common origin and a common insertion. Starting from the thorax and proceeding along the shoulder girdle and the humerus, the code identifier used in order to recognise each muscle is:

XXX-YZ

where:

XXX is the muscle identifier (initials of the muscle) and:

- Y name of origin bone(s)
- Z name of insertion bone(s)

Y and Z types:

T= Trunk

S= Scapula

C= Clavicle

H=Humerus

U=Ulna

R=Radius

The following groups have been addressed:

Group A

Muscles which have their origin on the trunk and their insertion on the scapula (see figure 2.7):

- Rhomboid Major (RHM-TS)
- Rhomboid minor (RHm-TS)
- Serratus Anterior Lower (SAL-TS)
- Serratus Anterior Upper (SAU-TS)
- Trapezius Lower Part (TLP-TS)

- Trapezius Middle Part (TMP-TS)
- Pectoralis minor (PEm-TS)
- Levator scapula (LES-TS)

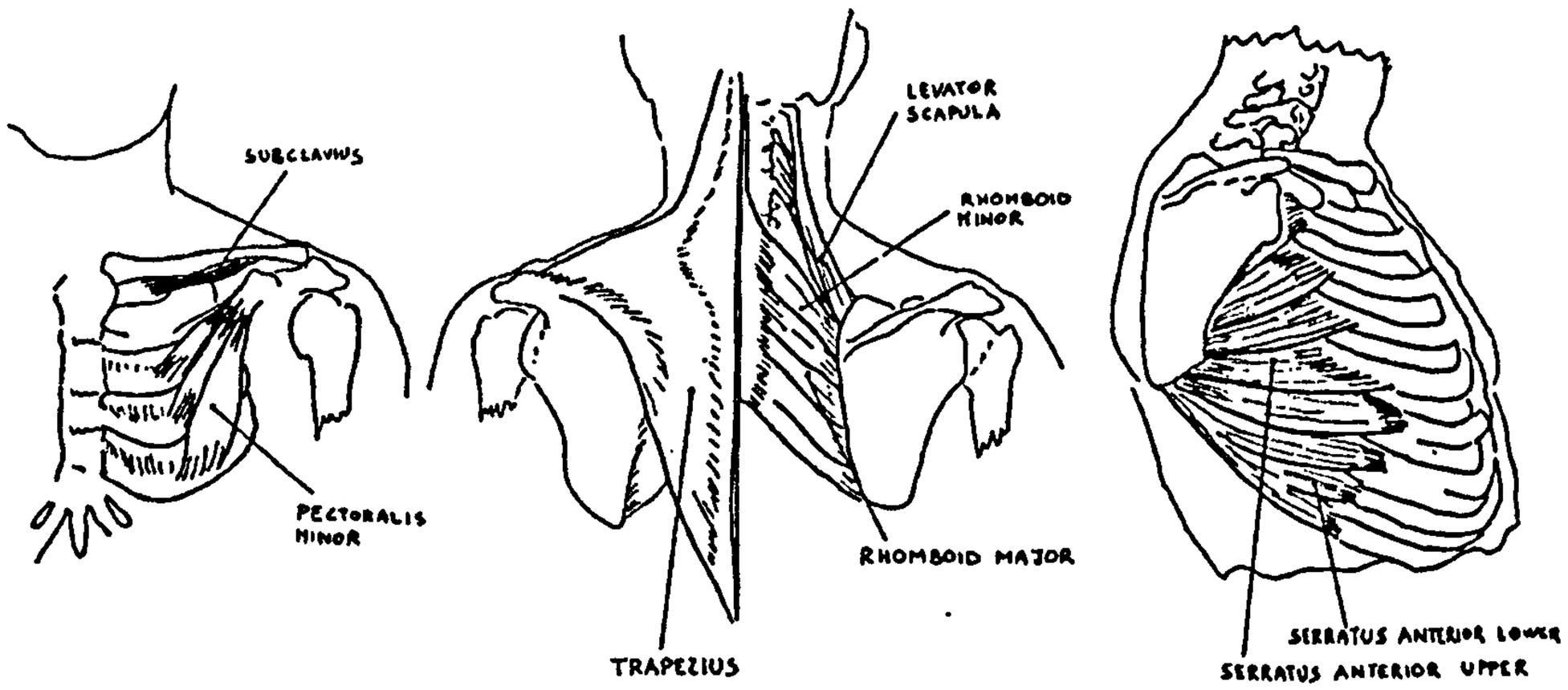

Figure 2.7: *Group A Muscles View*

Group B

Muscles which have their origin on the trunk and their insertion on the clavicle:

- Subclavius (SUB-TC) (see figure 2.7)
- Trapezius upper part (TUP-TC) (see figure 2.8)

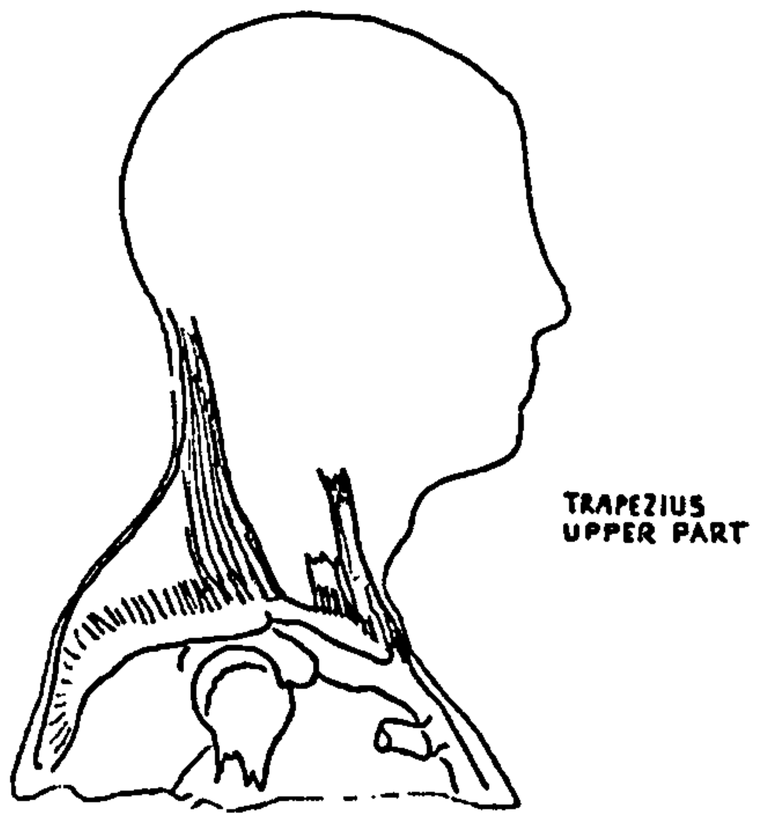

Figure 2.8: *Group B shoulder muscles*

Group C

Muscles which have their origin on the trunk and the insertion on the Humerus.

Pectoralis Major Sternocostal part (PMS-TH) (see figure 2.9)

Latissimus Dorsi (LAD-TH) (see figure 2.9)

Group D

Muscles which have their origin on the clavicle and the insertion on the Humerus.

- Deltoid Clavicular Part (DCP-CH) (see figure 2.10 a)
- Pectoralis Major Clavicular Part (PMC-CH) (see figure 2.9)

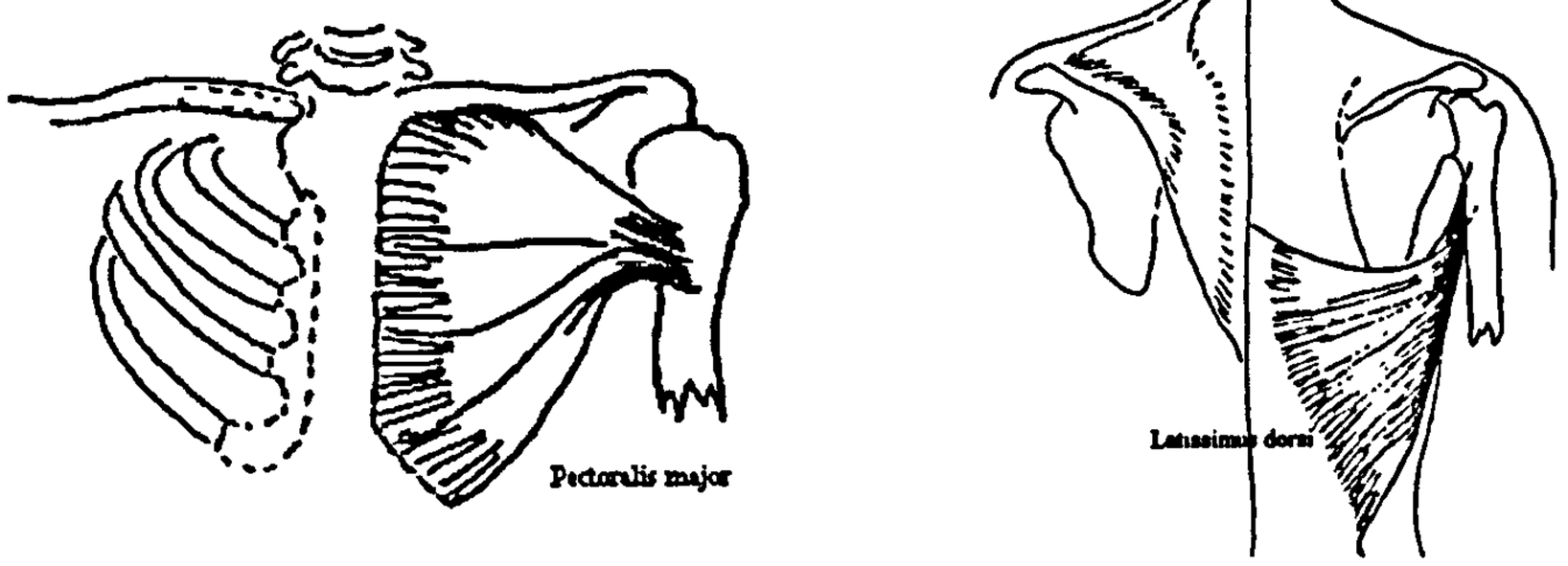

Figure 2.9: *Group C Shoulder Muscles*

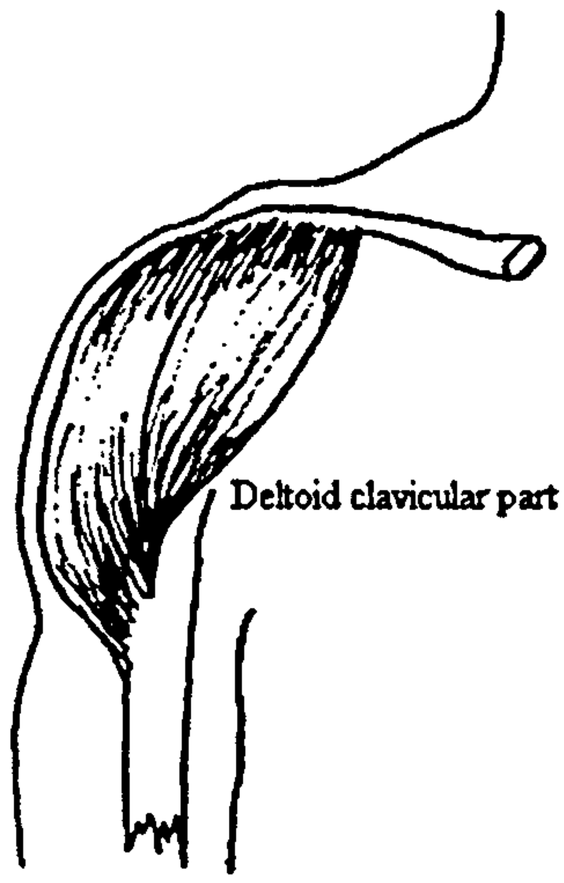

Figure 2.10 a: *Group D Shoulder Muscles*

Group E

Muscles having their origin on the scapula and which are inserted into the upper arm.

Sub-Group E1 Scapula-Humerus (Class XXX-SH) (see figure 2.10 b)

- Coracobrachialis (COR-SH)
- Deltoid Acromial Part (DAP-SH)
- Deltoid Scapular Part (DSP-SH)
- Infraspinatus (INF-SH)
- Supraspinatus (SUP-SH)
- Subscapularis (SUB-SH)
- Teres Major (TEM-SH)
- Teres minor (TEm-SH)

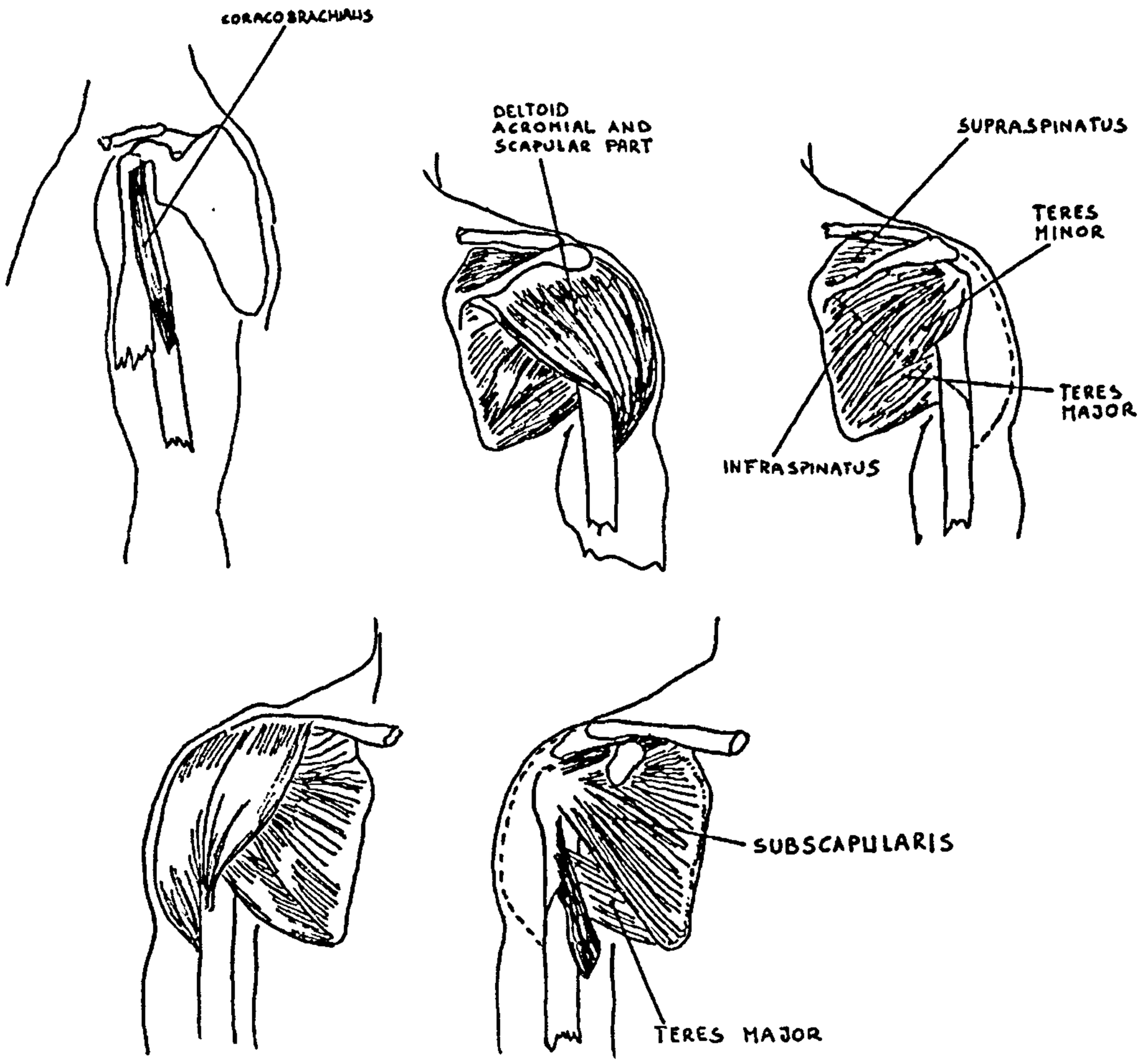

Figure 2.10 b: *Sub-Group E1: Scapula-Humerus Muscles*

Sub-Group E2 Scapula-Ulna (Class XXX-SU) (see figure 2.11)

- Triceps Long Head

Sub-Group E3 Scapula-Radio (Class XXX-SU) (see figure 2.11)

- Biceps Long Head (BLH-SR)
- Biceps Short Head (BSH-SR)

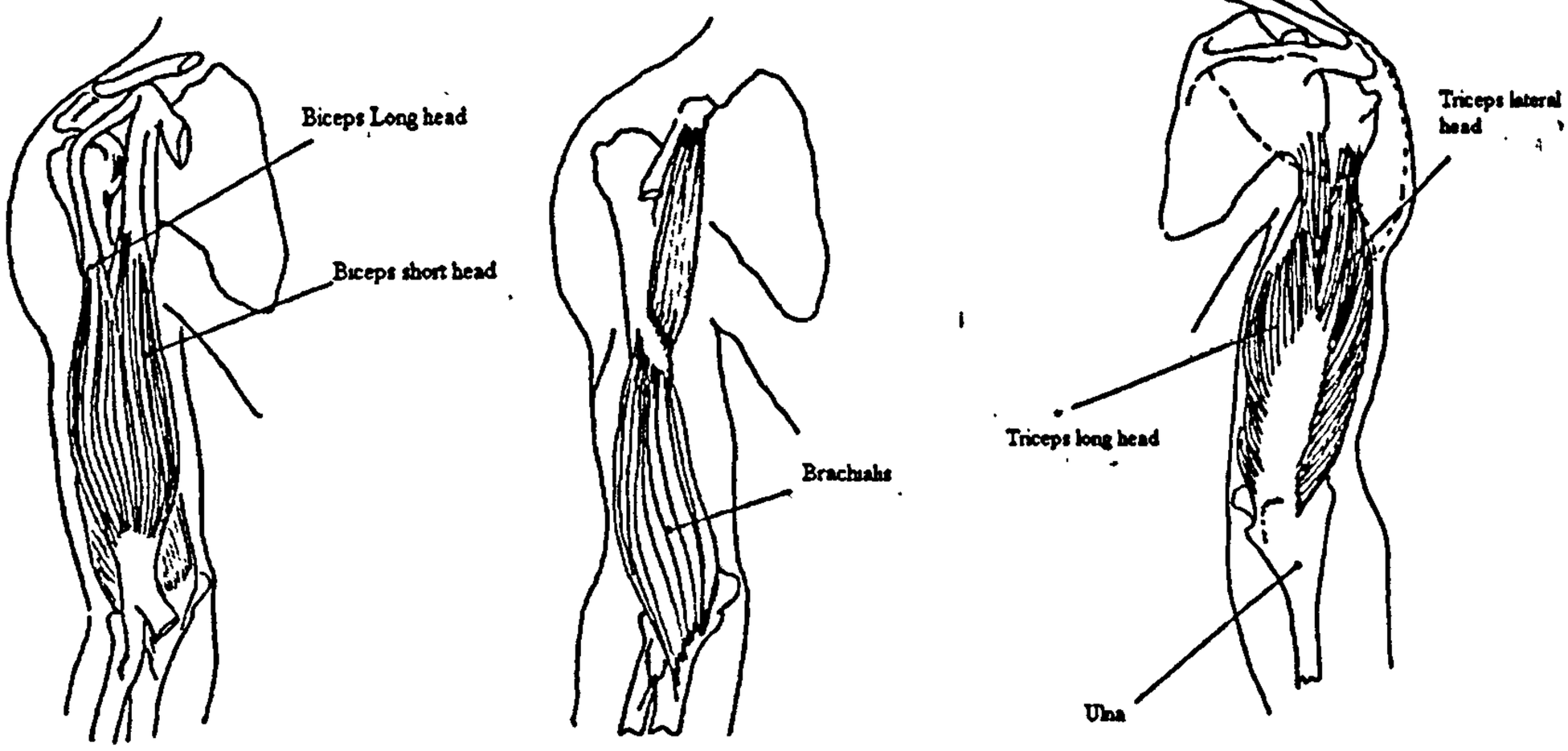

Figure 2.11: *Sub-Group E2-E3-F1 Shoulder Muscles*

Group F

Muscles having their origin on the Humerus and which are inserted into the lower arm (see figure 2.11).

Sub-Group F1 Humerus-Ulna (Class XXX-HU)

- Brachialis (BRA-HU)
- Triceps Lateral Head (TLH-HU)
- Triceps Medial Head (TMH-HU)

Sub-Group F2 Humerus-Radio (Class XXX-HR) (see figure 2.12)

- Brachioradialis (BRA-HR)

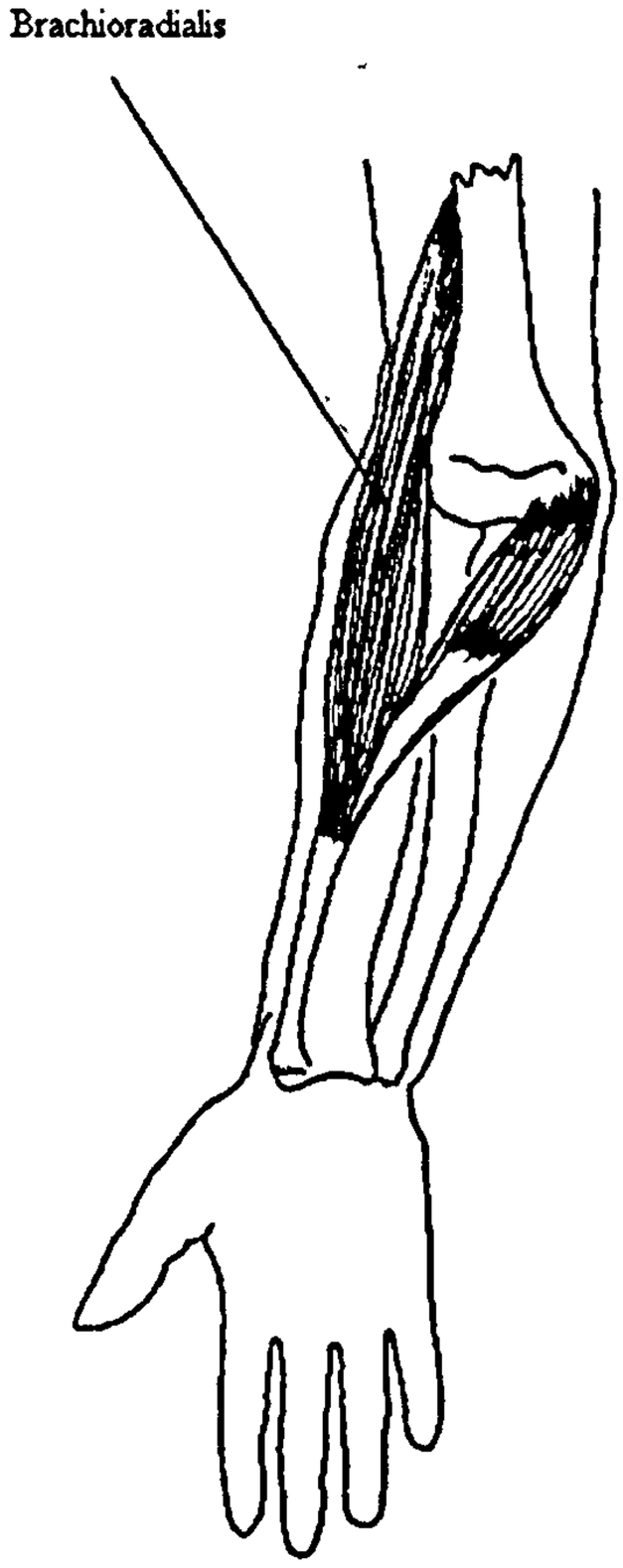

Figure 2.12: *Sub-Group F2 Shoulder Muscles (Humerus-Radio)*

2.3.2 Elbow Joint Muscles

The relevant muscles responsible for the motion of the elbow joint are depicted in figure 2.13. With reference to such figure, the three most important flexors are the following:

Brachioradialis;

Biceps Brachii;

Brachialis.

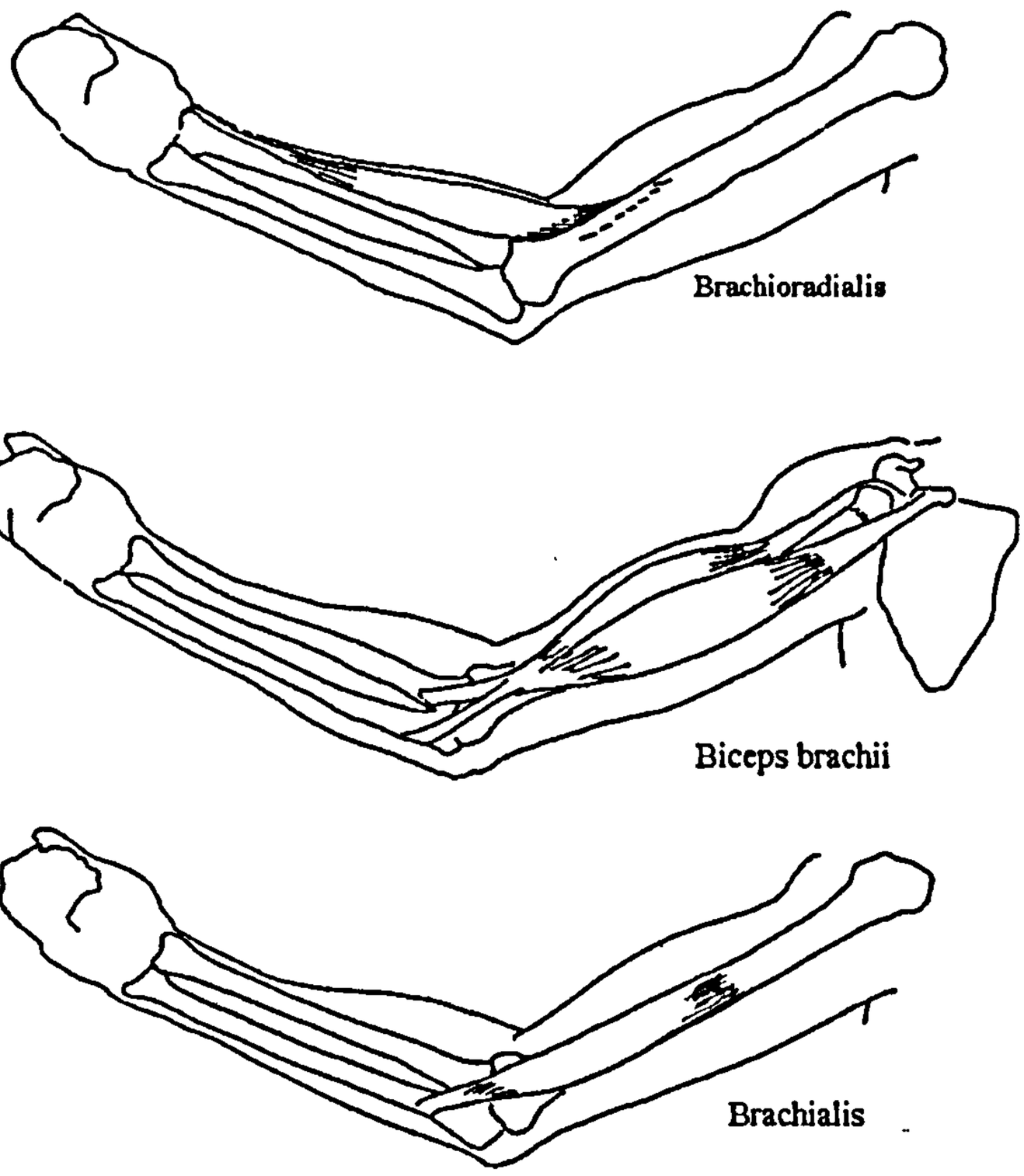

Figure 2.13: *Elbow joint Muscles*

Far from being an extensive treatise of the muscles of the arm, the above presentation is a general overview on the 'biomechanical actuator network' responsible for movement and stabilisation of the upper limb. Particular care has been given to the drawing representation to be considered as a powerful tool for a better understanding of the intimate connection between skin, skeletal and muscular apparatuses.

3 Forward Kinematics: Basic Rules, Definitions and Terminology

This Chapter introduces the notations used to describe the position and orientation of an object with respect to a fixed frame. It is an introduction to the formalism and notations used to describe the position and orientation of an object with respect to a fixed frame. The Denavit-Hartenberg notation widely accepted in robotics as a systematic method to extract information on a chain mechanism is here extensively described. The last section of the Chapter deals with the concept of workspace and of the attempts done in literature to measure the workspace of the arm.

Human locomotion is a theme that has attracted the most attention with researchers. This has been primarily due to the complexity of the movement and to the great relevance the study has with view to direct application to gait analysis and rehabilitation. Nevertheless in order to investigate human motion successfully, it is necessary to apply a strict formalism in the application of basic kinematic rules. In this chapter the upper limb is modelled as a variable geometry mechanical system formed by a set of rigid bodies connected through joints.
Links are here enumerated from 0 to N with respect to a base Cartesian frame. Joints are enumerated from 1 to N (see figure 3.1).
Degrees of freedom can be considered the number of independent joints or the number of independent variables necessary to specify the position of the mechanical system in the space.

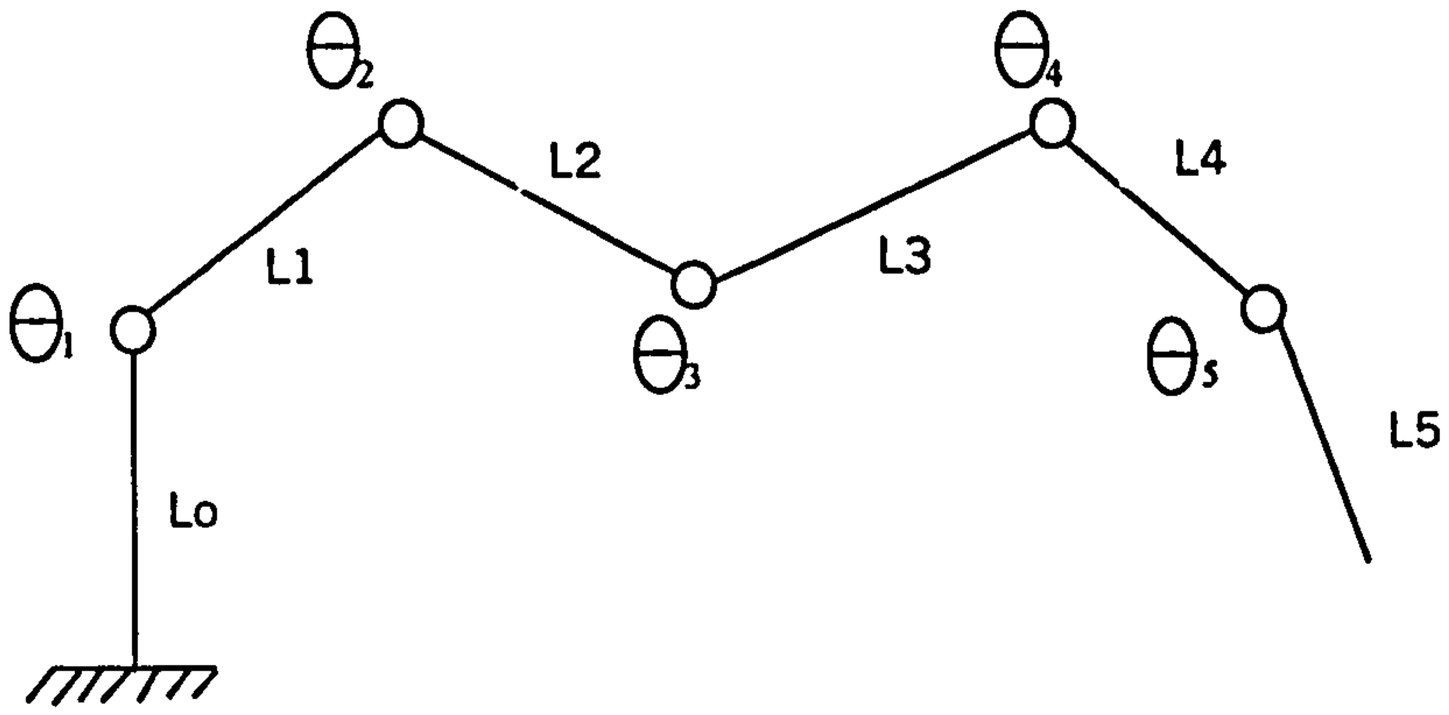

Figure 3.1: *Joints and Variables Enumeration*

An object in the space is completely localised through six independent parameters.

3.1 Formalism and Notations used for Spatial Description

3.1.1 Description of a Position (Cartesian frame)

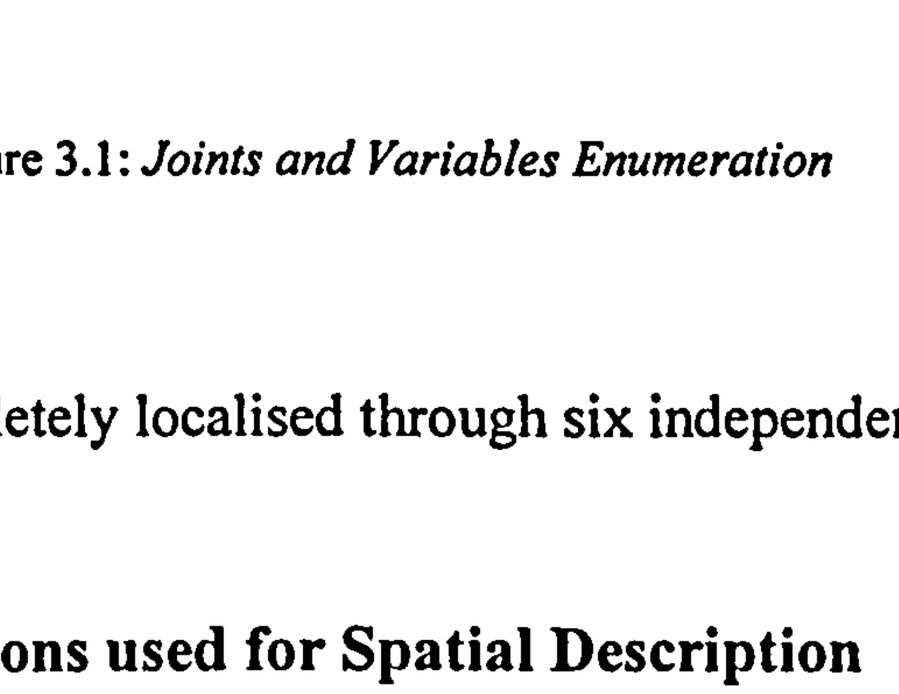

Fig. 3.2: *Cartesian Frame*

With respect to a Cartesian Frame A for the description of P in A we use (see figure 3.2):

$$ {}^{A}P = \begin{bmatrix} P_x \\ P_y \\ P_z \end{bmatrix} $$

3.1.2 Description of a Rotation

The orientation of an object in a base Cartesian Frame A can be described by means of the rotation of a frame B which is rigidly linked to the object. The rotation of a frame B in A can is defined by means of 3 unit vectors of B (X_b, Y_b, Z_b) in A.

Now we define:

$$^{A}R_B = (^{A}X_b, ^{A}Y_b, ^{A}Z_b)$$

which represents the rotation matrix of B with respect to A.

With reference to figure 3.3 if we want to describe B, which is rotated ϑ around Z_B we obtain:

$$^{A}X_B = \begin{pmatrix} \cos\theta \\ \sin\theta \\ 0 \end{pmatrix}$$

$$^{A}Y_B = \begin{pmatrix} -\sin\theta \\ \cos\theta \\ 0 \end{pmatrix}$$

$$^{A}Z_B = \begin{pmatrix} 0 \\ 0 \\ 1 \end{pmatrix}$$

$$^{A}R_B = \begin{pmatrix} \cos\theta & -\sin\theta & 0 \\ \sin\theta & \cos\theta & 0 \\ 0 & 0 & 1 \end{pmatrix}$$

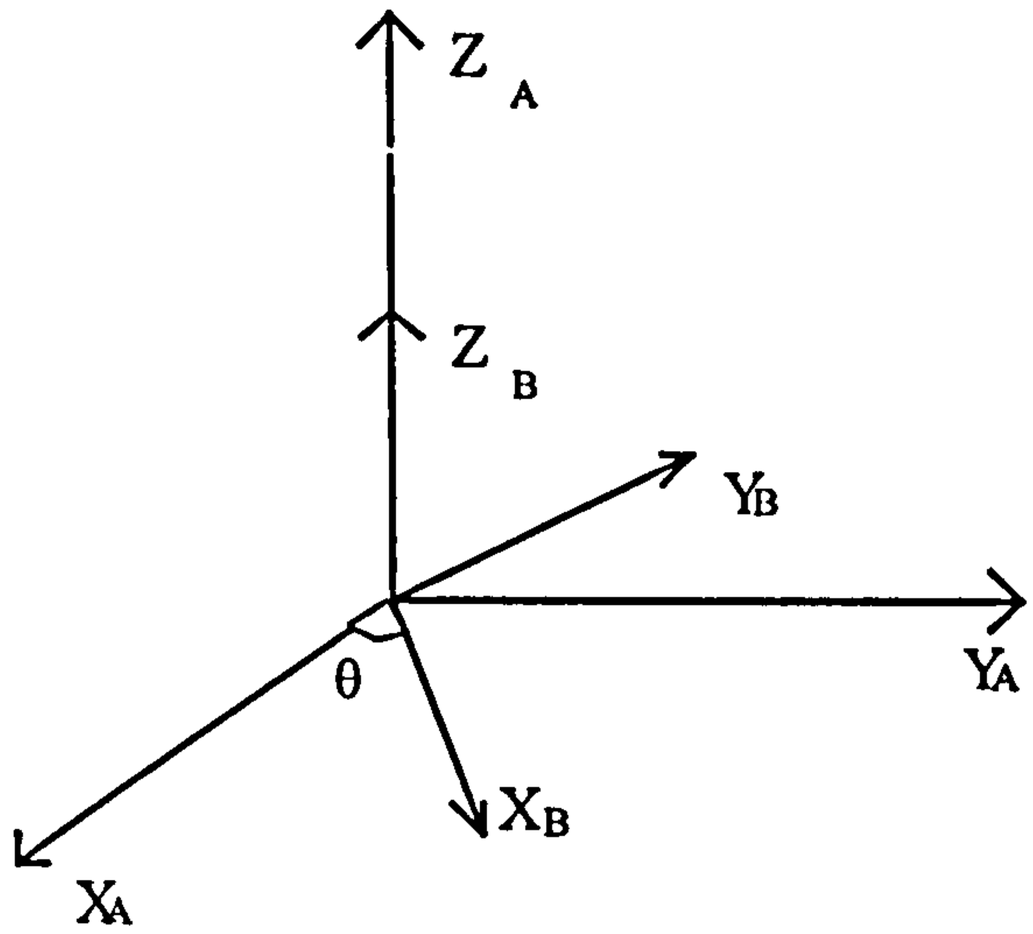

Fig. 3.3 *Description of a rotation*

3.1.3 Description of objects

A frame is determined by the position of its origin and by the rotation of its axes in the absolute base frame. We now define a couple position-orientation as an entity formed by 4 vectors providing information on position and orientation (see figure 3.4):

$\{{}^{A}R_B, {}^{A}P_{BO}\}$

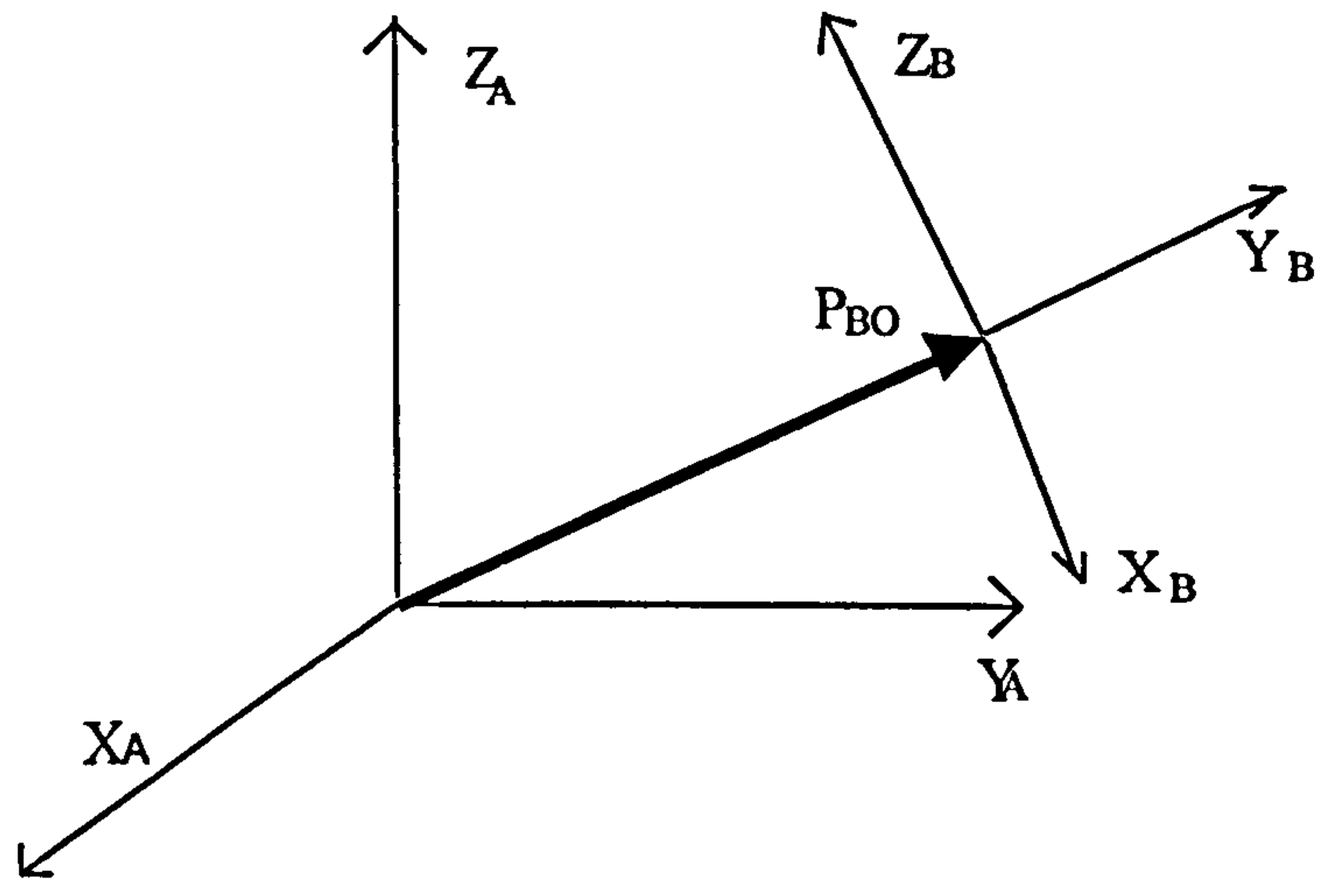

Fig. 3.4: *Definition of the couple position-orientation*

3.1.4 Transformations

Generally transformations are used to describe the motion of an object from a reference frame to another. The following cases can be distinguished:

Pure Translation

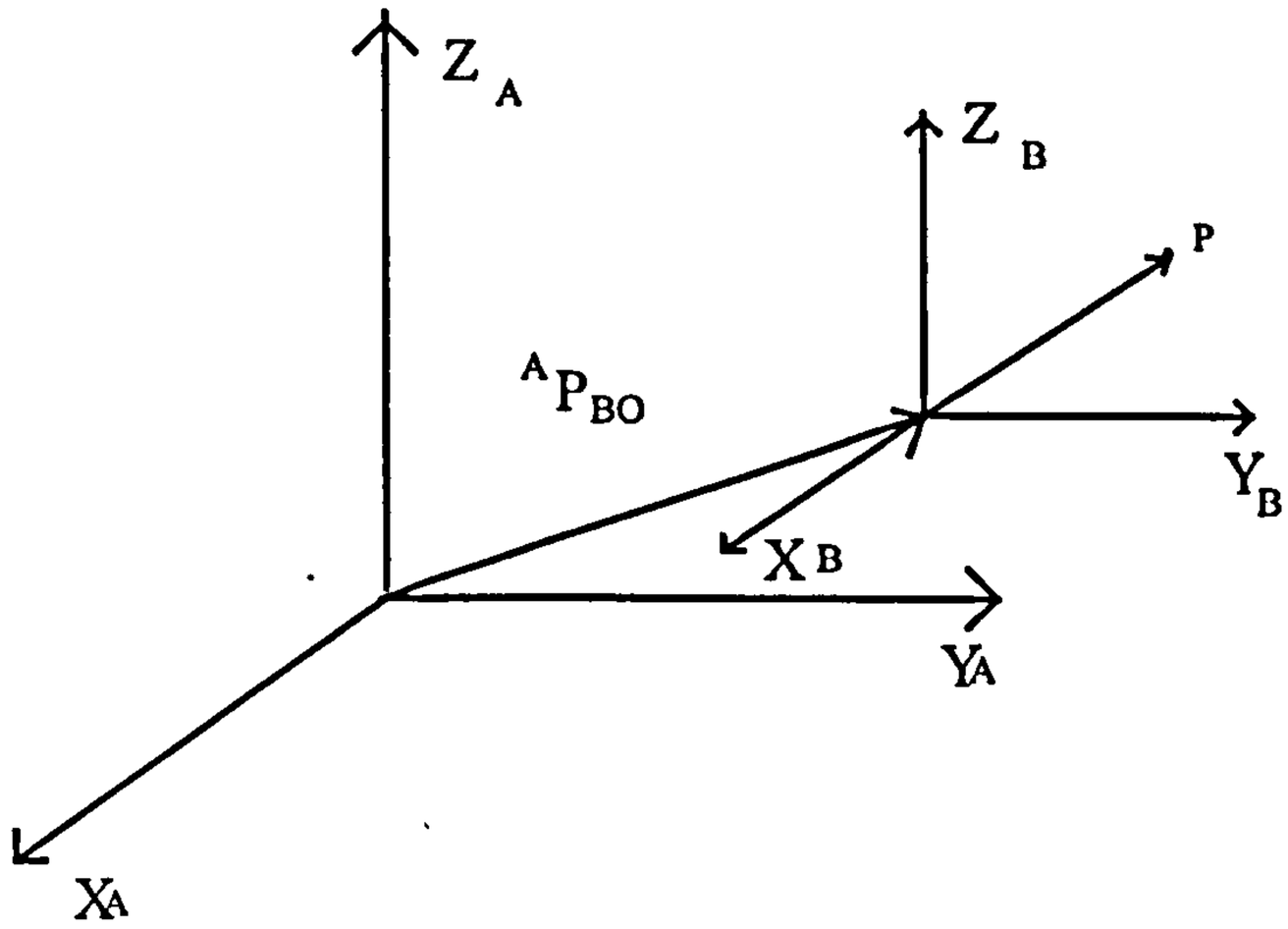

Figure 3.5: *Pure translation*

$$^{A}P = {}^{B}P + {}^{A}P_{BO}$$

Pure Rotation

In order to calculate ^{A}P (read P coordinates with respect to frame A) it can be noted that the components of a vector are *the components of the vector on the unit vectors of the reference frame.*

$$^{A}P_x = {}^{B}X_A \cdot {}^{B}P$$

$$^{A}P_y = {}^{B}Y_A \cdot {}^{B}P$$

$$^{A}P_z = {}^{B}Z_A \cdot {}^{B}P$$

$$^{A}P = \begin{pmatrix} ({}^{B}X_A)^T \\ ({}^{B}Y_A)^T \\ ({}^{B}Z_A)^T \end{pmatrix} \cdot {}^{B}P = ({}^{B}R_A)^T \cdot {}^{B}P = ({}^{B}R_A)^{-1} \cdot {}^{B}P = ({}^{A}R_B) \cdot {}^{B}P$$

Rotation +Translation

In the case of a frame B positioned in the space with respect to A we have:

$$^{A}P=^{A}P_{BO}+^{A}R_{B}.^{B}P$$

The above equation allows describing a vector from a reference frame to another. Nevertheless it would be better to define an operator matrix describing a generic transformation with:

$$^{A}P=^{A}T_{B}.^{B}P$$

This description of motion is an embedding of three-dimensional rigid body motion in $\Re^4$, where the homogeneous coordinates make possible the representation of both translation and rotation as a matrix multiplication.

It is now necessary to make a comparison between the Cartesian Space and the Homogeneous Space in order to find out the relationships between the two environments (Paul, 1981).

Cartesian Space	Homogeneous Space
$\begin{pmatrix} P_x \\ P_y \\ P_z \end{pmatrix}$	$\Rightarrow\Rightarrow\Rightarrow\Rightarrow\Rightarrow\Rightarrow\Rightarrow \begin{pmatrix} P_x \\ P_y \\ P_z \\ 1 \end{pmatrix}$
$\begin{pmatrix} V_x \\ V_y \\ V_z \end{pmatrix}$	$\Rightarrow\Rightarrow\Rightarrow\Rightarrow\Rightarrow\Rightarrow\Rightarrow \begin{pmatrix} V_x \\ V_y \\ V_z \\ 0 \end{pmatrix}$
$FRAME\{^{A}R_{B}, ^{A}P_{BO}\}$	$\Rightarrow \begin{pmatrix} ^{A}R_{B11} & ^{A}R_{B12} & ^{A}R_{B13} & ^{A}P_{BOx} \\ ^{A}R_{B21} & ^{A}R_{B22} & ^{A}R_{B23} & ^{A}P_{BOx} \\ ^{A}R_{B31} & ^{A}R_{B32} & ^{A}R_{B33} & ^{A}P_{BOx} \\ 0 & 0 & 0 & 1 \end{pmatrix}$

In $\Re^4$ it is easy to verify that $^{A}P=^{A}T_{B}{}^{B}P$

because

$$\begin{pmatrix} {}^{A}R_{B11} & {}^{A}R_{B12} & {}^{A}R_{B13} & {}^{A}P_{BOx} \\ {}^{A}R_{B21} & {}^{A}R_{C22} & {}^{A}R_{B23} & {}^{A}P_{BOx} \\ {}^{A}R_{B31} & {}^{A}R_{B32} & {}^{A}R_{B33} & {}^{A}P_{BOx} \\ 0 & 0 & 0 & 1 \end{pmatrix} \cdot \begin{pmatrix} {}^{B}P_x \\ {}^{B}P_y \\ {}^{B}P_z \\ 1 \end{pmatrix} = \begin{pmatrix} {}^{A}R_B{}^{B}P + {}^{A}P_{BO} \\ 1 \end{pmatrix} = \begin{pmatrix} {}^{A}P \\ 1 \end{pmatrix}$$

The 4*4 above matrix is called **Homogeneous Transformation.**

It allows the use of a simple multiplication matrix operator to represent a vector from A to B. Such transformations are useful to write compact equations, but their utilisation in calculating coordinates algorithms is not recommended because of the multiplication of 1 and zeros.

In Summary:

Homogeneous translations

$$Trans(d) = \begin{pmatrix} 1 & 0 & 0 & d_x \\ 0 & 1 & 0 & d_y \\ 0 & 0 & 1 & d_z \\ 0 & 0 & 0 & 1 \end{pmatrix}$$

Homogeneous Rotations

$${}^{A}Rot_B = \begin{pmatrix} r_{11} & r_{12} & r_{13} & 0 \\ r_{21} & r_{22} & r_{23} & 0 \\ r_{31} & r_{32} & r_{33} & 0 \\ 0 & 0 & 0 & 1 \end{pmatrix}$$

Homogeneous Roto-Translation

$${}^{A}T_B = \begin{pmatrix} r_{11} & r_{12} & r_{13} & d_x \\ r_{21} & r_{22} & r_{23} & d_y \\ r_{31} & r_{32} & r_{33} & d_z \\ 0 & 0 & 0 & 1 \end{pmatrix}$$

3.2 Kinematics of a multi-degree-of-freedom system

The kinematics of a *multiple degrees of freedom* system concerns the study of the geometric properties of the movements of the links in terms of translation, rotation, velocity, acceleration and jerk.

3.2.1 Forward kinematics

The purpose of the forward kinematics is to calculate the position and orientation of the end-effector with respect to a base frame reference.

The independent parameters are:

L_i = links length

ϑ_i=rotations

3.2.2 Inverse Kinematics

The purpose of inverse kinematics is to calculate the rotation of each joint corresponding to the position and orientation of the end effector. In general the configuration of a multi-degree-of-freedom system can be represented by:

a) Joint Space (vector of the joint variables) $\bar{\theta} \in \Re^N$

b) Cartesian Space (position and orientation of the end effector) $\bar{P} \in \Re^6$

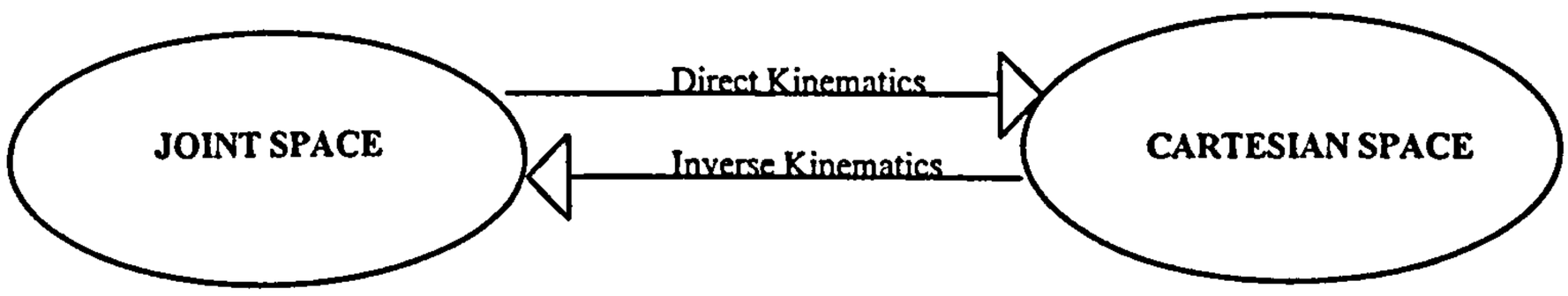

3.3 Kinematic Modelling [1]

The mathematical tools developed in the previous part can be applied to the kinematic modelling of manipulation arms to be treated as a series of rigid bodies connected through joints and forming a kinematic structure (see figure 3.6).

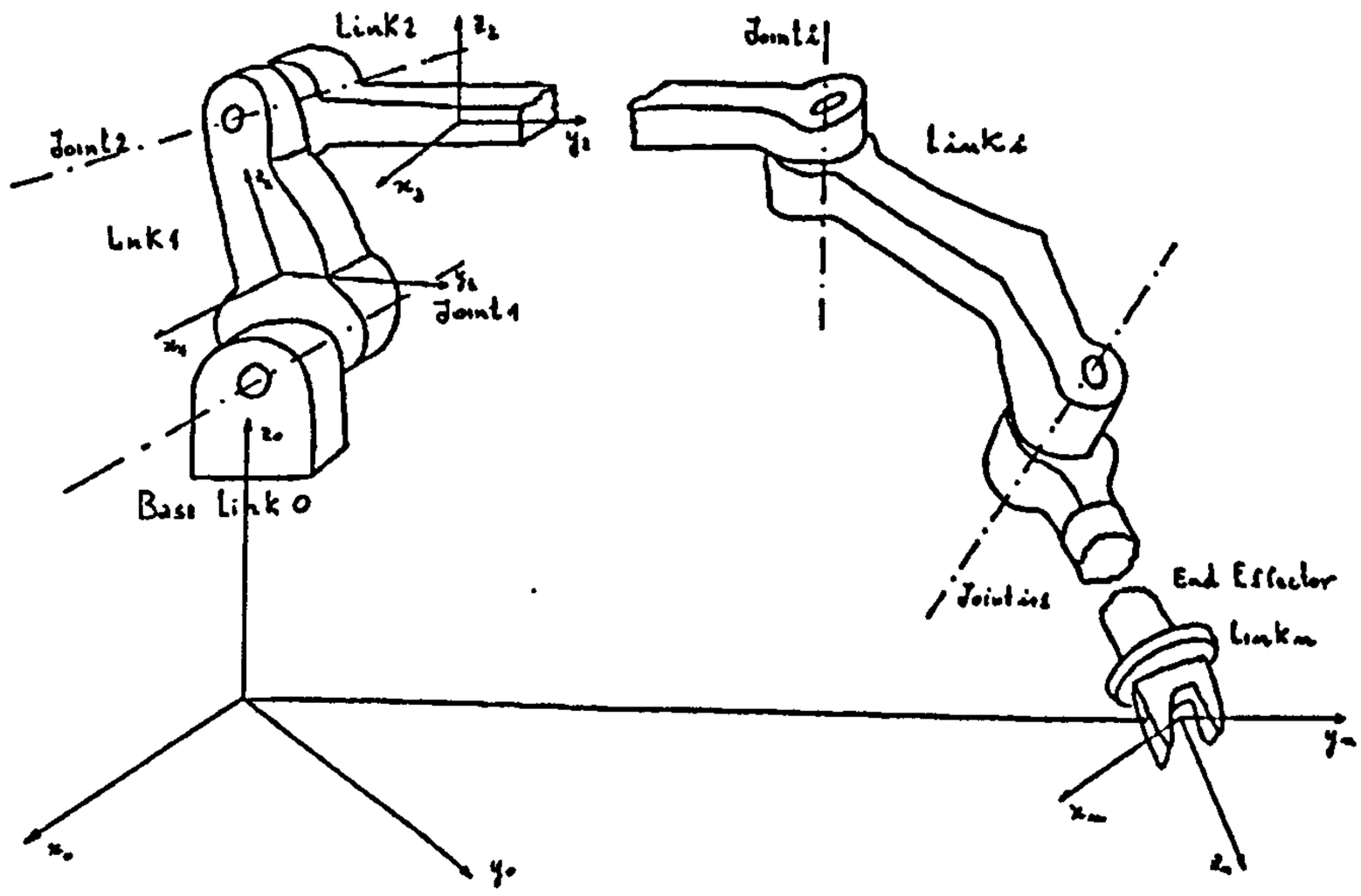

Figure 3.6: *Manipulation arm modelled as a serial linkage of rigid bodies*

In order to represent the position and orientation of the end-effector, we attach a coordinate frame O_n-$X_nY_nZ_n$ to the last link. The location of the coordinate frame is described with reference to another frame O_o-$X_oY_oZ_o$ fixed to the base link.

Motions of the intermediate joints between the base and the last link cause the end effector motion. Thus the end effector location can be determined by investigating the position and orientation of each link member in series. By attaching a coordinate frame to each link, namely O_i-$X_iY_iZ_i$ to link i, we can describe the position and orientation of the above frame

---

[1] The content of this chapter are based on Bergamasco (1994-1995).

relative to the previous frame O_{i-1}-$X_{i-1}Y_{i-1}Z_{i-1}$ by a 4x4 matrix describing the homogeneous transformation between these frames. The end effector position and orientation is then obtained by the consecutive homogeneous transformations from the last frame back to the base frame.

The motion of the joint connecting the two links causes the relative motion of the adjacent links.

There are a total of n joints involved in the manipulation arm consisting of (n+1) links.

We refer to the joint between link i-1 and link i as joint i.

3.3.1 The Denavit-Hartenberg Notation

The Denavit-Hartenberg (1955) notation is introduced as a systematic method of description of the kinematic relationship between a pair of adjacent links. The method is based on the 4x4 matrix representation of rigid body position and orientation. It uses a minimum number of parameters to describe completely the kinematic relationship.

In figure 3.7 a pair of adjacent links is shown. We can distinguish the following:

a) a pair of adjacent links: link i-1 and link i;

b) their associated joints: joint i-1, joint i, joint i+1;

c) line HiOi is the common normal to joint axes i and i+1.

The relationship between the two links is described by the transformation matrix indicating the relative position and orientation of the two coordinate frames attached to the two links.

In the Denavit-Hartenberg notation, the Origin of the (i_{th}) coordinate frame Oi is located at the *intersection of joint axis i+1 and the common normal between joint axis i and joint axis i+1.*

This means that the frame related to link i is at joint i+1 rather than at joint i.

The x_i axis is directed along the extension line of the common normal, while the z_i axis is along the joint axis i+1.

The y_i axis is chosen such that the resultant frame O_i-$X_iY_iZ_i$ forms a right hand coordinate system.

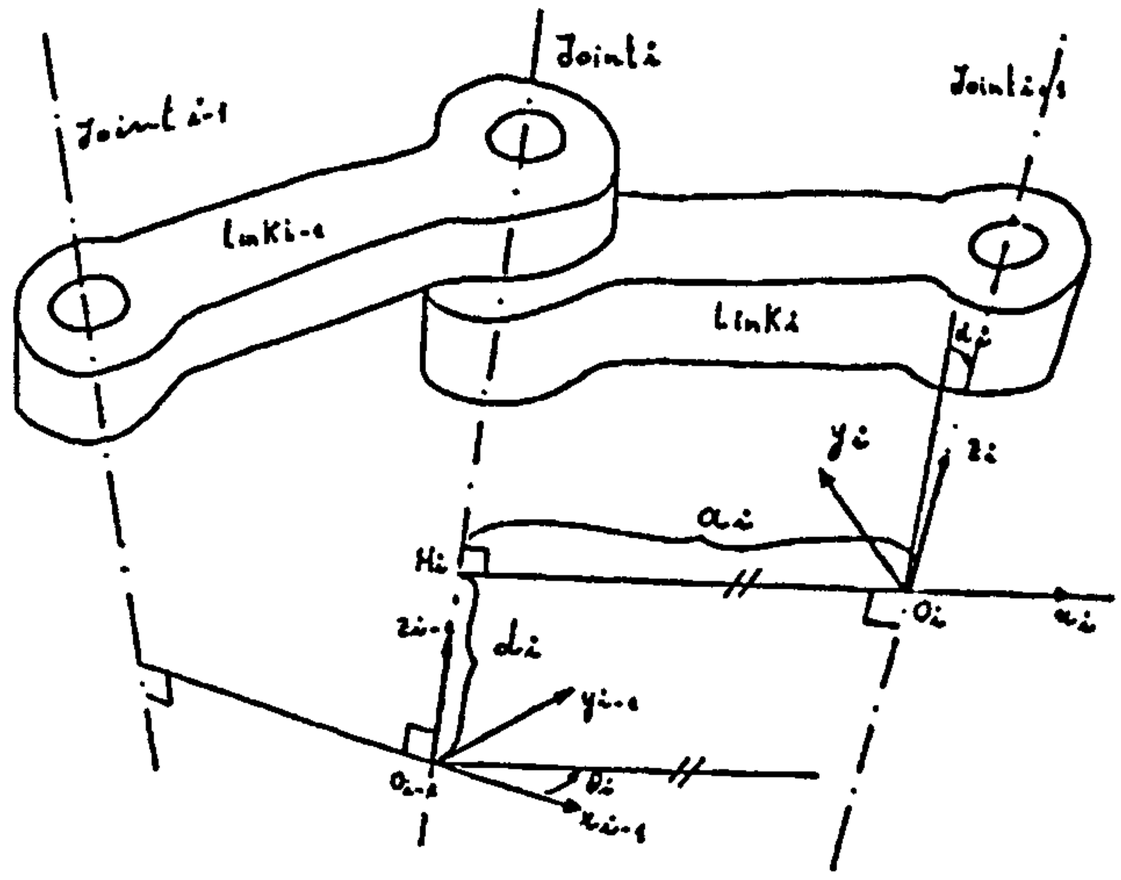

Figure 3.7: *Couple of adjacent links*

The relative location of the two frames can be completely determined by the following four parameters:

a_i the length of the common normal;

d_i the distance between the Origin Oi-1 and the point Hi;

α_i the angle between the joint axis i and the z_i axis in the right-hand sense;

ϑ_i the angle between the x_{i-1} axis and the common normal H_iO_i measured about the z_{i-1} axis in the right-hand sense.

The parameters a_i and α_i are constant parameters that are determined by the geometry of the link:

a_i represents the link length;

α_i is the twist angle between the two joint axes.

One of the other two parameters varies as the joint moves.

In general the typology of the joints is restricted to:

revolute joint: allows the rotation of the two links with respect to each other around the joint axis;

prismatic joint: allows the translation of the two links with respect to each other along the joint axis. In the case of a revolute joint, parameter ϑ_i is the variable that represents the joint displacement while parameter d_i is constant.In the case of a prismatic joint, on the other hand, parameter d_i is the variable representing the joint displacement, while ϑ_i is constant.

3.3.2 Kinematic Relationship

In the following, the kinematic relationship between two adjacent links using the 4x4 matrices is described. The 4x4 matrix representing the location of frame i relative to frame i-1 can be determined by considering the associated coordinate transformation (see figure 3.8). Let us assume the two frames:

o_i-$x_iy_iz_i$ fixed to link i

o_{i-1}-$x_{i-1}y_{i-1}z_{i-1}$ fixed to link i-1

and an intermediate coordinate frame $H_i - x'_{i-1}y'_{i-1}z'_{i-1}$ at H_i which is used to made calculations

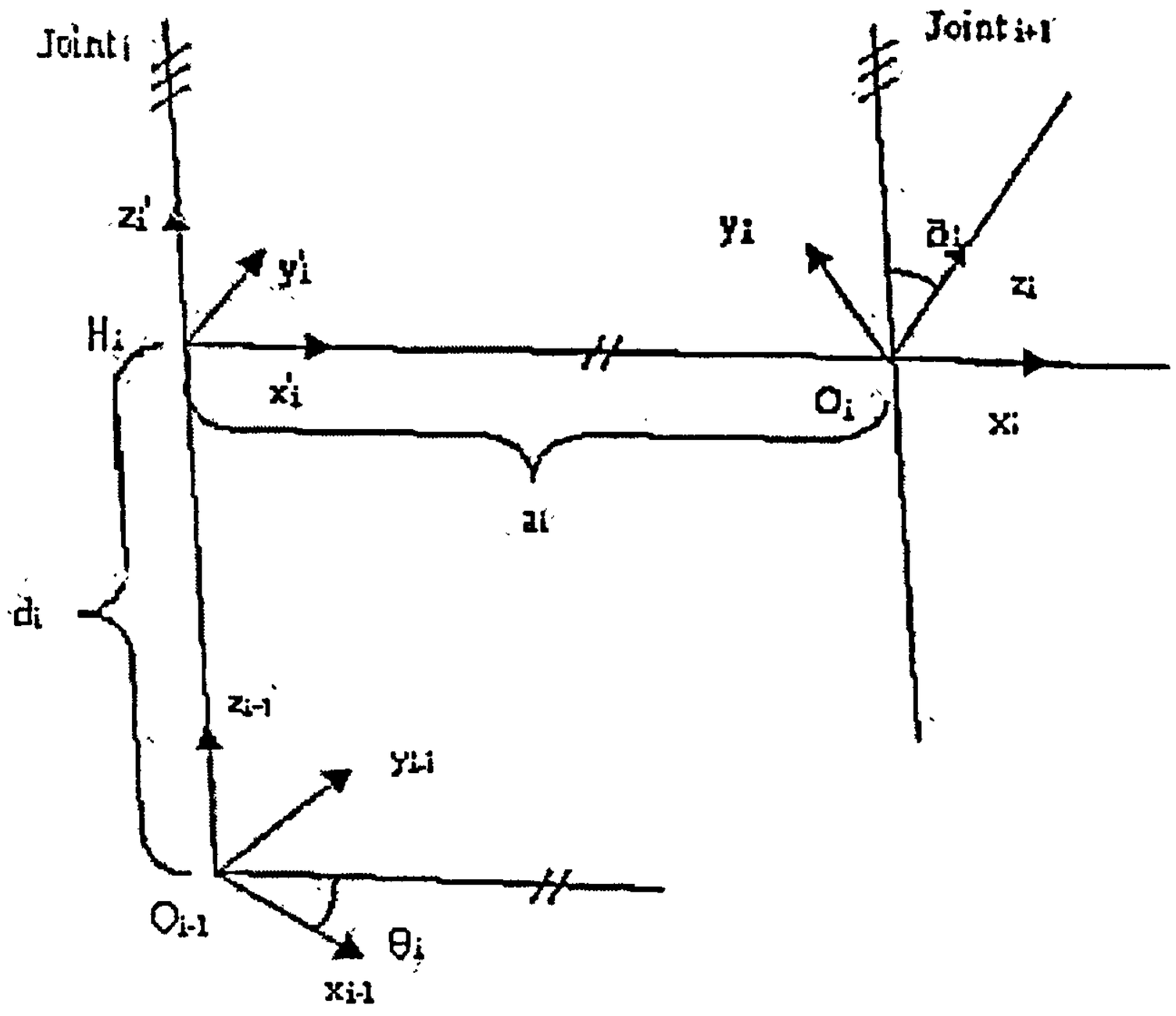

Figure 3.8: *Kinematic relationship between two adjacent links*

Let xi, x' and xi-1 be 4x1 position vectors in:

O_i-$x_iy_iz_i$ $\qquad$ $H_i - x'_{i-1}y'_{i-1}z'_{i-1}$ $\qquad$ O_{i-1}-$x_{i-1}y_{i-1}z_{i-1}$

The coordinate transformation from xi to x' is given by:

$$X' = A_i^{int} Xi$$

where the matrix A^{int} represents the transformation matrix between o_i-$x_iy_iz_i$ and o_{i-1}-$x_{i-1}y_{i-1}z_{i-1}$

$$A_i^{int} = \begin{bmatrix} 1 & 0 & 0 & a_i \\ 0 & \cos\alpha_i & -\sin\alpha_i & 0 \\ 0 & \sin\alpha_i & \cos\alpha_i & 0 \\ 0 & 0 & 0 & 1 \end{bmatrix}$$

similarly, the transformation from x' to x^{i-1} is given by:

$$X'^{-1} = A_{i-1}^{int} X'$$

where:

$$A_{i-1}^{int} = \begin{bmatrix} \cos\vartheta_i & -\sin\vartheta_i & 0 & 0 \\ \sin\vartheta_i & \cos\vartheta_i & 0 & 0 \\ 0 & 0 & 1 & d_i \\ 0 & 0 & 0 & 1 \end{bmatrix}$$

combining the two equations

$X' = A_i^{int} Xi$ $\qquad$ and $\qquad$ $X'^{-1} = A_{i-1}^{int} X'$

we obtain

$$X^{i-1} = A_i^{i-1} X^i$$

where

$$A_i^{i-1} = \begin{bmatrix} \cos\vartheta_i & -\sin\vartheta_i \cos\alpha_i & \sin\vartheta_i \cos\alpha_i & a_i \cos\vartheta_i \\ \sin\vartheta_i & \cos\vartheta_i \cos\alpha_i & -\cos\vartheta_i \sin\alpha_i & a_i \sin\vartheta_i \\ 0 & \sin\alpha_i & \cos\alpha_i & d_i \\ 0 & 0 & 0 & 1 \end{bmatrix}$$

The matrix A_i^{i-1} represents the position and orientation of frame i relative to frame i-1. The first 3 3x1 column vectors contain the direction cosines of the coordinate axes of frame i, while the last 3x1 column vector represents the position of the origin O_i with respect to the frame O_{i-1} X_{i-1} Y_{i-1} Z_{i-1}

3.3.3 Kinematic Equations

Using the Denavit-Hartenberg notation we express the position and orientation of the end-effector as a function of joint displacements.

The displacement of each joint is either angle ϑ_i or distance d_i depending on the joint type.

With revolute and/or prismatic joints, the chain of n+1 articulated links possesses n degrees of freedom, and a set of $q_1, q_2, \ldots q_n$ of n joint coordinates can be selected as a generalised coordinate system for the manipulator.

Let us define the binary parameter

$$\varepsilon_i = \begin{cases} 0 \\ 1 \end{cases}$$

0 for a revolute joint

1 for a prismatic joint

The i^{th} generalised coordinate can then be written as:

$$q_i = \bar{\varepsilon}_i \vartheta_i + \varepsilon_i d_i$$

with

$$\bar{\varepsilon}_i = 1 - \varepsilon_i$$

The configuration of the manipulator can then be described by the vector $\underline{\bar{q}}$ of components $q_1, q_2, \ldots q_n$ in the manipulator joint space.

$$q_i = \vartheta_i$$
$$q_i = d_i$$

for a revolute joint and a prismatic joint respectively.

The position and orientation of link i relative to link i-1 is then described as a function of q_i using the 4x4 matrix.

The pursued goal is to describe the position and orientation of the end effector with respect to the base frame as a function of joint displacements, $q_1, q_2, \ldots q_n$.

The manipulator arm consists of n+1 links from the base to the tip, in which relative locations of adjacent links are represented by the 4x4 matrices.

Considering the n consecutive coordinate transformation along the serial linkage, we can derive the end-effector location viewed from the base frame.

The position and orientation of the last link relative to the base frame is given by:

$$T = A_1^0(q_1) A_2^1(q_2) \ldots\ldots A_n^{n-1}(q_n)$$

where T is a 4x4 matrix representing the position and orientation of the last link with reference to the base frame.

This equation provides the relationship between the last link position and orientation and the displacements of all the joints involved in the open kinematic chain.

It is referred as the ***Kinematic Equation*** **of** the manipulator arm and governs the fundamental kinematic behaviour of the arm.

3.3.4 Exception to the Denavit-Hartenberg notation rule

There are several exceptions to the Denavit-Hartenberg rule. For example to define a coordinate frame attached to each link, the common normal between the two joint axes must be determined for the link. However, no such common normals exist for the base and the last links, since each of these links has only one joint axis.

For these two links, the coordinate frames are defined as follows:

Last link

The origin of the Coordinate frame can be chosen in any convenient point of the end effector. The orientation of the coordinate frame, however, must be determined so that the x_n axis intersects the last joint axis at a right angle. The angle α_n shown in figure 3.9 is arbitrary.

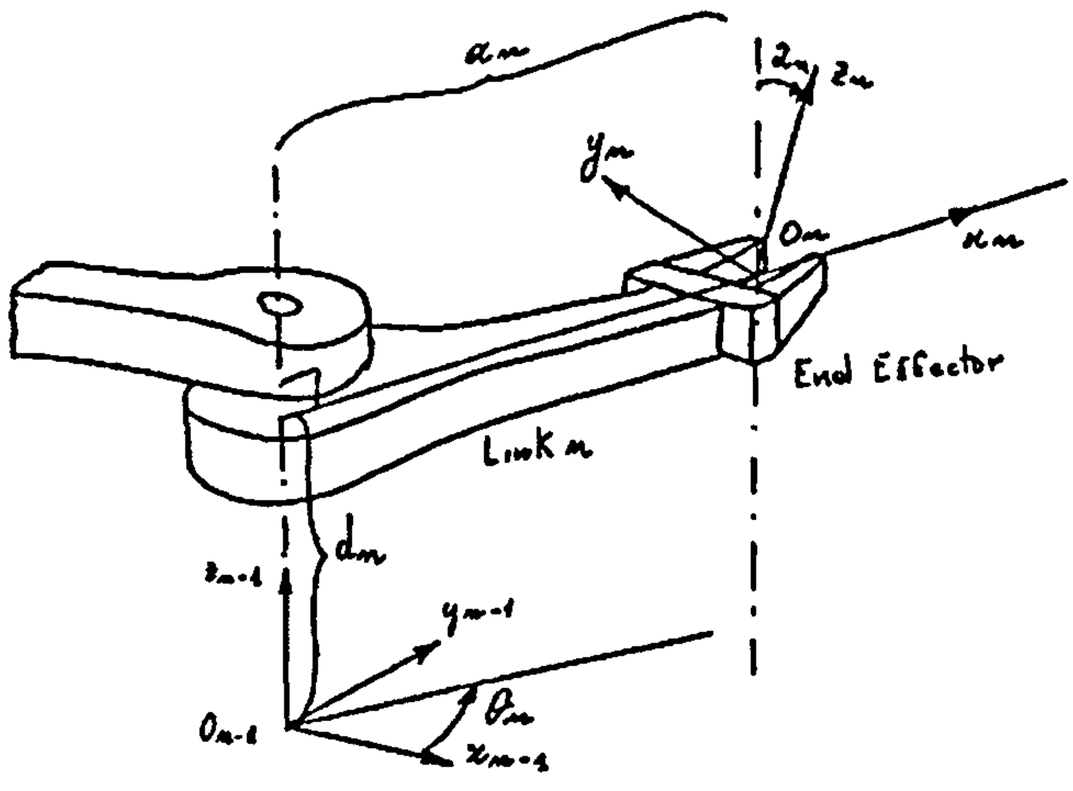

Figure 3.9: *Last link coordinate frame*

Base Link

The Origin of the coordinate frame can be chosen at an arbitrary point on the joint axis 1; the z_0 axis must be parallel to the joint axis, while the orientation of the x and y axes about the joint axes is arbitrary (see figure 3.10).

There are other two exceptions related to the intermediate links between the base and the last link.

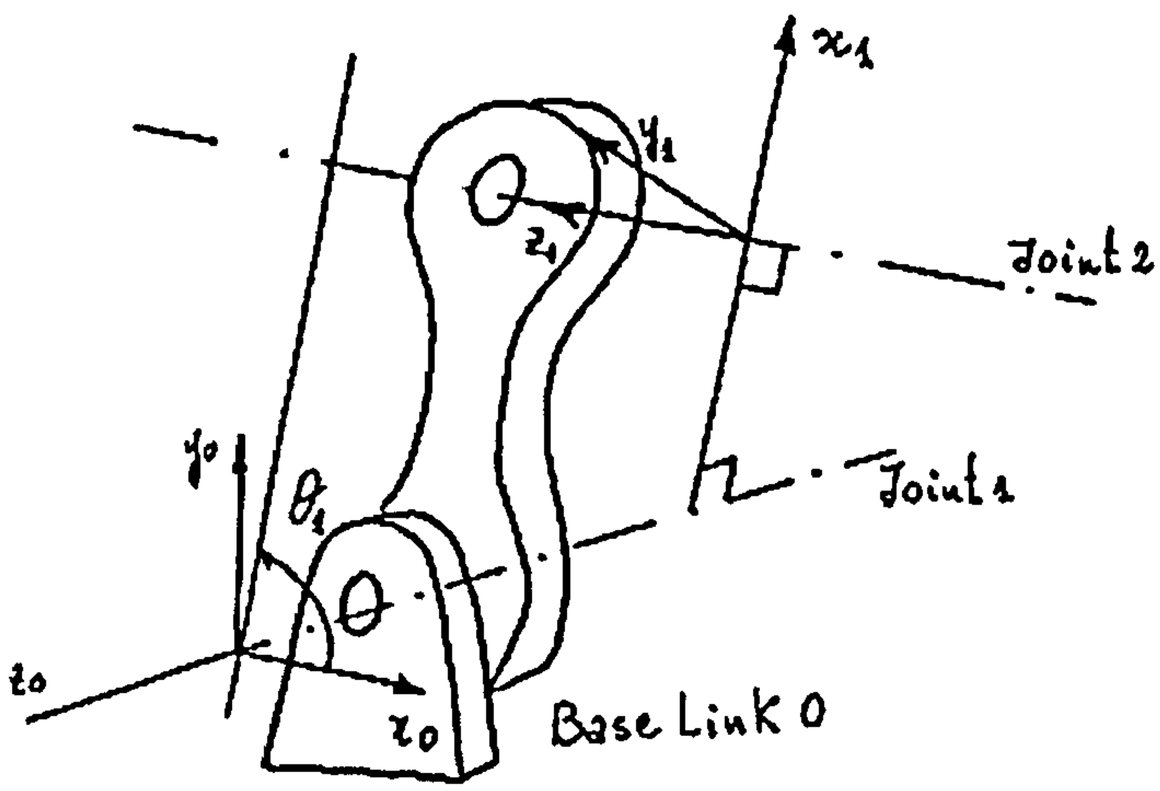

Figure 3.10: *Base link coordinate frame*

When the two joint axes are parallel, the common normal is not univocally determined. The choice of the common normal is then arbitrary.

Usually the common normal passing through O_{i-1} so that the distance di becomes zero.

The other exception concerns prismatic joints.

For a prismatic joint, only the direction of the joint axis is meaningful, hence the position of the joint axis can be chosen arbitrarily.

The above notations and basic rules are essential background information for investigating through a systematic approach on 3D kinematics and are used in the next sections in order to develop a model of the arm.

It is now interesting to review the researchers' attempts made for quantifying the workspace of the human arm. It will be shown that also in this field, because of lack of information on the kinematic chain of the arm and particularly on the clavicle motion, researchers used simplified models to extract information on the motion of the entire arm.

3.4 On the Workspace of the human arm

'The workspace can be considered the volume within which all points can be reached by a reference point of the end effector without considering its orientation'. This is the definition given by Kumar and Waldron in 1981 talking about manipulation arms.

Although such a definition is clear, workspace determination and evaluation is, in general, a complex and numerically time consuming problem. If all the characteristics of the internal workspace are requested, it is possible to use a method in which the number of operations is an exponential function of the number of the degrees of freedom. This method is based on the calculation of the position of the end effector for all combinations of values of joint coordinates inside their range of motion.

The interest this subject is due to the fact that a workspace that can be simulated, displayed and manipulated in real time on computer graphics is a useful and efficient tool for design and motion planning of mechanical manipulators as well as for analysis in ergonomics and architecture.

Only recently, an increased interest in the human arm has been shown by researchers who have modelled it as a geometric variable system. As a result, some techniques currently used for workspace detection have been applied for upper limb recording.

It is evident that a characterization of the workspace of the arm has immediate implications in medicine and rehabilitation as well as in ergonomics.

Although interesting and relevant from a clinical viewpoint, few data are available on this subject because of the intrinsic difficulties of measuring all the joint rotations of the kinematic chain, particularly the "shoulder complex".

It is worth mentioning that not all the attempts consider the real kinematics of the arm and therefore do not take into account either the geometry of the bones or the "non-visible" joints like the sterno-clavicular and acromioclavicular ones.

Dempster made a first attempt in 1955 with the design of aircraft cockpits for ergonomic purposes.

Although not complete, because of the lack of some relevant degrees of freedom, a quantitative result of the workspace has been obtained by Benati et al (1980).
As shown in figure 3.11 the model presented by Benati et al has two degrees of freedom at the sternoclavicular joint (abduction and elevation), while the acromioclavicular joint and the glenohumeral one are grouped in 3 coincident degrees of freedom.

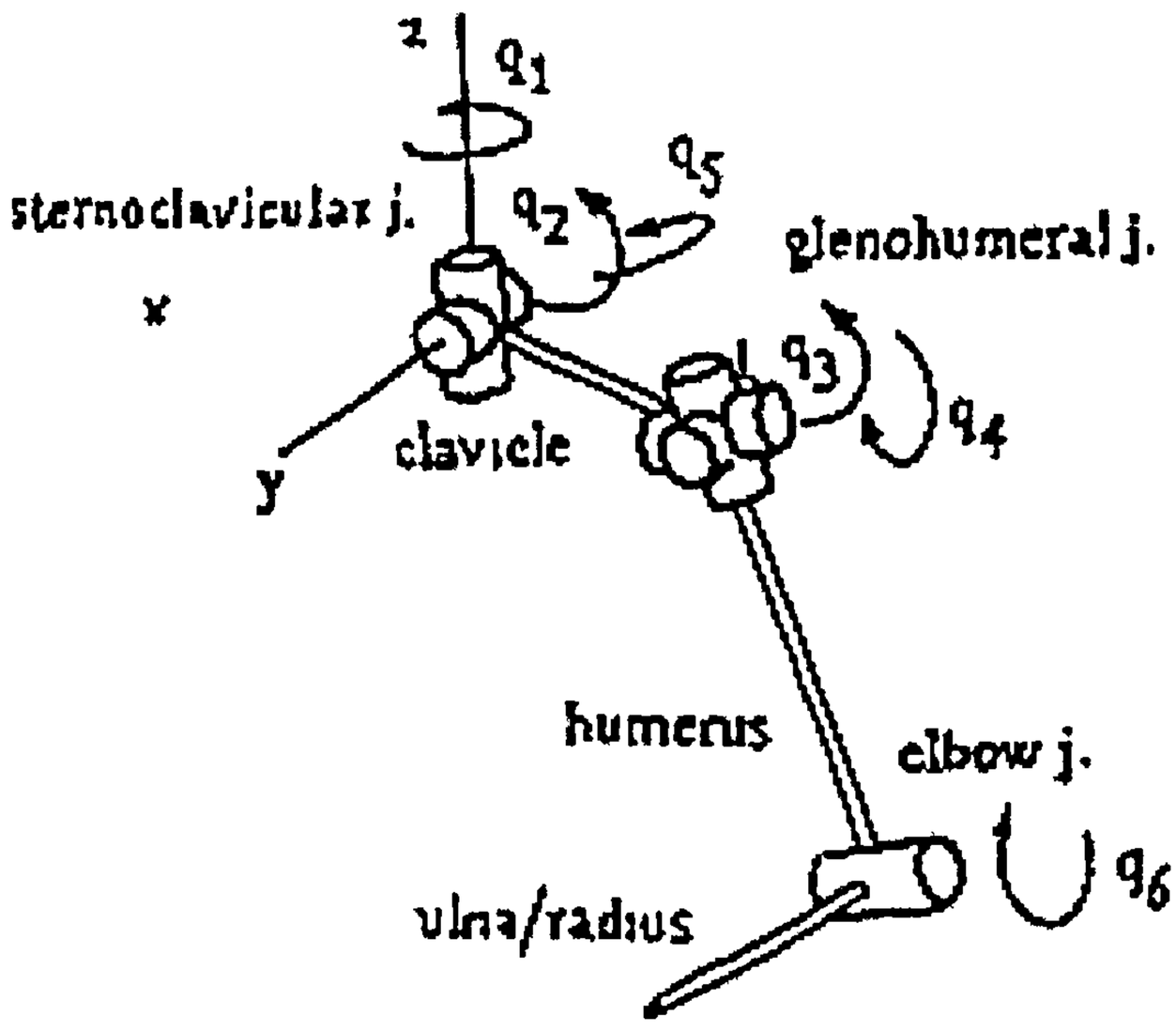

Fig. 3.11 *Kinematic model of the upper limb (Benati et al 1980)*

Data on human joints limited to the study of single joints or to the shoulder can be found also in the works of Engin and Chen (1986) and by Johnson and Gill (1987) who, by using the model proposed by Benati et al (1980) modelled the arm as a three segment seven degrees-of-freedom mechanism.
Other studies are due to Engin and Tumer (1989) and by Umek and Lenarcic (1991) who studied its properties with respect to the manipulability and kinematic index introduced by Yoshikawa (1985) and Angeles (1990) and finally by Kapandji (1994).

All of these studies are characterized by a simplification of the kinematics of the "shoulder complex".

Finally Wang et al (1998), by modelling the motion range of axial rotation of the arm, provided additional information to the statistical database proposed by Engin and Chen in 1986. Also in this case a simplification has been introduced by considering the clavicle-scapula and humerus interaction as a spherical joint.

It is interesting to note that all the attempts proposed in the literature introduce simplifications in order to analyse the motion of the limb because of the difficulty to have information on the motion of all the joints of the kinematic chain.

From the literature review carried out, it clearly emerges that the major advances in the quantification of the workspace have been due to investigation in robotics in order to optimise the design of robot kinematics. The attempts made in order to transfer such knowledge for the evaluation of the human arm have resulted in crude simplifications of the model. From the anatomical review carried out it is evident that, neglecting the translations occurring at each joint, a complete rotation model of the arm must consider 13 degrees of freedom, such as:

- 3 degrees of freedom at the sterno-clavicular joint
- 3 degrees of freedom at the acromio clavicular joint
- 3 degrees of freedom at the glenohumeral joint
- 2 degrees of freedom at the elbow joint (pronation-supination and flexion-extension)
- 2 degrees of freedom at the wrist joint

It seems also that either the geometry of the skeletal apparatus or the ligamentous structures play a fundamental role in the kinematic chain of the arm and although it can be agreed that the simplifications introduced by researchers do not affect much the end effector trajectories recorded, little is known about the mutual interaction of each joint during motion simply because the two kinematic chains are different. Therefore the

models previously studied cannot be used for the design of a consistent and complete biomechanical kinematic model of the arm which, in turn, hampers the possibility to obtain dynamic information from the analysis of the kinematics and muscle real behaviour. In this field it seems therefore that the complexity of the "shoulder complex" has hampered the birth of complete kinematic models of the human arm.

For the analysis of the kinematic chain it is convenient to use the Denavit-Hartenberg notation in order to decrease the number of parameters (see figure 3.12).

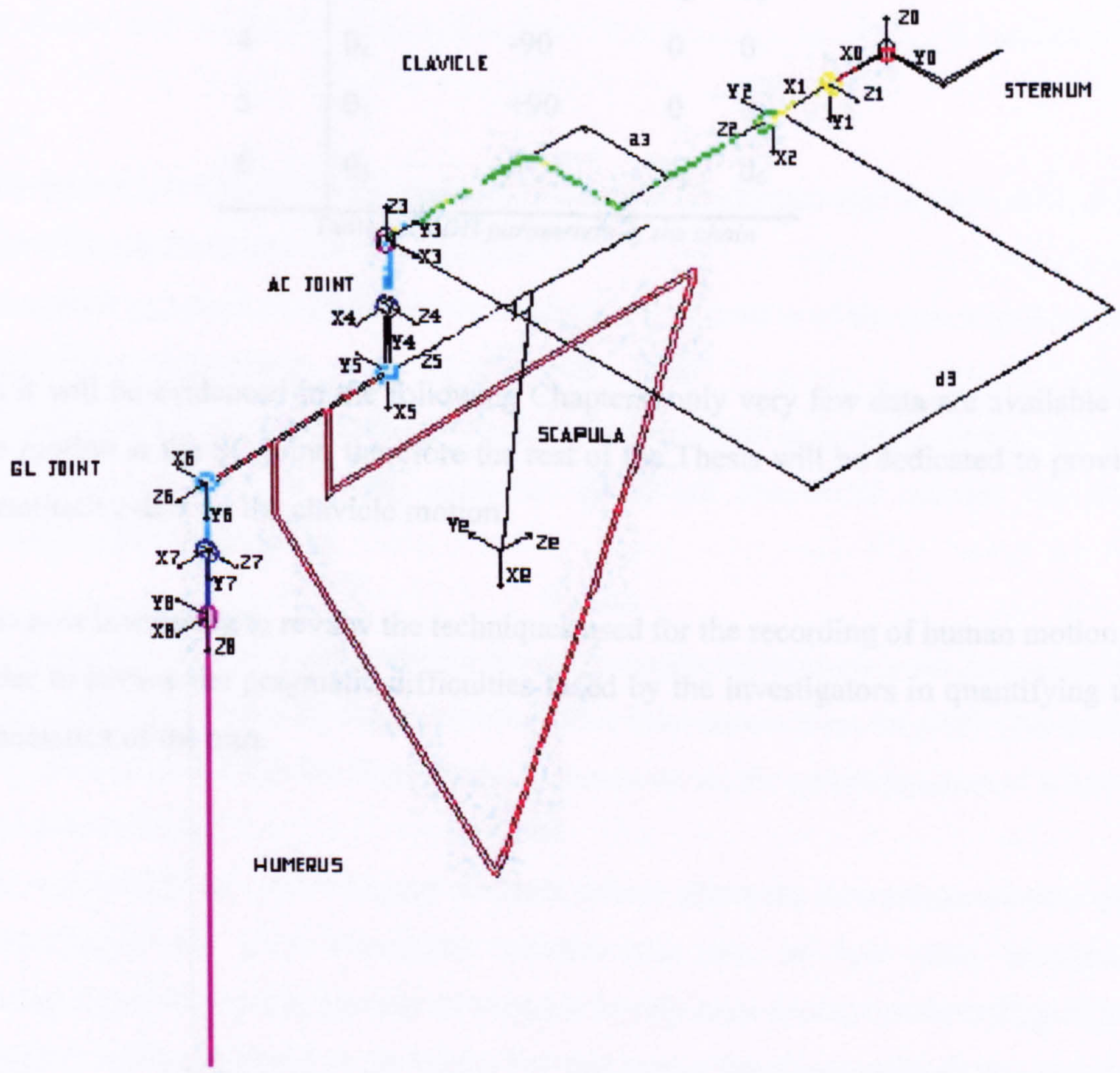

Figure 3.12 *Kinematic model of the human arm (Autocad 13)*

With reference to the above figure and to the notation used, the Denavit Hartenberg parameters for the first two joints of the "manipulator" at the SC and AC joints are given in table 3.13.

Link	*Variable*	$\alpha_{i\ (degrees)}$	a_i	d_i
1	θ_1	-90	0	0
2	θ_2	+90	0	0
3	θ_3	-90	a_3	d_3
4	θ_4	-90	0	0
5	θ_5	+90	0	0
6	θ_6	0	a_6	d_6

Table 3.13 *DH parameters of the chain*

As it will be evidenced in the following Chapters, only very few data are available on the motion at the SC joint, therefore the rest of the Thesis will be dedicated to provide quantitative data on the clavicle motion.

It is now interesting to review the techniques used for the recording of human motion in order to review the pragmatic difficulties faced by the investigators in quantifying the kinematics of the arm.

4 Techniques used to monitor joint rotation

In this Chapter, the techniques to monitor the joint rotations are reviewed. Advantages and drawbacks of each technique are extensively treated and the inadequacy of the methods proposed for the correct monitoring of "non-visible joints", like the SC, AC and clavicle scapula interaction, demonstrated. From the conclusions of the chapter, thus clearly emerges the need to have accurate information on the motion of non-visible joints in order to predict correctly the behaviour of the arm during motion[2].

As Marchese and Johnson (1997) pointed out, there are basically two approaches which can be used to make measurements of limb motion:

- the direct approach consisting of the analysis of the motion of the bones performed through x-ray analysis;
- the indirect approach performed by attaching transducers or markers on the skin or on the areas of well fitting garments which are considered suitable for the attachment of equipment.

It is worth mentioning that improvements in new emerging techniques such as magnetic resonance (MRI) or detection of direct proprioceptive information from the body (Pacinian corpuscle) would be useful in the future to get information on the spatial position of a limb with respect to the body.

Certainly radiographic or other imaging methods should allow the direct measurement of bone movements, but they commonly involve the use of low dose roentgen stereophotogrammetric motion pictures of subjects having high-density markers (typically small tantalum balls) implanted in the bones. For this reason the direct methods are useless

---

[2] This review has been re-arranged from a technical report of the European Project "Tremor" presented by Marchese and Johnson (1998).

in clinical practice and do not comply with the ethical and safety provisions of the Declaration of Helsinki. Such methods will be cited in the following section.

The indirect approach faces the problem of measurement of limb movements by accepting the limitations in precision and accuracy imposed by the physical attachments of transducers/markers on a non rigid structure (muscles, skin) changing shape and volumes during motion.

There are basically two indirect approaches which can be used to make measurements of limb motion: those that are mounted directly to the body and those that sense the movement remotely. Although both of them need equipment to be attached to the body (active sensors or markers) the latter tend to be optical systems or those that use sonic or electromagnetic technology.

In the following, both indirect approaches will be examined in depth outlining for each advantages and drawbacks. The review examines the historical development of the measurement methods; the former evolving with the improvements in sensor technology, the latter starting with the development of tracking systems used for military purposes to more recent equipment for applications in virtual reality scenarios. In addition, specific attention is given to differentiate sensor-based technologies by sonic, electromagnetic or video camera based systems.

The simplest device is the goniometer or electro-goniometer, defined as an angle measuring instrument, which is attached to a limb segment. Individual goniometers normally measure only a single degree of freedom but they may be produced in assemblies to measure movement at multiple degree of freedom joints. They may be based on a number of technologies but electrical resistance measurement is the most common. While the commonest and simplest approach has been to use rotary or linear potentiometers, there can be significant practical difficulties when attaching these devices across joints having either more than one degree of freedom or a variable centre of rotation (e.g. the glenohumeral joint). While assemblies of more than one potentiometer have been used for the measurement of joint motion, Chao (1980) has pointed out the difficulties which can arise because of the non-commutative nature of finite rotations. A strong limitation the

successful use of such devices is represented by their physical size. Gomes et al (1999) used a triaxial goniometer for the determination of upper arm orientation demonstrating the applicability of gyroscope-based methods for the recording of the shoulder motion.
Such problems moved the researchers' attention to the development of other designs and, in particular to the flexible electrogoniometer. This device, first described by Nicol (1987), consists of a thin square flexible beam which has a continuous strain gauge attached along pairs of opposite faces. Analysis of the output of these strain gauges reveals that the output is proportional to the relative rotation of the two ends, and is independent of deformed shape. Although the problem related to alignment has been resolved, the physical size of the sensors is big and robustness in state-of-the-art devices does not allow an easy use in clinical practice.

Alternative angular measurements can be made using position transducers in conjunction with mechanical systems that convert angular movements to linear displacements. Such devices fall into high accuracy oscillator/demodulator types or into potentiometric devices. Low cost LVDT devices are precision displacement transducers. The linear variable differential transformers are based on the variation in mutual inductance between a primary winding and each of the two secondary windings. A signal-conditioning amplifier has to be used which adds to the bulk and weight of the transducer system. These devices are generally energy-expensive and require mains power (i.e. 110 V or 220 V). Again their physical size does not allow their use in assembly to measure more than one degree of freedom.
Recently Bergamasco et al (1992) developed a new sensor-based device for monitoring joint rotation at the level of the hand. Such sensors have been applied to monitor finger adduction-abduction movements. They exploit the Hall effect and are miniaturised although the permitted range of motion is 45 degrees that is not sufficient to cover the range of motion of most of human joints. The operating principle of such sensors is extensively described in section 5.

4.1 Electromagnetic measurement systems

These systems, which rely upon the analysis of electromagnetic fields, can measure 6 degrees of freedom within a single sensor. Measurements are made relative to an axis system and origin based in the electromagnetic source, which may or may not be attached to the subject. Multiple sensor systems are available. There are two commercially available systems, one of which uses low frequency AC magnetic fields while the other uses a pulsed DC field. The advantage of the latter is that it is far less susceptible to errors caused by the proximity of metal. The receivers of these systems are typically 35 mm cubes with a mass of 20 gm. The transmitter is much heavier but need not be attached to the subject. These measurement devices have been used extensively in Virtual Reality applications but also in biomechanics. In particular, their use has been reported for the measurement of upper limb kinematics. The technology is improving very rapidly in this field, with consequent reduction of the size of the transmitter and the receiver (An et al (1988); Johnson and Anderson (1990) and Barnett et al (1999)).

4.2 Camera-based systems

The use of video/cine cameras is well established in the field of experimental biomechanics but is used relatively infrequently in the clinical setting. The one exception is probably its use in Gait Analysis in conjunction with force measurement platforms and/or electromagnetic signals (emg). Exceptions are represented by Wang et al (1996,1998) who analysing the upper limb during sport activities, tried to characterise the normal functional range of motion of the upper limb during different daily living activities. These systems normally rely on the automatic recognition of pre-defined markers attached to the limb segments. The markers may either be passive reflective or else active. Infrared lighting is frequently used to ensure maximum image contrast. The kinematic data from cameras is digitised for post-processing at the end of the experiment. Three or more cameras are frequently required, the number depending on the nature and complexity of movement.

Three-dimensional reconstruction of image co-ordinates is normally achieved using the Direct Linear Transform method.

Marchese and Johnson (1997) grouped camera-based systems into three main categories:

1. On-line digitisation of active markers;
2. On-line digitisation of passive reflective markers;
3. Post- processing of video data.

The drawbacks of such systems are the number of cameras to be used in order to cope with the problems related to the visibility of the markers, their relative high cost and the time necessary to set up an analysis in clinical practice. This has resulted in their poor applicability in routine clinical analyses.

As repeatedly above mentioned, both the indirect methods must unavoidably cope with the attachment of equipment to a non-rigid structure characterised by a variation of volumes and shapes with motion and loads applied to the structure. This means that a given spatial configuration of the arm can correspond different spatial positions of sensors and markers with a consequent error.

Of all the techniques available, only cinematography, cineradiography, sonic digitizers, electromagnetic devices and instrumented linkages offer practical methods for measuring general spatial motion. As pointed out by Bergamasco et al (1991), the critical key factor that reduces the usability of current technology in this field and in the field of man-machine interfaces in general, is the physical size of the mechanical attachment to humans.
As evidenced in the review of the systems able to monitor limb motion, all the techniques reviewed for the monitoring of the upper limb unavoidably face the pragmatic problem of measurement. Skin and soft tissue deformation combined with the indeterminate location of each joint centre of revolution prevent to determine accurately the relevant variables under examination (rotations, speed, etc.).

In this section the indirect methods used to obtain information on the upper limb kinematics have been reviewed. The next logical step is therefore to show the results obtained using the above measurement systems for the recording of the shoulder motion.

4.3 The Shoulder Complex

The interaction between clavicle, scapula, humerus and thorax is called "the shoulder complex". It is formed by four independent articulations, the sternoclavicular, acromioclavicular, scapulothoracic and glenohumeral joints. Although the scapulothoracic articulation cannot be considered a joint, the elevation of the extremity both in flexion and in abduction, at the glenohumeral articulation seems simultaneously accompanied by movements occurring in the interaction between scapula and thorax (see figure 4.1). Therefore, analysis of the mechanism of the shoulder results in the understanding of the sequence of motion, which occurs at its component joints.

In the following, a chronological literature review to highlight the main features of the shoulder kinematics is given.

The shoulder has attracted the interest of researchers of the 18th Century. Early qualitative observations can be found in the works of Duchenne (1867), Cleland (1881) and Cathcart (1884) who was the first to introduce the concept of synchronous movements of humerus and scapula. Such a concept was extensively shown by Codman (1934) who coined the term "the shoulder rhythm" to best describe the combined motion of the two bones.

Although important, all these studies are not measurement of scapula motion, but only descriptive observation of motion.

Flecker (1929) carried out the first quantitative investigation on the scapula motion during the arm movements. He investigated the rotation of scapula in the coronal plane and despite the individual variation of the three subjects tested, he identified a trend of motion (figure 4.2).

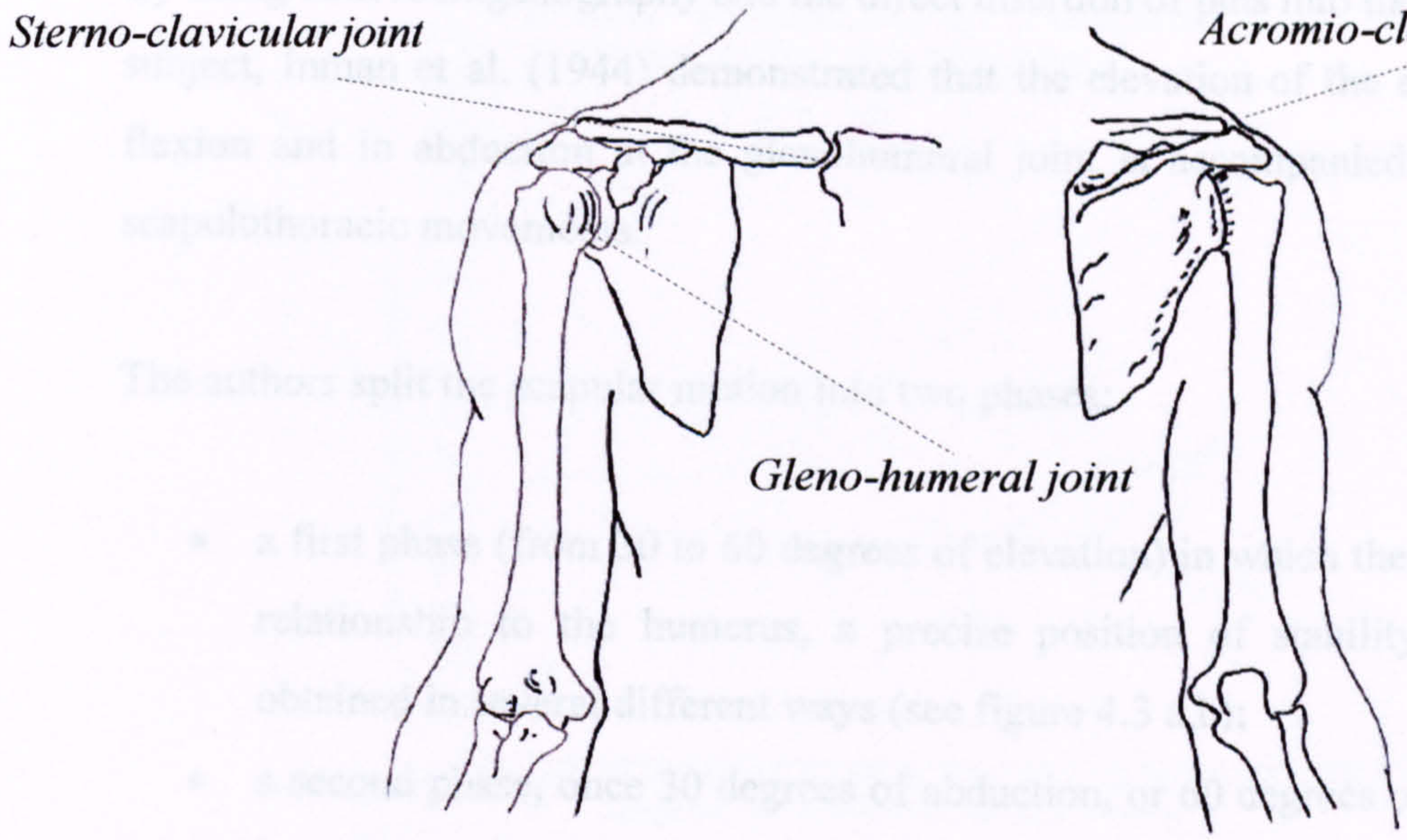

Fig. 4.1: *The shoulder complex frontal and dorsal views*

This study was followed one year after by Lockart (1930) who carried out a series of tests on normals and pathological subjects with the help of X-rays demonstrating the synchronization of motion of scapula and humerus four years before the publication of Codman.

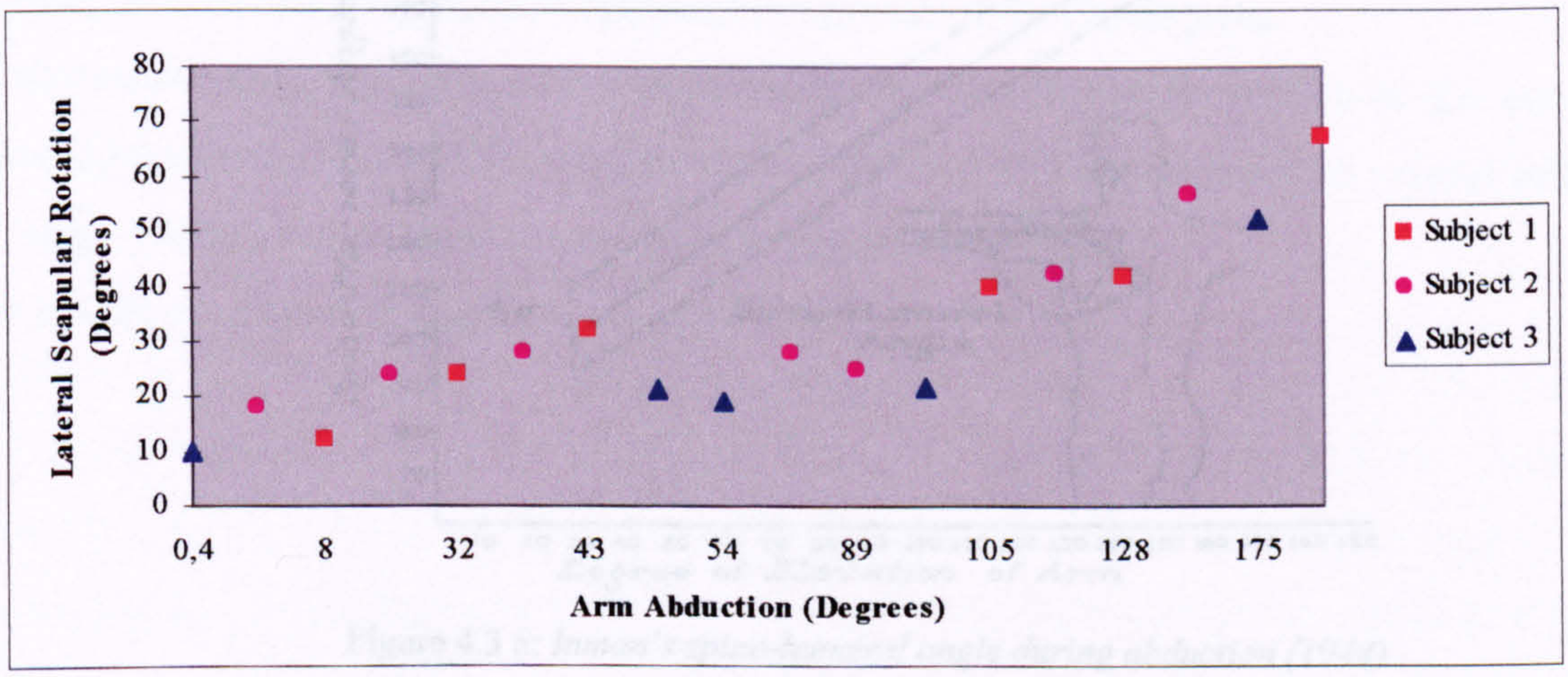

Figure 4.2: *Scapula rotation in the coronal plane (Flecker 1929)*

By using both roentgenography and the direct insertion of pins into the bones of a living subject, Inman et al. (1944) demonstrated that the elevation of the extremity, both in flexion and in abduction at the glenohumeral joint is accompanied by simultaneous scapulothoracic movements.

The authors split the scapular motion into two phases:

- a first phase (from 30 to 60 degrees of elevation) in which the scapula seeks, in relationship to the humerus, a precise position of stability which may be obtained in several different ways (see figure 4.3 a,b);
- a second phase, once 30 degrees of abduction, or 60 degrees of forward flexion have been reached, in which the relationship between scapular and humeral motion remains remarkably constant (see figures 4.3 a,b).

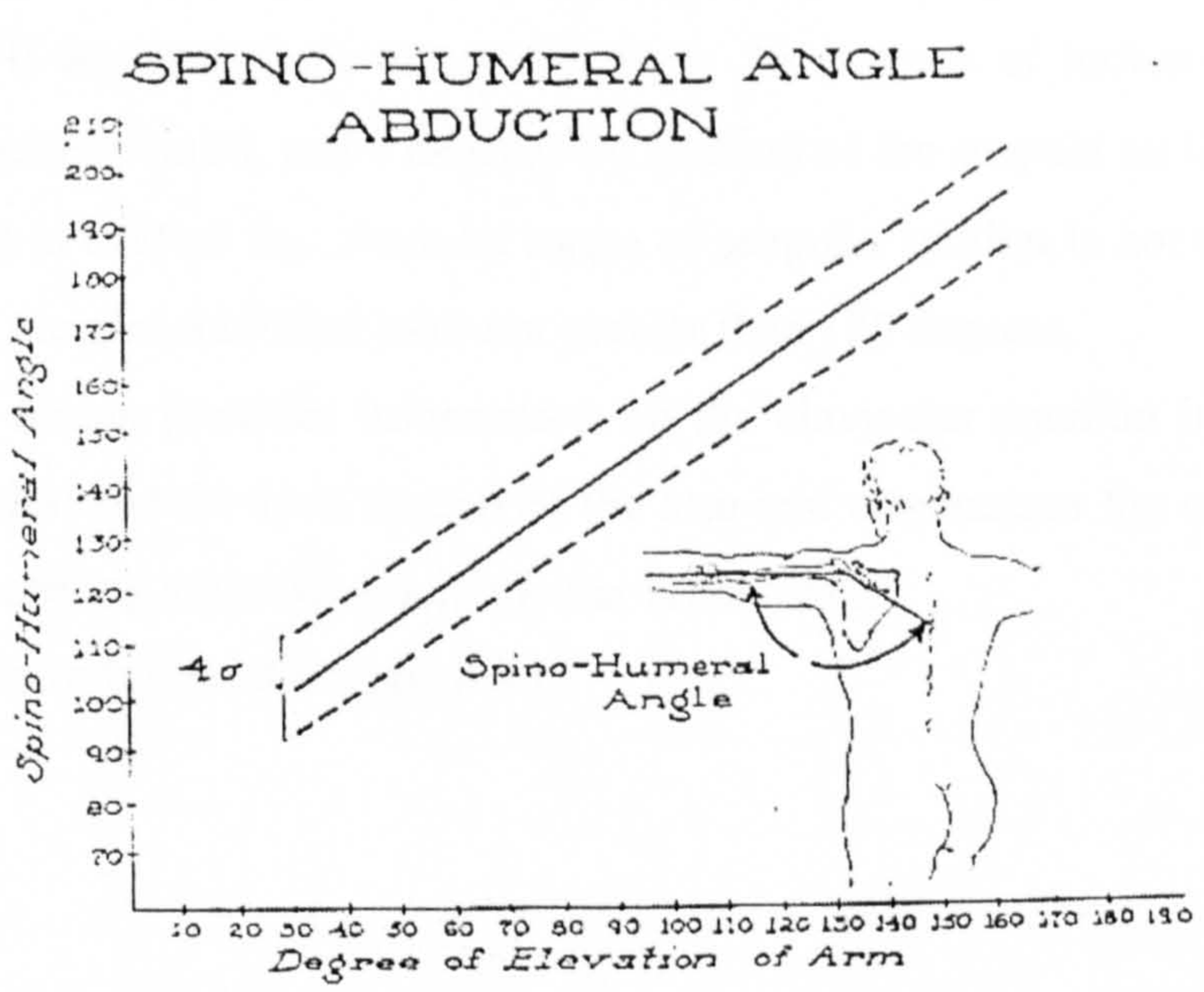

Figure 4.3 a: *Inman's spino-humeral angle during abduction (1944)*

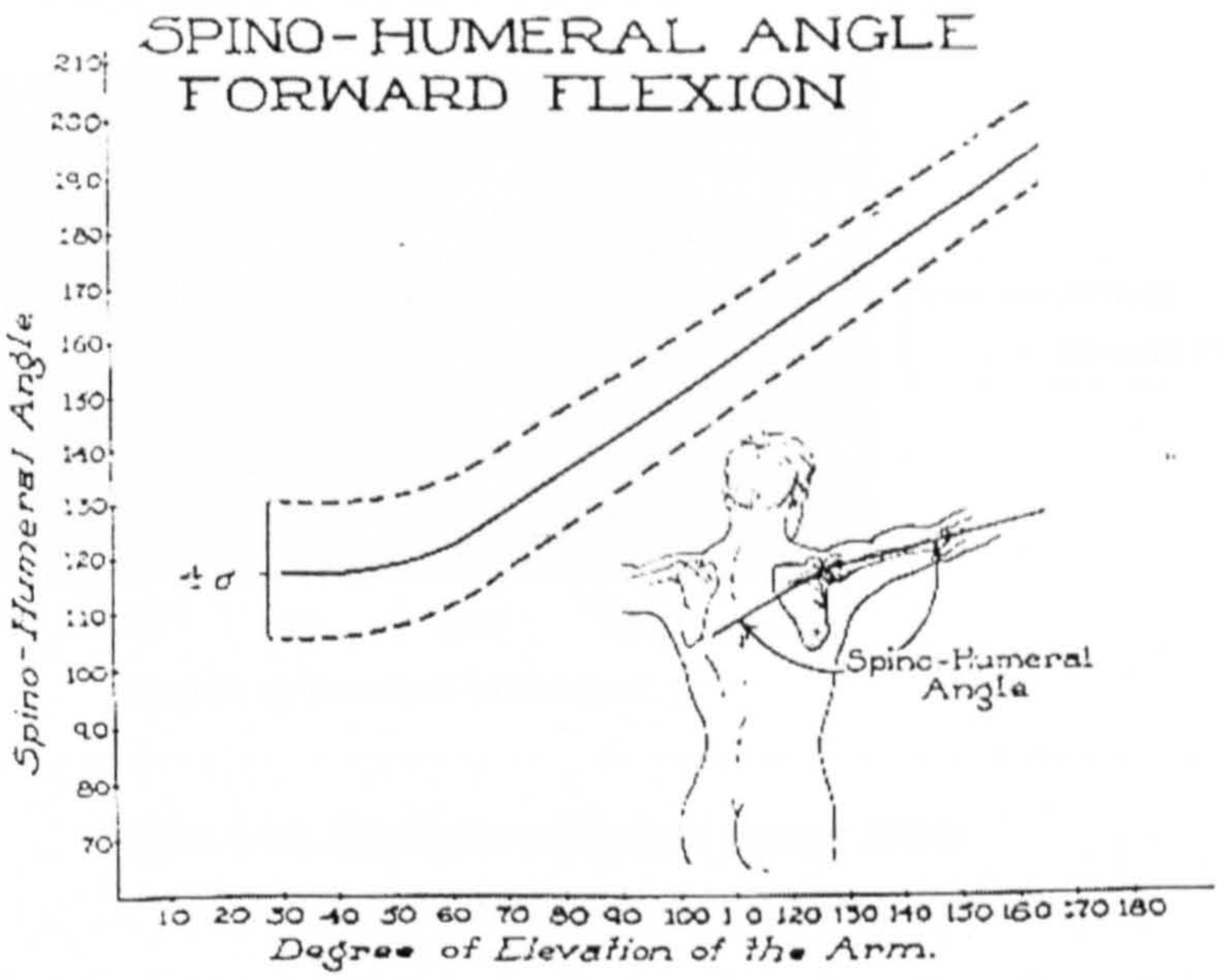

Figure 4.3 b *Inman's spino-humeral angle in forward flexion (1944)*

Thereafter they suggest a ratio of two of humeral to one of scapular motion; and thus between 30 and 170 degrees of elevation, for every 15 degrees of motion, 10 degrees occurs at the glenohumeral joint, and 5 degrees by rotation of the scapula on the thorax. As this ratio pertains, it is evident that the total range of scapular motion is not more than 60 degrees, and that of the glenohumeral joint not greater than 120 degrees.

In the same paper, Inman provides information on the clavicular rotation in the coronal plane during abduction and forward flexion of the arm and emphasizes the crucial role of the axial rotation occurring at the sterno-clavicular articulation.

His results are shown in figures 4.4 a and 4.4 b.

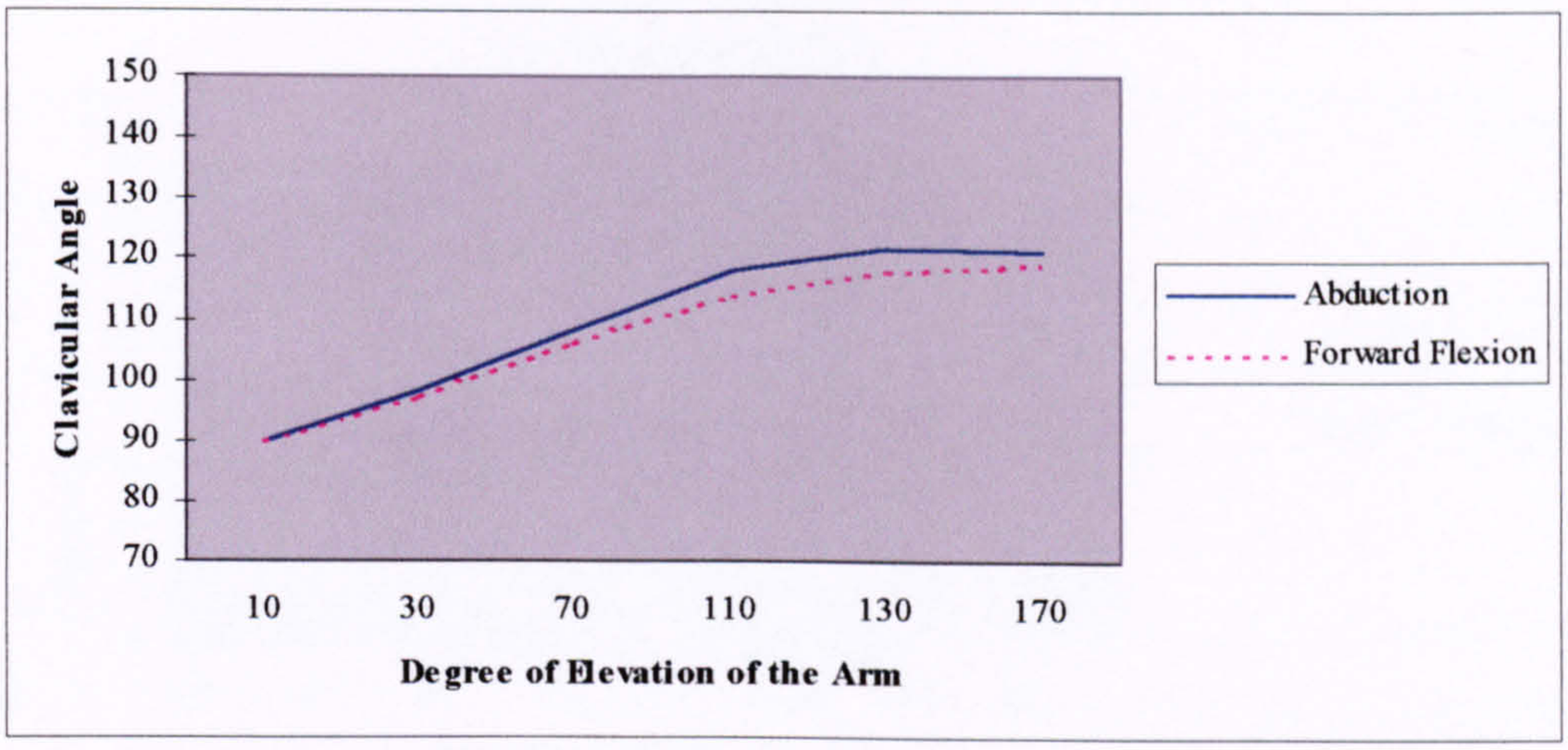

Figure 4.4 a: *Clavicular abduction (Inman 1944)*

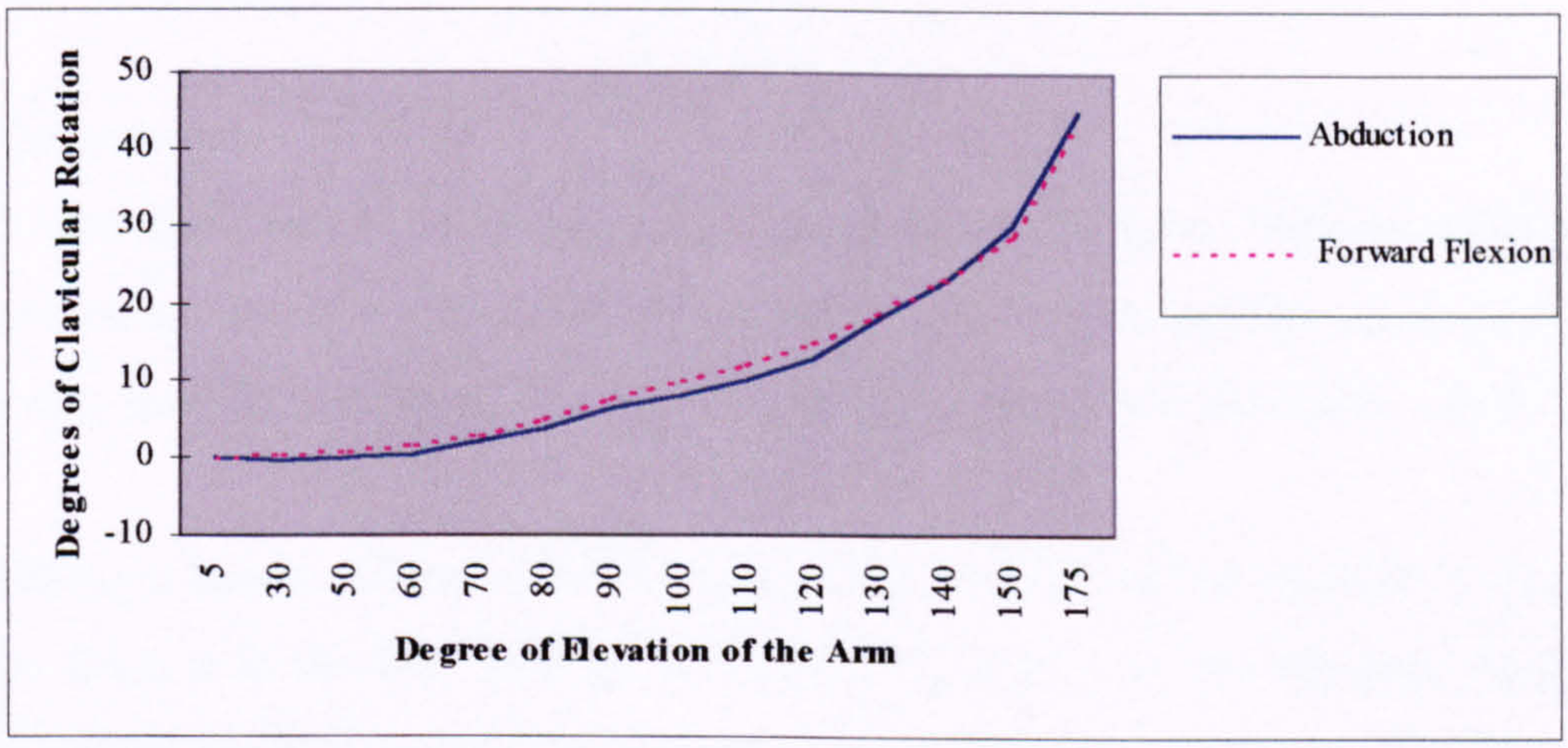

Figure 4.4 b: *Clavicle axial rotation (Inman 1944)*

Additionally, information on the motion occurring at the acromio-clavicular joint are given. With reference to figure 4.5, the author calls the motion occurring at the acromion "spino-clavicular angle" defined as the angle between the spine of scapula and a straight line connecting the sterno-clavicular to the acromio-clavicular angle. It is interesting to note that already in the 1944, preliminary features of all the articulations involved are outlined. It is, indeed, the first paper in which the scapular spatial position is considered as the result of two combined rotations: one occurring at the sternoclavicular joint and the other one at the acromioclavicular articulation (see figure 4.5).

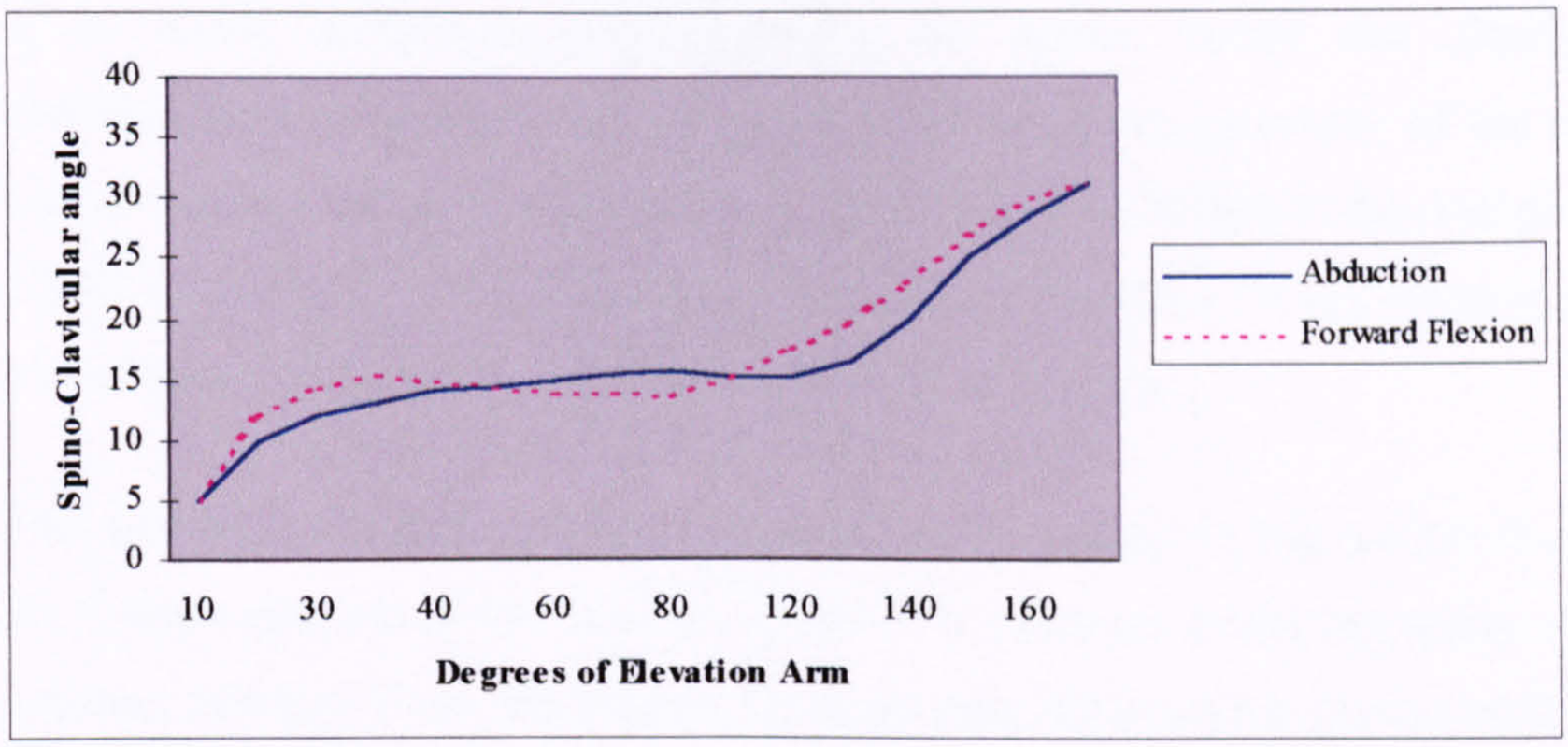

Figure 4.5: *Spino-clavicular angle in the coronal plane (Inman 1944)*

Citing the authors:

> "*Clavicular motion is more complicated than has been hitherto suspected. The continuous rotation of the scapula on the thoracic wall during elevation of the extremity is only possible because of the motion permitted at the two clavicular joints*".

Although Inman did not provide detailed information on the method used to perform the tests, it is the first attempt in which information on the shoulder complex as a kinematic chain is given. The author gives a pragmatic demonstration of the motion occurring at the acromio-clavicular joints presenting two case studies in a publication of 1946 (Inman and Saunders) in which, because of traumatic injuries occurring at the acromio-clavicular joint of two subjects, a reduction of the arm range of motion (ROM) together with discomfort at the sterno-clavicular joint was noticed. He stated:

> "*…From the observations it is clear that apart from serving as a link in the pectoral girdle, the fundamental and most important function of the clavicle is related to the existence of its curvatures. It is these curves, especially the lateral, which bring this bone into relationship with the scapula and indeed are responsible for the necessary freedom which the scapula must possess to provide the niceties of rhythm which are so characteristic of shoulder movement*".

It is worth mentioning, that although the author points out clearly that the functionalities of the entire complex are affected by the geometry of the clavicle and that any modification to such geometry are promptly reflected in the change of the total ROM of the arm, all the future studies mainly focussed on the scapula, model the clavicle, as a straight line between the SC and AC joints.

Fisk (1944) in the same period carried out another study on the scapula by performing an X-Rays analysis of the bone at a number of positions during elevation and internal-external rotation. From the images, by measuring the apparent change of dimension of scapula in the coronal plane, he studied both the lateral rotation in the coronal plane and the rotation in the sagittal plane. Here a preliminary evidence of the 3 dimensional nature of scapula motion has been presented. Although such evidence has been reiterated by Saha (1950) who strongly pointed out that the scapula plane (defined as the plane that is obtained with a cross section of the scapula containing its widest surface) was not fixed during motion, such findings have been nearly ignored by many authors who continued to quantify motion through analyses performed in a single plane. Moreover, as already mentioned, researchers focussed their attention on the scapula motion, treating the bone as if it was completely disconnected by the rest of the kinematic chain of the arm.

In 1956, Jones studied scapular motion during abduction-adduction through an X-Rays analysis (see figure 4.6). Either the "setting phase" or the ratio scapula-humerus motions are similar to those ones measured by Inman.

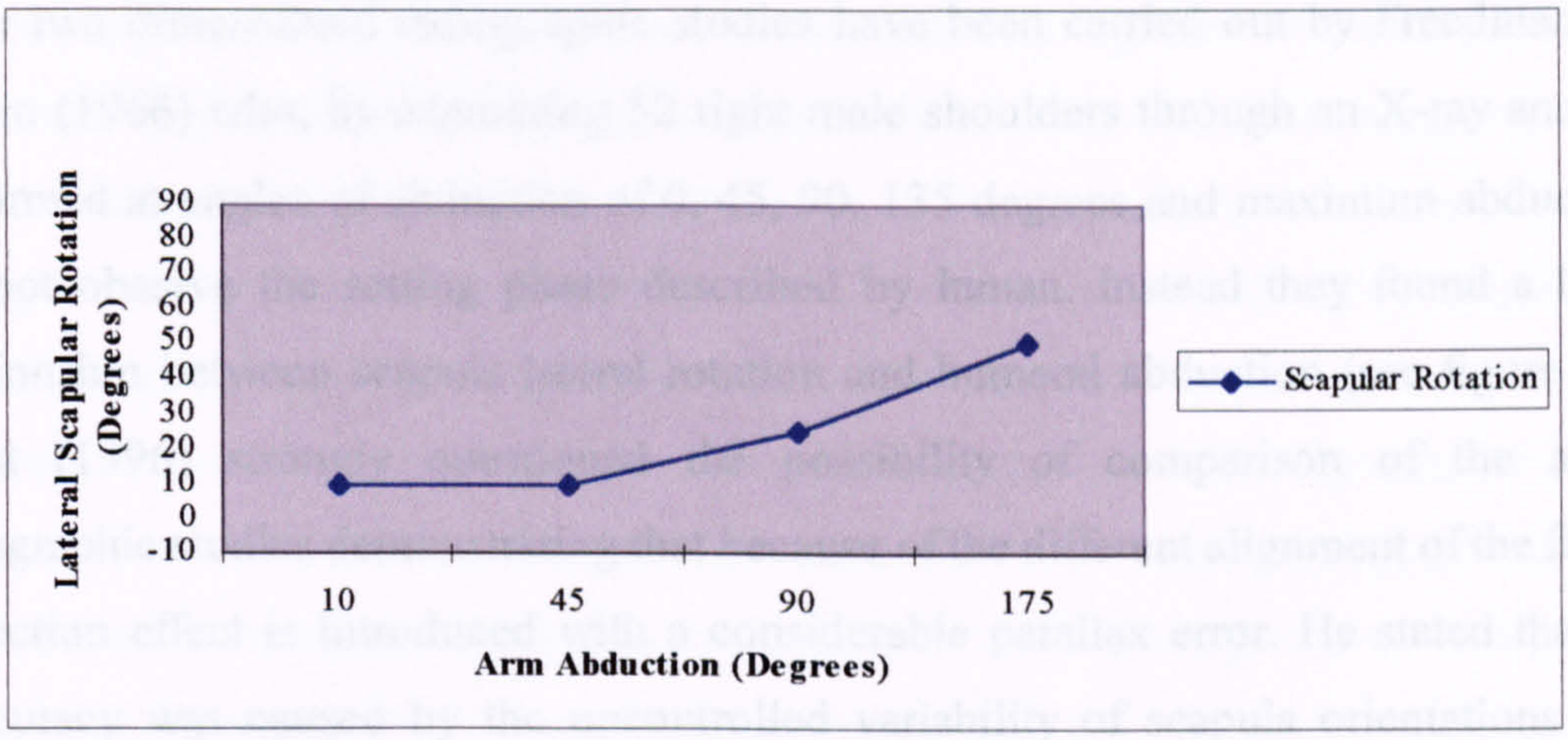

Figure 4.6: *Lateral rotation of scapula during abduction (Jones, 1956)*

The importance of the movement occurring at the SC and AC joints has been reiterated by Conway in 1961 who developed two simple apparatuses based on angular goniometers to measure starting angles at SC and AC versus humerus abduction. The measurements obtained by the examination of 60 subjects have shown a third degree of freedom occurring at the SC joint (the posterior one): " *the clavicle at the sterno clavicular joint has a posterior and superior movement during elevation. The superior movement is greater in amount than the posterior movement* ". The author presents data in the form of a table giving the range of motion occurring at the two joints as measured in female and male subjects. No data were given in relation to humeral motion or the axial rotation of the clavicle.

A summary of his findings regarding clavicle motion is given in the following table:

Clavicle motion (degrees)	Pro-retraction	Abduction-adduction
SC	10-17	20-30
AC	8-10	8

Table 4.1: *Average values of motion at the Sterno-clavicular and Acromio-clavicular joints (Conway 1961)*

Other two dimensional radiographic studies have been carried out by Freedman and Munro (1966) who, by examining 52 right male shoulders through an X-ray analysis performed at angles of abduction of 0, 45, 90, 135 degrees and maximum abduction, did not observe the setting phase described by Inman. Instead they found a linear relationship between scapula lateral rotation and humeral abduction (see figure 4.7). Groot (1996) strongly questioned the possibility of comparison of the above radiographic studies demonstrating that because of the different alignment of the film, a projection effect is introduced with a considerable parallax error. He stated that the inaccuracy was caused by the uncontrolled variability of scapula orientations with respect to the camera and by the problems of landmark recognition in the X-ray images.

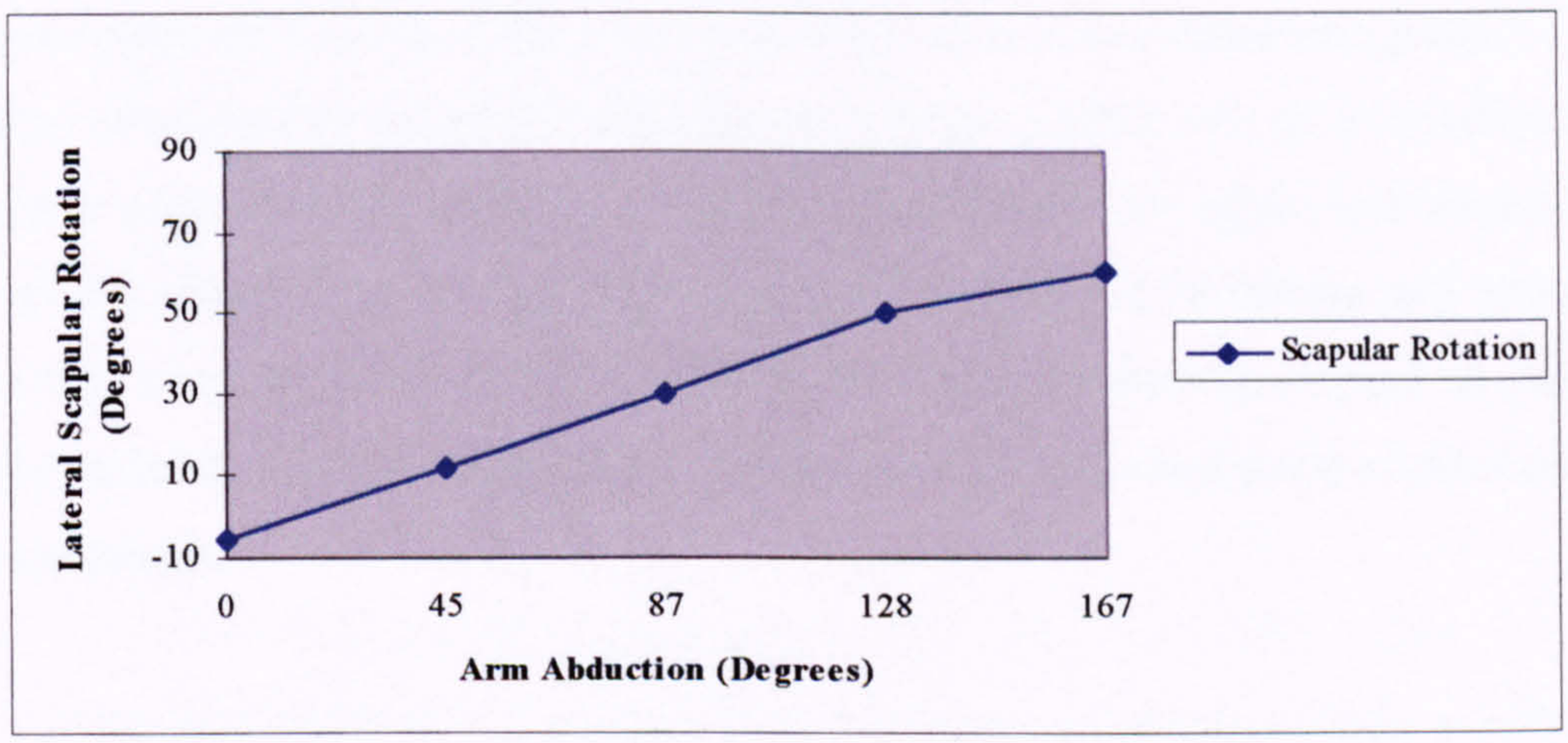

Figure 4.7: *Lateral rotation of scapula during arm abduction (Freedman and Munro 1966)*

Another two dimensional non-invasive technique has been used by Doody et al. (1970b) to study scapular motion in relation to humeral motion. Using a "scapulo-humeral goniometer" they studied abduction in the scapula plane. Their results evidence a non-linear relationship between scapular and humeral motion.

A further study, carried out by Poppen and Walker (1976) using the X-ray technique, showed results in accordance with those of Freedman and Munro.

In 1978, Dvir and Berme developed a qualitative kinematic model of the shoulder complex in elevation measuring the rotation of scapula from coronal radiographs at

each 15 degrees of humeral abduction. Using such data together with data previously published, they modelled clavicle and scapula motion using a mechanism approach and provided data for the coordinates of the root of the scapular spine. Data are given throughout a range motion from 0 to 180 degrees at increments of 15 degrees. In constructing their model, as pointed out by the authors: "*...use was made of the following relevant findings:...the clavicle has two modes of motion. The initial rotation about an anterior-posterior axis through the sterno-clavicular joint...followed by a second rotation along the long axis of the bone...*" and although the third degree of freedom at the sterno-clavicular joint is not accounted, they found two distinguished phases of motion: "*...the initial phase of elevation is strongly dependent on the scapulothoracic and acromioclavicular joint, while the later phase of the motion becomes more dependent on the gleno-humeral and acromio-clavicular joints*".

Another non-invasive technique was presented by Ito (1980), who developed a system using two potentiometers attached at the scapula spine and the upper arm respectively. The results obtained are shown and compared to those of Freedman and Munro in figure 4.8. Scapular rotations are smaller with respect to those presented in previous studies probably because of the relative motion between skin and point of attachment of the transducers.

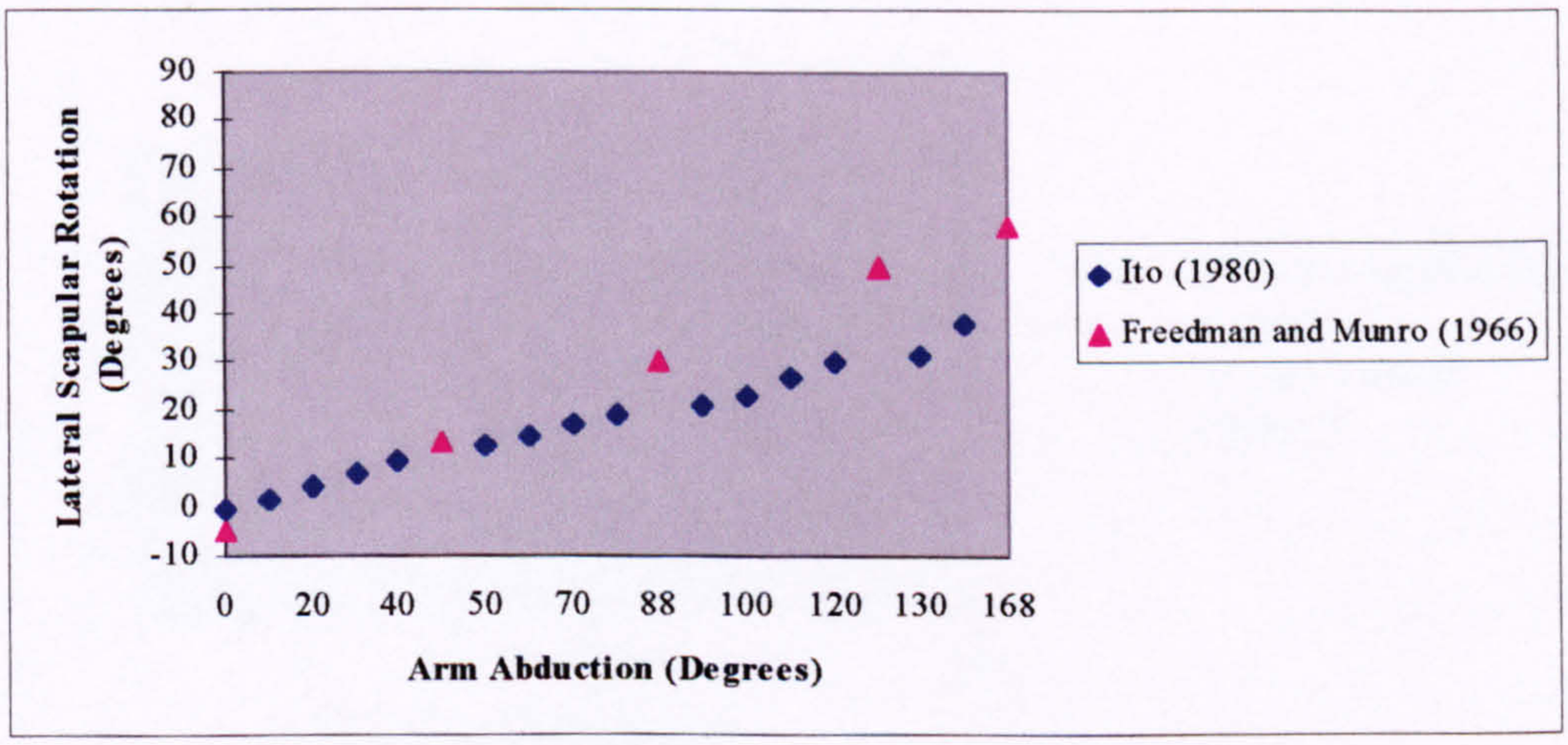

Figure 4.8: *Scapular rotation during humeral abduction (Ito 1980)*

Although the three-dimensional nature of clavicle-scapula motion was described by Inman, discovered by Fisk in 1944 and reiterated by Saha (1950), the first attempt to quantify a three dimensional scapular and clavicular motion took place only in 1982 with the study of Wallace and Johnson (1982) who used two X-ray sources to perform tests in the sagittal and coronal planes respectively. The results were presented as projections onto three orthogonal views; an anterior-posterior view (front to back), plan view and lateral view. The results shown in figure 4.9a,b,c, evidence again the motion of the clavicle that must be taken into account in quantifying the motion of the bones.

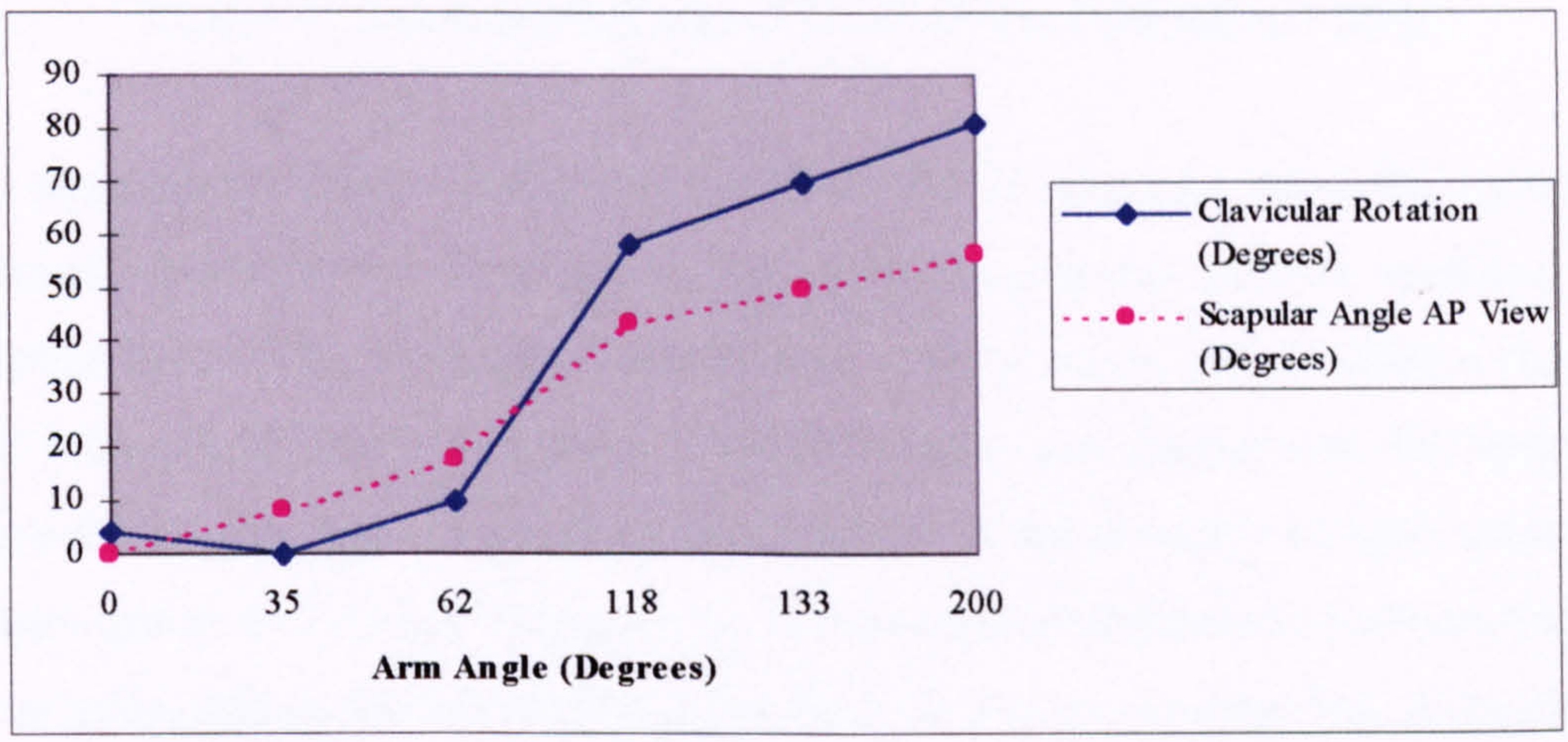

Figure 4.9a: *Rotations of scapula and clavicle* (*Wallace and Johnson 1982)*

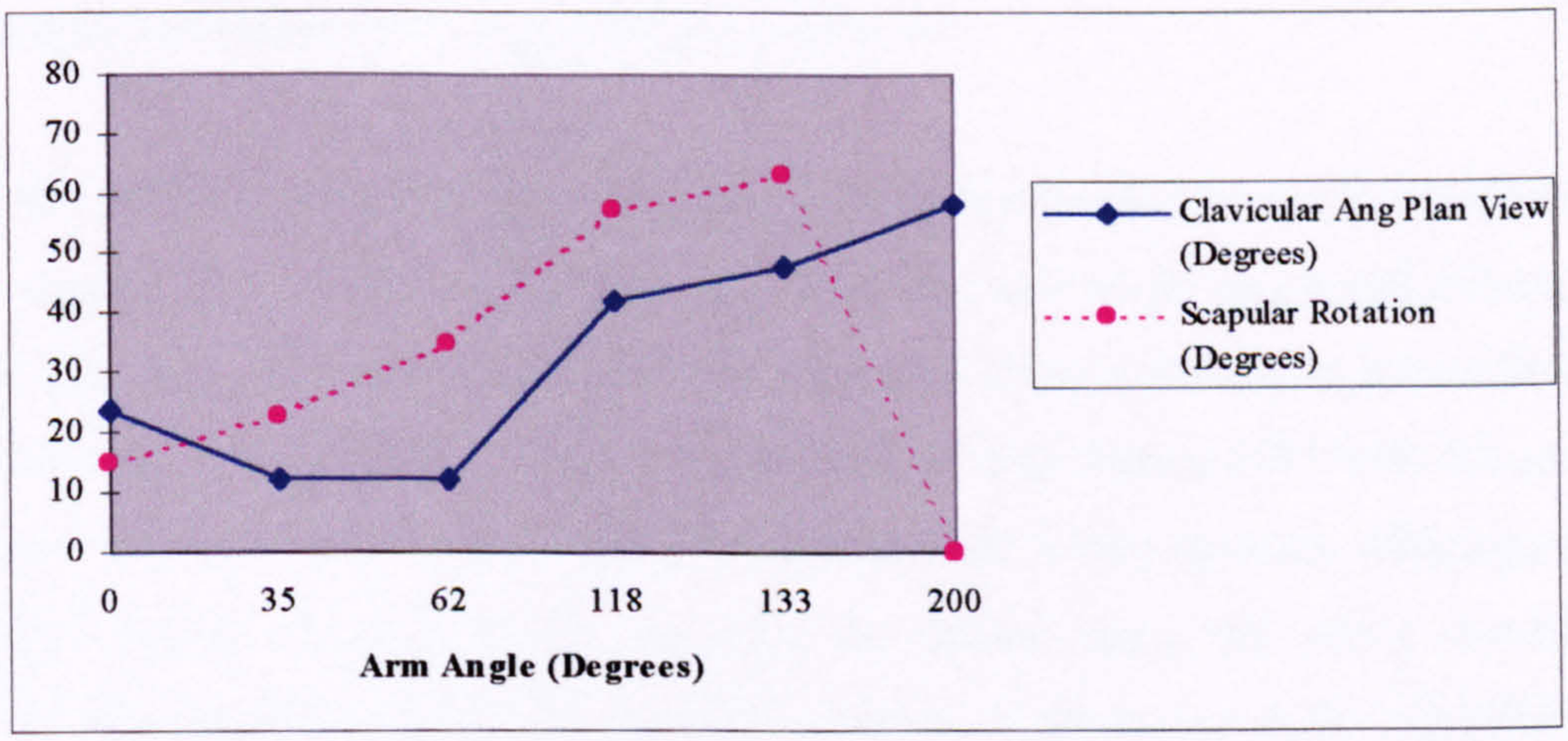

Figure 4.9b: *Rotations of scapula and clavicle* (*Wallace and Johnson 1982)*

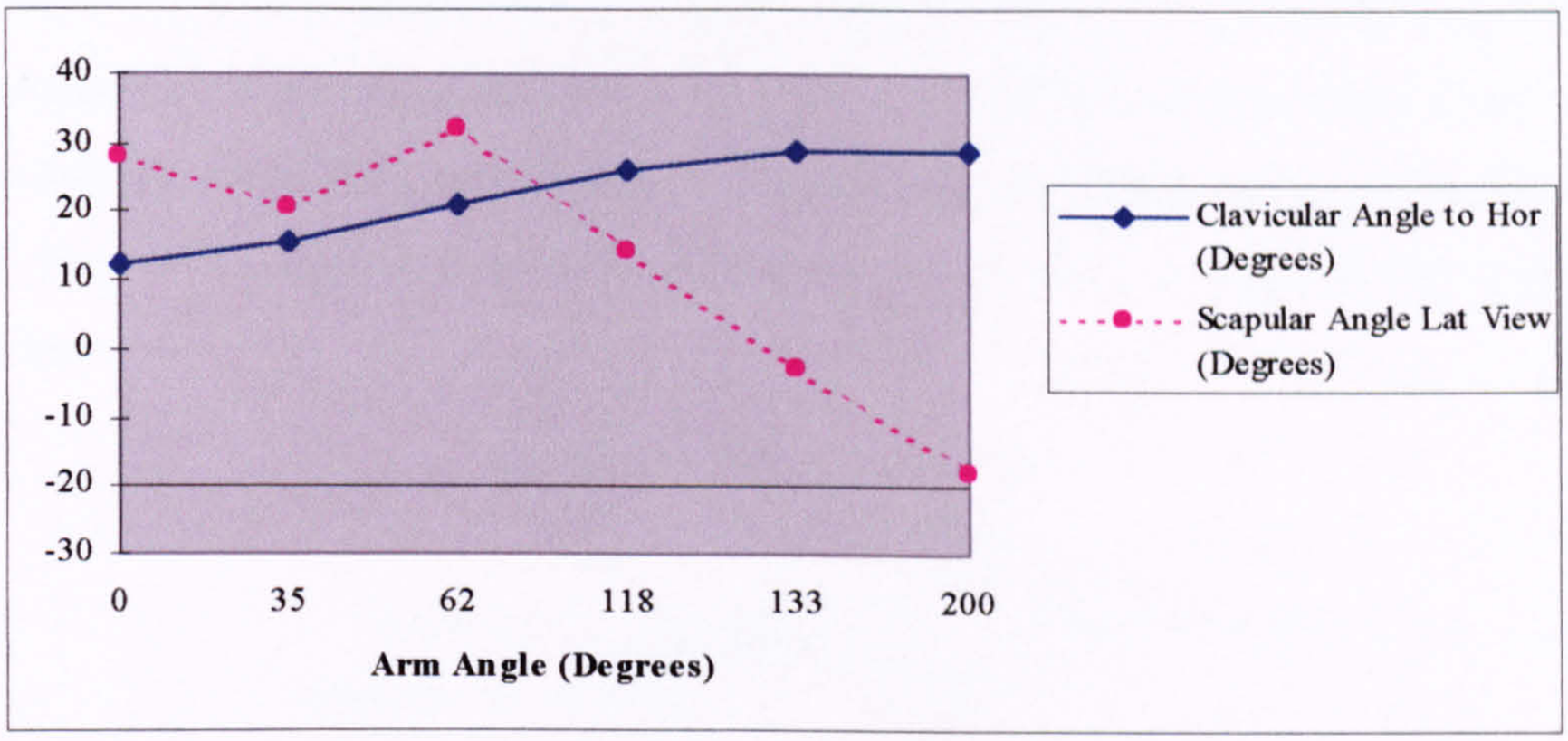

Figure 4.9c: *Rotations of scapula and clavicle* (*Wallace and Johnson 1982)*

In the same period, Engin (1980), Engin et al. (1984), Engin and Chen (1986) presented a research program for determining the three-dimensional passive resistive joint properties beyond the shoulder complex sinus. This research has provided a shoulder model with quantitative descriptions of the individual joint sinus cones. The technique proposed is a sonic digitising technique consisting of the assembly of sonic emitters to the torso and to the arm cuff respectively. A redundant arrangement of sensors together with selection and optimisation criteria has been used to process the data. Although this study represents an improved description of the shoulder, the model does not provide information on the simultaneous motions of the shoulder bones in that sterno-clavicular and acromioclavicular motion are not accounted for.

In 1987, another program was developed by Hogfors et al. who used optimisation techniques to predict the forces in the muscles, modelled as straight or curved strings, as functions of the static arm position and the external loads. From a kinematic point of view, the program is interesting because it was validated with in vivo data in 1991 with the use of implants in the bones of small tantalium balls together with X Ray analysis. Although this program deals with force prediction in muscles, the author, using the above described technique, demonstrated that while the absolute position of the bones varies significantly between individuals, their relative displacements exhibit similarities and consistently the rhythm was very stable and insensitive to small hand-loads.

In 1989 Engin and Tumer proposed a new interesting model shown in figures 4.10a and b, which represented the shoulder complex as a serial chain of links and revolute joint. Links have been defined as straight lines between two neighbouring articulating joints. Thus the clavicular link is a straight line between the sternoclavicular joint and the acromio-clavicular one.

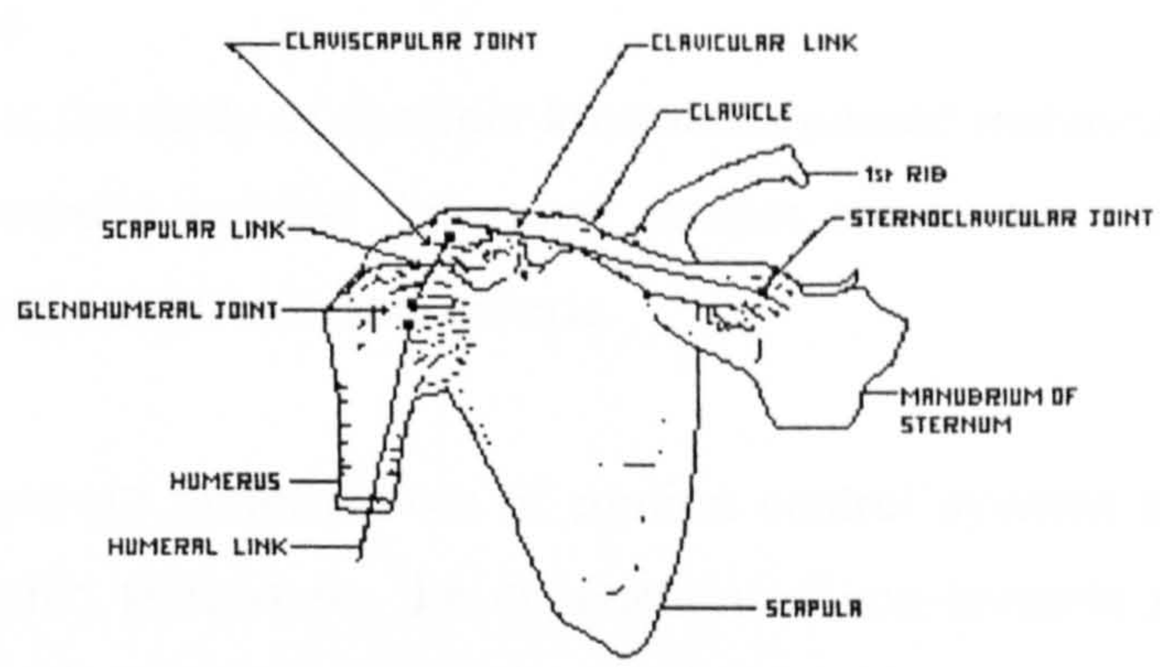

Fig. 4.10a: *Anatomical model of the shoulder complex (Engin and Tumer 1989)*

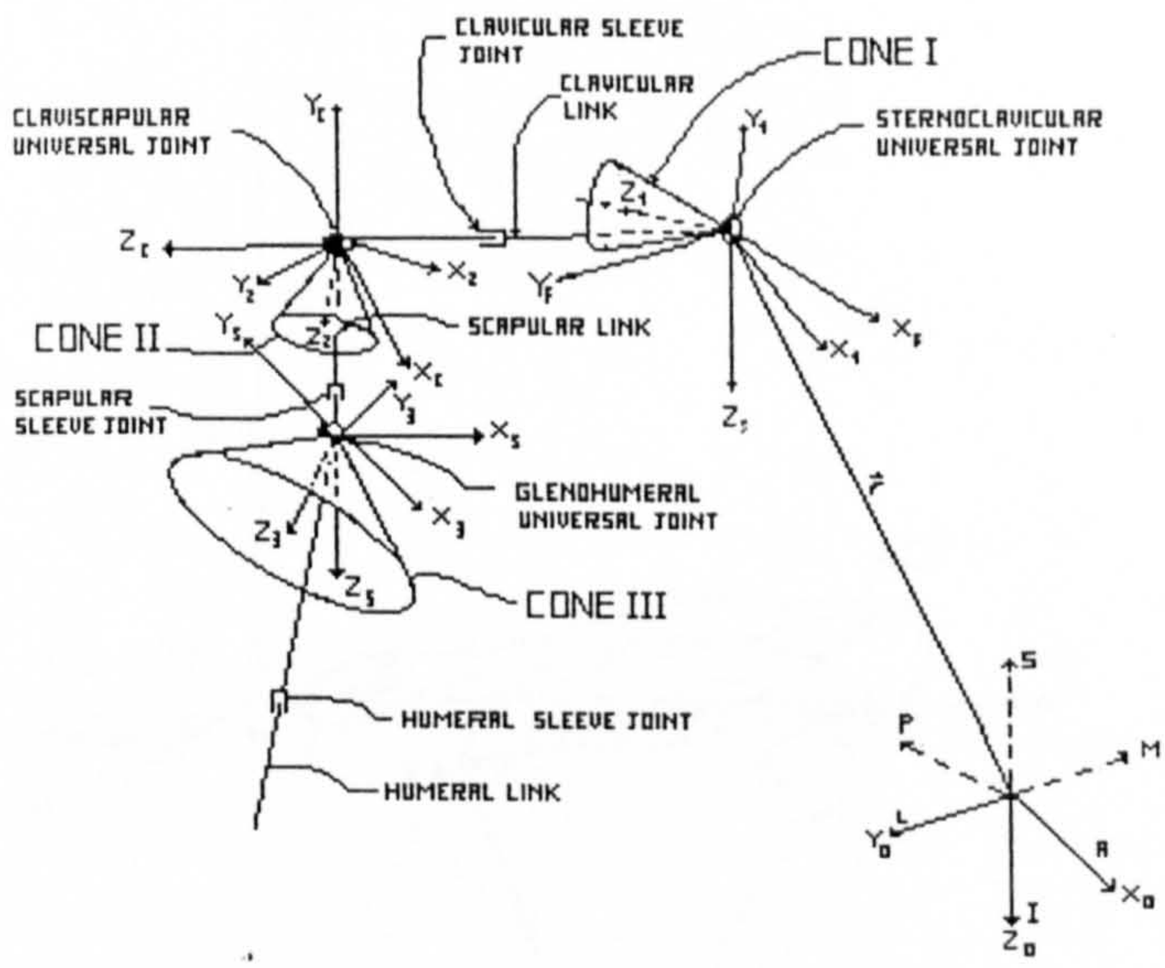

Fig. 4.10b: *Biomechanical model of the shoulder complex (Engin and Tumer 1989)*

The model treats the shoulder complex as a nine-degree-of-freedom open chain mechanism where it is possible to identify: a sternoclavicular universal joint (two degrees of freedom) and a clavicular sleeve joint (one degree of freedom); a claviscapular universal joint and a

scapular sleeve joint; a glenohumeral universal joint and a humeral sleeve joint. This model seems to be consistent with the real in-vivo model assuming to neglect the translations occuring at each joint. Nevertheless in the determination of the joints sinus cones, the geometry of the clavicle joint is not accounted for and the method utilises a database previously developed on specimen together with an optimisation model. No proper in vivo validation study is given.

The difficulties in the study of shoulder kinematics pushed researchers to investigate dynamics applying computer-assisted dynamical studies combined with finite element analysis methods and various optimisation criteria.

As a result of the improved performances of motion control systems and of the lesser popularity of radiographic techniques, the application of non-invasive methods became prevalent. In 1989 Pronk and van der Helm carried out a study on the role of the coracoclavicular mechanism, in the motion pattern between scapula and clavicle.

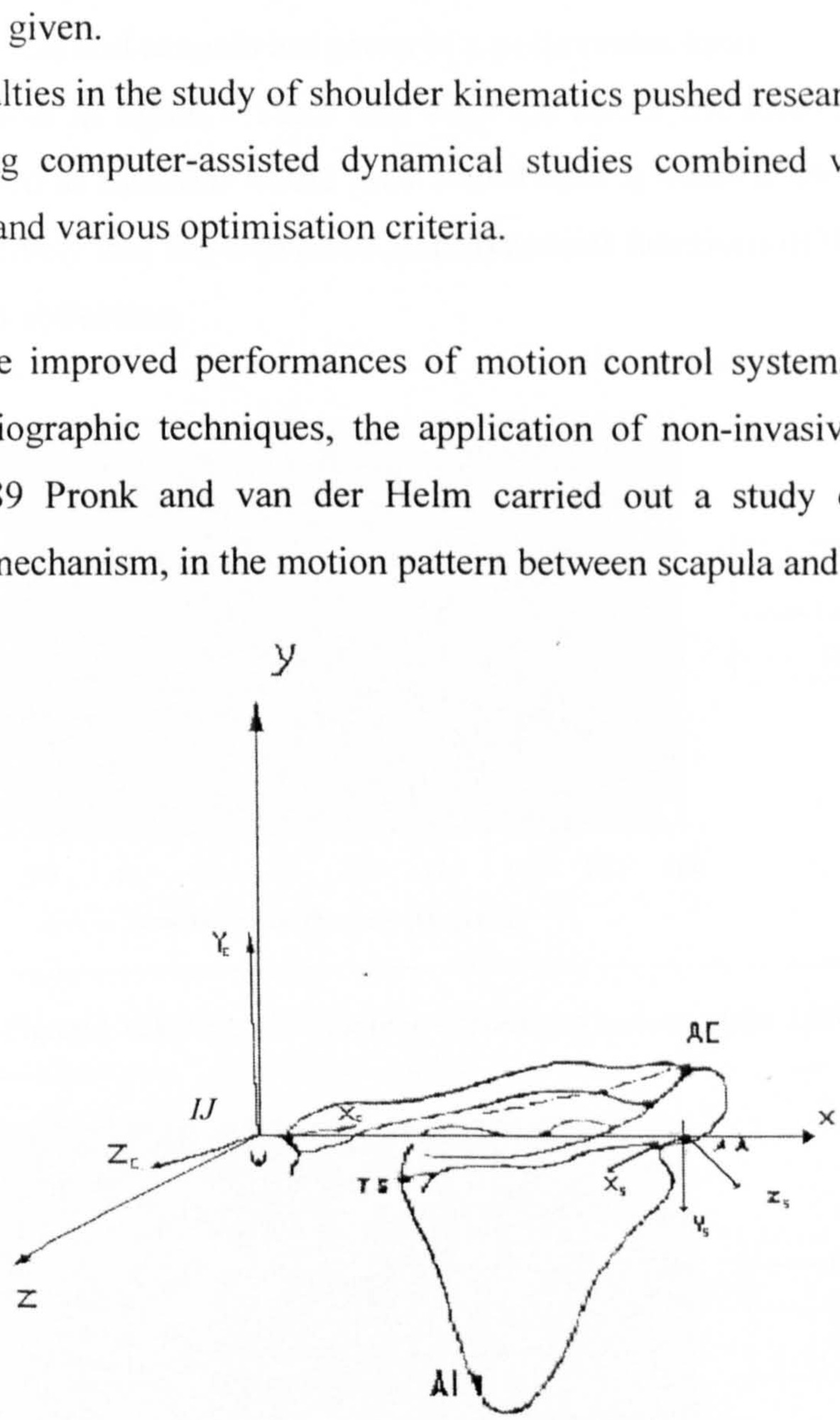

Figure 4.11: *Definition of global and local coordinate systems (Pronk, van der Helm 1989)*

It is worth mentioning that the authors realised the importance of the clavicle ligamentous structure in the kinematic behaviour of the shoulder complex.

Although the palpation technique used is not described in depth, with reference to the global coordinate system fixed at the Incisura Jugularis (IJ) and local coordinate systems fixed to the scapula (x_s,y_s,z_s) and to the clavicle (x_c,y_c,z_c) respectively shown in figure 4.11, the rotations of clavicle and scapula are given in a polynomial form.

The results are shown in figure 4.12a,b and 4.13 a,b where the rotations of scapula and clavicle are described as rotations in the local coordinate systems in the sequence Y, z_s, x_s and Y,z_c, x_c respectively and are expressed as polynomial functions of the humerus during forward flexion and abduction.

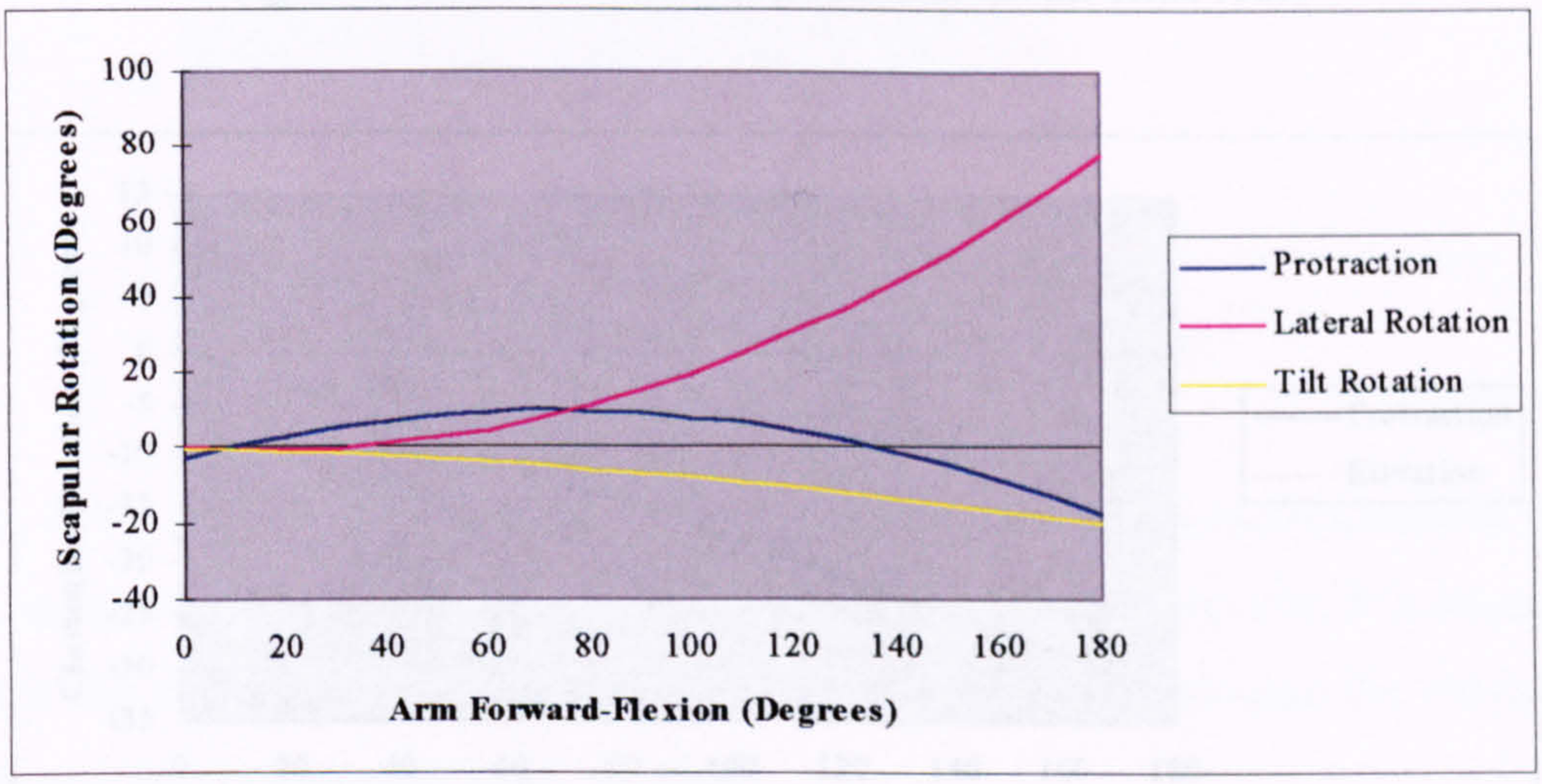

Figure 4.12a: *Scapular rotations (Pronk and van der Helm 1989)*

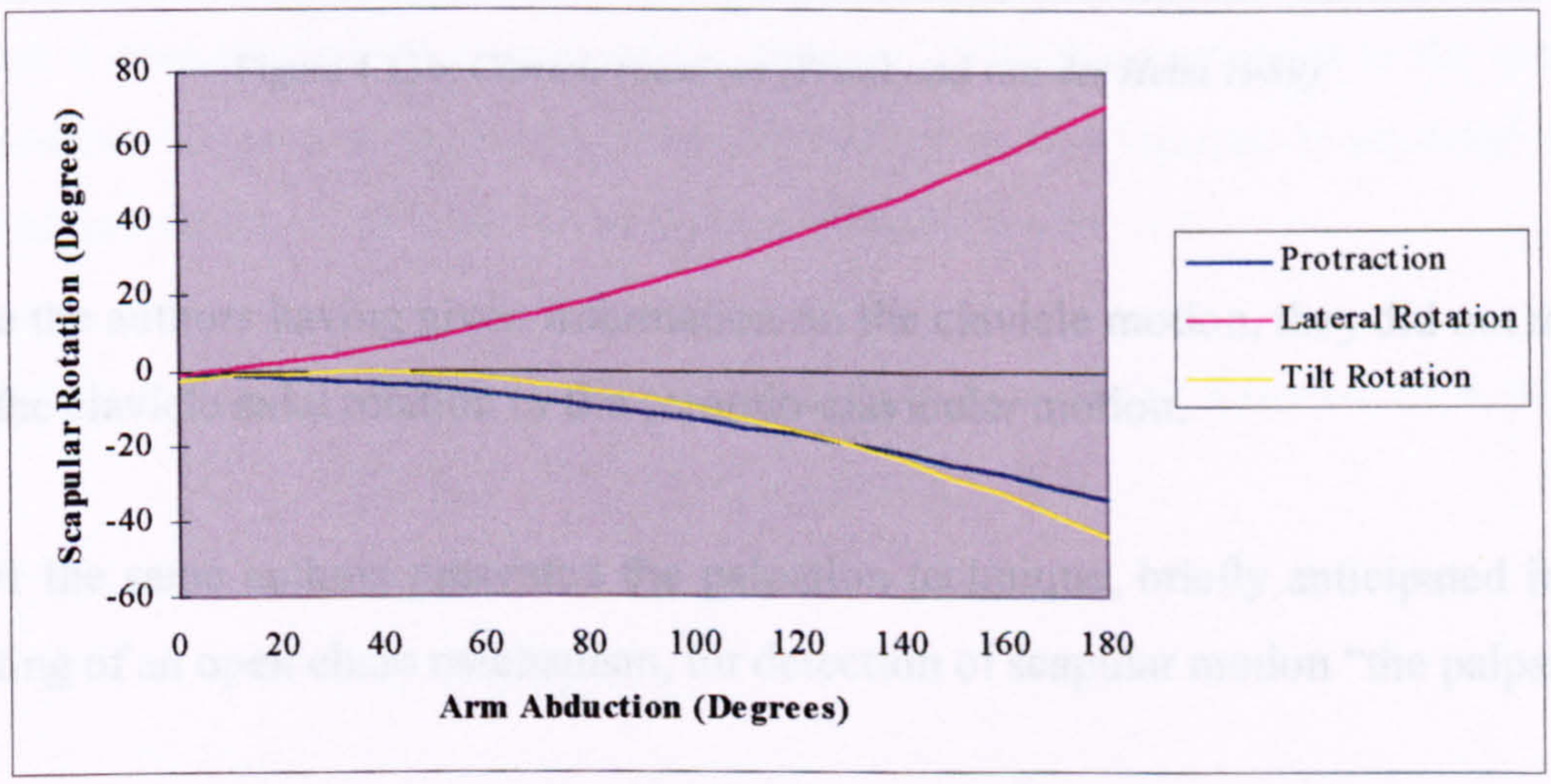

Figure 4.12b: *Scapular rotations (Pronk and van der Helm 1989)*

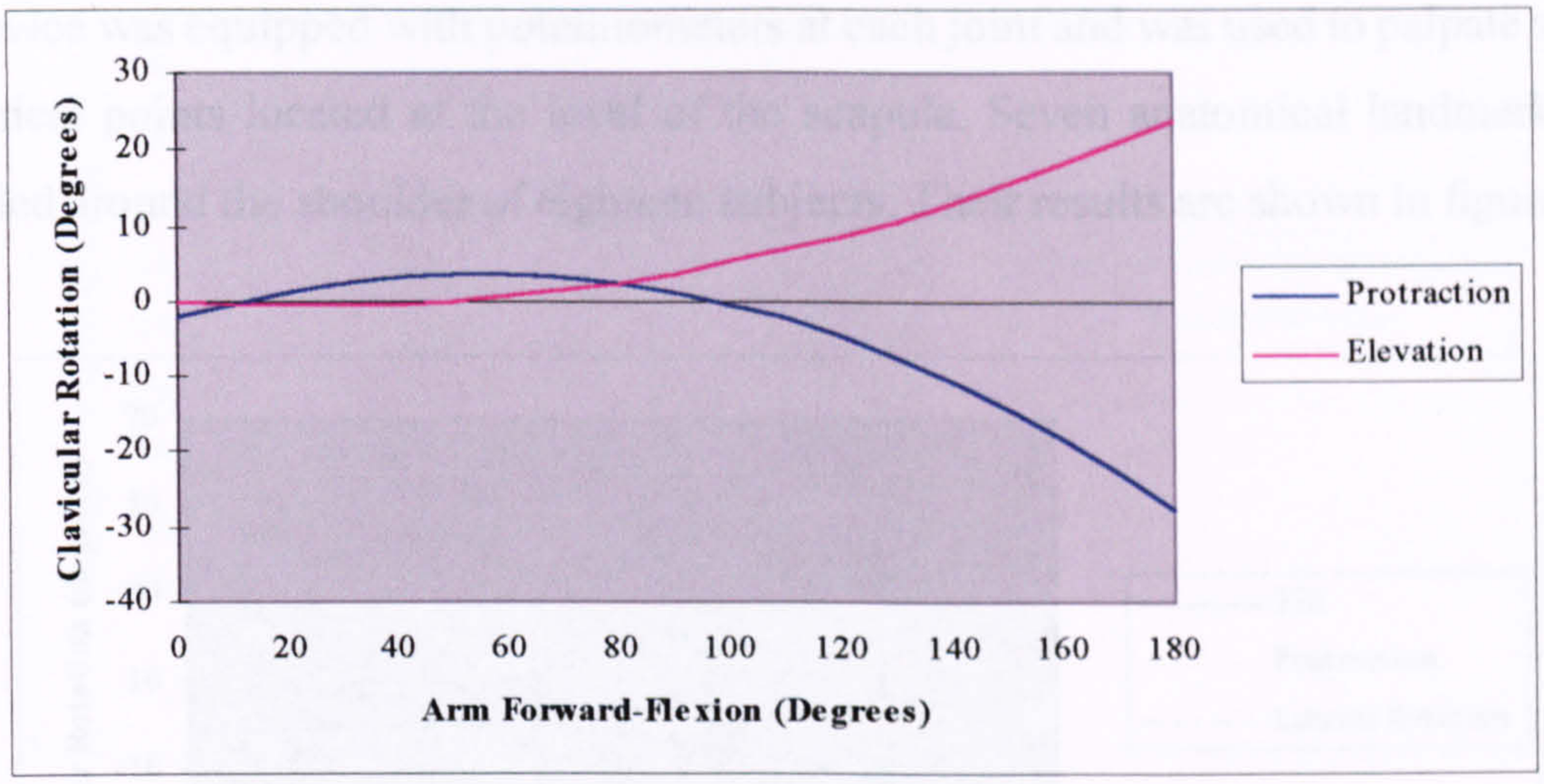

Figure 4.13a: *Clavicle rotations (Pronk and van der Helm 1989)*

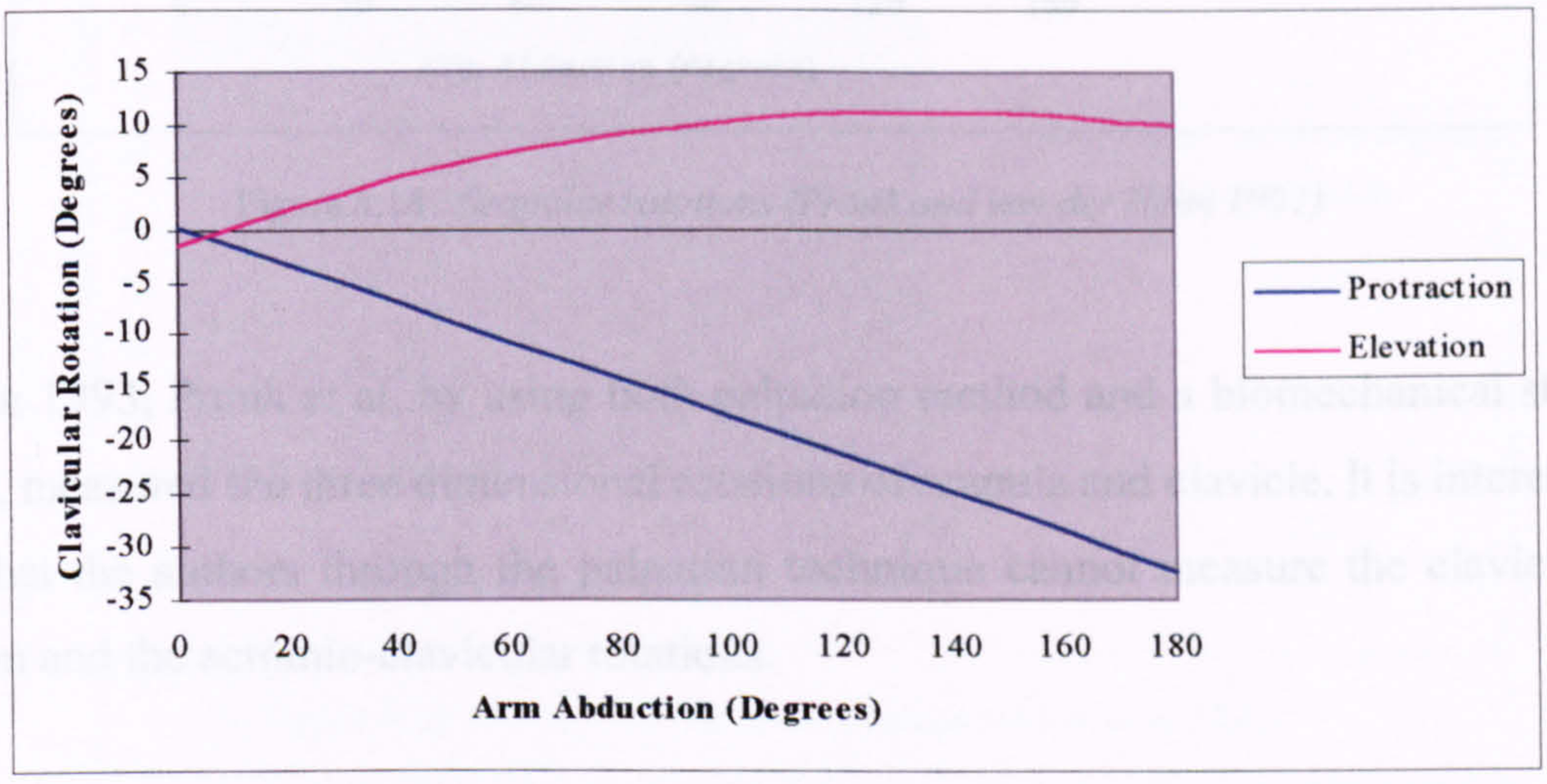

Figure 4.13b: *Clavicle rotations (Pronk and van der Helm 1989)*

Despite the authors having given information on the clavicle motion, they did not measure either the clavicle axial rotation or the acromio-clavicular motion.

In 1991 the same authors presented the palpation technique, briefly anticipated in 1989, consisting of an open chain mechanism, for detection of scapular motion "the palpator".

The device was equipped with potentiometers at each joint and was used to palpate specific anatomical points located at the level of the scapula. Seven anatomical landmarks were identified around the shoulder of eighteen subjects. Their results are shown in figure 4.14.

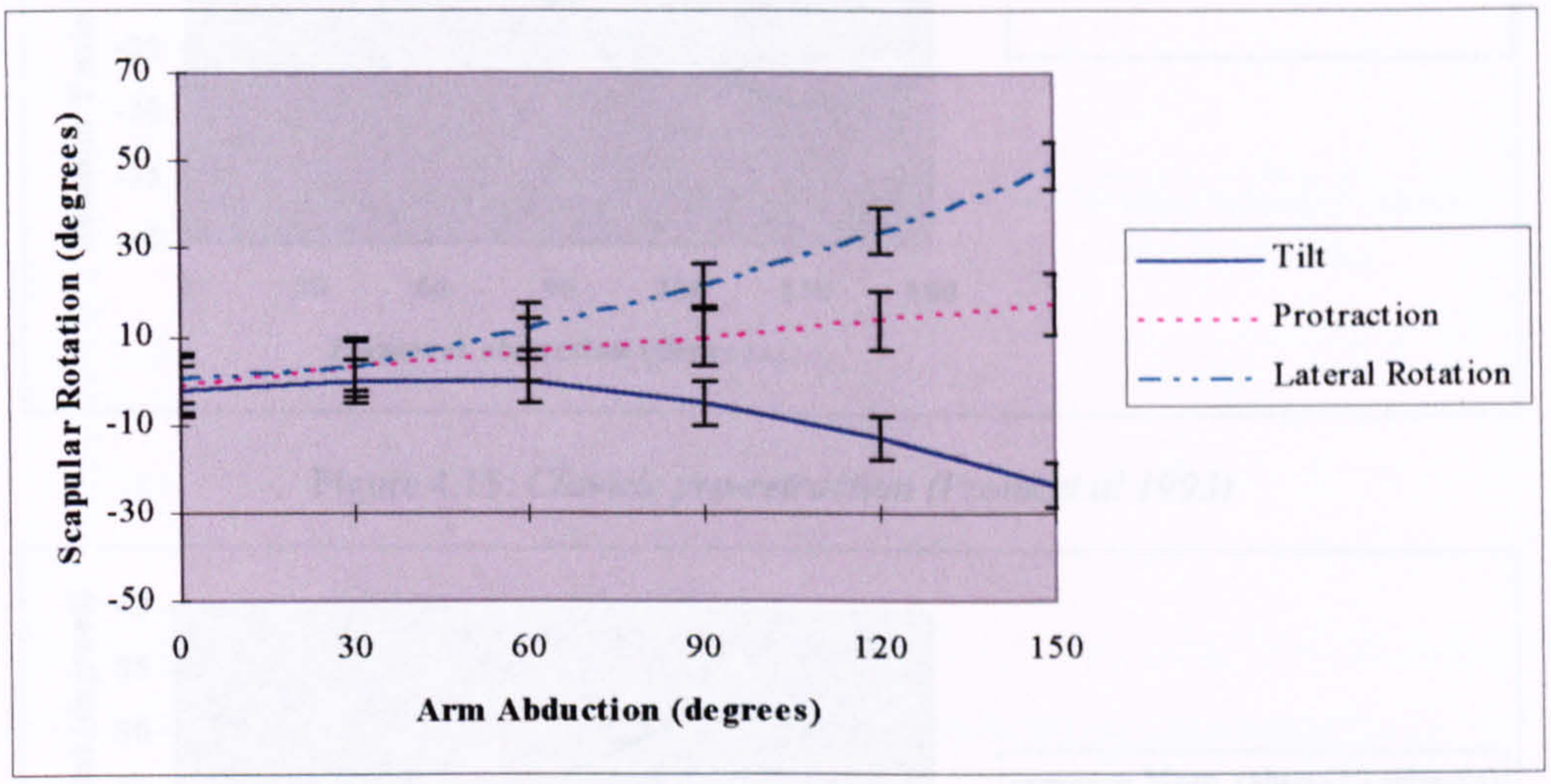

Figure 4.14: *Scapular rotations (Pronk and van der Helm 1991)*

Only in 1993, Pronk et al, by using both palpation method and a biomechanical shoulder model, measured the three dimensional rotations of scapula and clavicle. It is interesting to note that the authors through the palpation technique cannot measure the clavicle axial rotation and the acromio-clavicular rotations.

They use a musculoskeletal model, which imposes additional constraint to the motion. In fact a contact between scapula and thorax (modelled as an ellipsoid) is imposed together with a minimization of the rotations at the acromio-clavicular joint.

The clavicle motion, measured during arm abduction is shown in figures 4.15, 4.16, 4.17.

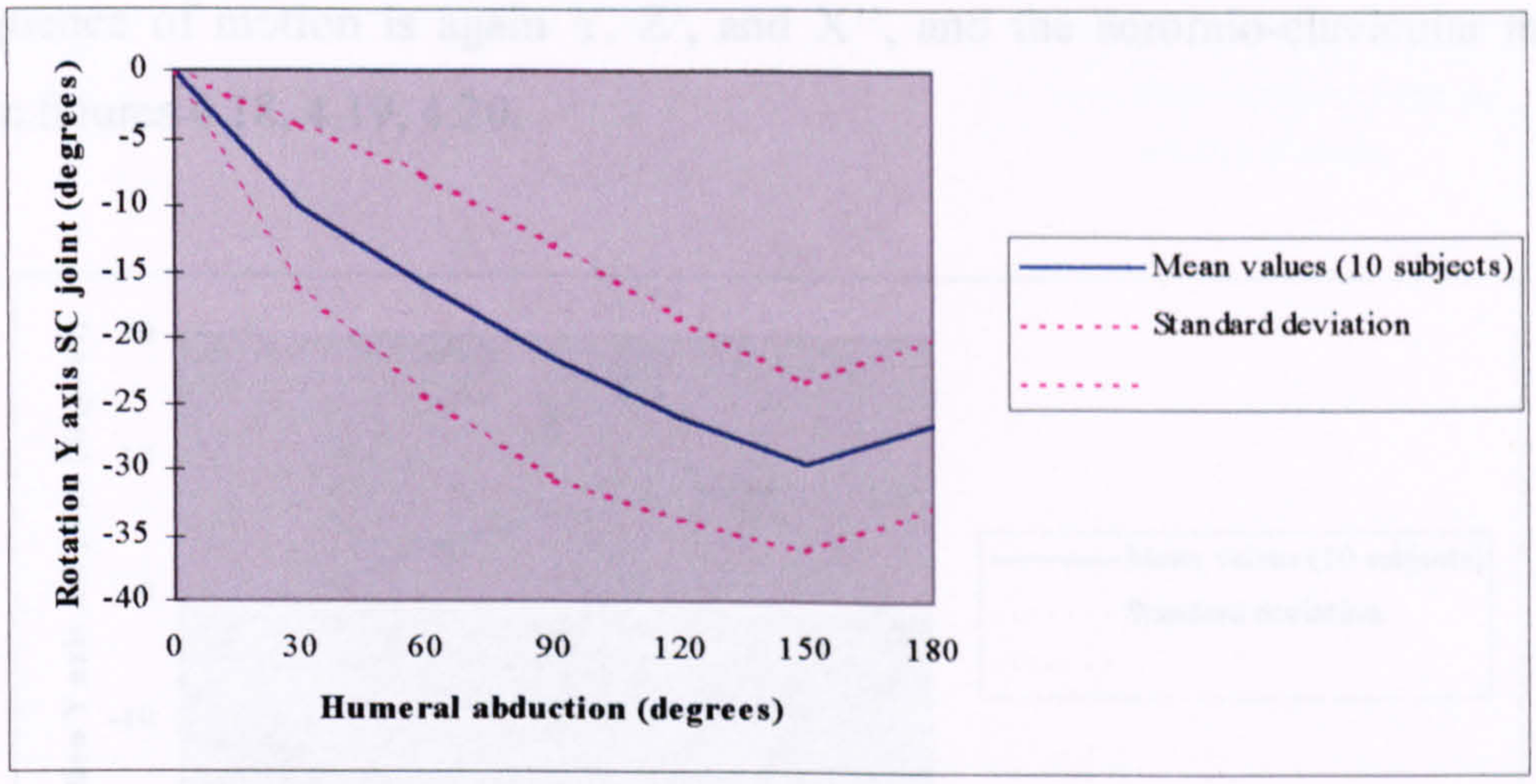

Figure 4.15: *Clavicle pro-retraction (Pronk et al 1993)*

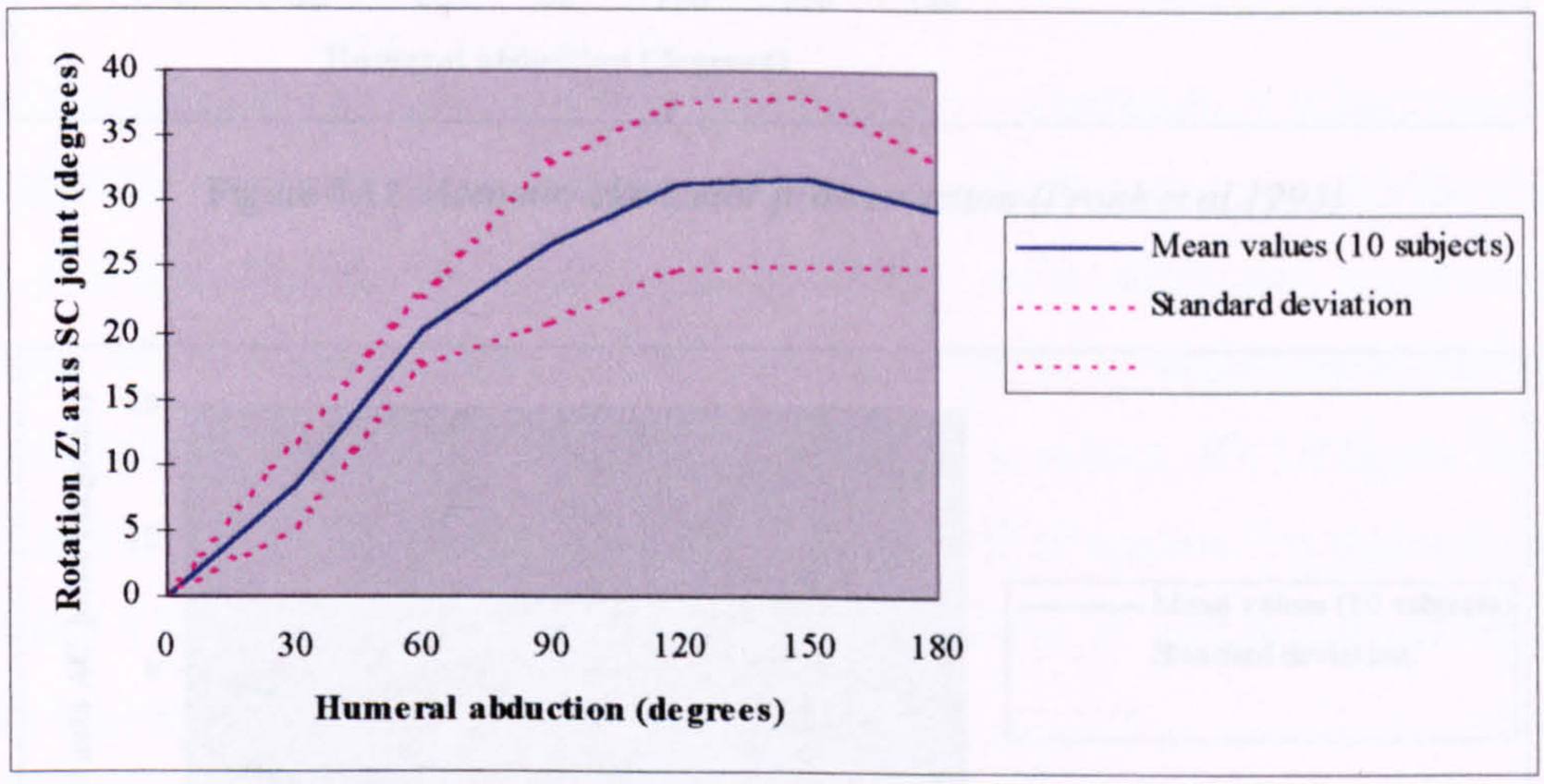

Figure 4.16: *Clavicle elevation-depression (Pronk et al 1993)*

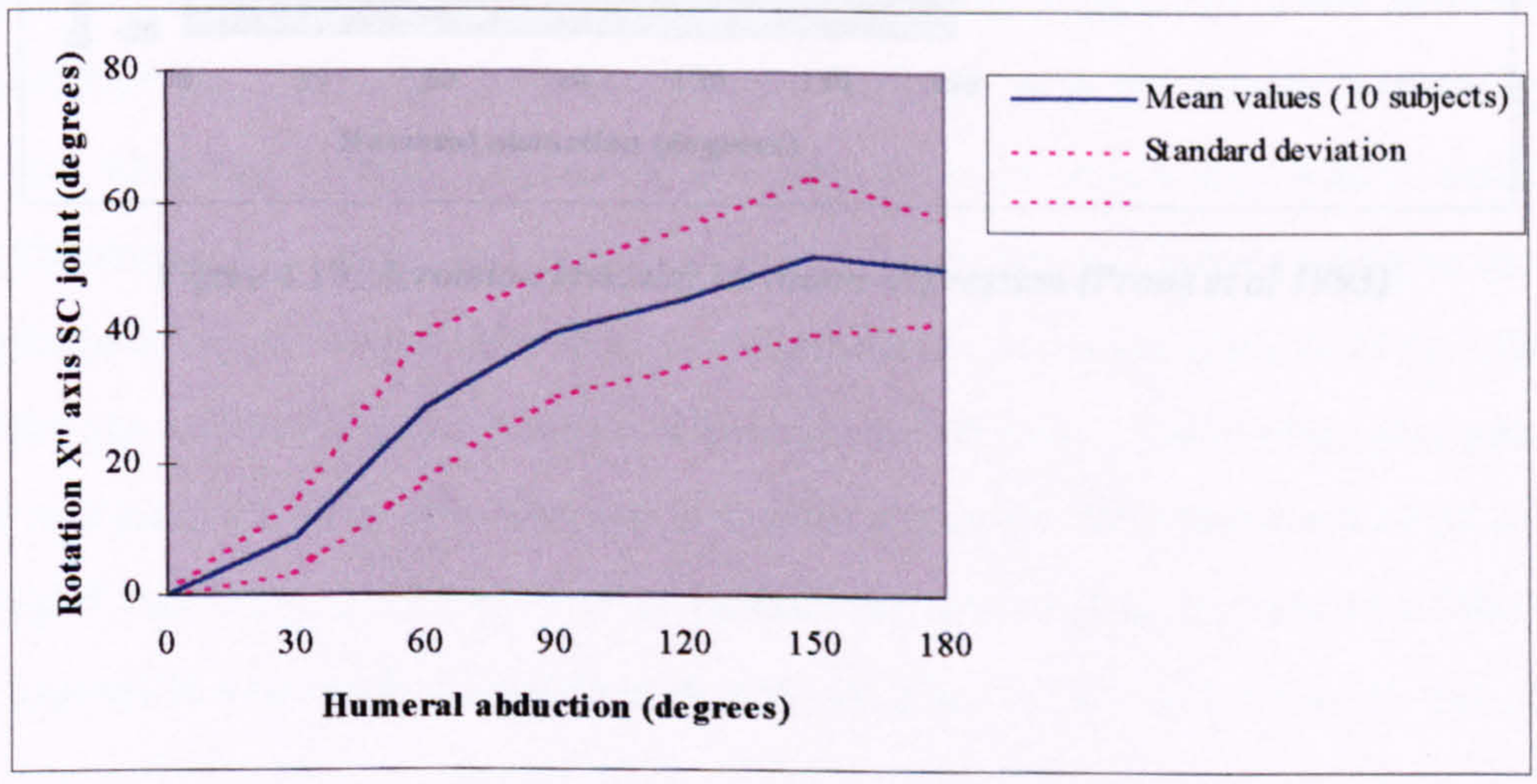

Figure 4.17: *Clavicle axial rotation (Pronk et al 1993)*

The sequence of motion is again Y, Z', and X'', and the acromio-clavicular motion is shown in figures 4.18, 4.19, 4.20.

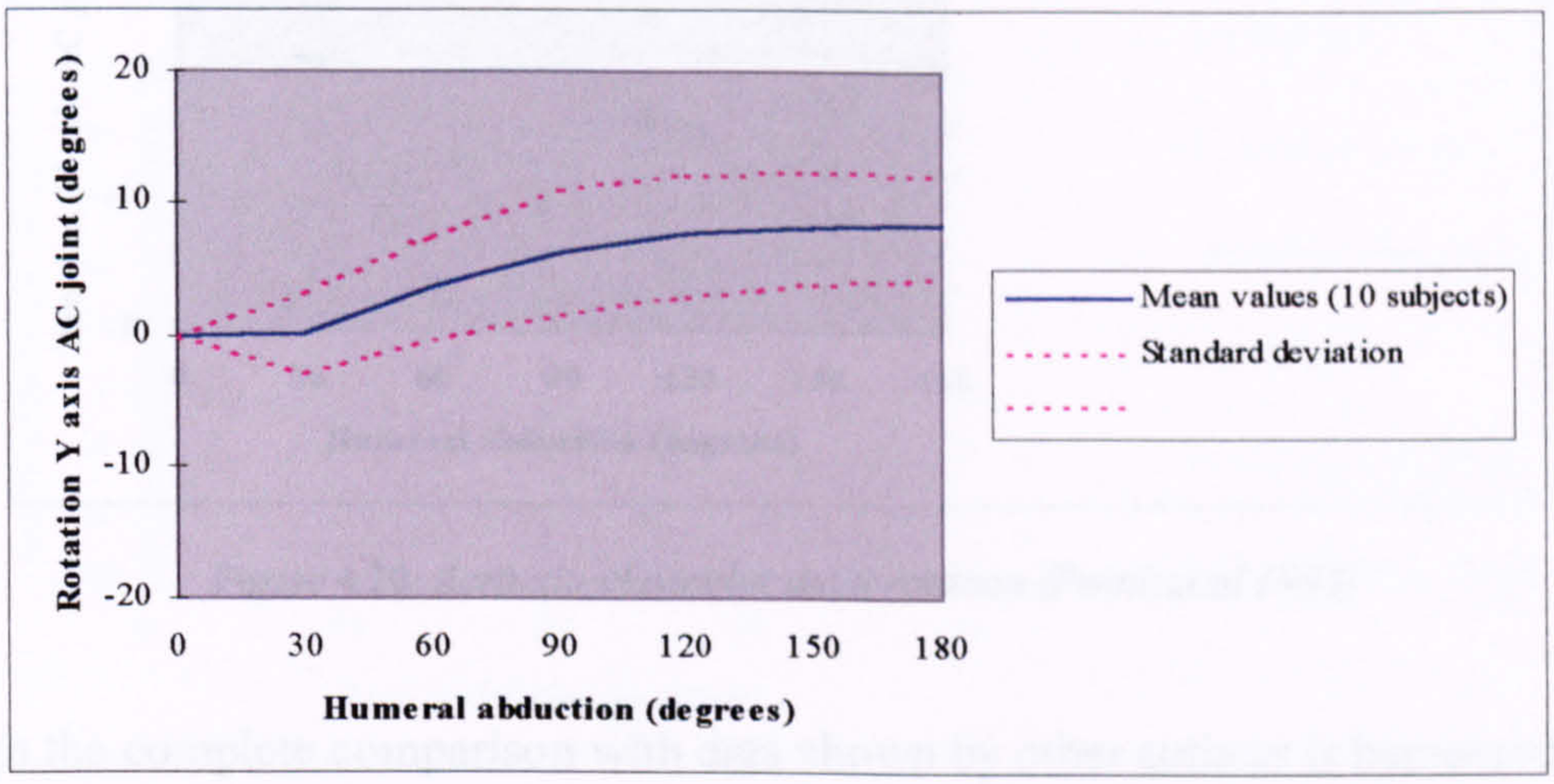

Figure 4.18: *Acromio-clavicular pro-retraction (Pronk et al 1993)*

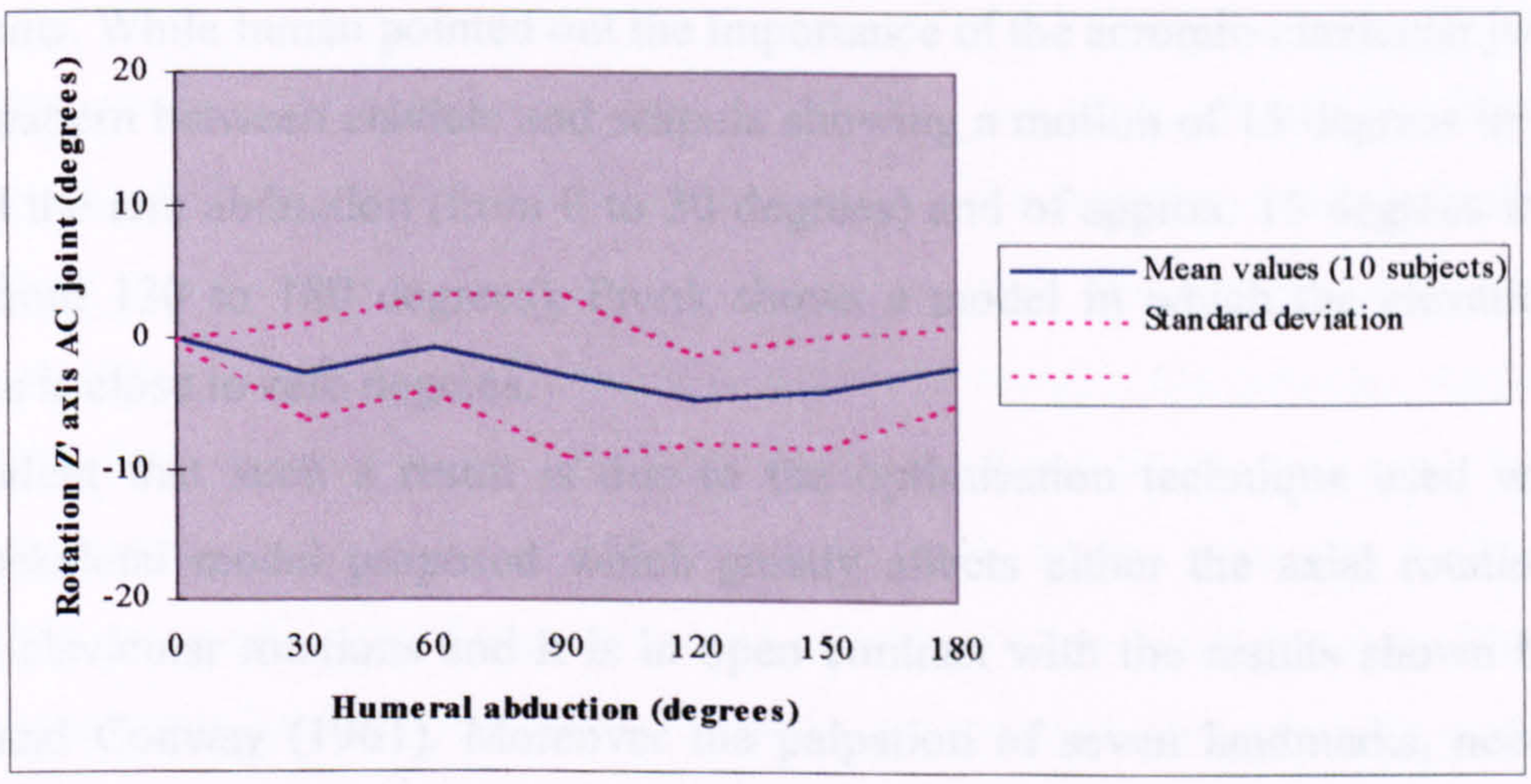

Figure 4.19: *Acromio-clavicular elevation-depression (Pronk et al 1993)*

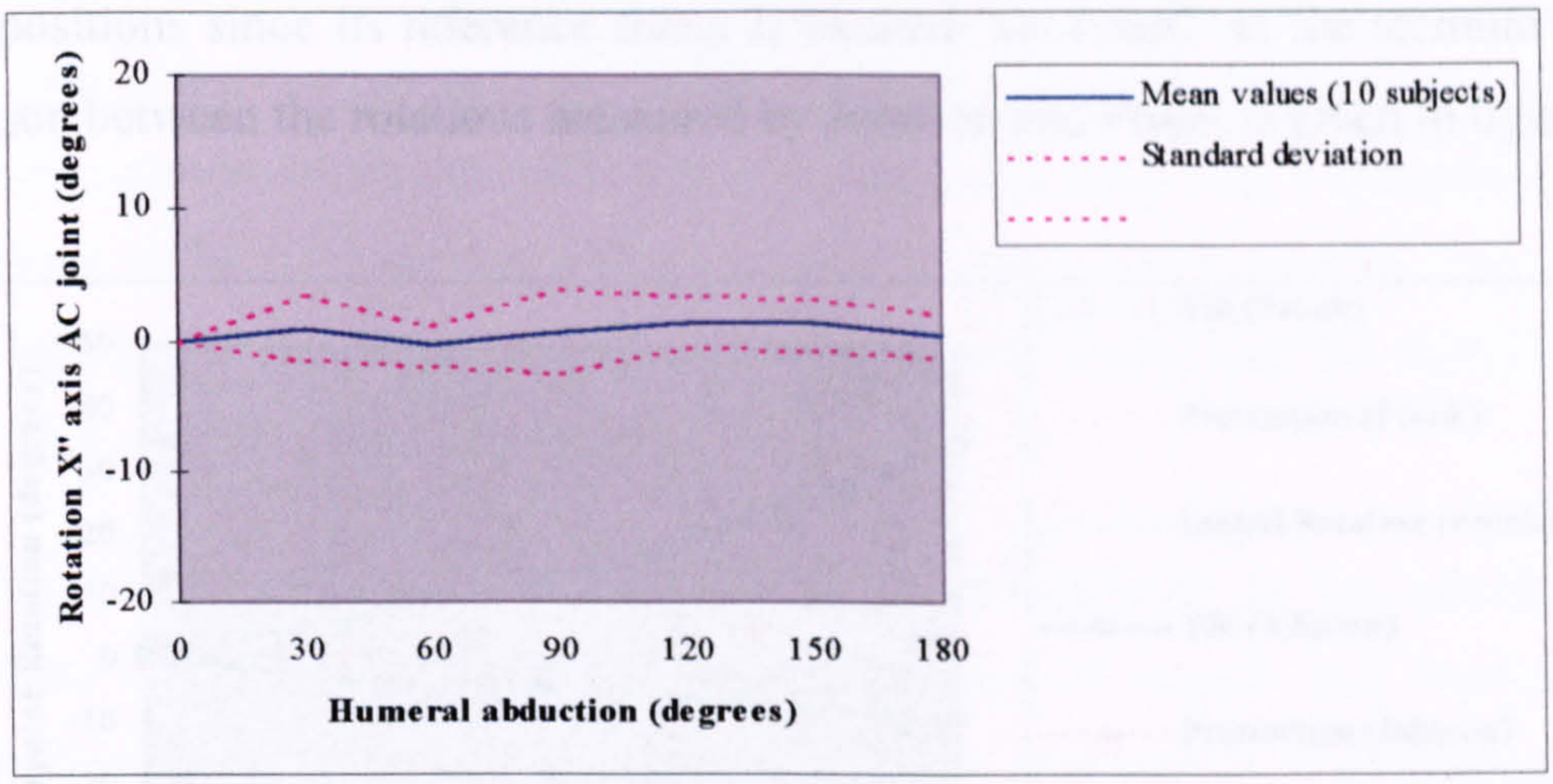

Figure 4.20: *Acromio-clavicular axial rotation (Pronk et al 1993)*

Although the complete comparison with data shown by other authors is hampered because of the different reference frames, it is interesting to note some remarkable differences between the data shown by Inman and by Pronk concerning the acromio-clavicular movements. While Inman pointed out the importance of the acromio-clavicular joint in the motion pattern between clavicle and scapula showing a motion of 15 degrees in the early phase of the arm abduction (from 0 to 30 degrees) and of approx. 15 degrees in the last phase (from 130 to 180 degrees), Pronk shows a model in which the elevation at the acromion is close to zero degrees.

It is evident that such a result is due to the optimisation technique used within the musculoskeletal model proposed which greatly affects either the axial rotation or the acromio-clavicular rotations and it is in open contrast with the results shown by Inman (1944) and Conway (1961). Moreover the palpation of seven landmarks, necessary to achieve information on a single position, is time consuming and induces fatigue in subjects. To overcome these problems related to scapula motion, Johnson et al. in 1993 developed a new technique based on a six-degree-of-freedom electromagnetic system equipped with a receiver mounted close to the sternum and with a transmitter assembled to an adjustable three legged mechanical fixture used to palpate the anatomical landmarks of the scapula. Such a system is extremely versatile and it is not affected by errors due to the change of

subject positions since its reference frame is located "on board" at the sternum level. A comparison between the rotations measured by Johnson and Pronk is given in figure 4.21.

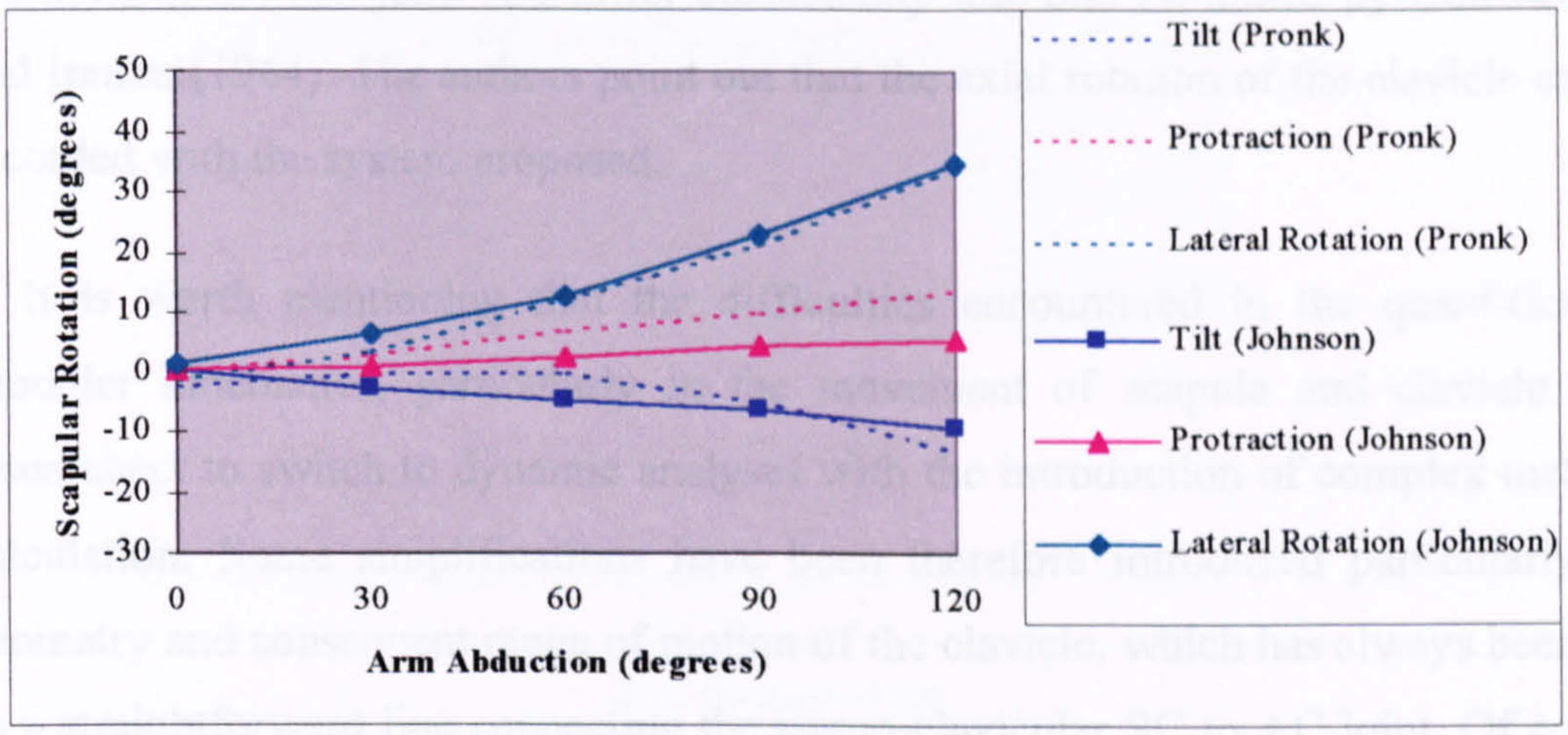

Figure 4.21: *Rotations of scapula measured by Johnson (1991) and by Pronk (1993)*

Although the shoulder rhythm was investigated by other authors like Badler et al. (1993) who, by applying statistical results, tried to formulate the clavicular and scapular elevations as functions of the humeral abduction, their relationships only apply for a given motion and are not sufficient to describe realistically the complex motion of the shoulder. A complete dynamic shoulder model has been finally suggested by van der Helm by means of the finite element method in 1994. In this approach, the bones were modelled, as usual, as rigid segments connected by ball and socket joints. The specific scapulo-thoracic joint was modelled as a triangular structure constrained in contact on an ellipsoid. All muscles and ligaments were taken into account and modelled as straight or curved lines of action between their connections on the bones. A previous analysis had provided a discretization method for the modelling of muscles with large attachment sites. Geometrical and mechanical parameters were also collected to enable the kinematic and dynamic analysis of the shoulder. From this analysis, a further step in human shoulder description has been established by van der Helm and Pronk (1995) and validated, where possible, on the basis of anatomical, practical, minimization criteria and experimental results. Kinematic data therefore appear on the movement of the shoulder

complex in a limited subset of the workspace and it is interesting to notice that again, the rotations of the "virtual clavicle" (which connects with a line the Incisura-Jugularis (IJ) and the acromio-clavicular (AC) joint) are estimated imposing a minimization of the rotations in the AC joint and differ consistently that one estimated by Conway (1961) and Inman (1944). The authors point out that the axial rotation of the clavicle cannot be recorded with the system proposed.

It is worth mentioning that the difficulties encountered in the quantification of shoulder kinematics, particularly in the movement of scapula and clavicle has led researchers to switch to dynamic analyses with the introduction of complex methods of calculation. Some simplifications have been therefore introduced particularly in the geometry and consequent range of motion of the clavicle, which has always been treated as a straightforward line connecting the sterno-clavicular SC to AC joint. Of course, as pointed out by Inman (1946), the geometry of the bone plays an important role either from the kinematic point of view, because it affects the real movement of the entire arm, or from a dynamic one, because its surface acts as an important site for muscle attachment. These geometric properties, in all the previous studies mentioned, have never been taken into account.

Another interesting fact, which represents a leitmotiv of all these studies, is that the experimental data has been obtained in a very limited workspace and not always a proper statistical analysis has been conducted in order to extrapolate the results.

In 1996 Barnett, using the same technique developed by Johnson, modelled the scapula as a six-degree-of-freedom and quantified its motion in a subset of the workspace of the human arm. Data have been extracted from an extensive validation study and by applying a proper statistical analysis. Scapular rotations are presented as surface functions of the humeral motion in a subset of the workspace. The data shown by Barnett are well in accordance with the data shown by Pronk (see figure 4.22a,b,c).

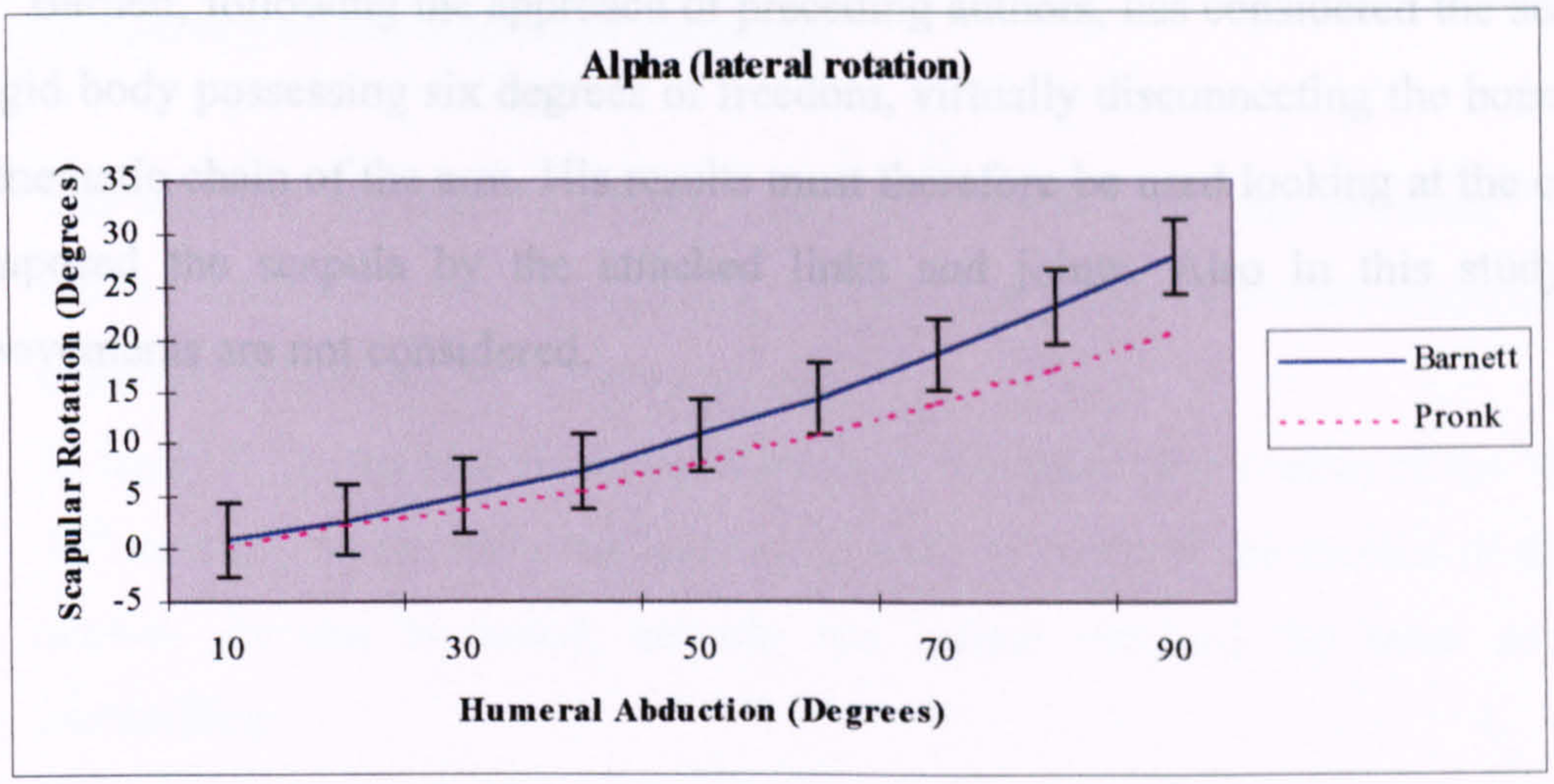

Figure 4.22 a *Scapular rotations comparison between the work of Pronk (1991) and Barnett (1996)*

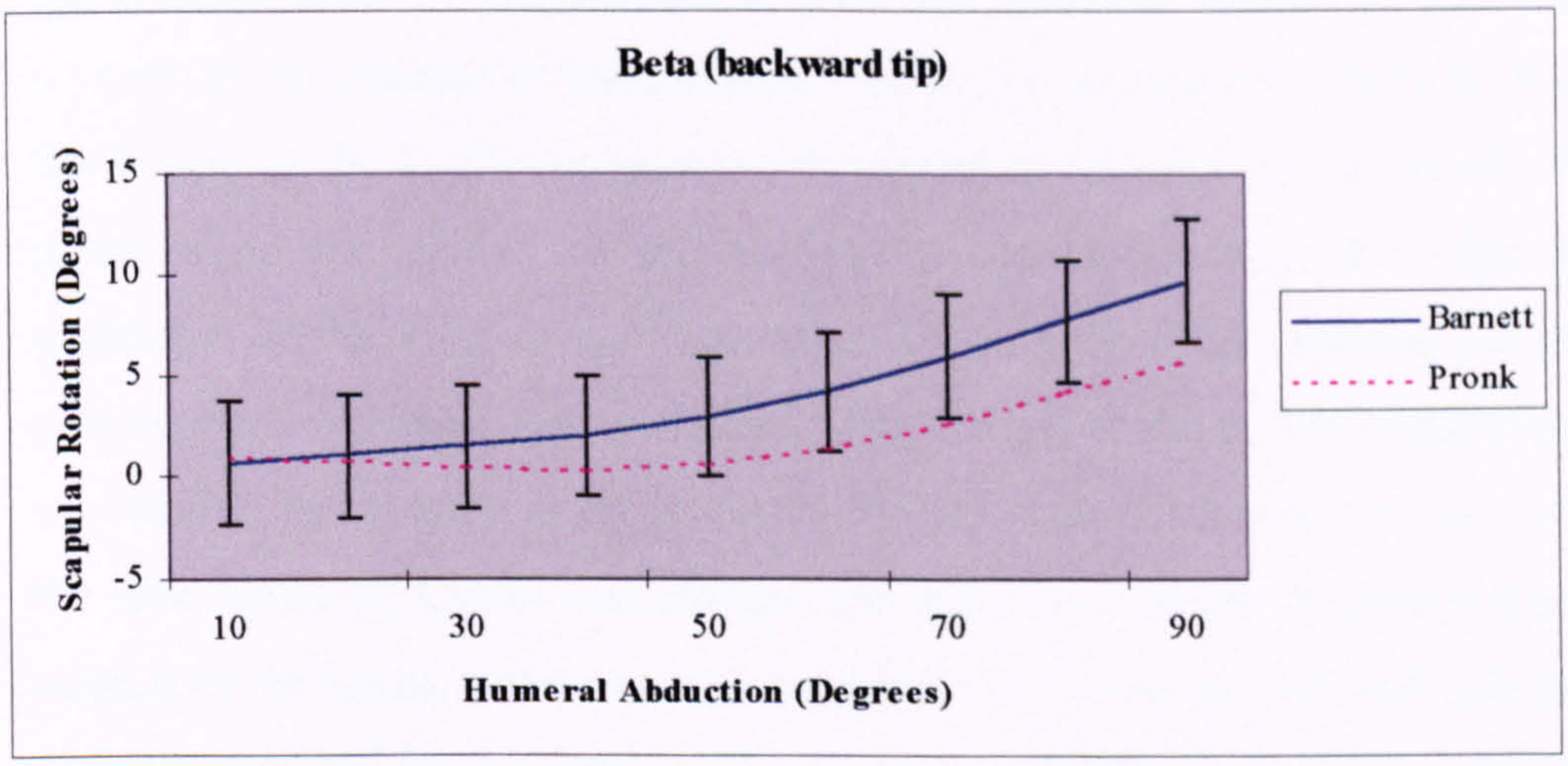

Figure 4.22 b *Scapular rotations comparison between the work of Pronk (1991) and Barnett (1996)*

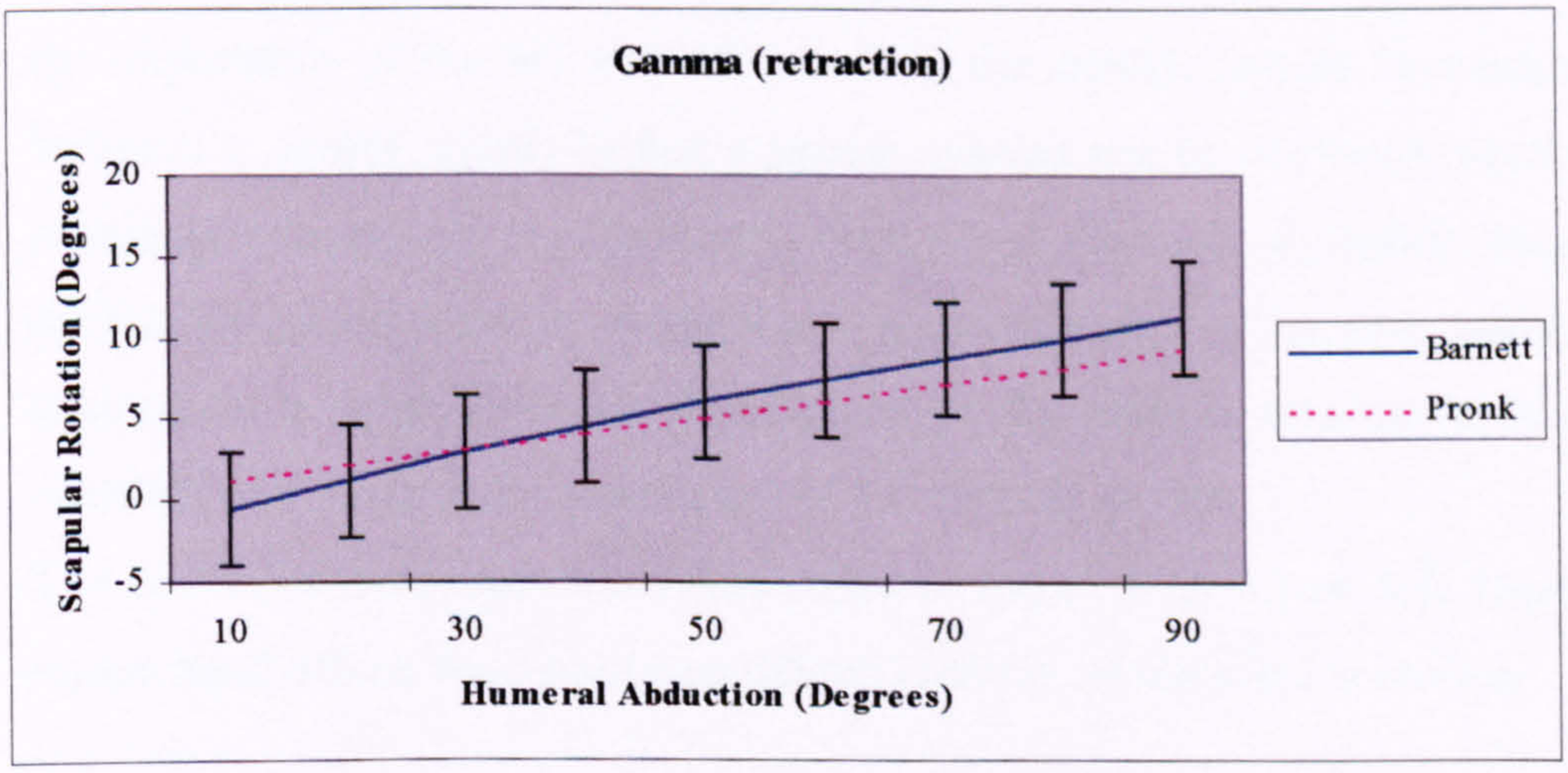

Figure 4.22 c *Scapular rotations comparison between the work of Pronk (1991) and Barnett (1996)*

Barnett, following the approach of preceding authors, has considered the scapula as a rigid body possessing six degrees of freedom, virtually disconnecting the bone from the kinematic chain of the arm. His results must therefore be used looking at the constraints imposed the scapula by the attached links and joints. Also in this study clavicle movements are not considered.

4.4 Summary of the Relevant Findings

The shoulder complex has been object of intense study and research. The complex motion interaction between scapula, clavicle and humerus pushed researchers to apply different techniques for motion analysis.

In figure 4.23, the historical evolution from the qualitative studies of the 18th and early 19th century, to the different techniques used to quantify the motion of the scapula is shown. As can be noted, scapula has indeed received the most attention from researchers.

The most relevant findings are undoubtedly the 3D features of the scapula motion and the constant relationship between scapula and humerus called "the shoulder rhythm". Despite the kinematics of the shoulder was finally presented in 1993 by Pronk and van der Helm, as far as the kinematics of the entire complex is concerned, few data are given about the motion of the clavicle at the sterno-clavicular joint. In fact, the geometry of the bone is not accounted for and its axial rotation calculated by an optimisation technique that minimizes the motion at the acromio-clavicular joint and constrained the scapula to rotate on the thorax wall. Such data are not consistent with the data shown by Inman who stressed the importance of the clavicle in the harmonious motion of the bones. What has been suggested by Inman in 1946 and reiterated by Saha in 1950 was an investigation on the *clavi-scapulo-humeral rhythm* which could be a more accurate definition of shoulder kinematics. From many of the studies carried out, the importance of the SC and AC joints in the motion pattern between scapula and humerus is clearly stated. In fact scapular rotation can be obviously seen as a sum of rotations occurred at the proximal bone (the clavicle). Probably because of the difficulties encountered by researchers in quantifying on "in vivo subjects" clavicle kinematics, a main focus has been given to the scapula rotation with a very poor attention to the kinematic assessment of the clavicle motion.

The historical challenges are summarised in figure 4.23 where it is highlighted how researchers' efforts have been concentrated mainly on the scapula motion.

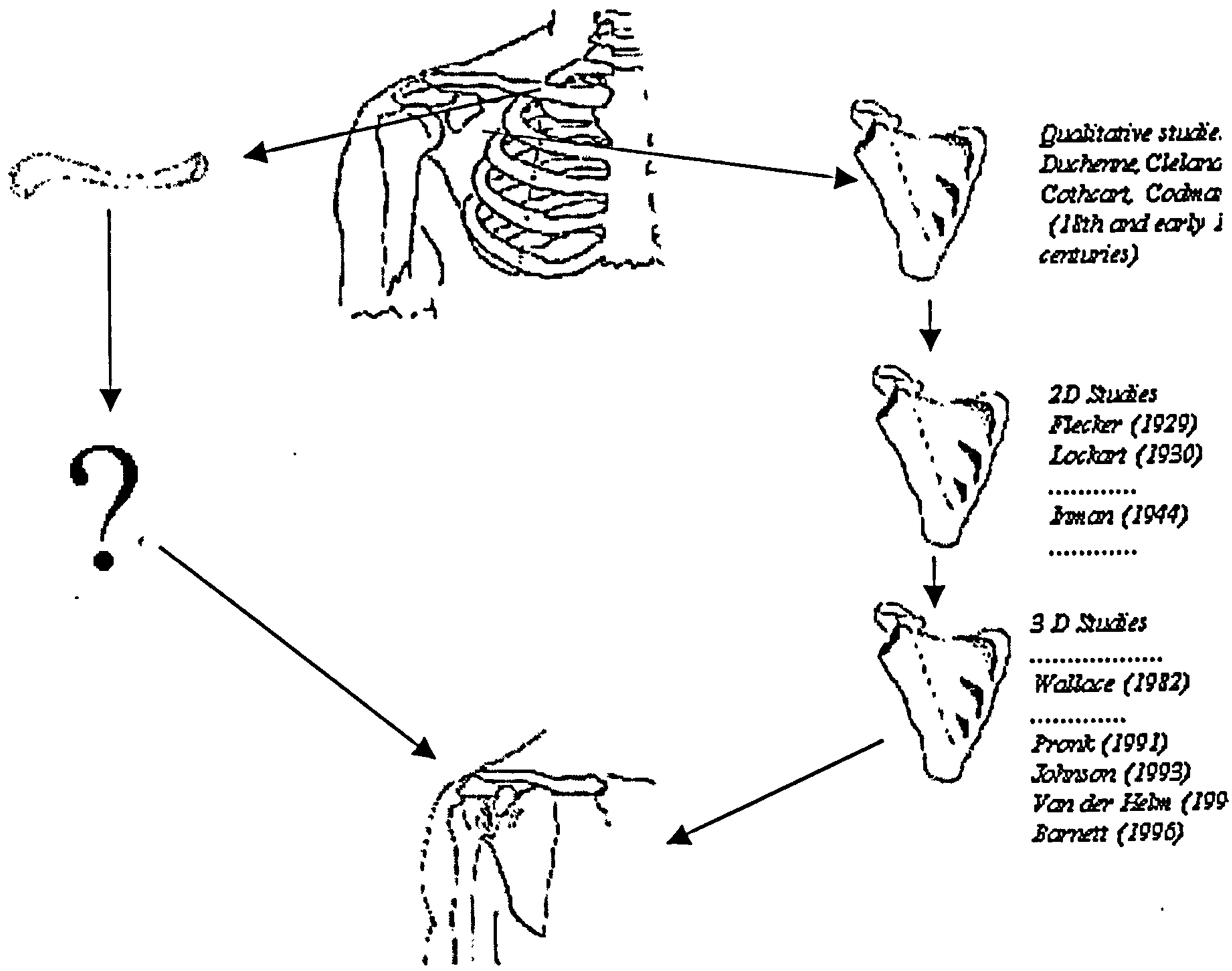

Clavi-scapulo-humeral kinematics

Figure 4.23: *Historical studies of the shoulder complex*

Therefore, despite the extensive research carried out, the kinematics of the clavicle still hides its main features, which, in turn, being the clavicle the first bone of the kinematic chain of the arm, means a lack of information on the motion of the entire arm.

5 Materials and Methods

In the previous chapter, it has been shown that currently available techniques do not allow the monitoring of multi-degree-of-freedom joints like the shoulder complex. The most affecting constraint is represented by the allowed surfaces of the body where sensitive apparatuses must be attached for proper recording. The miniaturised size of markers or of active devices is therefore a pre-requisite to attach them to humans.

The motion of the clavicle is completely hidden by skin and soft tissues, therefore this section aims at exploiting any possible methodological approach for the design of a kinematic structure to be positioned close to the subject and capable of providing information that can be converted through an algorithm in the three rotations of the clavicle. It is demonstrated that in order to approach the problem correctly it has been necessary to dedicate considerable efforts to the design and development of new miniaturised sensors whose small size would allow their assembly in a kinematic arrangement in order to provide information on invisible joints.

Therefore, using the new sensors developed, the clavicle, which is probably the most difficult bone to be recorded on an in vivo subject, has been addressed for the research designing and developing the "*clavicle movement detector*".

All the phases of design, development and necessary improvements of the sensors and of the detector developed are described in the present Chapter.

5.1 Preliminary design steps

As previously shown, few data are available on the movement of the clavicle. Some information can be found in the work of Inman (1944), who pointed out the crucial

role of the axial rotation of the bone. This rotation is caused by the marked curvature of the outer third of the clavicle and by the spatial position of the inner third of the bone.

The preliminary idea for the development of a device capable of monitoring the SC joint has been suggested by Inman's words (1944): "*...Because of the marked curvature of the outer third of the clavicle, we could envisage a relative elongation of the coracoclavicular ligament, only by the clavicle rotating on its long axis, so as to allow this curvature to act as a crankshaft*".

The kinematic model proposed exploits the above geometric characteristics of the clavicle in order to extract information on its three rotations. The bone has been modelled as a crankshaft possessing three degrees of freedom located in the centre of the sterno-clavicular articulation.

In this configuration the problem is still unresolved because the axial rotation is not visible. Moreover, the volumes surrounding the sternum do not allow either the positioning of sensors and markers or their arrangement in a complex kinematic chain. Therefore the main questions still remain: "Is it possible to arrange a kinematic chain in order to have information on the axial rotation of the joint? Are the volumes located close to sternum sufficient to integrate such kinematic structure? Is it possible to use existing sensor devices?

With reference to figure 5.0, the axial rotation of the clavicle θ_3 can be expressed as a function of θ_1 and θ_2 and if we assume two sensors located along the abduction-adduction axis and maintaining the contact with the inner and outer third of the clavicle respectively, we can say that:

if

$$\theta_1=\theta_2 \Rightarrow \theta_3=0$$

and if

$\theta_1 \neq \theta_2 \Rightarrow \theta_3 \neq 0$

where, in the last case $\theta_3 = f(\theta_1, \theta_2, R, b)$

The above equation will be examined in depth later in this chapter.

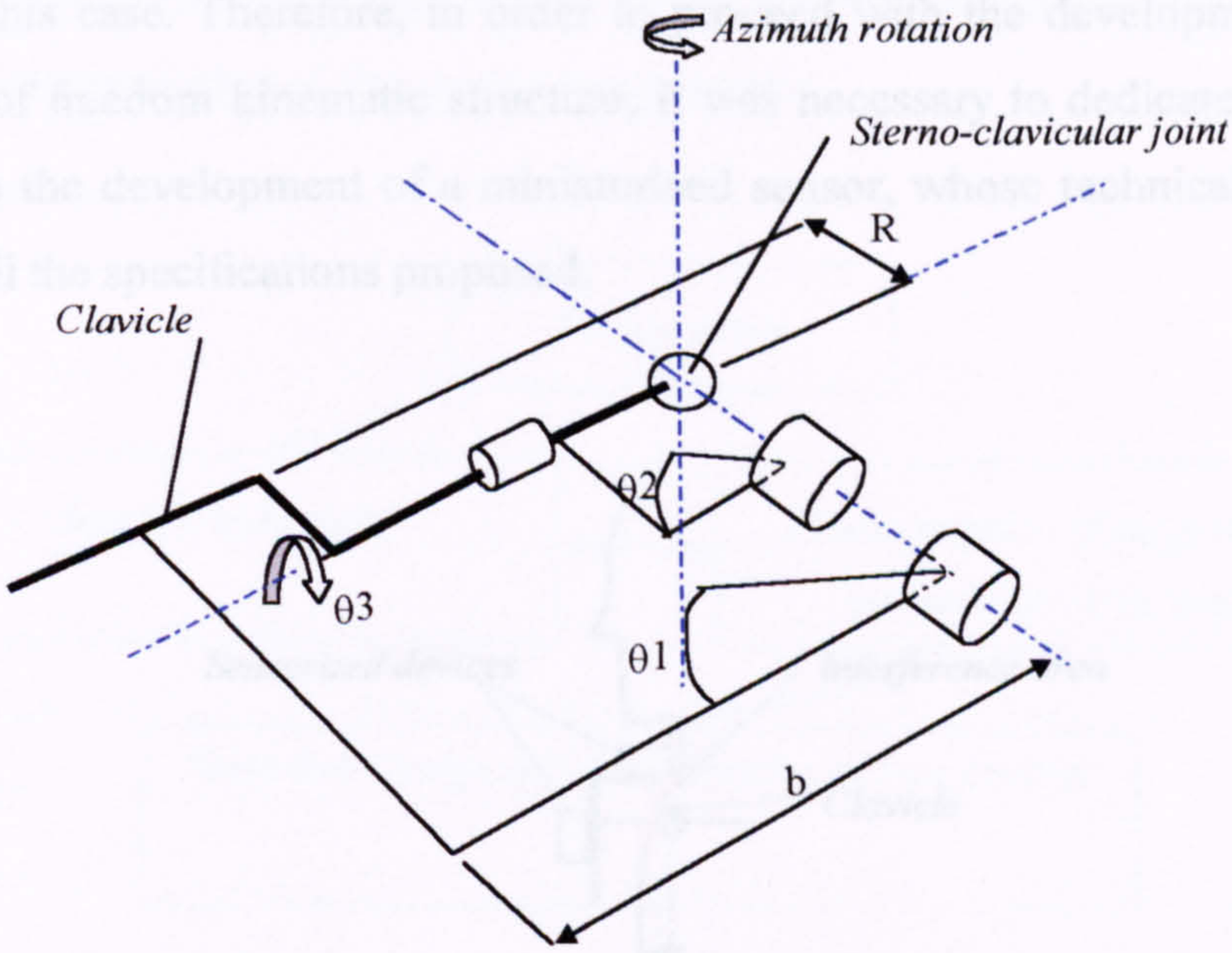

Fig. 5.0: *Model of the clavicle*

With reference to figure 5.0 it seems possible to find a sensor arrangement that can provide information on the clavicle motion. The most difficult problem to be addressed is the design of a miniaturised kinematic structure that can be interfaced in a way to allow the monitoring of the three degrees of freedom of the SC joint. In order to highlight the main requirements of the sensors and of the mechanical structure, a study on the definition of the interface characteristics of the device has been carried out. As shown in figure 5.1, the most difficult part is the proper positioning of the rotation axis of the device coincident with the azimuth anatomical axis. This problem is represented by the proper monitoring of the pro-retraction

movement (rotation along the azimuth axis), because of the physical presence of the body that prevents location of devices in the proximity of the joint.

In particular the device to be aligned to the anatomical axis (pro-retraction) should be designed in a way to have its axis very close to a side of the device in order to avoid interference with the subject's neck (see figure 5.1).

With reference to the literature research carried out in Chapter 4, it is clear that the sizes of state-of-the-art devices commonly used to measure joint rotation prevent their use in this case. Therefore, in order to proceed with the development of a multi-degree of freedom kinematic structure, it was necessary to dedicate a considerable effort to the development of a miniaturised sensor, whose technical characteristics can fulfil the specifications proposed.

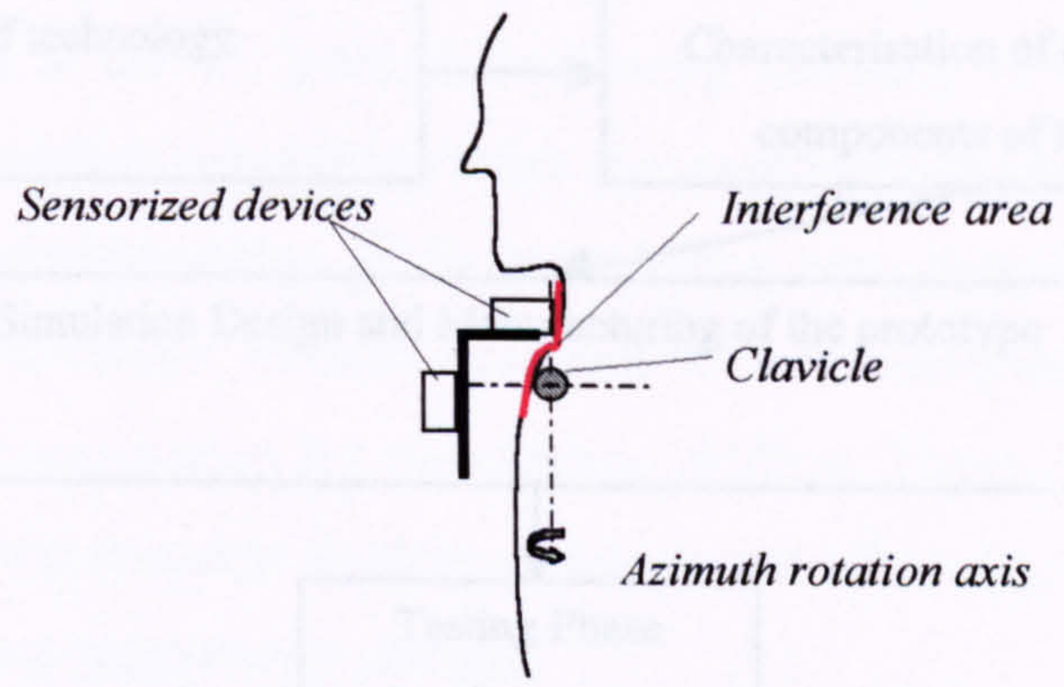

Fig. 5.1: *Allowed volumes surrounding the sterno-clavicular joint*

An intense phase of design has therefore been dedicated to the design and development of new miniaturised electro-goniometers whose development phases will be extensively treated in the next section.

5.2 Sensor Development

In the development of a new measurement system it is necessary to follow strictly design steps able to characterise the device to be developed. With reference to figure 5.2 the phases of development are described:

a) a design phase in which the technical specifications of the device are specified;

b) a choice of the technology able to satisfy the main requirements;

c) a characterisation of the sensor components;

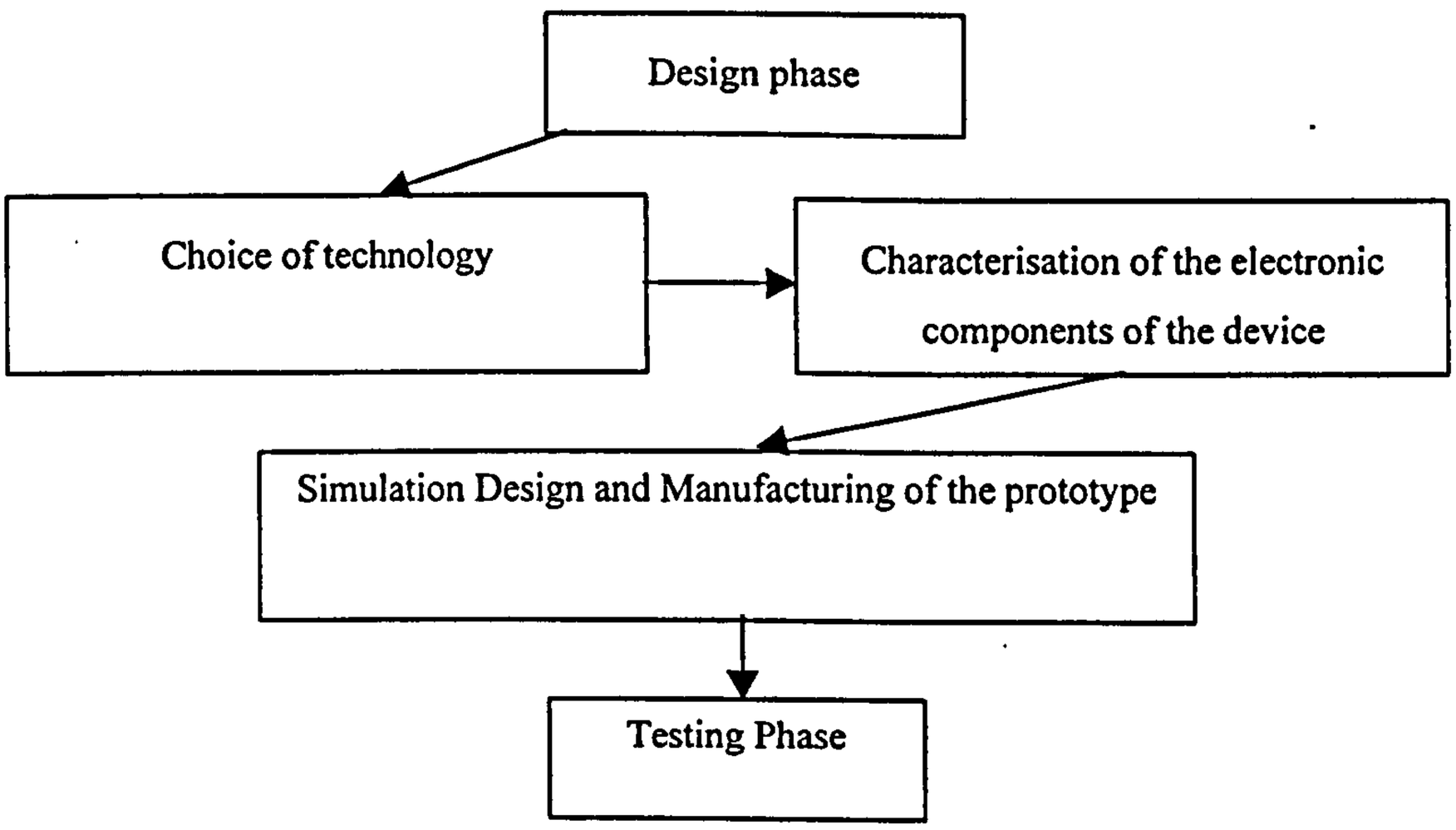

Fig. 5.2 *Development phases of the sensorized device*

d) a phase of simulation, design and manufacturing in which a first prototype has been manufactured;

e) a testing phase able to characterise the first prototype and to compare the results with the simulation curve previously obtained.

5.3 Design phase

The more restrictive constraint for a proper recording of the movements on subjects through any indirect method relates to the allowed volumes to locate passive or active devices. In the case of the clavicle, because of its anatomical position in the body and the small size of the bone, the interface of passive or active devices for the proper localisation and recording of the 3 degrees of freedom located at the SC joint is a difficult task. State of the art technology, as shown in chapter 4, is inadequate to solve the problem because the size of either sensor or passive devices does not allow an arrangement suitable for our purposes.

Therefore it was decided to consider the possibility to develop a new miniaturized sensor capable to record angular rotations and to arrange it in a kinematic chain that can record the 3 degrees of freedom at the SC joint. After having carefully reviewed the technologies available, the most attractive seemed to be that one exploiting the Hall effect because of its higher possibility of miniaturization. Such devices have been improved in the last ten years and are available as electronic devices equipped with an integrated amplification of the signal and intrinsic compensation for temperature drifting. These characteristics make the difference between potentiometric devices which do not allow a great miniaturization and are not protected against temperature drifting.

The Hall effect, discovered by E. H. Hall in 1879, consists of the generation of a difference in electric potential between the sides of a conductor or semiconductor through which a current is flowing while in a magnetic field perpendicular to the current.

Among the different devices available on the market, that one combining smaller size and pre-amplification features has been chosen and tested.

In broad terms, the sensors, sketched in figure 5.3a, are made by: an electronic device (a) capable to give a signal proportional to the magnetic field generated by a magnet (b) where the output varies with the displacement of the magnet and the gap between the magnet and the sensor. The output is a bell shape curve that can be exploited in its linear zone. The

displacement of the magnet can occur in two directions: "Head-on" when the movement is along the perpendicular axis to electronic device, and "Slide-by" when the movement is parallel to the device. The electronic device is sensitive to both movements varying its output voltage. The output of the device is a function of the displacement of the magnet on it.

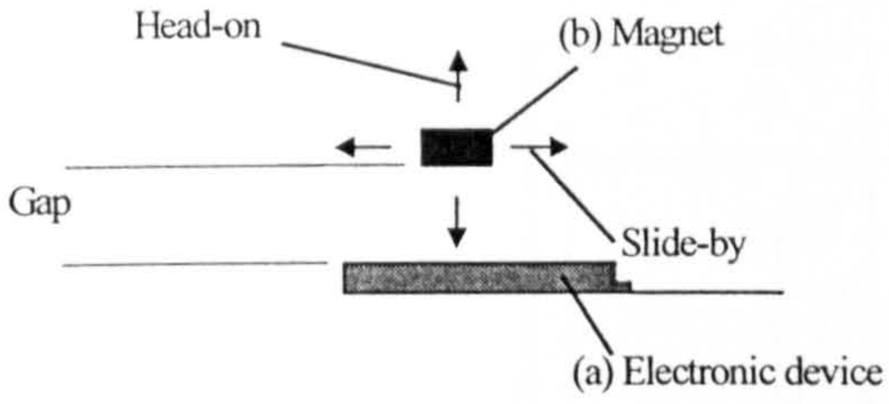

Figure 5.3a: *Hall Effect Device*

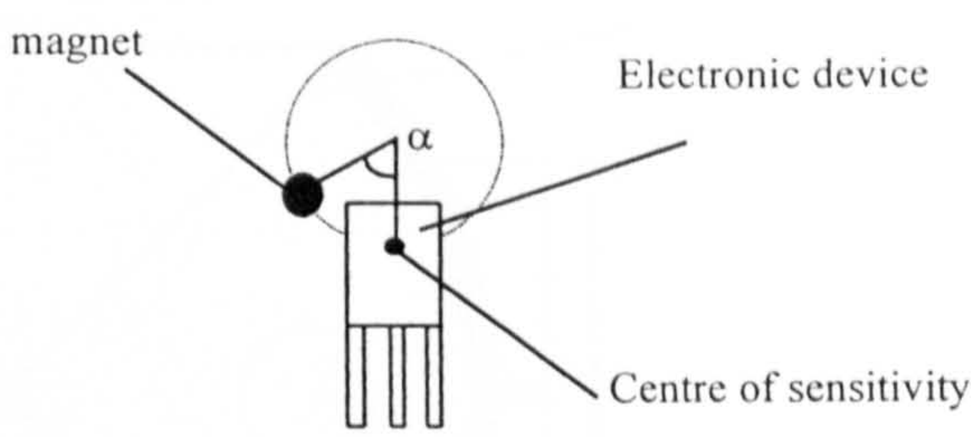

Figure 5.3b: *Working Principle*

The main idea is to exploit the sensor characteristics in order to design a rotating device by imposing the movement of the magnet on a circumference of fixed radius as sketched in figure 5.3b.

The magnet is constrained by a mechanical arrangement to rotate on a circumference of fixed radius with respect to the centre of sensitivity of the sensor.
The transducer input is the angular position of the magnet with respect to the centre of sensitivity of the sensor. It is therefore necessary to find the relationship between the input variable α and the output of the electronic device.
In order to characterise the behaviour of the device it is necessary to obtain the output of the sensor versus the angle α covered by the magnet for a fixed radius and for a fixed gap.
A purposely-conceived bench test has been set up in order to characterise the sensor behaviour. The first step was the design of a testing device whose mechanical drawing of the testing device is shown in figure 5.4.

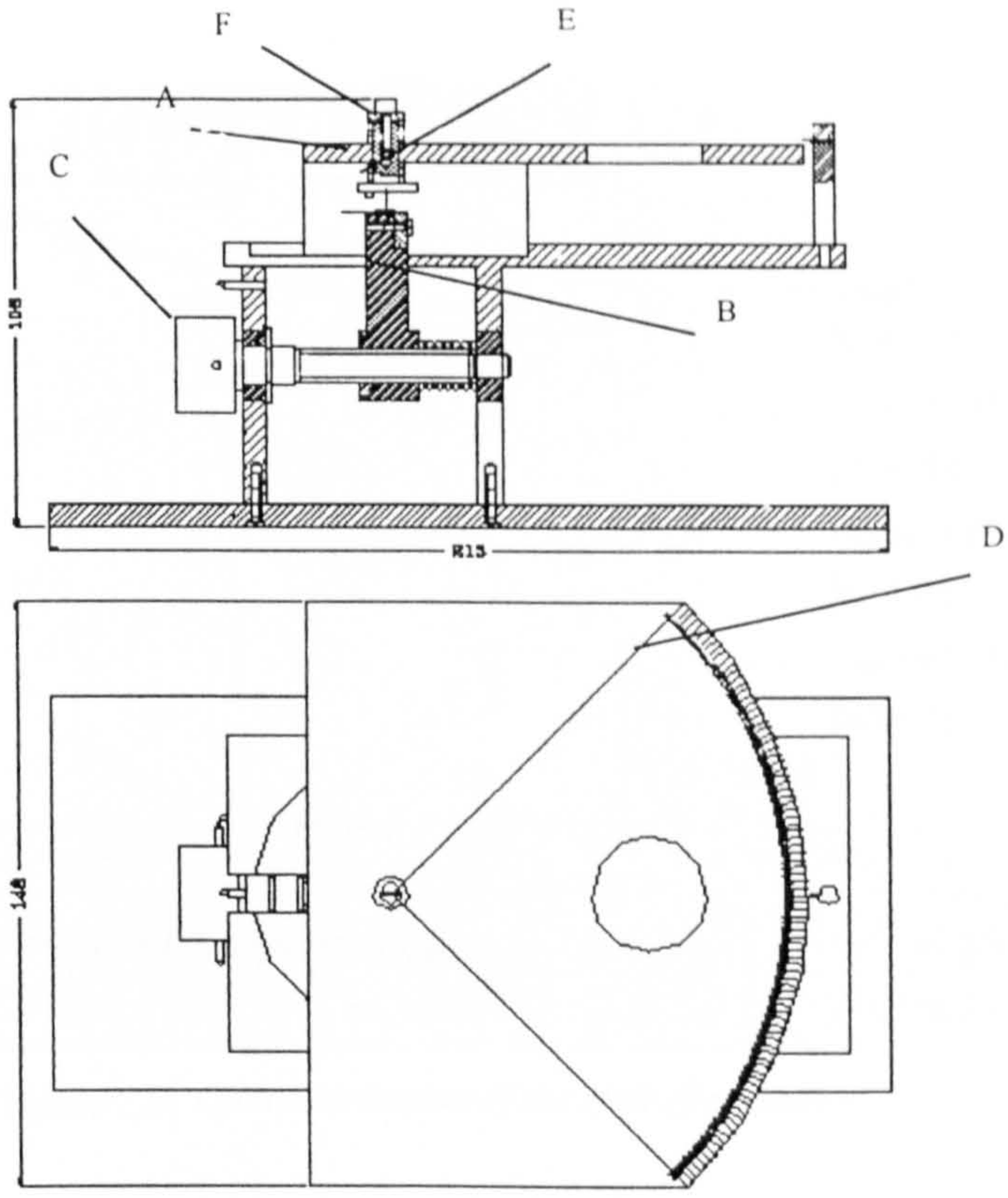

Figure 5.4: *Mechanical drawing of the testing device*

In this figure, a three-degree-of-freedom device possessing two adjustable linear axes and a rotating one has been designed and manufactured. The electronic device (sensitive element) is positioned on a linear axis that can be moved by the screw (C) in order to position the centre of sensitivity of the sensor on a fixed radius R with respect to the centre of rotation of the member (D). The magnet is glued on an aluminium plate (A) on the same radius R. The distance between the aluminium plate (A) and the Hall effect sensor (E) can be varied by introducing calibrated spacers (F).

The sensor behaviour has been characterised by rotating the magnet, which is rigidly linked to the member (D). Different trials at different radii with respect to the centre of sensitivity of the Hall effect sensor have been performed.

The results obtained are shown in figure 5.5, where the output is plotted versus the rotating angle α. Different sensors have been tested changing the gap between the magnet and the sensor.

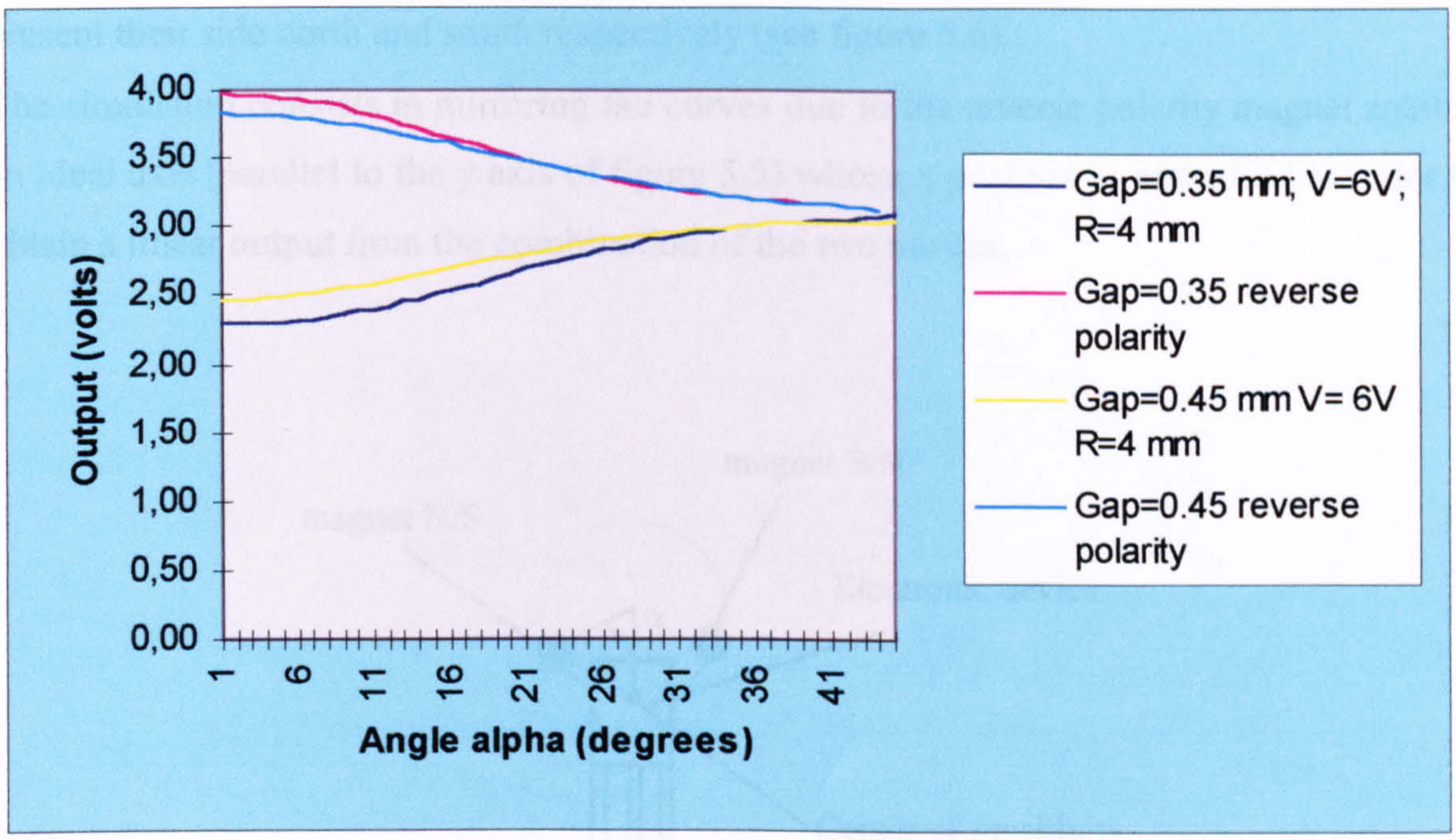

Figure 5.5: *Characterization of the Hall effect sensor*

As is shown in the above figure, the magnetic field generated loses its effect after approximately 40 degrees where the sensor output becomes a constant function of the supply voltage (6 Volts). The two bell shape curves show a linear range between 10 and 35 degrees. As it can be noted, the linear useful range of the sensor is 25 degrees. In order to obtain a rotating device able to cover the range of motion of most of the human joints it is necessary to expand coherently such a range.

The next section will deal with the design steps, which have lead to obtain a sensor capable to monitor a range of 180 degrees.

5.4 Sensor modelling

In order to obtain **an enlarged linear area** of the curve a simulation aimed at determining the angular distance between two magnets positioned at the same radius and arranged in a

way to provide a linear behaviour has been carried out. The magnets are located in a way to present their side north and south respectively (see figure 5.6).

The simulation consists in mirroring the curves due to the reverse polarity magnet against an ideal axis (parallel to the y axis of figure 5.5) whose x position is optimised in order to obtain a linear output from the combination of the two curves.

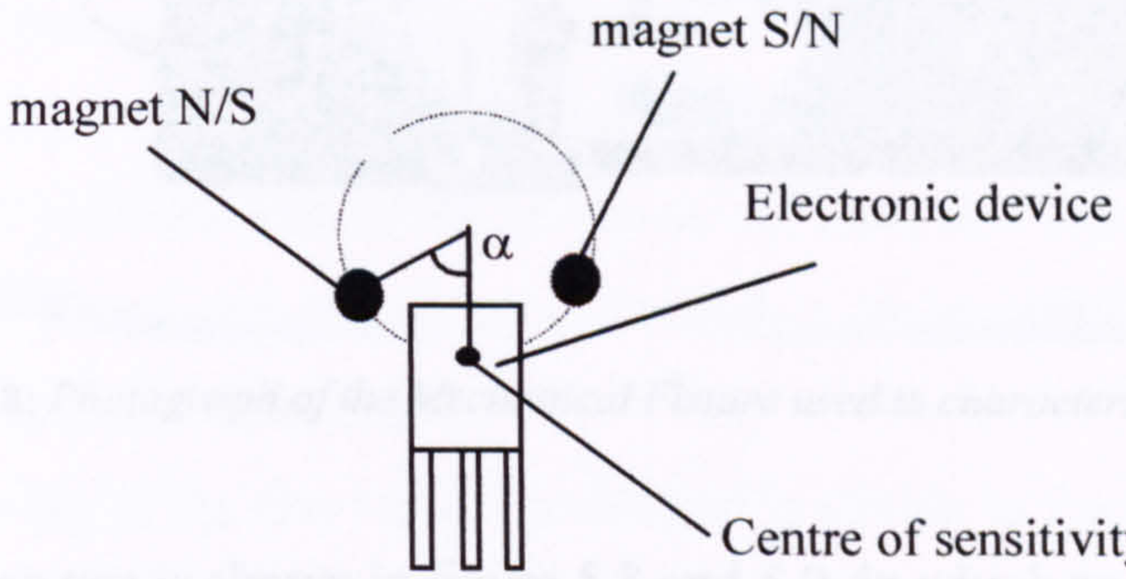

Figure 5.6: *Arrangement of two magnets placed on a radius R at an angular distance alpha*

A simulation of the sensor behaviour with an arrangement of two magnets placed at a radius of 4 mm at an angular distance of 81 degrees with a comparison with the real behaviour of the sensor are given in figure 5.7.

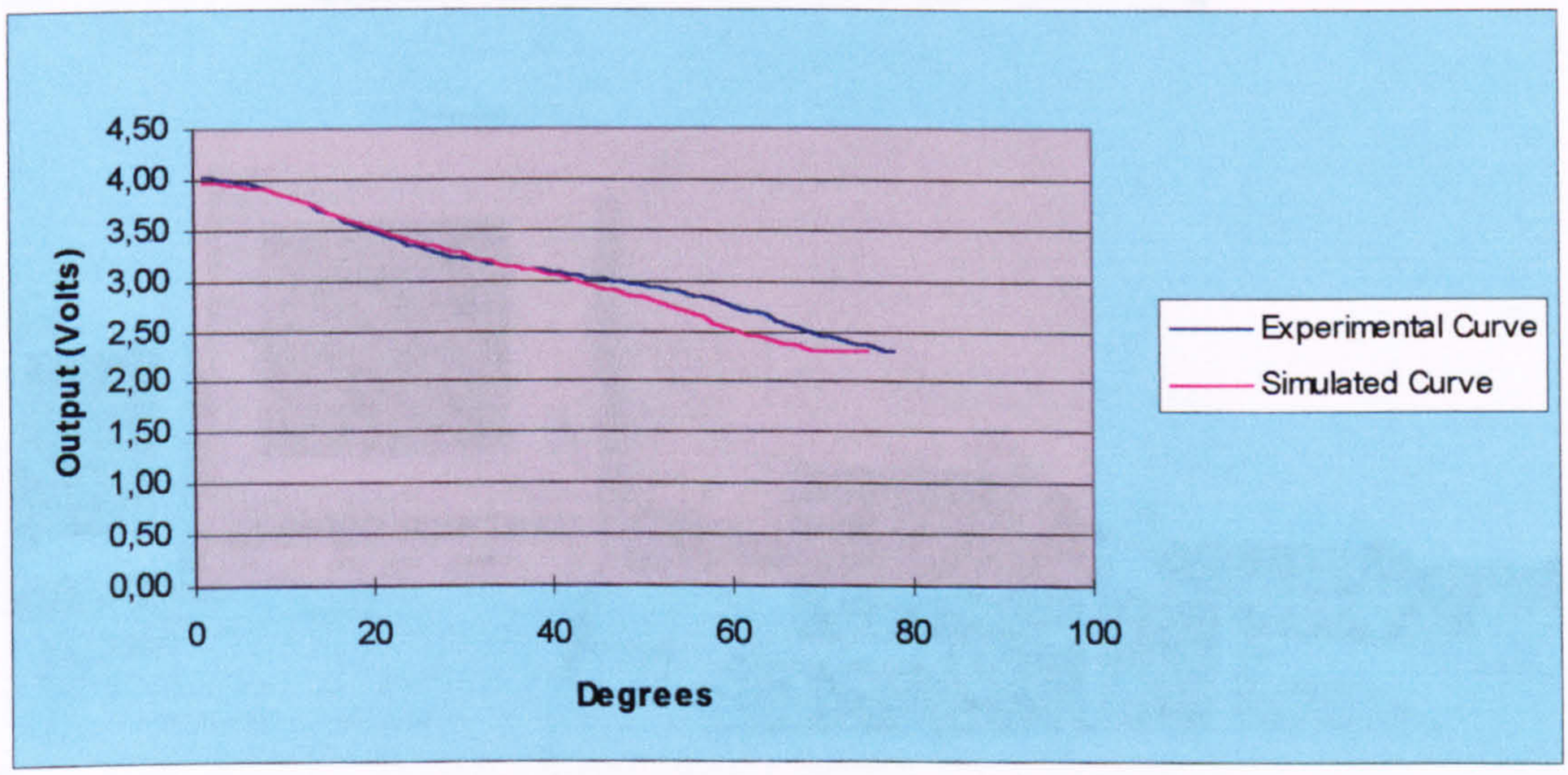

Figure 5.7: *Comparison between the experimental and simulated curve*

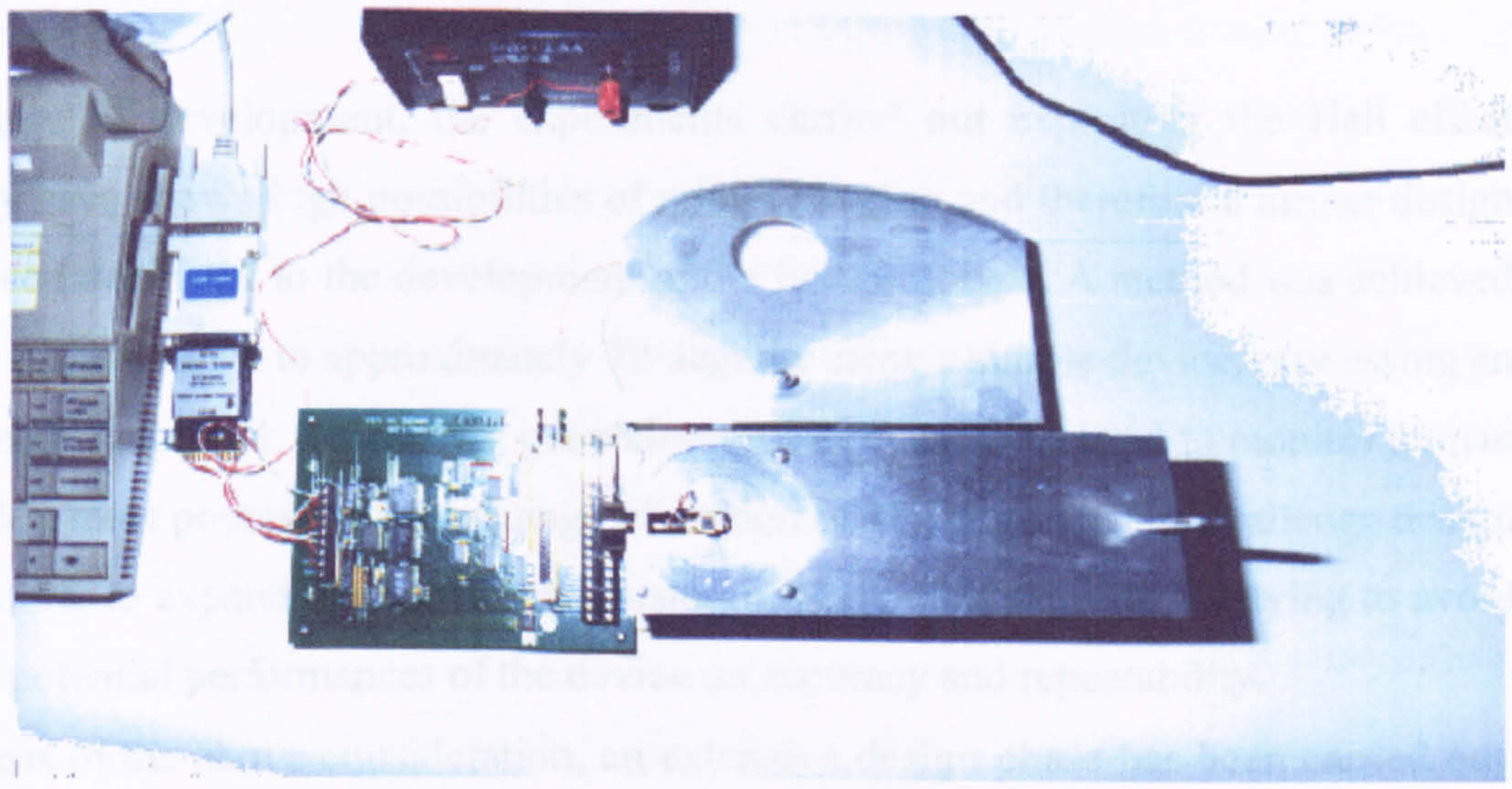

Figure 5.8: *Photograph of the Mechanical Fixture used to characterize the sensors*

The complete bench test is shown in figure 5.8 and 5.9, in which an electronics acquisition board has been interfaced to the sensors and to a portable PC. The calibration mechanical fixture containing the magnets can be manually rotated with respect to the Hall effect sensors and the signal acquired at each degree of rotation.

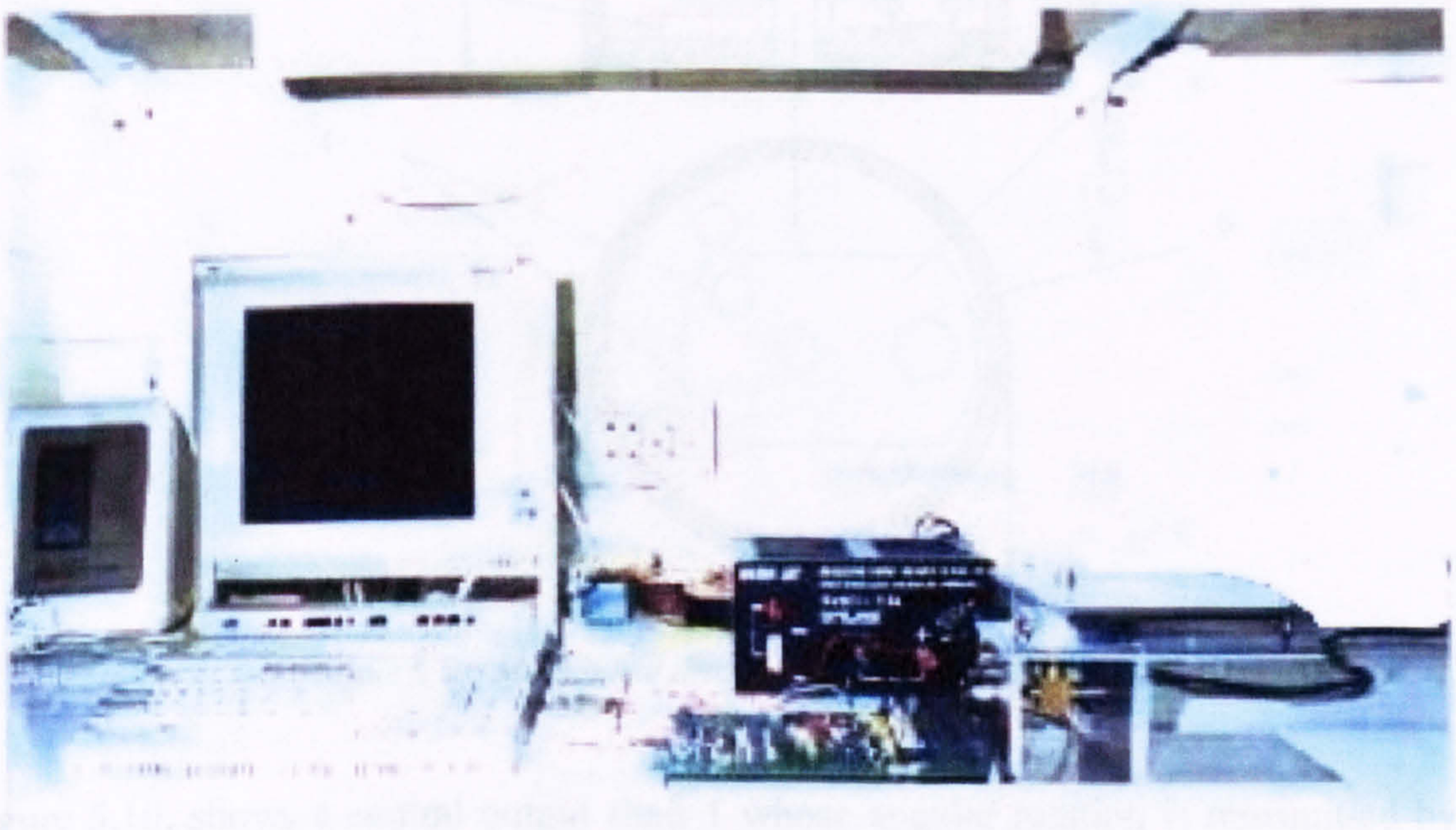

Figure 5.9: *Bench Test*

5.5 Mechanical Design of a rotating device

At this stage of development, the experiments carried out exploiting the Hall effect technology have shown high possibilities of miniaturisation and therefore a further design step has been dedicated to the development of the first prototype. A method was achieved to expand a linear range to approximately 70 degrees using a simple device, possessing an output already amplified. However, a general-purpose device to be used to monitor human joint rotation must possess at least a range of motion of 180 degrees. The challenge design was, therefore, to expand the above range using a mechanical ratio of 1/3 trying to avoid losing the potential performances of the device on accuracy and repeatability.

On the basis of the above consideration, an extensive design phase has been carried out, which has led to a first series of sensors.

The assembly drawing of the first sensor developed is shown in figure 5.10.

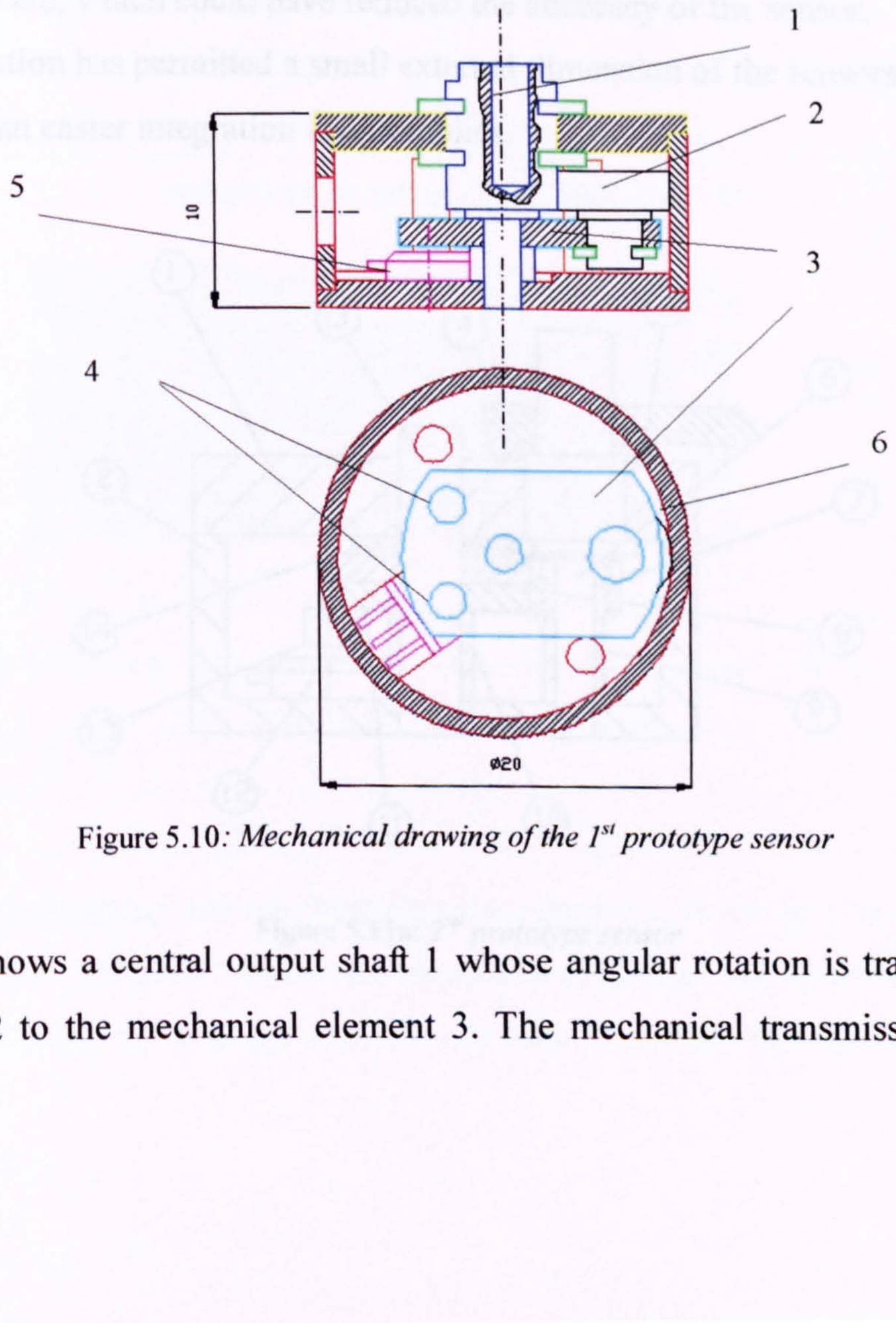

Figure 5.10: *Mechanical drawing of the 1st prototype sensor*

Figure 5.10, shows a central output shaft 1 whose angular rotation is transmitted by the satellite gear 2 to the mechanical element 3. The mechanical transmission is made by

friction between the elements 1, 2, and 3 of the chain. The two magnets 4 are embedded in 3 and can rotate around the output shaft axis. Their rotation provides a change in the output of sensor 5 proportional to the angular rotation.

With this mechanical configuration, because of the mechanical transmission performed through a satellite gear, the maximum reduction ratio within the minimum volumes has been obtained. On the other hand, since the mechanical transmission is performed through friction, a very high dimensional precision is required between the elements 1, 2, 3, 6 of the chain. After a short amount of tests it became evident that the mechanical transmission performed by friction did not guarantee a repeatable angular movement.

It was therefore decided to use a mechanical transmission based on miniaturised gears with a ratio of 1/3. With reference to figure 5.11a, the output shaft (6) has been moved to a side of the mechanical structure. Two pairs of gears have been used. On gear (8), two magnets (13) are glued presenting a reverse polarity to the sensor (12) assembled on the inferior plate (2). A miniaturised spring-based system has been chosen in order to avoid backlash between the gears, which could have reduced the accuracy of the sensor.

This configuration has permitted a small external dimension of the sensors (20x10x14 mm), which allows an easier integration in assemblies.

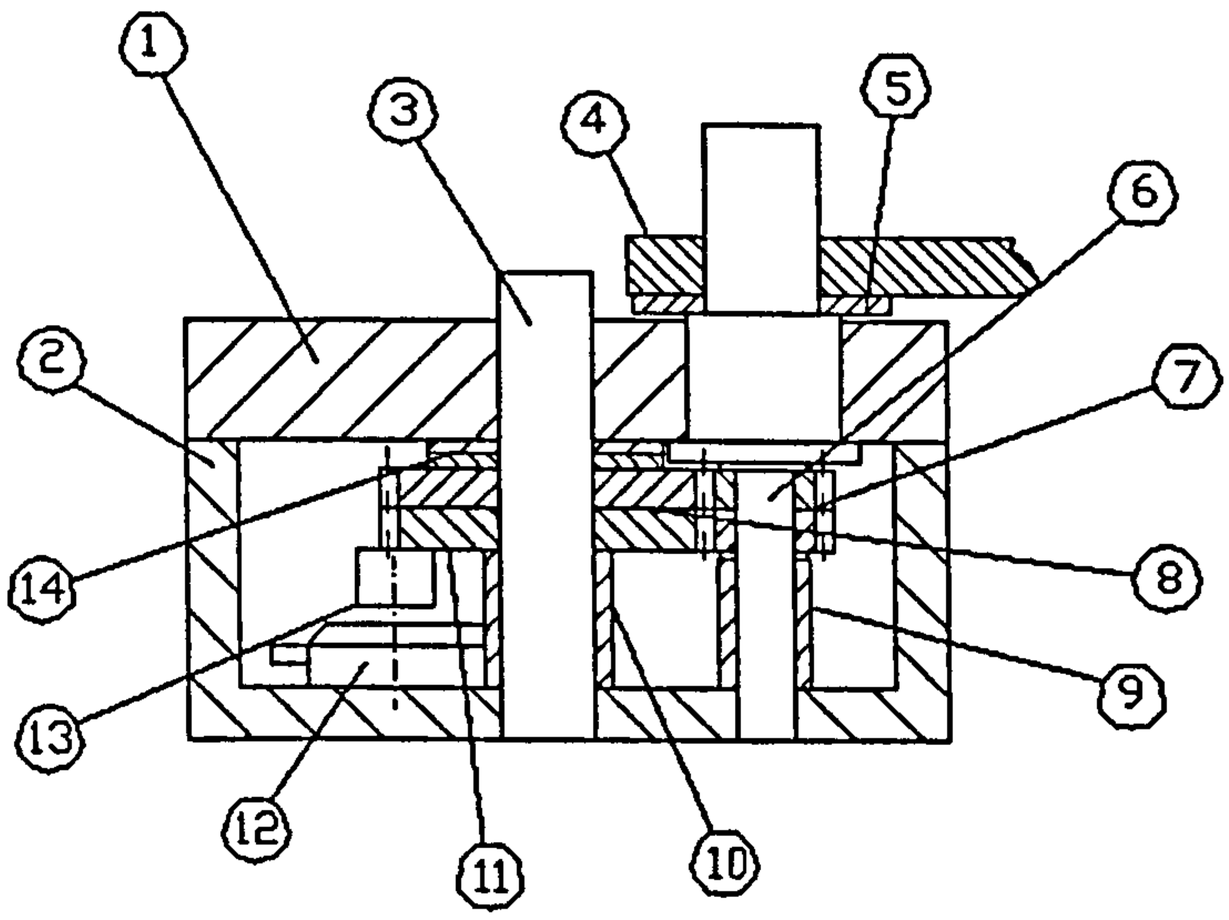

Figure 5.11a: *2nd prototype sensor*

An important mechanical feature is the position of the output shaft 6, which allows, as it is reported in the next section, to locate the main axes of the sterno-clavicular detector coincident with the anatomical axes of the sterno-clavicular joint.
A sensor prototype is shown in figure 5.11b where its miniaturized sized can be noted.

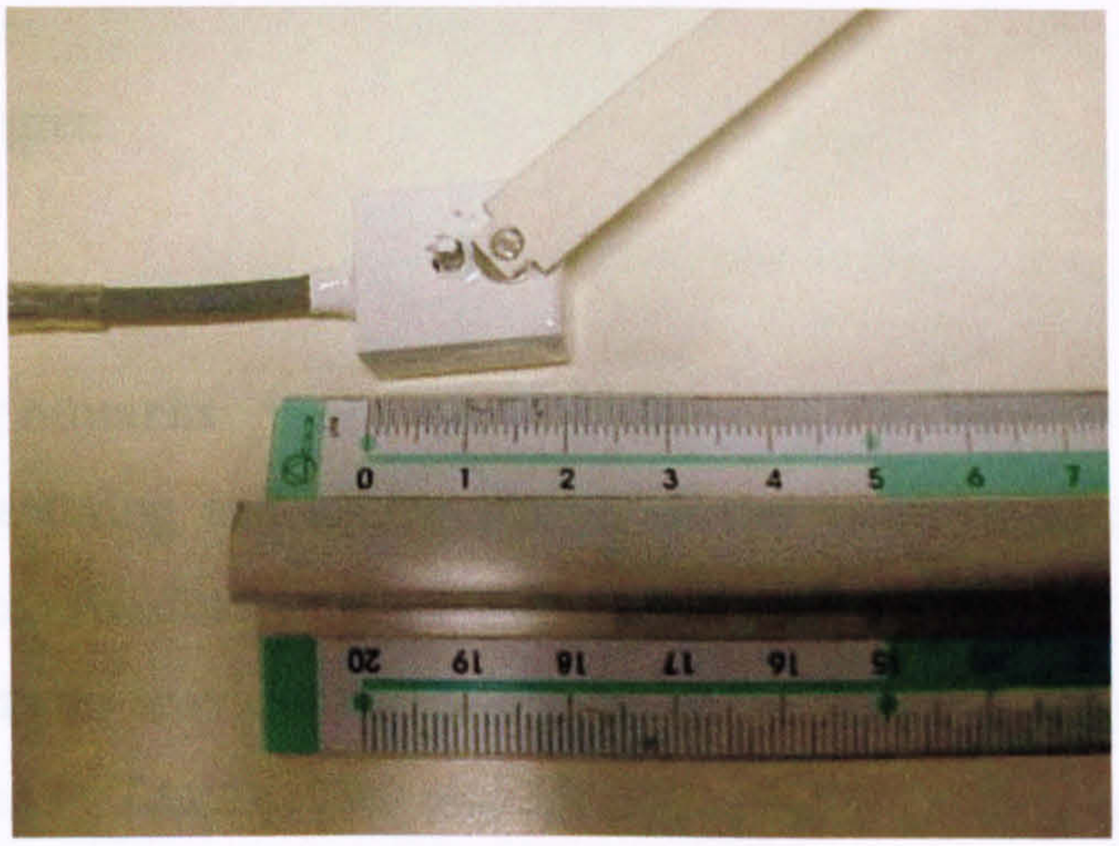

Figure 5.11b: *2nd prototype sensor*

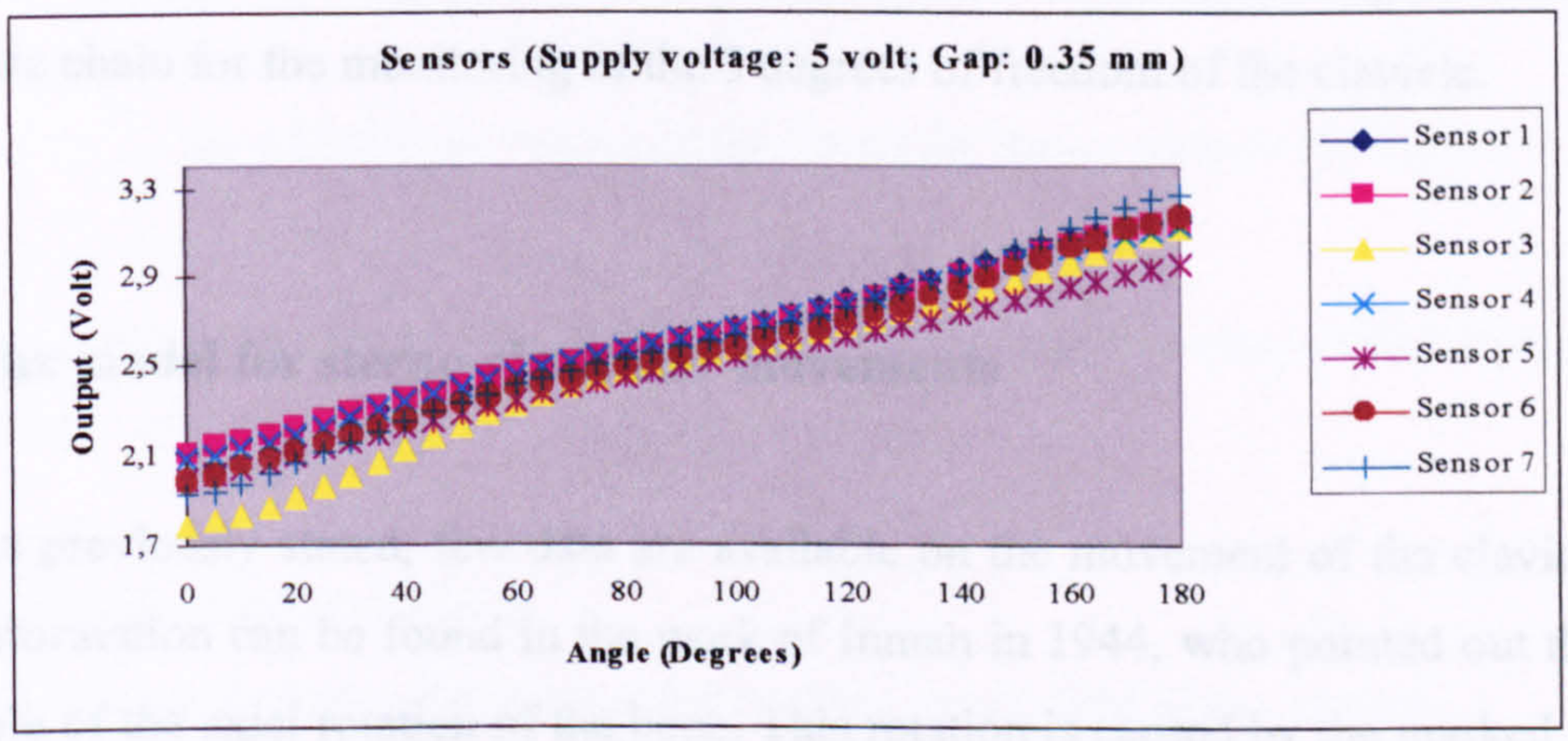

Figure 5.12: *Comparative curves*

In order to verify accuracy and repeatability of the device a simple test has been set up. Using a graduated scale, the output was measured clockwise and counter-clockwise each five degrees of rotation. Five repetitions were then executed. The results were analysed

through a standard statistical software package (Excel 97) and the results obtained are shown in figure 5.12.

From the tests carried out, the technical specifications of the sensor have been obtained:
accuracy within the range of motion: 1 degree;
precision 0.5 degree
resolution: 7 mV/degree

5.5.1 Concluding remarks

The design, manufacturing and testing phases of the sensor have been carried out. The small dimensions of the device allow the possibility to assemble them according to a kinematic chain that can provide information on the anatomical rotation of the clavicle. In fact, as demonstrated by Chao (1980) and Marchese et al (1997), a useful approach for the monitoring of difficult human joints like the shoulder or the knee is to link the anatomic chain to an external kinematic chain designed in a way to avoid hindrances to the natural range of motion of the subject. The next section deals with the modelling of such external kinematic chain for the monitoring of the 3 degrees of freedom of the clavicle.

5.6 The model for sterno-clavicular movements

As previously stated, few data are available on the movement of the clavicle. Some information can be found in the work of Inman in 1944, who pointed out the crucial role of the axial rotation of the bone. This rotation is caused by the marked curvature of the outer third of the clavicle and by the spatial position of the inner third of the bone. As discussed in the previous Chapter, the kinematic model proposed exploits the above geometric characteristics of the clavicle in order to extract information on its three rotations. The bone, as depicted in figure 5.13, has been sketched as a

crankshaft possessing 3 degrees of freedom located in the centre of the sterno-clavicular articulation.

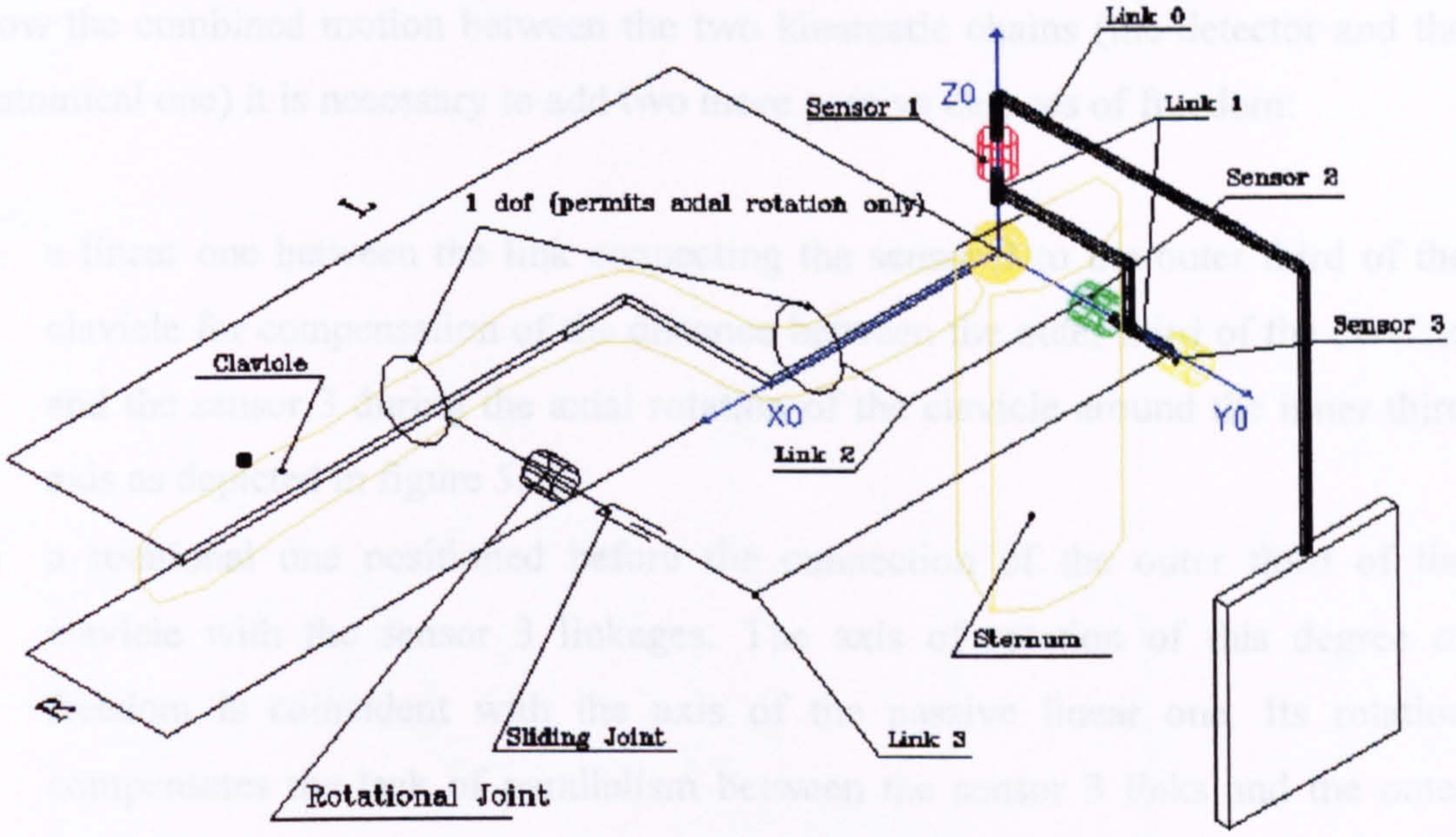

Fig. 5.13: *Kinematic model of the detector for sterno-clavicular movements*

With reference to the above figure, the geometric characteristics of the clavicle are:

L = *length of the clavicle*

R = *distance between the inner third and the outer third of the clavicle*

The proposed model consists of a three-degree-of-freedom frame whose centre of rotation is coincident with the centre of rotation of the clavicle. This frame is positioned close to the sternum in a way to avoid motion during the arm movement. The sensors are positioned on a structure according to a serial-parallel chain. Sensor 1 permits a pure rotation in the transverse plane, Sensors 2 and 3 permit a pure rotation

in the coronal plane and are connected to the inner and outer third of the clavicle respectively in the local coordinate frame. The connections to the bone that, in reality are not physically possible because of the presence of skin and muscles, have been approximated with single rotational degrees of freedom which permit the rotation of the clavicle around the inner third and the outer third axes respectively. In order to allow the combined motion between the two kinematic chains (the detector and the anatomical one) it is necessary to add two more passive degrees of freedom:

- a linear one between the link connecting the sensor 3 to the outer third of the clavicle for compensation of the distance between the outer third of the clavicle and the sensor 3 during the axial rotation of the clavicle around the inner third axis as depicted in figure 5.13;
- a rotational one positioned before the connection of the outer third of the clavicle with the sensor 3 linkages. The axis of rotation of this degree of freedom is coincident with the axis of the passive linear one. Its rotation compensates the lack of parallelism between the sensor 3 links and the outer third of the clavicle because of the axial rotation of the clavicle during motion.

The theoretical solution, which expresses the rotations of the clavicle as functions of the rotations of the detector, has been therefore found.

With reference to figures 5.13 and 5.14 we have:

α_r = *clavicle axial rotation*

α_a = *clavicle abduction-adduction in the coronal plane*

α_t = *clavicle rotation in the transverse plane*

$\vartheta_1, \vartheta_2, \vartheta_3$ = *rotations of sensor 1, sensor 2 and sensor 3 respectively*

L = *clavicle length*

R = Clavicle radius (distance between the inner third and the outer third

and by applying trigonometric rules of spherical geometry, we have

$$\alpha_r = arcsin\left(\frac{L}{R}\cdot\frac{sin\vartheta_3 - sin\vartheta_2}{\cos\vartheta_2}\right)$$

$$\alpha_a = \vartheta_2$$

$$\alpha_t = \vartheta_1$$

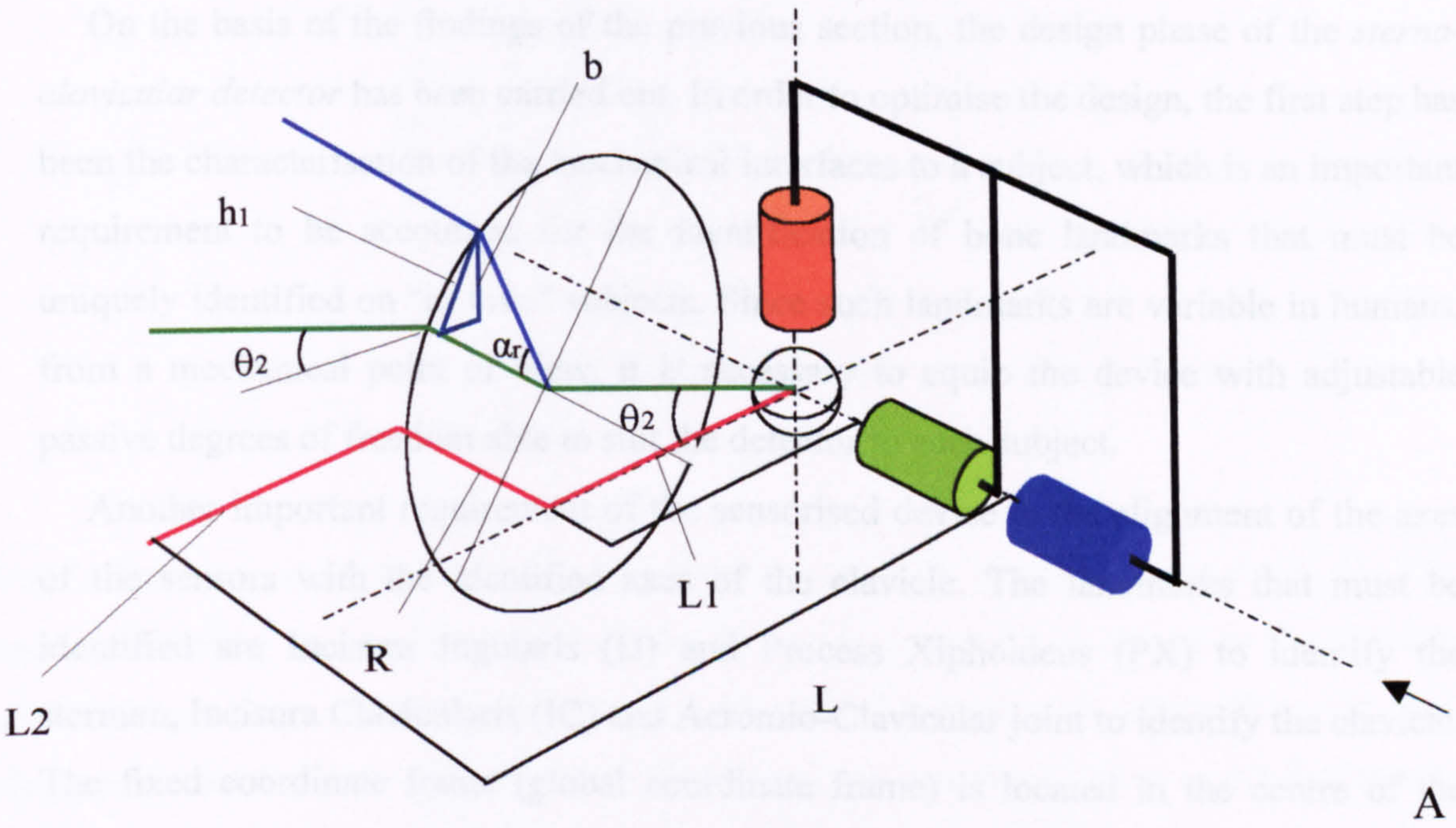

View from A

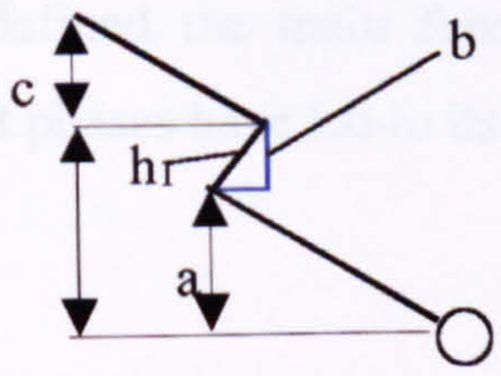

$L = L_1 + L_2$

$a = L_1 \sin\theta_2$

$b = h_1\sin(90-\theta_2) = h_1\cos\theta_2 = R\sin\alpha_r\cos\theta_2$

$c = L_2\sin\theta_2$

$L\sin\theta_3 = L_1\sin\theta_2 + R\sin\alpha_r\cos\theta_2 + L_2\sin\theta_2$

$R\sin\alpha_r\cos\theta_2 = L\sin\theta_3 - (L_1 + L_2)\sin\theta_2$

$R\sin\alpha_r\cos\theta_2 = L\sin\theta_3 - L\sin\theta_2$

Fig. 5.14 *Algorithm demonstration*

The above demonstrates that the axial rotation of the clavicle can be expressed as a function of θ_2 and θ_3. As it is shown in the above formula the geometric parameters affect the reading through the amplification factor L/R that represents length and radius of the clavicle. It is therefore necessary to find a method to measure accurately these parameters.

5.7 Design of the detector of sterno-clavicular movements

On the basis of the findings of the previous section, the design phase of the *sterno-clavicular detector* has been carried out. In order to optimise the design, the first step has been the characterisation of the mechanical interfaces to a subject, which is an important requirement to be accounted for the identification of bone landmarks that must be uniquely identified on "in vivo" subjects. Since such landmarks are variable in humans, from a mechanical point of view, it is necessary to equip the device with adjustable passive degrees of freedom able to suit the detector to each subject.

Another important requirement of the sensorised device is the alignment of the axes of the sensors with the identified axes of the clavicle. The landmarks that must be identified are Incisura Jugularis (IJ) and Process Xiphoideus (PX) to identify the sternum, Incisura Clavicularis (IC) and Acromio-Clavicular joint to identify the clavicle. The fixed coordinate frame (global coordinate frame) is located in the centre of the Incisura Clavicularis, which is modelled as a pure spherical joint.

Having defined the main functional requirements of the device, the design and development phases have led to its mechanical assembly shown in figure 5.15.

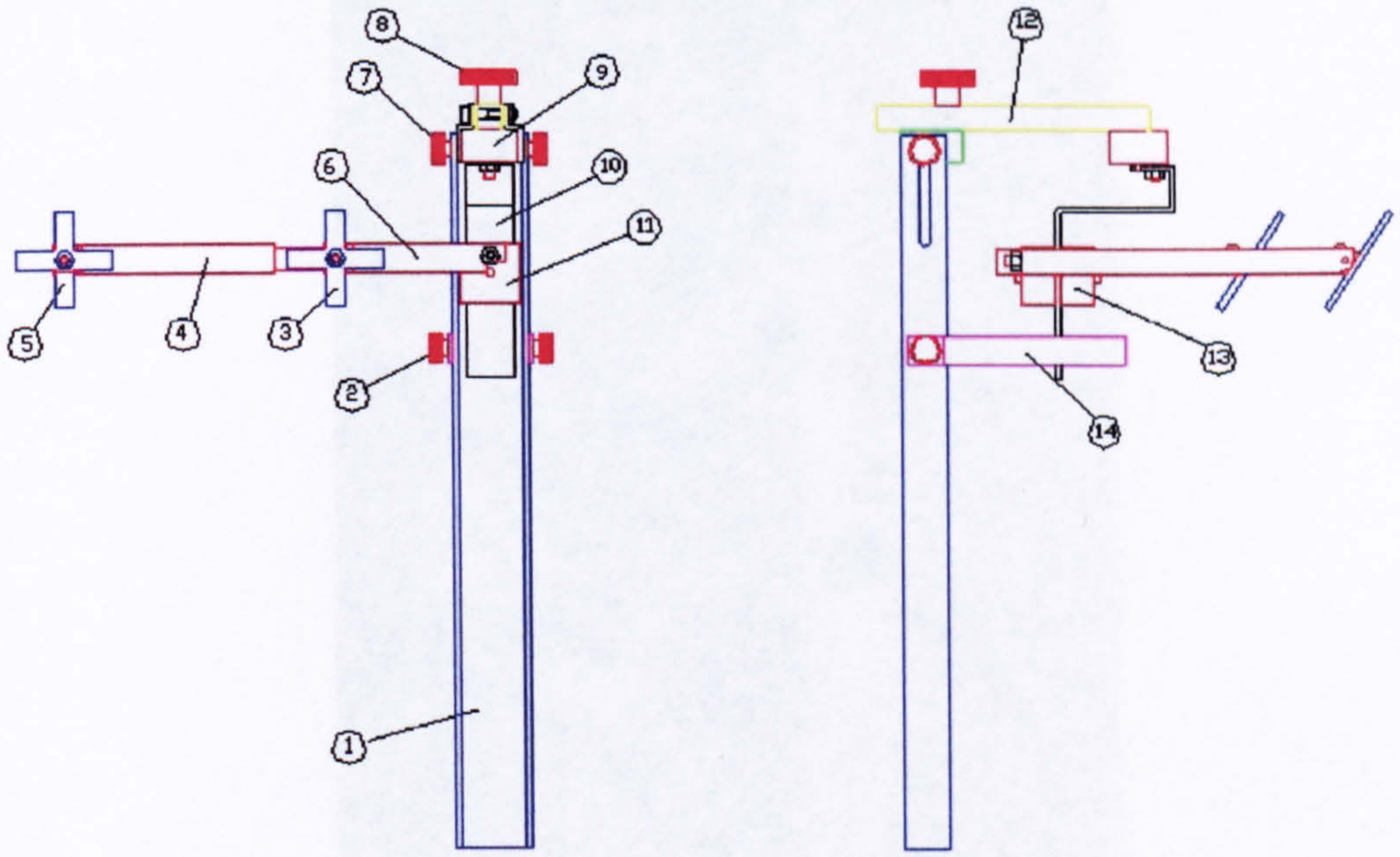

Figure 5.15 *Assembly drawing of the sterno-clavicular movement detector*

With reference to such figure, the structure possesses three sensors (particular 9, 11, 13) located according to a serial parallel chain. Sensor 9 is capable of recording the angular rotation around the azimuth, while sensor 11 and 13 outputs are attached to the two adjustable links 4 and 6 of the structure. Such links are positioned close to the landmarks identified according to the procedures described in the next chapter (section 6.4). The structure must be positioned on the subject in a way that the intersection point of the axes of the sensors is coincident with the anatomical SC axes. The photograph of the device is shown in figure 5.16.

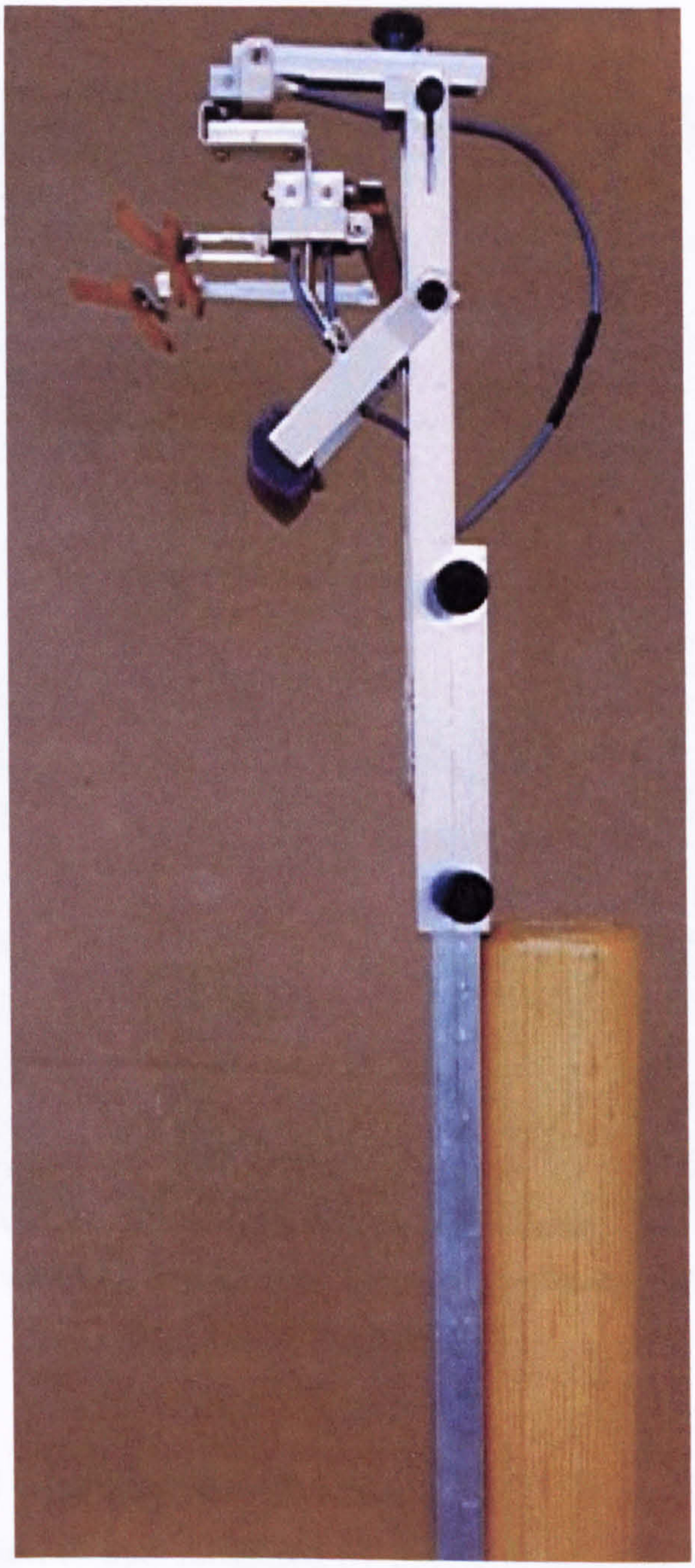

Figure 5.16 *Photograph of the sterno-clavicular detector*

As it is shown in figure 5.17 the apparatus is equipped with the 3 sensors, 4 passive linear adjustments and 1 passive rotational adjustment. In order to adjust the device to different subjects, two additional passive degrees of freedom have been added.

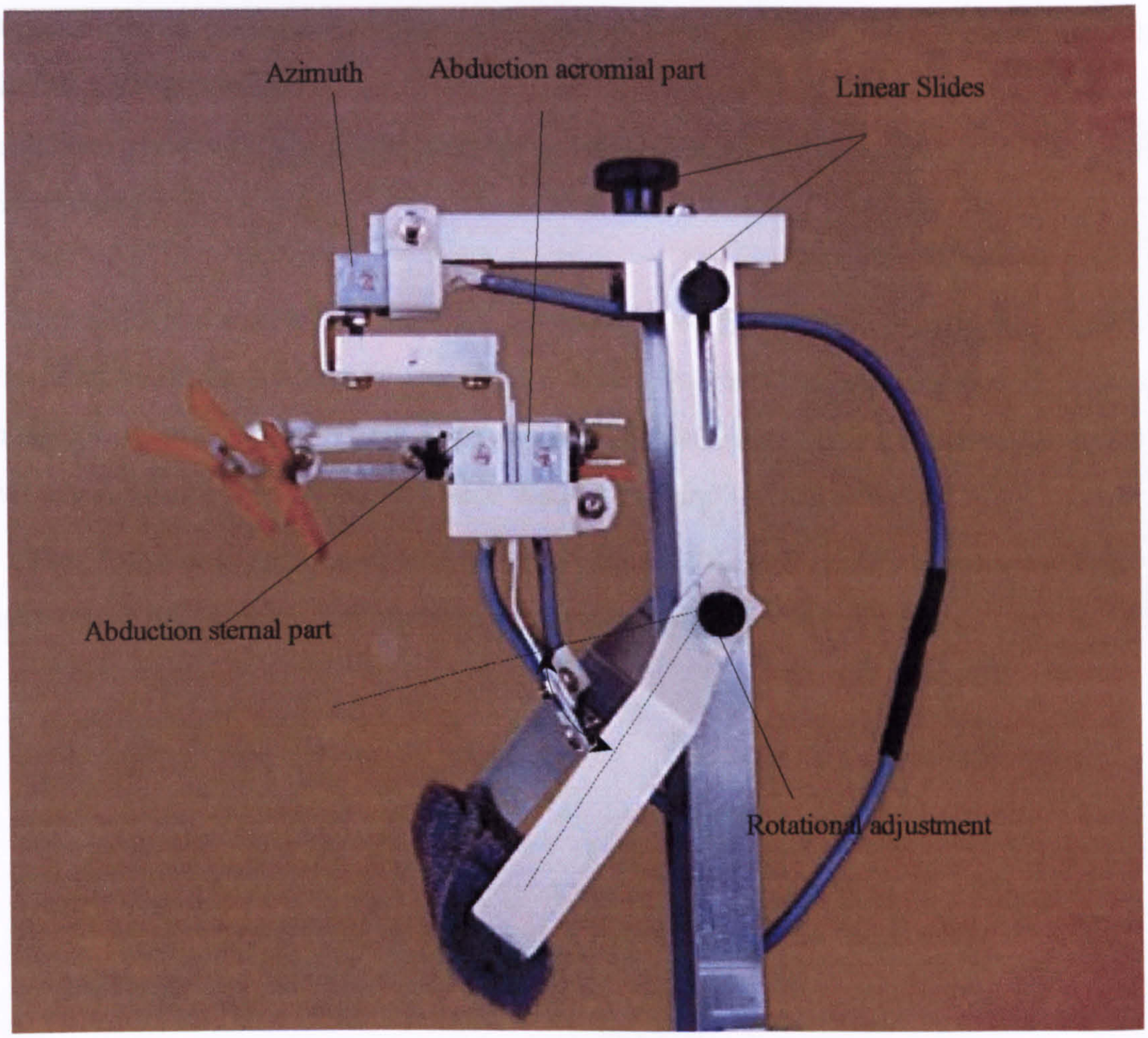

Figure 5.17: *Photograph of the sterno-clavicular detector*

5.8 Global and Local Coordinate Systems

The cross evaluation of data measured by different apparatuses is often hampered because of different descriptions of the three dimensional motion involved. With reference to recent work of van der Helm (1999), who proposes a standardised protocol to the International Standard of Biomechanics (ISB) for motion recording of the shoulder, the following suggestions are given in order to allow a proper comparison of data:

- definition of a global and local coordinate system with respect to bony landmarks;

- description of the reference frame and order of rotation;
- to consider the global coordinate and local coordinate systems of the bone aligned in the initial resting position;
- rotations should be given with respect to well recognisable axes which are more easily interpreted.

The sterno-clavicular detector provides information with reference to a global coordinate frame fixed at incisura jugularis (see figure 4.11). The local coordinate system is aligned with the global coordinate system in the anatomical position. The rotations as given by the device are Azimuth with respect to the Y axis and z_S and x_S respectively.

The following section is dedicated to the validation studies carried out for the assessment of precision, accuracy and repeatability of the new system.

6 Validation Studies

The clinical use of any new measurement system must be validated through a set of experiments to determine accuracy, precision, repeatability and reproducibility. To this purpose, technical and clinical trials have been performed in order to identify and quantify all the sources of errors affecting the reading.

Particular attention has been paid to establish inter-and intra-operator errors and by applying standard statistical techniques for the proper analysis of the results and the consequent determination of a mean value and a confidence interval of the variable under examination.

Before starting with the procedures used to analyse the results obtained, it is preferable to provide the reader with definitions that lead to a validation of a measuring system such terms very often being improperly used. With reference to a publication of Pallas-Areny and Webster (1991) the following definitions are given:

Accuracy is the quality that characterises the capacity of a measuring instrument for giving results close to the true value of the measured quantity. The "true", "exact" or "ideal" value is obtained when measurements are made using an ideal method. A measurement method is considered to be ideal when experts agree that its results are sufficiently accurate for the intended application of the measurement data.

Any difference between the true value for the measured quantity and the instrument reading is called an error.

Precision is the quality that characterises the capability of a measuring system of giving the same reading when repeated measurements are performed. Precision is a condition necessary but not sufficient for accuracy. In figure 6.1 is shown a measurement situation where in case a) there is a higher accuracy and a low precision because the repeated results obtained (represented by the white stars) are more close to the exact value. In case b) although there is a higher precision because of a smaller variance of the read value, the accuracy is very poor because the difference between the read value and the exact value is always higher than the case represented in a).

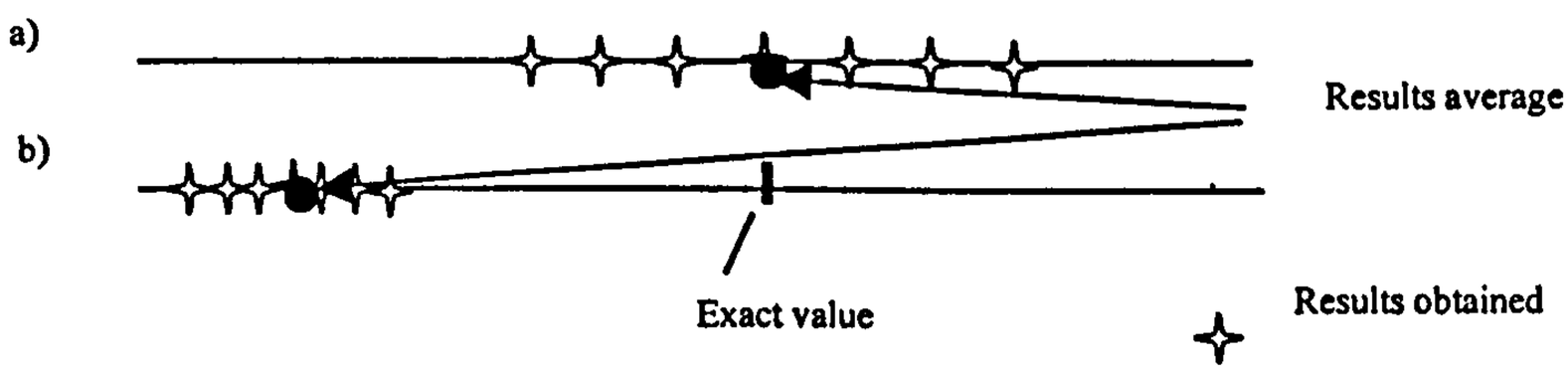

Figure 6.1: *Measurement situations*

The *repeatability* is the closeness of agreement between successive results obtained with the same method under the same conditions and in short time interval. Quantitatively the repeatability is the minimum value that exceeds, with a specified probability, the absolute value of the difference between two successive readings obtained under the specific conditions. If it is not stated, it is assumed that the probability is 95 %.

The *reproducibility* is also related to the degree of coincidence between successive readings when the same quantity is measured with a given method but with a long term set of measurements or with measurement carried out by different people or in different laboratories. Quantitatively the reproducibility is the minimum value that exceeds, with a specified probability, the absolute value of the difference between two successive readings obtained under the above-mentioned conditions. If it is not stated, it is assumed that the probability is 95 %.

In broad terms accuracy is usually determined by means of calibration processes against measurement standards which are known quantities. Their values are generally at least ten times more accurate than that of the sensor or system under examination.

In our case, although such a method has been applied for determining the accuracy and precision of the sensors, it is not possible to assess the accuracy of the sterno-clavicular movement detector against standard or measurable values to be compared in the clinical setting because of a complete lack of data on the examined subject. This means that we are forced to accept all the drawbacks of the indirect measurement performed.
In order to cope with this fact, it is necessary to apply appropriate statistical techniques taking into account all the sources of errors that are unavoidably generated during the execution of the tests. In practical terms it is necessary to find out a procedure through which we can estimate an unknown variable trying to obtain an estimate of the variable, which in turn will provide us with information on the precision of the method, but not on its accuracy.

6.1 Applicability of a statistical model

Whatever statistical model is used for the validation of a measurement system, it must take into account all the sources of errors that can be generated during the tests. For this reason it is worth mentioning all the key factors affecting the system under study:

- errors due to the algorithm and to the resolution of the measurement system;
- misalignment errors due to a misalignment between the anatomical axis and the axis of the device; such error can be caused either by a wrong assembly of the device or by a different estimate of the examiner (inter-and intra-operator errors);

- estimation of the clavicle parameters L and R which lead to a variation of the read angles;
- movement of the device during motion, which causes a displacement of the axes of the device vs. the anatomical ones (this error can be considered a misalignment error).

In order to validate the measurement system, all the above-mentioned errors are to be quantified in a consistent subset of the allowable workspace of the clavicle. Repeated measurements are therefore necessary to establish a mean and a variance of the measurement plotted against different humeral positions. Each test will therefore provide a point estimate of the investigated variable which will be linked to the real mean value with a confidence interval.

A key role in the minimisation of the errors generated during the test is played by the standardisation of the test procedure that must be performed in the full respect of a specific testing protocol. Therefore, the tests presented in the following have been designed to quantify the errors and to provide the final users of the apparatus with a standard procedure that can allow accurate and repeatable results.

6.2 Validation of the algorithm

The verification of the algorithm which is, in turn, a verification of the validity of the electro-mechanical device built has been pursued according to the following technique: a wooden mock-up of the clavicle has been linked with the sterno-clavicular detector as shown in figure 6.2 and a further sensor, with an accuracy of 0.5 degrees has been located coincident with the axial rotation axis of the mock-up in order to perform a cross evaluation. The comparison of motion is performed in the allowed workspace, with the sensor rigidly linked to the abduction – adduction axis of the device as sketched in figure 6.2 a and b.

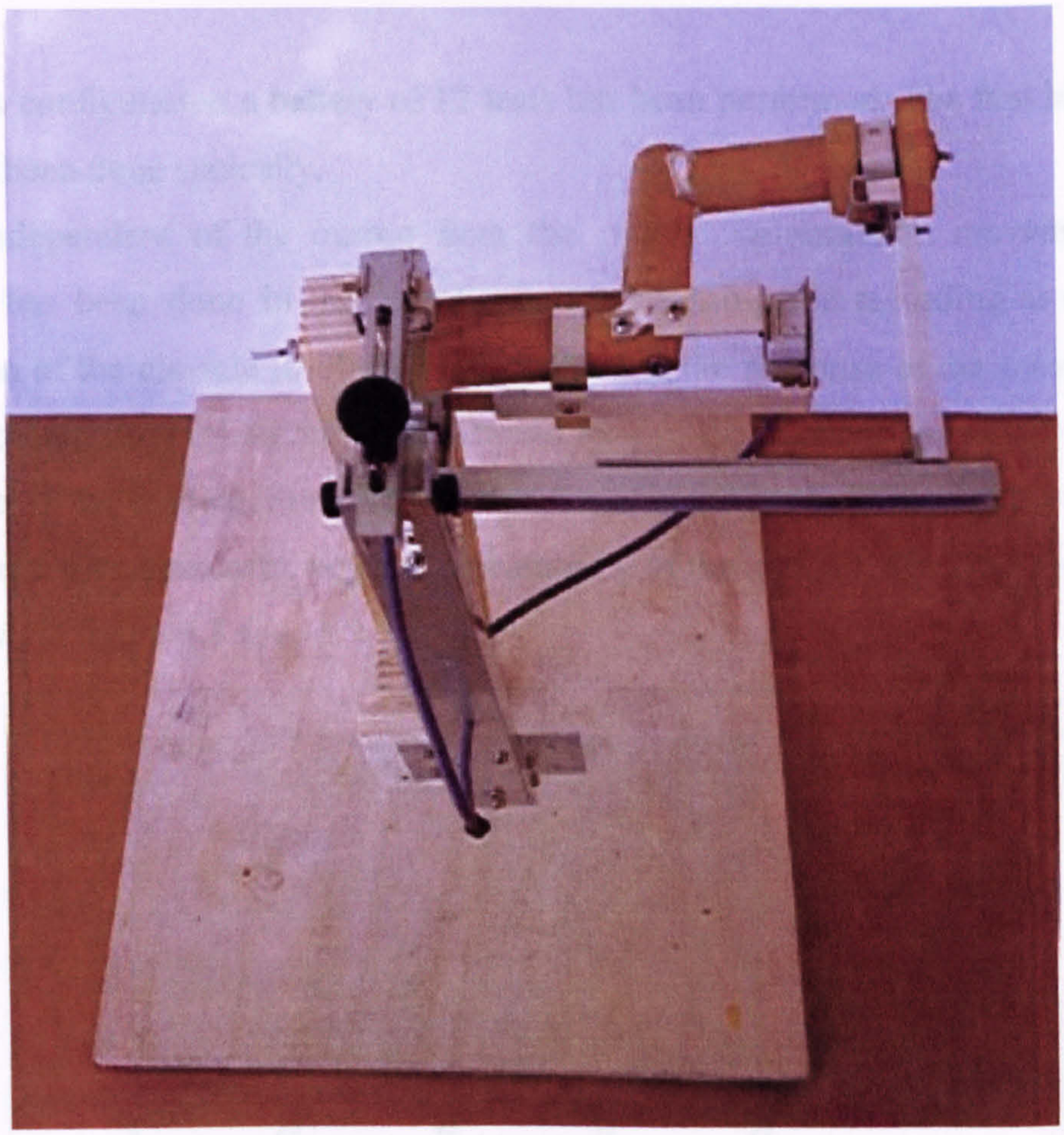

Figure 6.2 a: *Wooden mock-up*

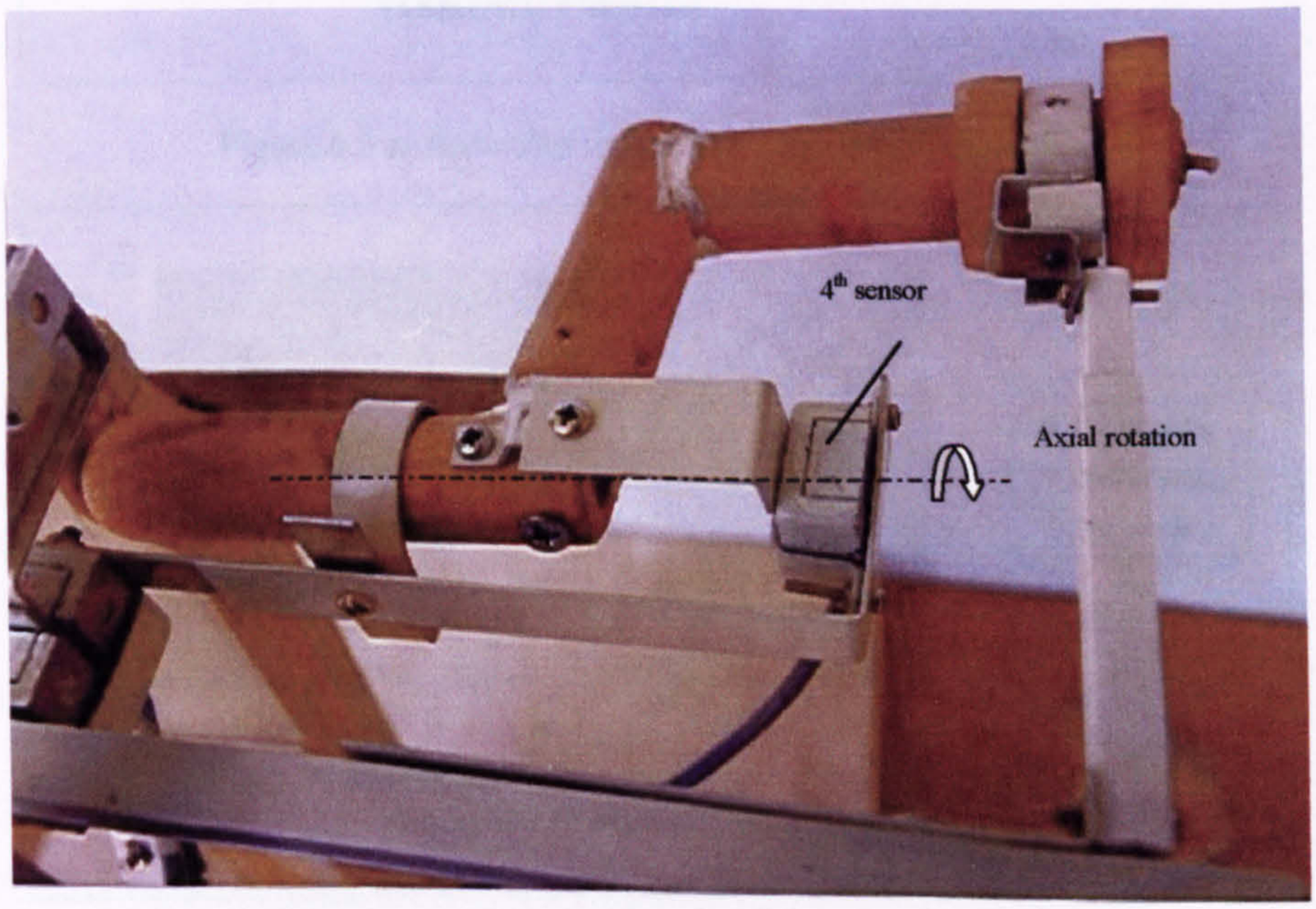

Figure 6.2 b: *Wooden mock-up*

With this configuration a battery of 12 tests has been performed. The first battery of tests has been done statically.

Being independent of the output from the protraction-retraction movement, the analysis has been done in the frontal plane performing the recording at different abduction of the clavicle (0-30-60) and evaluating the response of the sensors. The sensor located directly on the axial rotation axis of the clavicle has been used as a reference for the reading. For each position 3 readings have been recorded in order to characterise precision, accuracy and repeatability of the method. The results obtained are shown in figure 6.3 a, b, c.

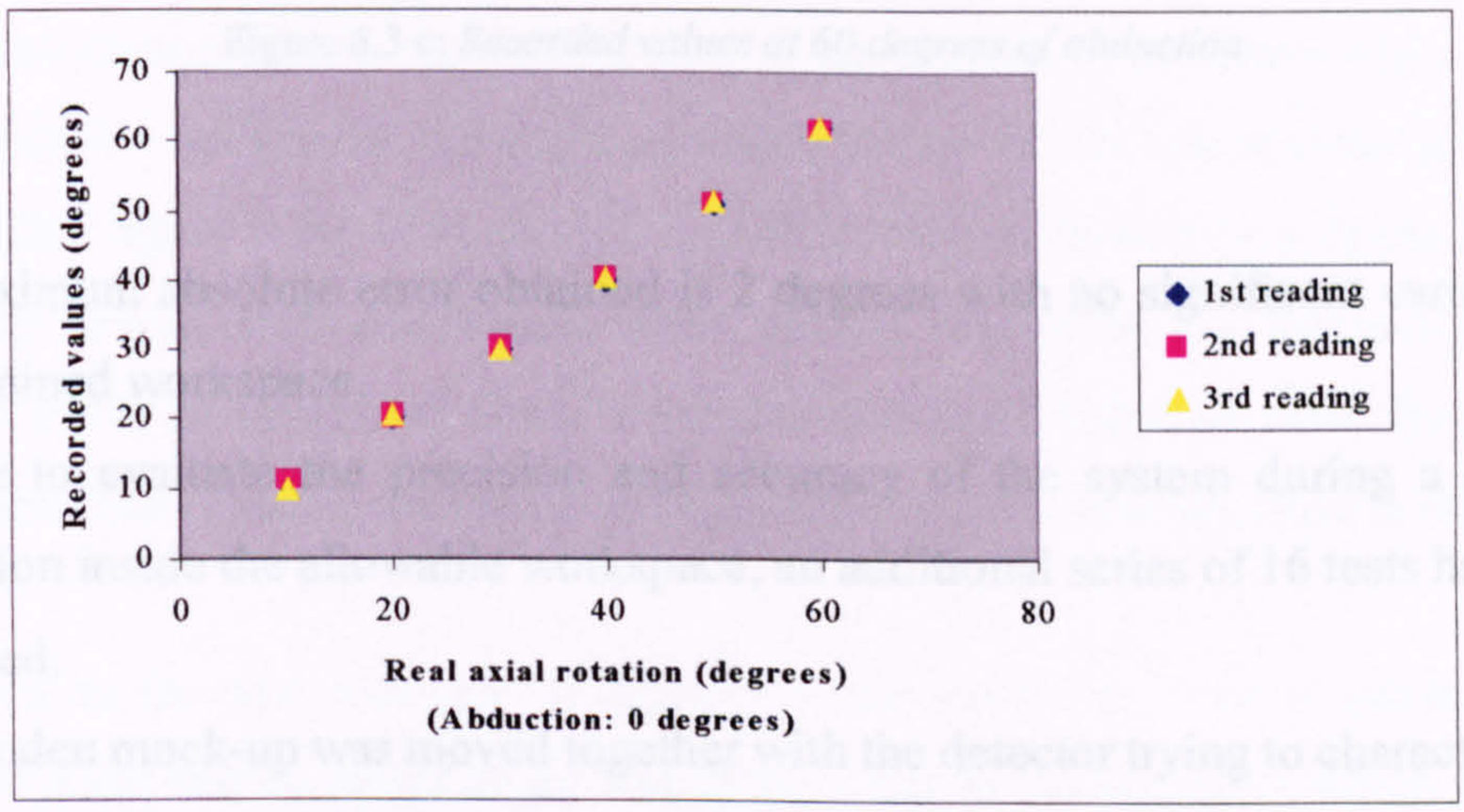

Figure 6.3 a: *Recorded values at 0 degrees of abduction*

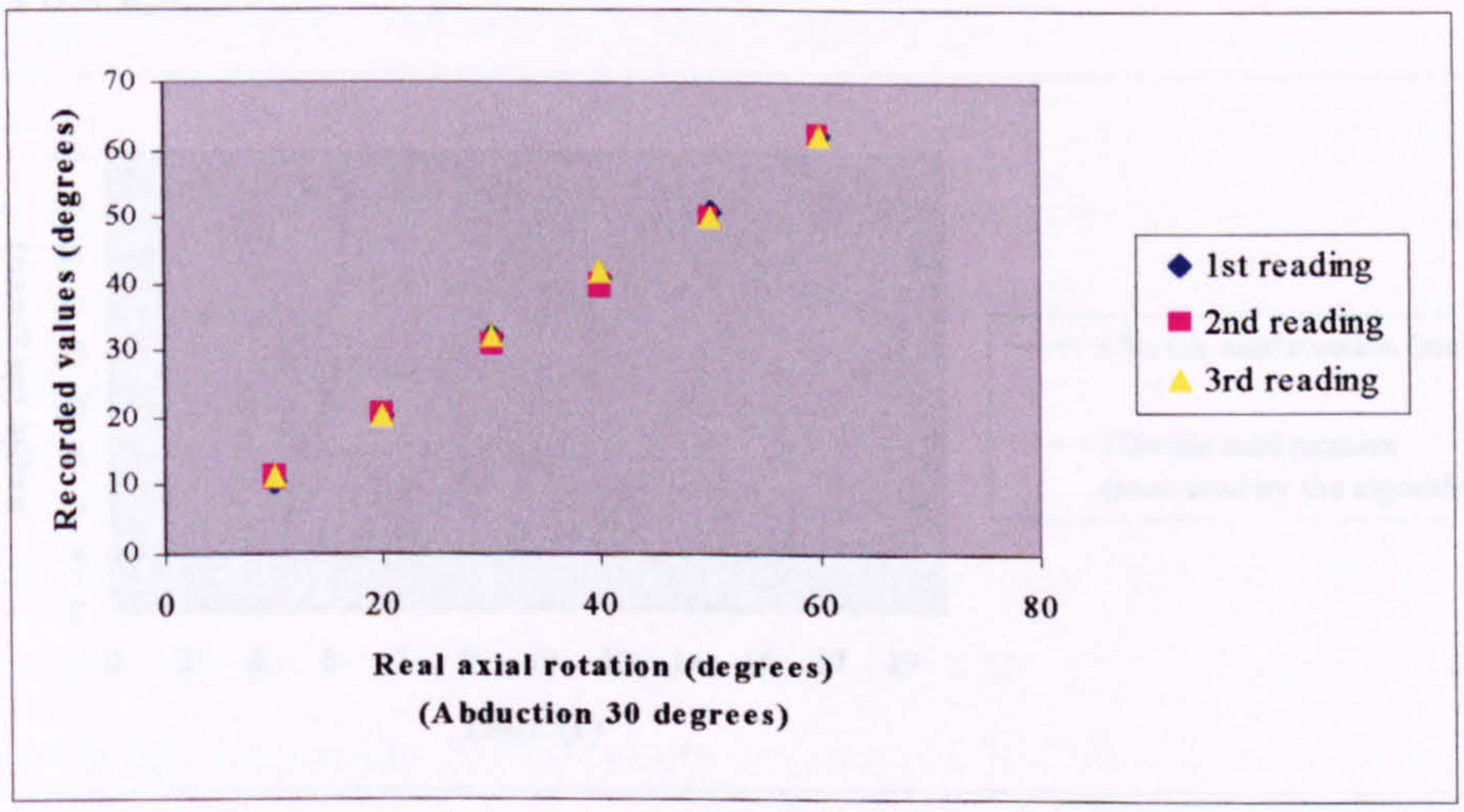

Figure 6.3 b: *Recorded values at 30 degrees of abduction*

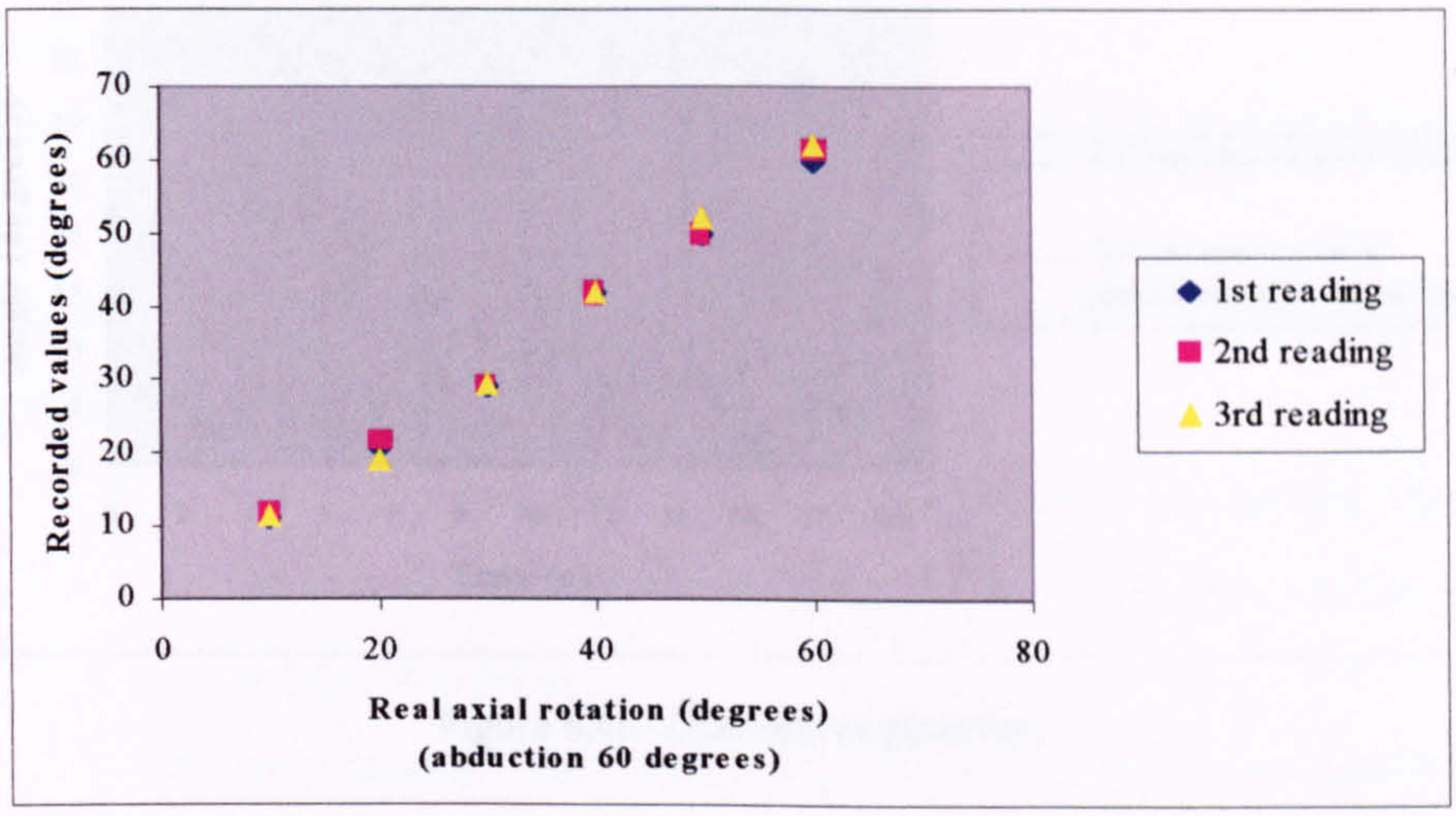

Figure 6.3 c: *Recorded values at 60 degrees of abduction*

The maximum absolute error obtained is 2 degrees with no significant variations in the examined workspace.

In order to evaluate the precision and accuracy of the system during a dynamic acquisition inside the allowable workspace, an additional series of 16 tests have been performed.

The wooden mock-up was moved together with the detector trying to characterise the behaviour of the two systems. Example of the results obtained is shown in the graphs of figures 6.4 a,b.

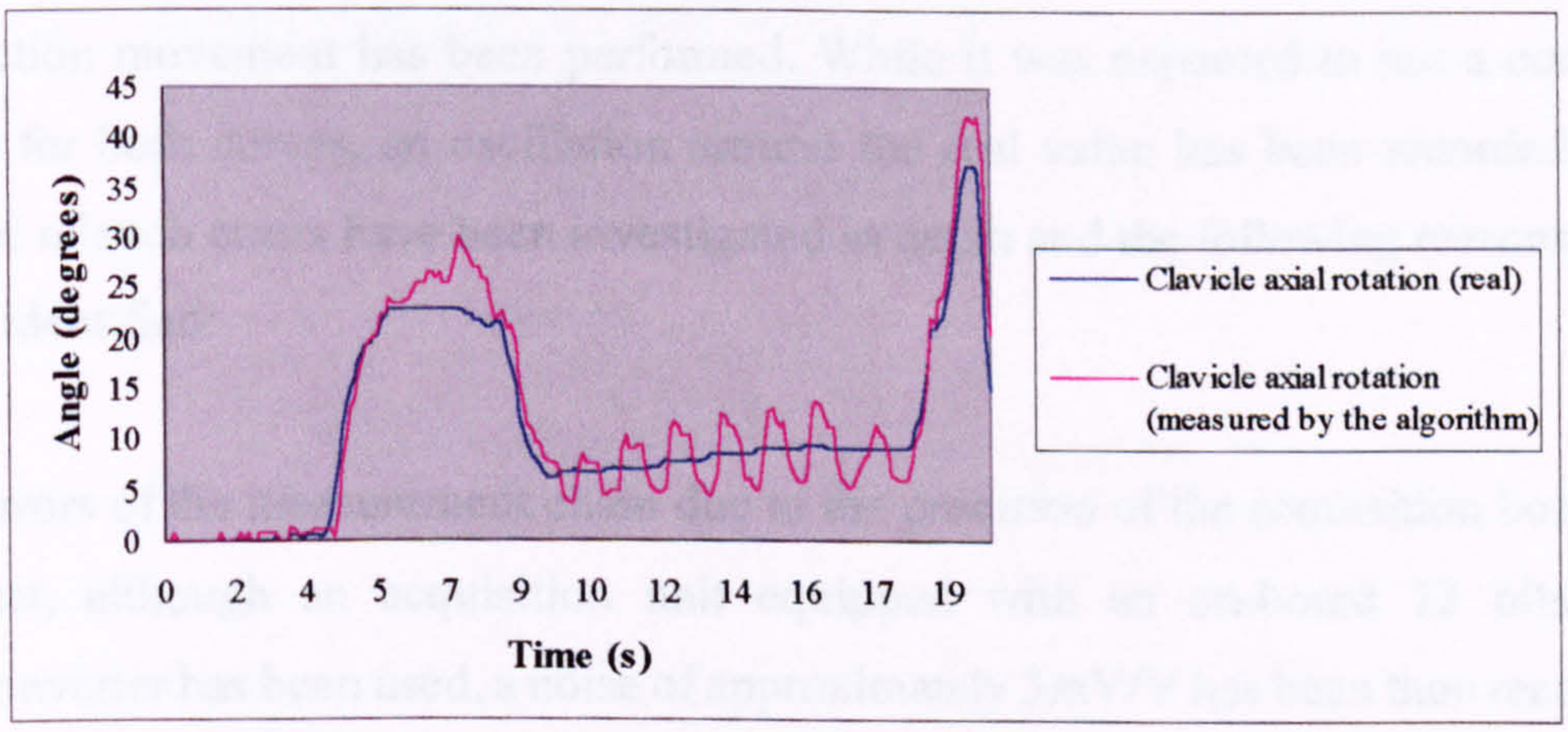

Figure 6.4a: *Dynamic acquisition*

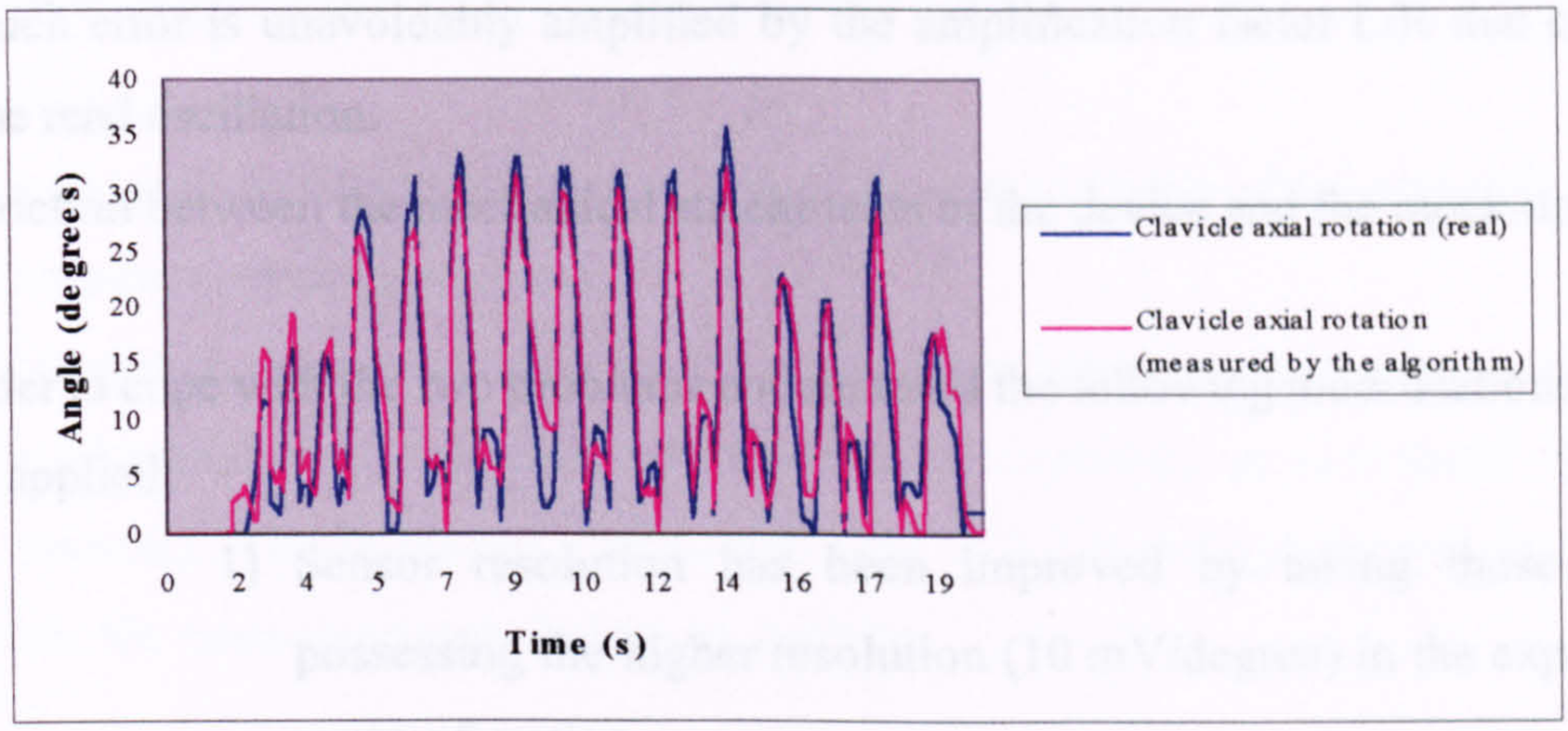

Figure 6.4b: *Dynamic acquisition*

The results obtained have shown that there is an increase of the errors (max absolute error inside the workspace: 4.5 degrees) either in case of a constant value of the axial rotation (see figure 6.4a) or in case of high frequency of motion (see figure 6.4b). As described below, such errors have been caused mainly by the following factors: accuracy of the measurement chain in the first case and friction between the mock-up and the detector together with poor stiffness of the mechanical structure in the second one.

As shown in the first example of figure 6.4 the source of error is caused by the accuracy of the measurement chain that, in turn, due to the algorithm which acts as an amplification factor (L/R), increases the errors. In fact as it can be noted, by maintaining a constant axial rotation (represented by the blue line), an abduction-adduction movement has been performed. While it was expected to see a constant value for both curves, an oscillation around the real value has been recorded. The causes of such errors have been investigated in depth and the following reasons have been identified:

a) Errors of the measurement chain due to the precision of the acquisition board. In fact, although an acquisition unit equipped with an on-board 12 bits A/D converter has been used, a noise of approximately 3mV/V has been then recorded.

Such error is unavoidably amplified by the amplification factor L/R that causes the read oscillation.

b) Friction between the mechanical attachments of the device and the mock-up.

In order to cope with the two problems encountered the following modifications have been applied:

1) Sensor resolution has been improved by taking those ones possessing the higher resolution (10 mV/degree) in the exploited range of motion.
2) the detector has been re-designed increasing the stiffness of the bars.

As far as friction is concerned, some lubricant has been used between the mock-up surfaces interfaced to the clavicle detector (see figure 6.2 a, b).

Another battery of 8 tests have been then executed with a consistent decrease of the amplitude of the oscillations, an example is shown in figure (see 6.5) where it can be noted that the behaviour of the two curves is much similar.

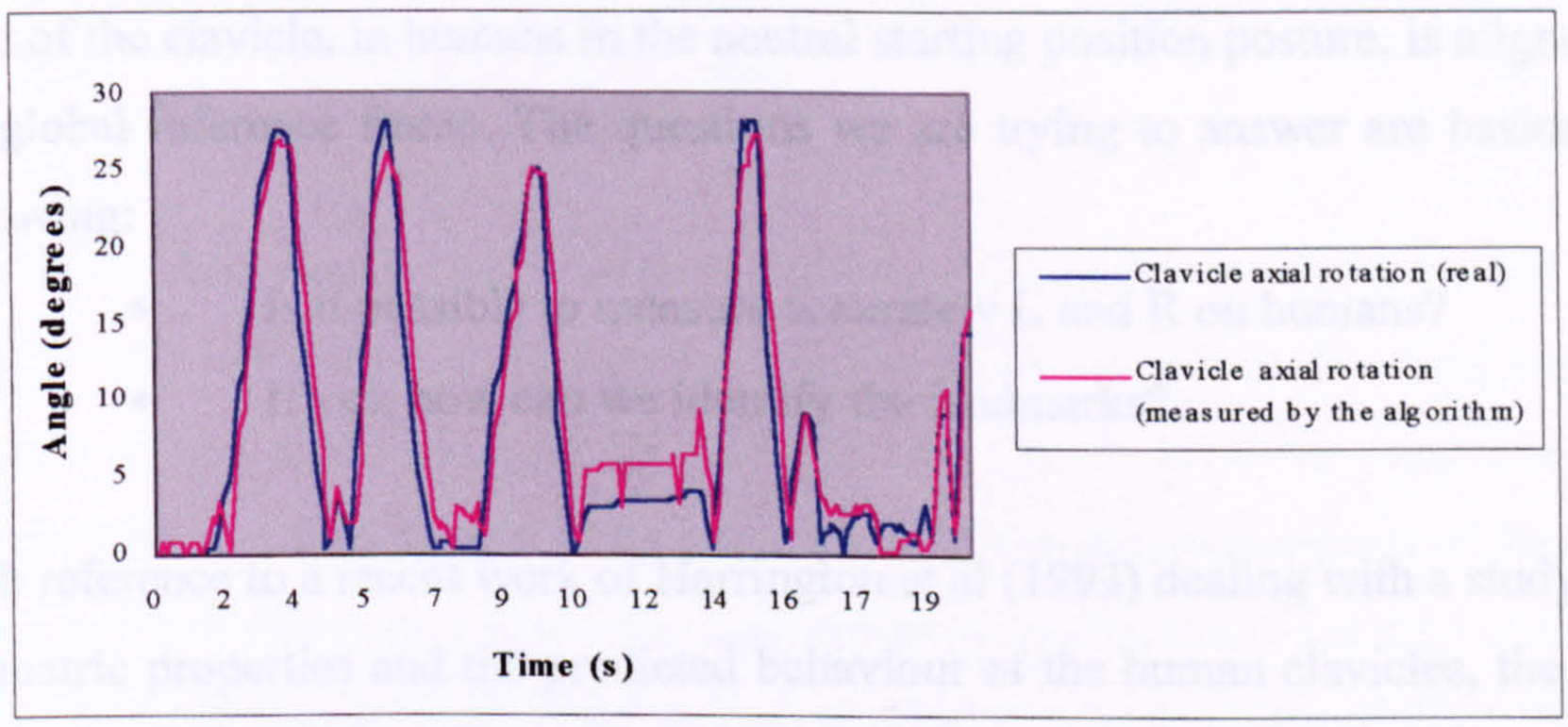

Figure 6.5 *Test performed with the modified equipment*

6.2.1 Concluding remarks

The tests performed with the test rig have shown the validity of the algorithm and of the measurement equipment used.

The maximum errors obtained using a quasi-static technique within the investigated range of motion was 2 degrees, which has been considered an acceptable result for our purposes. The following section will deal with the tests performed in order to validate the measurement technique on humans.

6.3 Sensitivity of the algorithm to the variation of the parameters L/R

A key factor which can greatly affect the algorithm is the estimation of two parameters of the bone L and R where L is the orthogonal projection of the distance between the Sterno-Clavicular joint and the acromio-clavicular on the frontal plane and R is the projection of the distance of the same joints in the sagittal plane respectively (see Figure 5.2). Our assumption is based on the hypothesis that the inner third of the clavicle, in humans in the neutral starting position posture, is aligned with the global reference frame. The questions we are trying to answer are basically the following:

- Is it possible to measure accurately L and R on humans?
- If yes, how can we identify the landmarks?

With reference to a recent work of Harrington et al (1993) dealing with a study on the geometric properties and the predicted behaviour of the human clavicles, the second moments of area of discrete sections of the clavicle are given. By examining histomorphometric properties of 15 adult male and female clavicles they demonstrated that the clavicle cross-sectional geometry changes from a circular, vertically oriented shape sternally to a flat, horizontal orientation acromially. As can be seen in the table below taken from the above paper, the anatomical second moment

of area are given for some sections expressed as percentages of the total length of the clavicle.

Length (%)	Area (cm^2)	$I_{AP}(cm^4)$	$I_{CC}(cm^4)$
5	0,74±0,61	0,84±0,70	0,72±0,67
10	0,37±0,21	0,46±0,31	0,40±0,27
15	0,44±0,26	0,33±0,20	0,26±0,17
20	0,51±0,21	0,23±0,10	0,18±0,08
25	0,53±0,21	0,17±0,07	0,13±0,05
30	0,57±0,21	0,15±0,06	0,12±0,04
35	0,54±0,19	0,13±0,05	0,10±0,04
40	0,67±0,31	0,13±0,05	0,12±0,08
45	0,62±0,19	0,11±0,06	0,11±0,05
50	0,67±0,18	0,10±0,05	0,12±0,06
55	0,70±0,20	0,10±0,06	0,14±0,08
60	0,76±0,24	0,10±0,05	0,17±0,12
65	0,86±0,30	0,12±0,07	0,24±0,16
70	0,87±0,32	0,13±0,07	0,29±0,16
75	0,84±0,32	0,14±0,09	0,33±0,15
80	0,74±0,21	0,12±0,06	0,32±0,10
85	0,68±0,33	0,14±0,09	0,40±0,25
90	0,60±0,38	0,17±0,14	0,45±0,36
95	0,25±0,05	0,11±0,05	0,32±0,08
100	0,36±0,26	0,18±0,15	0,45±0,31

Table 6.1: *Geometry data for all clavicles by % of total length as measured from the sternal length of the bone (Harrington et all 1993)*

The above data can be used in order to extract information on the bony landmarks. Consistently with the data shown by Harrington et al. (1993), the two centres of rotation of the acromio-clavicular joint and the sterno-clavicular joint are located respectively at 5 % and 90 % of the total length. *Since the cross section of the clavicle has an elliptic form, we can use the data shown in the Table 6.1 relative to the areas of the relevant section and of the second moment of area in order to determine, with simple calculations, the length of the two axes of the ellipses at SC and AC respectively.* Since such part of the bone is in intimate connection with the skin we have direct information on the position of the landmarks as shown in figure 6.6.

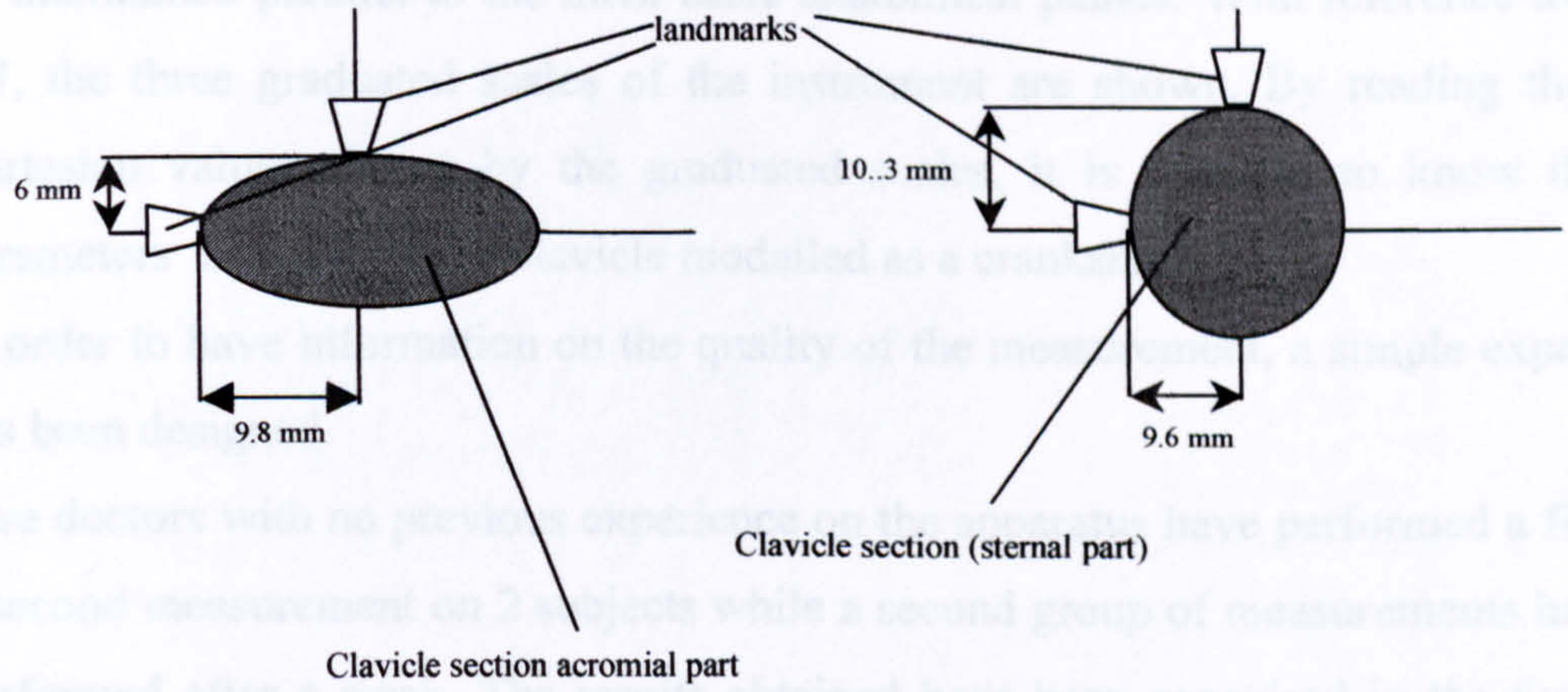

Figure 6.6 *Landmark position a) acromial part; b) sternal part*

The above functional specifications have been used as guidelines for the design and development of a three degrees of freedom adjustable ruler (shown in figure 6.7) that can be used for measuring the left and the right clavicle.

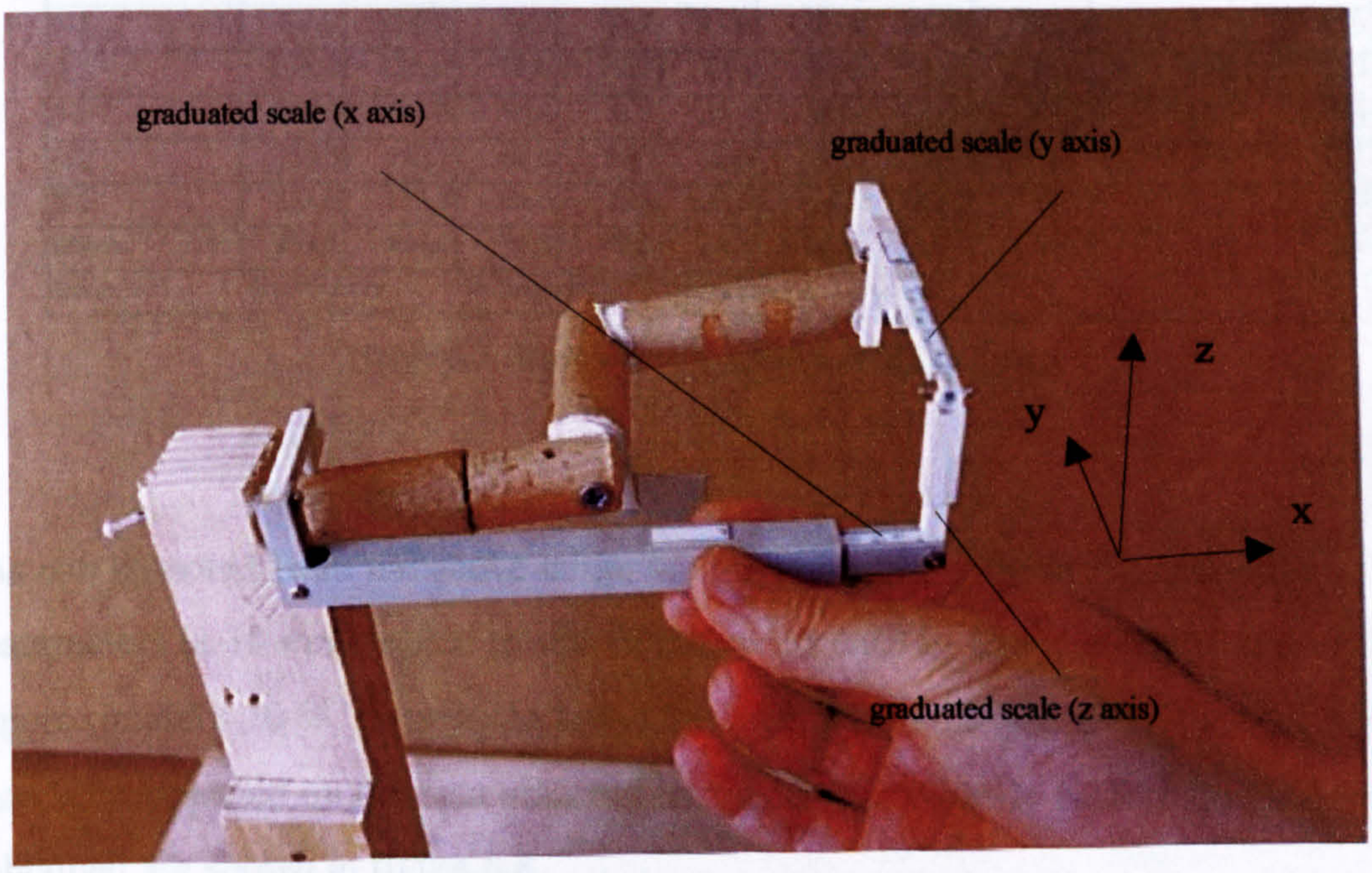

Figure 6.7: *Locator of the acromio-clavicular joint*

The equipment is used together with a small inclinometer which allows the locator to be maintained parallel to the three basic anatomical planes. With reference to figure 6.7, the three graduated scales of the instrument are shown. By reading the three Cartesian values shown by the graduated scales, it is possible to know the two parameters L and R of the clavicle modelled as a crankshaft.

In order to have information on the quality of the measurement, a simple experiment has been designed.

Five doctors with no previous experience on the apparatus have performed a first and a second measurement on 2 subjects while a second group of measurements has been performed after a week. The results obtained have been organised in the form of a table below.

Observation	L 1st	L 2nd	l 1st	l 2nd	h 1st	h 2nd	R 1st	R 2nd	L/R 1st	L/R 2nd
1-1	135,0	133,0	40,0	37,0	15,0	20,0	42,7	42,1	3,2	3,2
2-1	140,0	142,0	44,0	38,0	15,0	18,0	46,5	42,0	3,0	3,4
3-1	145,0	144,0	42,0	40,0	18,0	18,0	45,7	43,9	3,2	3,3
4-1	142,0	135,0	40,0	43,0	19,0	15,0	44,3	45,5	3,2	3,0
5-1	144,0	140,0	45,0	45,0	22,0	16,0	50,1	47,8	2,9	2,9
Mean	**141,2**	**138,8**	**42,2**	**40,6**	**17,8**	**17,4**	**45,9**	**44,3**	**3,1**	**3,1**
1-2	152,0	154,0	73,0	76,0	34,0	38,0	80,0	82,0	1,9	1,9
2-2	155,0	155,0	75,0	70,0	30,0	36,0	83,0	78,7	1,9	2,0
3-2	152,0	154,0	70,0	75,0	30,0	32,0	81,0	81,5	1,9	1,9
4-2	153,0	156,0	68,0	68,0	28,0	33,0	78,0	75,6	2,0	2,1
5-2	155,0	153,0	70,0	75,0	35,0	33,0	75,0	81,9	2,1	1,9
Mean	**153,4**	**154,4**	**71,2**	**72,8**	**31,4**	**34,4**	**79,4**	**80,0**	**1,9**	**1,9**
Code X-Y	X=Observer		Y=Subject		Measurement unit=mm					

Table 6.2: *Measurements taken from two subjects*

As can be noted from the above table, the max absolute error in the estimation of the parameters is 10 mm, which results in the worst case in an error of the ratio L/R of approximately 10 %. In order to know the max error obtained a variation of ± 10 % has been imposed on the data obtained by the tests previously performed. The results obtained are shown in figure 6.8.

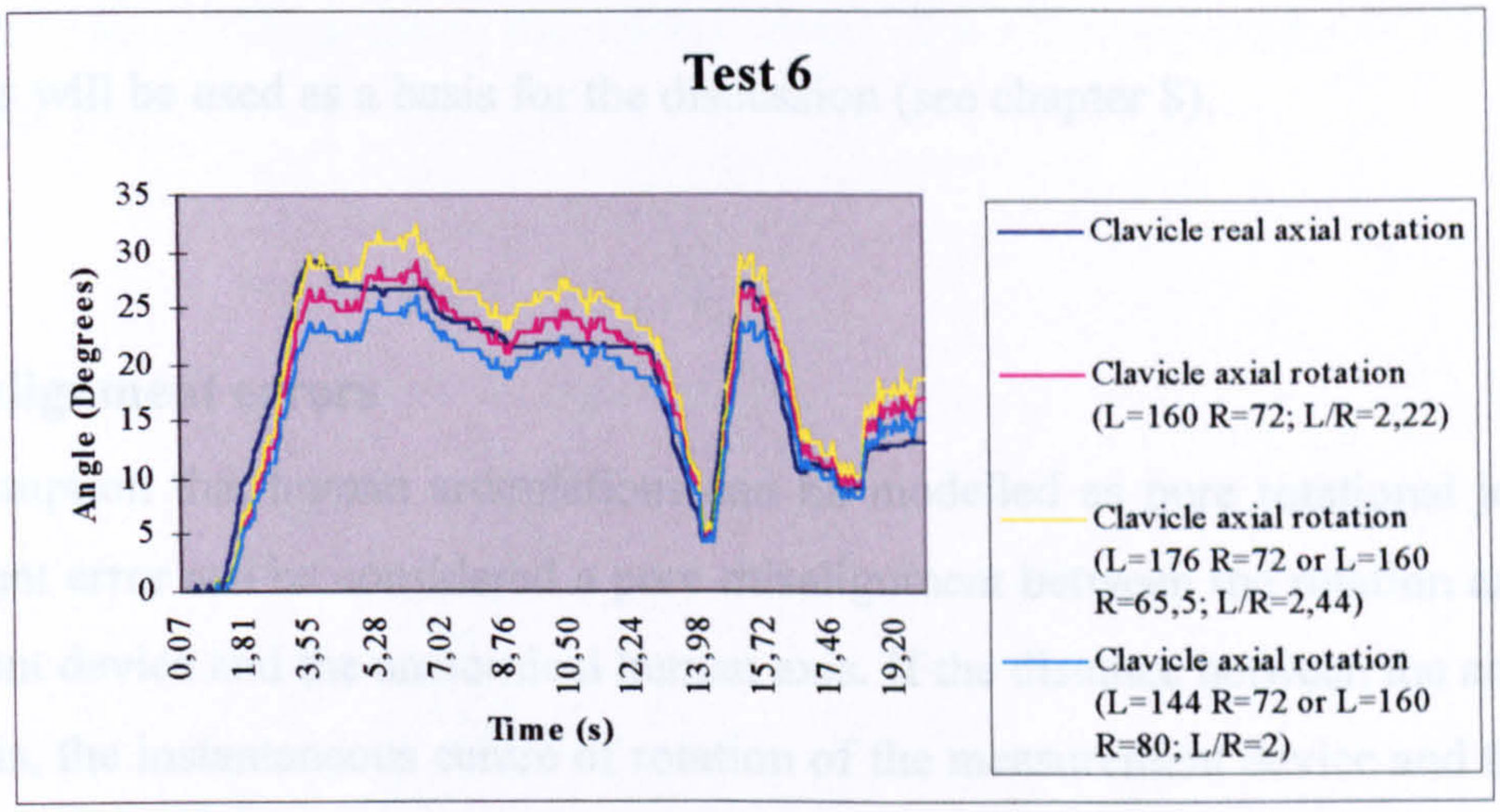

Figure 6.8 *Influence of 10 % variation on the axial rotation*

Consistently with the assumption that the clavicle is from a geometrical point of view a highly variable bone, a set of measurements taken from 21 subjects has been performed (mean age 28, variance 17). As can be seen in the following table the ratio L/R is highly variable ranging from 1.6 to 3.2.

Subj.	Weight (kg)	Height (cm)	L (mm)	l (mm)	h (mm)	R (mm)	L/R (mm)
1	80,0	178,0	135,0	40,0	15,0	42,7	3,2
2	84,0	170,0	140,0	70,0	15,0	71,6	2,0
3	75,0	168,0	130,0	52,0	17,0	54,7	2,4
4	78,0	173,0	150,0	54,0	20,0	57,6	2,6
5	68,0	174,0	142,0	60,0	24,0	64,6	2,2
6	70,0	175,0	140,0	52,0	15,0	54,1	2,6
7	92,0	186,0	155,0	75,0	30,0	80,8	1,9
8	82,0	178,0	154,0	64,0	23,0	68,0	2,3
9	81,0	179,0	135,0	52,0	25,0	57,7	2,3
10	70,0	175,0	140,0	55,0	20,0	58,5	2,4
11	61,0	170,0	135,0	48,0	25,0	54,1	2,5
12	78,0	165,0	130,0	45,0	18,0	48,5	2,7
13	74,0	171,0	140,0	63,0	30,0	69,8	2,0
14	70,0	170,0	135,0	48,0	25,0	54,1	2,5
15	64,0	165,0	125,0	77,0	13,0	78,1	1,6
16	77,0	179,0	140,0	63,0	22,0	66,7	2,1
17	76,0	180,0	152,0	65,0	26,0	70,0	2,2
18	72,0	170,0	134,0	60,0	25,0	65,0	2,1
19	76,0	168,0	135,0	80,0	18,0	82,0	1,6
20	76,0	180,0	158,0	55,0	20,0	58,5	2,7
21	80,0	172,0	135,0	63,0	20,0	66,1	2,0

Table 6.3: *Subjects anthropometrics data*

Such results will be used as a basis for the discussion (see chapter 8).

6.4 Misalignment errors

In the assumption that human articulations can be modelled as pure rotational joints, the misalignment error can be considered a pure misalignment between the rotation axis of the measurement device and the anatomical human axis. If the distance between the anatomical rotation axis, the instantaneous centre of rotation of the measurement device and the length of the bar attached to the movable joint are known, we can apply the model depicted in figure 6.9.

Let us assume that A is the instantaneous centre of rotation of the device attached through a bar of length l to the skin and B is the anatomical centre of rotation which in theory should be coincident with A, but in practice it is located at a distance r from it. B represents the centre of rotation of the device through which we would like to read the rotation angle α'. But since the two rotation axes are not coincident we will read the angle β' instead of α. Under this assumption the mechanism formed by two joints (A, B) and 2 links can rotate only if we allow in C a rotation and a translation which is the simulation of presence of soft tissues and muscles which do not allow a rigid connection between the two devices. The relationship between α' and β' can be found as follows (see figure 6.9):

$$y = l*\sin(\alpha-\alpha')$$

$$z = r-l*\cos(\alpha-\alpha')$$

$$y = z*\tan(\beta+\beta') = (r-l*\cos(\alpha-\alpha'))*\tan(\beta+\beta')$$

$$l*\sin(\alpha-\alpha') = [r-l*\cos(\alpha-\alpha')]*\tan(\beta+\beta')$$

$$\tan(\alpha-\alpha') = r*\tan(\beta+\beta')/(l*\cos(\alpha-\alpha'))-\tan(\beta+\beta')$$

In the assumption that the maximum parallax error is that related to the difficulties in locating the SC joint and taking, in the less favourable case, the maximum absolute error, we can have a point estimate of r.

By applying the above formulae, it is therefore possible to have information on the error occurred during the reading. As an example, by providing values to the parameters l = 50

mm, r=10 mm and α= 70 degrees, the results obtained for the two angles α' and β' are shown in figure 6.10.

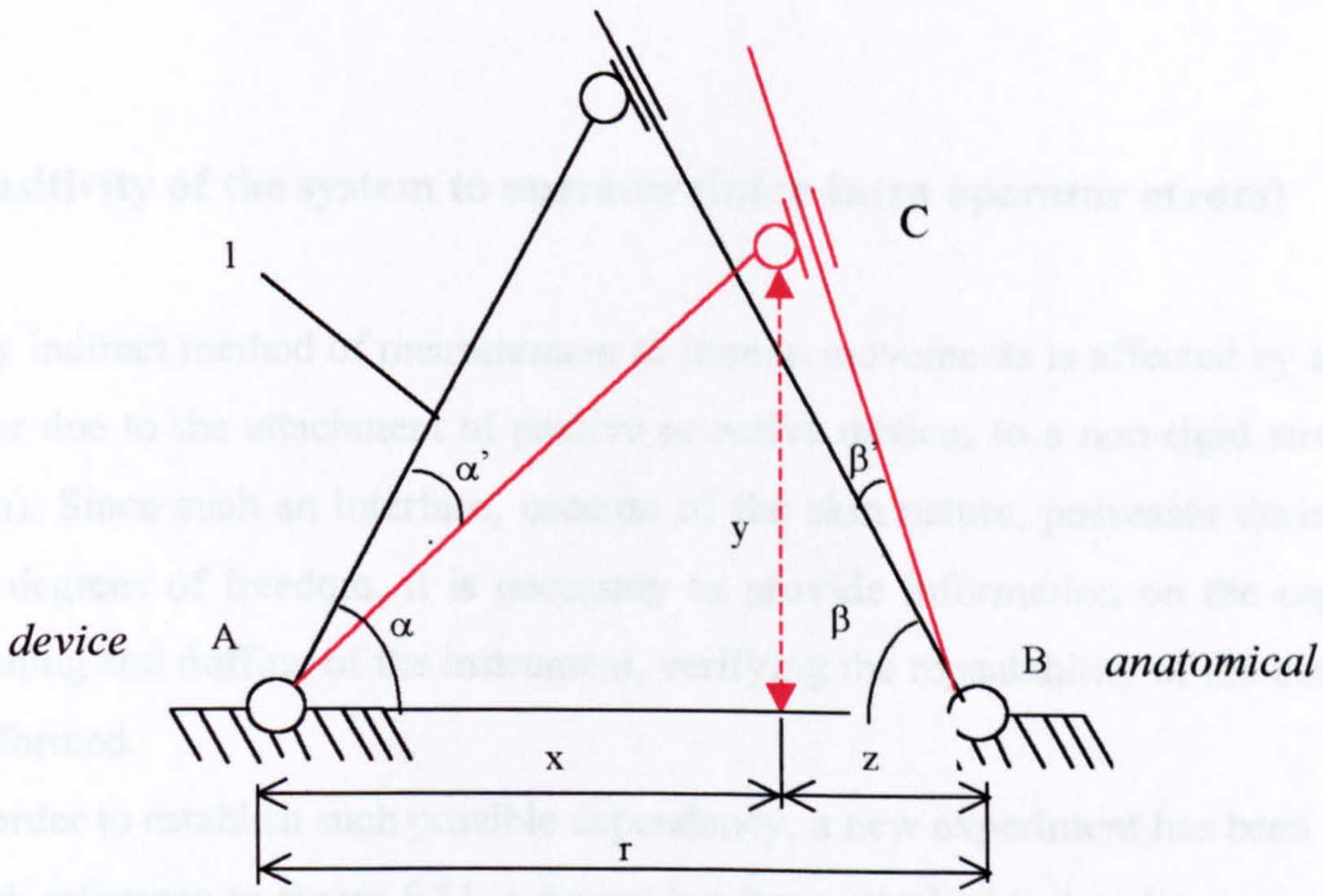

Figure 6.9: *Misalignment errors*

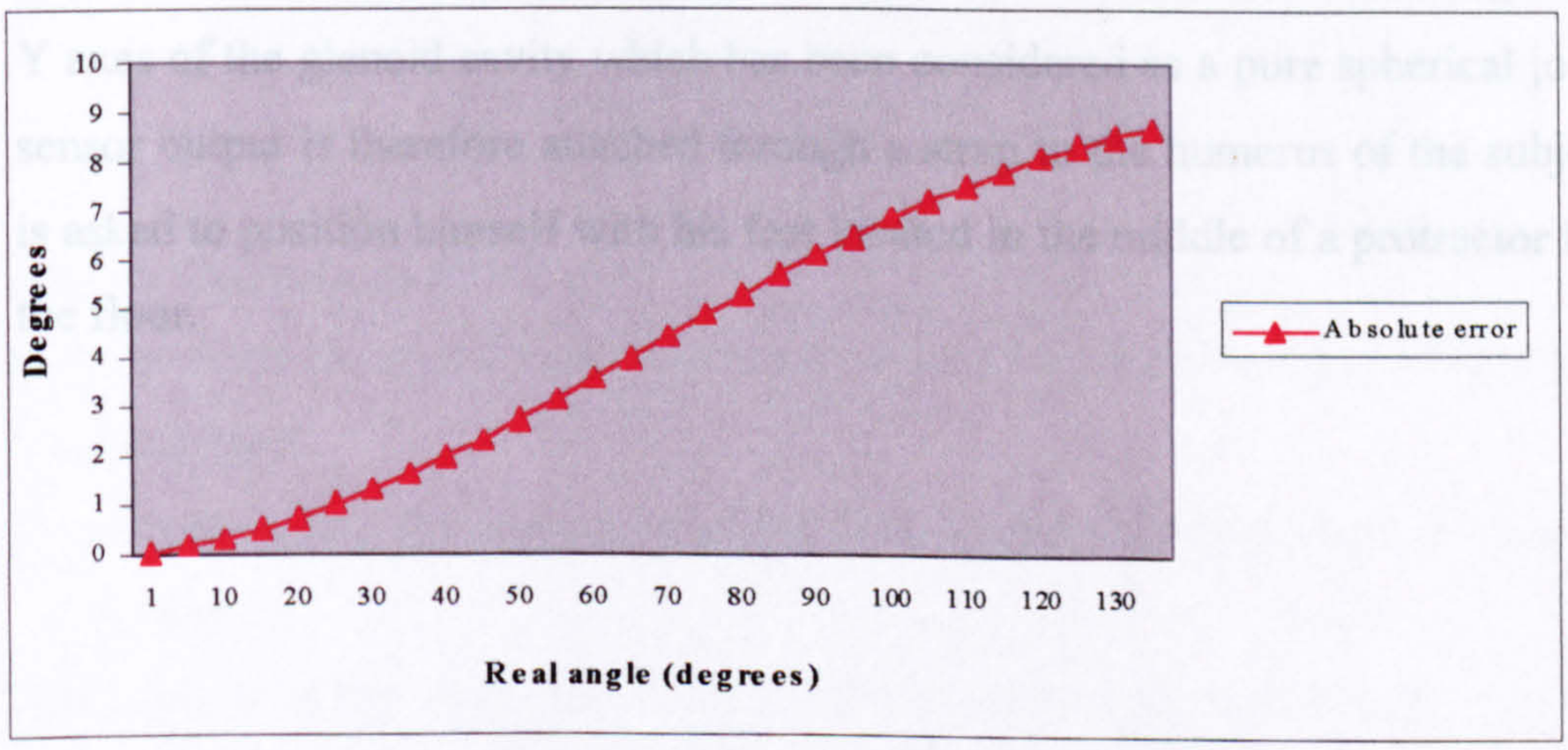

Figure 6.10: *Difference between the read and the real angle*

As far as the clavicle is concerned, since the maximum angle read by the sensors is approximately 50 degrees, we are in an area of the curve where the error is limited (maximum error: 3.3 degrees).

It is worth mentioning that between 0 and 30 degrees the maximum error obtained is less than 1.5 degrees.

6.5 Sensitivity of the system to operator (inter-intra operator errors)

Any indirect method of measurement of human movements is affected by an intrinsic error due to the attachment of passive or active devices to a non-rigid structure (the skin). Since such an interface, because of the skin nature, possesses during motion, six degrees of freedom, it is necessary to provide information on the capability of donning and doffing of the instrument, verifying the repeatability of the measurement performed.

In order to establish such possible dependency, a new experiment has been set up.

With reference to figure 6.11, a sensor has been attached to two linear passive slides attached to the wall in a way to allow a linear displacement along the direction x, y. The slides have been located in order to compensate the translations along the X and Y axes of the glenoid cavity which has been considered as a pure spherical joint. The sensor output is therefore attached through a strap to the humerus of the subject who is asked to position himself with his feet located in the middle of a protractor fixed on the floor.

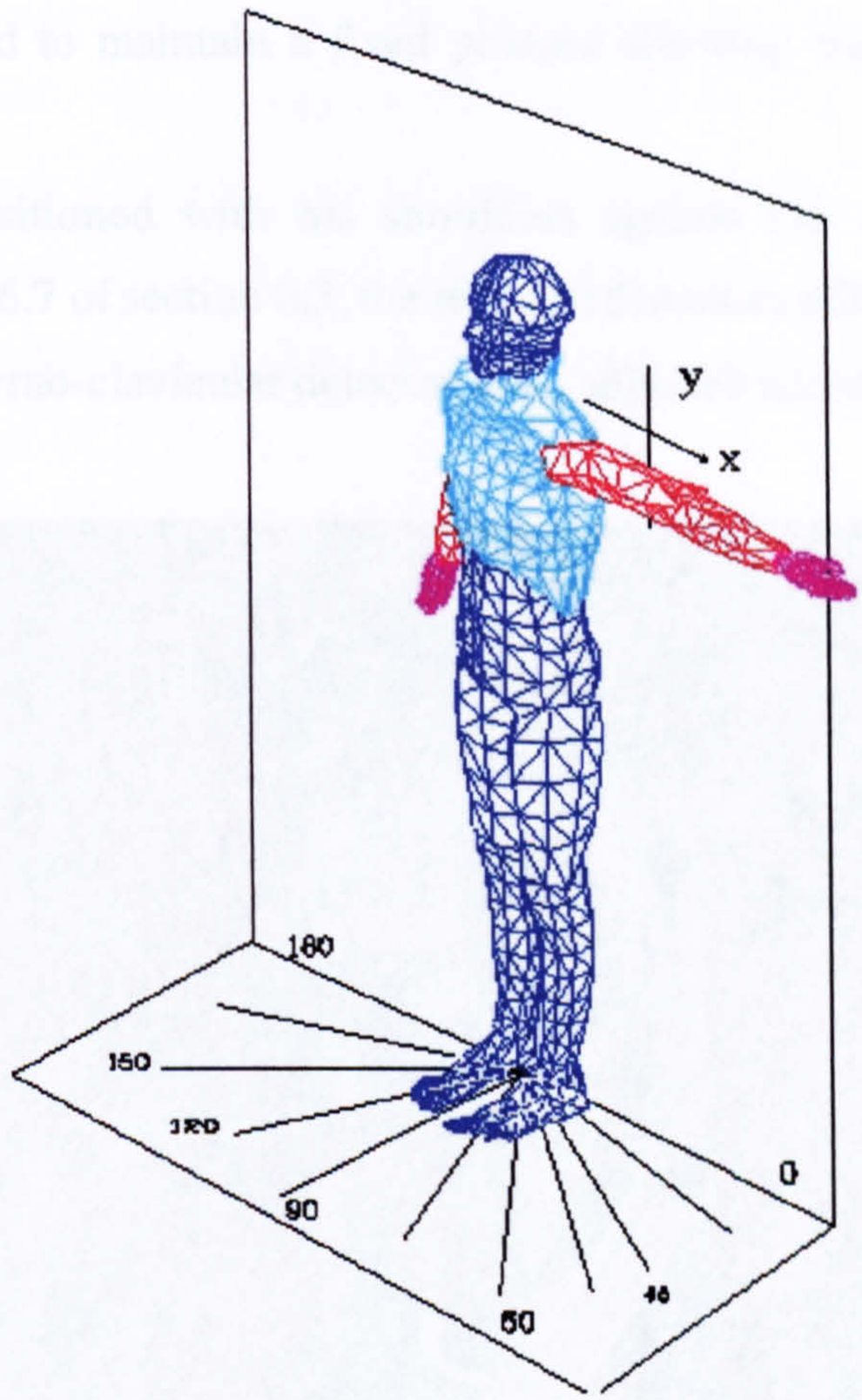

Figure 6.11 *Sketch of the test (Mannequin)*

The two linear slides allow:

a) to position the sensor axis coincident with the moving anatomical humeral axis of the subject;

b) to compensate the movement of the gleno-humeral joint during the elevation of the arm.

This equipment has been used to record the angular displacement of the humerus at different azimuth rotations. The information taken from the sensor attached to the slides has been also cross-evaluated by using a liquid goniometer.

The above described procedure has been used in order to decrease fatigue on subjects during repetitive measuring. In fact, despite the sensor located on the two slides has the same role of the liquid goniometer, we have decreased the time in which the

subject was obliged to maintain a fixed posture allowing the operator to read the measure.

The subject is positioned with his shoulders against the wall. Using the ruler described in figure 6.7 of section 6.3, the relevant distances of the subject clavicle are detected and the sterno-clavicular detector links adjusted accordingly.

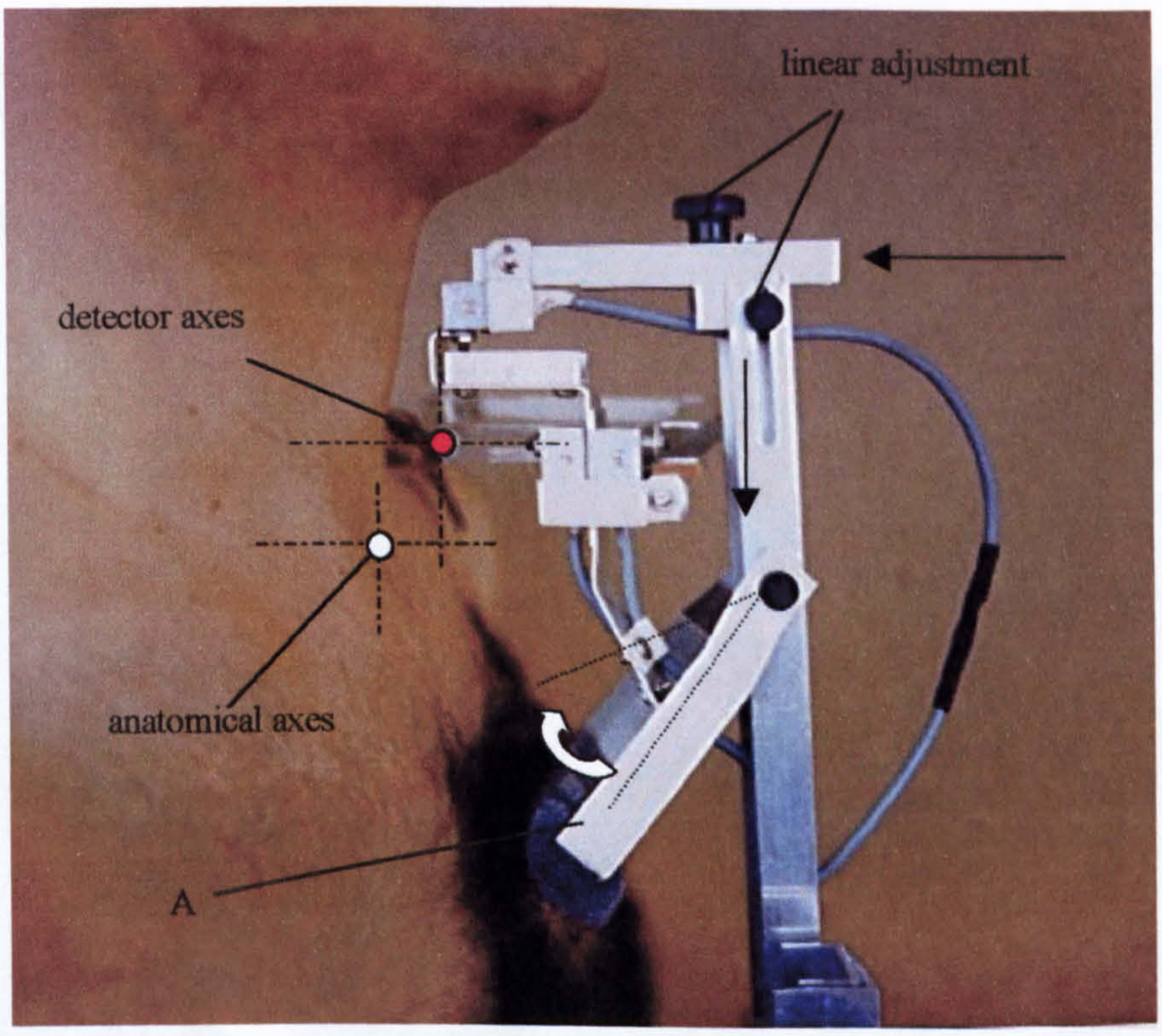

Figure 6.12 *Particular of the test*

As soon as the mechanical structure has been adjusted according to the anatomical distances of the patient the detector, fixed to a rigid structure, is located close to the subject trying to align the axes of the device to the subject anatomical axes. With reference to figure 6.12 the adjustments are made by moving the structure through the linear slides in the direction indicated by the vertical and horizontal rows shown in figure 6.12. When a satisfactory position is reached, the device is referenced to the subject by acting on the angular passive degrees of freedom (A), which hampers the free swinging of the subject in the horizontal direction (e.g. the shoulders of the subject are in contact with the wall). In these conditions the two links of the structures are preliminarily connected to the subject

using adhesive bands as shown in figure 6.13. Humeral adduction-abduction (in the case of the figure) together with the 3 degrees of freedom of clavicle are then recorded simultaneously. The sensor detecting humeral elevation is attached to two passive slides (2 degree-of-freedom system) necessary to compensate the movement of the gleno-humeral joint during motion and allowing a consistent movement between the anatomical chain and the recording system.

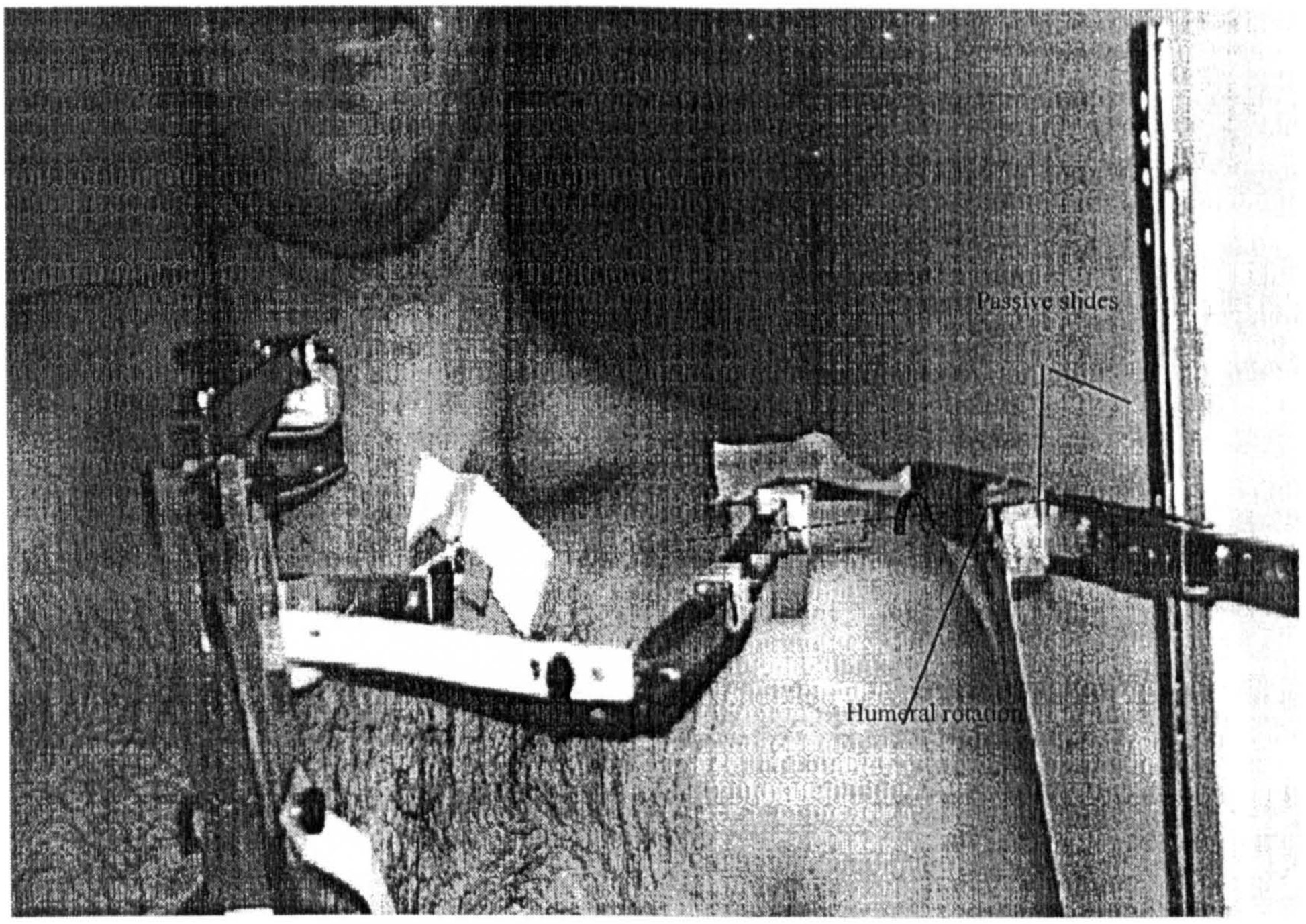

Figure 6.13 Photograph of the test

In order to avoid a relative movement between skin and the landmarks, the adhesives are manually maintained in contact during motion by the observer. The subject is then asked to rotate the body 45 degrees (counter clockwise with reference to figure 6.11) and the test is repeated. Measurements are therefore taken at 0, 45, 90 azimuth degrees inside the workspace.

This procedure has been used to assess inter and intra operator errors by executing a set of trials on each subject as follows:

Two observers each recorded 3 replicate measurements on a random sample of 10 subjects (mean age 27 SD=6). Data have been collected in a static way at increments of 10 degrees.

The hierarchical model used is shown in figure 6.14.

Data have then been analysed with a standard statistical model. A 2^{nd} order fitting technique has been used to compare the results, which are shown in the following graphs.

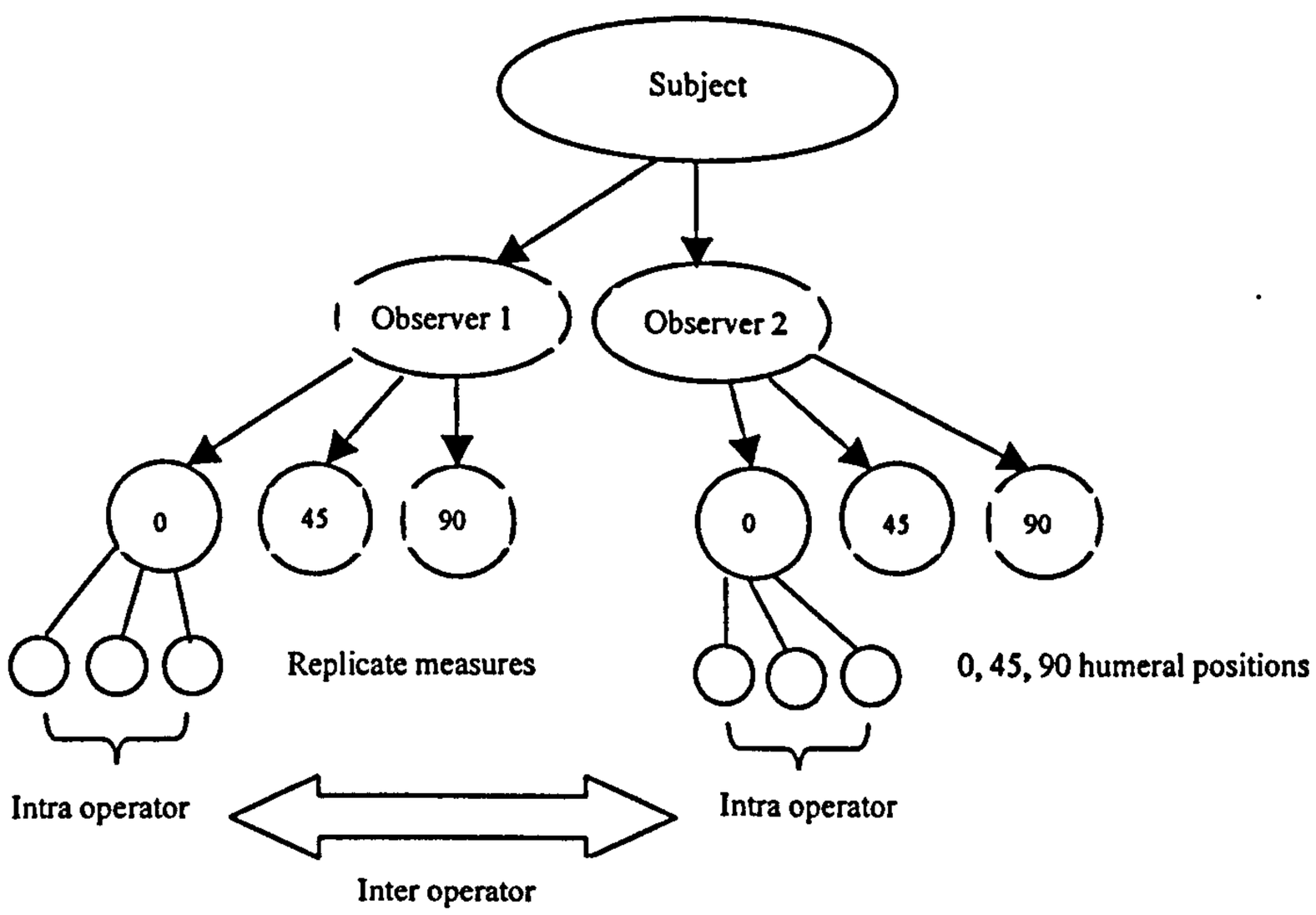

Figure 6.14 *Tree diagram of the hierarchical model*

The graphs from figure 6.15 to figure 6.23 have been taken from three subjects while the complete tests are given in Appendix 1 together with the complete set of data.

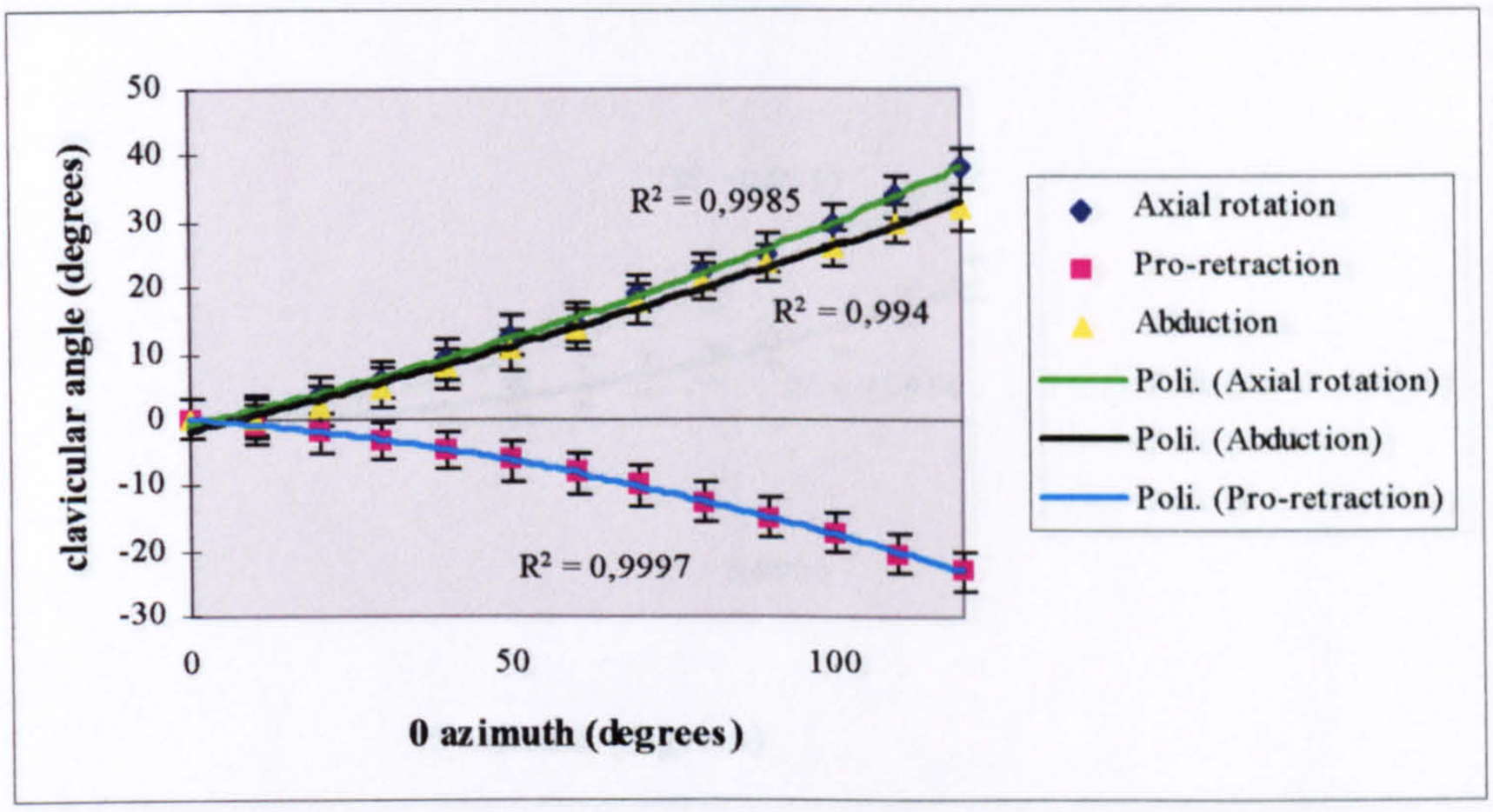

Figure 6.15 a: *Subject 1(L/R=2,46) - 0 degrees azimuth observer 1*

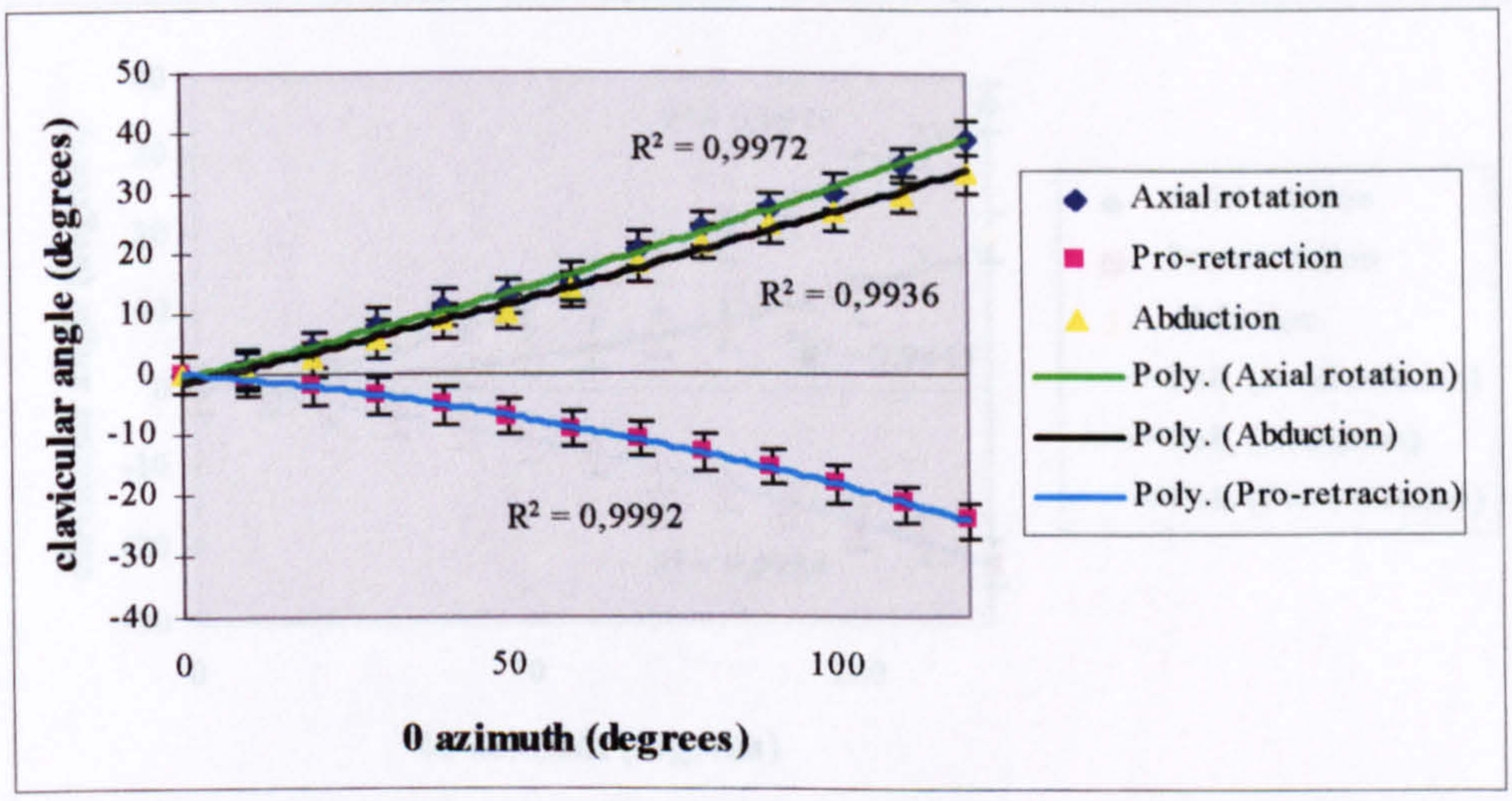

Figure 6.15 b: *Subject 1(L/R=2,46) - 0 degrees azimuth observer 2*

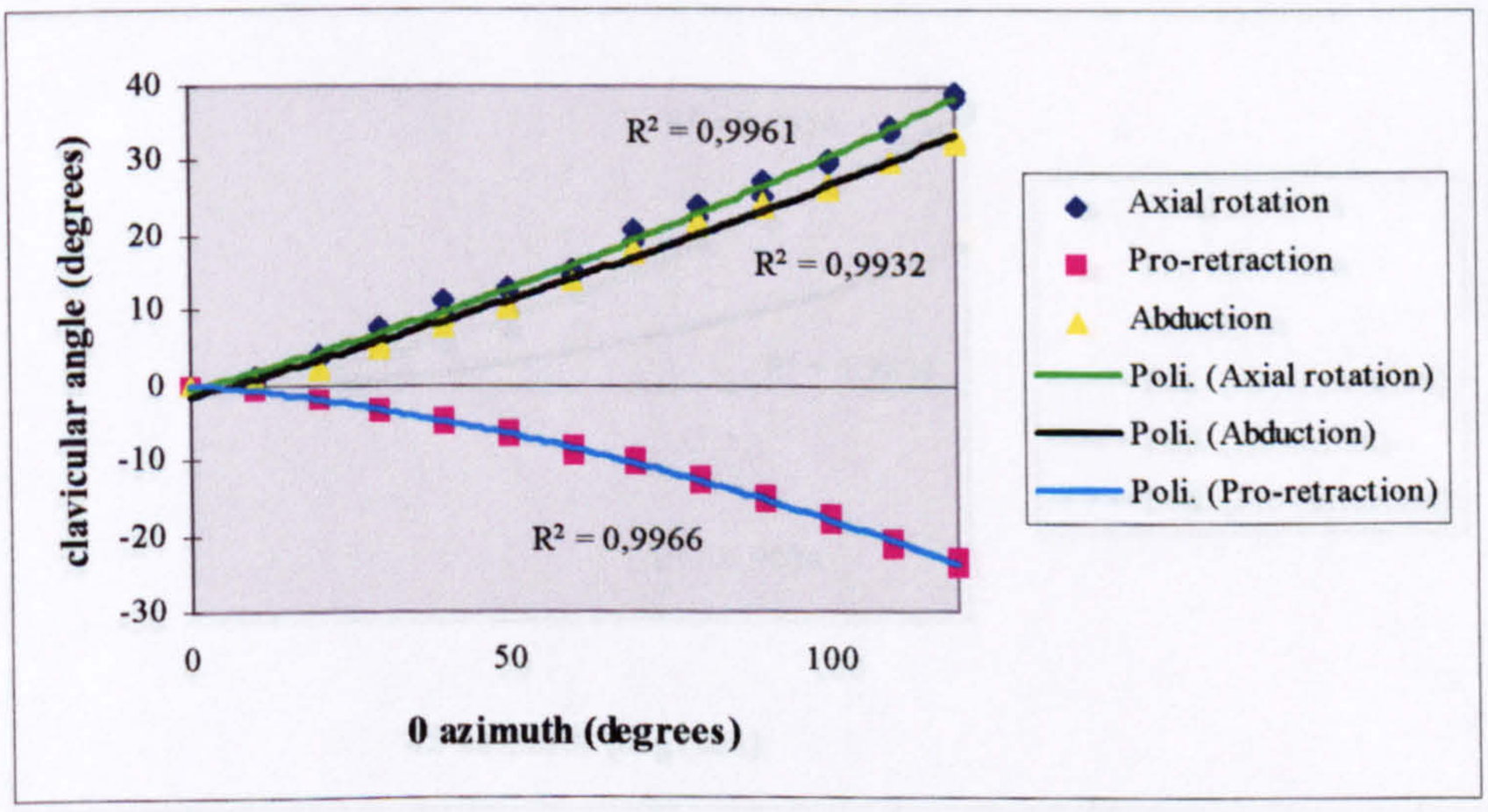

Figure 6.15 c: *Subject 1(L/R=2,46) - 0 degrees azimuth inter observer*

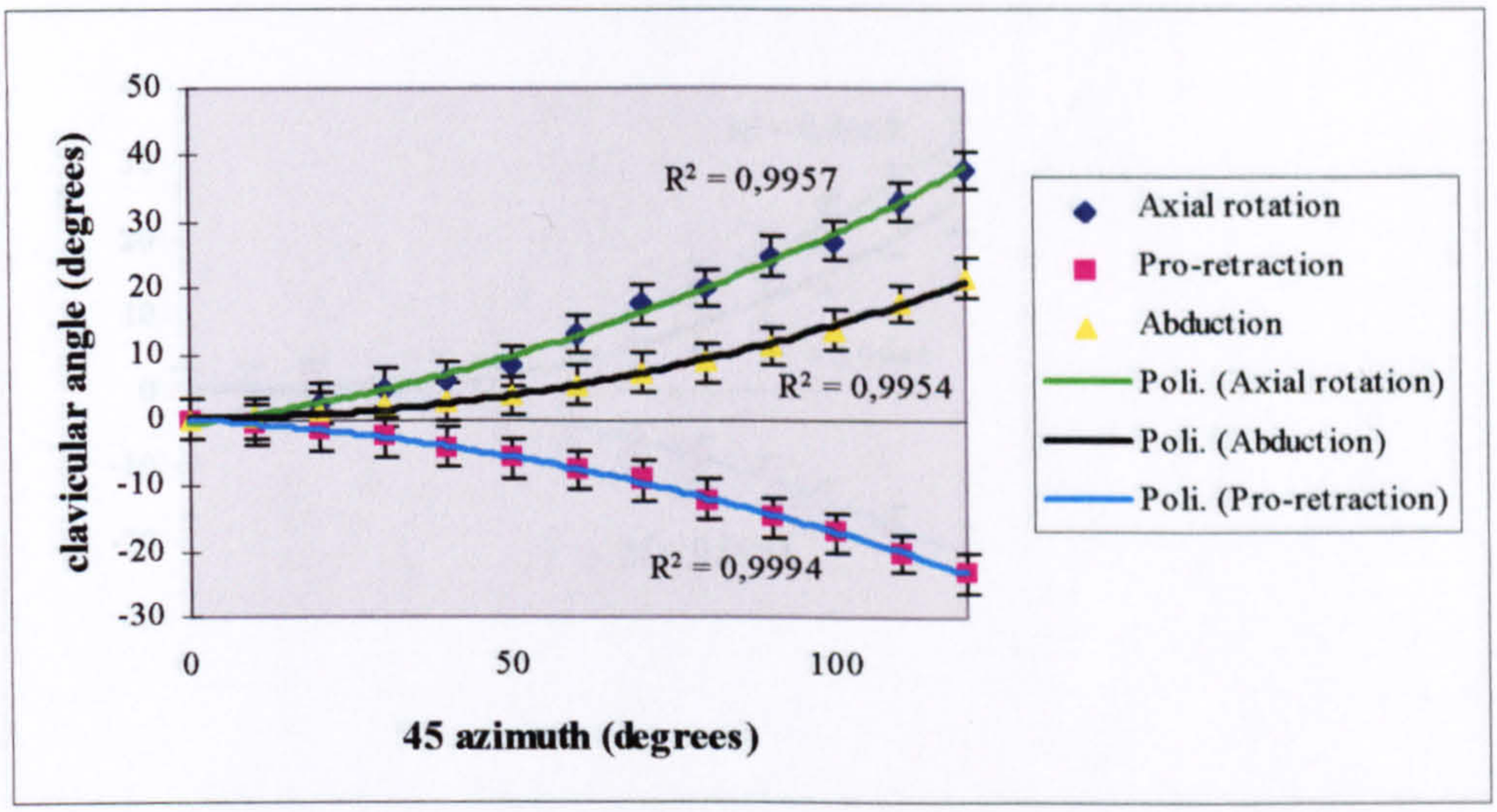

Figure 6.16 a: *Subject 1 (L/R=2,46) - 45 degrees azimuth observer 1*

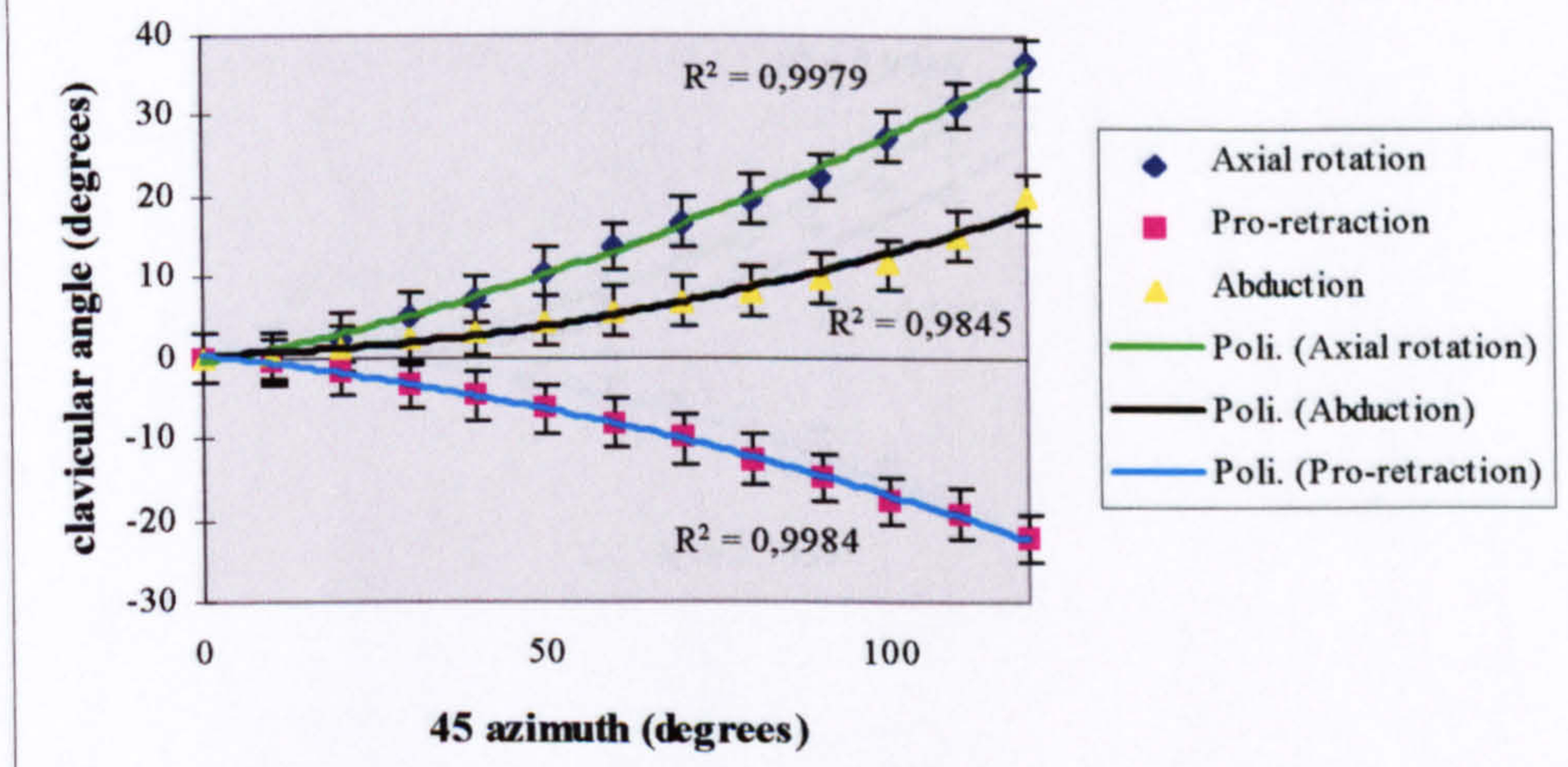

Figure 6.16 b: Subject 1 *(L/R=2,46) - 45 degrees azimuth observer 2*

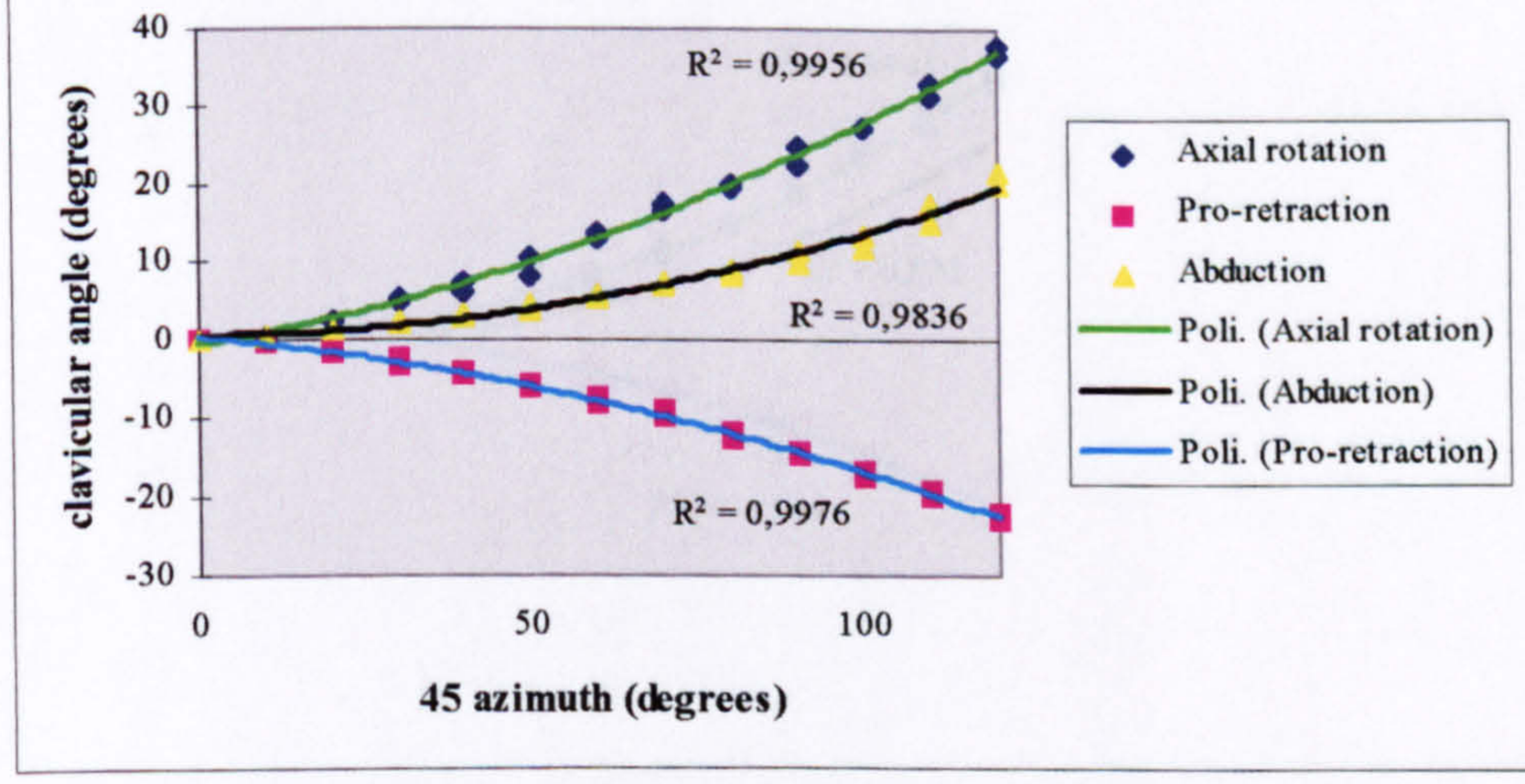

Figure 6.16 c: *Subject 1 (L/R=2,46) - 45 degrees azimuth inter observer*

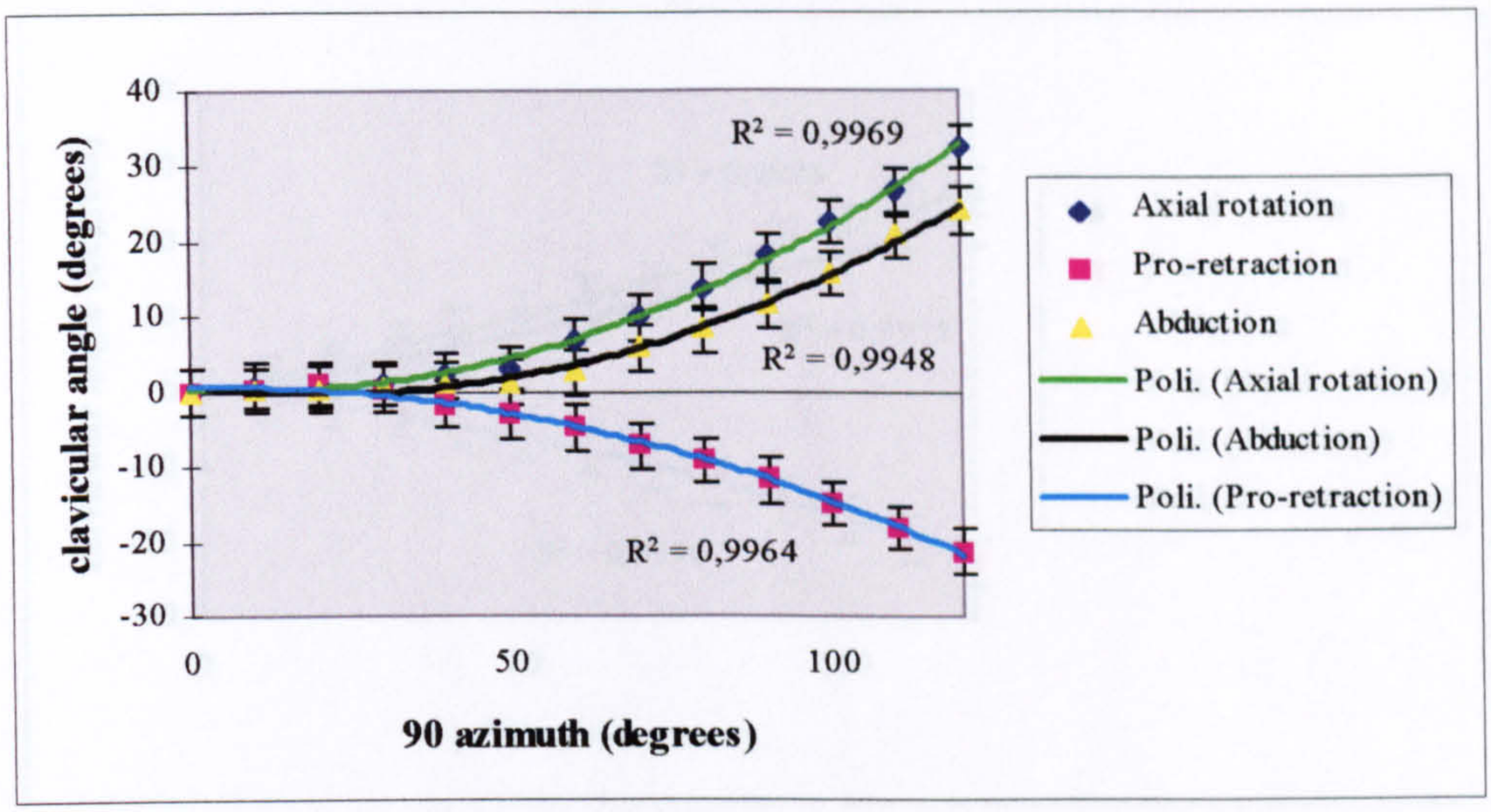

Figure 6.17 a: *Subject 1(L/R=2,46) - 90 degrees azimuth observer 1*

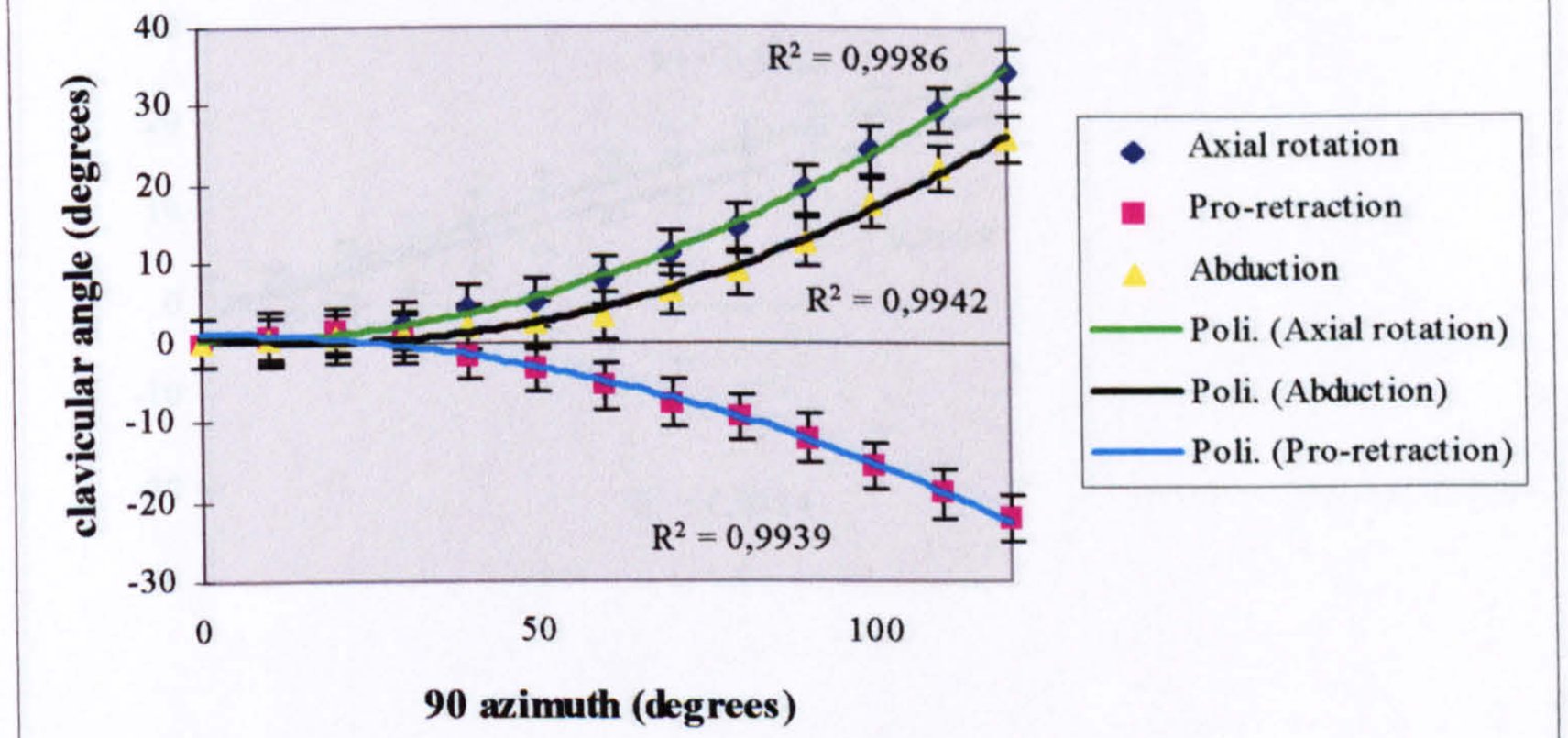

Figure 6.17 b: *Subject 1(L/R=2,46) - 90 degrees azimuth observer 2*

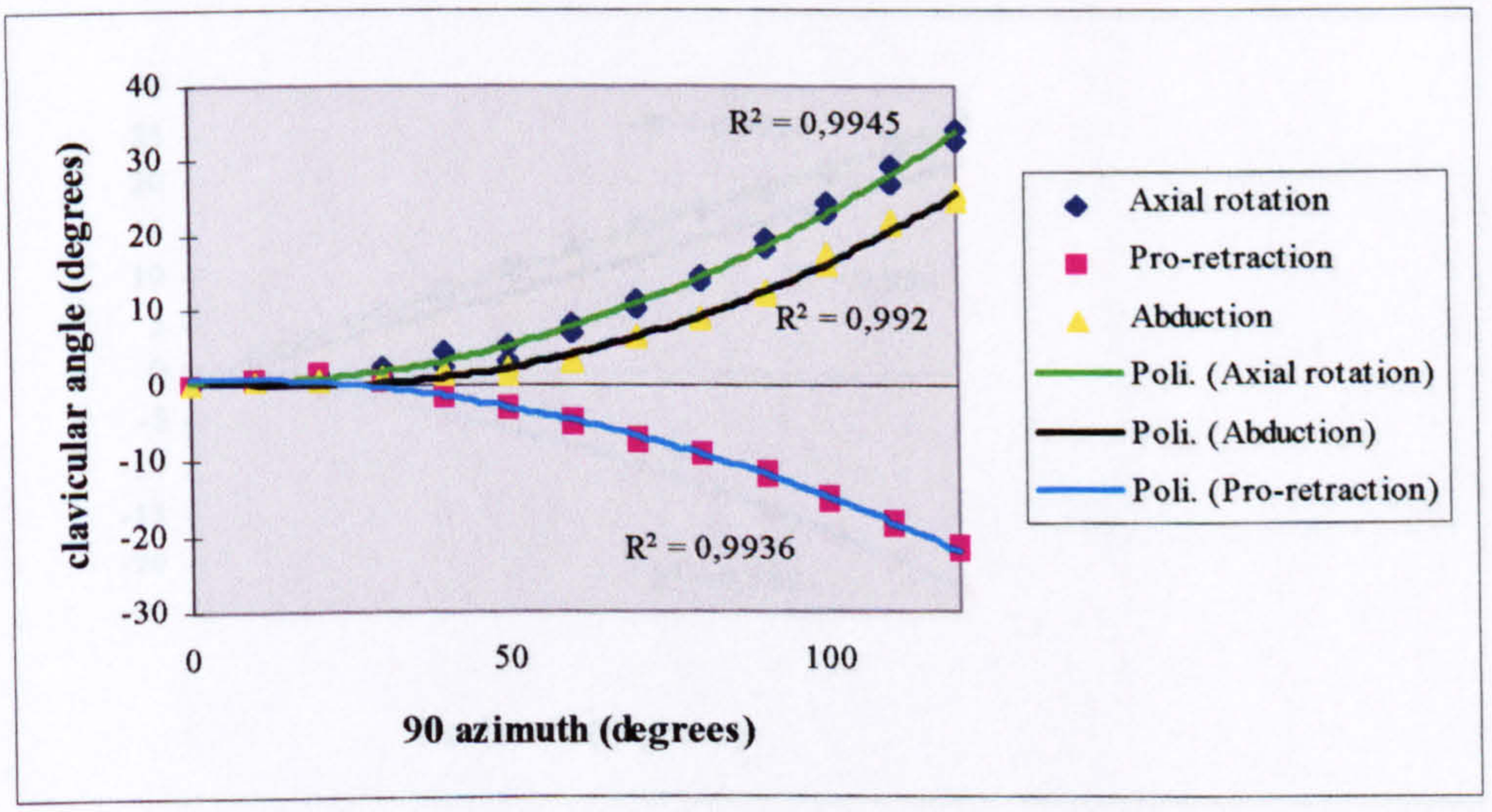

Figure 6.17 c: *Subject 1 (L/R=2,46) - 90 degrees azimuth inter observer*

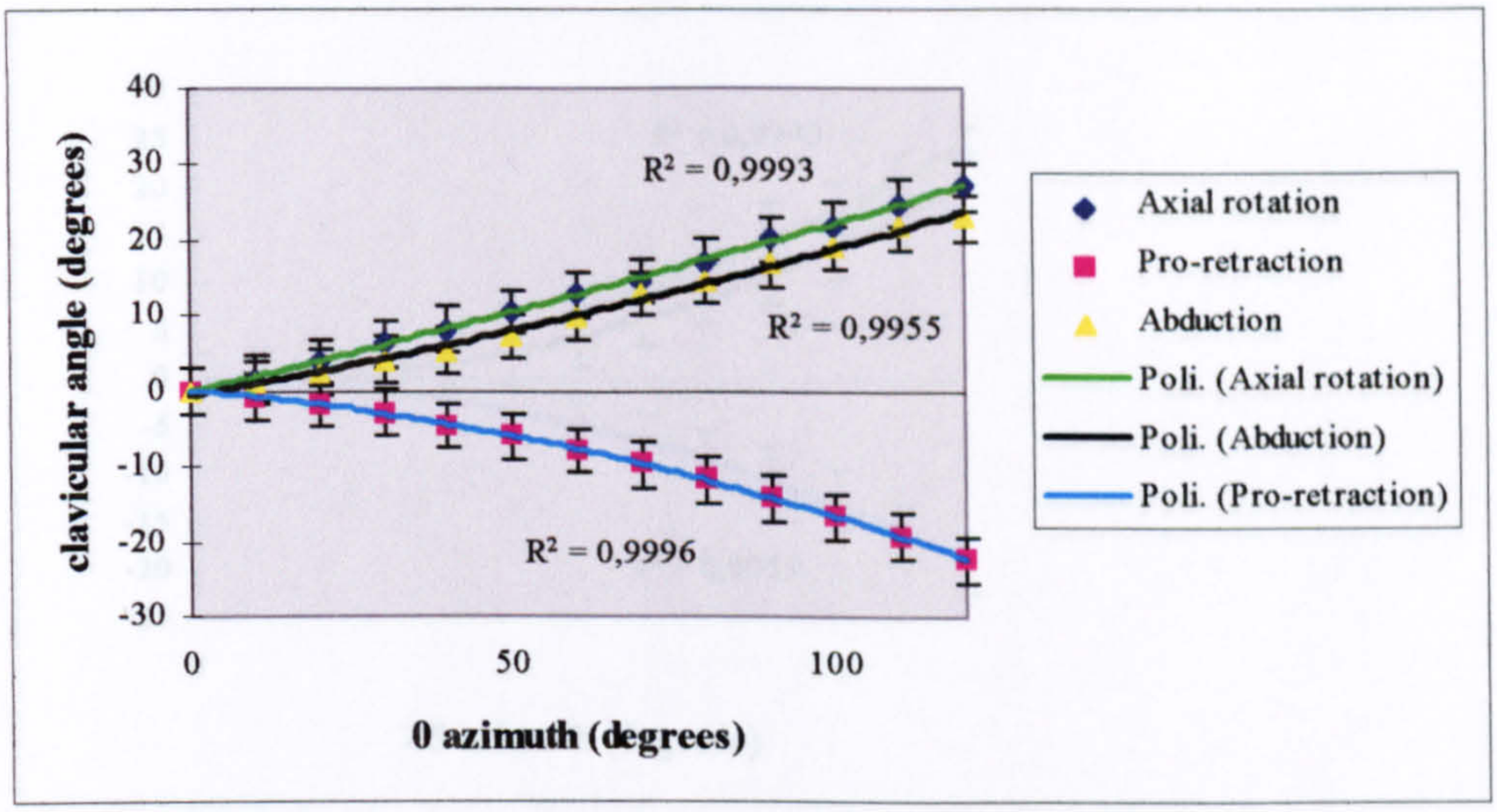

Fig. 6.18 a: *Subject 2 (L/R=1.6) - 0 degrees azimuth observer 1*

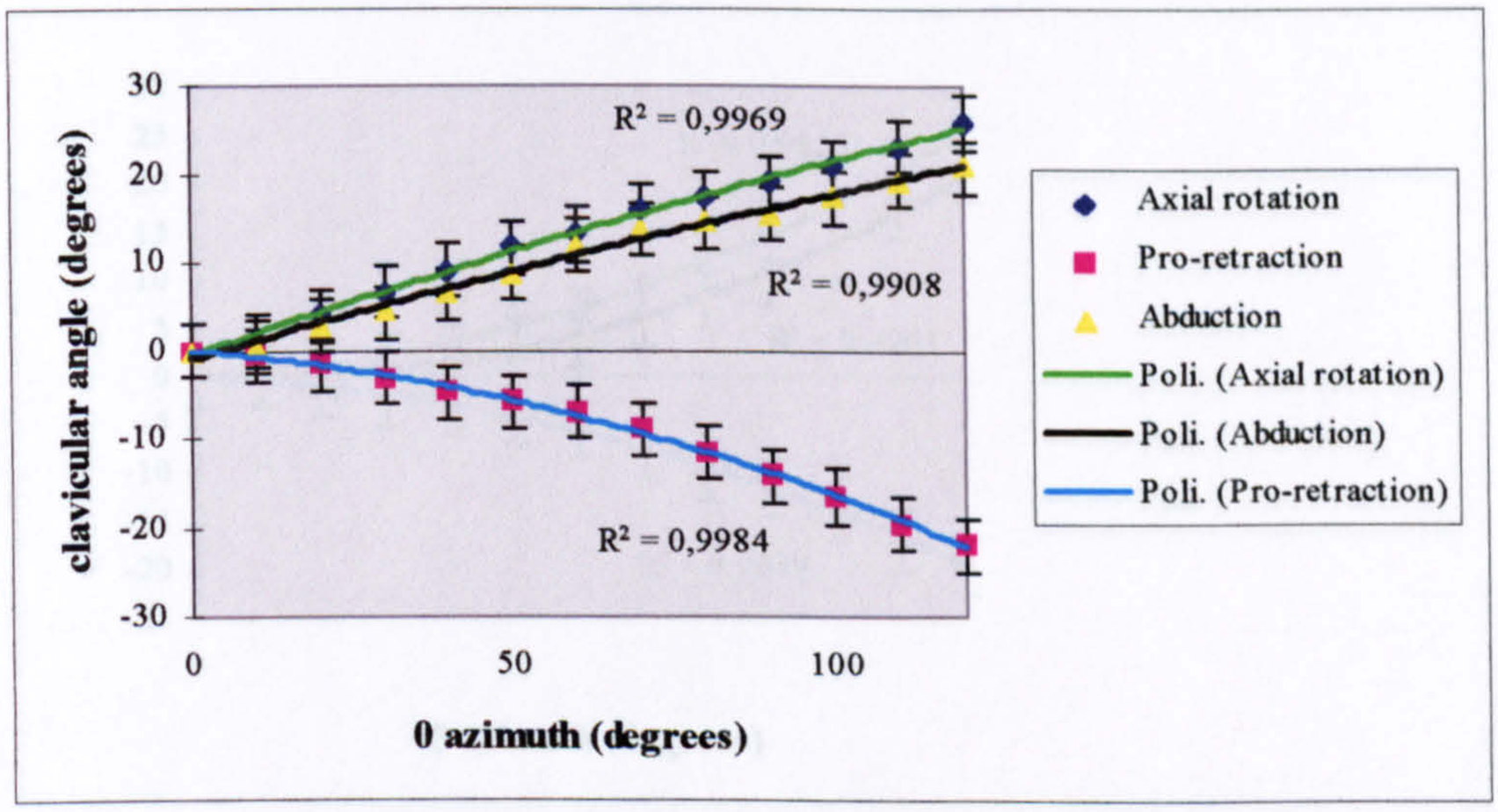

Fig. 6.18 b: *Subject 2 (L/R=1.6)- 0 degrees azimuth observer 2*

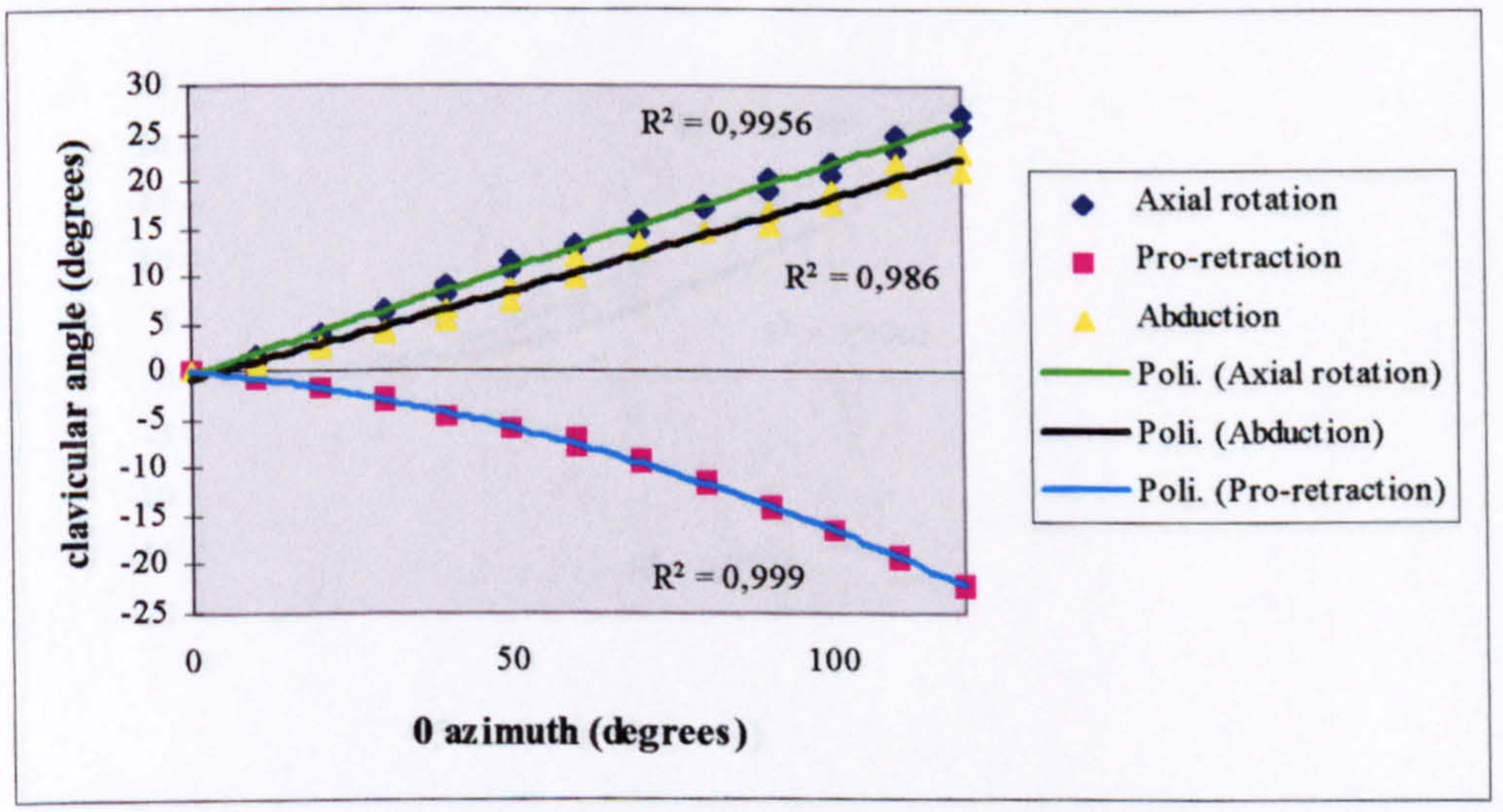

Fig. 6.18 c: *Subject 2 (L/R=1.6) - 0 degrees azimuth inter observer*

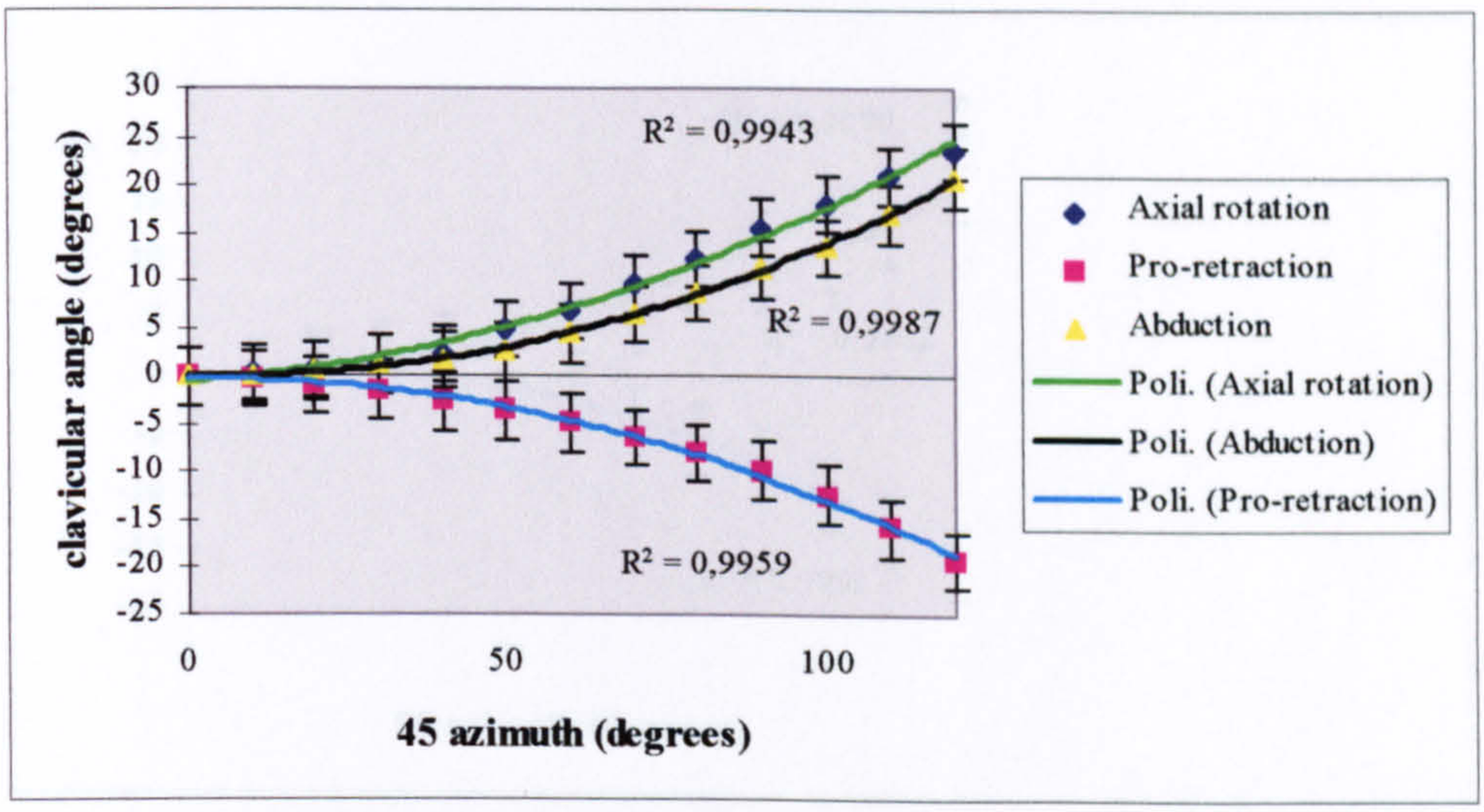

Fig. 6.19 a: *Subject 2 (L/R=1.6) - 45 degrees azimuth observer 1*

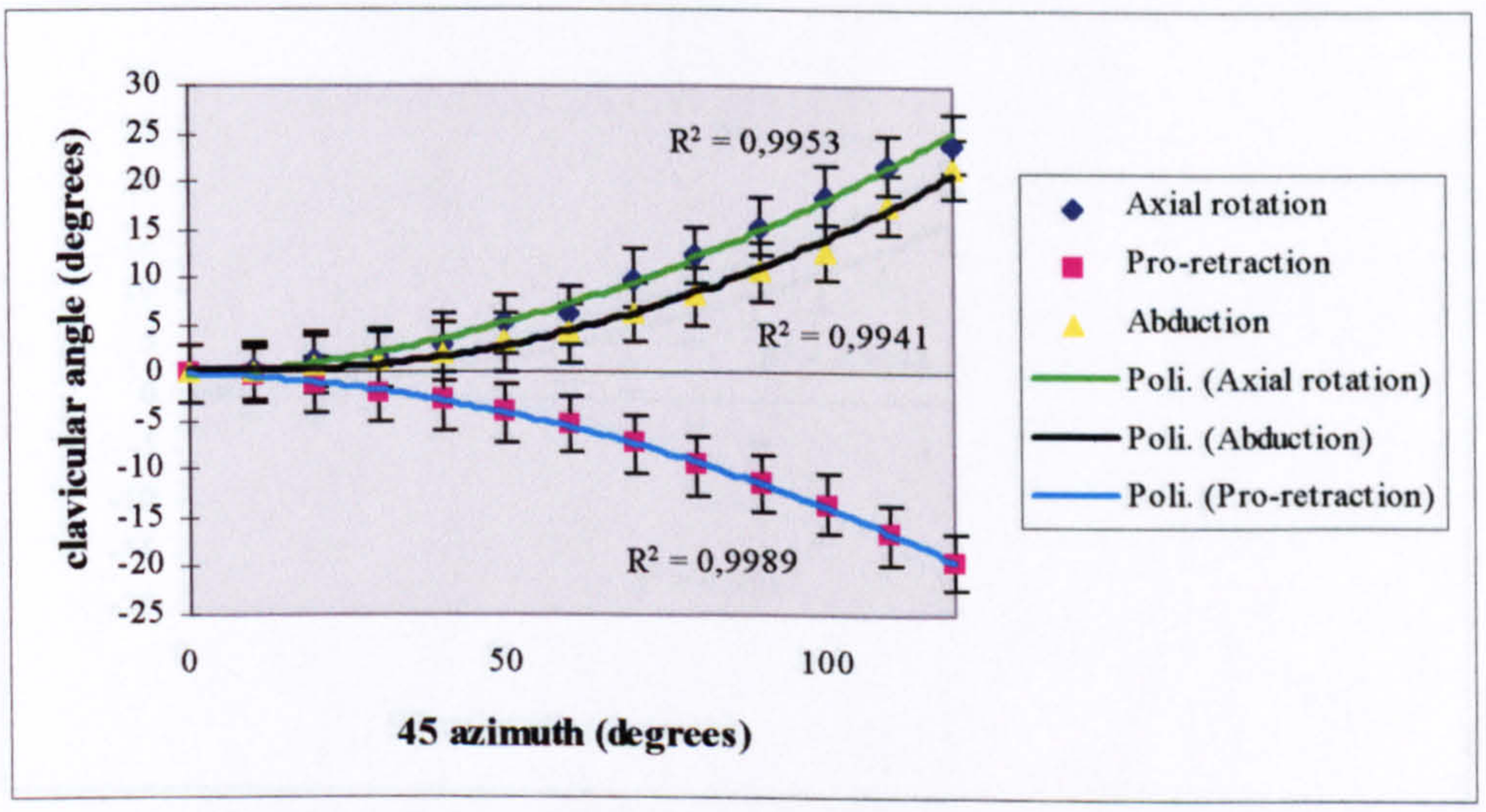

Fig. 6.19 b: *Subject 2 (L/R=1.6) - 45 degrees azimuth observer 2*

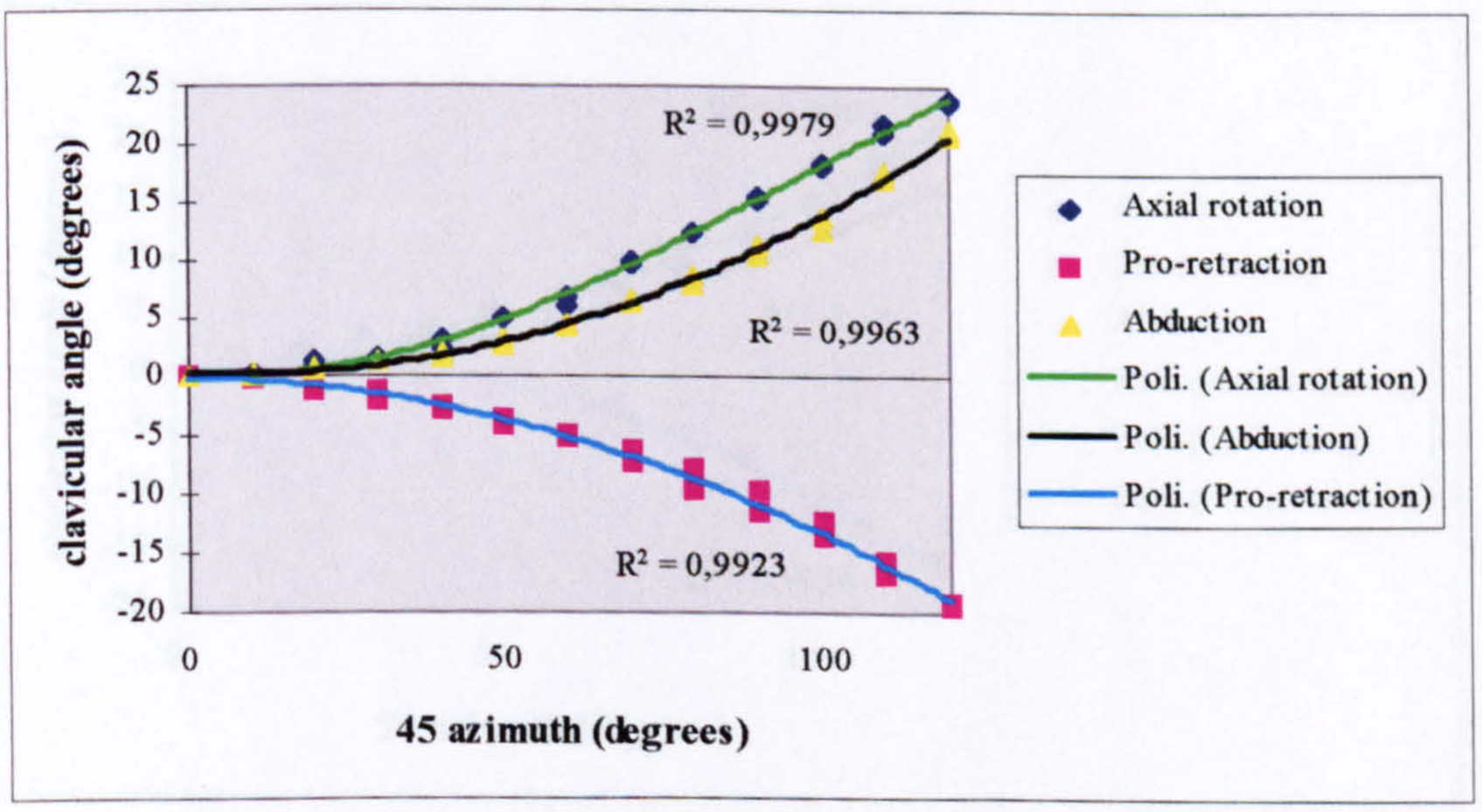

Fig. 6.19 c *Subject 2 (L/R=1.6) - 45 degrees azimuth inter observer*

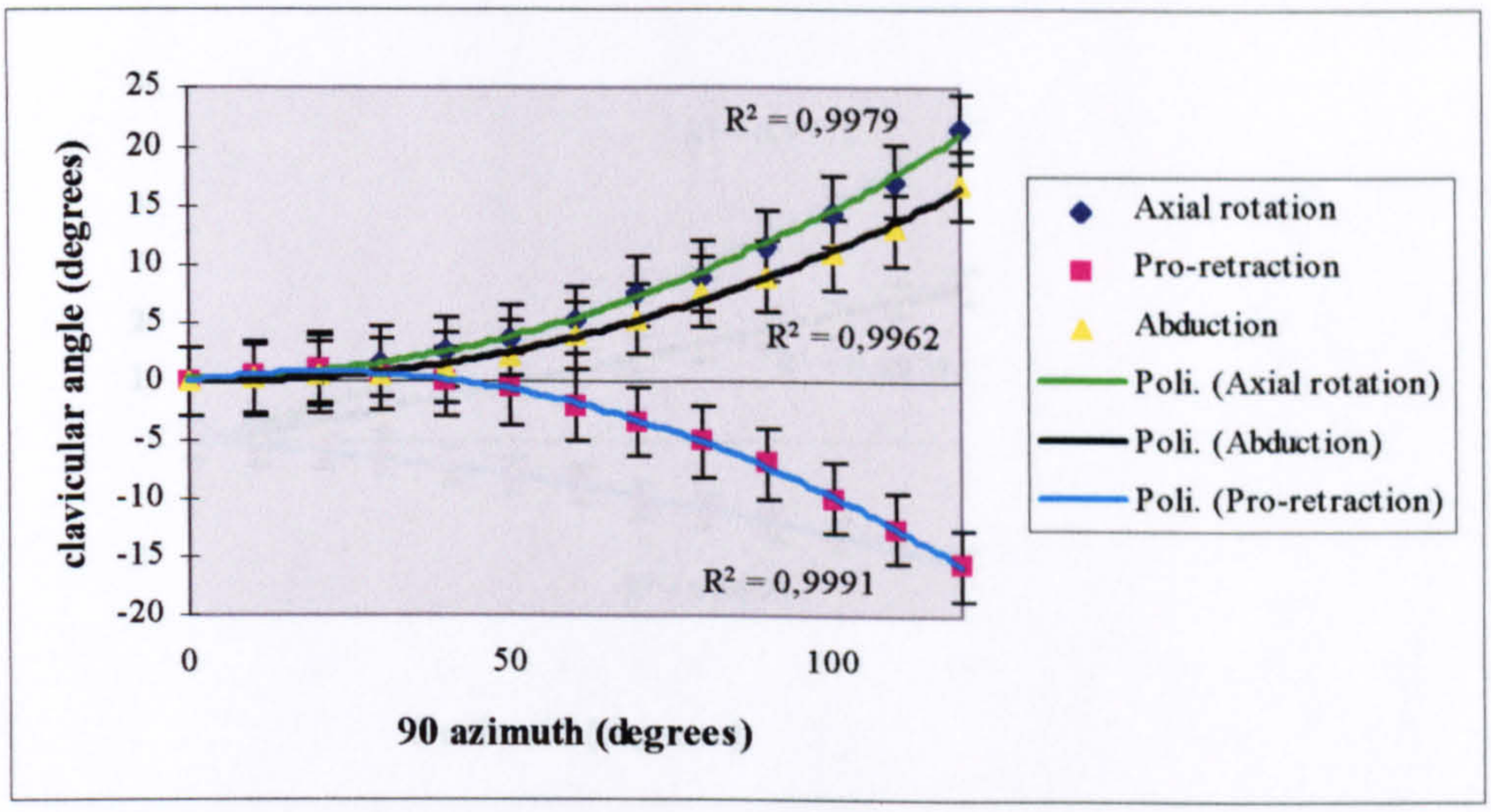

Fig. 6.20 a: *Subject 2 (L/R=1.6) - 90 degrees azimuth observer 1*

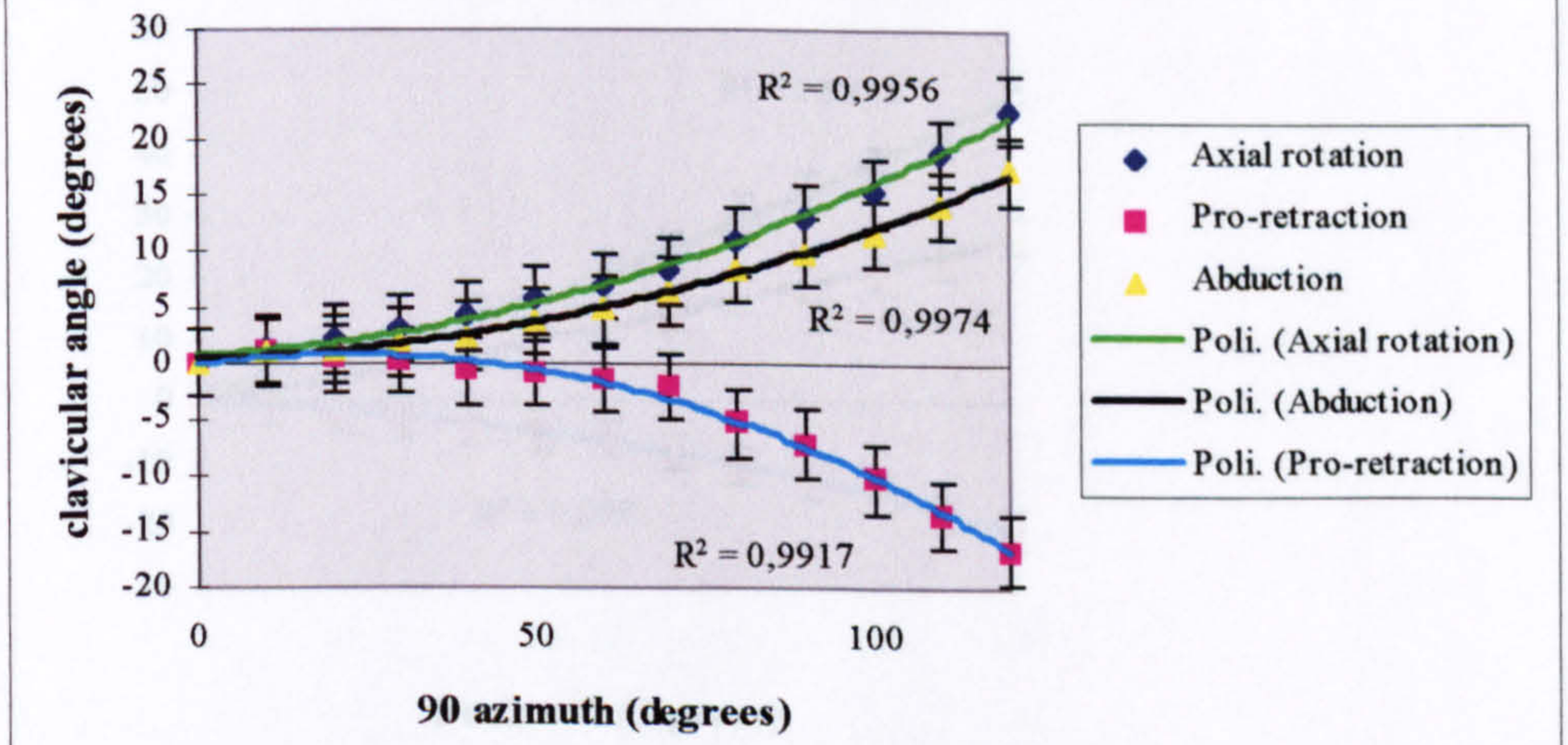

Fig. 6.20 b: *Subject 2 (L/R=1.6)- 90 degrees azimuth observer 2*

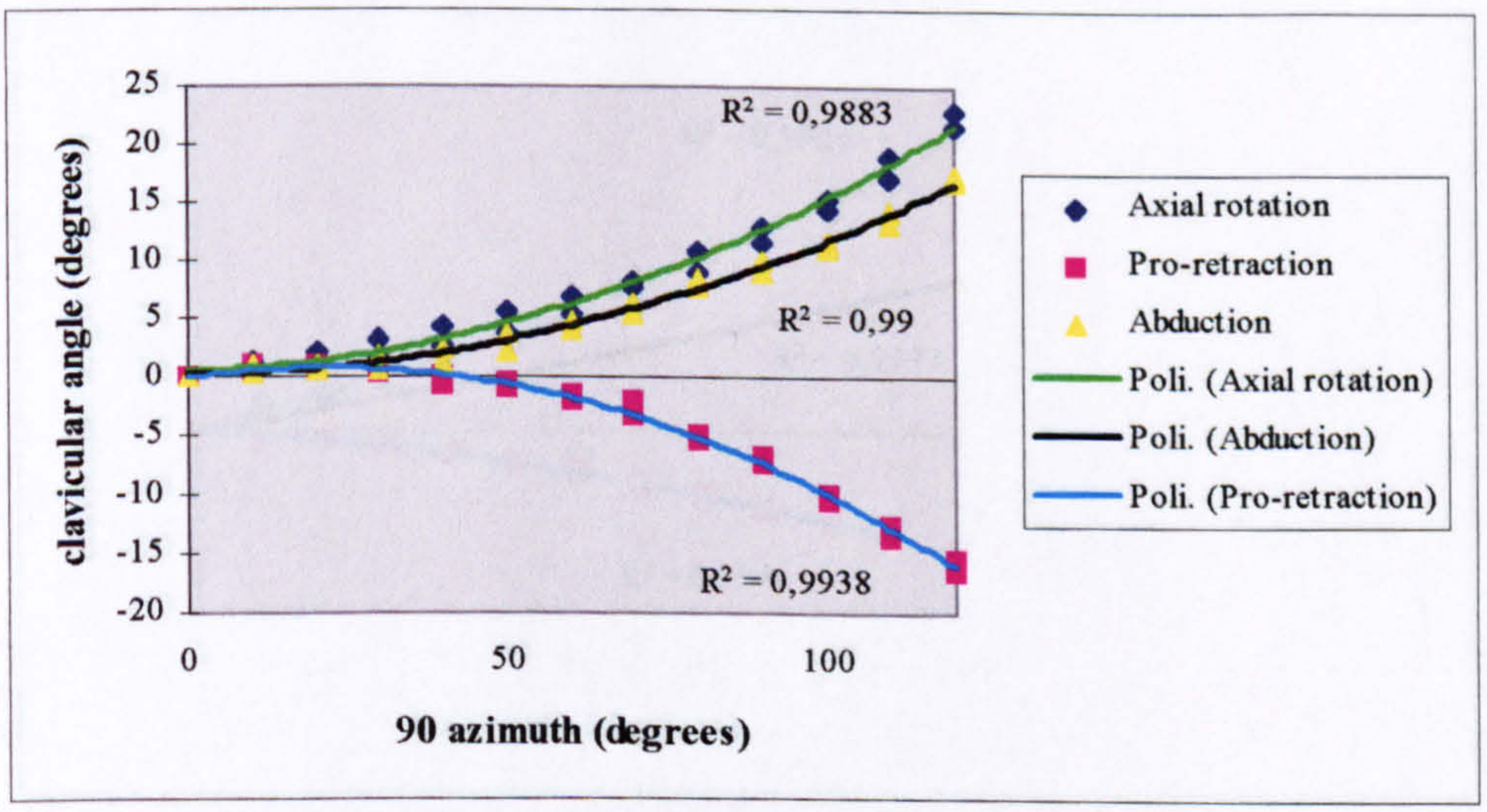

Fig. 6.20 c: *Subject 2 (L/R=1.6) - 90 degrees azimuth inter observer*

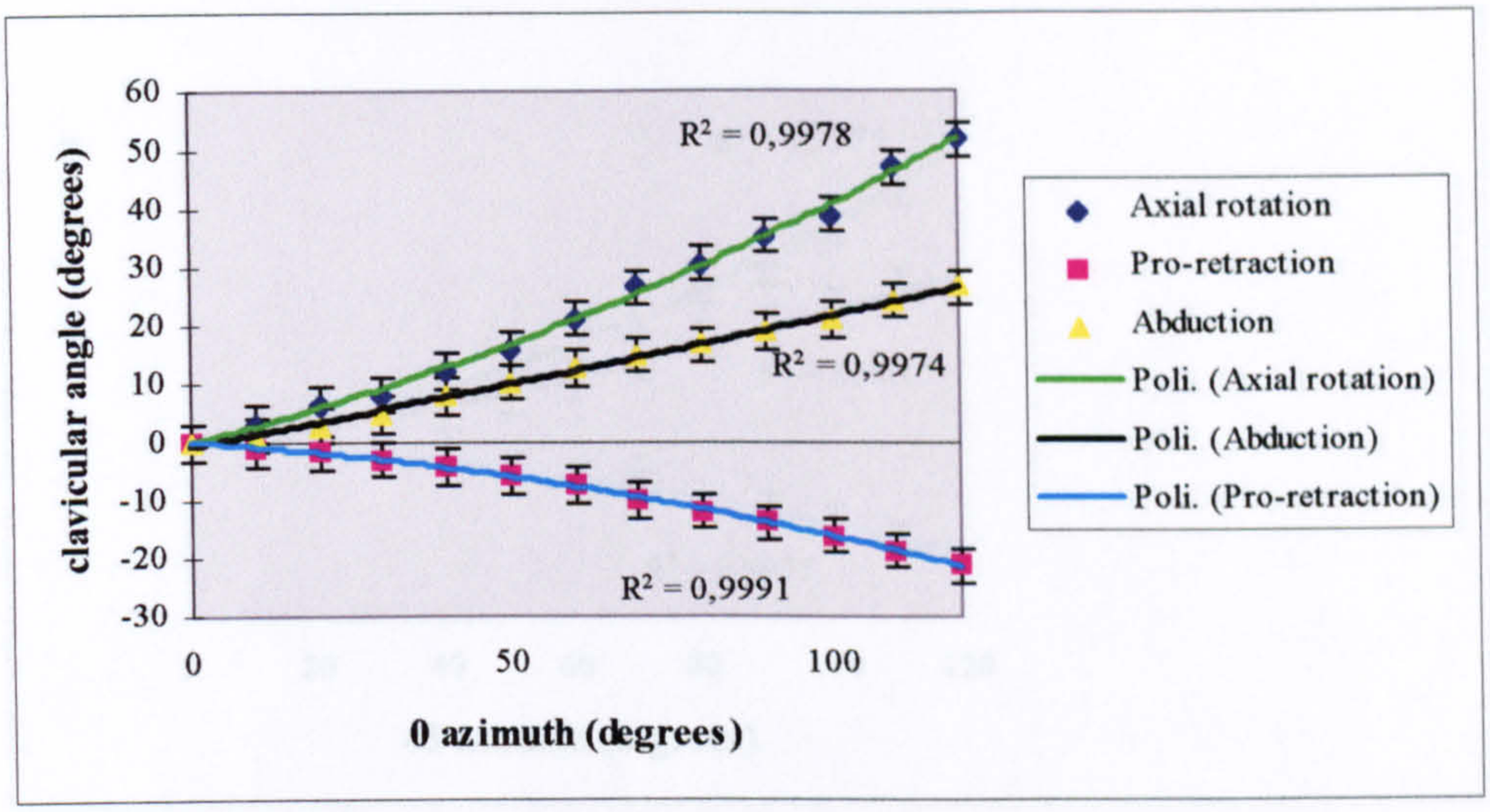

Fig. 6.21 a: *Subject 3 (L/R=2.74) - 0 degrees azimuth observer 1*

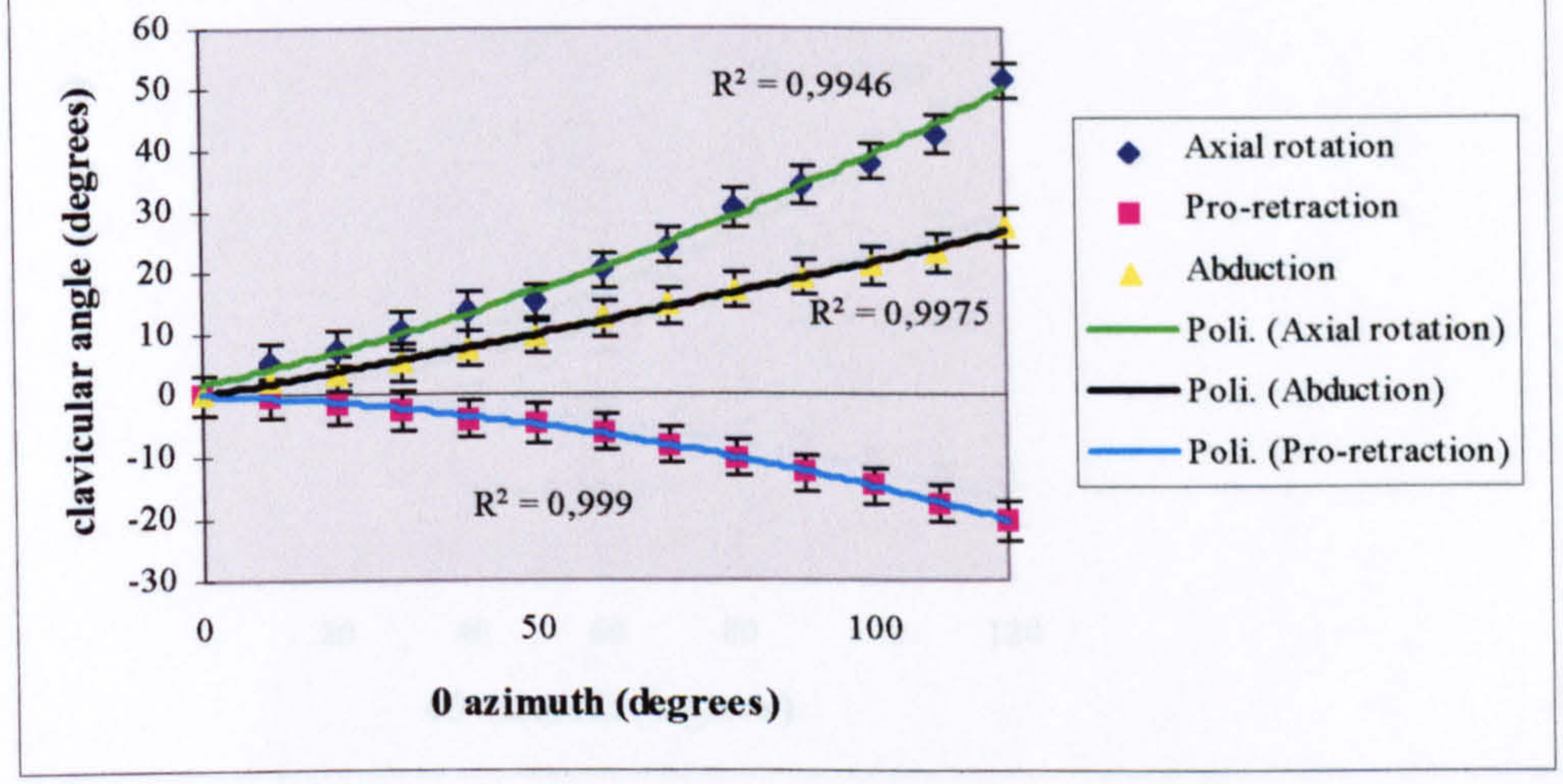

Fig. 6.21 b: *Subject 3 (L/R=2.74) - 0 degrees azimuth observer 2*

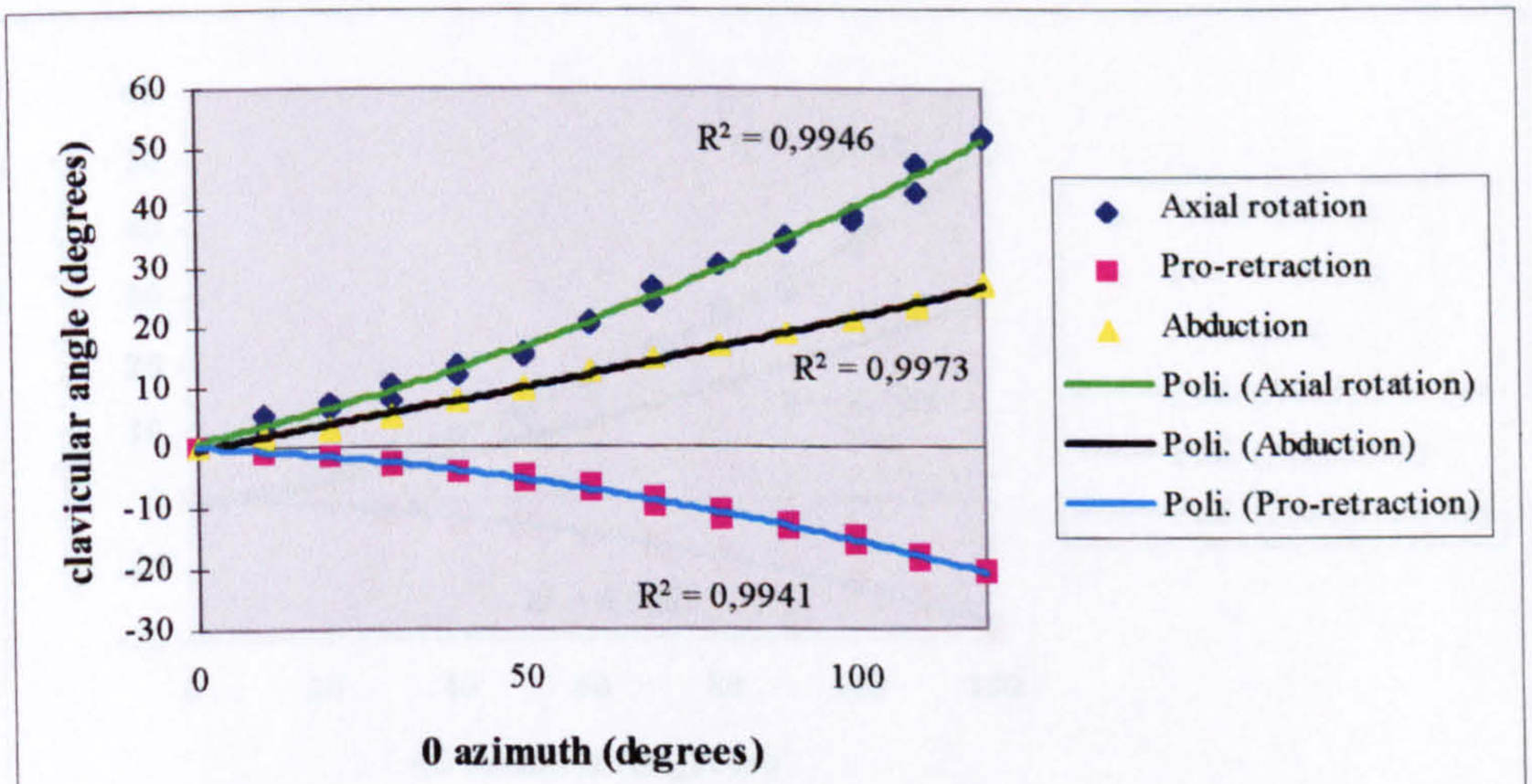

Fig. 6.21 c: *Subject 3 (L/R=2.74) -0 degrees azimuth inter observer*

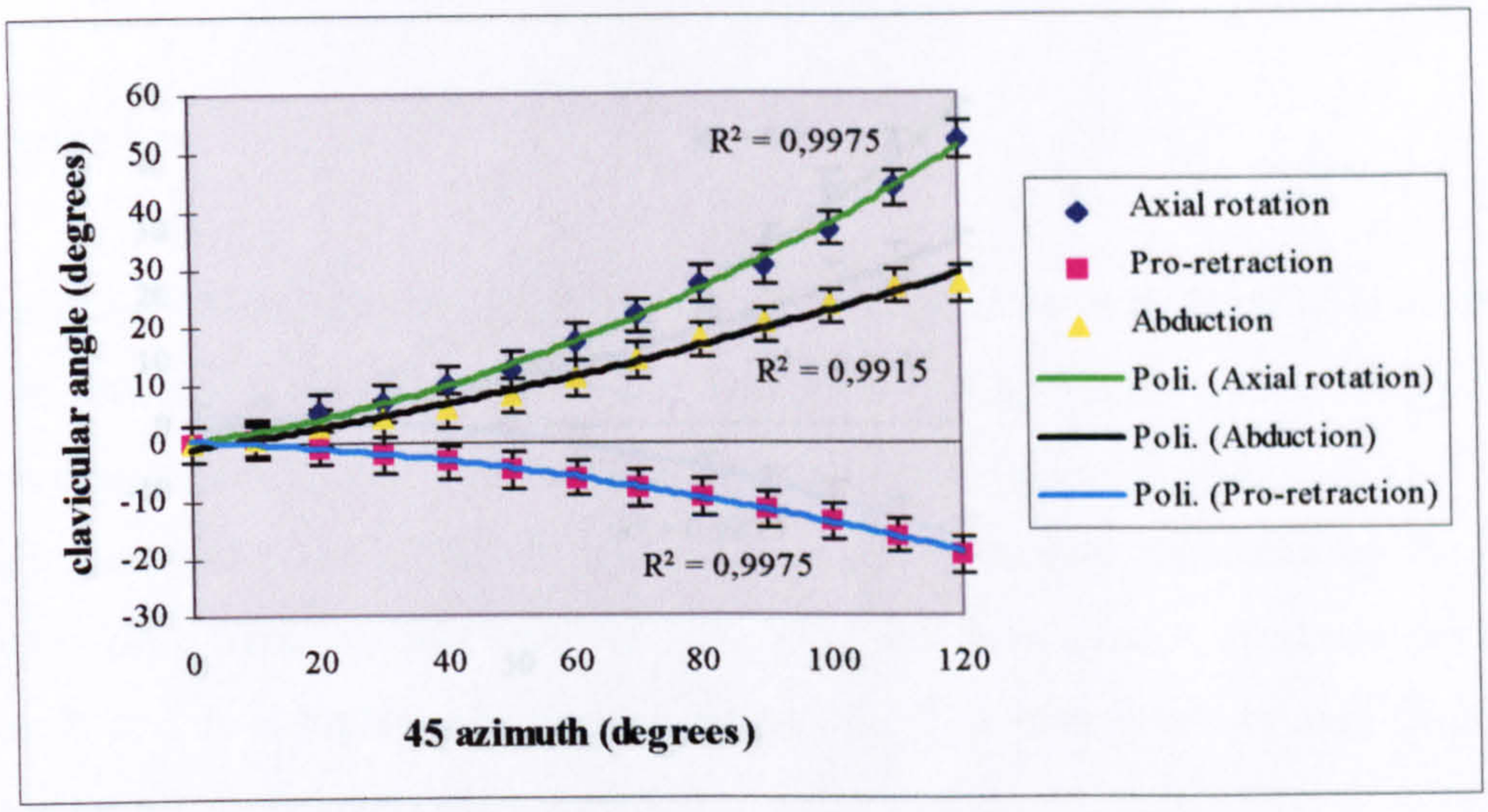

Fig. 6.22 a *Subject 3 (L/R=2.74) - 45 degrees azimuth observer 1*

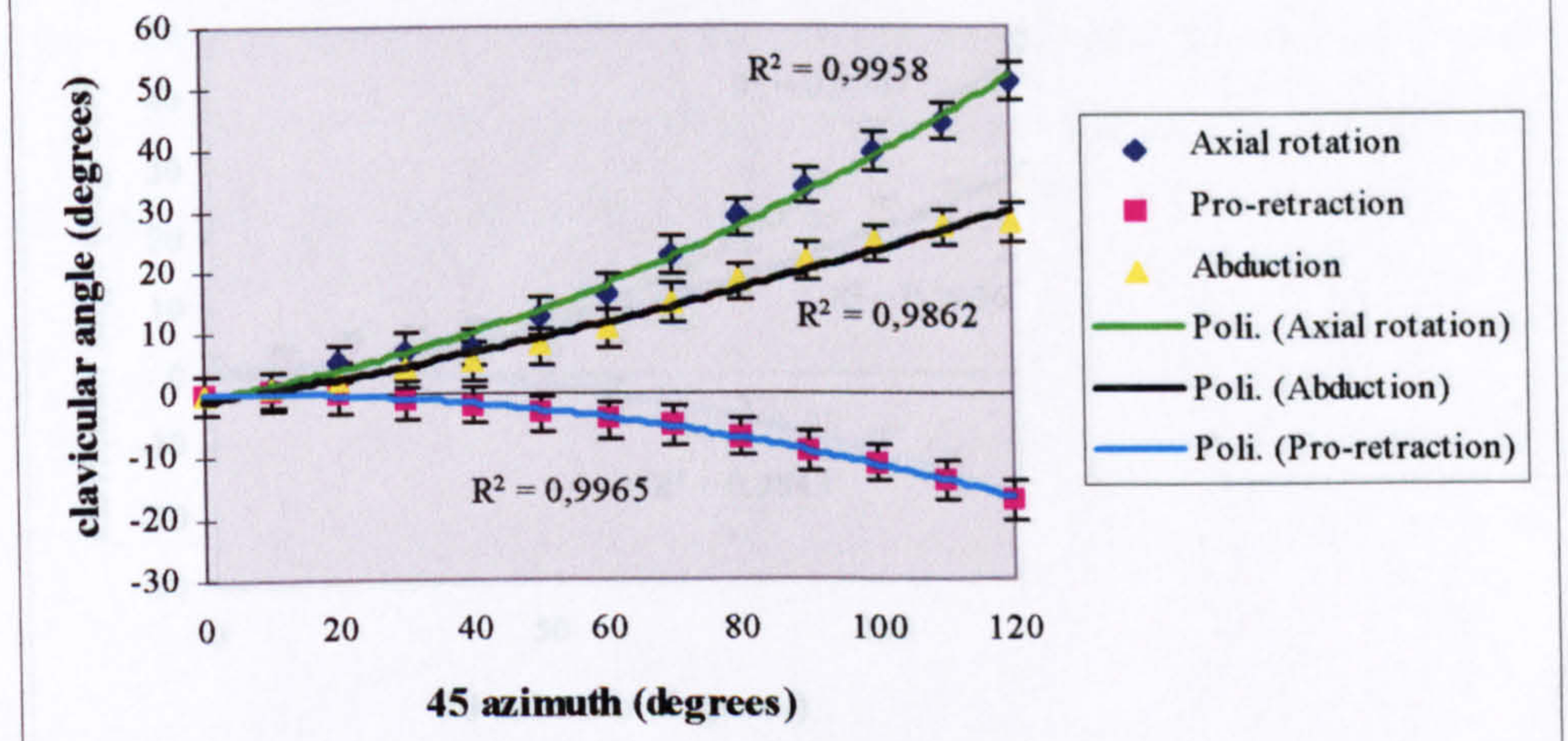

Fig. 6.22 b *Subject 3 (L/R=2.74) - 45 degrees azimuth observer 2*

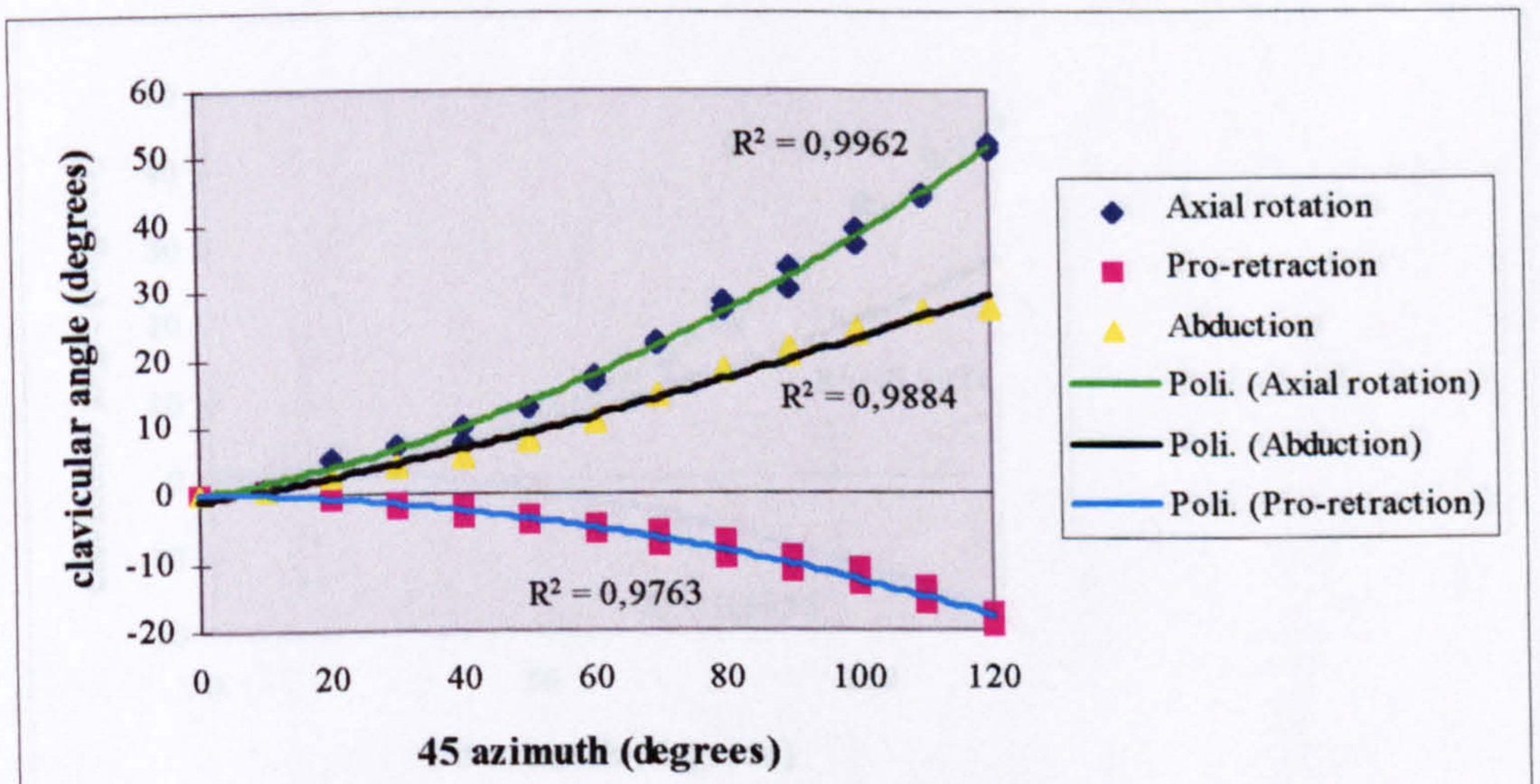

Fig. 6.22 c *Subject 3 (L/R=2.74) - 45 degrees azimuth inter observer*

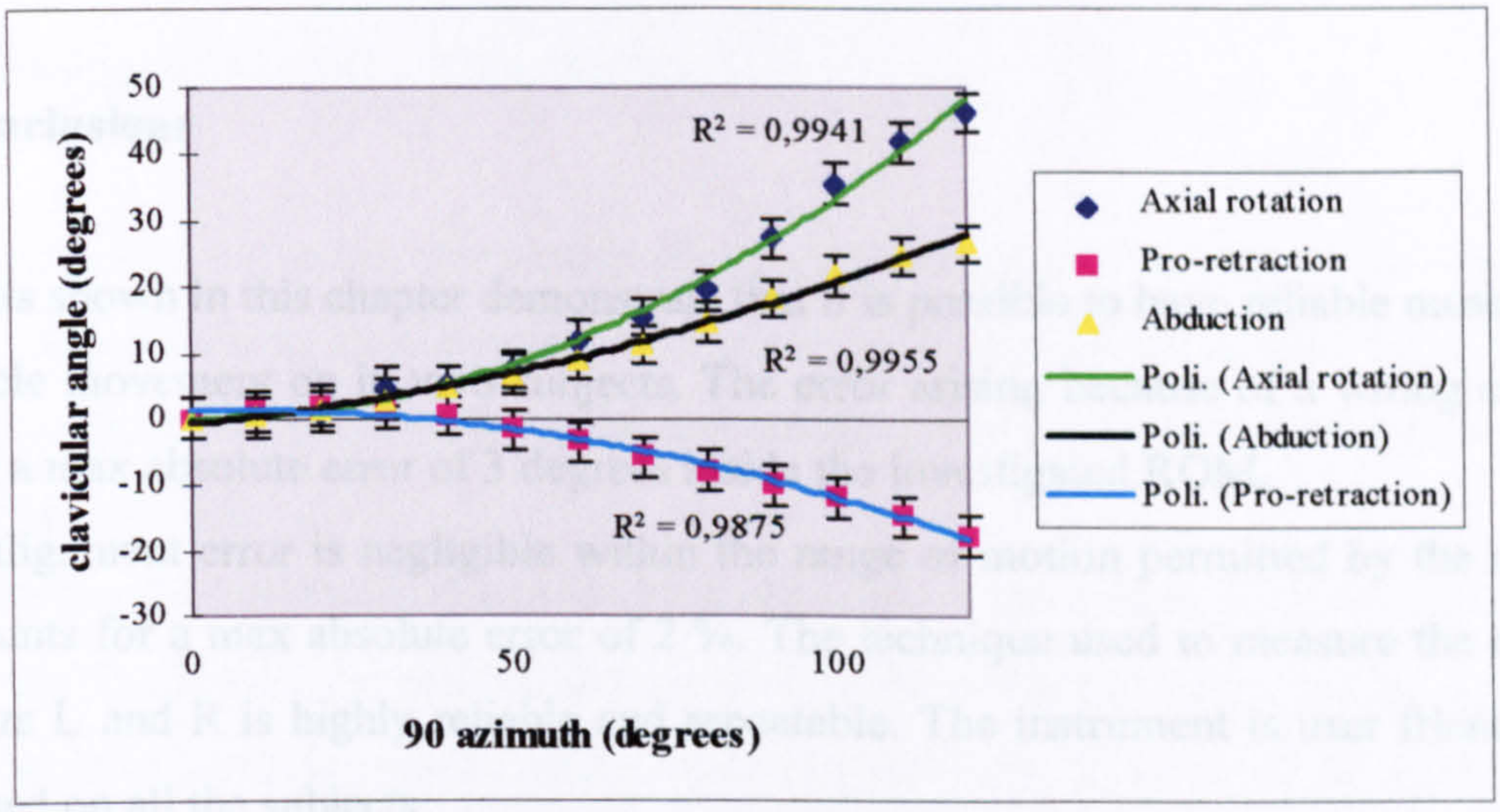

Fig. 6.23 a *Subject 3 (L/R=2.74) - 90 degrees azimuth observer 1*

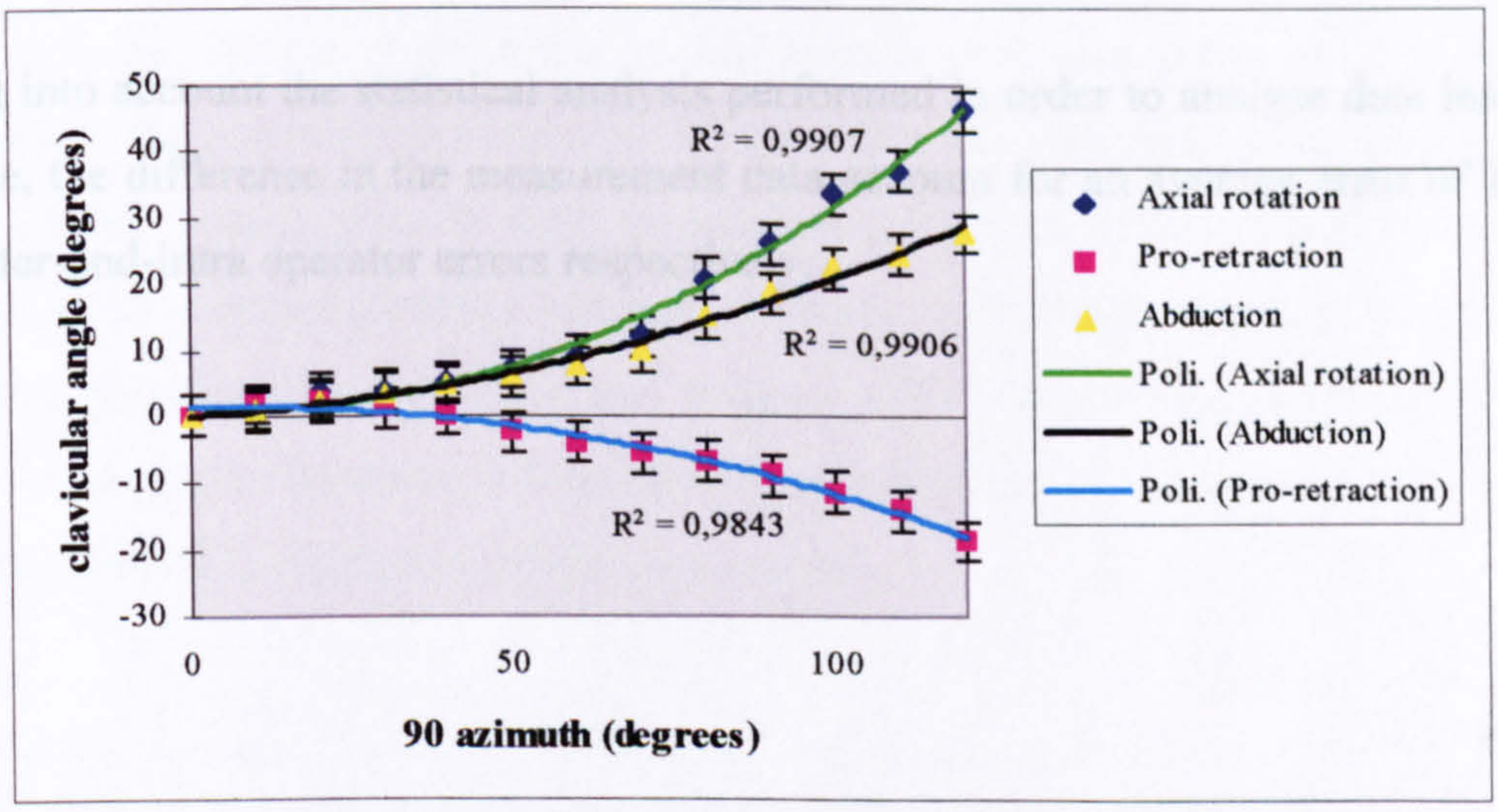

Fig. 6.23 b *Subject 3 (L/R=2.74) - 90 degrees azimuth observer 2*

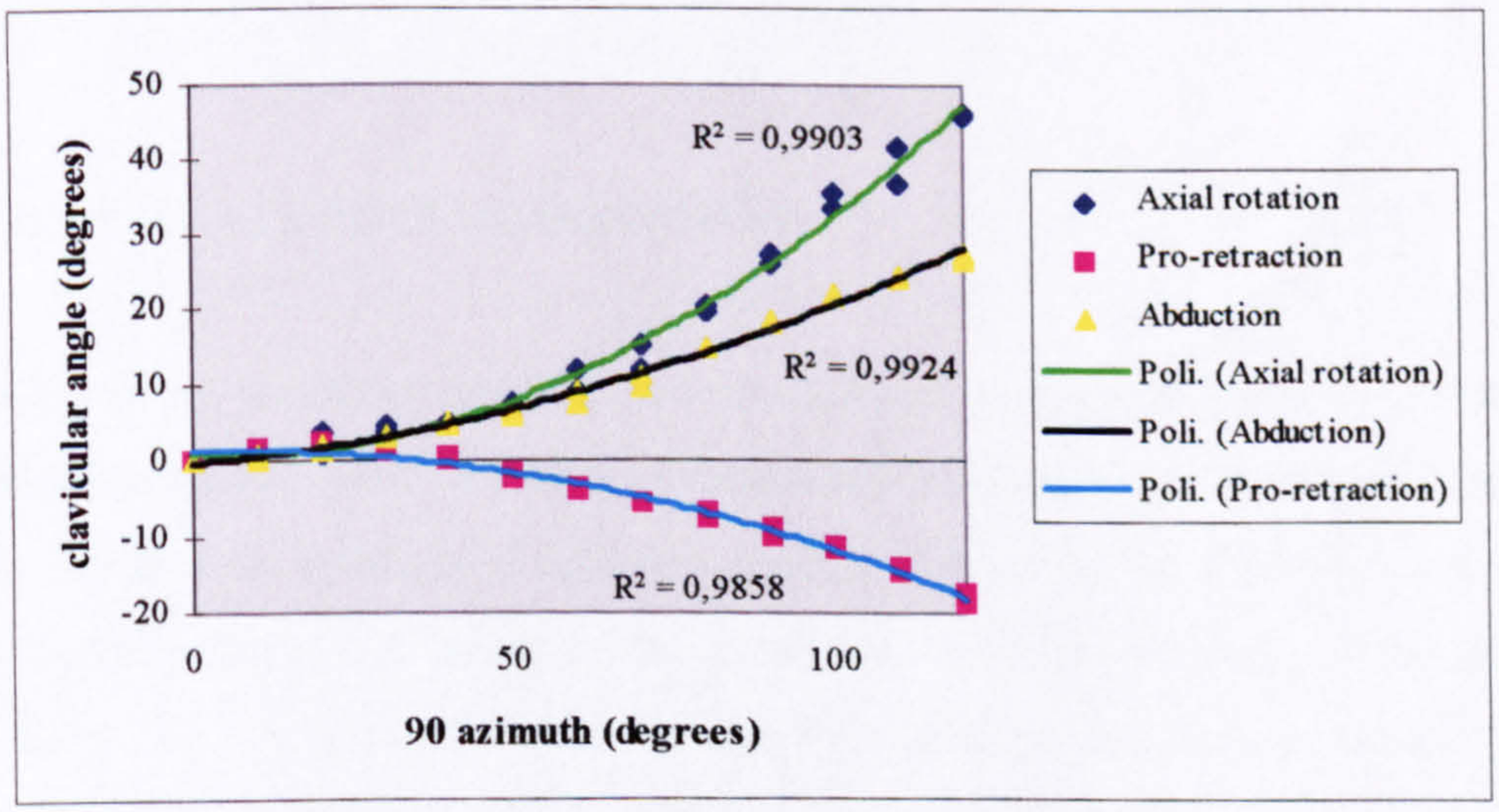

Fig. 6.23 c *Subject 3 (L/R=2.1) - 90 degrees azimuth inter observer*

6.6 Conclusions

The results shown in this chapter demonstrate that it is possible to have reliable measures of the clavicle movement on in vivo subjects. The error arising because of a wrong estimate results in a max absolute error of 3 degrees inside the investigated ROM.

The misalignment error is negligible within the range of motion permitted by the clavicle and accounts for a max absolute error of 2 %. The technique used to measure the clavicle parameters L and R is highly reliable and repeatable. The instrument is user friendly and can be used on all the subjects.

By taking into account the statistical analysis performed in order to analyse data inside the workspace, the difference in the measurement data account for an average error of 1% and 3% for inter-and-intra operator errors respectively.

7 Modelling of clavicle kinematics

The possibility to have information on the three-dimensional movements of the clavicle of "in vivo" subjects opens new avenues in clinical measurement. This may be either for diagnostic purposes or for quantifying the real outcome of a rehabilitative treatment after a functional impairment.

It is known that the clavicle is the most fractured bone of the human body and because of its anatomical position, in almost all the cases no orthopaedic treatment can be applied to fix the bone. This technique can be easily applied to highlight the effect of such therapeutic choice with a comparison between the healthy and affected clavicle after treatment.

Despite the many clinical applications in the neurological and orthopaedic fields, the measurement of the clavicle rotations at the SC joint fills the existing knowledge gap on the kinematic of the human arm. In fact, in order to obtain complete information on the kinematics of the shoulder complex, existing measurement methods can now be applied to investigate in depth on this matter. To this purpose a 3D interpolation technique has been applied to highlight the behaviour of the clavicle as a function of the humeral position in a subset of the allowable workspace of the human arm.

7.1 Development of a Mathematical Model

In order to develop a predictive model based on a subject database of the movement of the clavicle, an investigation based on experimental trials performed on 10 subjects has been carried out. It has been possible to compare clavicle kinematics on different subjects for identical humeral position and to extract the mean and confident intervals of the resulting motion patterns. By analysing the data set and by applying a regression technique, the

mathematical model is generated which accepts the humeral coordinates as inputs and provides a prediction of the movement of the clavicle expressed in a polynomial form.

A subset of the humeral workspace considered representative for daily activity movements has been considered. In order to provide a graphical representation of the workspace examined, in the assumption that the gleno-humeral joint can be represented as a pure 3 degrees of freedom rotational joint fixed in space, we can locate a sphere whose centre is coincident with the GH joint centre.

With reference to figure 7.1, the examined workspace is shown. Starting from the neutral zero position and by using the hierarchical model presented in section 6, the following position have been recorded:

- 3 repetitive measurements at 0 degress azimuth for each of the two observers within a ROM of 0-120 degrees with constant intervals of 10 degrees;
- 3 repetitive measurement at 45 degrees azimuth for each of the two observers within a ROM of 0-20 degrees with constant intervals of 10 degrees;
- 3 repetitive measurements at 90 degrees azimuth for each of the two observers within a ROM of 0-20 degrees with constant intervals of 10 degrees.

On each subject 216 static measurements, which have been analysed through a standard software package (Excel 97), have been performed using the hierarchical model presented in Chapter 6.

The mean value obtained for each subject has been compared with the mean values of the other subjects obtaining a mean curve for each azimuth position recorded.

The angles of the clavicle can therefore be expressed as surfaces, which are functions of the humeral position. In order to have evidence of the dependence, if any, of the clavicle

motion as a function of the humeral internal and external rotation the following experiment has been carried out on 4 subjects. The sterno-clavicular detector has been assembled as per figures 6.11, 6.12 and for each humeral position recorded inside the workspace according to the method above described, the subject has been asked to perform a humeral internal and external rotation with the elbow 90 degrees flexed while the operator by using a palpation method maintained the detector in constant contact with the bony landmarks.

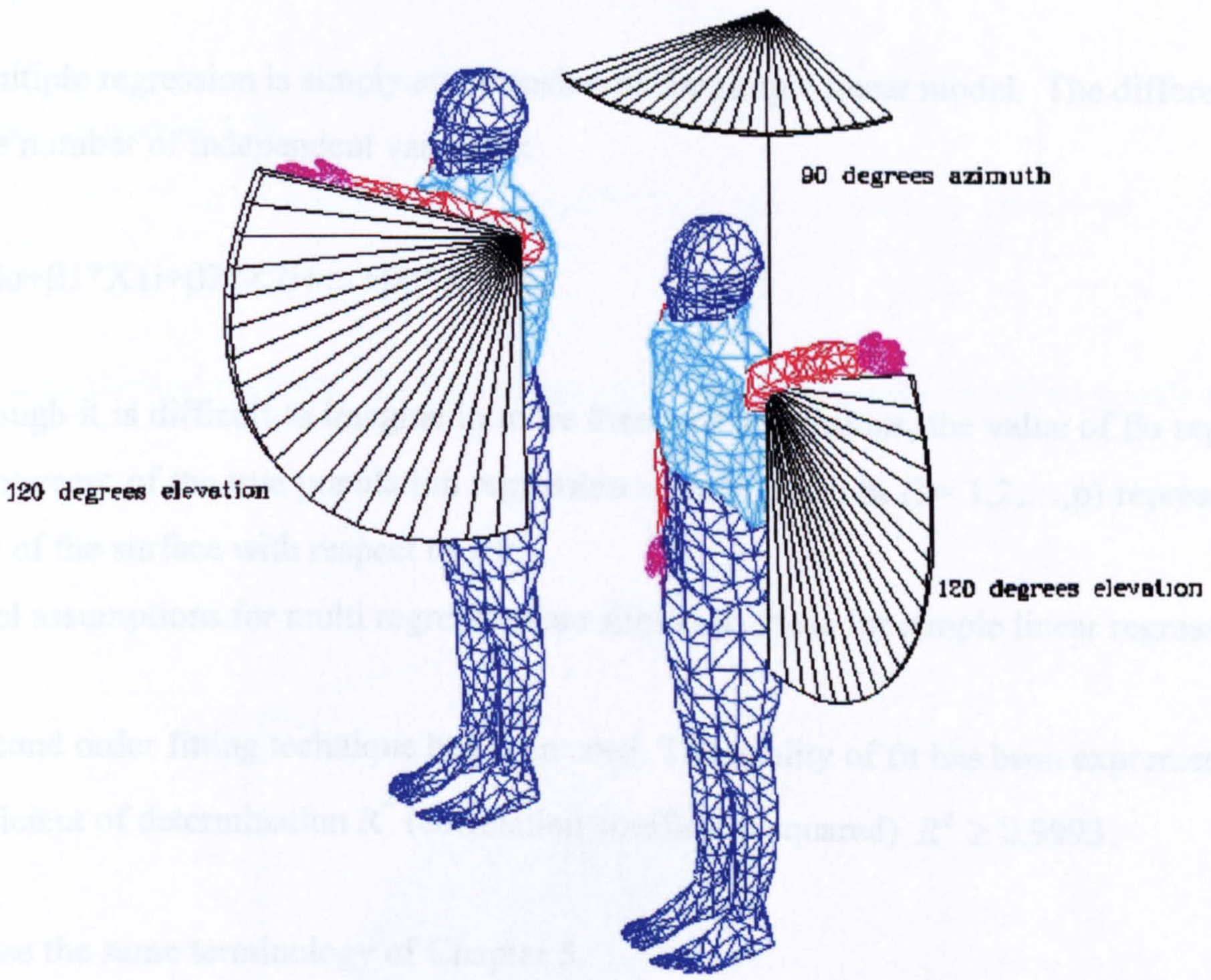

Figure 7.1 *Examined workspace (Mannequin)*

The results obtained have shown an independence of the clavicle motion from the humeral internal and external rotation, which has led to the motion equations, which express in a polynomial form the clavicle rotations as a function of the humeral motion. All the above data are given in Chapter 12.

7.2 Data Collection

The objectives pursued were to collect a data set representative of the workspace of the clavicle.

A second order fit polynomial multi-regression technique has been applied through a standard software package (MATHCAD) whose code is given in Appendix C.

By using multiple regression we can express the three clavicle rotations as functions of the two humeral rotations in a polynomial form.

A multiple regression is simply an extension of the simple linear model. The difference lies in the number of independent variables:

$$Yi=\beta o+\beta 1*X1i+\beta 2*X2i+\ldots+\beta p*Xpi+\varepsilon i$$

Although it is difficult to imagine in more than two dimensions, the value of βo represents the intercept of the true population regression surface. Each β_k (k= 1,2,…,p) represents the slope of the surface with respect to Xk.

Model assumptions for multi regression are similar to those for simple linear regression.

A second order fitting technique has been used. The quality of fit has been expressed by the coefficient of determination R^2 (correlation coefficient squared) $R^2 \geq 0.9993$.

We use the same terminology of Chapter 5.

α_r = clavicle axial rotation

α_a = clavicle adduction-abduction

α_t = clavicle azimuth

β = humeral elevation

γ = humeral azimuth

Axial rotation (equation 7.1):

$$\alpha_r = 1.38 \cdot 10^{-3} \cdot \beta^2 - 2.849 \cdot 10^{-4} \cdot \gamma^2 - 4.762 \cdot 10^{-4} \cdot \beta \cdot \gamma + 0.153 \cdot \beta + 2.076 \cdot 10^{-3} \cdot \gamma + 0.685$$

R=0.995

Abduction-adduction (equation 7.2):

$$\alpha_a = 1.077 \cdot 10^{-3} \cdot \beta^2 + 2.279 \cdot 10^{-4} \cdot \gamma^2 - 2.381 \cdot 10^{-4} \cdot \beta \cdot \gamma + 0.08 \cdot \beta - 0.035 \cdot \gamma + 0.804$$

R=0.993

Azimuth (equation 7.3):

$$\alpha_t = -1.299 \cdot 10^{-3} \cdot \beta^2 + 3.609 \cdot 10^{-4} \cdot \gamma^2 + 1.832 \cdot 10^{-4} \cdot \beta \cdot \gamma - 0.04 \cdot \beta - 5.006 \cdot 10^{-3} \cdot \gamma - 0.648$$

R=0.995

The results shown in figures 7.2, 7.3, 7.4 are surfaces representing the above equations.

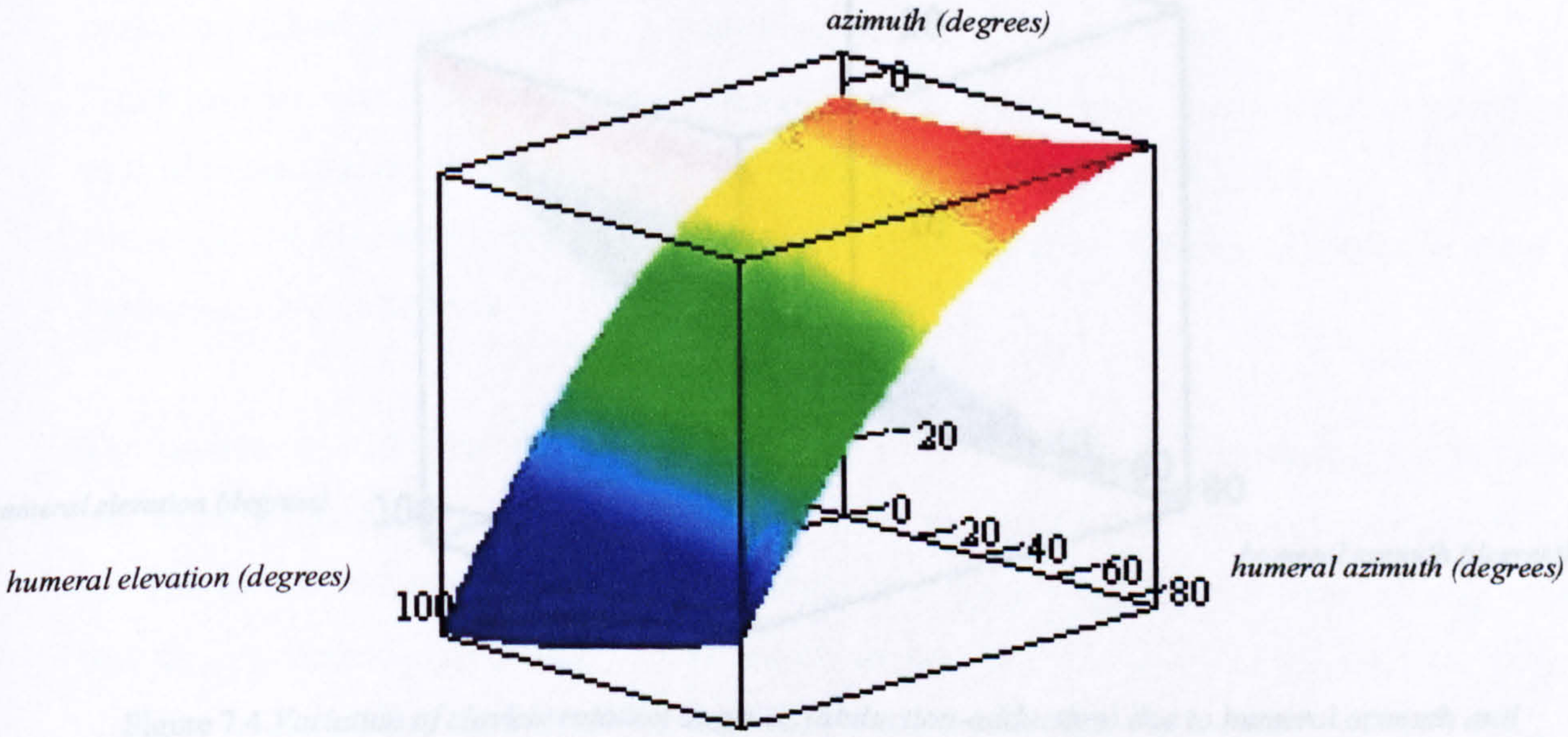

Figure 7.2 *Variation of clavicle rotation angle α_t (azimuth) due to humeral azimuth and elevation*

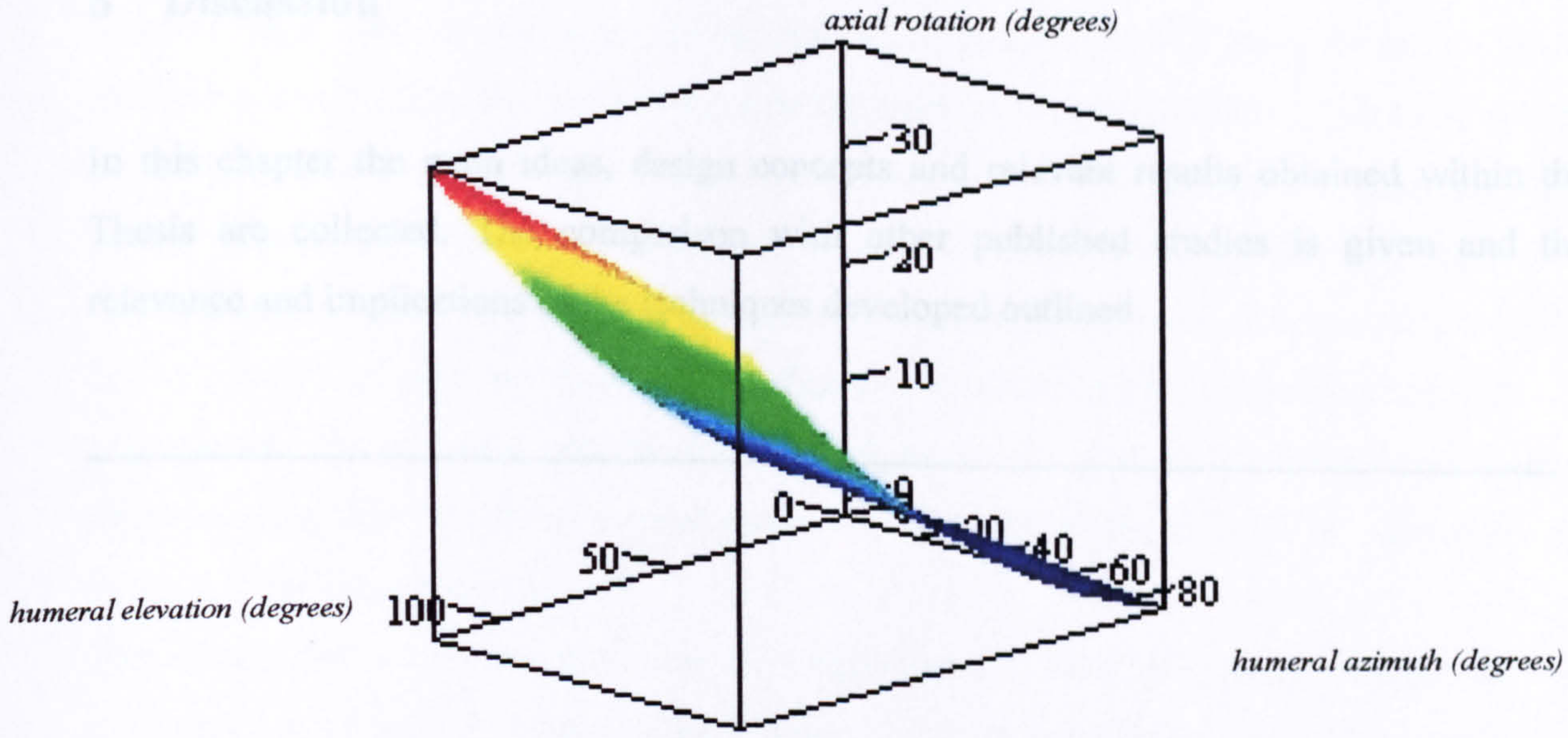

Figure 7.3 *Variation of clavicle rotation angle α_γ (axial rotation) due to humeral azimuth and elevation*

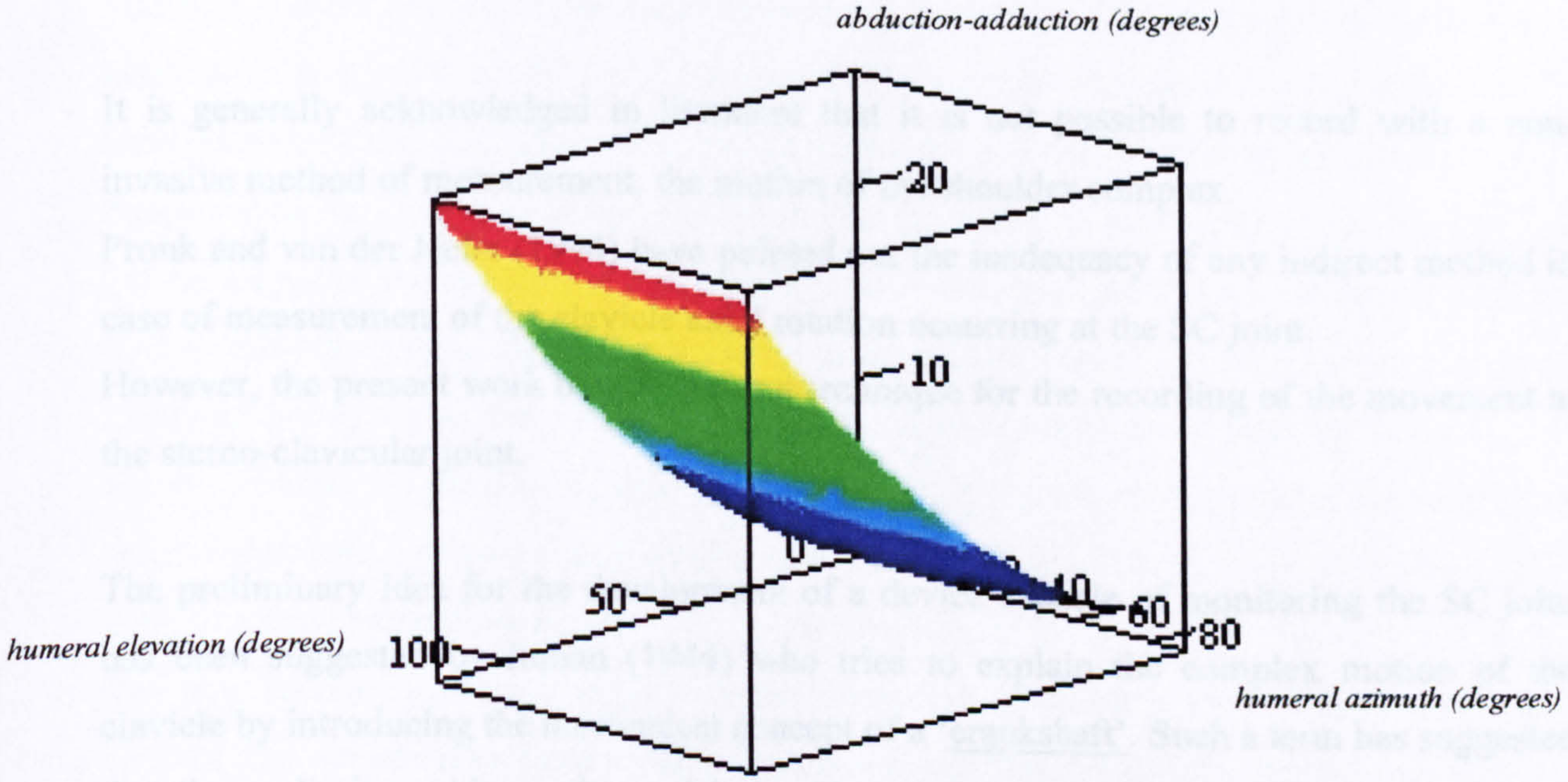

Figure 7.4 *Variation of clavicle rotation angle α_a (abduction-adduction) due to humeral azimuth and elevation*

The meaning of the above results is discussed in Chapter 8.

8 Discussion

In this chapter the main ideas, design concepts and relevant results obtained within the Thesis are collected. The comparison with other published studies is given and the relevance and implications of the techniques developed outlined.

8.1 Thesis Leitmotiv

It is generally acknowledged in literature that it is not possible to record with a non-invasive method of measurement, the motion of the shoulder complex.
Pronk and van der Helm (1994) have pointed out the inadequacy of any indirect method in case of measurement of the clavicle axial rotation occurring at the SC joint.
However, the present work demonstrates a technique for the recording of the movement at the sterno-clavicular joint.

The preliminary idea for the development of a device capable of monitoring the SC joint has been suggested by Inman (1944) who tries to explain the complex motion of the clavicle by introducing the mechanical concept of a 'crankshaft'. Such a term has suggested that the preliminary kinematic model should exploit the geometric characteristics of the clavicle modelled as a crankshaft in order to extract information on its three rotations. As is evidenced in Chapter 5, because of the allowed volumes surrounding the clavicle, the design of any external kinematic chain presents several difficulties.

For the above reason a careful review of the existing devices and techniques used to measure joint rotation has been carried out. Unfortunately the volumes surrounding the clavicle did not allow the use of any existing method of measurement. Therefore it was decided to investigate different technologies used to develop miniaturized sensors. Such review has demonstrated the inadequacy of state-of-the-art systems and has led to the development of the new miniaturized Hall effect-based sensor, which has represented the "core" device of a more complex mechanical structure able to monitor the clavicle movements. The technical specifications, which have been used to guide the entire design of the device, have allowed a mechanical arrangement of the sensors in assemblies to monitor a 3D spherical joint.

The sensor 'per se' represents a new electrogoniometer that can be easily adapted for the measurement of all the joints of the human body. Its mechanical design has combined characteristics that are often in antithesis such as miniaturized size and robustness.

The device has been calibrated, determining its accuracy and resolution. The use of coupled anti-backlash miniaturized gears has permitted an accuracy of 0.5 degrees with a resolution ranging from 7 to 10 mV/degree. A range of 180 degrees has been obtained exploiting the arrangement of two magnets positioned on a radius of 4 mm at an angular distance of 81 degrees with an inverse polarity with respect to the centre of sensitivity of the device. The typical output of the sensor together with the tests carried out are shown in Chapter 5 and 6.

It is worth mentioning that today, with microprocessors capable of being incorporated in measurement systems, there is more interest in repeatability than in linearity because it is always possible to produce a look-up table giving input values corresponding exactly to measured values. By using interpolation techniques, it is possible to reduce the size of that table to a reasonable dimension.

The new sensor developed presents some interesting advantages with respect to existing devices like potentiometers and strain-gage based electrogoniometers currently used in the fields of neurology and orthopaedics. In fact the device does not need any further amplification, it does not drift with temperature and allows a direct assembly to body landmarks because of its flat external surfaces.

As soon as the development phase of the sensors has provided relevant information on the definitive size of the 'sterno-clavicular detector', a new technique for "in vivo" measurement of the clavicle motion has been established. The technique exploits the geometry of the bone through a sensor arrangement according to an external kinematic chain. This allows the recording of the clavicle motion modelled as a pure 3-degree-of-freedom joint. As described in Chapter 5, in order to give information on the axial rotation of the bone, the external chain is arranged with two co-axial abduction-adduction sensors attached to the inner third and outer third of the bone respectively. The motion recorded by the sensors is therefore processed by an algorithm, which provides information on all the rotations at the SC joint. An extensive mechanical design phase aimed at the characterization of the interfaces with the human body has been carried out in order to define the technical specification of the electro-mechanical device.

As a result, a first prototype has been obtained and tested in order to quantify resolution, accuracy and repeatability of the technique. The method is extensively described in Chapter 6.

The results have shown that the key factors affecting the reading of the system under study are:

- errors due to the algorithm and to the resolution of the measurement system;
- errors due to a misalignment between the anatomical axis and the axis of the device; such error can be caused either by a wrong assembly of the device or by a different estimate of the examiner (inter and intra operator errors);
- errors in estimation of the clavicle parameters L and R which lead to a variation of the read angles;
- movement of the device during motion which causes a displacement of the axes of the device vs. the anatomical ones (this error can be considered a misalignment error).

All the above errors have been quantified in a consistent subset of the allowable range of motion of the clavicle. Repetitive measurements have been used to establish the mean and variance of the measurement plotted against different humeral position.

The validation studies have demonstrated that it is possible to have reliable measures of the clavicle movement. With reference to the validation studies carried out in Chapter 6, the error due to a wrong estimate of the parameters L and R affecting the algorithm results in a maximum absolute error of 3 degrees inside the investigated range of motion.
The misalignment error is negligible within the range of motion permitted by the clavicle and accounts for a maximum absolute error of 2 degrees.

All the above have demonstrated that the technique used to measure the clavicle parameters L and R is highly reliable and repeatable. The instrument is user-friendly and can be used on all subjects.
By taking into account the statistical analysis performed in order to analyse data inside the workspace, the differences in the measurement data account for an average error of 1 degree and 3 degrees for inter-and intra-operator errors respectively.

8.2 Mathematical modelling

A spatial interpolation technique has been applied to predict the movement of the clavicle as a function of the humeral position in a subset of the allowable workspace of the human arm.
A mathematical model based on the analysis of experimental data taken on a sample of ten subjects has been developed using the hierarchical approach proposed in Chapter 6. It has been possible to compare clavicle kinematics on different subjects for identical humeral positions and to extract the mean and confident intervals of the resulting motion patterns. By analysing the data set and by applying a regression technique, the mathematical model

is generated which accepts the humeral coordinates as inputs and provides a prediction of the movement of the clavicle expressed in a polynomial form.

A subset of the humeral workspace considered representative for daily activity movements has been considered. In order to provide a graphical representation of the workspace examined, in the assumption that the gleno-humeral joint can be represented as a pure three-degree-of-freedom rotational joint fixed in space, we can locate a sphere whose centre is coincident with the GH joint centre.

The angles of the clavicle can therefore be expressed as surfaces, which are functions of the humeral position. As described in section 7, these results are valid within the workspace examined (see figure 7.1).

The rotations of the clavicle are given with respect to the local coordinate frame where the sequence of rotations is Y, z_c, y_c.

8.3 Clavicle Motion

Very little is known about the anatomical or biomechanical function of the clavicle. It is worth mentioning that feline animals do not possess the bone. As pointed out by Inman (1946), some researchers consider the clavicle as a sort of flexible outrigger, which serves as a "propeller" for the shoulder, thus establishing the conditions necessary for free actions of the arm. Whatever its function is, it cannot be discovered without a deep understanding of the shoulder as a whole mechanism. In fact the clavicle, thanks to its unique shape, allows a wide range of motion for the arms supplying, for each trajectory, a connection point which provides the widest triangle base necessary to transfer the loads acting from the arms to the body. Therefore the optimal combination of motion and structural integrity is obtained. All the studies carried out until now have not considered the geometry of the bone as an intrinsic property of the mechanism. In fact it is due to such geometric features and to the kinematic constraints imposed by the ligamentous structure between clavicle and scapula that the SC joint assumes particular characteristics of motion.

In order to understand better all these important biomechanical functions it is convenient to start from pure anatomical considerations.

Let us assume to locate a global coordinate frame at the Sterno clavicular joint (Incisura Jugularis (IJ)) and another frame in correspondence of the AC joint. As shown in figure 8.1, by considering the anatomical data taken from a sample of 21 subjects, (see Table 6.3 in Chapter 6 - Section 6.3) the mean distances between the two frames x_l=140 mm; y_l=21 mm; z_l=59.1 mm are obtained. This means that with the body standing in the neutral starting position (anatomical position), the clavicle is rotated approximately 20 degrees around the X axis with respect to the XZ plane.

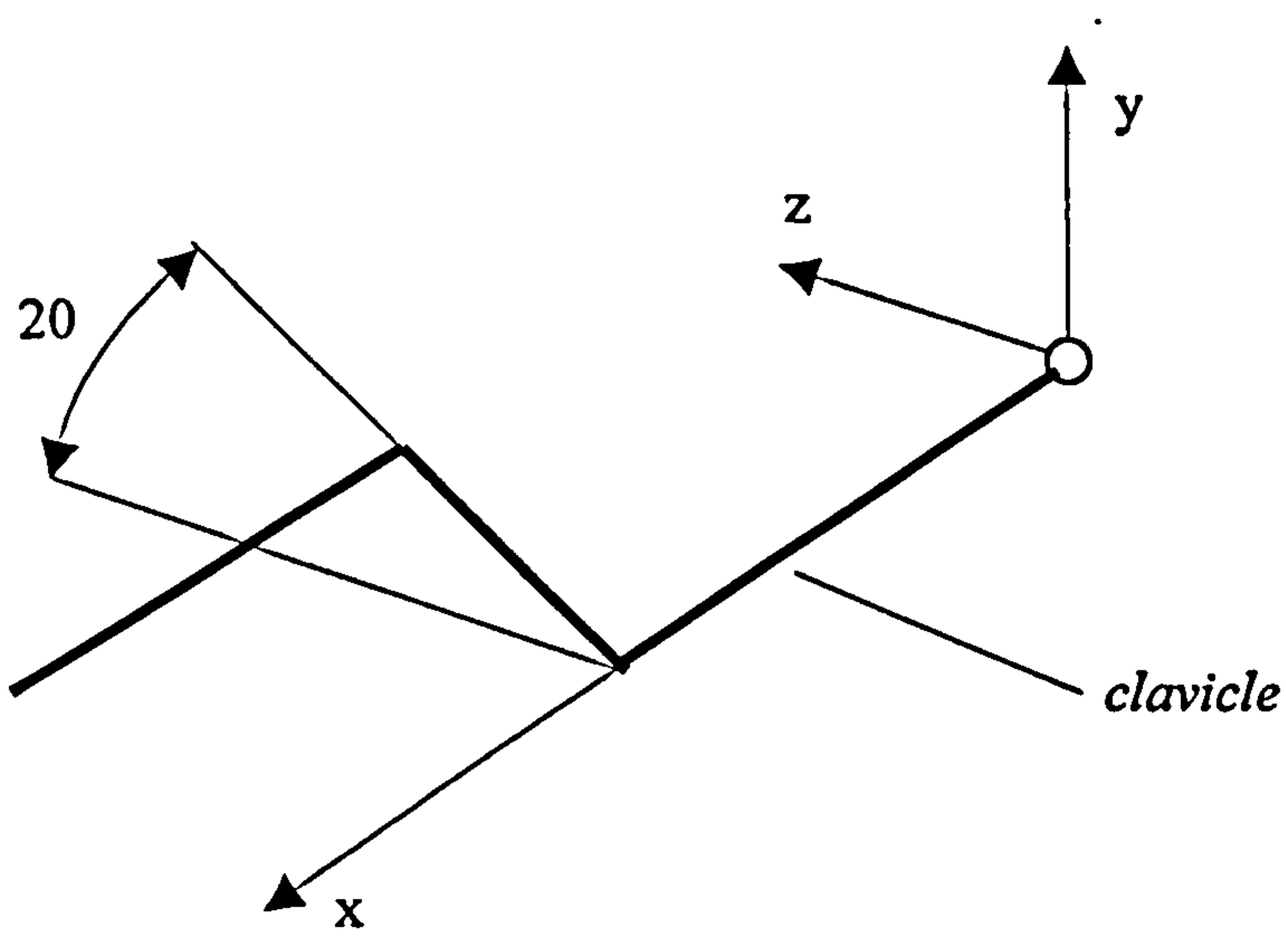

Figure 8.1 *Clavicle in the anatomical position*

The complete sequence of motion of the shoulder complex during elevation is shown in figure 8.2 where the sense of rotation is represented.

As can be noted during humeral abduction, because of the geometry of the clavicle and of the constraints imposed by the trapezoid and conoid ligaments, the permitted sense of axial

rotation of the clavicle is only that one shown in figure 8.2. Such rotation is accompanied by a retraction and a considerable elevation at the sterno-clavicular joint.

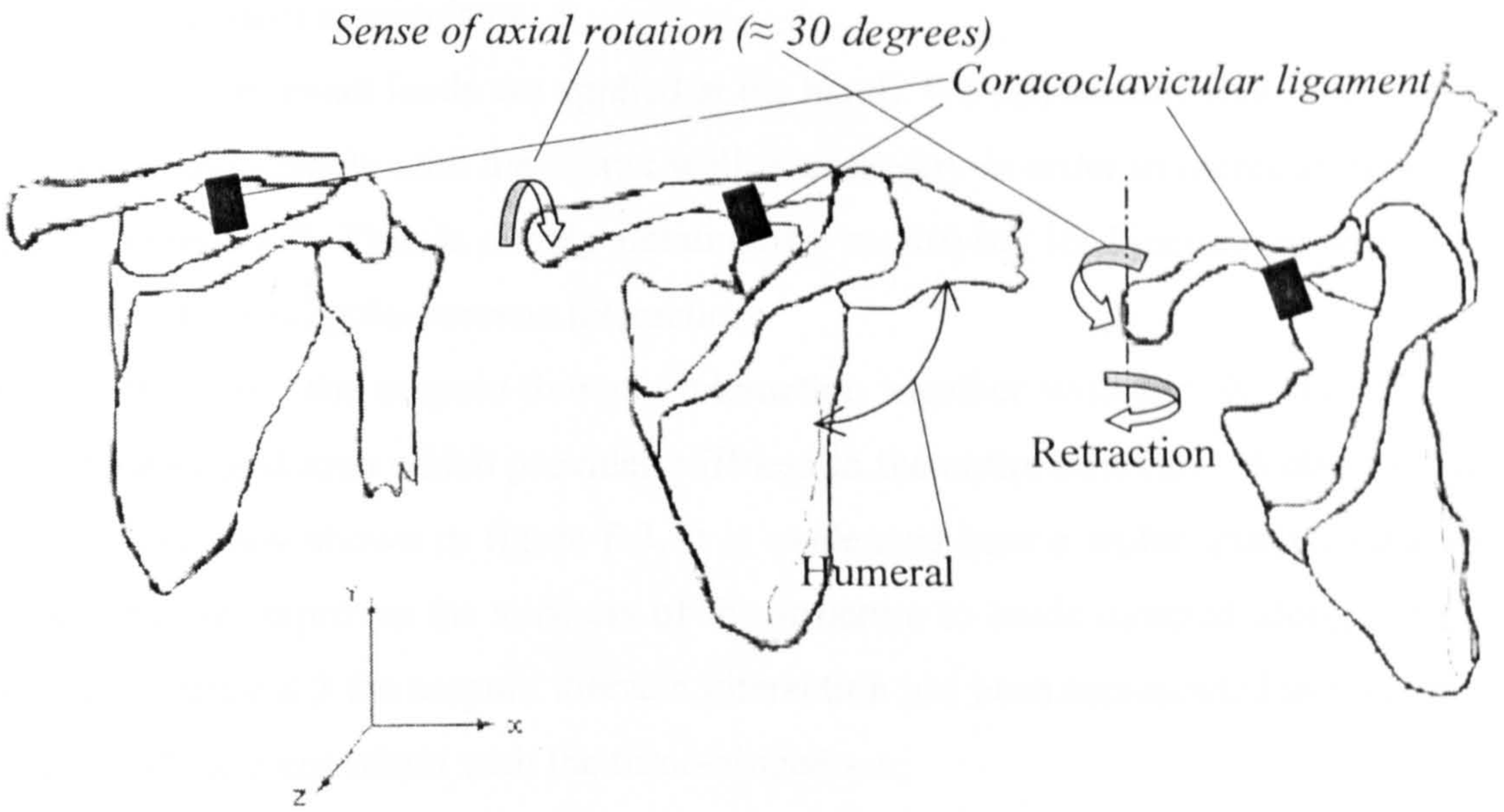

Figure 8.2 *Sequence of motion occurring at the sterno-clavicular joint*

In fact, during elevation of the arm, the spatial position of the acromio-clavicular joint with respect to the global frame, is characterized by an increased displacement along the Y and Z axes which can result only if a great elevation at the sterno-clavicular joint has occurred, the axial rotation of the clavicle acting in the opposite sense.

The coraco-clavicular ligament plays a fundamental role in forcing the sense of the axial rotation of the clavicle and consequently in increasing the elevation of the inner third of the bone. The costo-clavicular ligament, on the other hand, acts as a limiting factor of the clavicle elevation at the SC joint. According to Poirier (1890), Cave (1961) and Bearn (1967) a further elevation at the SC joint is only possible by a translation of the clavicular head in an inferior direction which is arrested by tension in the superior fibres of the sterno-clavicular joint capsule. In the proposed model the SC joint is considered a pure three-degree-of-freedom joint, therefore such translations are neglected.

But why does the clavicle have an S curvature?

It is thanks to such curvature that the full exploitation of the axial rotation of the bone at the SC joint is obtained.

In order to understand this concept better, with reference to figure 8.3, we can model the arm as an open chain manipulator.

What happens if relevant loads are applied at the hand? We can assume that in this case the interaction of the scapula with the thorax wall is necessary in order to increase the stiffness of the "manipulator". This is simply obtained by modifying its kinematics with the full exploitation of the scapulo-thoracic interaction.

In fact in this case, the scapulo-thoracic interaction together with the SC and AC joints, form a three hinged arch which provides stiffness to the entire structure. With reference to the partial top view shown in figure 8.3, it is evidenced how a wider triangle base of the triple hinged arc improves the stiffness of the structure to loads directed along the z axis. Note that in figure 8.3 the scapulo thoracic interaction has been represented as a hinge joint in order to allow comparison with the three-hinged arc.

During the humeral elevation, the clavicle performs an axial rotation of approximately 30 degrees. Such movement is helpful and necessary in order to obtain the correct spatial position of the scapula in its interaction with the thorax and therefore in obtaining the best structural position which provides the increased mechanical stiffness to the arm.

It can be concluded that:

"The S curvature of the clavicle allows the widest triangle base of the three hinged arc formed by ST, SC and AC joints for each static spatial position of the humerus. Such geometric feature adds another degree of freedom at the SC joint which increases the motion possibilities occurring at the AC joint within a restricted volume and helps in the determination of optimal interaction between scapula and thorax in order to improve mechanical stiffness".

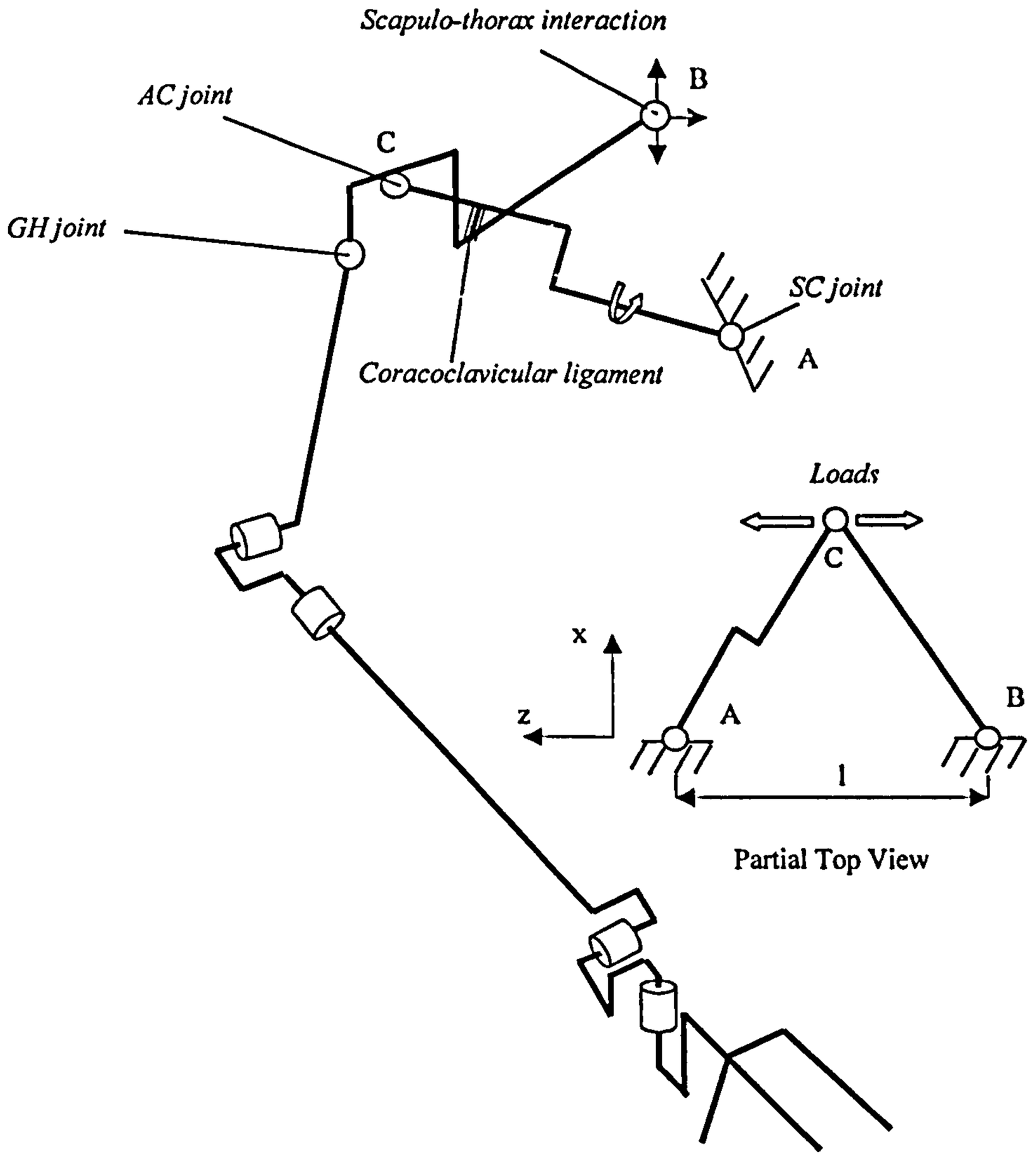

Figure 8.3: *Model of the shoulder complex*

As described above, the geometry of the bone plays a fundamental role in the amount of rotation occurring at the acromioclavicular joint. Indeed, the experimental data have shown that the axial rotation is the large rotation occurring at the SC joint.

In the following, the rotations occurring at the SC joint are given together with a comparison with data obtained from literature.

8.4 Comparison with data of literature

As previously stated, few published data are available on the movement of the clavicle and comparison of data is often hampered by a lack of a standardized description of spatial

kinematics. Moreover, the examined works treat the bone as a straight line between SC and AC, without taking into account its geometry and its wide influences on the kinematic and dynamic behaviour of the shoulder complex. Such data often result from an approximate solution to an indeterminate problem caused by the presence of redundant joints of the kinematic chain that cannot be recorded through an indirect method on an "in vivo" subject. The first researcher who examined the movement of the clavicle, emphasizing the crucial role of axial rotation was Inman (1944) who, by inserting pins directly in the bone of a living subject, tried to quantify the movement of the clavicle. He did not include information on the measurement method used to quantify the rotations and for this reason it is not possible to discuss the reasons for differences between the data extracted by his work and those measured by the sterno-clavicular detector (see figures 8.4 and 8.5). With reference to such figures it can be noted that the data related to clavicle abduction obtained by Inman correlates well with the data obtained by the sterno-clavicular detector, while the axial rotation measured by Inman is considerably less (see figure 8.5).

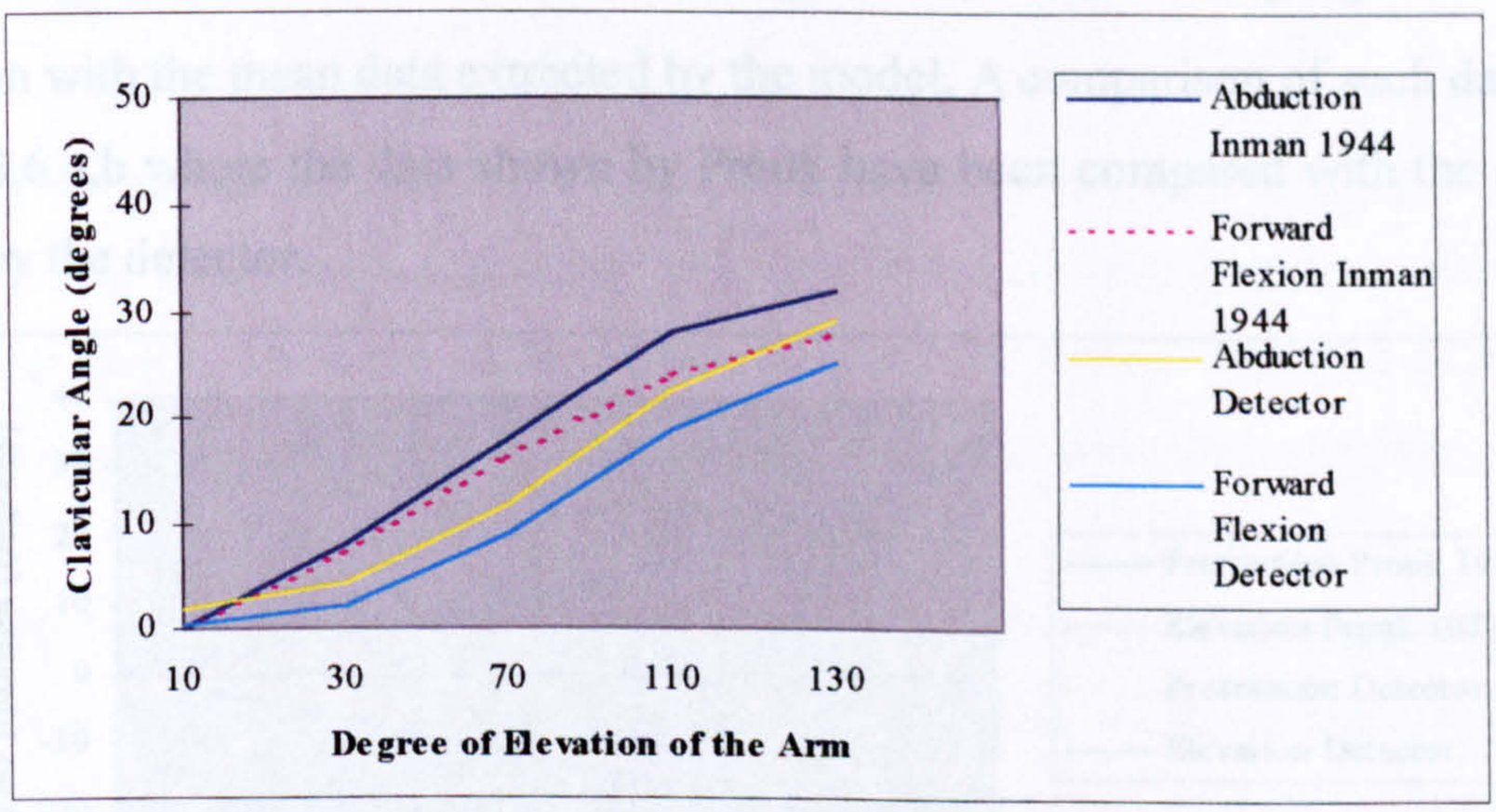

Figure 8.4: *Clavicle Abduction. Comparison with the data presented by Inman (1944)*

A more consistent comparison can be given with the data presented by Pronk (1989) who, based on the measurements of 18 male subjects and using spatial motion patterns, calculated the motion of scapula and clavicle.

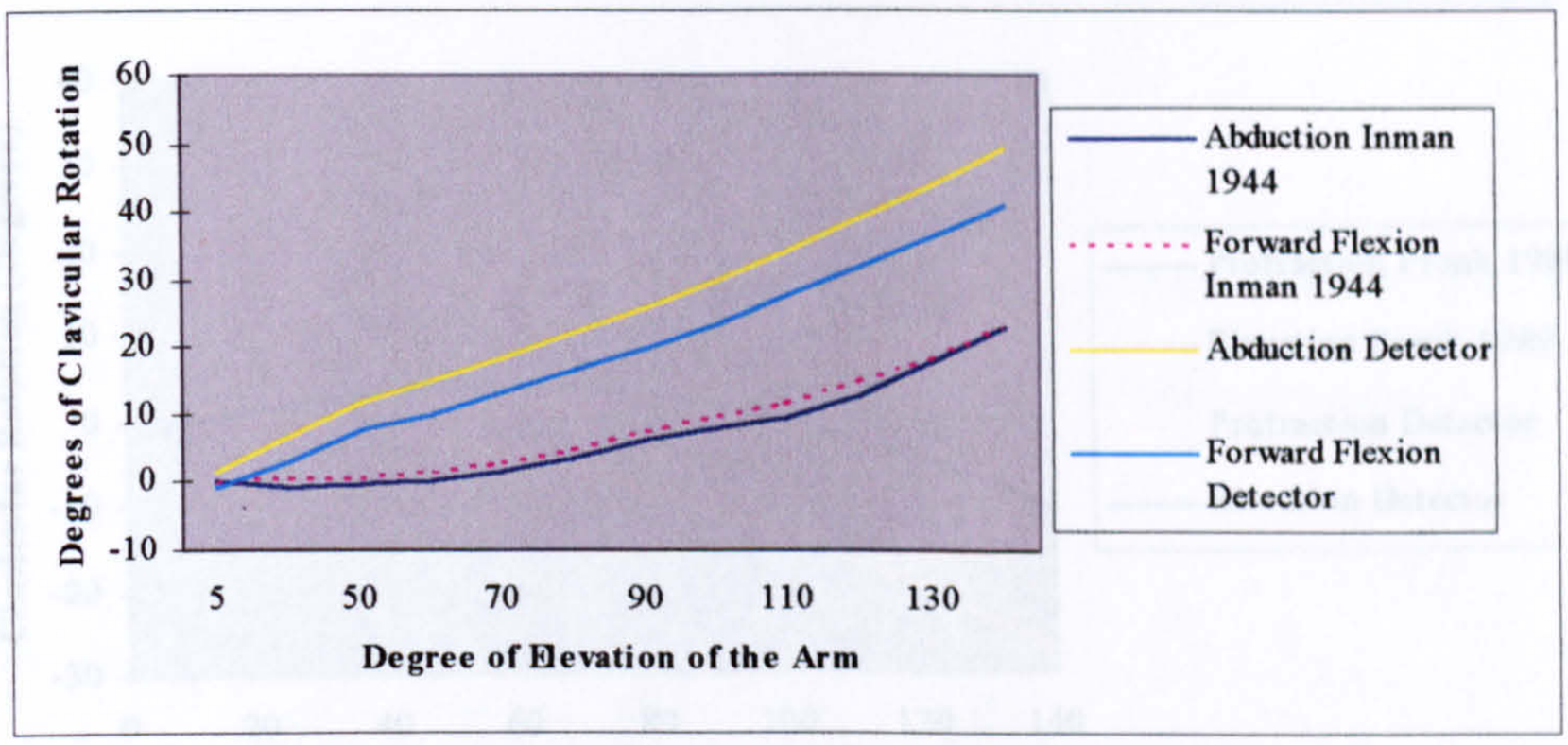

Figure 8.5: *Clavicle Axial Rotation. Comparison with the data presented by Inman (1944)*

Although the axial rotation of the clavicle is not given, the protraction-retraction and elevation of the clavicle have been expressed in a polynomial form as functions of humeral elevation in forward flexion and abduction of the humerus. The rotations of the clavicle have been described as rotations in the local coordinate systems fixed to the bone as shown in figure 8.1. The sequence of rotations proposed by Pronk Y, z_c, x_c allows a direct comparison with the mean data extracted by the model. A comparison of such data is given in figure 8.6 a,b where the data shown by Pronk have been compared with the mean data obtained by the detector.

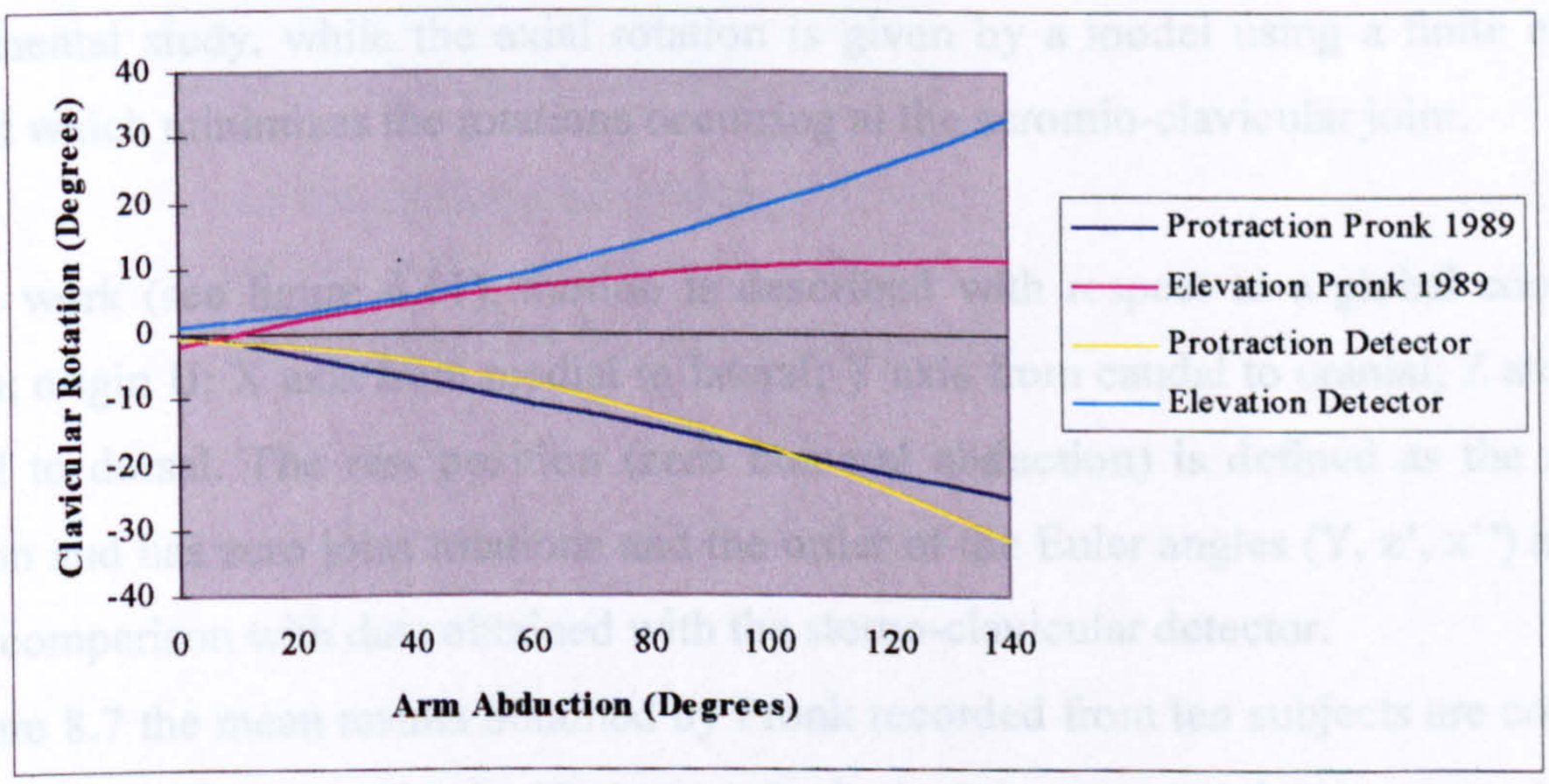

Figure 8.6a: *Clavicle Adduction and protraction in arm abduction. Comparison with data of Pronk 1989*

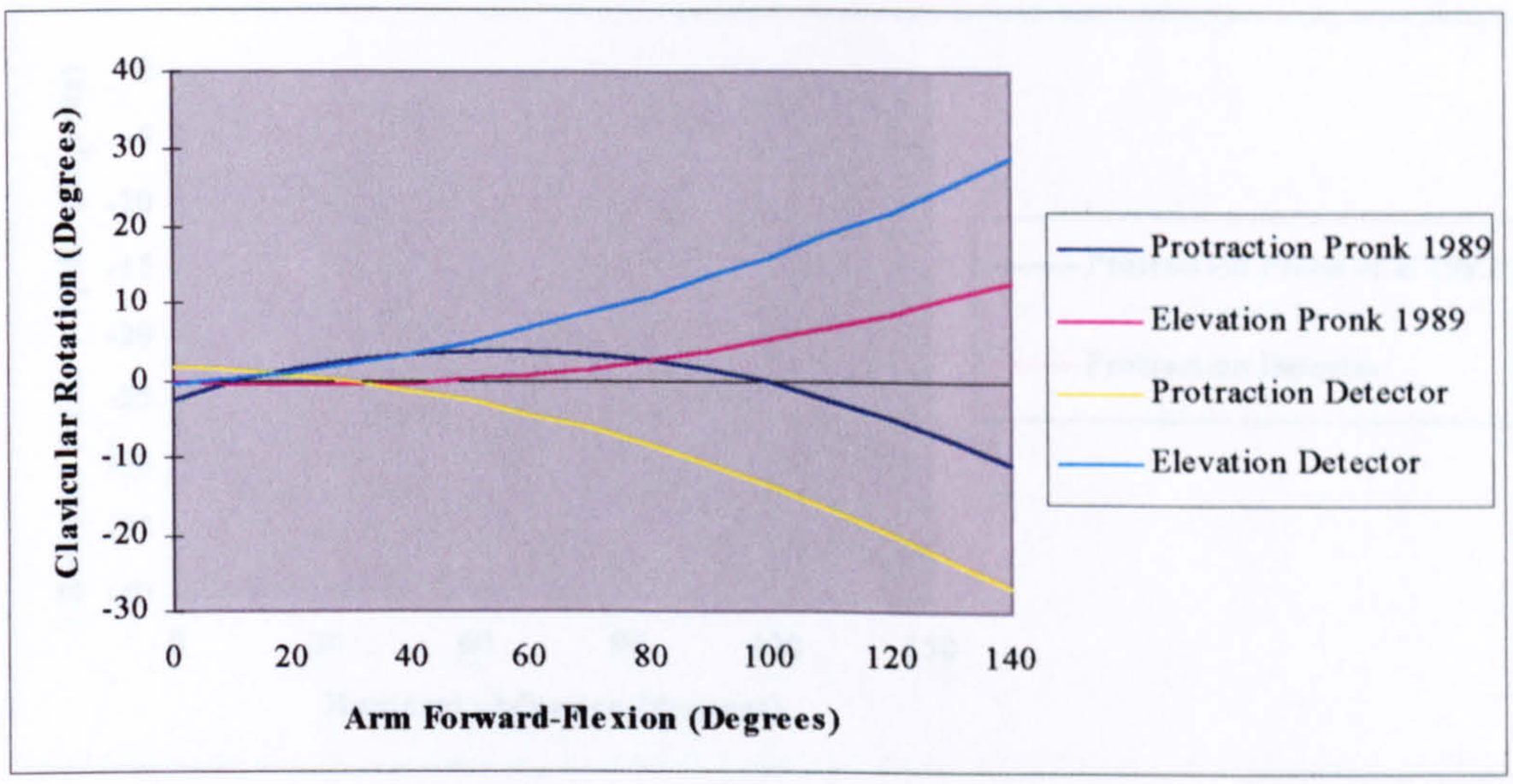

Figure 8.6b: *Clavicle adduction and protraction in arm forward flexion Comparison with data of Pronk 1989*

Pronk (1989) provides information on two of the three rotations occurring at the sterno-clavicular joint. It can be noted that there is a difference of the abduction-adduction movement as well as of the pro-retraction of the clavicle during abduction and flexion-extension of the arm.

Pronk in 1993 and van der Helm (1994) updated the above data including the axial rotation of the clavicle. Abduction-adduction and pro-retraction rotations are given by an experimental study, while the axial rotation is given by a model using a finite element method which minimizes the rotations occurring at the acromio-clavicular joint.

In this work (see figure 4.11), motion is described with respect to a global coordinate system: origin IJ; X axis from medial to lateral; Y axis from caudal to cranial; Z axis from ventral to dorsal. The rest position (zero humeral abduction) is defined as the starting position and has zero joint rotations and the order of the Euler angles (Y, z', x'') allows a direct comparison with data obtained with the sterno-clavicular detector.

In figure 8.7 the mean results obtained by Pronk recorded from ten subjects are compared with the mean results obtained with the sterno-clavicular movement detector recorded from 12 subjects.

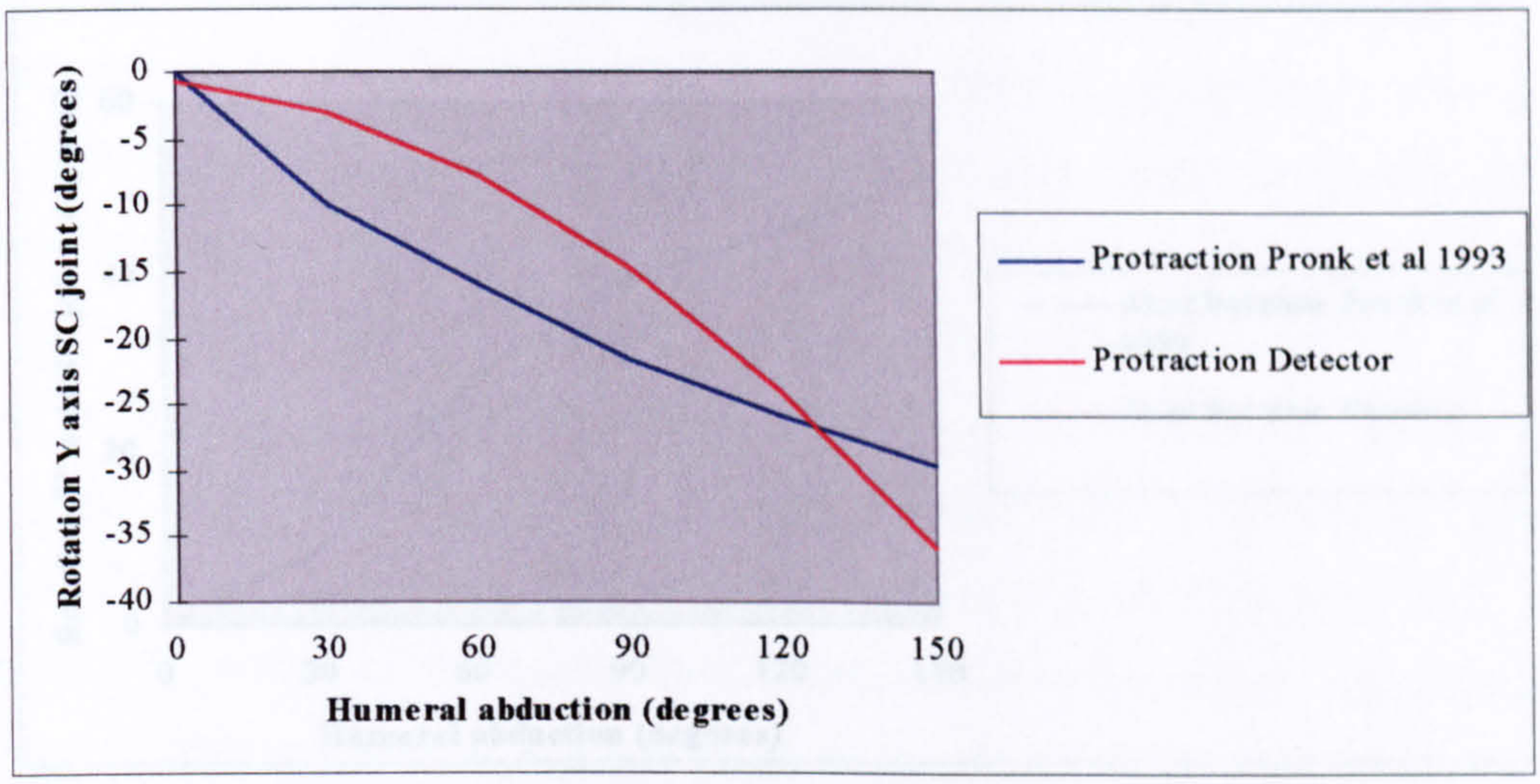

Figure 8.7a: *Clavicle protraction. Comparison with Pronk 1993*

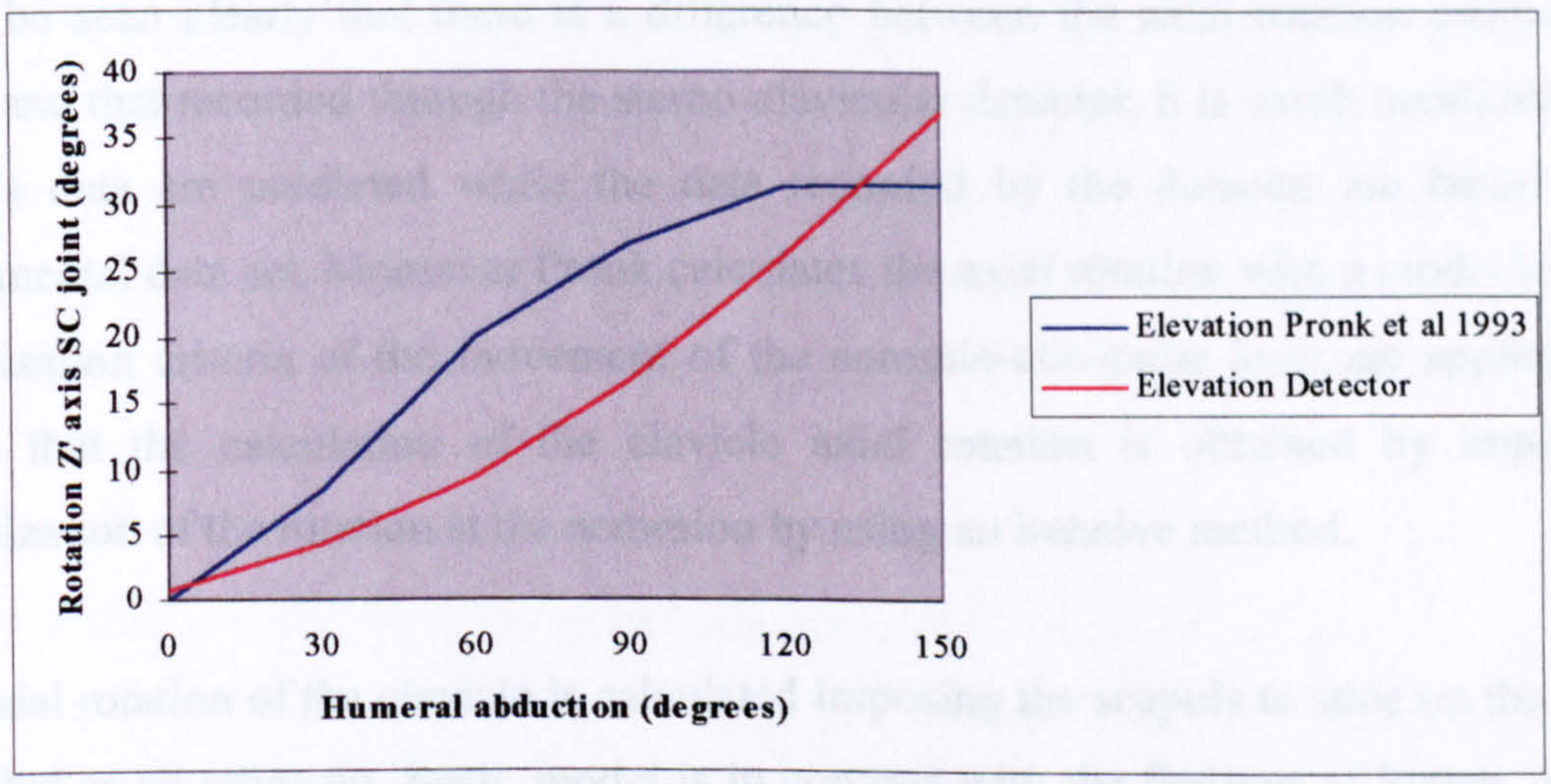

Figure 8.7b: *Clavicle abduction. Comparison with Pronk 1993*

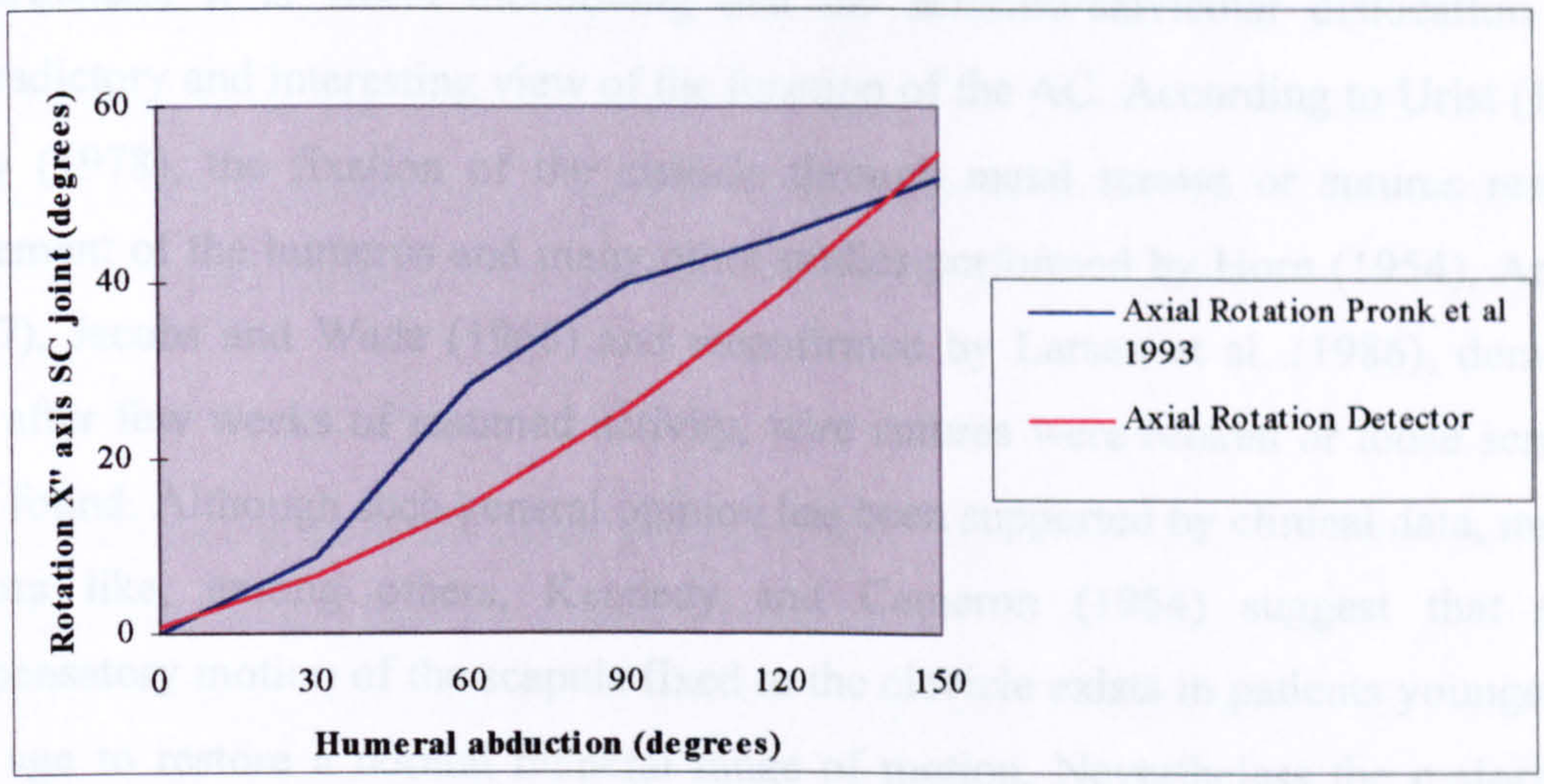

Figure 8.7c: *Clavicle axial rotation. Comparison with Pronk 1993*

It can be seen clearly that there is a difference between the axial rotation estimated by Pronk and that recorded through the sterno-clavicular detector. It is worth mentioning that Pronk's data are predicted while the data recorded by the detector are based on an experimental data set. Moreover Pronk calculates the axial rotation with a model in which minimisation criteria of the movement of the acromio-clavicular joint are applied. This means that the calculation of the clavicle axial rotation is obtained by imposing a minimization of the rotation at the acromion by using an iterative method.

The axial rotation of the clavicle is calculated imposing the scapula to slide on the thorax, modelled as an ellipsoid. Such model is in contrast with the findings of Inman, who has shown, through clinical examples, the importance of the rotation at the AC joint. In fact, an actual surgical technique is to treat a dislocation at the AC joint by inserting a metal screw from the lateral head of the clavicle directly in the base of the coracoid process. One patient treated according to this technique was unable to elevate the arm above 110 degrees. The same subject, while running, slipped and fell, forcibly abducting the arm above his head. Following an immediate pain he found that he re-gained a complete range of motion. X rays revealed that the screw has been bent and avulsed from the coracoid permitting the clavicle to rotate freely. This is a pragmatic demonstration of the role of the AC joint.

Nevertheless, it is worth mentioning that the acromio-clavicular dislocation yields a contradictory and interesting view of the function of the AC. According to Urist (1946) and Perry (1978), the fixation of the clavicle through metal screws or sutures restricts the movement of the humerus and many other studies performed by Horn (1954), Arner et al. (1957), Jacobs and Wade (1966) and reconfirmed by Larsen et al. (1986), demonstrated how after few weeks of resumed activity, wire sutures were broken or loose screws have been found. Although such general opinion has been supported by clinical data, many other authors like, among others, Kennedy and Cameron (1954) suggest that sufficient compensatory motion of the scapula fixed to the clavicle exists in patients younger than 50 year age to restore a normal humeral range of motion. Nevertheless the majority of the clinical studies carried out agree that there is a considerable range of motion at the AC joint.

The model proposed by Pronk and Van der Helm to provide a complete kinematic model of the arm for in vivo subjects, presents a solution that minimises the motion at the AC, that is in open contrast with the surgical studies presented. The loosening of screws or wire sutures seems a clear indication of the rotation occurring between clavicle and scapula at the AC joint. It is evident that the model proposed by Pronk starts from two hypotheses that clearly affect the results:

1) the sliding joint between thorax and scapula in all the range of motion.
2) the clavicle axial rotation calculated with an iterative method, which minimises the rotations at the AC joint.

Let us assume that the contact between scapula and thorax occurs when it is necessary to transmit high loads from the arm to the trunk. In this case, the contact between scapula and thorax closes the kinematic chain by offering to the external load a triangle base as a resistive mechanical structure. In the case of free motion of the arm, this contact seems not necessary at all.

As far as the AC joint is concerned, it seems that a compensatory rotation occurs at this joint particularly in abduction and adduction. Further studies are certainly necessary by

recording the movement of the clavicle and of the scapula on the same subject in order to obtain information on the complete motion of the arm. Certainly it is possible to use the proposed constraint equations in order to obtain a complete model of the upper arm. A theoretical approach based on the constraint equation proposed is given in the following Chapter.

It is now interesting to make some pure kinematic considerations on the motion at the sterno-clavicular joint. Since the distance between the AC and the SC joint is constant (if translations at the SC joint are not considered), the head of the clavicle moves around a sphere. In figure 8.8a it is plotted the motion of the head of the clavicle obtained by applying the equations 7.1, 7.2 and 7.3). The red dots represent the sequence of Cartesian positions assumed by a point located in the centre of rotation of the AC joint with respect to a global coordinate frame located in the centre of rotation of the SC joint, while in figure 8.8 b,c,d the projections D0, D1, D2 with respect to the frontal (coronal), sagittal and transverse planes are given. Data have been obtained by applying the equations 7.1, 7.2 and 7.3 to a clavicle modelled as per figure 8.1. The distance between the two frames has been obtained by using the mean values of table6.3.

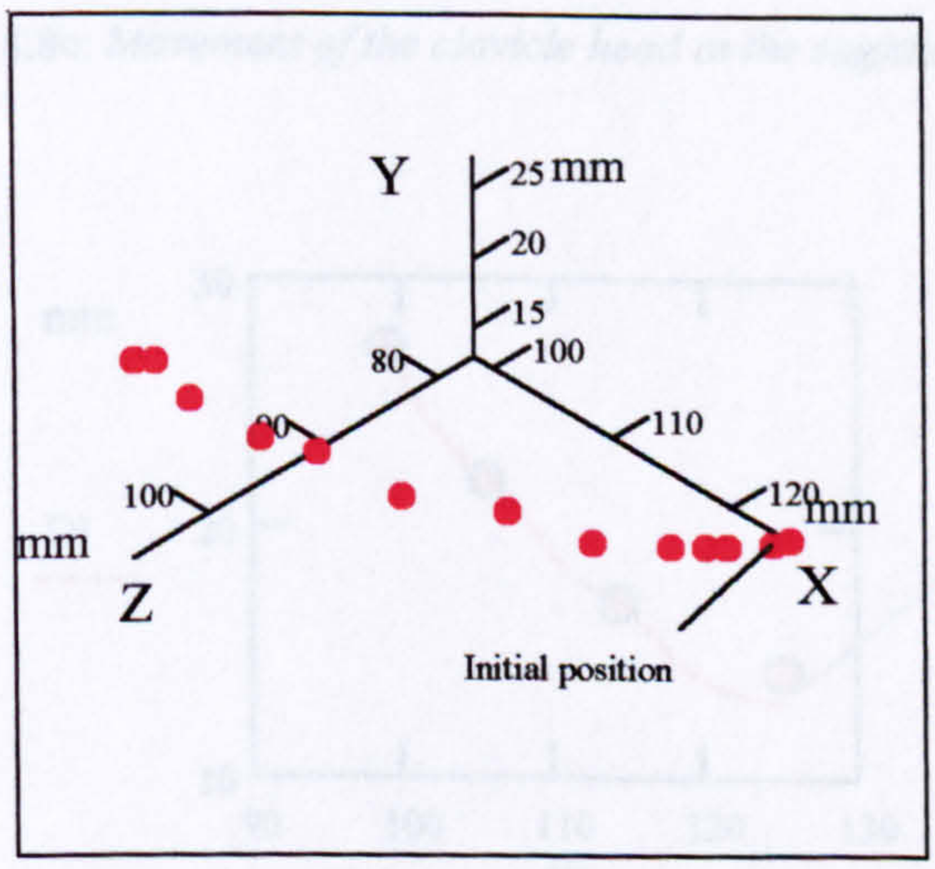

D2, D0, D1

Figure 8.8a: *Movement of the clavicle head (stick figures)*

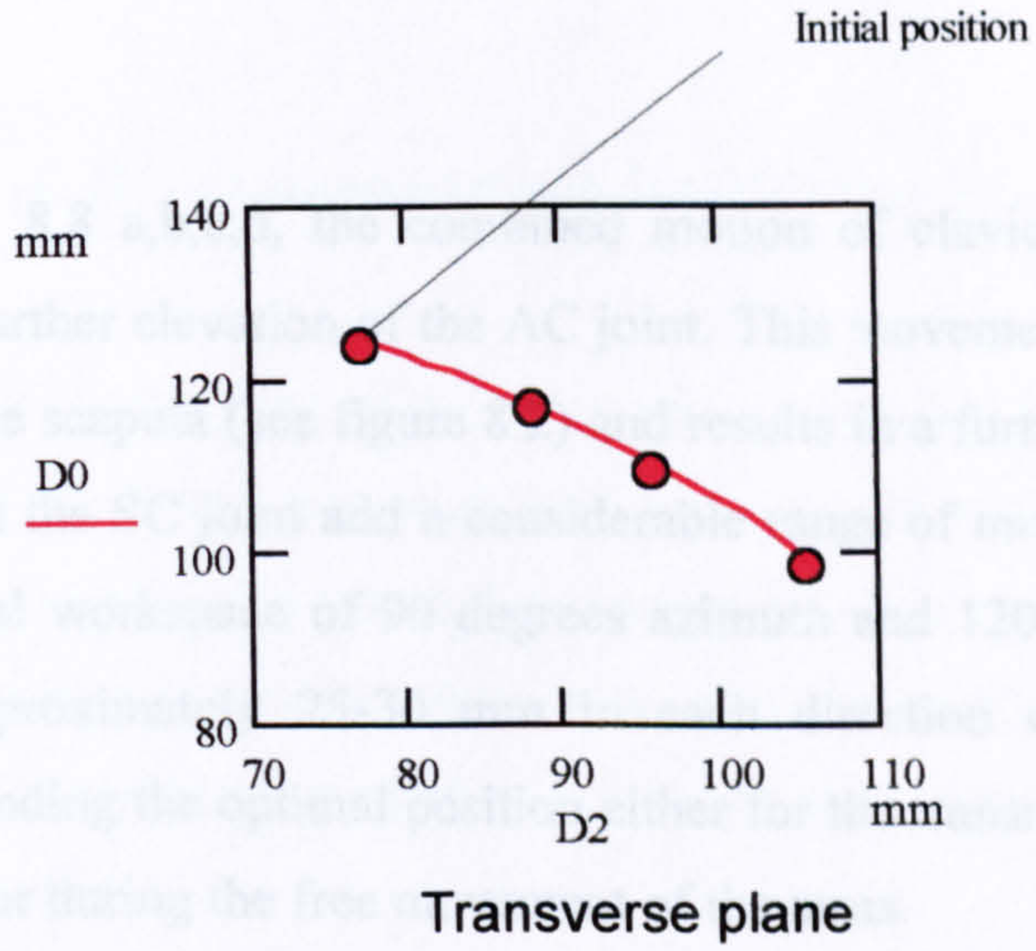

Figure 8.8b: *Movement of the clavicle head in the transverse plane*

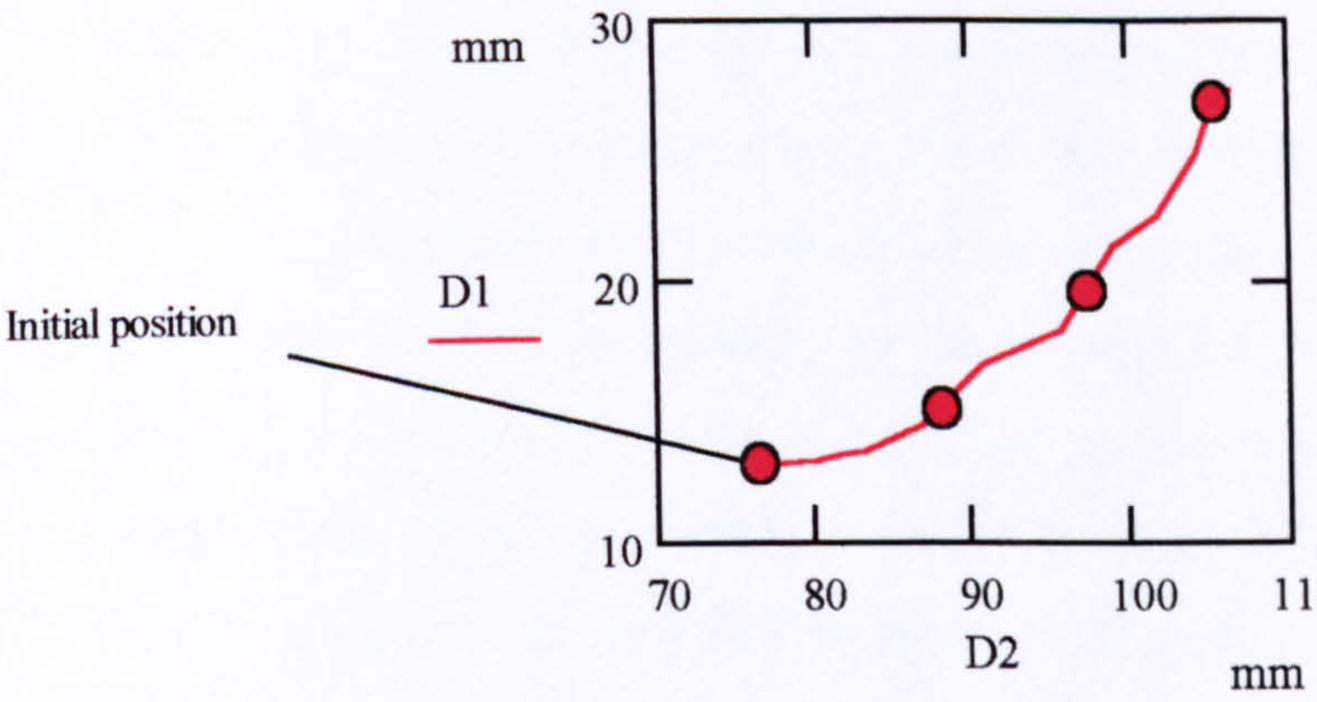

Figure 8.8c: *Movement of the clavicle head in the sagittal plane*

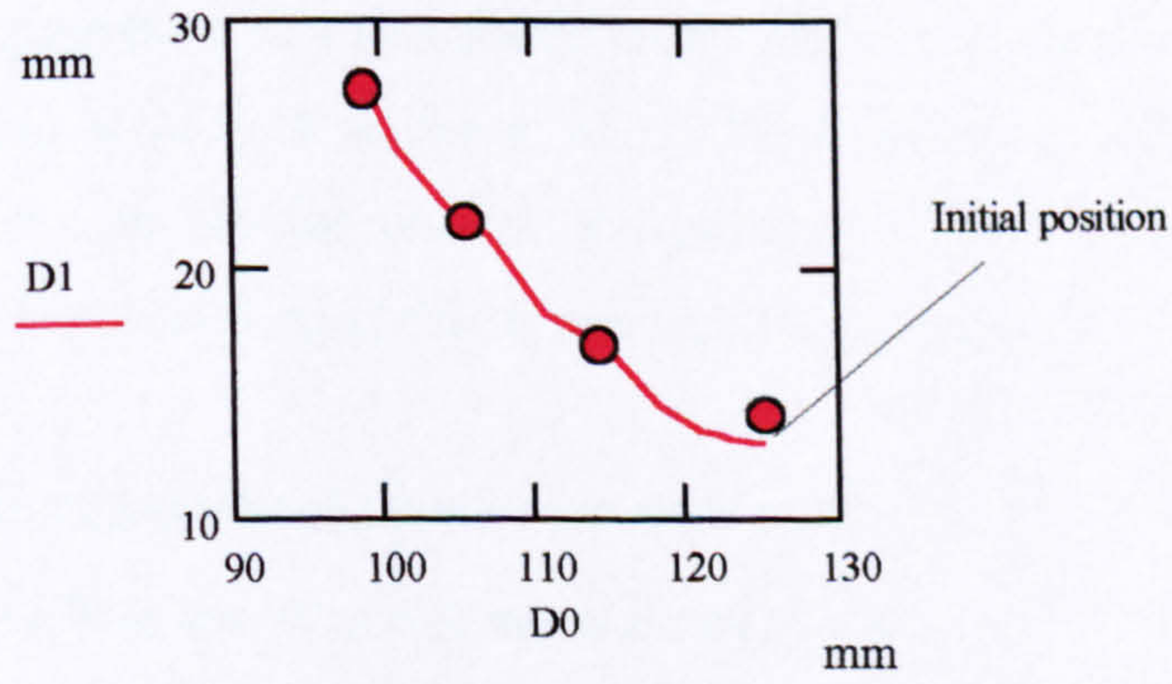

Figure 8.8d: *Movement of the clavicle head in the frontal plane*

As shown in figures 8.8 a,b,c,d, the combined motion of clavicle abduction and axial rotation results in a further elevation of the AC joint. This movement acts as a natural help to the abduction of the scapula (see figure 8.2) and results in a further elevation of the GH joint. The rotations at the SC joint add a considerable range of motion at the AC joint. In fact, within a humeral workspace of 90 degrees azimuth and 120 degrees elevation, AC displacements of approximately 25-30 mm in each direction can be obtained. Such movement helps in finding the optimal position either for the transmition of loads from the humerus to the body or during the free movement of the arms.

9 Conclusions and Recommendations for Future Work

The present work has focussed on the kinematics of the clavicle.

The first part of the Thesis has dealt with the study of anatomy of the arm as the necessary background to understand the complex kinematics of the upper limb. Both skeletal and muscular apparatuses have been overviewed trying to put in evidence, with the help of a systematic support of drawings, the intimate relationship of bones and muscles with skin.

Despite the many attempts, the complexity of the anatomy has hampered the identification of a consistent and accurate biomechanical model of the human arm. This is strongly demonstrated by the wide variety of limb models that can be found in literature. Some models judged the most accurate have been reviewed in depth.

As a result of the study of the published biomechanical models, it has been realised that a complete and unifying theory of the kinematics of the upper limb has not been presented yet. In fact although many attempts have been devoted to identify the kinematic chain of the upper limb, an orthodox kinematics seems to be not available. This is due mainly to the lack of information related to the movement of the clavicle.

In order to approach the problem from a theoretical point of view, the arm has been modelled as a geometric variable system. For this reason an entire chapter has been dedicated to the basic terminology currently used in robotics in order to characterise manipulator kinematics. The chapter ends with an extensive explanation of the Denavit-Hartenberg notation as a systematic method of description of the kinematic relationship between a pair of adjacent links. Such notation will be useful to researchers who wish to use the constraint equations of the clavicle in order to characterize the motion occurring at the acromio-clavicular joint.

The present work has dealt with the following topics:

- study of the skeletal and muscular apparatuses of the arm;
- review of the biomechanical models of the shoulder complex;

- study of the forward kinematics of a geometric variable system;
- study of manipulator workspace and of its main properties;
- development of a technique able to record the SC motion;
- design and development of a new miniaturized electrogoniometer as a necessary step for the application of the technique;
- design and development of a device able to record the 3 degrees of freedom at the sternoclavicular joint;
- validation phase dedicated to highlight the precision and accuracy of the new system proposed;
- development of a mathematical model through which the clavicle rotations are expressed in a polynomial form function of the humeral positions.

9.1 Results

A new measurement technique which exploits the geometry of the limb has been presented and a new system for investigating spatial clavicle-humeral kinematics developed. The system has been validated through an intensive set of validation studies.

An intense design and development phase has been tailored to the development of miniaturized rotation sensors. Such development has been carried out in order to cope with the "allowed volumes" in proximity of the sternum. In fact the pragmatic difficulties encountered in interfacing a sensorised device able to record the rotations at the SC joint has guided the development of the sensitive element.

Based on the above device, an electromechanical device has been designed and manufactured where the sensors have been assembled according to a serial/parallel kinematic chain. The accuracy and repeatability of the *sterno-clavicular detector* has been verified by a purposely conceived set of bench test experiments as well as on subjects.

A predictive model of the behaviour of the clavicle has been finally developed using a regression technique. The results compared favourably with the data of Inman (1944),

Pronk (1993) and van der Helm (1994) although some differences concerning the shape of the curve have been found particularly with the data shown by Pronk. Such differences may be attributed to the optimisation technique used by the author, who detects the clavicle axial rotation by minimizing the movement at the sterno-clavicular joint.

Concerning the kinematics of the clavicle, the main conclusions can be summarised as follows:

1. The rotation of the humerus causes a combined motion between clavicle and scapula, which can be coined as a *clavi-scapulo-humeral rhythm*. The sense of axial rotation of the clavicle is constrained by the conoid and trapezoid ligaments, which play a fundamental role in the motion pattern between clavicle, scapula and humerus.
2. Either abduction or forward flexion of the humerus causes a three dimensional combined motion of the clavicle: *axial rotation* along an axis coincident with the inner third of the bone (sternal part), *abduction-adduction* and a considerable *pro-retraction.*
3. The larger movement is the axial rotation followed by a considerable abduction, which permits an elevation of the acromion during motion.
4. Any representative model of the arm should consider the coracoclavicular ligament which plays a fundamental role in the motion pattern between scapula and clavicle offering an additional constraint that is to be accounted in the model. It is easy to understand how any articular problem involving such ligamentous structure can cause a difficult reorganization of the network of muscles responsible for the dynamics of the movement of the shoulder complex;
5. The internal-external rotation of the humerus has not measurable effects on the clavicle motion.

9.2 Technical development

The development of a new system of measurement has been carried out with an intensive validation phase aimed at determining its accuracy and repeatability.

The technique developed exploits the geometry of the clavicle for gaining essential information on the axial rotation occurring at the sterno-clavicular joint. The model basic hypothesis is that the sternal part of the clavicle, modelled as a line, lies in the corononal plane in the anatomical position.

The importance of the coordinate system has been demonstrated particularly for the comparison of the results.

The electromechanical system has been developed together an acquisition unit and software designed using C++ for Windows 95/98 environments.

The data have been analysed using standard software as MathCAD and Excel.

9.3 Recommendations for future work

It is common belief that any research generates more questions than findings. Therefore a list of recommendation is given in the following in order to suggest to future researchers possible development for a better understanding of the kinematics of the arm.

9.3.1 Increased workspace

The workspace investigated is a subset of the workspace of the arm; therefore the validity of the relationships should be checked also in an increased workspace. In particular the slope of the polynomial curve used does not fit outside the examined workspace.

9.3.2 Arm kinematics

A complete investigation on the arm kinematics can now be achieved. From a kinematic point of view, any future biomechanical model should take into account the geometry of the "links" which play a fundamental role in the interaction between the joints. Particular attention should be taken in the role played by the ligamentous structure of the arm, which is, indeed, an additional constraint of motion.

In order to highlight the main features of the arm kinematics, it is recommended that the Denavit-Hartenberg notation should be used and that the local coordinate frames should be located along the anatomical joints (SC, AC, GH) in order to have evidence of the motion of each link. The combined application of the clavicle detector and of any "non invasive method" for the scapular measurement should demonstrate, once forever, the effective existence of the scapulothoracic joint also during motion of the unloaded arm.

To this purpose a key idea should be the application of a theoretical approach based on predictive models of clavicle and scapula motion as those developed in this work and by Barnett (1996). The kinematics of the arm can be modelled as per figure 3.12 and 9.1. In the hypothesis that the first two joints of the shoulder complex formed by clavicle, scapula and humerus can be modelled as a six-degree-of-freedom open chain "manipulator" possessing three degrees of freedom at the SC and three degrees of freedom at the AC joint respectively.

It follows that the SC and the AC can be modelled as pure spherical joints as depicted in figure 9.1.

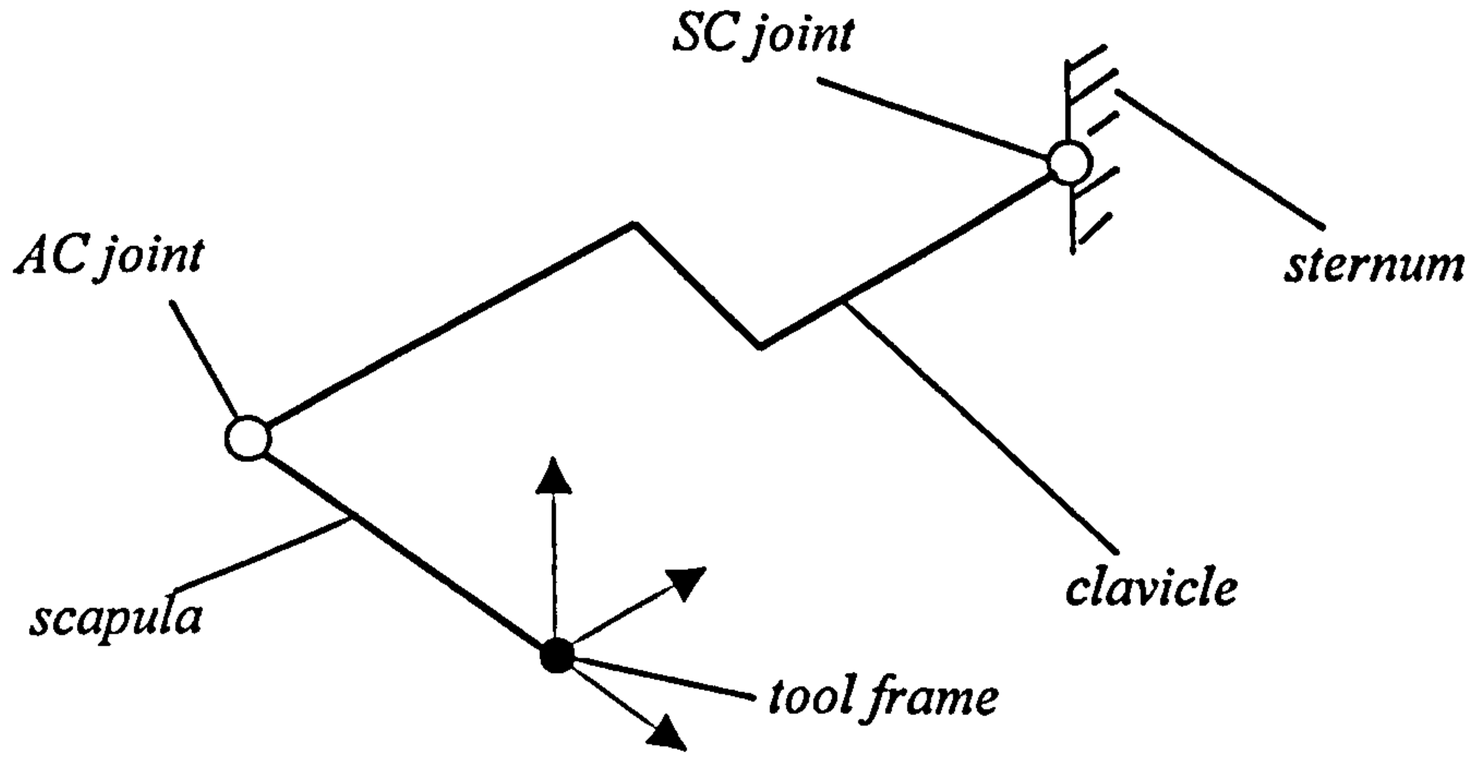

Figure 9.1: *Model of clavicle and scapula*

With reference to figure 9.1 and 3.12 and to the notations used in Chapter 3, the Denavit-Hartenberg notation can be applied to the manipulator as follows (see Table 3.13):

Data:

1) Spatial position of the AC joint with respect to a frame located at the SC joint with the body in the anatomical position. Such mean data can be extracted from Table 6.3 in Chapter 6. From these data the Denavit-Hartenberg parameters related to the geometry of the clavicle can be extracted (see Table 9.1).
2) With reference to the model developed by Barnett (1996) and to figure 9.1, the six coordinates α, β, γ, X, Y, Z of the scapula referred to a frame located at the SC joint and expressed in a polynomial form as functions of a (azimuth), e (elevation) and r (roll) of the humerus can be obtained.

Since such data are given for a sequence of known humeral positions, the spatial position of the scapula (considered as a rigid body) with respect to the sternum is known for each humeral position. This means that, if the geometry of the manipulator is known, the Denavit-Hartenberg notation together with an inverse kinematics can be applied to know, for each humeral position, the six rotations at the SC and AC joints that are necessary to locate the scapula in the known position.

Using the above models it will be possible to obtain from the sequence of positions assumed by the scapula (the end effector of the manipulator) for each humeral position the angles at the SC and AC respectively and therefore to know the complete kinematics of the arm.

10 References

Abdel-Rahman E. and Hefzy M.S. (1993) A Two Dimensional Dynamic Anatomical Model of the Human Knee Joint. *Journal of Biomechanical Engineering. Transactions of the ASME* **115**, 357-365

An, K.N., Jacobsen, M.C., Berglund, L.J. and Chao, E.Y.S. (1988) Application of a magnetic tracking device to kinesiologic studies. *J. Biomechanics* **21**, 613-620.

Angeles, J. (1990) A Scale-Independent and Frame-Invariant Index of Kinematic Conditioning for Serial Manipulator; *Proc. of the 2nd Workshop on Advances in Robot Kinematics, Linz, Austria.*

Arner, O., Sandahl, U. and Ohrling, H. (1957) Dislocation of the acromio-clavicular joint. review of literature and report of 56 cases. Acta Chir. Scand. **113**, 140-152.

Badler, N.I., Phillips, C.B. and Webber, B.L. (1993) Simulating Humans. Pub. Oxford University Press.

Bagg, S.D., and Forrest, W.J.1988 "A biomechanical analysis of scapular rotation during arm abduction in the scapular plane, Am. J. Phys. Med. Rehab., **67**, 238-245.

Barker, T.M., Nicol, A.C., Kelly, I.G. and Paul, J.P. (1996) Three dimensional joint co-ordination strategies of the upper limb during functional activities. *J. Eng. Med., Proc. IMechE, Part H*, **210**, 17-26.

Barnett, N.D. (1996) Measurement and modelling of three dimensional scapulohumeral kinematics. *PhD Thesis*, University of Newcastle upon Tyne.

Barnett N.D., Duncan R.D.D. and Johnson G.R. (1999) The measurement of three dimensional scapulo-humeral kinematics – a study of reliability. *Clinical Biomechanics* **14**, 73-76

Bearn, J.G. (1967) Direct observations of the function of the capsule of the sterno-clavicular joint in clavicular support. *J. Anat.* **101**, 159-170.

Benati, M., Gaglio, S., and Morasso, P., Tagliasco, T., and Zaccaria, R. (1980) Anthropomorphic Robotics. *Biological Cybernetics* **38**, 125-140.

Bergamasco, M. (1994-1995) Lectures on Robot Kinematics. "Scuola Superiore S'Anna, Italy. Internal Report"

Bergamasco, M., De Micheli, D.M., Parrini, G., Salsedo, F. and Scattareggia Marchese S. (1991) Design Considerations for Glove-like advanced Interfaces. IEEE Proc. of International Conference on Advanced Robotics, Pisa, Italy, 162-167.

Bergamasco, M., Scattareggia Marchese S., Salsedo F., and Parrini G. Device for monitoring the configuration of a distal physiological unit to be used as an advanced interface for machines and computers"; Patent n° TO- 92A000941-8th October 20th November 1992.

Braune, W. and Fischer, O. (1888) Über den Antheil, den die einzelnen Gelenke des Schultergürtels am der Beweglichkeit des menschlichen Humerus Haben. *Abh. math-phys. Cl. d. k. Sächs Gesellsch. d. Wiss.* **14**, 393-410.

Cathcart, C.W. (1884) Movements of the shoulder girdle Involved in those of the Arm on the Trunk. *J. Anat. and Physiol.* **18**, 210-218.

Cave, A.J.E. (1961) The nature and morphology of the costoclavicular ligament. *J. Anatomie* **95**, 170-179.

Chao, E.Y.S. (1980) Justification of triaxial goniometer for the measurement of joint rotation. *J. Biomechanics* **13**, 989-1006.

Chao, E.Y.S., Ljnch, J.D., Vanderploeg M.J. (1993) Simulation and Animation of Muskuloskeletal Joint System'. *Bioengineering Conference, Forum on the 20th Anniversary of ASME Biomechanics Symposium, Breckenridge*, 25-29.

Cleland, J. (1881) Shoulder Girdle and its Movements *The Lancet* **7**, 283-284.

Codman E.A. (1934) The Shoulder. Rupture of the Supraspinatus Tendon and other Lesions in or about the Sub-Acromial Bursa, Boston: Thomas Todd Company.

Cole, G. K., Nigg, B.M., Ronsky, J.L. and Yeadon, M.R. (1993) Application of the joint coordinate system to three dimensional joint attitude and movement representation: a standardization proposal. *Journal of Biomechanical Engineering.*, **115**, 344-349

Conway, A. M. 1961 " Movements at the sterno-clavicular and acromio-clavicular joint. *Phys. Ther. Rev.*, **11**, 421-432.

Culham, E. and Peat, M. (1993) Spinal and shoulder complex posture. I: Measurement using the 3Space Isotrak. *Clin. Rehab.* **7**, 309-318.

Dempster, W.T. (1955) *Space requirements of the seated operator* WADC-TR-55-159, Aerospace MEDICAL Research Laboratories.

Denavit, J. and Hartenberg,R.S. (1955) "A kinematic notation for lower pair mechanisms based on matrices" *Journal of Applied Mechanics* **22**, 215-221

Doody, S.G., Waterland, J.C. and Freedman, L. (1970a) Prosthetics, Orthotics and Devices. Scapulo-humeral Goniometer. *Arch. Phys Med Rehab.* **51**, 711-713.

Doody, S.G., and Freedman, L. Waterland, J.C. (1970b) Shoulder Movements during abduction in the Scapular Plane. *Arch. Phys Med Rehab.*, **51**, 595-604.

Duchenne, G.-B. (1867) *Physiologie des mouvements* pub. Paris: Bailliere

Dvir, Z. and Berme (1978) N. The Shoulder Complex in Elevation of the Arm: a Mechanism Approach. *J. Biomechanics* **11**, 219-225

Engin, A. E. and Tumer S. T. (1989) Three-Dimensional Kinematic Modelling of the Human Shoulder Complex- Part I: Physical Model and Determination of Joint Sinus Cones. *Journal of Biomechanical Engineering.* **111**, 107-112

Engin, A.E. (1980) On the biomechanics of the shoulder complex. *J. Biomechanics* **13**, 575-590.

Engin A.E., Peindl,R.D., Berme,N. and Kaleps, I. (1984) Kinematic and force data collection in biomechanics by means of sonic emitters-I. Kinematic data collection methodology. *Journal of Biomechanical Engineering* **106**, 204-211.

Engin, A.E. and Chen, S.M. (1986) Statistical database for the biomechanical properties of the human shoulder complex – I Kinematics of the shoulder complex. *Journal of Biomechanical Engineering* **108**, 215-221.

Engin, A.E. and Peindl, R.D. (1987) On the biomechanics of human shoulder complex - I. Kinematics for determination of the shoulder complex sinus. *J. Biomechanics* **20**, 103-117.

Engin, A.E. and Tumer, S.T. (1989) Three-dimensional kinematic modelling of the human shoulder complex - II. Mathematical modelling and solution via optimisation. *Journal of Biomechanical Engineering* **111**, 113- 121.

Fisk, J.H. (1944) Some Observations of Motion at the Shoulder Joint. *Canadian Med. Assn J* **50**, 213-216.

Flecker, H. (1929) Roentgenographic Study of the Movements of Abduction at the Normal Shoulder Joint. *Med. J. Australia*, 122-123.

Fraietta N. (1991) Uomo e Movimento Meccanica e organizzazione sistemica degli organi di moto - *Ed. Marrapese Roma.*

Freedman, L. and Munro, R.R. (1966) Abduction of the Arm in Scapular Plane: Scapular and Glenohumeral Movements *J. Bone Jt. Surg.* **48-A**, 1503-1510.

Fukuda K, Graig EV, An KN, Cofield RH, Chao EY (1986): Biomechanical study of the ligamentous system of the acromioclavicular joint. *J. Bone Jt. Surg.* **68A**, 434-439

Galen and Brock (1916), A. J. *On the natural faculties. With an English translation by Arthur John Brock* London: Heinemann

Gallasch, E., Rafolt, D., Moser, M., Hindinger, J., Eder, H., Wiesspeiner, G. and Kenner, T. (1996) Instrumentation for assessment of tremor, skin vibrations, and cardiovascular variables in MIR space missions. *IEEE Transactions on Biomedical Engineering* **43**, 328-333.

Gerhardt, J. J. and J. Rippstein Measuring and Recording of Joint Motion- Hogrefe & Huber Publishers, Toronto

Giordano G., Lanza (1989) Atlante di Anatomia Edizioni Scientifiche Florio, Napoli

Gomes G.T. S.S. Marchese and Johnson G.R. (1999) Determination of upper arm orientation using a triaxial goniometer. Proceedings International Society of Biomechanics XVII World Congress, Calgary, Canada 452

Gupta K. C. (1984) On the Nature of Robot Workspace *Conference on Mechanical Engineering, Haifa, Israel.*

Haken H. (1996) Principles of Brain Functioning. A synergetic approach to brain activity behavior and cognition. Springer-Verlag Berlin

Hall, E.H. (1879) On the new action of the magnet on electric current. *American Journal of Mathematics*, **2**, 287-294

Harrington M. A. Jr, Keller T.S.;Weikert D.R.; Moljanto E.; and Scwartz H.S (1993) Geometric Properties and the Predicted Mechanical Behaviour of Adult Human Clavicle. *J. Biomechanics* **26**, 417-426

Hippocrates and Littré, E. (1839-61) Oeuvres completes d'Hippocrate. Paris: Bailliére

Hogfors C., Sigholm, G., P. Herberts P. (1987) Biomechanical Model of the Human Shoulder, I. Elements. *J. Biomechanics* **20**, 157-166.

Hogfors, C., Karlsson, D. and Peterson B. (1995) Structure and Internal Consistency of a Shoulder Model. *J. Biomechanics*, **28** 767-777

Hogfors, C., Peterson, B. Sigholm G. and P. Herberts (1991) Biomechanical Model of the Human Shoulder Joint-II. The Shoulder Rythm – *J. Biomechanics* **24**, 669-709.

Hogfors, C., Peterson, B. Sigholm, G. and Herberts, P. (1991) Biomechanical Model of the Human Shoulder Joint, II. The Shoulder Rhythm. *J. Biomechanics* **8**, 699-709.

Horn, J.S. (1954) The traumatic anatomy and treatment of acute acromio-clavicular dislocation. *J. Bone Jt. Surg.* **36-B**, 194.

Inman, V. T., Saunders M. and L. C. Abbott (1944) Observations on the Function of the Shoulder Joint - *J. Bone Jt. Surg.* **26**, 1-30

Inman, V.T. and Saunders, J.B. (1946) Observations on the functions of the clavicle. *Calif. Med.* **65**, 158-166.

Ito, N. (1980) Electromyographic Study of Shoulder Joint. *Jpn. Orthop. Assoc.* **54**, 1529-1540.

Jacobs, B. and Wade, P.A. (1966) Acromioclavicular joint injury. *J. Bone Jt. Surg.* **48-A**, 475-486.

Jensen, R.K. (1993) Human Morphology: Its Role in the Mechanics of Movement. *J. Biomechanics* **26**, 81-84.

Johnson, G.R. and Anderson, J.M. (1990) Measurement of three dimensional shoulder movement by an electromagnetic sensor. *Clinical Biomechanics* **5**, 131-136.

Johnson, G.R. and Gill, J. M. (1987) Predictions of the range of hand positions available to a patient with movement restrictions at the joints of the upper limb. *International Journal of Rehabilitation Research* **10**, Supplement 5.

Johnson, G.R., Spalding, D., Nowitzke, A. and Bogduk, N. (1996) Modelling the muscles of the scapula: morphometric and coordinate data and functional implication. *J. Biomechanics* **29**, 1039-1051.

Johnson, G.R., Stuart, P.R. and Mitchell, S. (1993) A method for the measurement of three-dimensional scapular movement. *Clinical Biomechanics*, 269-273.

Johnson, G.R. and Barnett, N.D. (1996) The measurement of three dimensional movements of the shoulder complex. *Clinical Biomechanics* **5**, 131-136

Jones, L. (1956) The Shoulder Joint. Observations on Comparative Anatomy, Physiology and Treatment. California Medicine **84**, 185-192

Jou, T. M. and Waldron, K. J. (1983) Geometric Design of Manipulators using Interactive Computer Graphics *Proc. 6th World Congress on Theory of Machines and Mechanisms* 949-954.

Kapandji, I.A. (1994) Physiologie Articulaire. Tome 1: Membre Supérieur, 5th Edition. Maloine

Karlsson, D. and Peterson, B. (1992) Towards a Model for Force Predictions in the Human Shoulder *J. Biomechanics* **25** 189-199

Kennedy, J.C. and Cameron, H. (1954) Complete dislocation of the acromioclavicular joint. *J. Bone Jt. Surg.* **36-B**, 202-208.

Kinzel, G.L. and Gutkowski, L.J. (1983) Joint Models, Degrees of Freedom and Anatomical Motion Measurement. *Journal of Biomechanical Engineering* Transactions of ASME **105**, 59-62

Kumar, A., Waldron, K. J. (1981) The Workspaces of a Mechanical Manipulator *Journal of Mechanical Design* **103**, 665-672.

Langrana N. A. (1981) Spatial Kinematics Analysis of the Upper Extremity Using a Biplanar Videotaping Method. *Journal of Biomechanical Engineering* **103**, 11-17.

Larsen, E., Bjerg-Nielsen, A. and Christensen, P. (1986) Conservative or surgical treatment of acromial dislocation. *J. Bone Jt. Surg.* **68-A**, 552-555.

Laumann, U. (1982) Kinesiology of the Shoulder Electromyographic and Stereophotogrammetric Studies. In: Bateman and Walsh, (eds.) Surgery of the Shoulder. 6-11.

Lenarcic, J., Stanic, U. and Oblak P. (1989) Some Kinematic Considerations for the Design of Robot Manipulators. *Robotics & Computer Integrated Manufacturing* **5**, 235-241

Leonardo Da Vinci Corpus degli Studi Anatomici nella Collezione di Sua Maestà la Regina Elisabetta II nel Castello di Windsor Vol. I Facsimili di Tavole di Concordanza Giunti Barbera Editore.

Lockart, R.D. (1930) Movements of the Normal Shoulder Joint and a Case with Trapezius Paralysis Studied by Radiogram and Experiments in the Living. *J. Anat.* **64**, 288-302.

Luria A.R. Come Lavora il Cervello. Ed. Il Mulino, 1997

Luria A.R. Le Funzioni Corticali Superiori dell'Uomo. Giunti Barbera Universitaria, 1967

Marchese, S. S., Buckley, M.A., Valleggi, R. and Johnson G.R (1997) An optimised design of an active orthosis for the shoulder. An iterative approach Proceeding of *International Conference on Rehabilitation Robotics Bath, UK* 14-15 .

Marchese, S.S. and Johnson G.R. (1997) State of the Art Analysis of Measurement Systems in Rehabilitation. Technical Report. *Development and Validation of New Assistive Devices for the Treatment of Disability Caused by Tremor "Tremor"* European Project n. DE 3216 Telematics Applications Programme

Marey, E.J. (1885) La Methode Graphique. 2nd ed. Paris: G. Masson Editeur

Nicol, A.C. (1987) A new flexibie goniometer with widespread applications. In: *Biomechanics XB*, 1029-1033. Illinois: Human Kinetics.

Pallas–Areny, R. and Webster, J.G (1991) Sensor and Signal Conditioning, New York: *John Wiley and Sons.*

Panjabi, M.M., Goel, V. K., Walter, S.D. and Schick (1982) S. Errors in the Centre and Angle of Rotation of a Joint. An Experimental Study. *Journal of Biomechanical Engineering. Transactions of the ASME* **104**, 232-237

Paul, R.P.(1981) *Robot manipulators (Mathematics, programming and control),* MIT Press: Cambridge, Mass.

Peindl, R.D. and Engin, A.E. (1987) On the biomechanics of human shoulder complex - II. Passive resistive properties beyond the shoulder complex sinus. *J. Biomechanics* **20**, 119-134.

Perry, J. (1978) Normal Upper extremity kinesiology. *Phys. Ther.* **53**, 265-278.

Poirier, P. (1890) La clavicle et ses articulations. Bourses séreuses des ligament costo-claviculaire trapezoide en conoide. *J. D'Anatomie* **26**, 82-103.

Poppen, N.K. and Walker P.S. (1976) Normal and Abnormal Motion of the Shoulder. *J. Bone Jt. Surg.* **58-A**, 195-201

Pronk, G.M. and van der Helm, F.C.T. (1989) The role of the coracoclavicular mechanism in the motion pattern between scapula and clavicle. Proceedings of the 12th International congress of biomechanics. Los Angeles, USA, 654-655.

Pronk, G. (1991) The shoulder girdle. Ph.D Thesis, University of Delft, Netherlands

Pronk, G.M. and van der Helm, F.C.T. (1991) The palpator: an instrument for measuring the positions of bones in three dimensions J. Med. Eng. Tech. **15**, 15-20.

Pronk, G.M., van der Helm, F.C.T. and Rozendaal, L.A. (1993) Interaction between the joints in the shoulder mechanism: the function of the costoclavicular, conoid and trapezoid ligaments. Presented at the International seminar on "Biomechanics and joint replacement in the upper limb". London.

Raikova, R.A. (1992) General Approach for Modelling and Mathematical Investigation of the Human Upper Limb. *J. Biomechanics* **25**, 857-867.

Safaee-Rad, R., Shwedyk, E., Quanbury, O. and Cooper, J.E. (1990) Normal Functional Range of Motion of Upper Limb Joints during performance of Three Feeding Activities. *Arch. Phys. Med. Rehabil.* **71**, 505-509.

Saha, A.K. Mechanism of Shoulder Movements and a Plea for the Recognition of the "Zero Position" of the Glenohumeral Joint. *Clin. Orthop.* **173**, 3-10

Savelberg H.H.C.M., Otten J.D.M., Kooloos J.G.M.; Huiskes R. and Kauer J.M.G. (1993) Carpal Bone Kinematics and Ligament Lengthening Studied for the full Range of Joint Movement. *J. Biomechanics* **26**, 1389-1402.

Sherrington, C. S. (1933) *The brain and its mechanism* Cambridge: University Press.

Sherrington, C.S. (1973) *The integrative action of the nervous system* New York: Arno Press

Smith S. (1986) Anatomia, Prospettiva e Composizione Trattato di Disegno Professionale Specializzato ed. Editemme.

Sprigings, E., Marshall, R., Elliott, B. and Jennings, L. (1994) A 3D Kinematic Method for determining the Effectiveness of Arm Segment Rotations in Producing Racquet Head Speed. *J. Biomechanics* **27**, 245-254.

Timmer, J., Gantert, C., Deuschl, G. and Honerkamp, J. (1993) Characteristics of hand tremor time series. *Biological Cybernetics* **70**, 75-80.

Thomas, D.B. The first Negatives. London. HMSO, 1964

Umek A., Lenarcic, J. (1991) Recent Resulis in Evaluation of Human Arm Workspace IEEE *Proc. of International Conference on Advanced Robotics*, Pisa, Italy 237-242.

Urist, M.R. (1946) Complete dislocation of the acromio-clavicular joint. *J. Bone Jt. Surg.* **28**, 813-837.

Van der Helm F.C.T., Veeger H. E.J., Pronk G. M., van der Woude, L.H.W and Rozendal, R. H. (1992) Geometry parameters for musculoskeletal modelling of the shoulder mechanism. *J. Biomechanics* **25**, 129-144.

Van der Helm, F.C.T. (1994a) A finite element musculoskeletal model of the shoulder mechanism. *J. Biomechanics*, **27**, 551-569.

Van der Helm, F.C.T. (1994b) Analysis of the kinematic and dynamic behavior of the shoulder mechanism. *J. Biomechanics* **27**,527-550.

van der Helm, F.C.T. A standardized protocol for motion recordings of the shoulder. http://www.fbw.vu.nl/research/Lij...oulder/isg/proposal/protocol.html

van der Helm, F.C.T. and Pronk, G.M. (1995) Three- dimensional recording and description of motions of the shoulder mechanism. *Journal of Biomechanical Enginecring* **117**, 27-40.

van der Helm, F.C.T. and Veenbaas, R. (1991) Modelling the mechanical effect of muscles with large attachment sites: Application to the shoulder mechanism. *J. Biomechanics*, **27**, 1151-1163.

van der Helm, F.C.T., Veeger, H.E.J., Pronk, G.M., van der Woude, L.V.H. and Rozendal, R.H. (1992) Geometry parameters for musculoskeletal modelling of the shoulder system. *J. Biomechanics*, **25**, 129-144.

Van Der Helm, F.T.C. (1994) Analysis of the Kinematic and Dynamic Behaviour of the Shoulder Mechanism. *J. Biomechanics*. **27**, 527-550.

Verstraete, M.C. and Soutas-Little R.W (1990) Method for Computing the Three Dimensional Angular Velocity and Acceleration of a Body Segment from Three Dimensional Position Data. *Journal of Biomechanical Engineering* **112**, 114-118

Vijaykumar, R., Tsai, M. J. and Waldron, K. J. (1985) Geometric Optimisation of Serial Chain Manipulators Structures for Working Volume and Dexterity. *Int Conference on Robotics and Automation* 228-236

Wallace, W.A and Johnson F. (1982) A bionechanical Appraisal of the Acromioclavicular Joint. In: Bailey and Kessel. (eds.) *Shoulder Surgery*, 179-182.

Wang L., Wu, H., Chang, Su and Lo (1996) Three dimensional kinematic analysis of upper extremity in the soft-tennis forehand drive. In: Haake, *The Engineering of Sport*, 141-146. Rotterdam: Balkema.

Wang, X., Maurin, M., Mazet, F., De Castro Maia, N., Voinot, K., Verriest, J.P. and Fayet, M. (1998) Three-dimensional modelling of the motion range of axial rotation of the upper arm. *J. Biomechanics* **31**, 899-908.

Winter D. A. (1990) Biomechanics and Motor Control of Human Movement. *Pub*: *Wiley Interscience Publication.*

Wirhead R. (1982) Athletic Ability and the Anatomy of Motion *Pub*: *Wolfe Medical Publications ltd.*

Wood, J.E., Meek S.G., and Jacobsen S.C. (1989) Quantitation of Human Shoulder Anatomy for Prosthetic Arm Control, II Anatomy Matrices *J. Biomechanics* **22**, 309-325

Wuelker, N. Wirth, C. J., Plitz, W.and Roetman, B. (1995) A Dynamic Shoulder Model: Reliability Testing and Muscle Force Study *J. Biomechanics* **28**, 489-499.

Yoshikawa, T. (1985) Manipulability of Robotics Mechanisms. *Journal of Robotics Research*. **4**, 3-9.

Young, D.C.H. and Lee T.W. (1984) Heuristic Combinational Optimisation in the Design of Manipulator Workspace, *IEEE Trans. on Syst., Man. and Cybern.* **14**, 571-580.

11 Appendix A

This appendix contains the graphs of the tests performed on the subjects. Data related to the graphs are given in Appendix B.

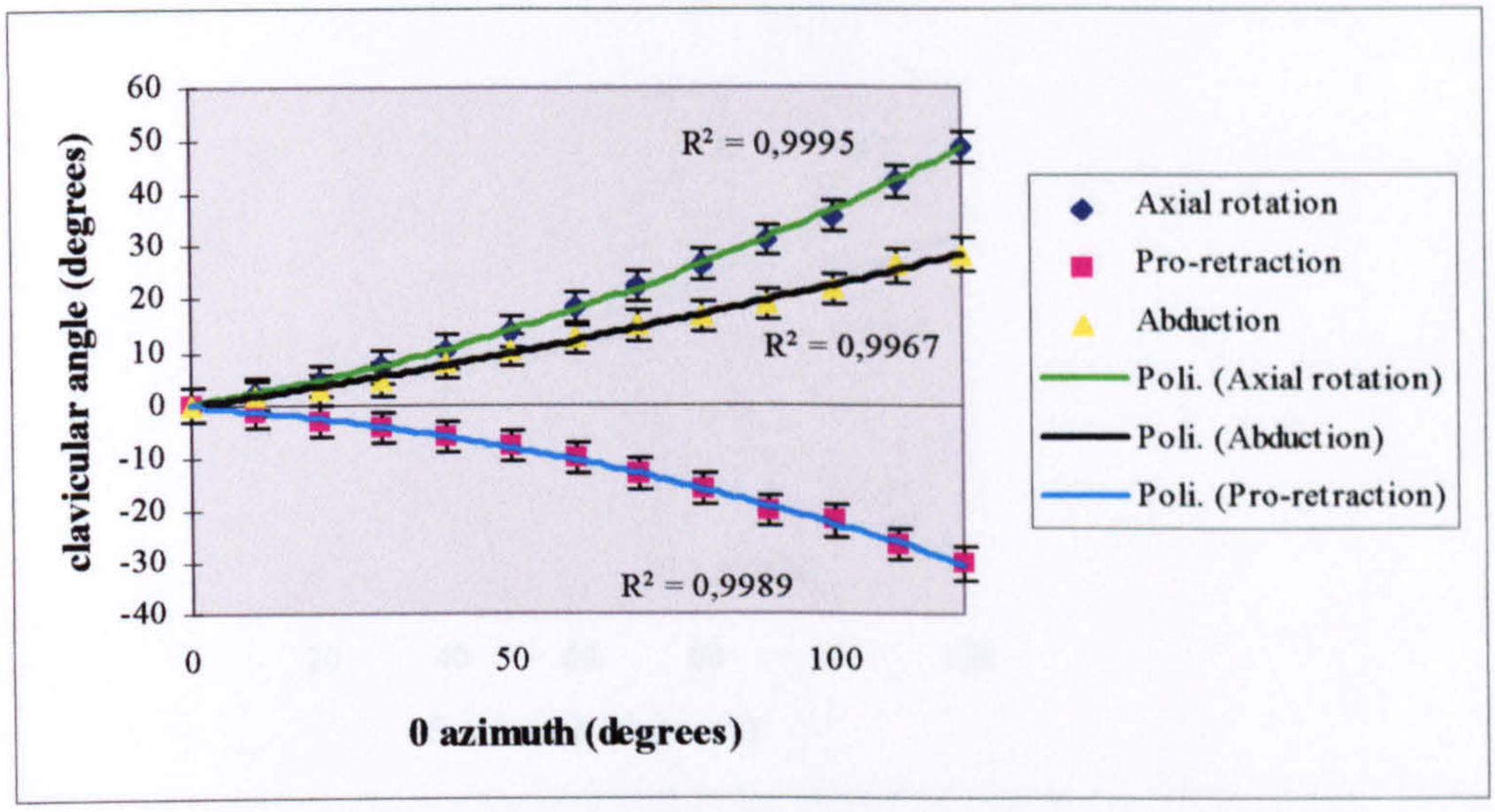

Figure 11.1 a: *Subject 4 (L/R=2,37) - observer 1*

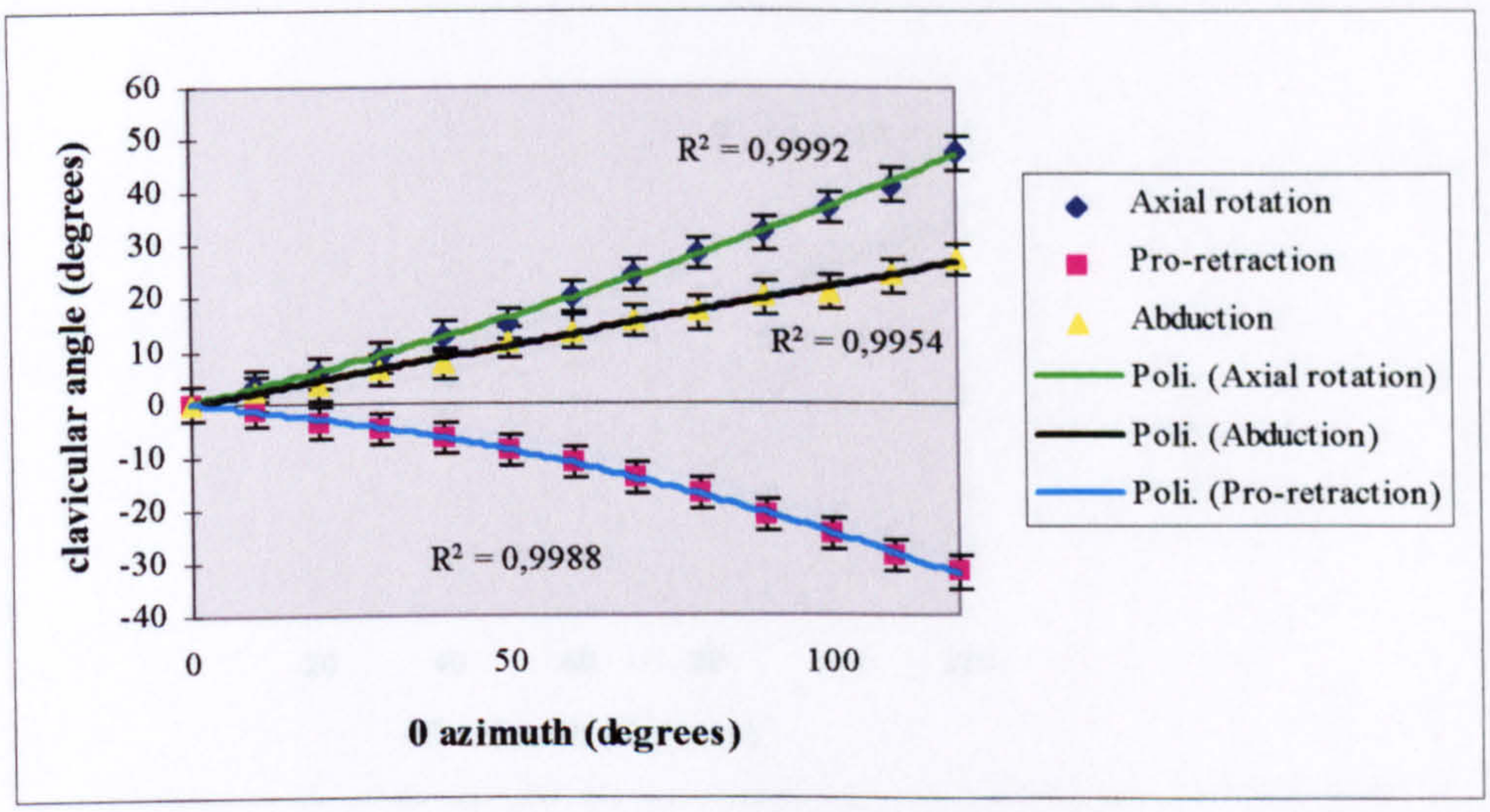

Figure 11.1 b: *Subject 4 (L/R=2,37) - observer 2*

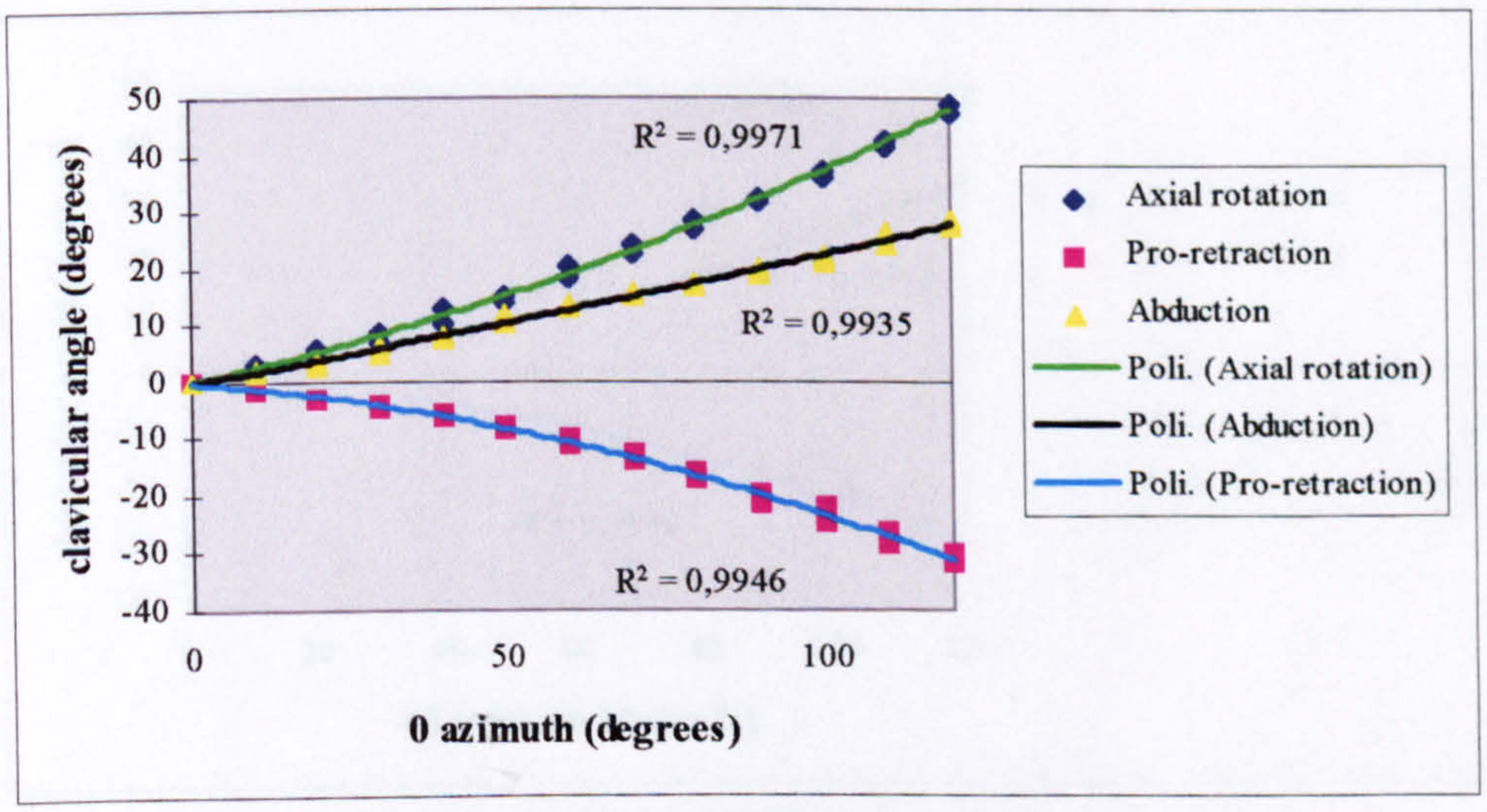

Figure 11.1 c: *Subject 4 (L/R=2,37) - inter observer*

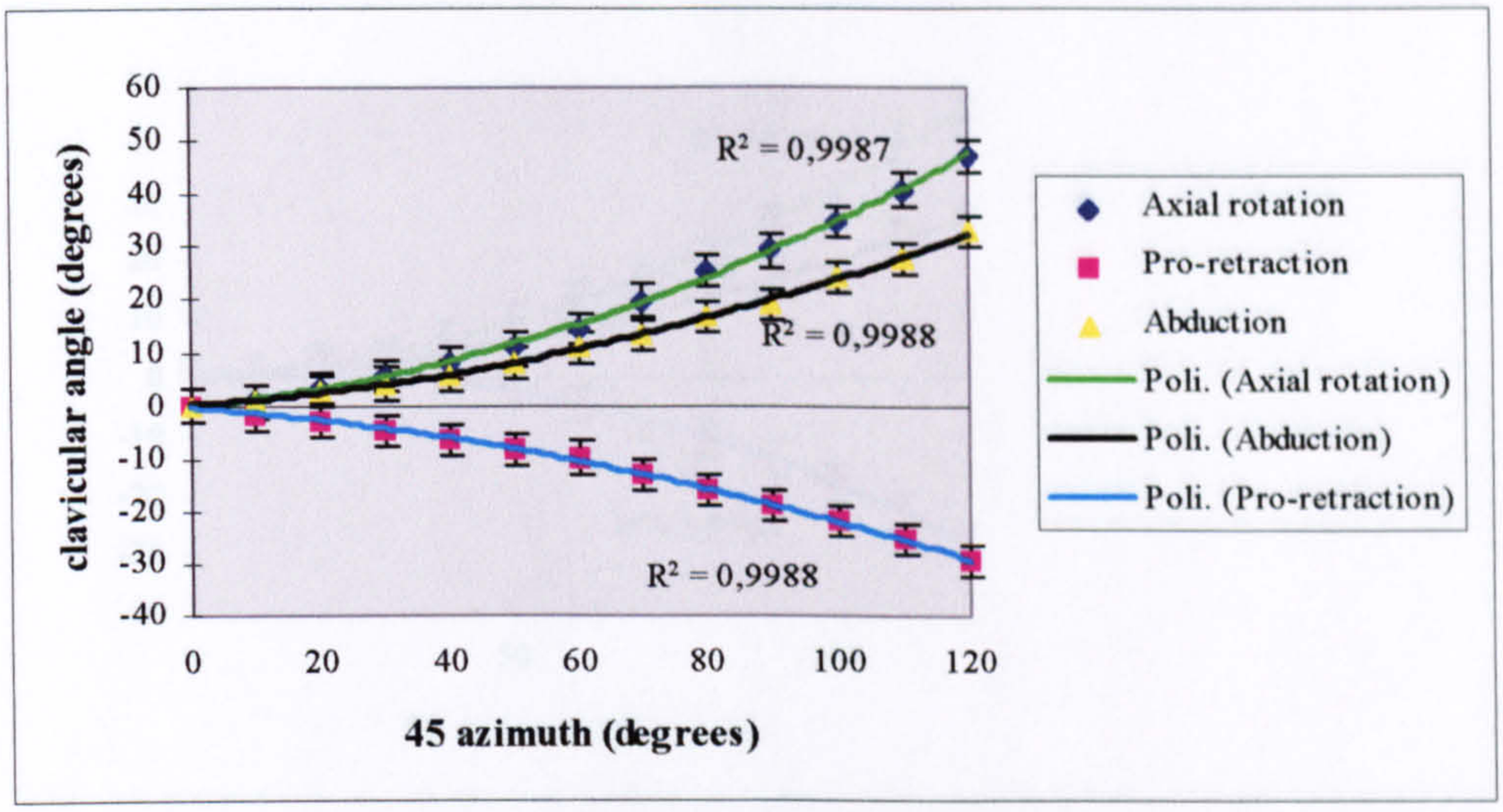

Figure 11.2 a: *Subject 4 (L/R=2,37) - observer 1*

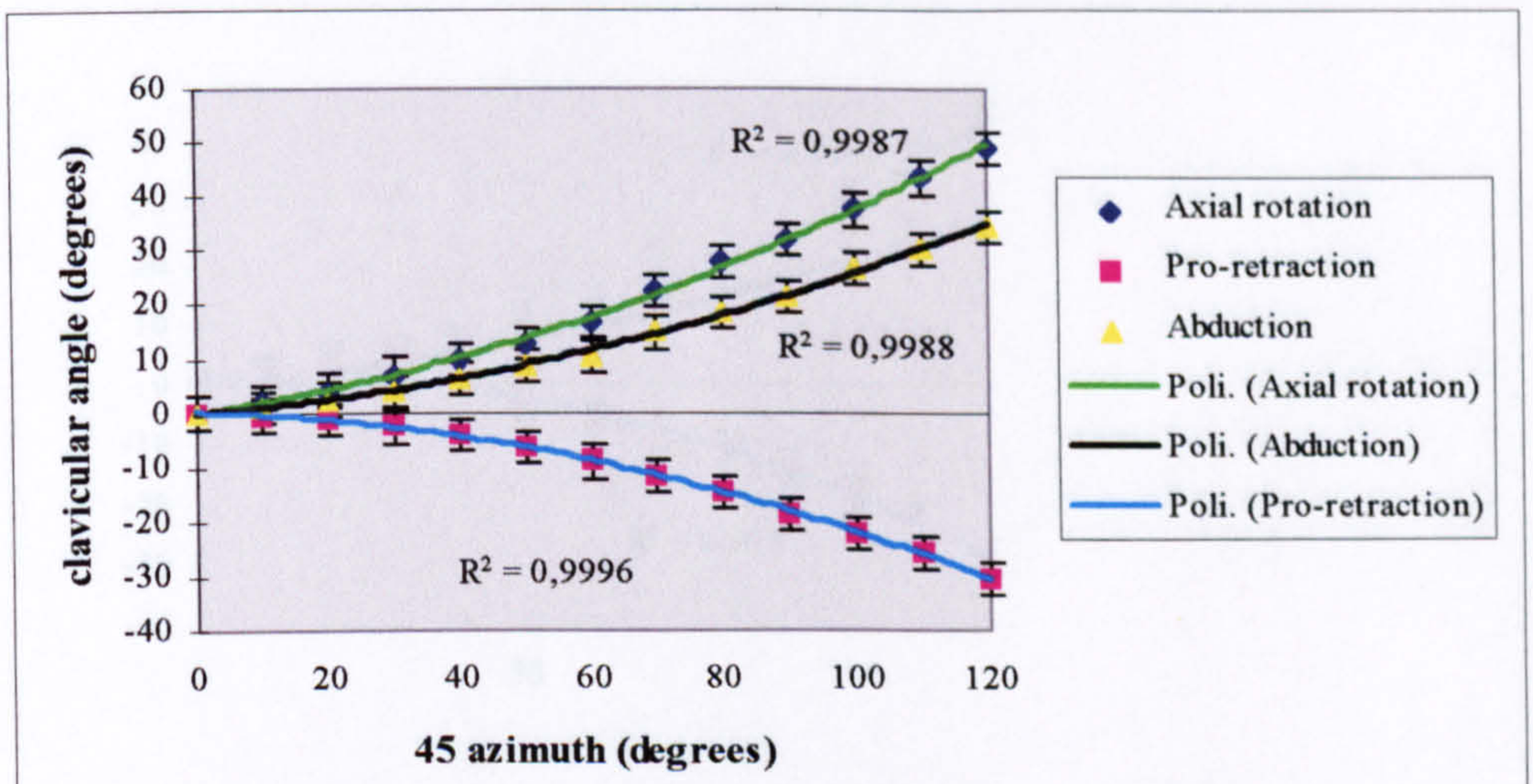

Figure 11.2 b: *Subject 4 (L/R=2,37) - observer 2*

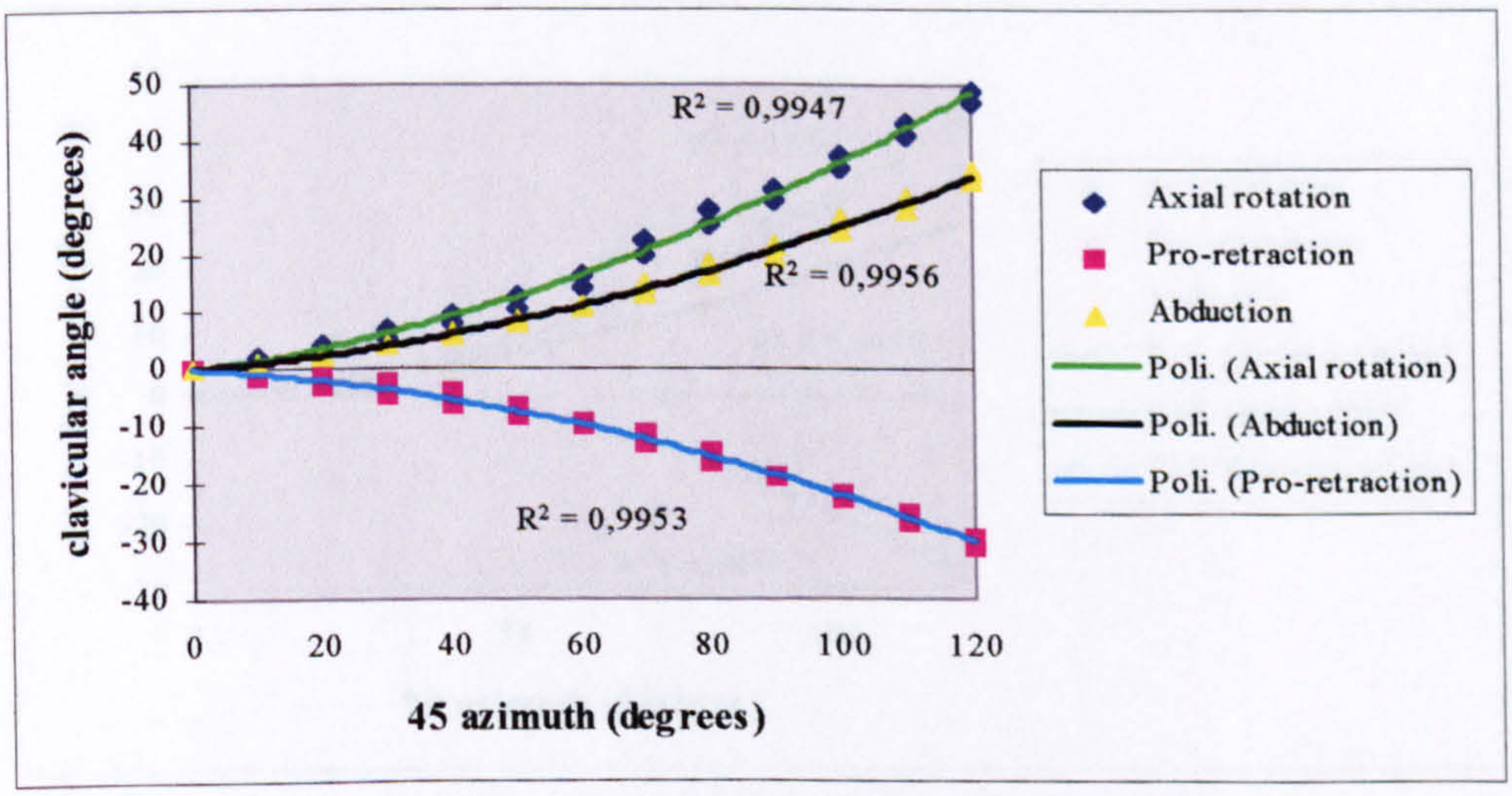

Figure 11.2 c: *Subject 4 (L/R=2,37) - inter observer*

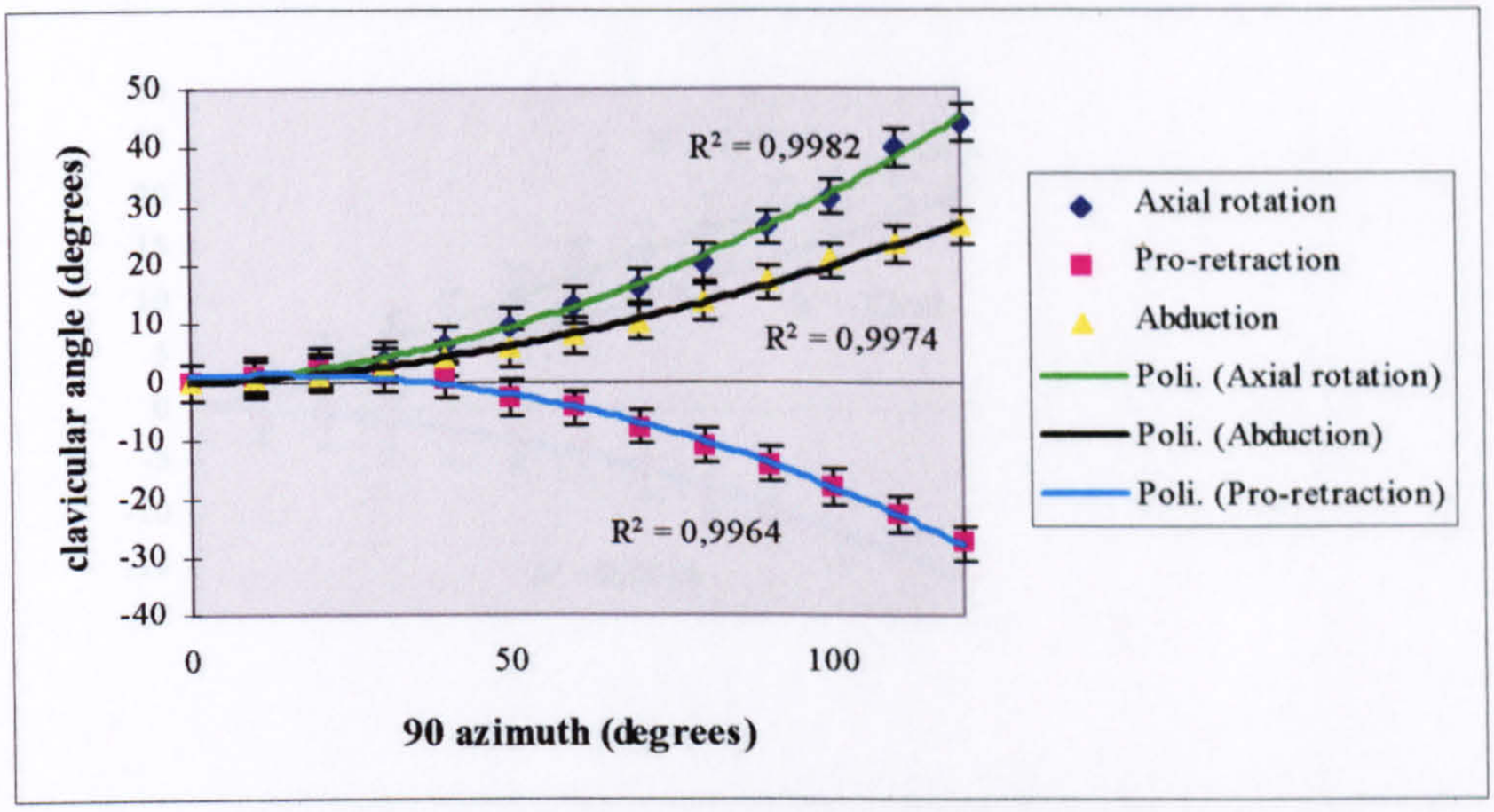

Figure 11.3 a: *Subject 4 (L/R=2,37) - observer 1*

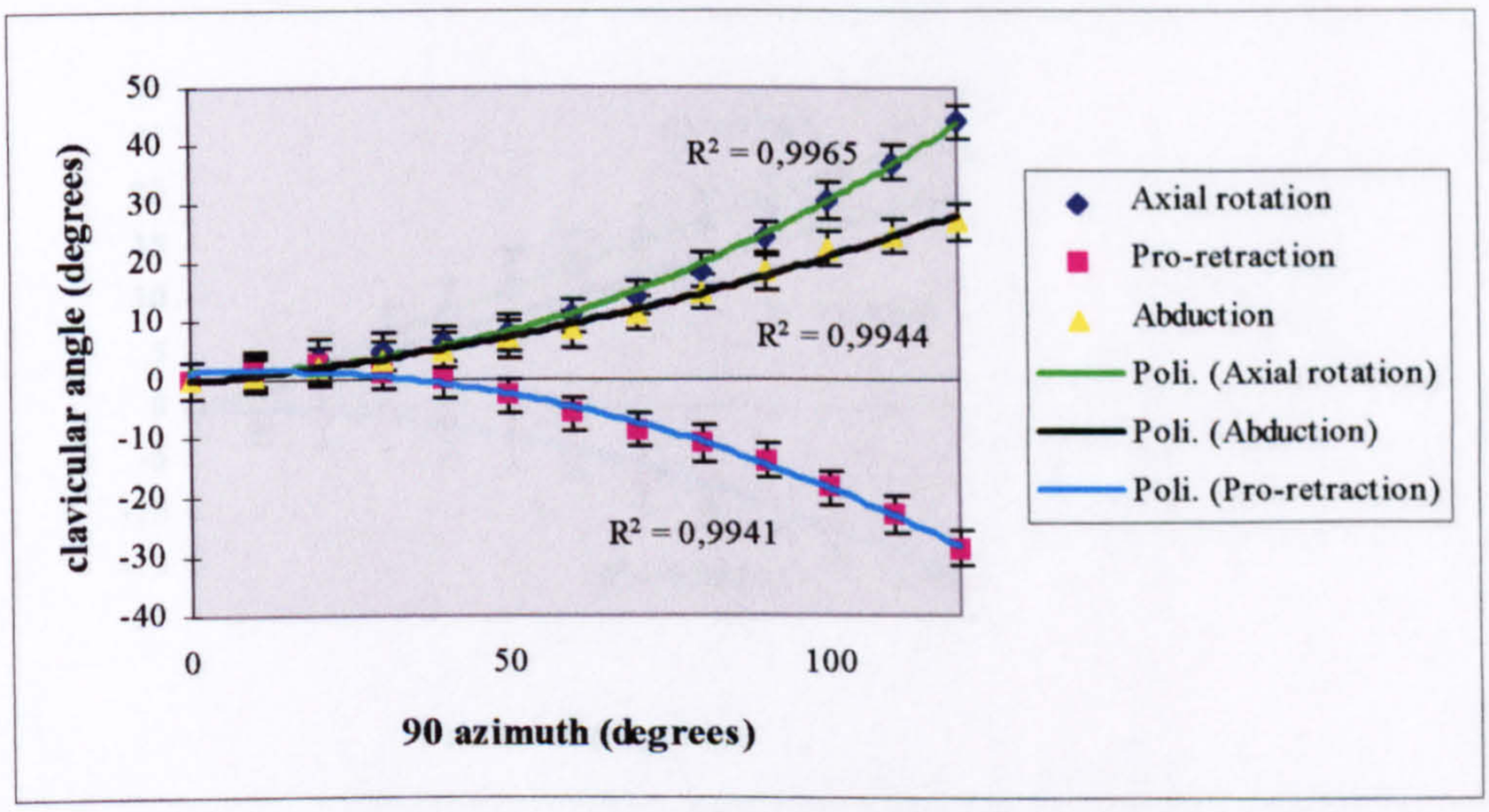

Figure 11.3 b: *Subject 4 (L/R=2,37) - observer 2*

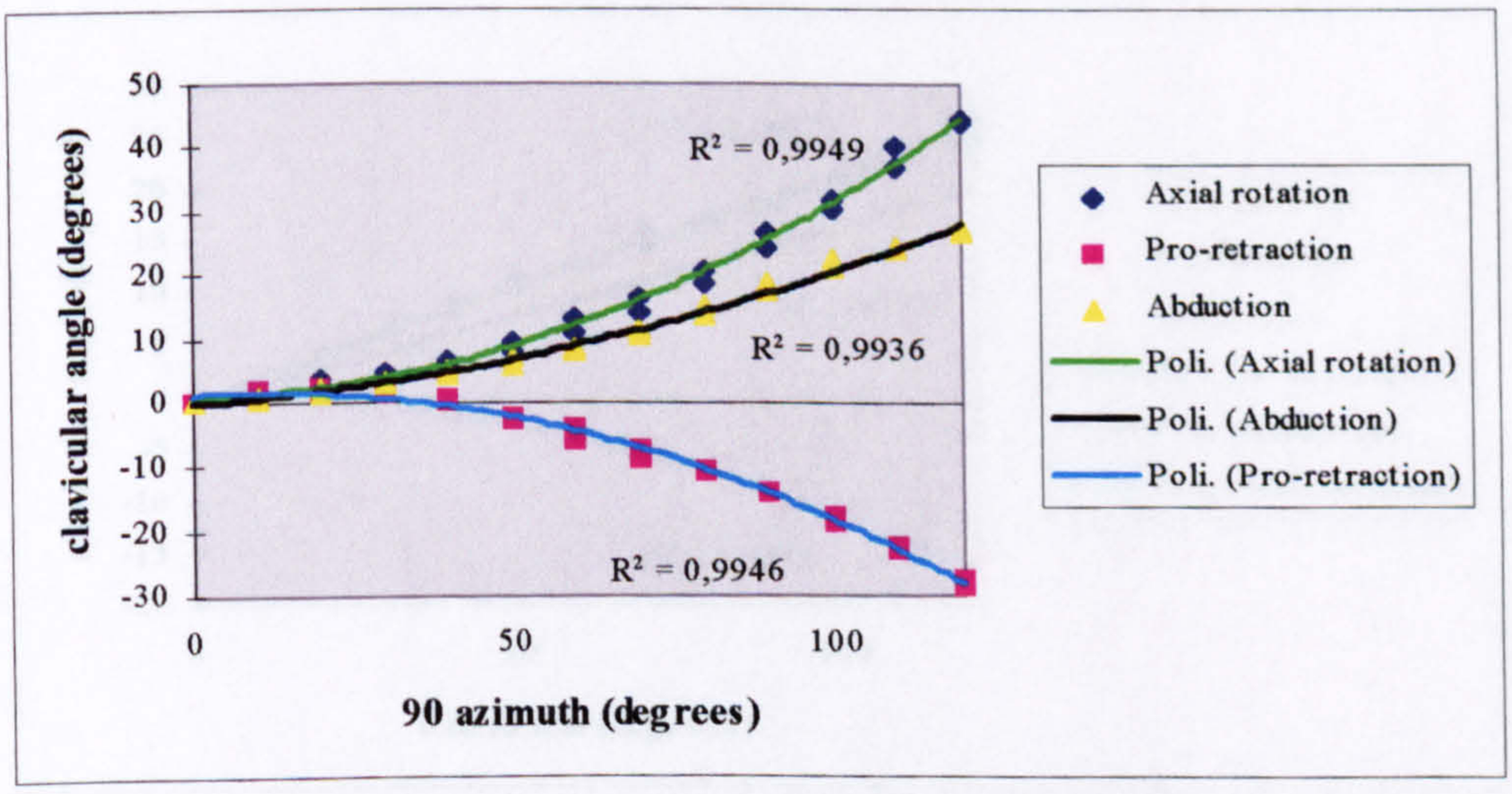

Figure 11.3 c: *Subject 4 (L/R=2,37) - inter observer*

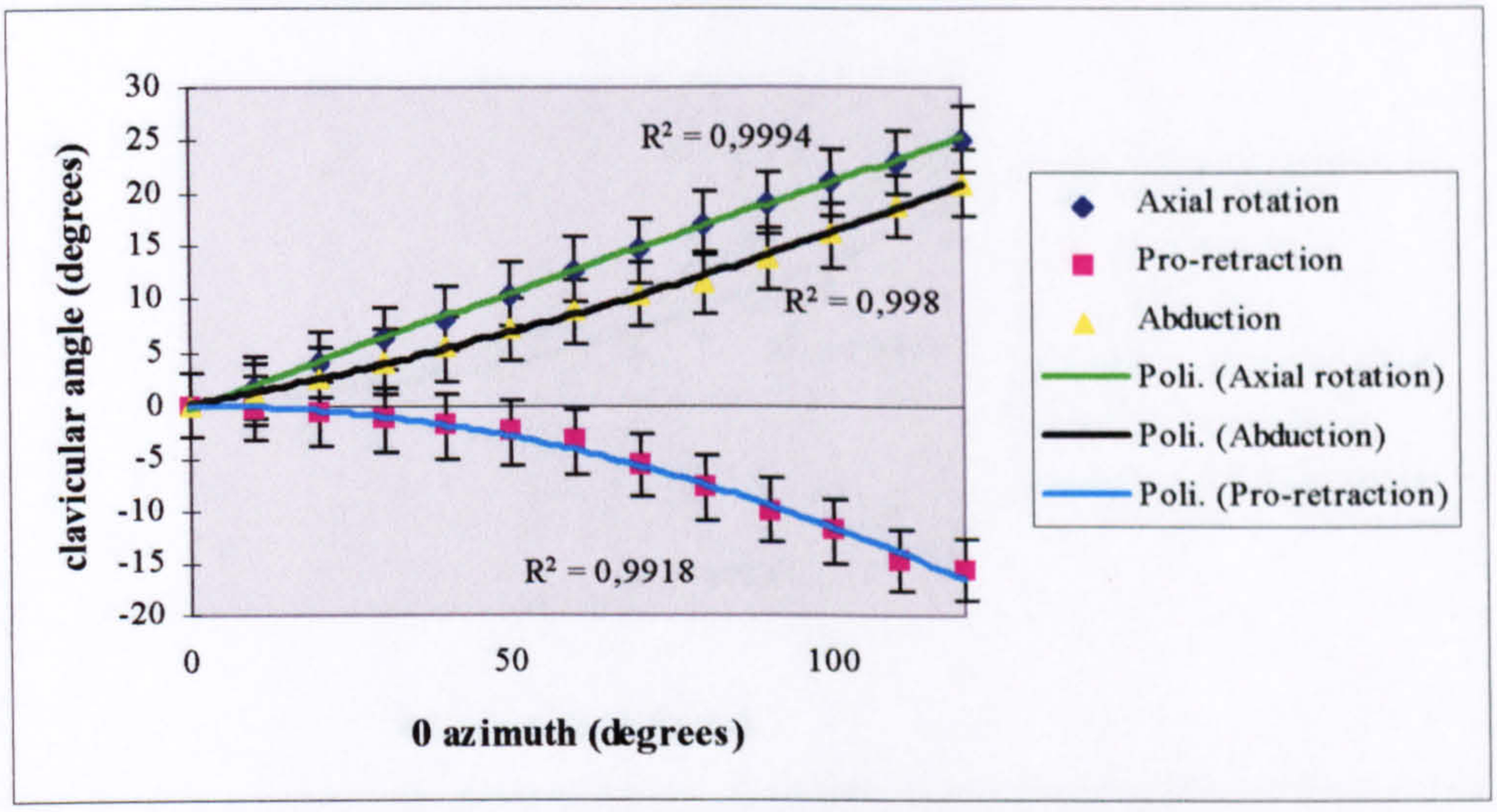

Figure 11.4 a: *Subject 5 (L/R=1,92) - observer 1*

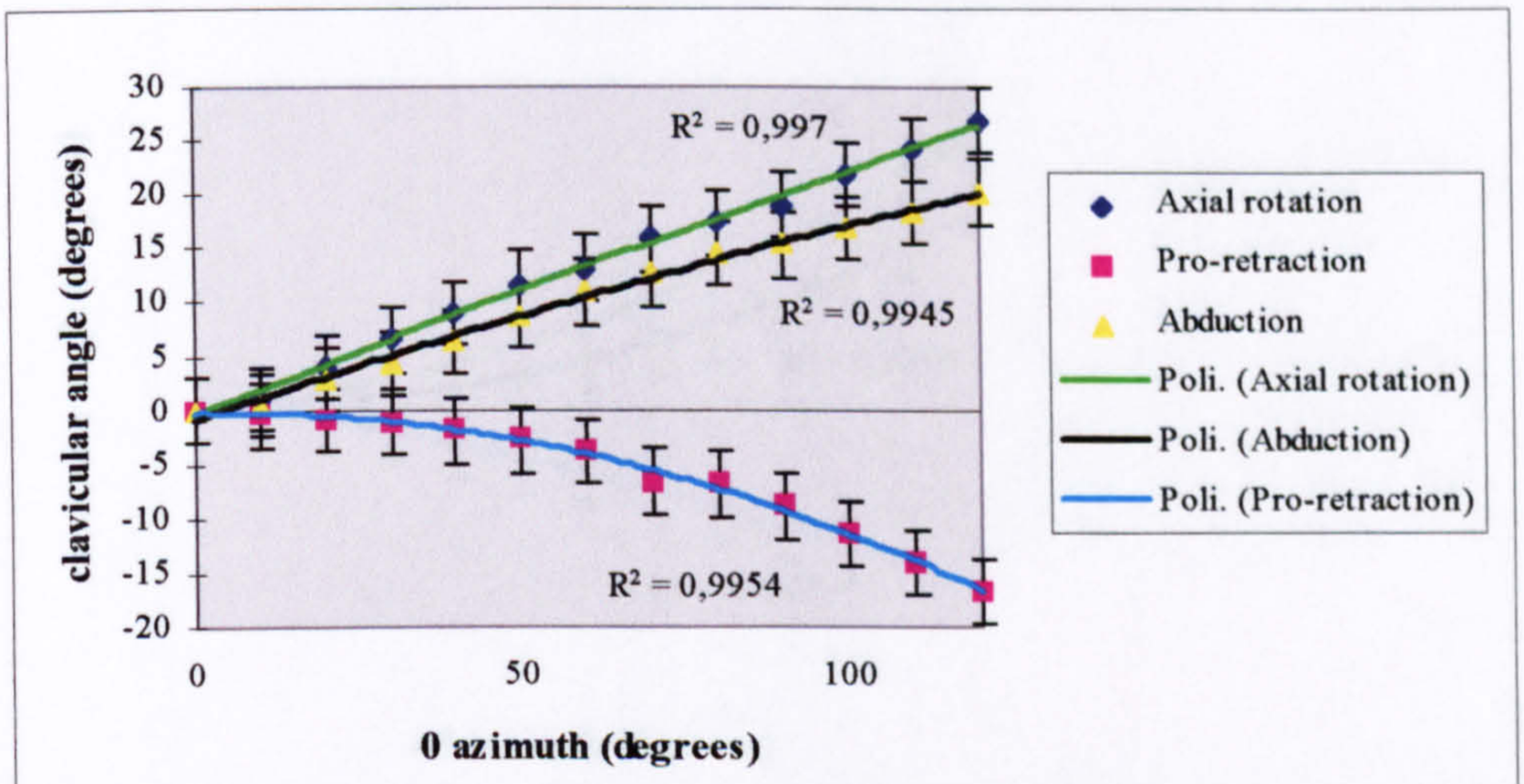

Figure 11.4 b: *Subject 5 (L/R=1,92) - observer 2*

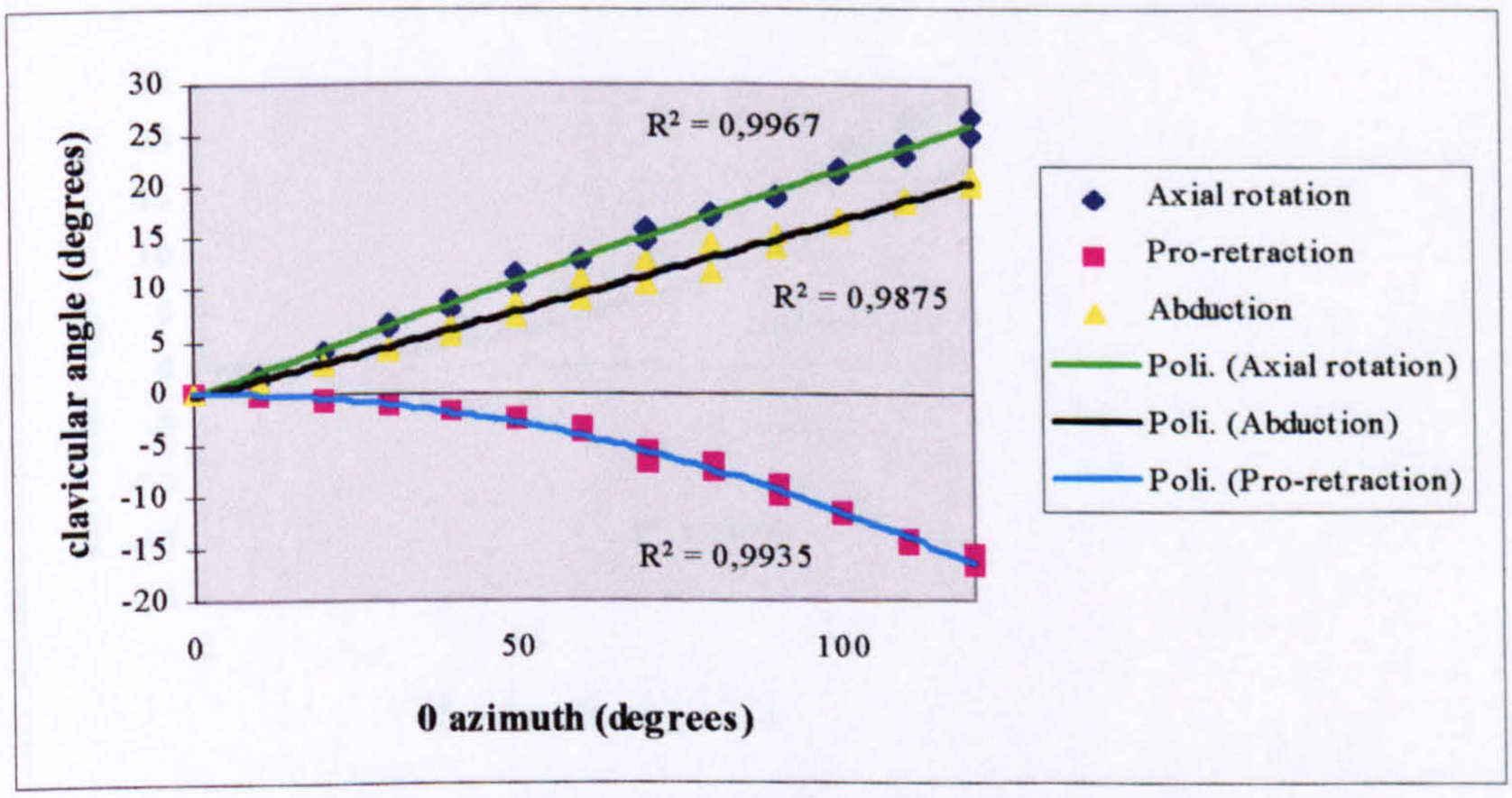

Figure 11.4 c: *Subject 5 (L/R=1,92) - inter observer*

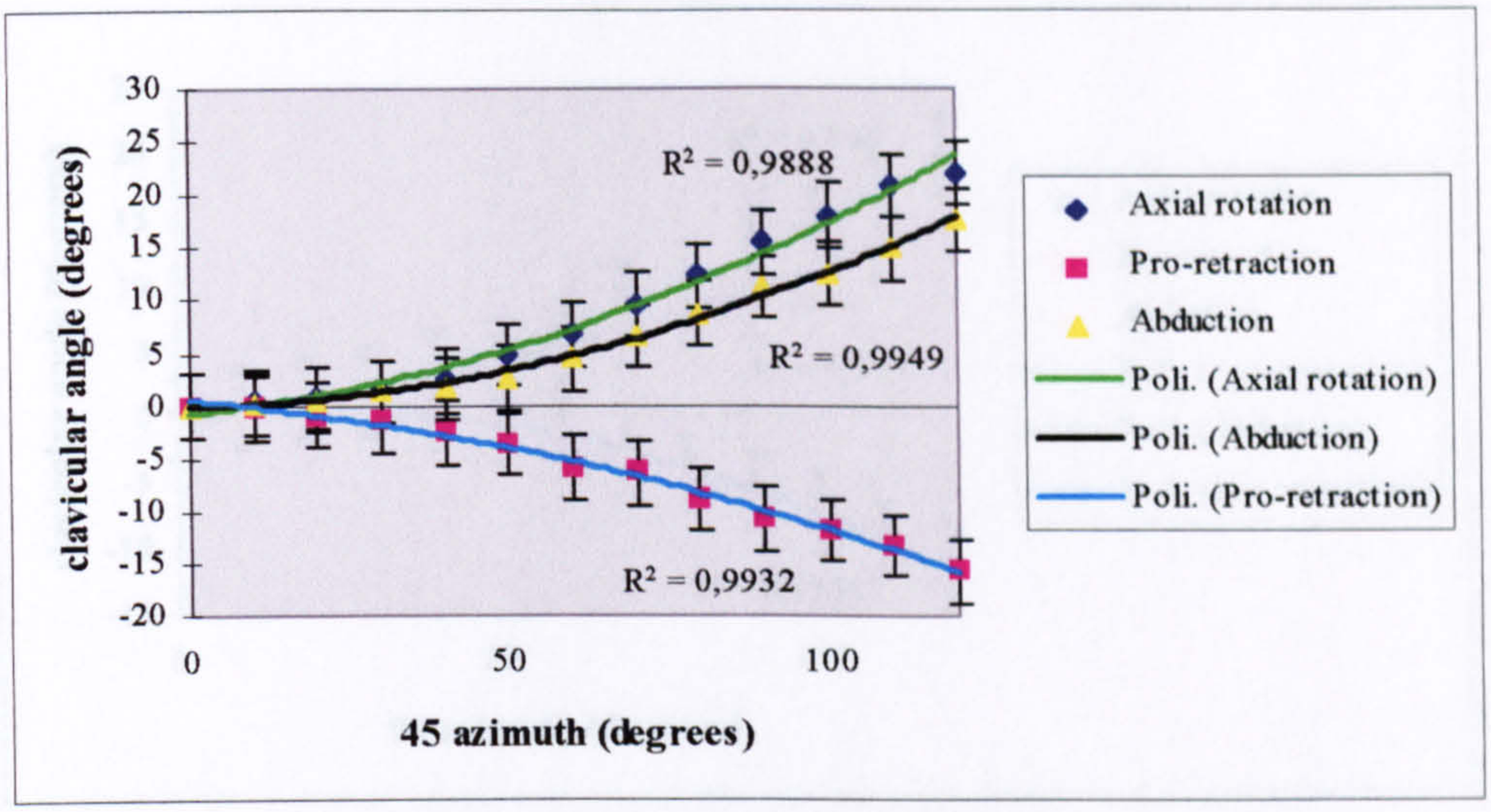

Figure 11.5 a: *Subject 5 (L/R=1,92) - observer 1*

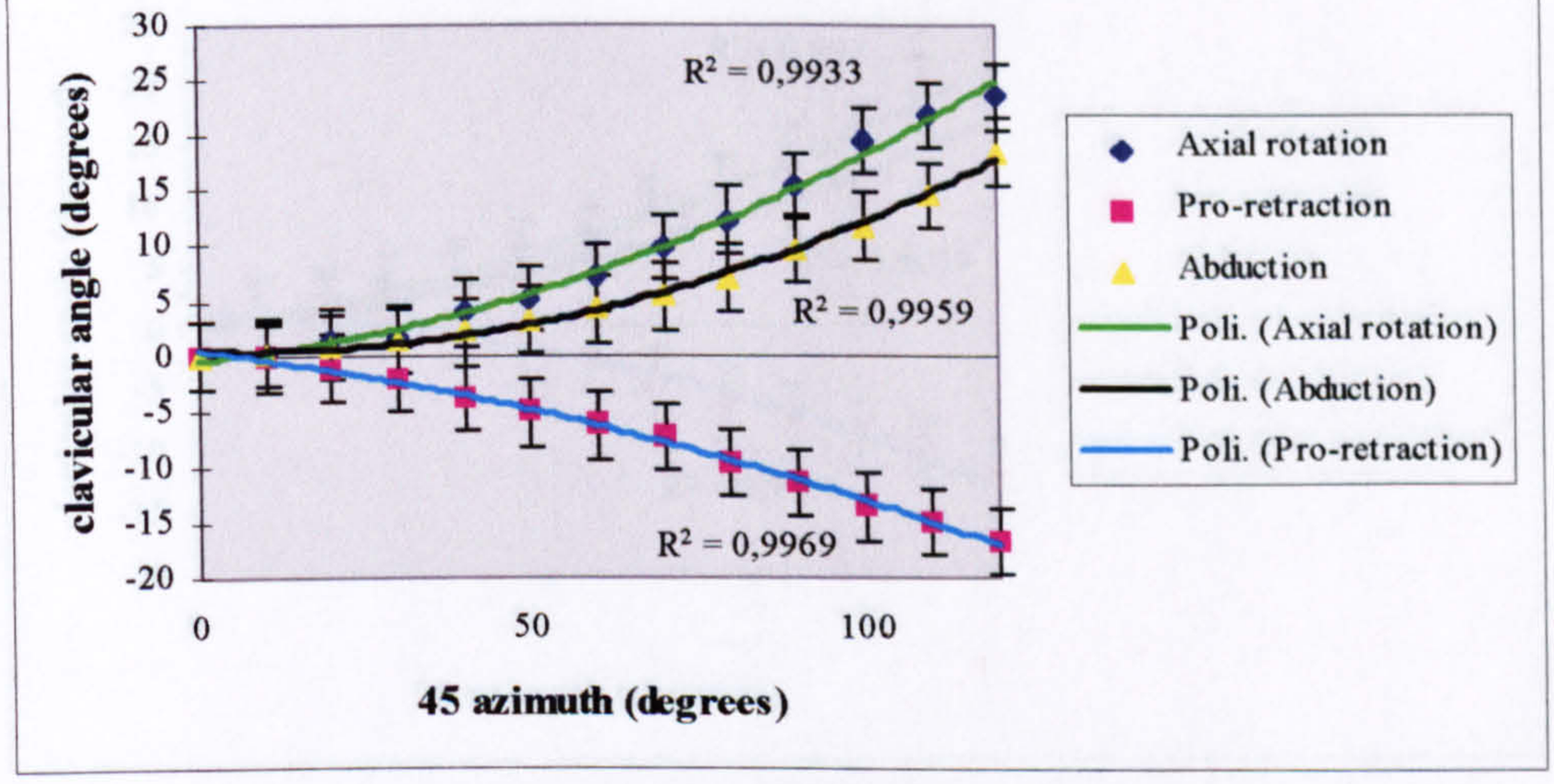

Figure 11.5 b: *Subject 5 (L/R=1,92) - observer 2*

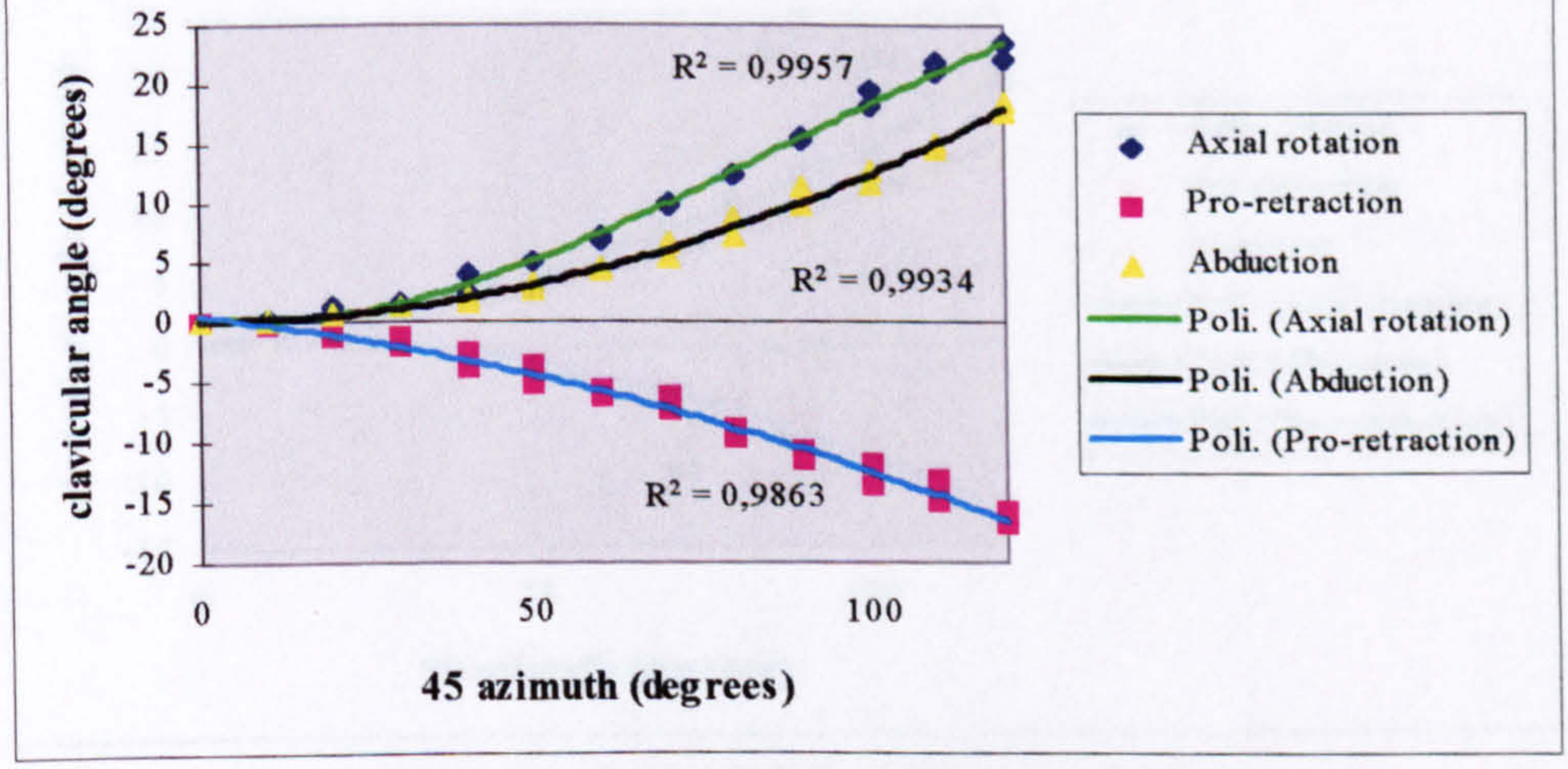

Figure 11.5 c: *Subject 5 (L/R=1,92) - inter observer*

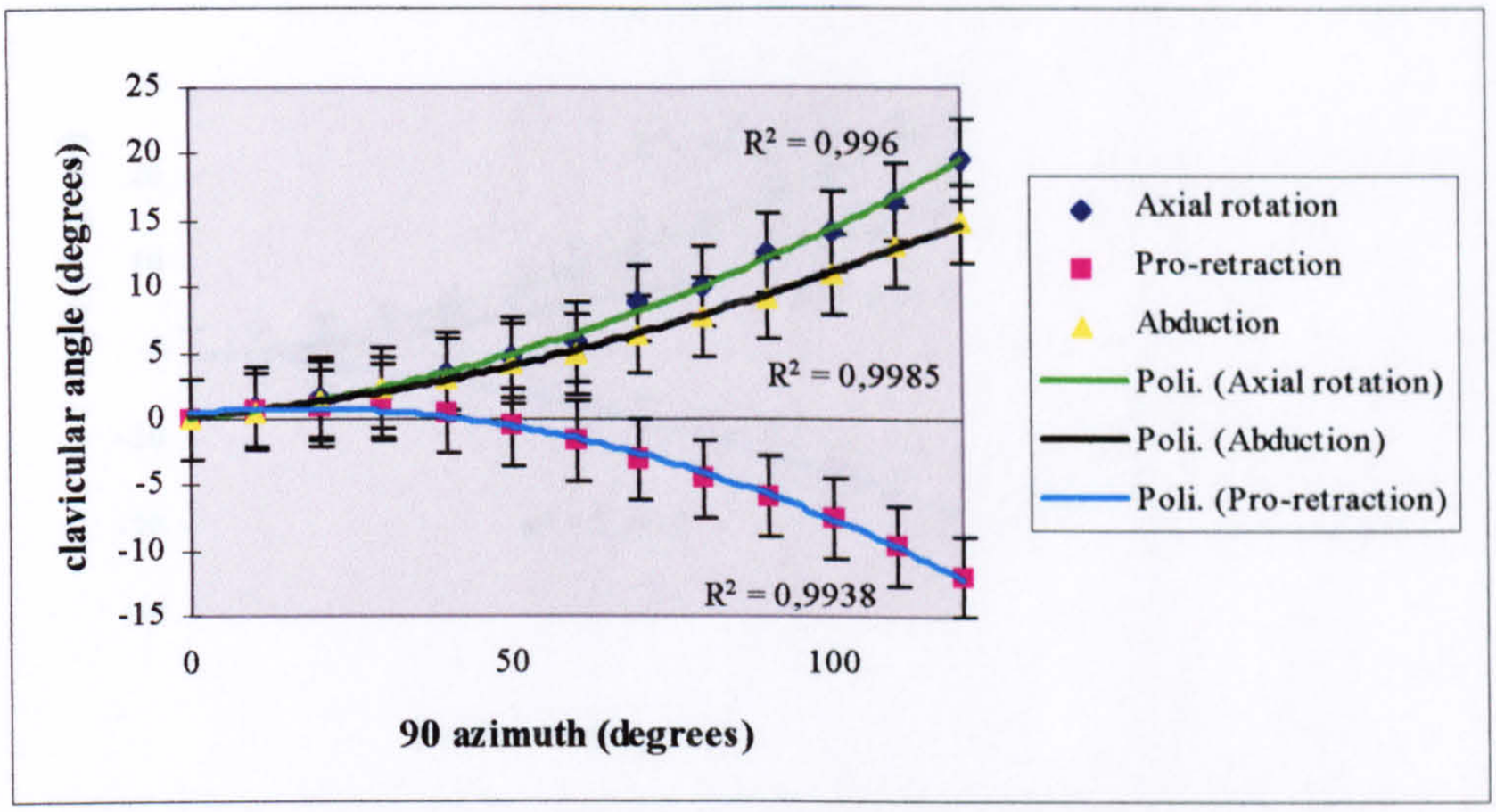

Figure 11.6 a: *Subject 5 (L/R=1,92) - observer 1*

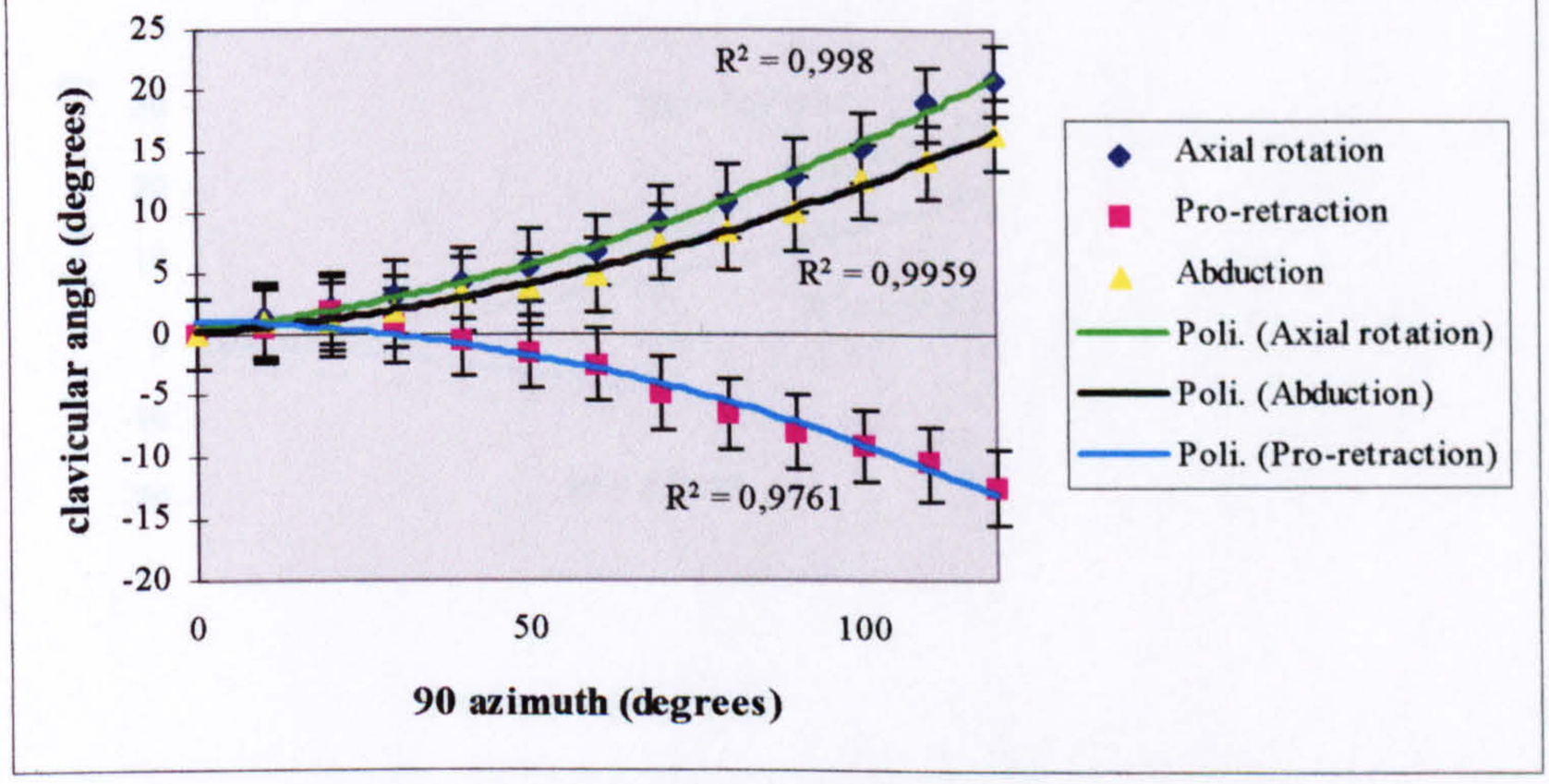

Figure 11.6 b: *Subject 5 (L/R=1,92) - observer 2*

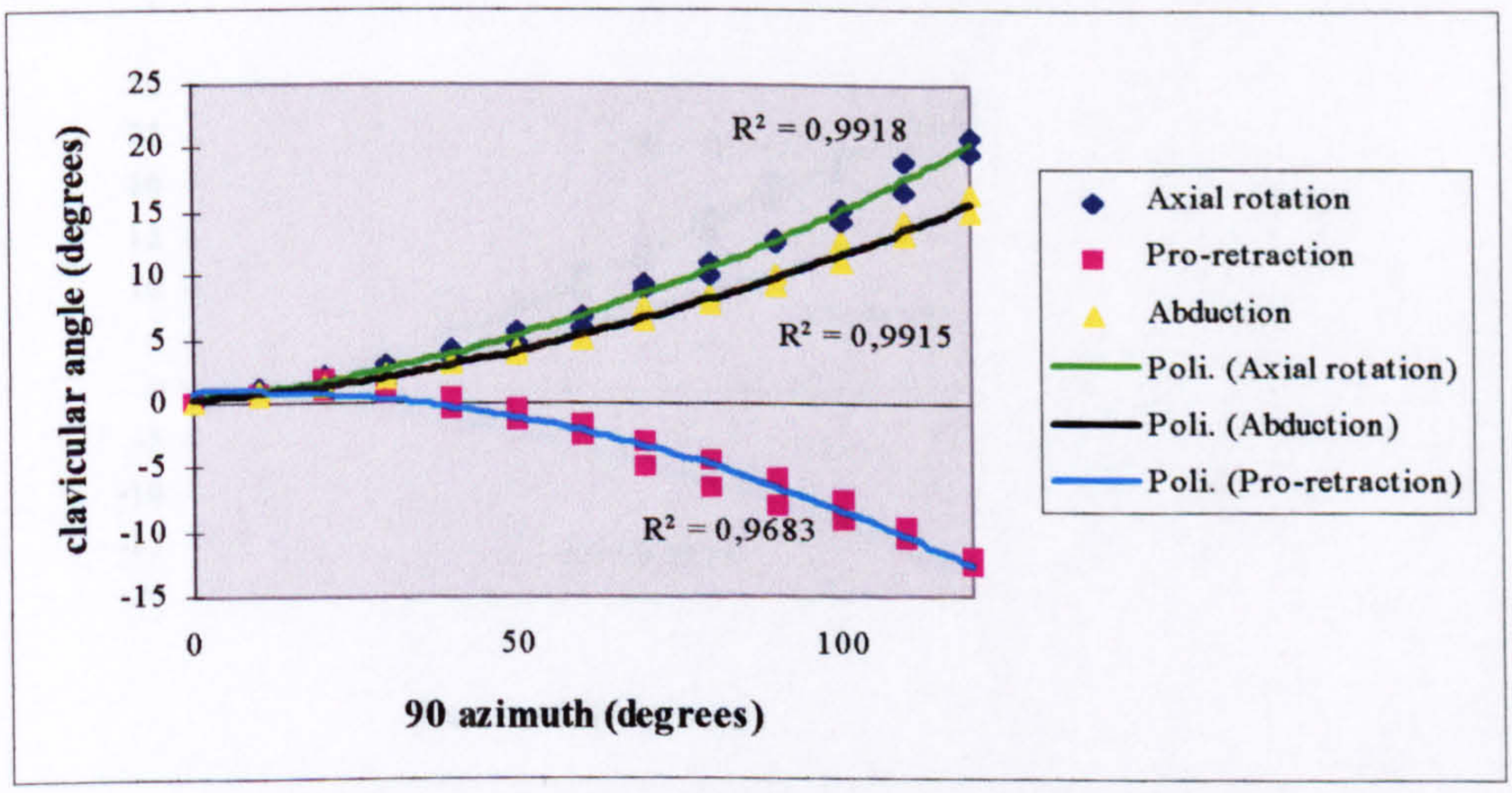

Figure 11.6 c: *Subject 5 (L/R=1,92) - inter observer*

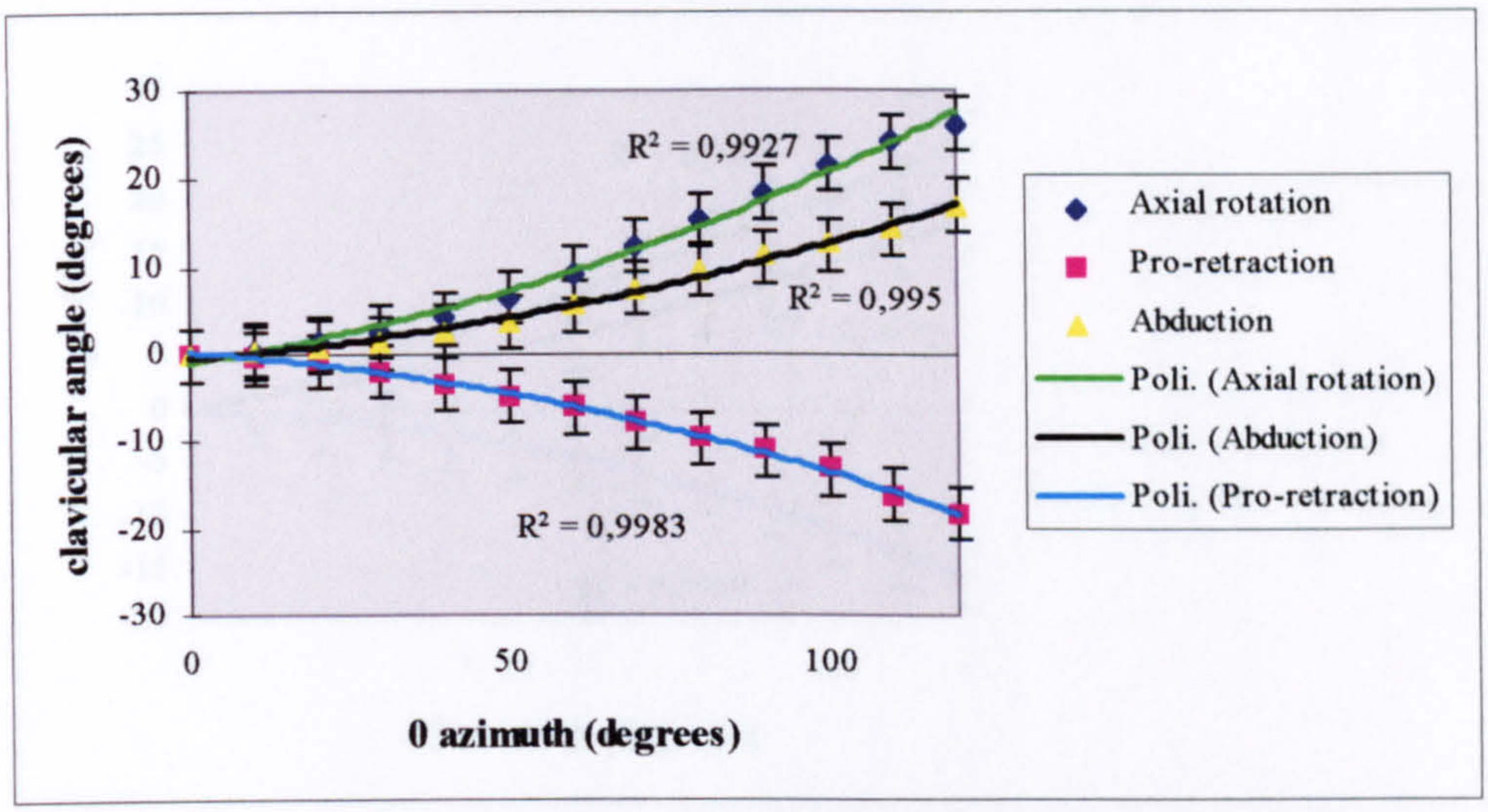

Figure 11.7 a: *Subject 6 (L/R=1,96) - observer 1*

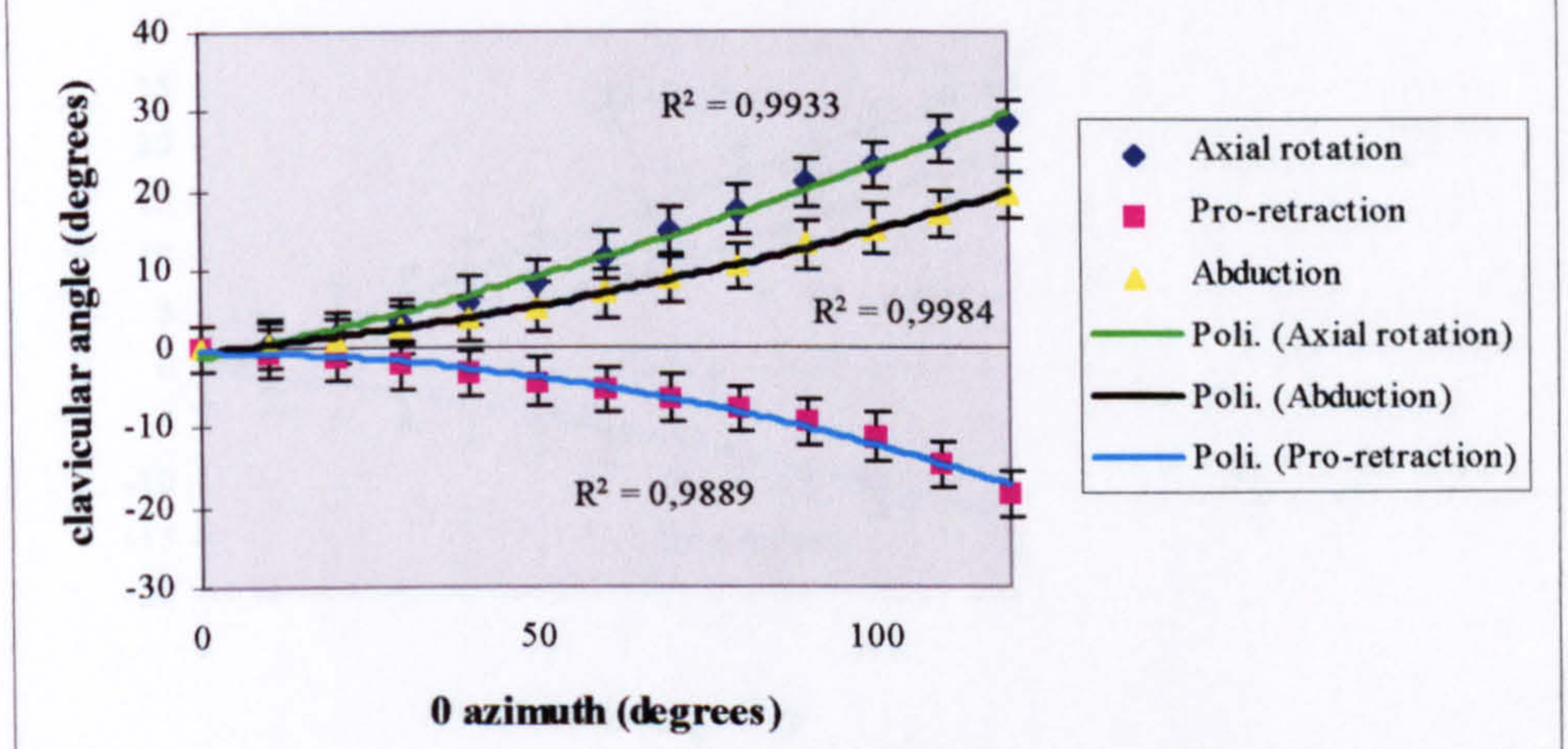

Figure 11.7 b: *Subject 6 (L/R=1,96) - observer 2*

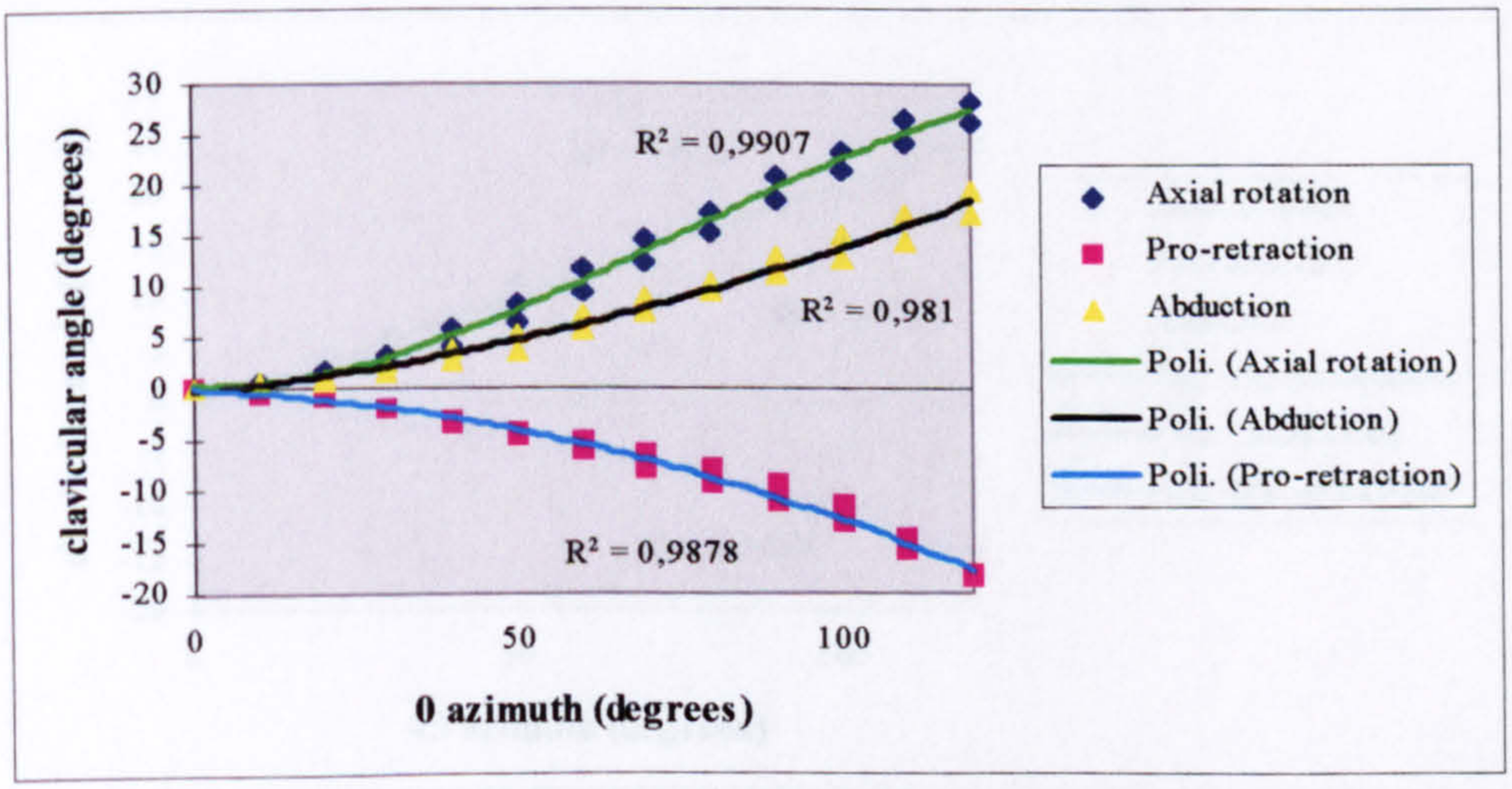

Figure 11.7 c: *Subject 6 (L/R=1,96) - inter observer*

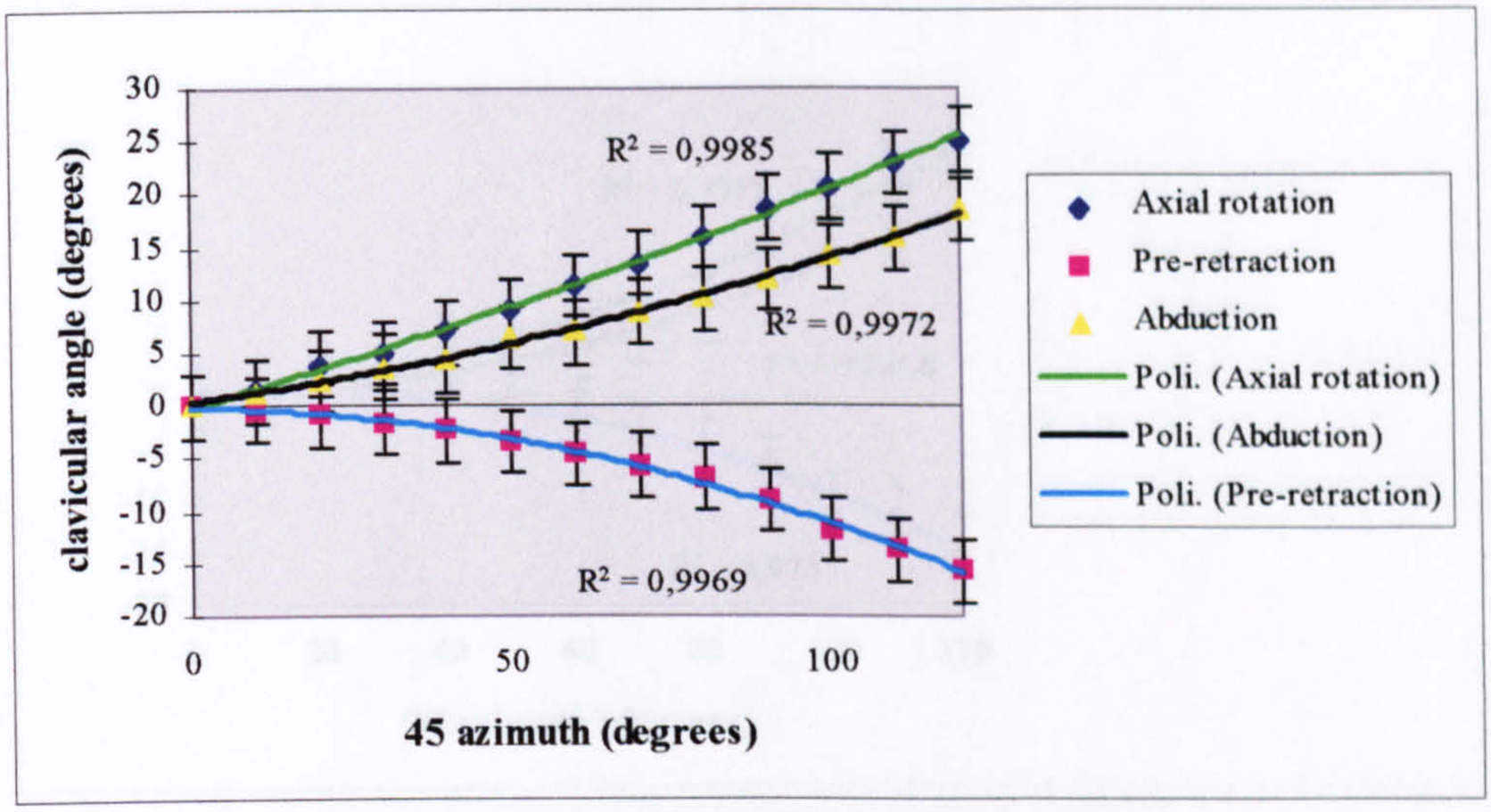

Figure 11.8 a: *Subject 6 (L/R=1,96) - observer 1*

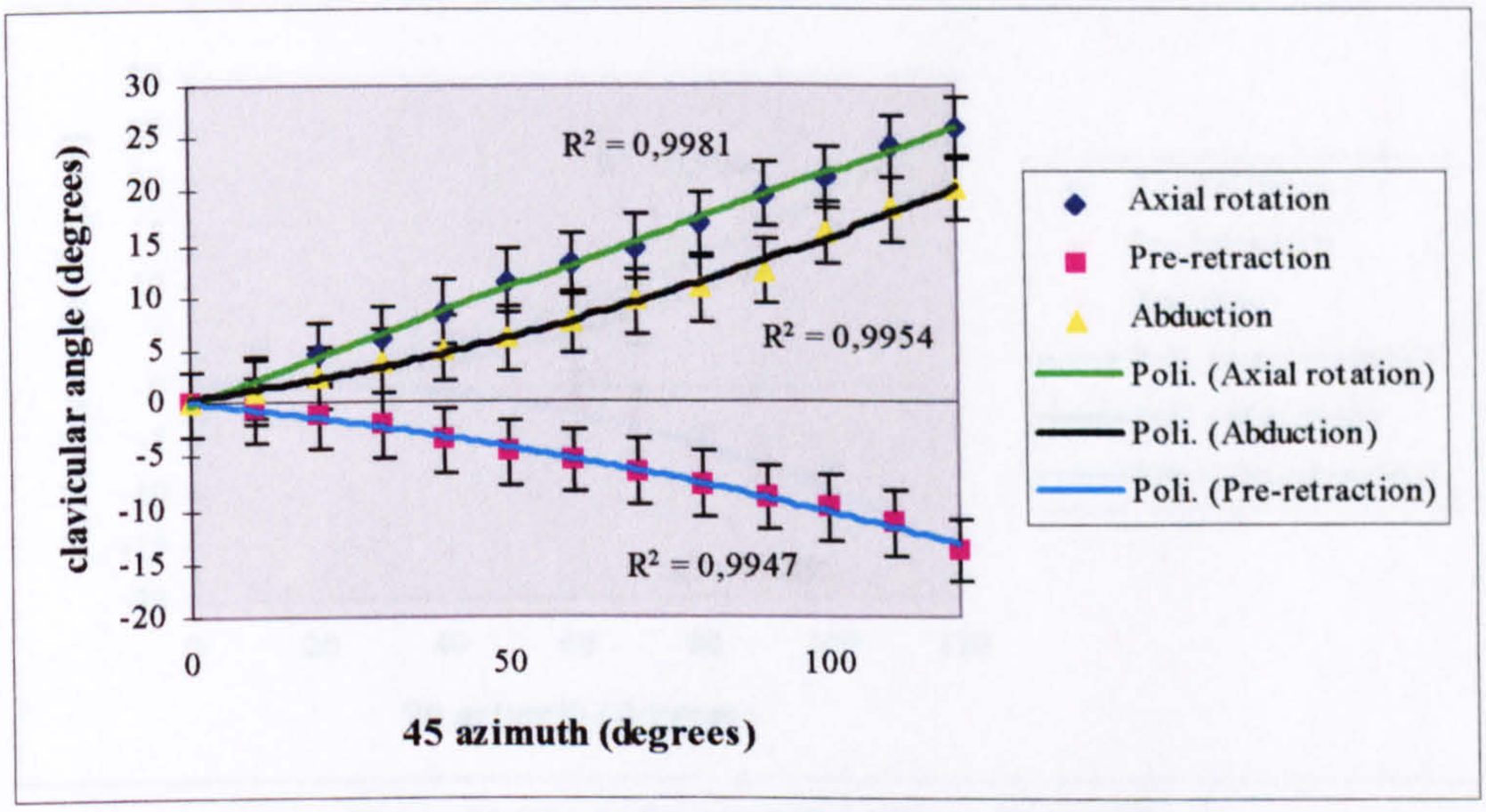

Figure 11.8 b: *Subject 6 (L/R=1,96) - observer 2*

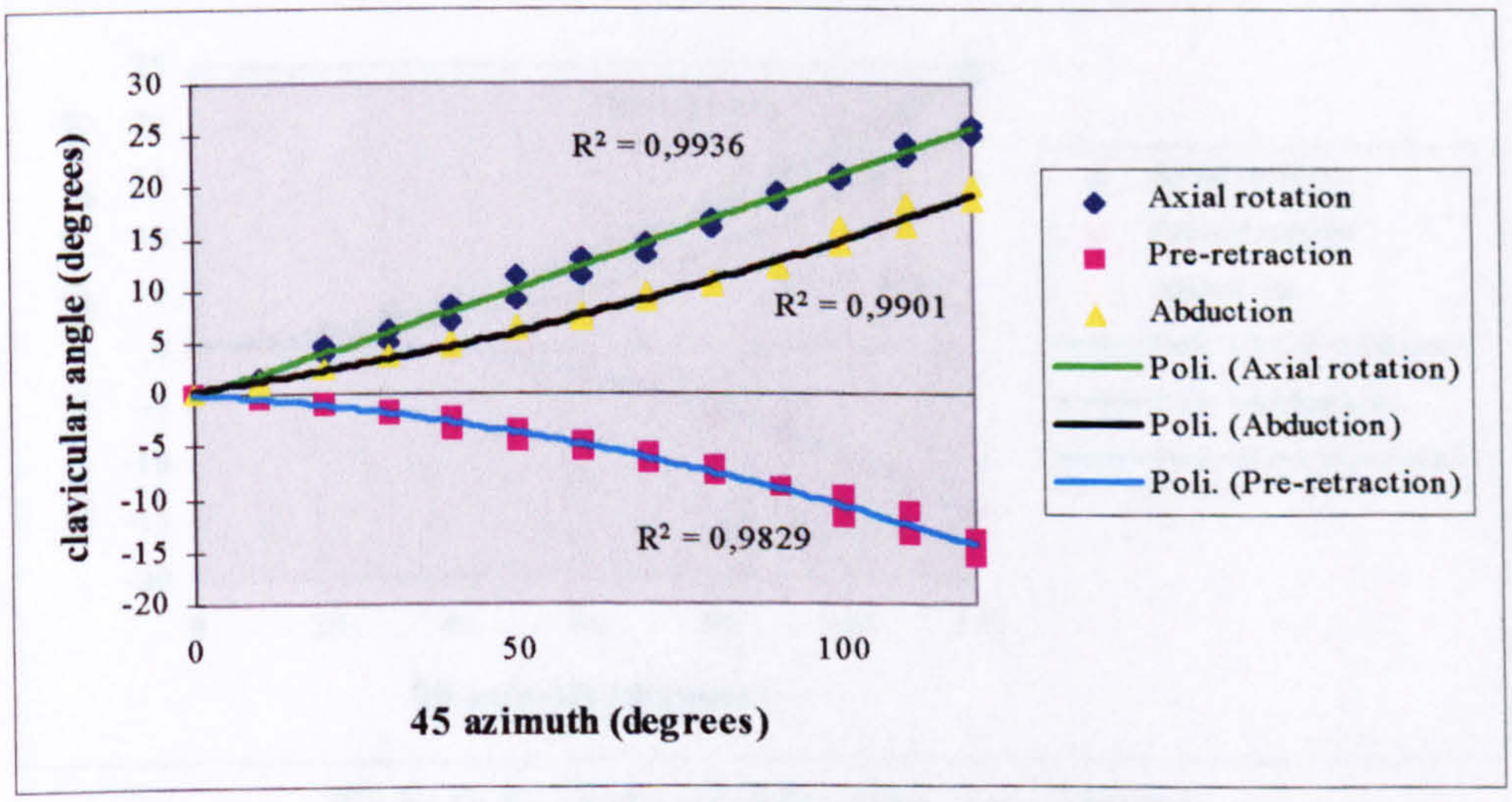

Figure 11.8 c: *Subject 6 (L/R=1,96) - inter observer*

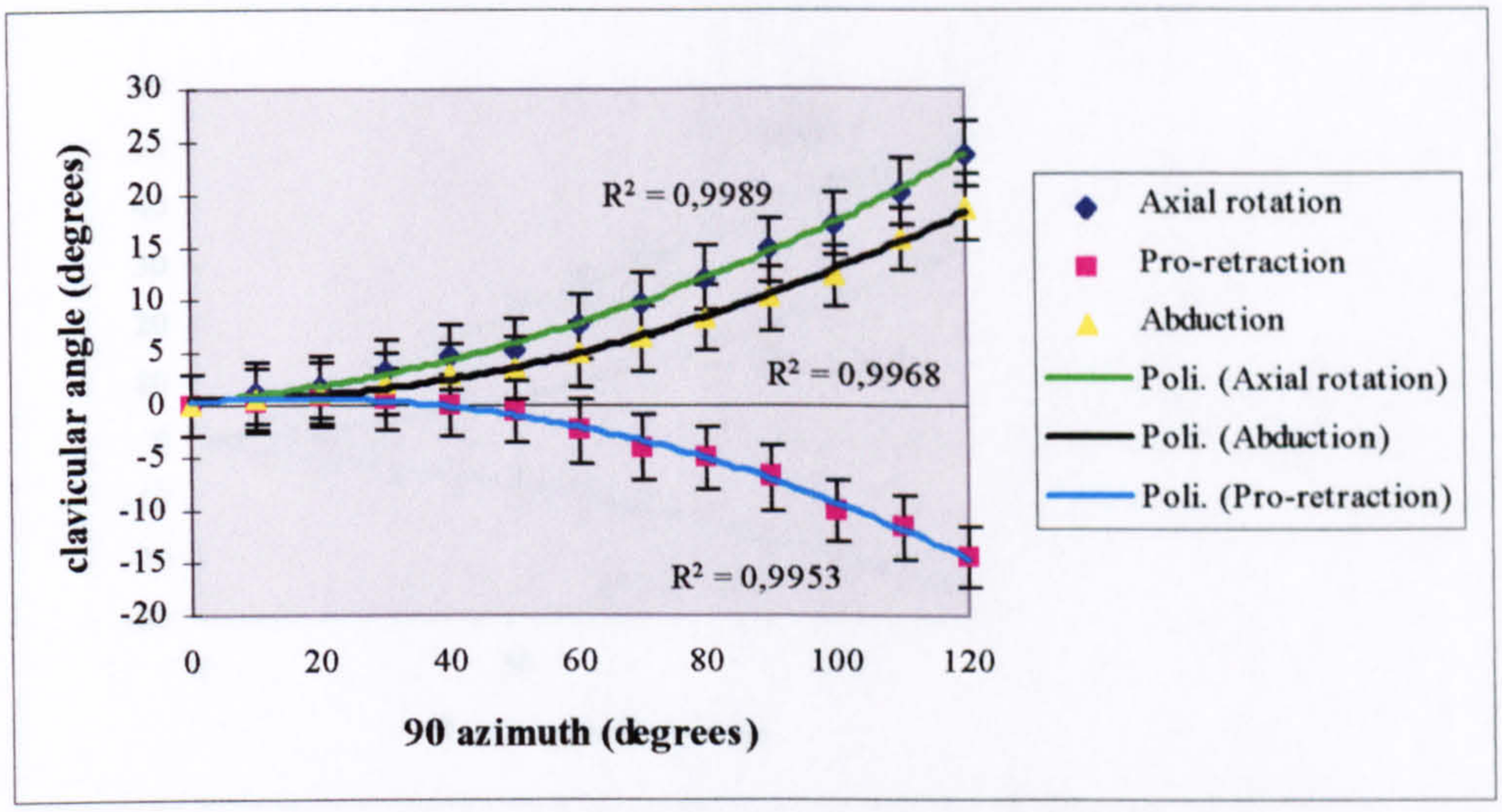

Figure 11.9 a: *Subject 6 (L/R=1,96) - observer 1*

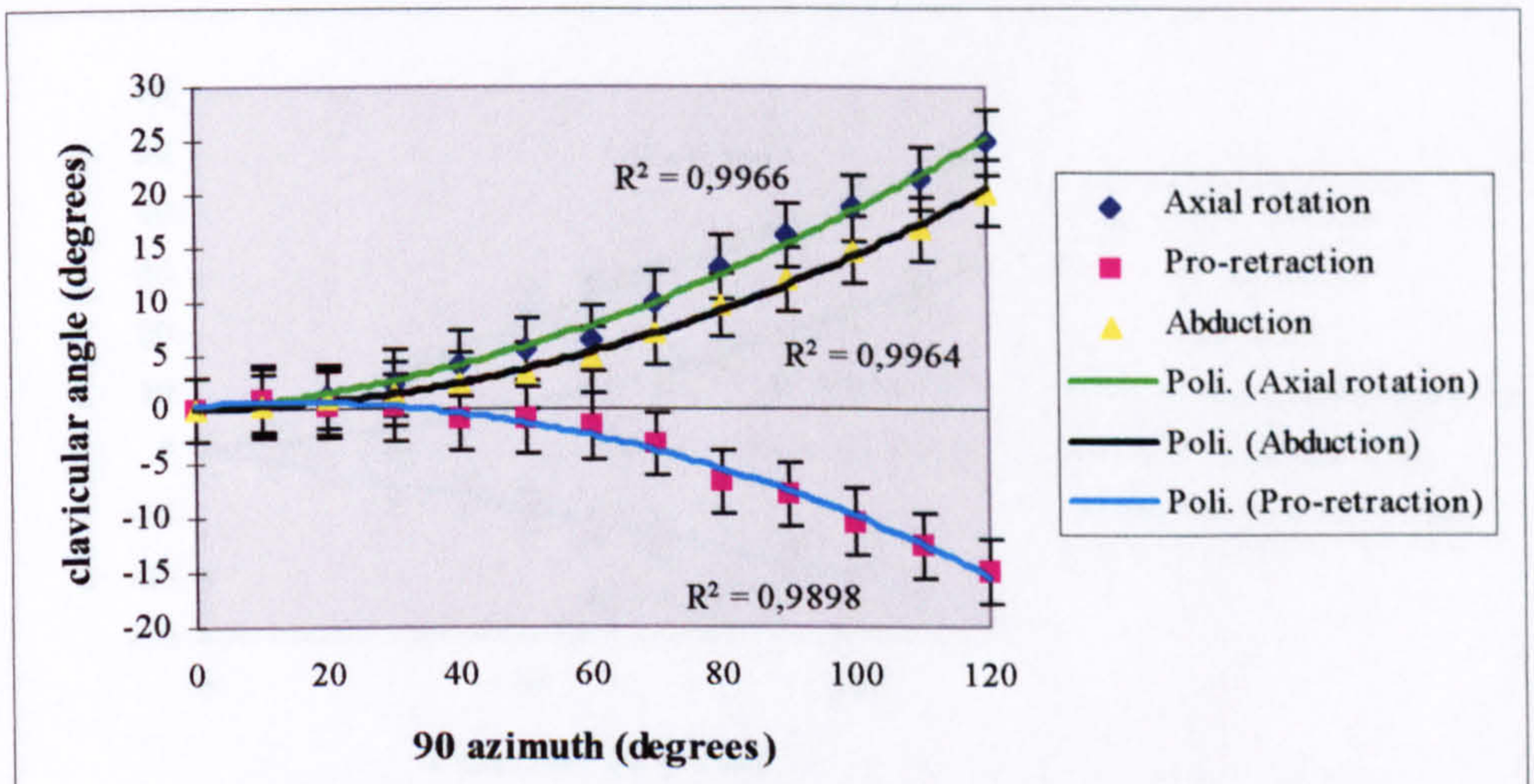

Figure 11.9 b: *Subject 6 (L/R=1,96) - observer 2*

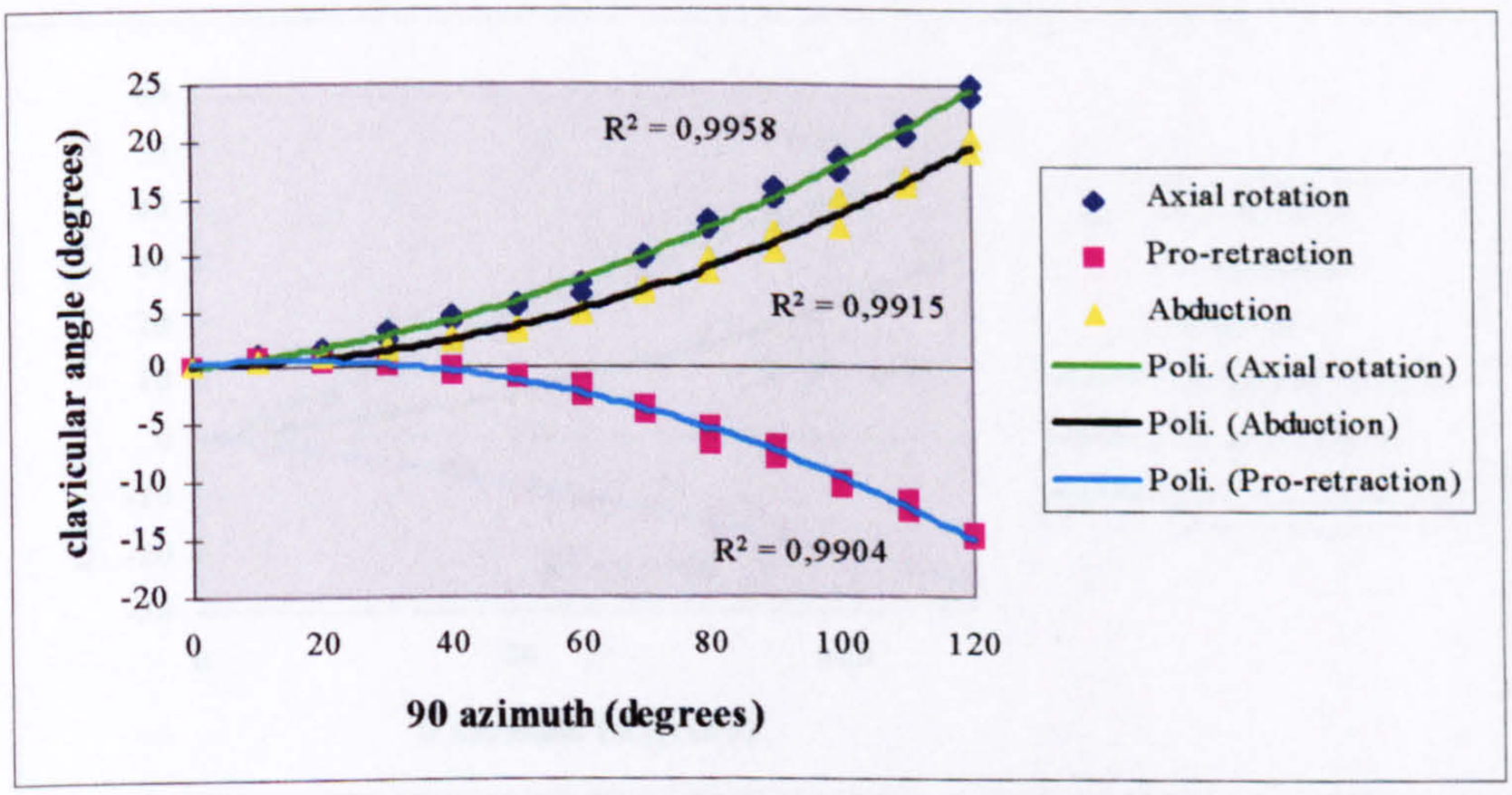

Figure 11.9 c: *Subject 6 (L/R=1,96) - inter observer*

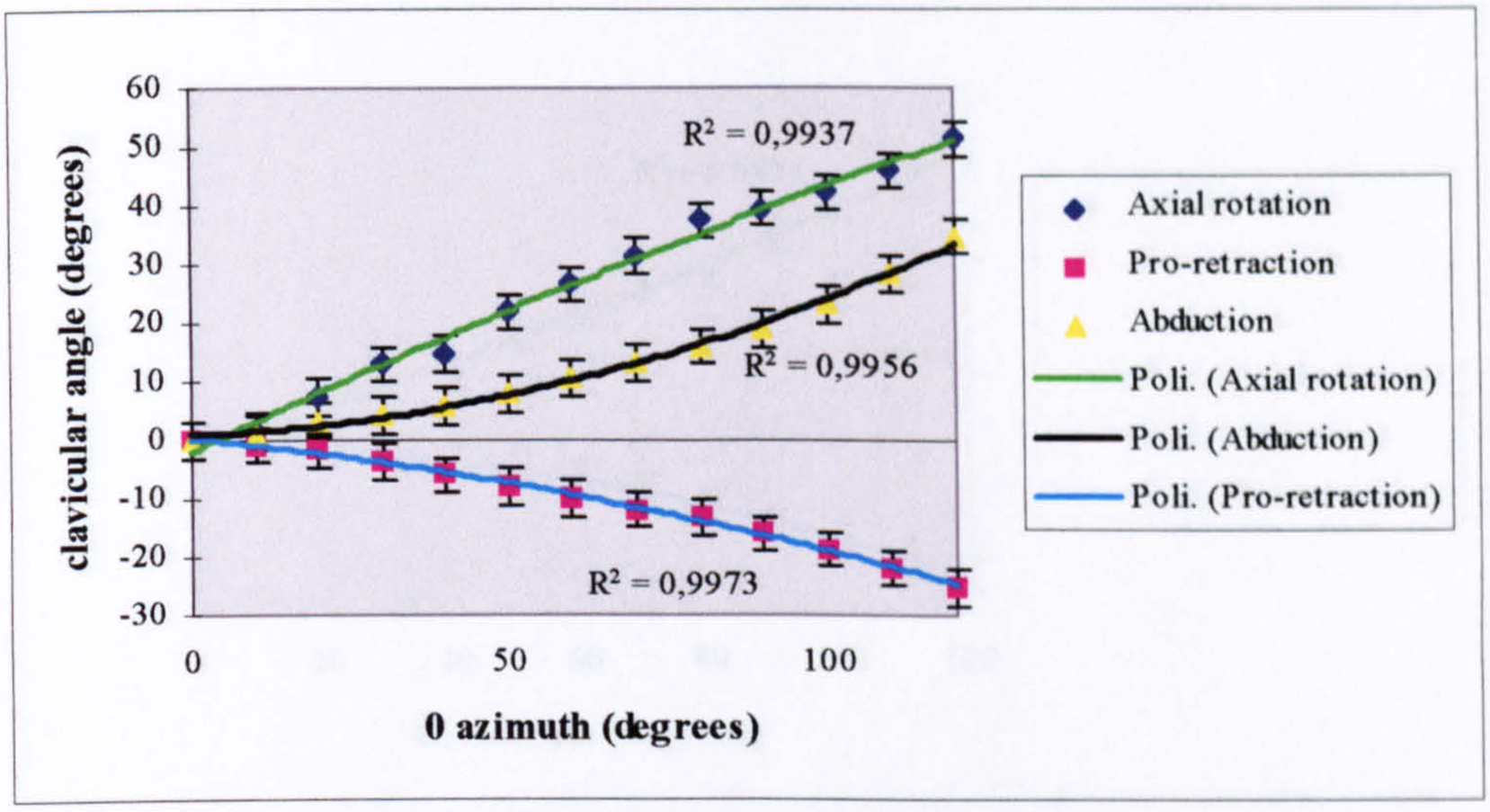

Figure 11.10 a: *Subject 7 (L/R=2,73) - observer 1*

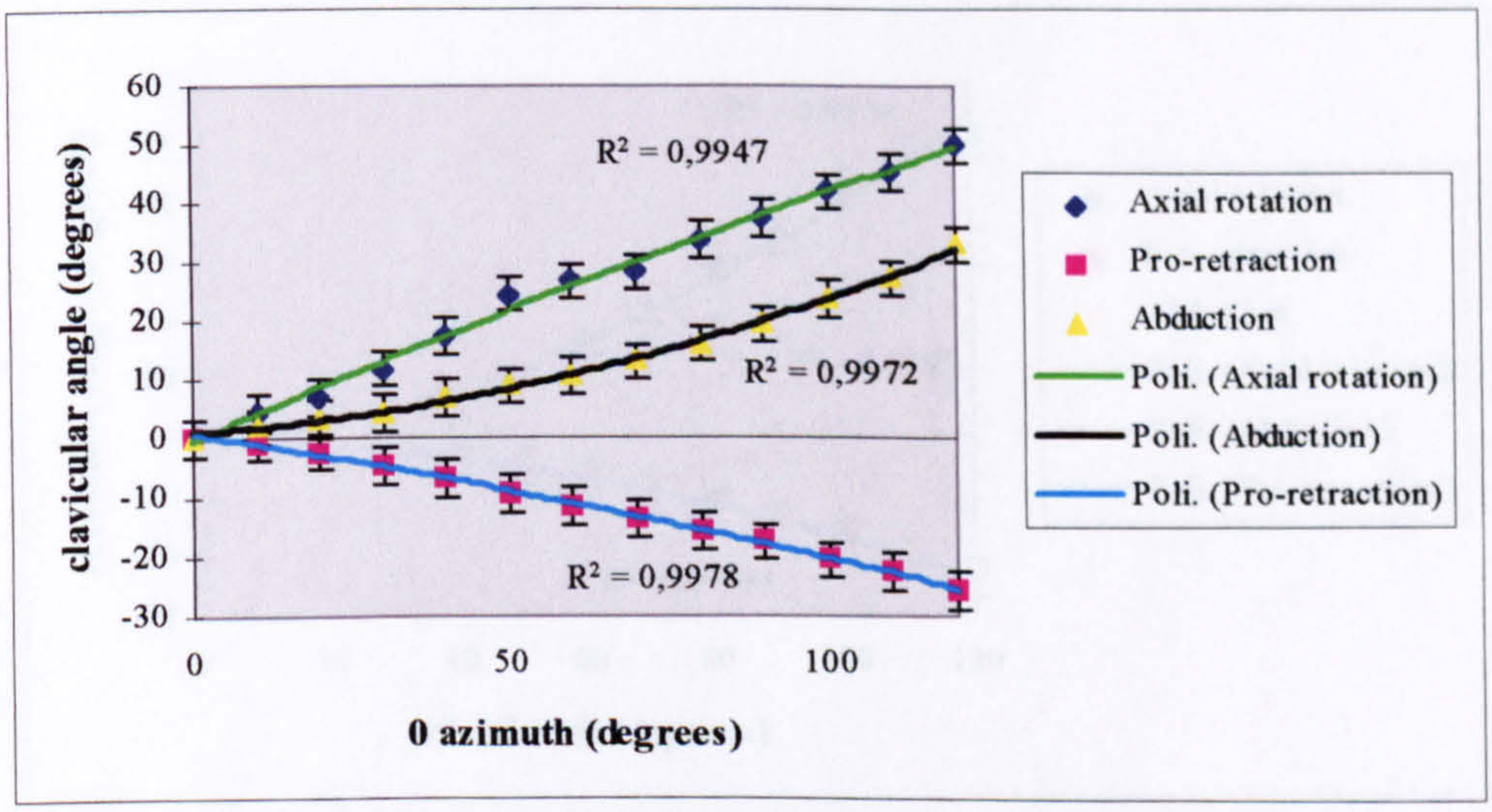

Figure 11.10 b: *Subject 7 (L/R=2,73) - observer 2*

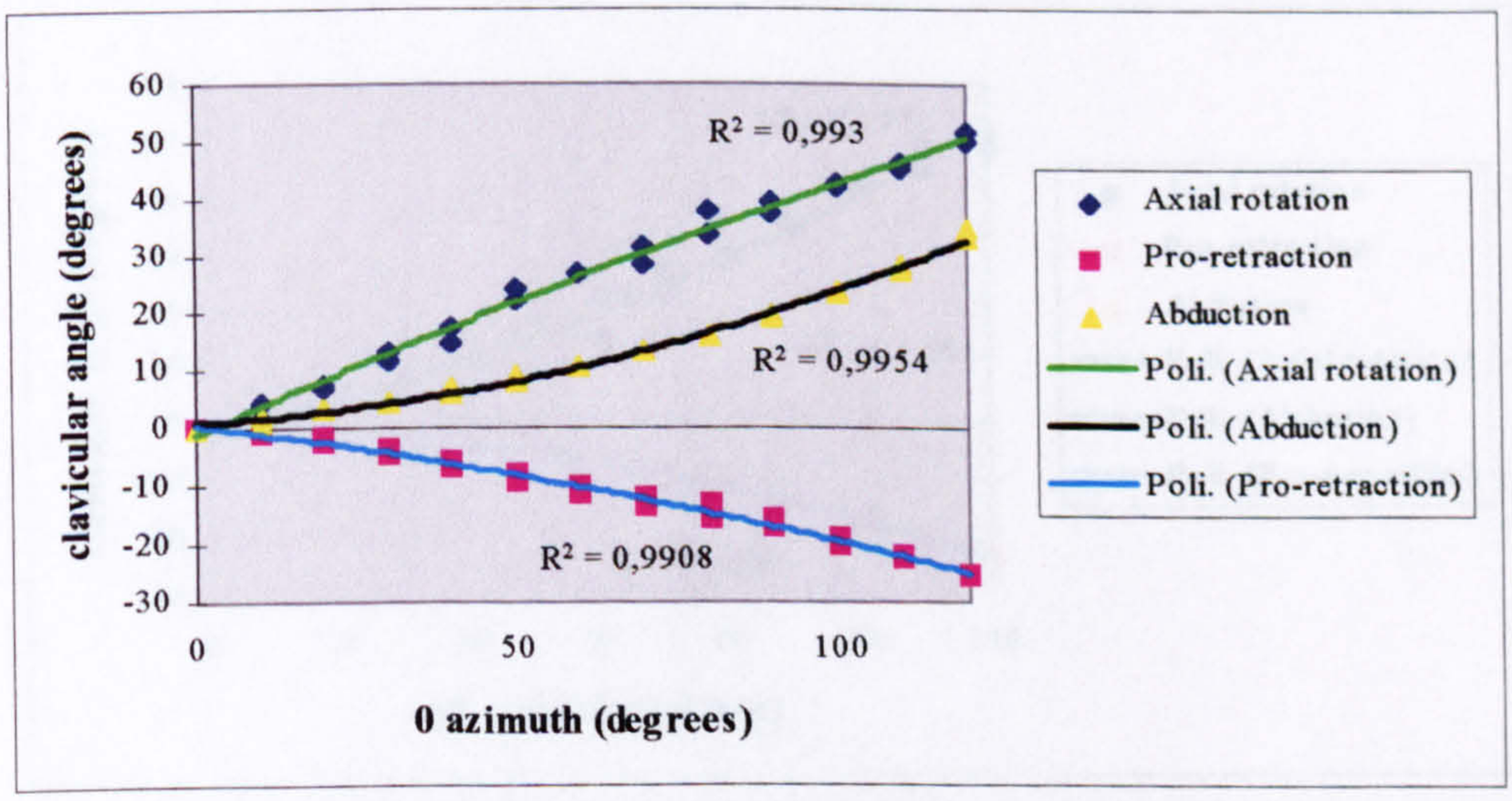

Figure 11.10 c: *Subject 7 (L/R=2,73) - inter observer*

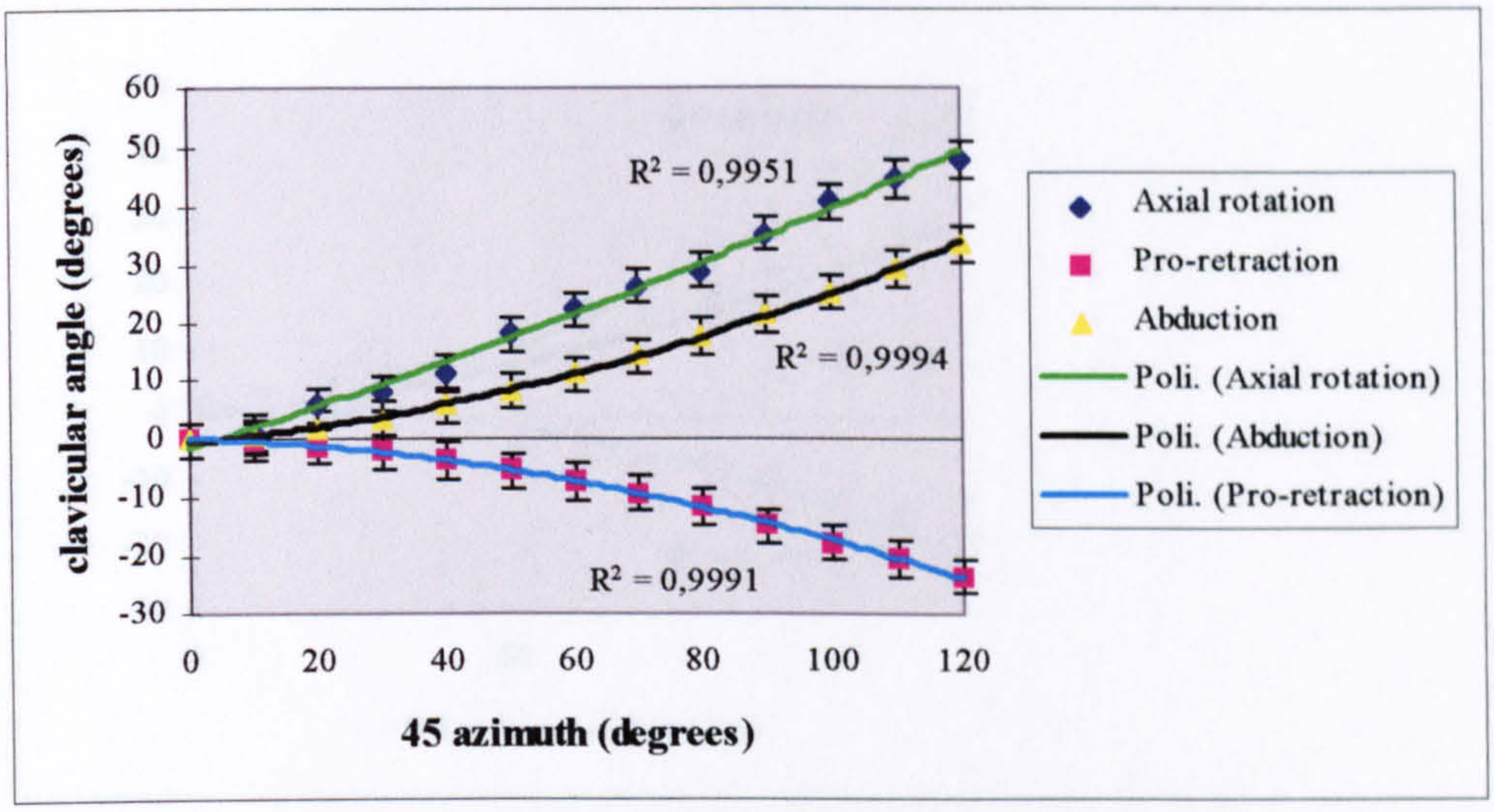

Figure 11.11 a: *Subject 7 (L/R=2,73) - observer 1*

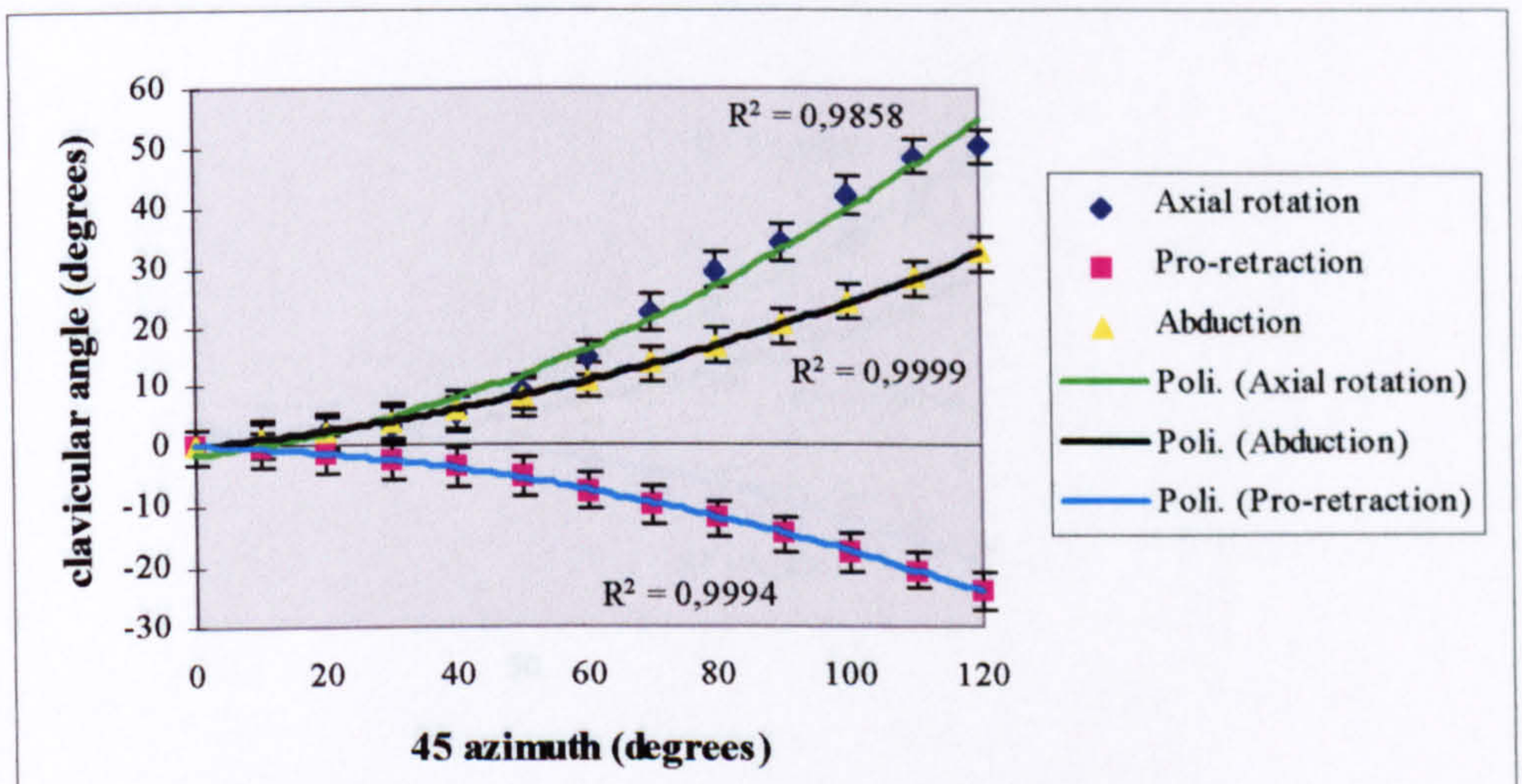

Figure 11.11 b: *Subject 7 (L/R=2,73) - observer 2*

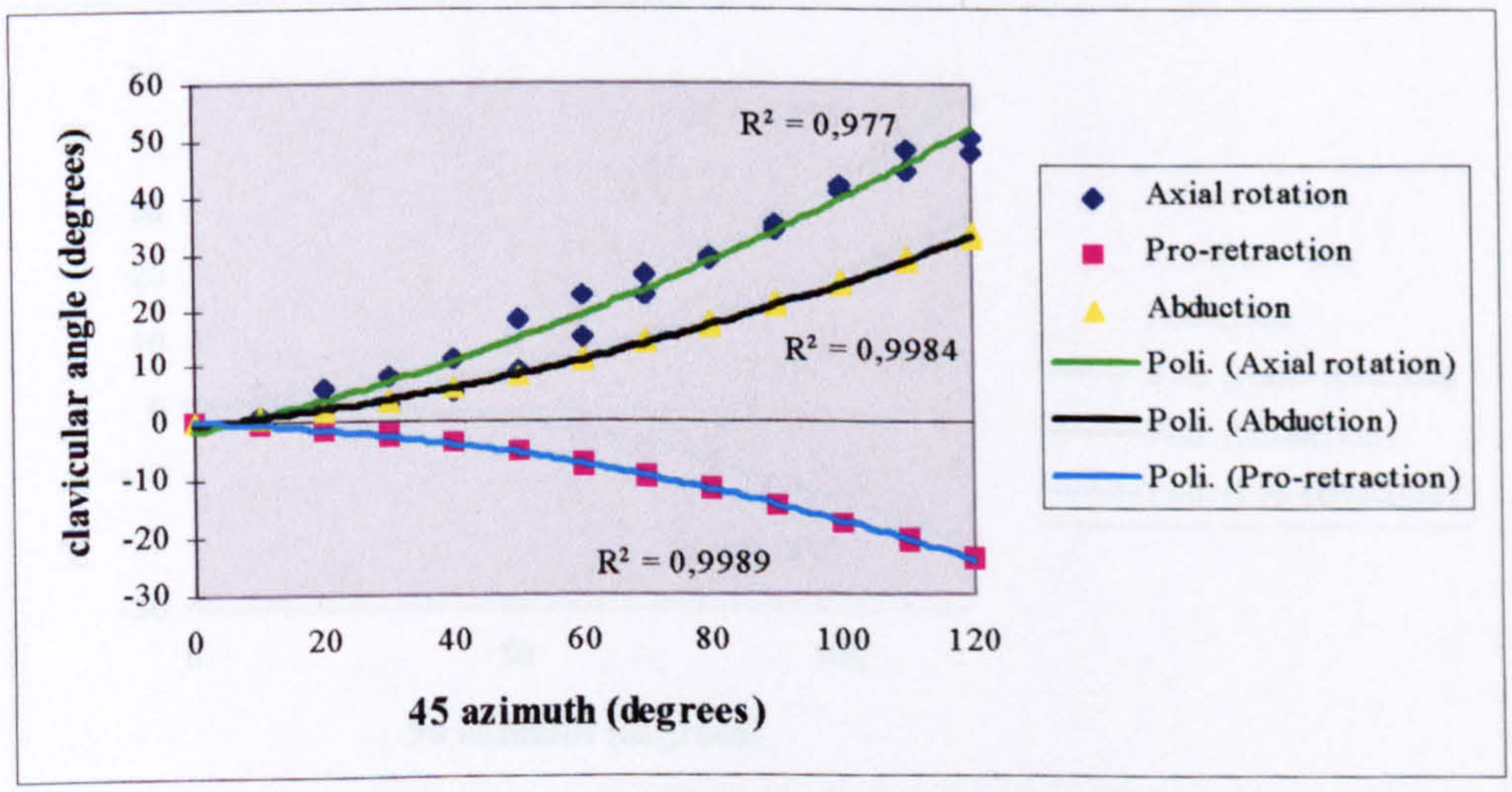

Figure 11.11 c: *Subject 7 (L/R=2,73) - inter observer*

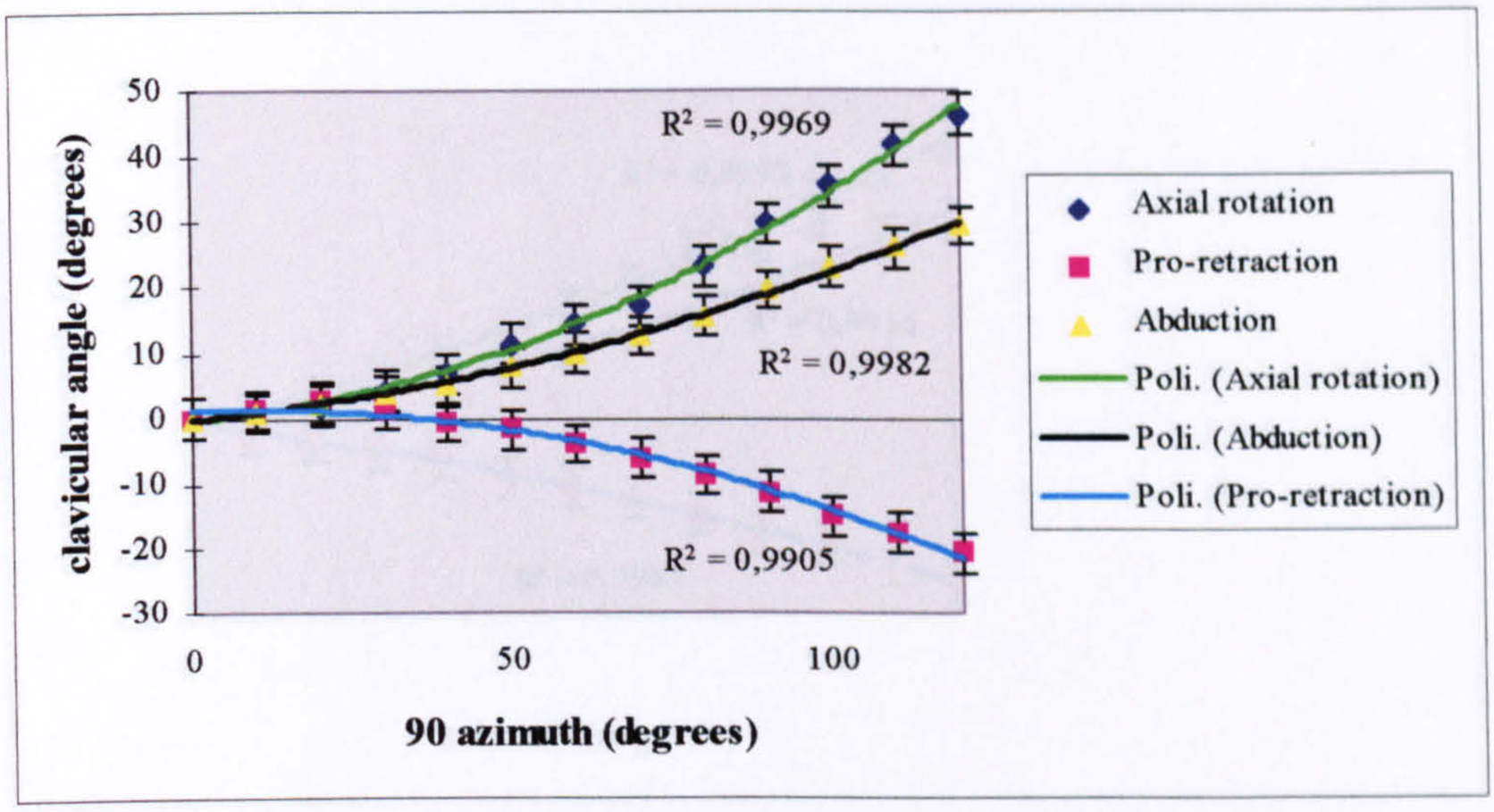

Figure 11.12 a: *Subject 7 (L/R=2,73) - observer 1*

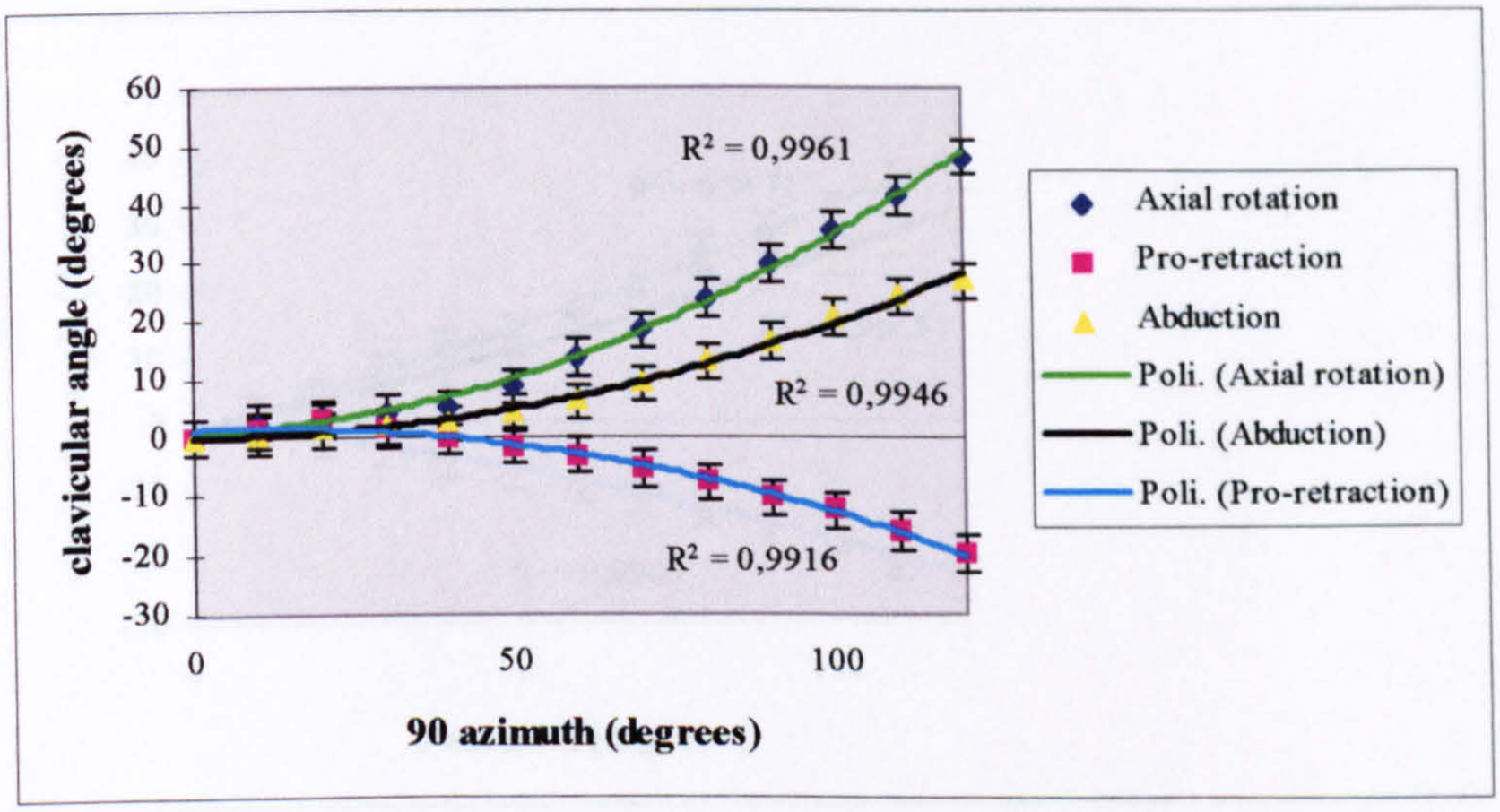

Figure 11.12 b: *Subject 7 (L/R=2,73) - observer 2*

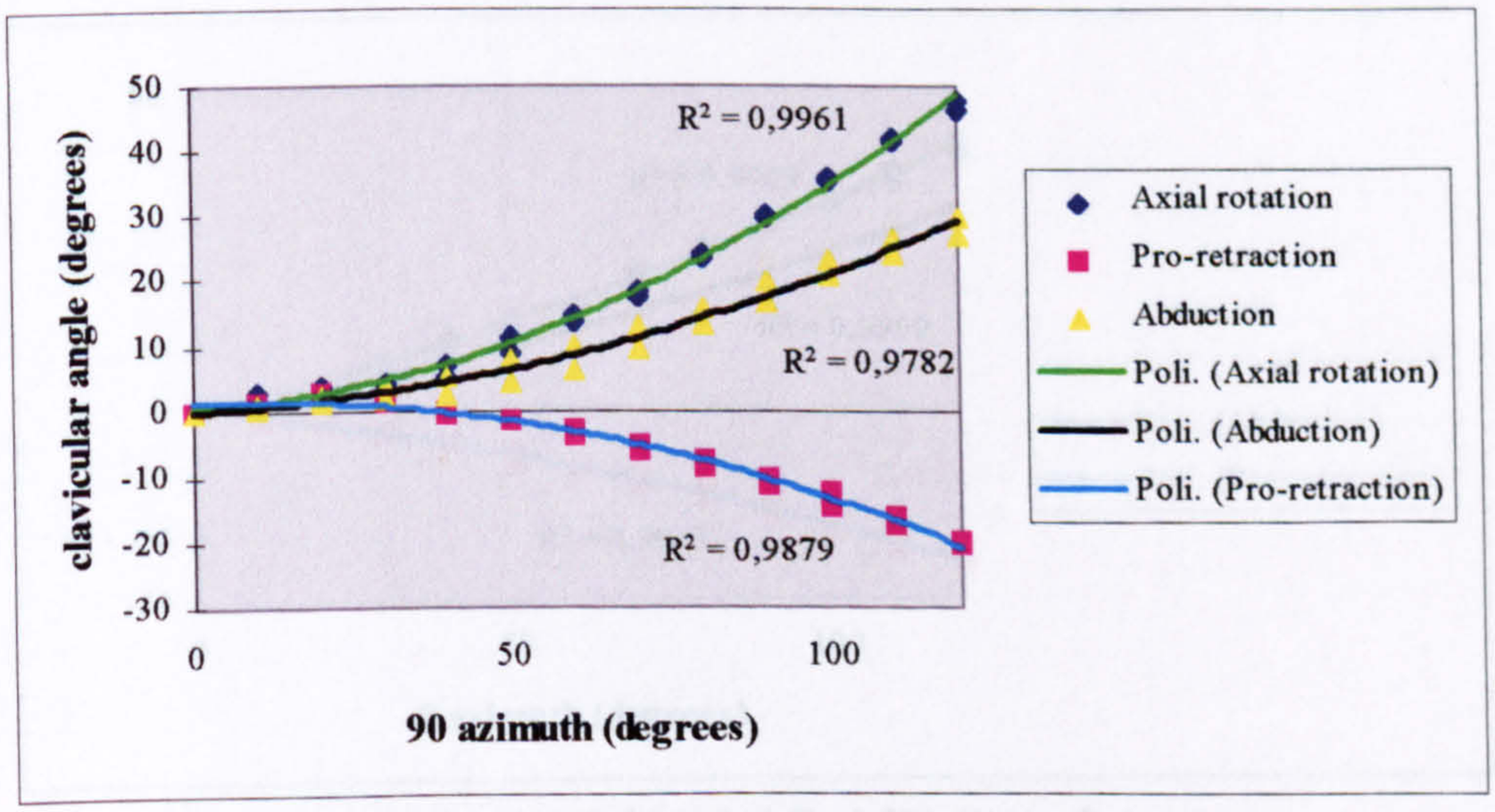

Figure 11.12 c: *Subject 7 (L/R=2,73) - inter observer*

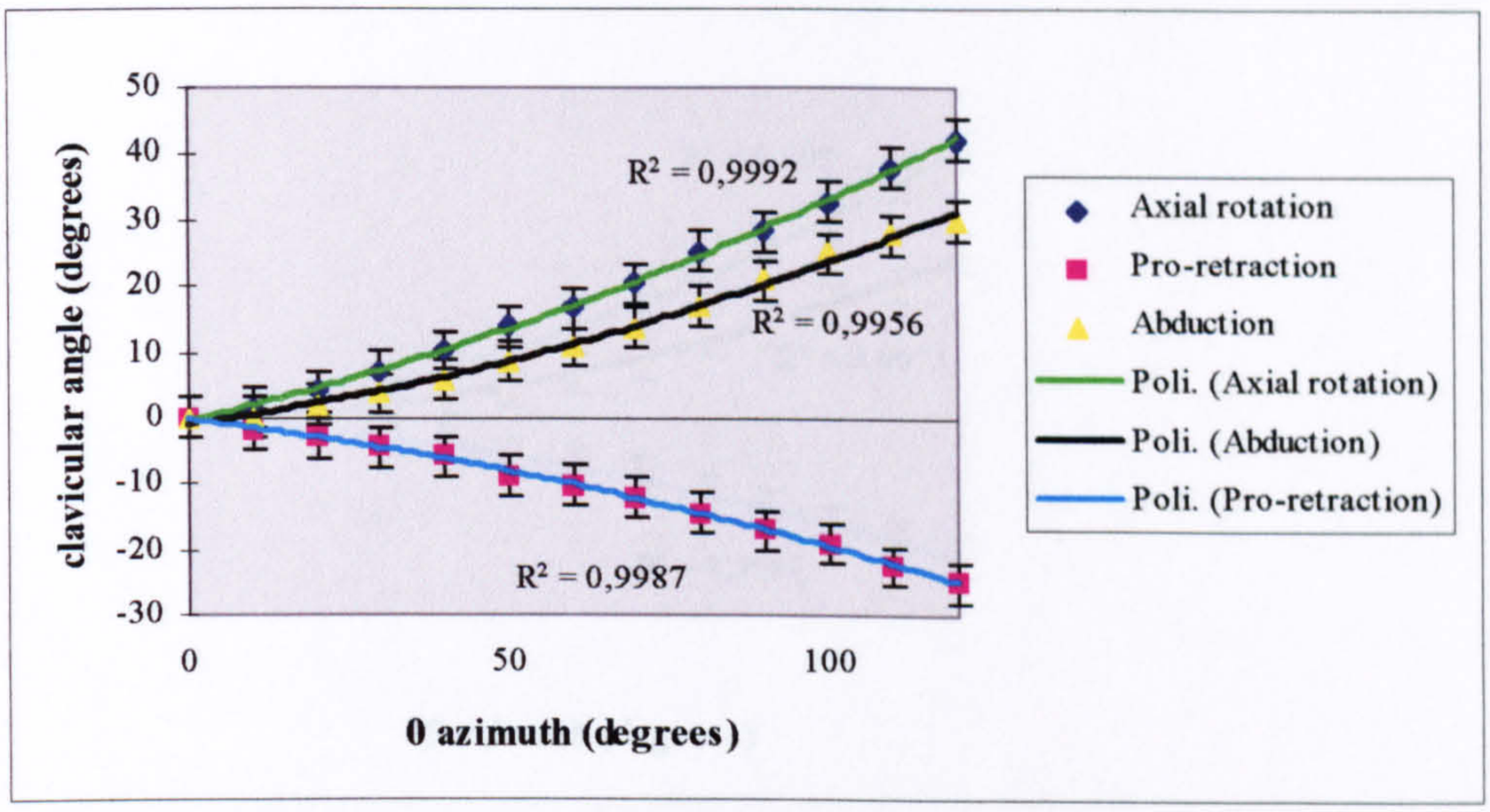

Figure 11.13 a: *Subject 8 (L/R=2,39) - observer 1*

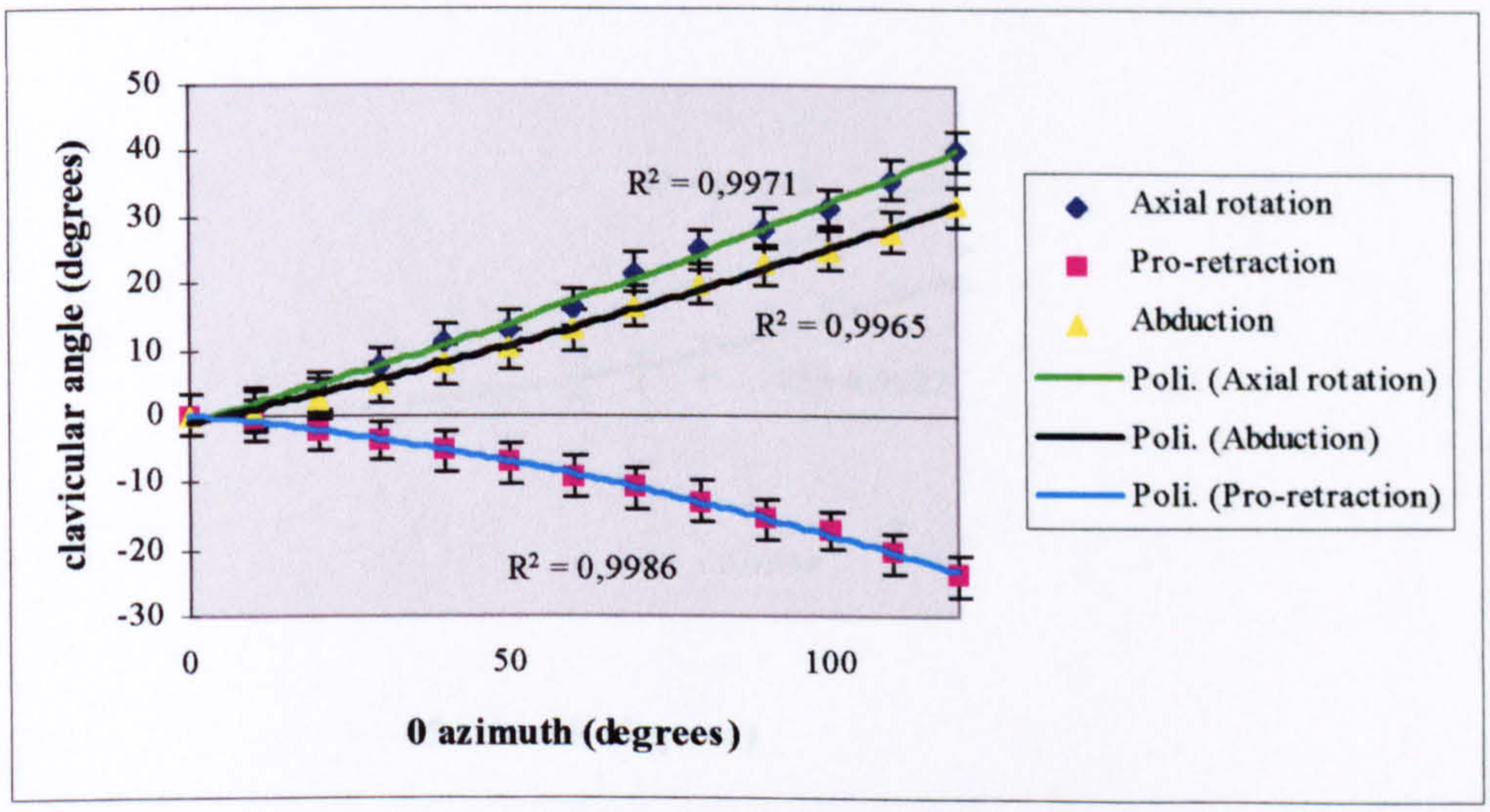

Figure 11.13 b: *Subject 8 (L/R=2,39) - observer 2*

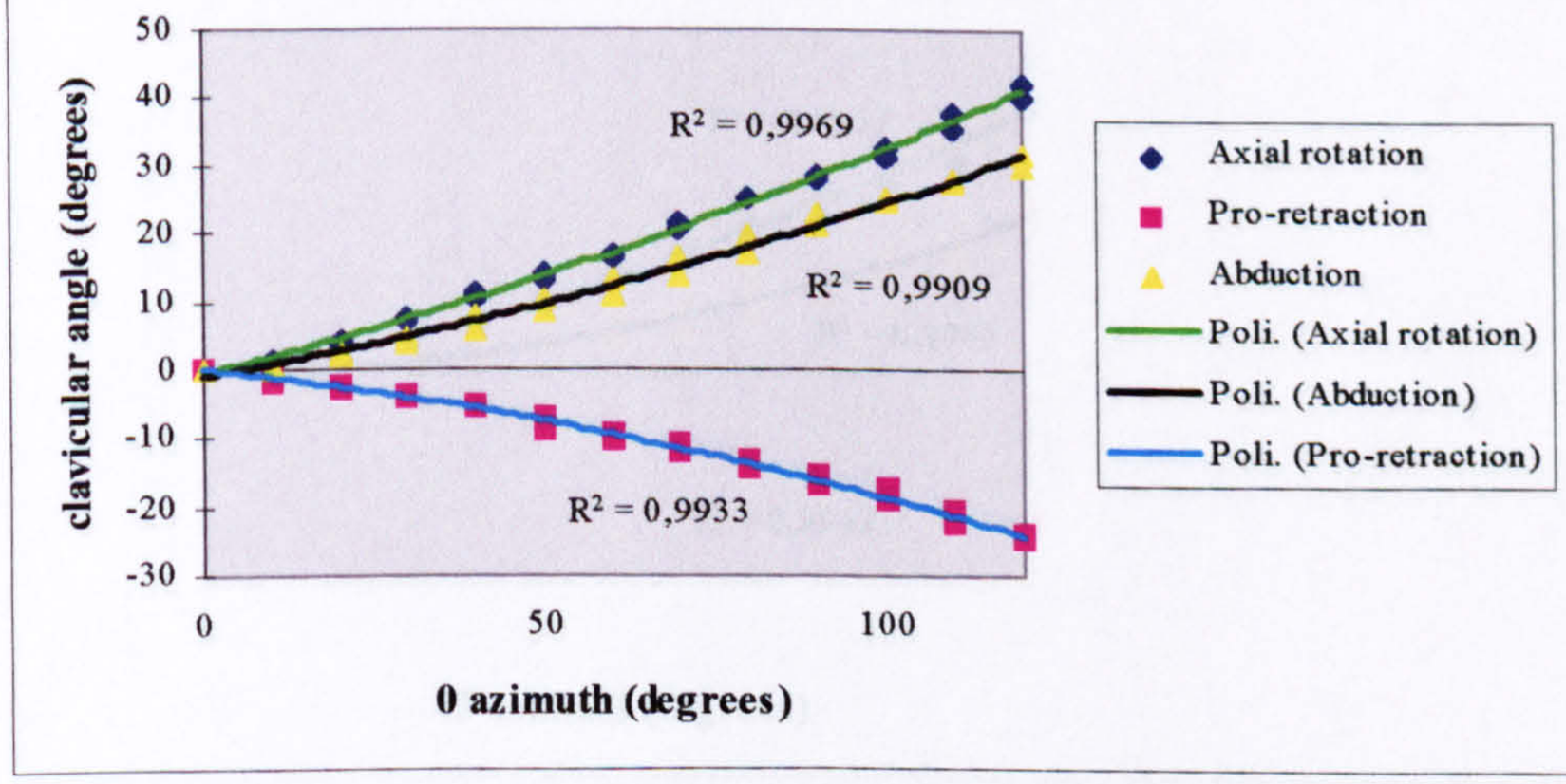

Figure 11.13 c: *Subject 8 (L/R=2,39) - inter observer*

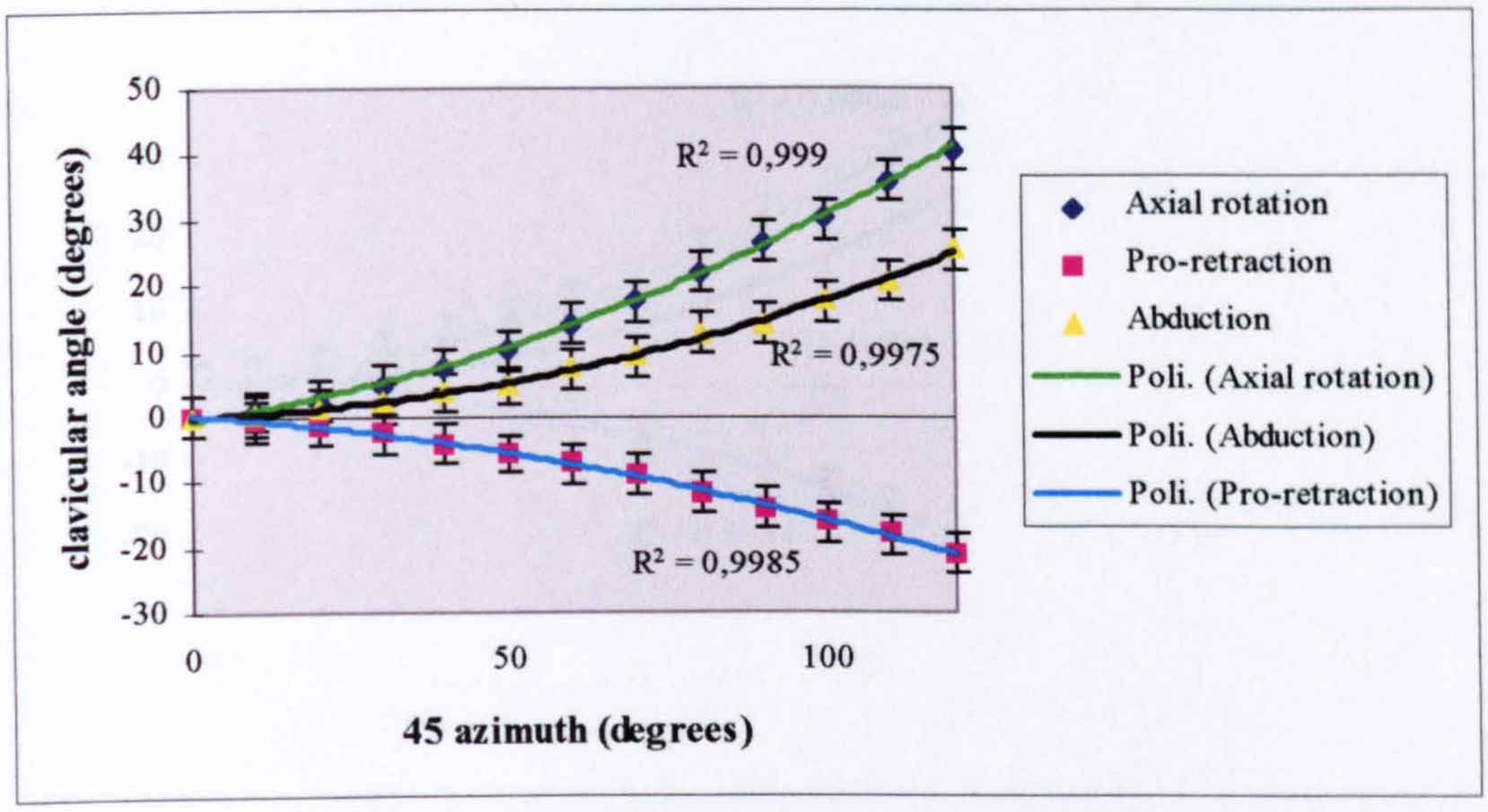

Figure 11.14 a: *Subject 8 (L/R=2,39) - observer 1*

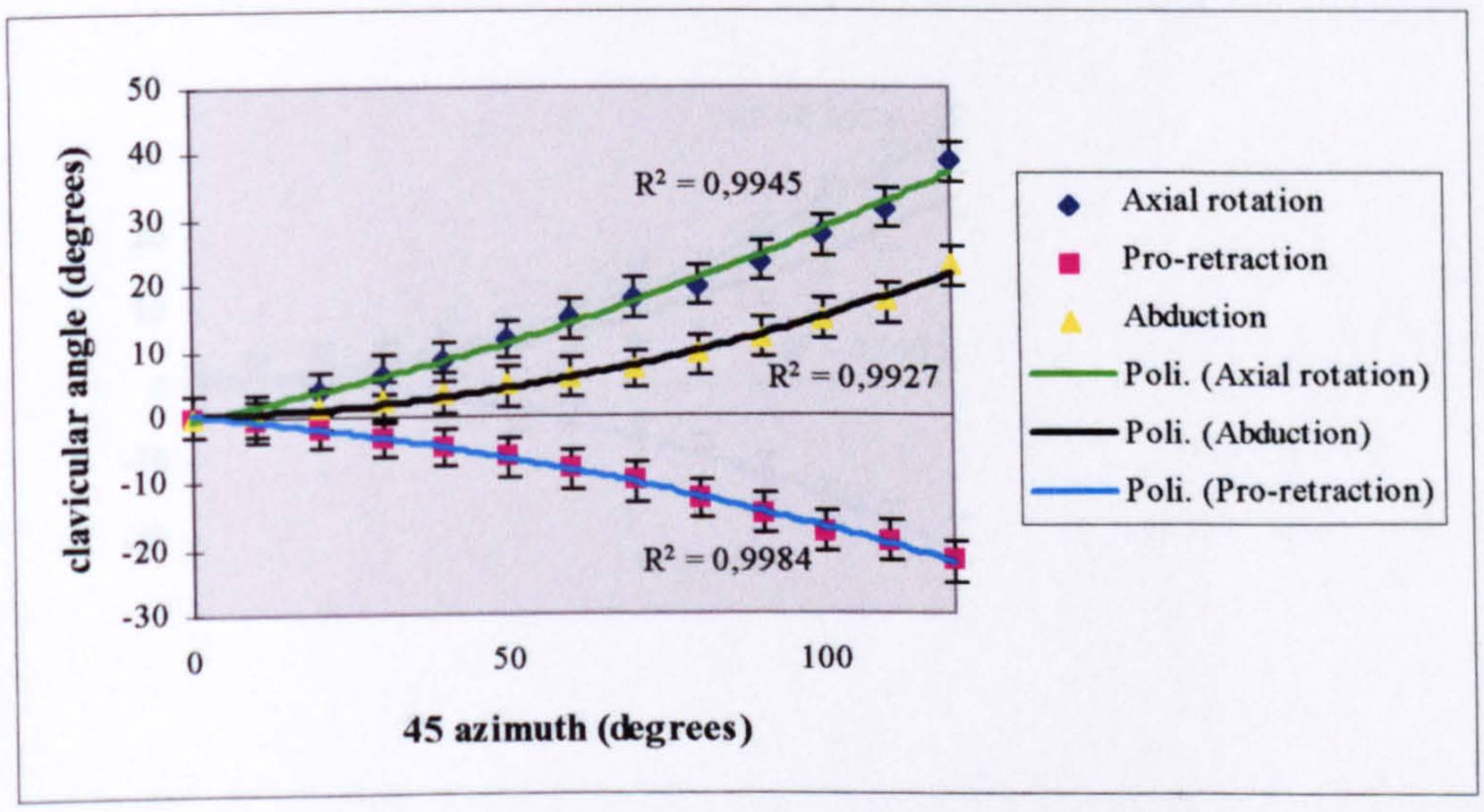

Figure 11.14 b: *Subject 8 (L/R=2,39) - observer 2*

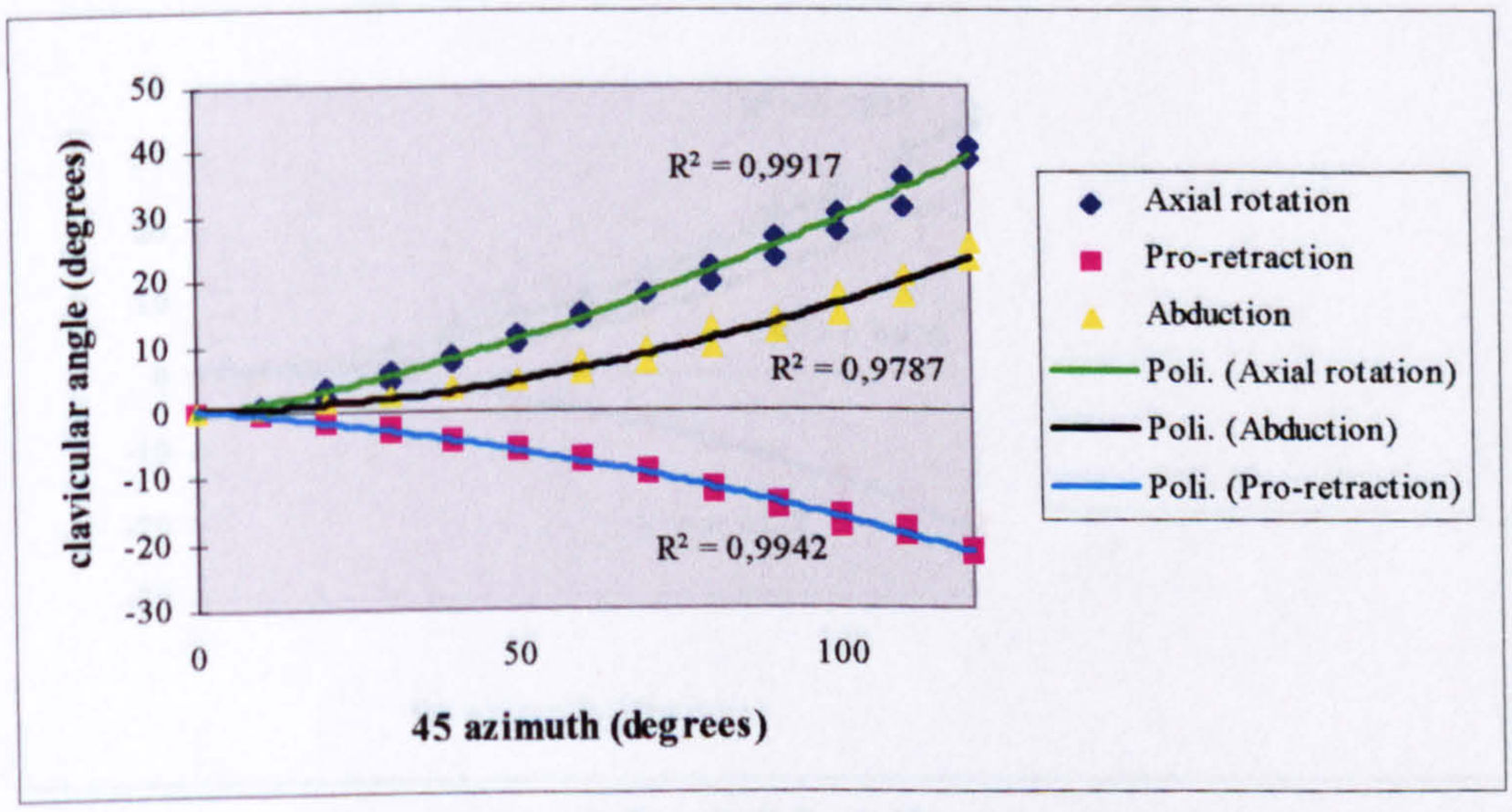

Figure 11.14 c: *Subject 8 (L/R=2,39) - inter observer*

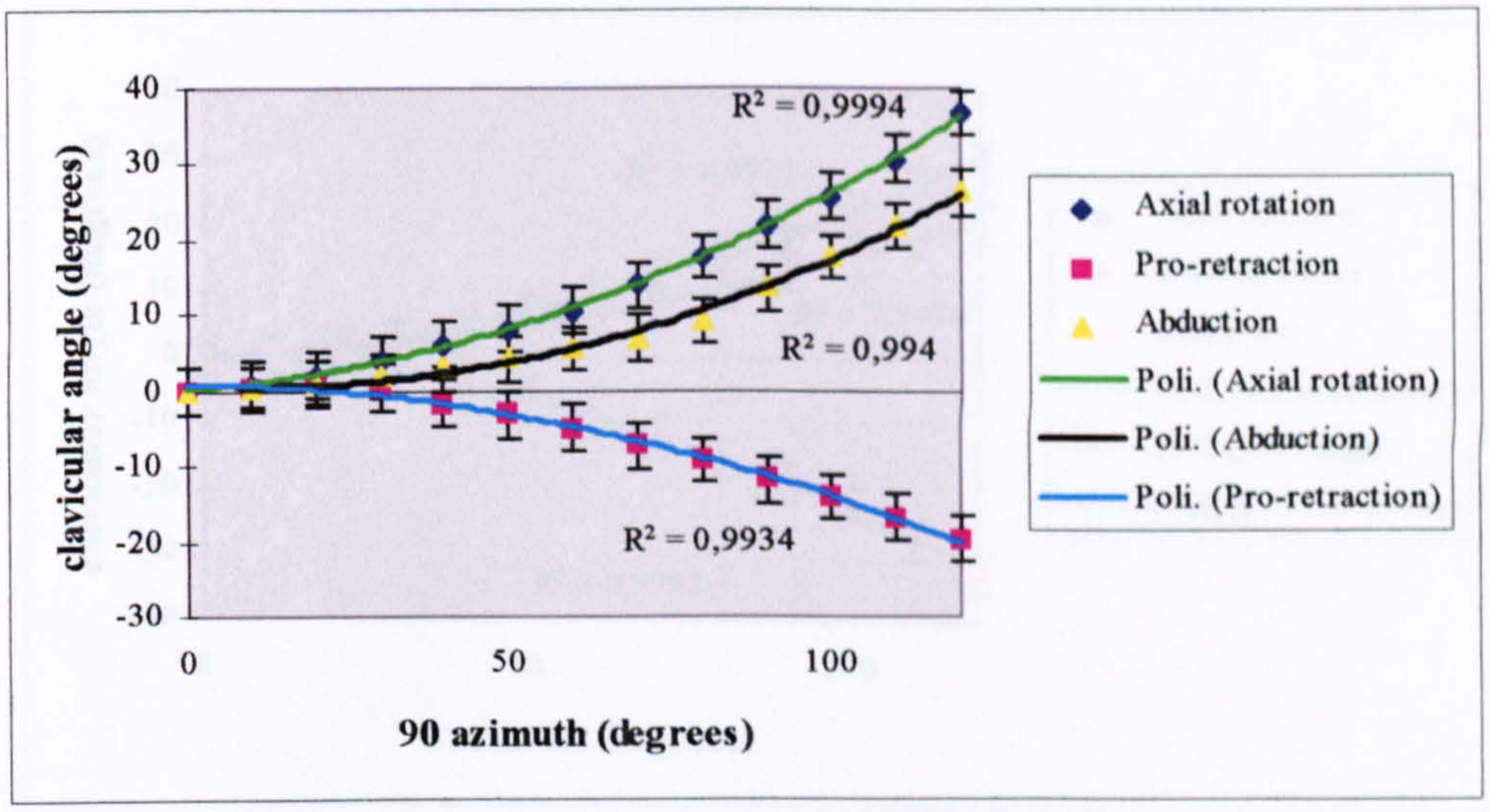

Figure 11.15 a: *Subject 8 (L/R=2,39) - observer 1*

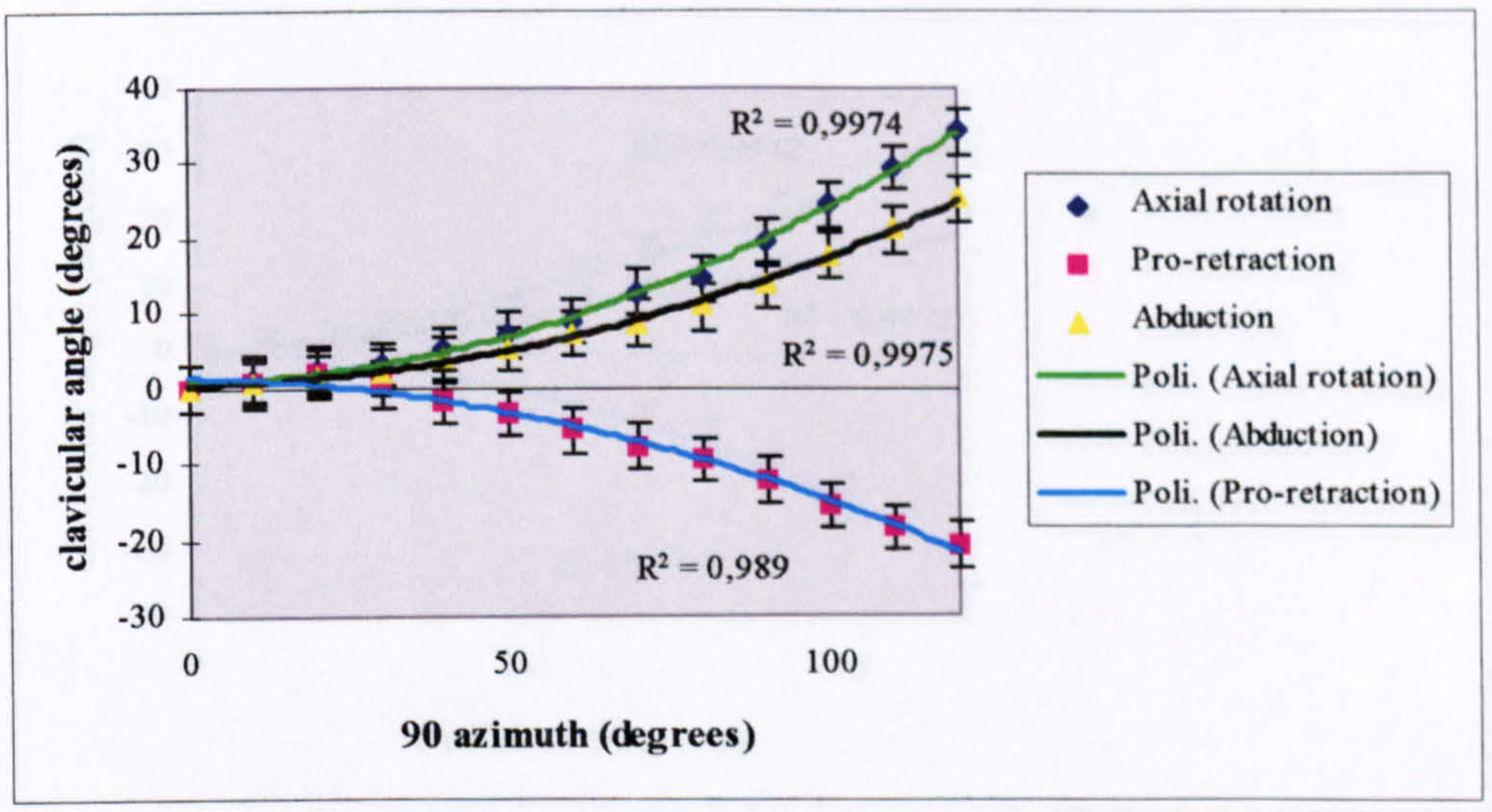

Figure 11.15 b: *Subject 8 (L/R=2,39) - observer 2*

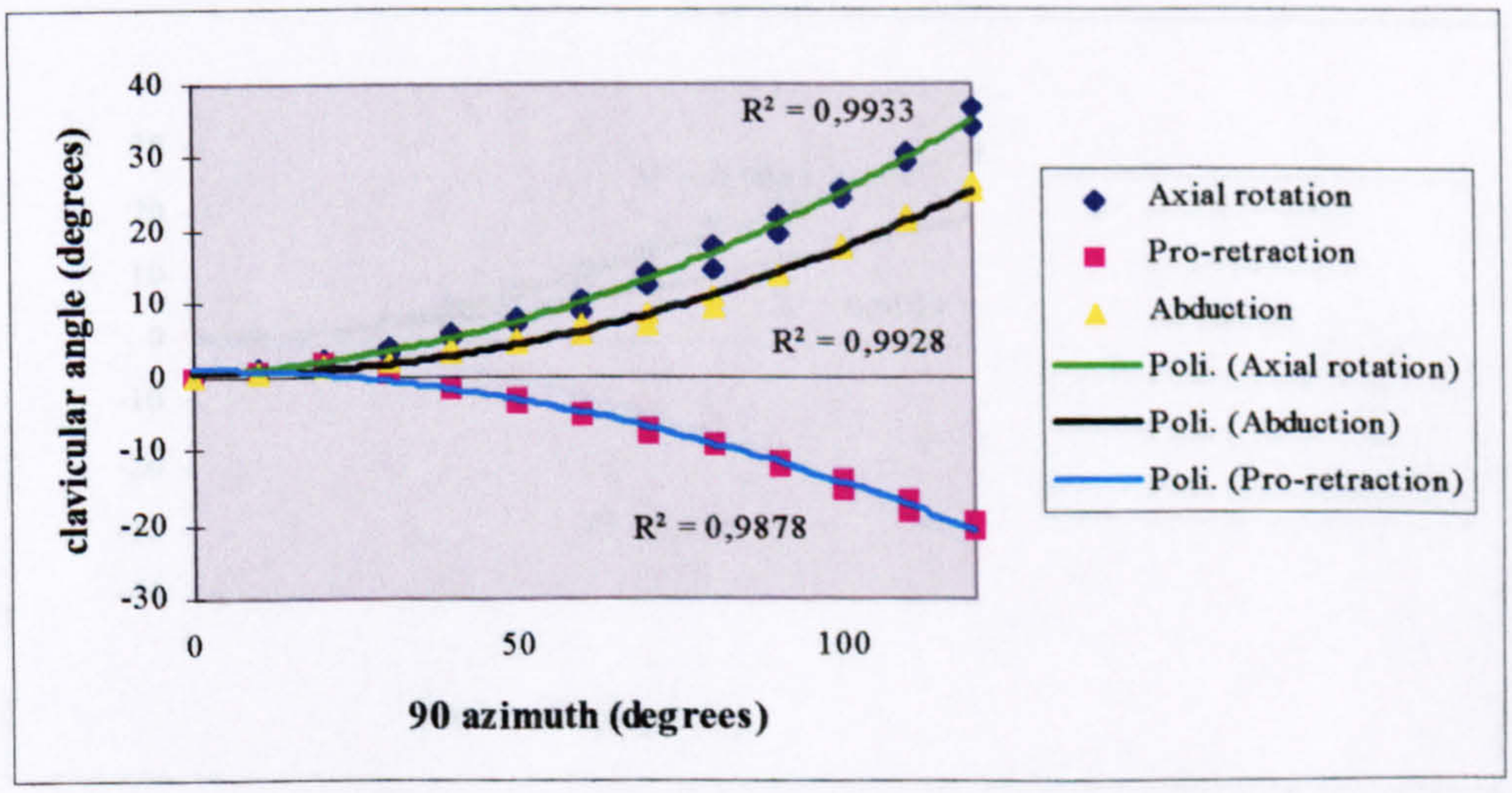

Figure 11.15 c: *Subject 8 (L/R=2,39) - inter observer*

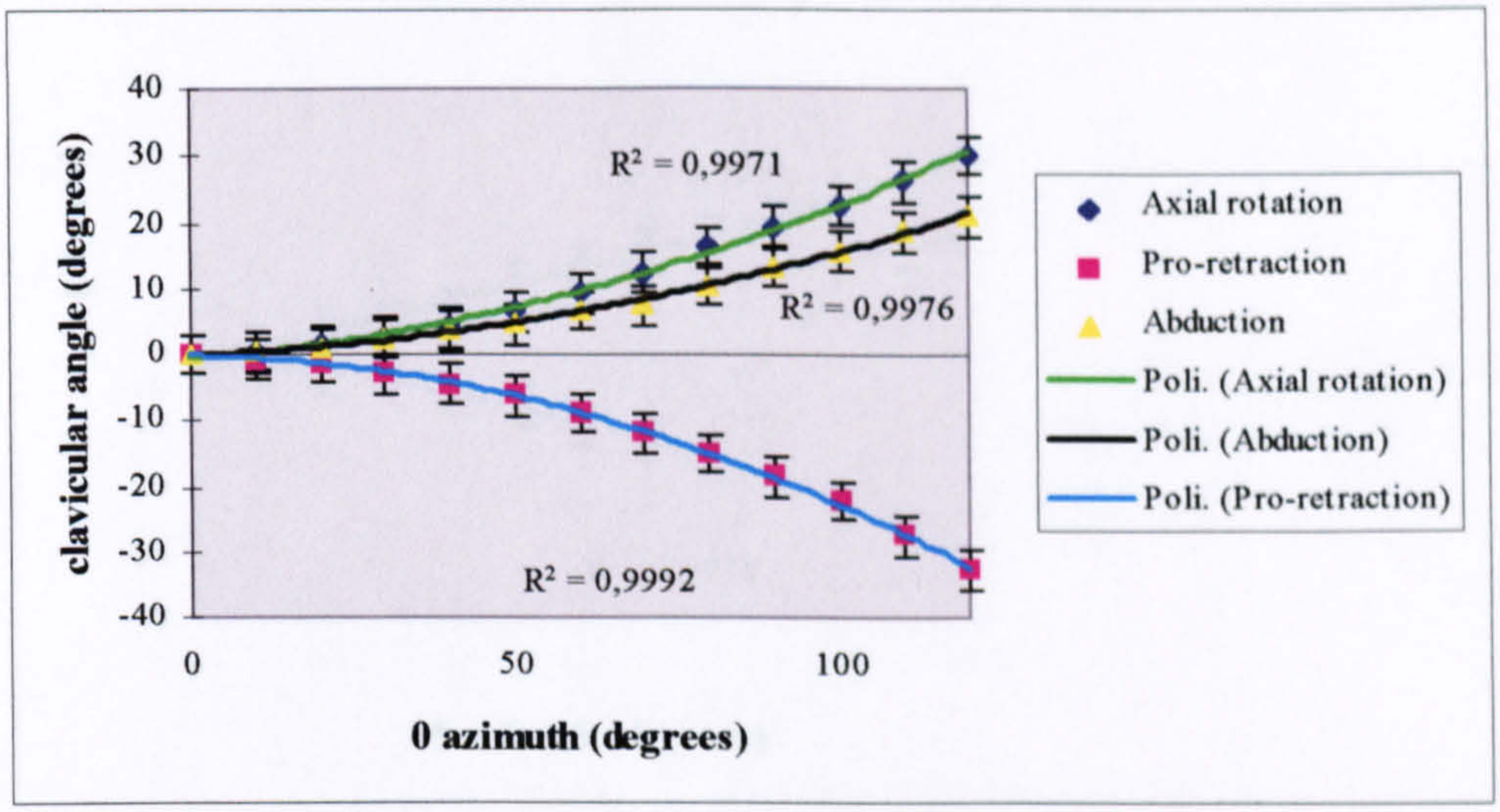

Figure 11.16 a: *Subject 9 (L/R=2,26) - observer 1*

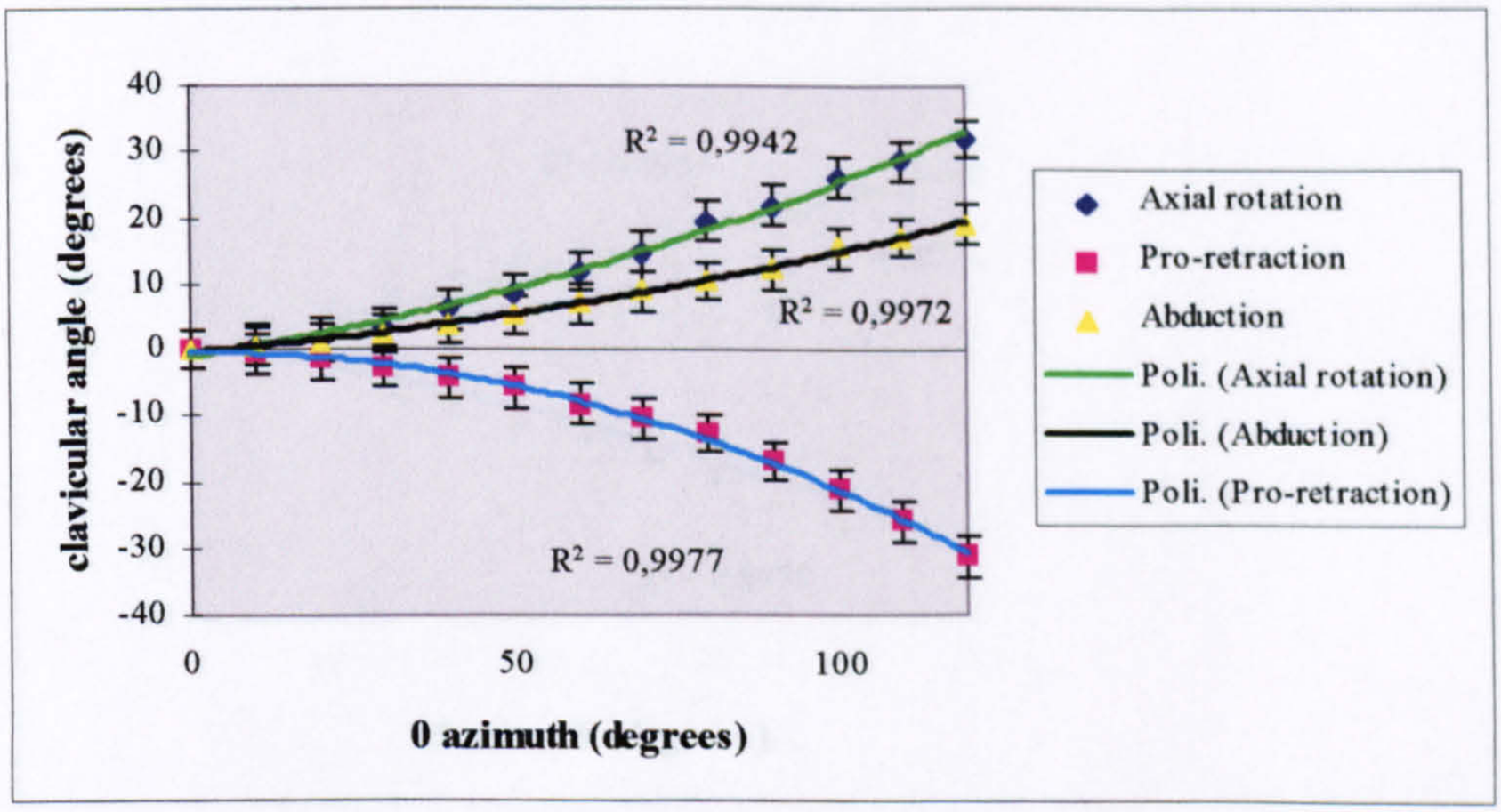

Figure 11.16 b: *Subject 9 (L/R=2,26) - observer 2*

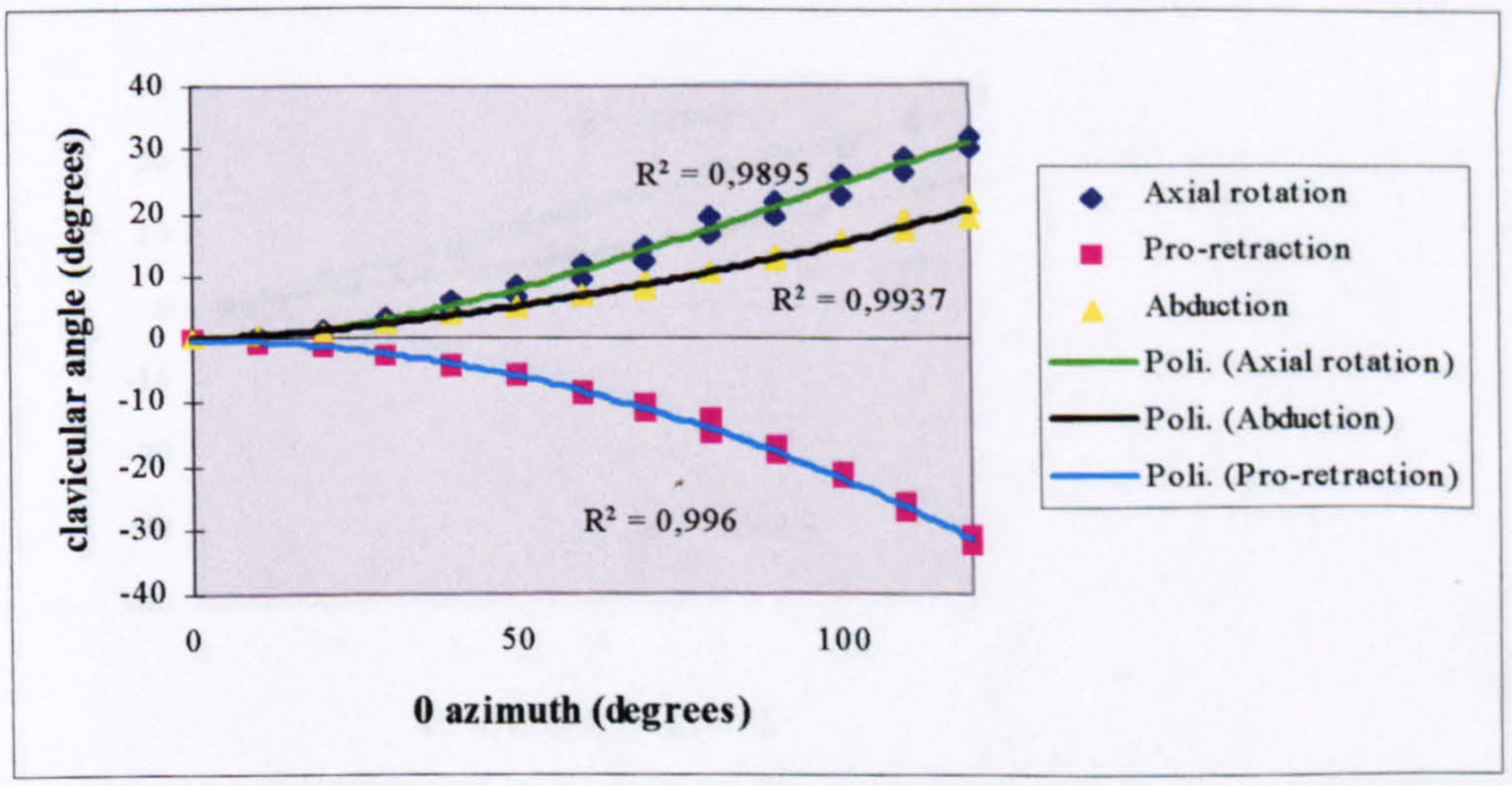

Figure 11.16 c: *Subject 9 (L/R=2,26) - inter observer*

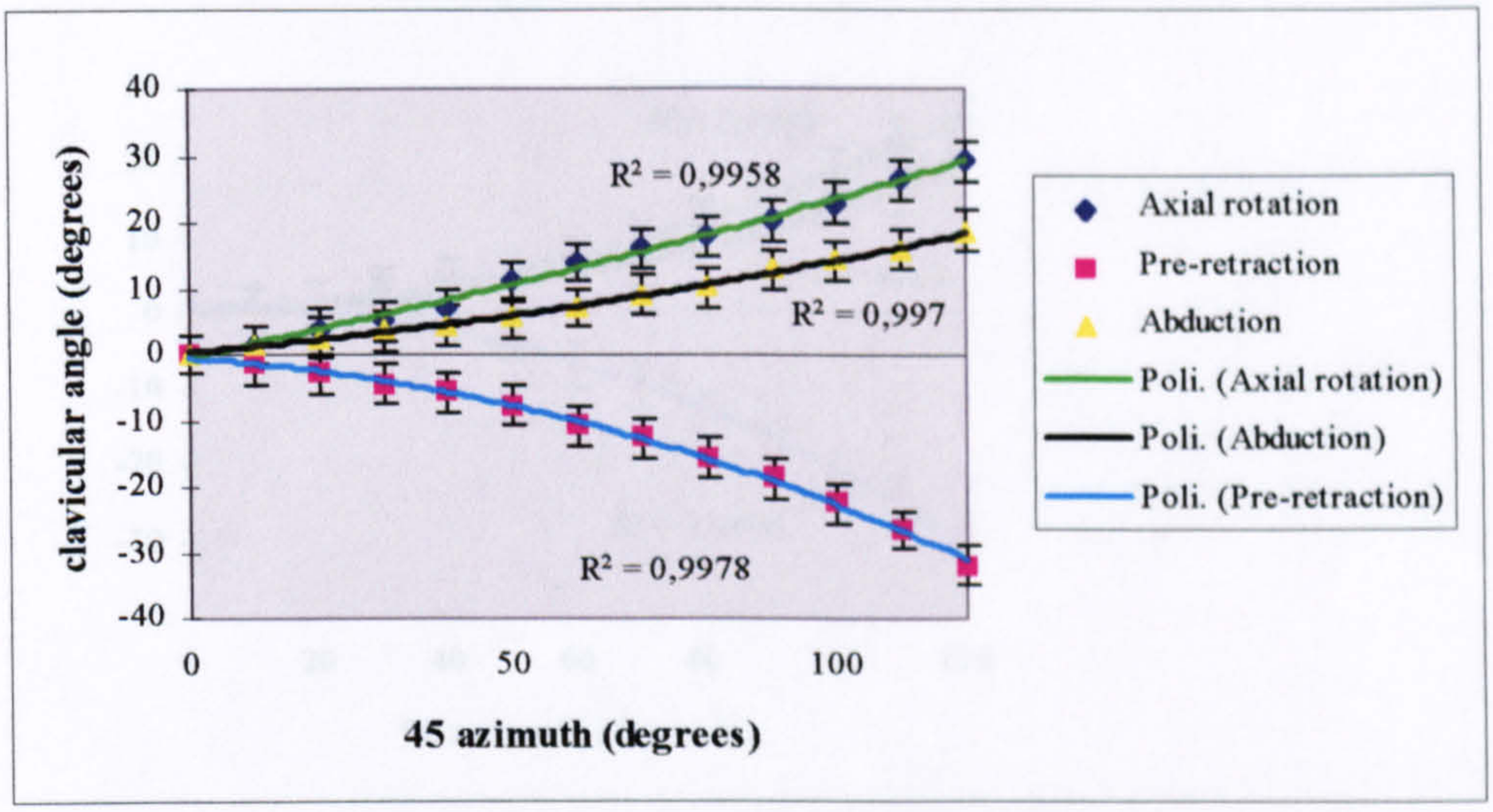

Figure 11.17 a: *Subject 9 (L/R=2,26) - observer 1*

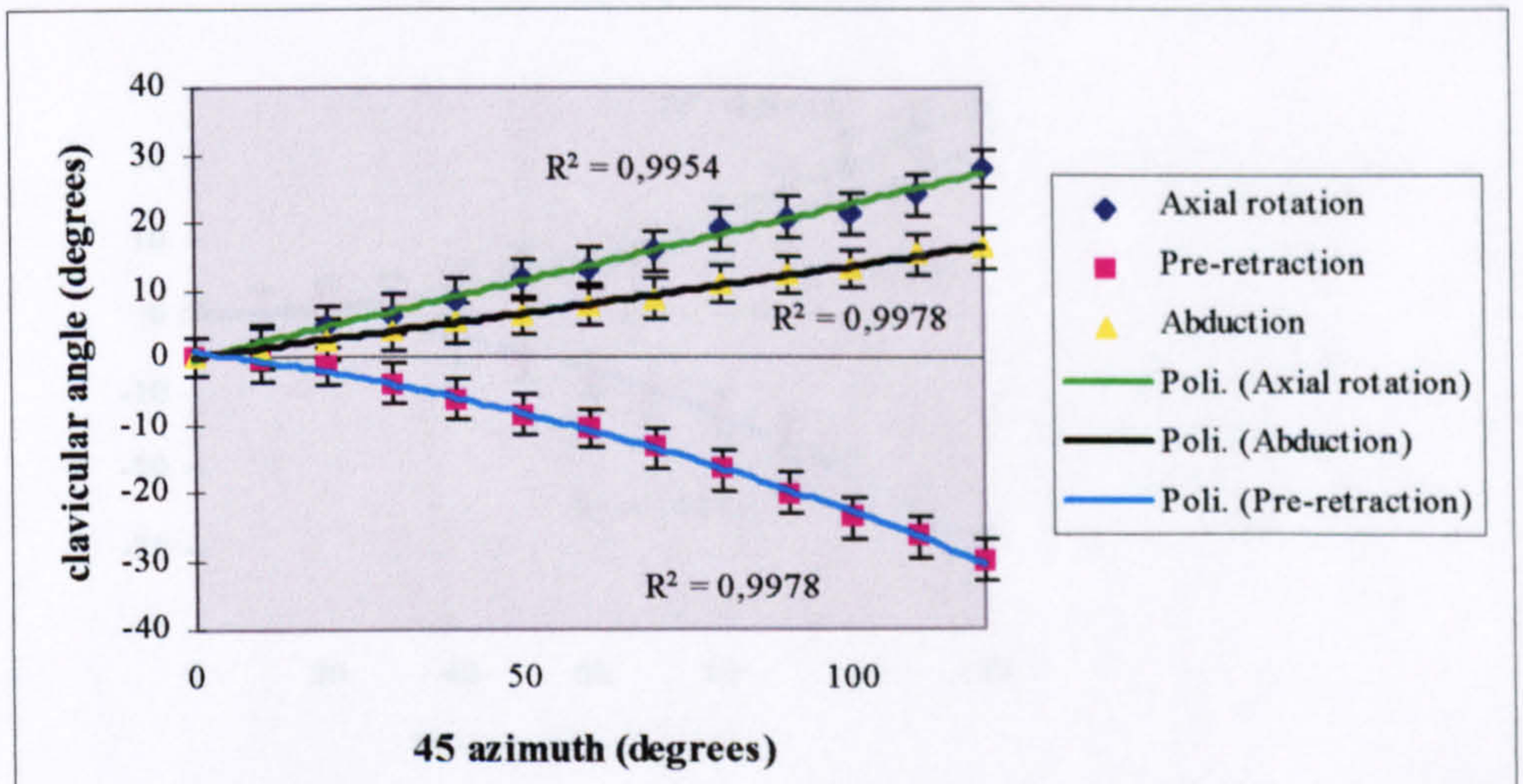

Figure 11.17 b: *Subject 9 (L/R=2,26) - observer 2*

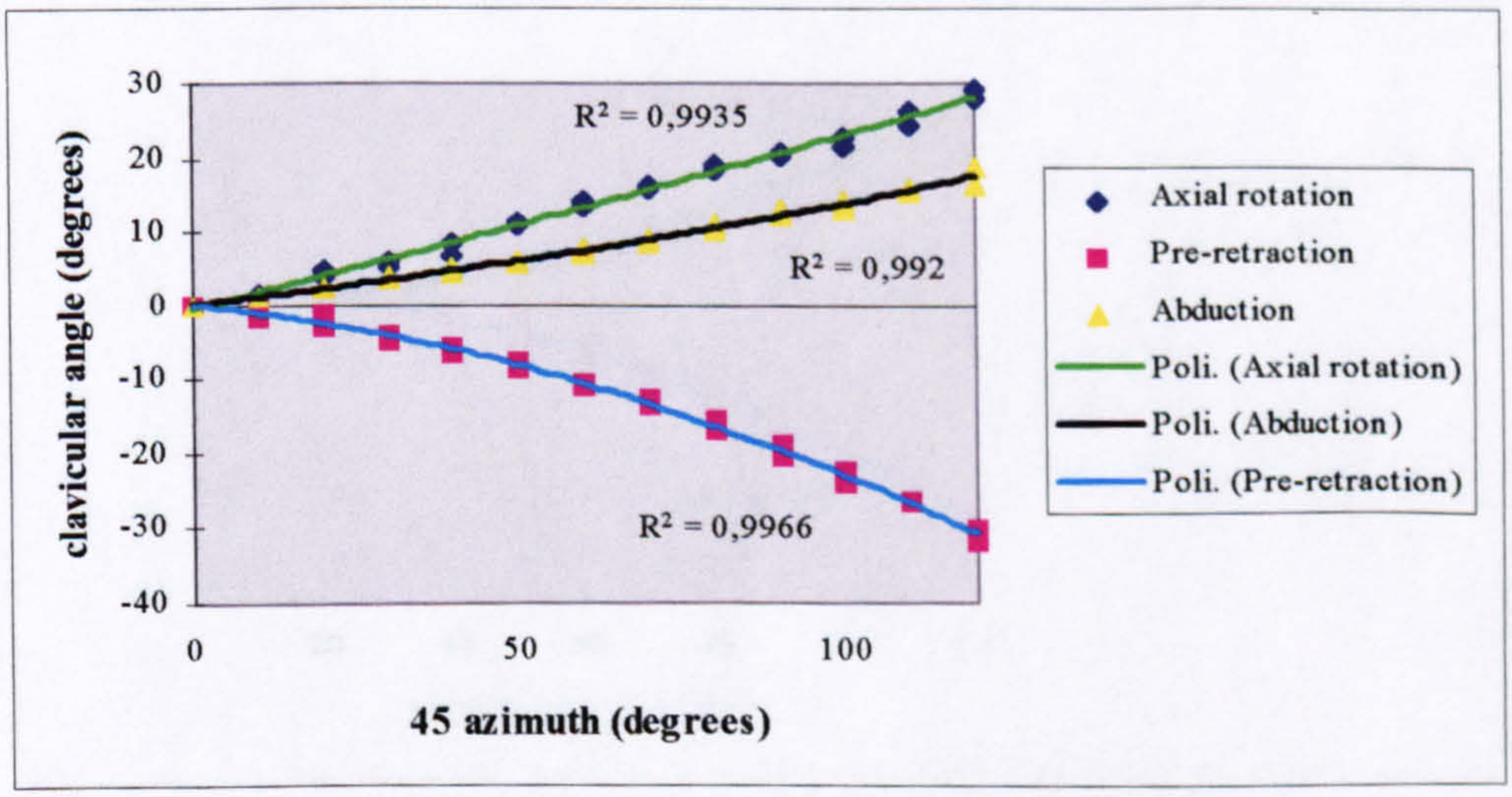

Figure 11.17 c: *Subject 9 (L/R=2,26) - inter observer*

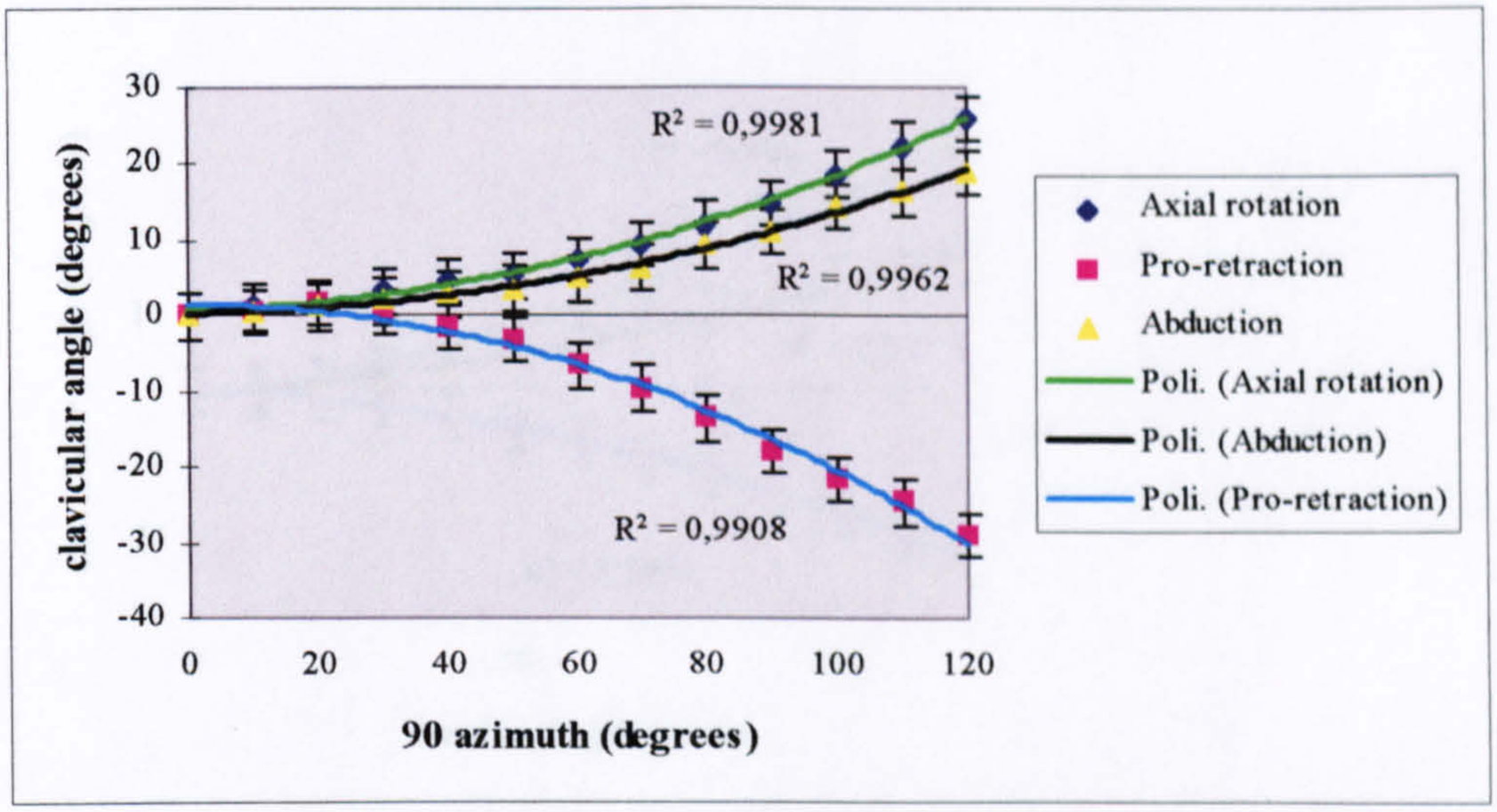

Figure 11.18 a: *Subject 9 (L/R=2,26) - observer 1*

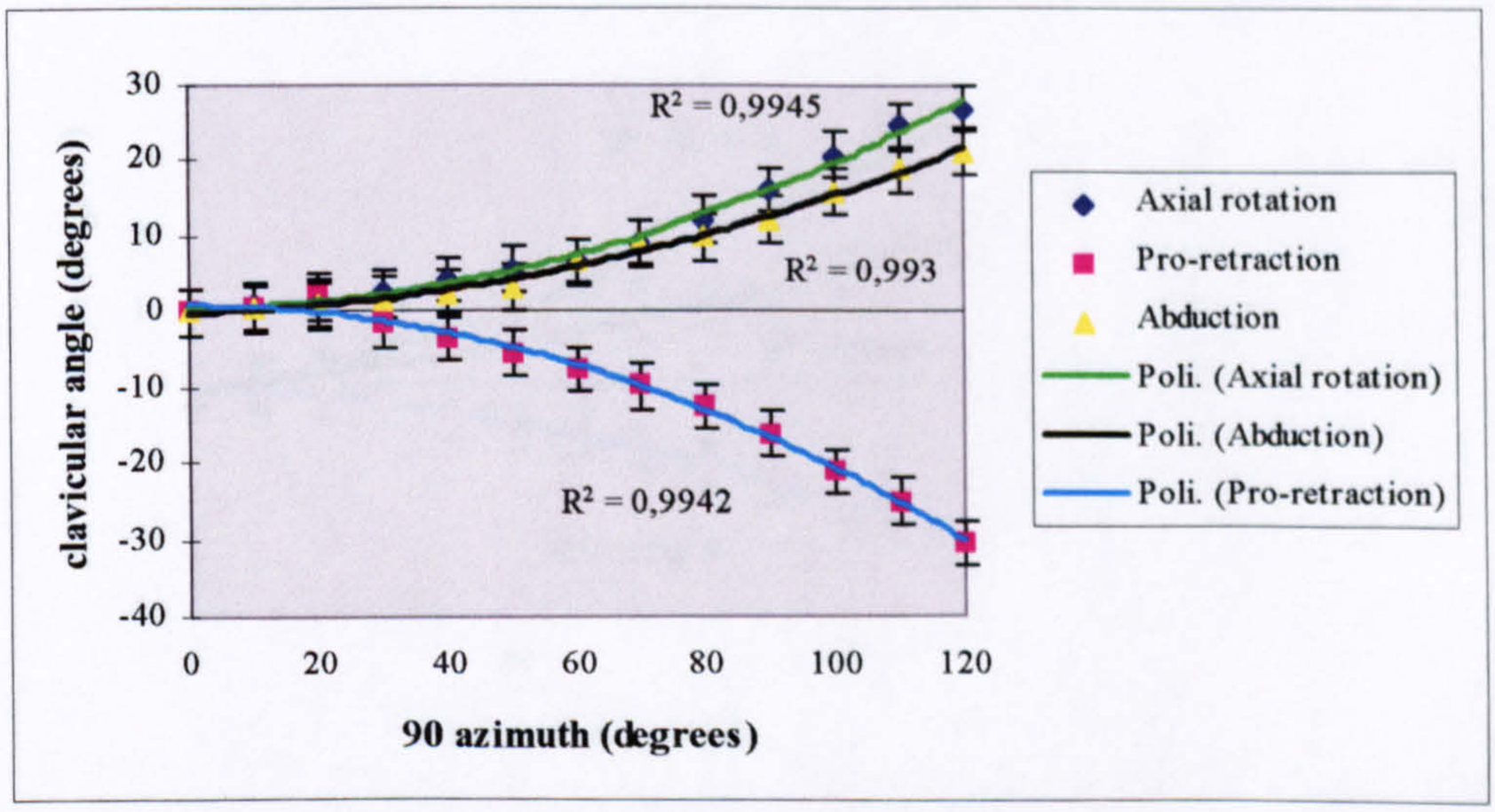

Figure 11.18 b: *Subject 9 (L/R=2,26) - observer 2*

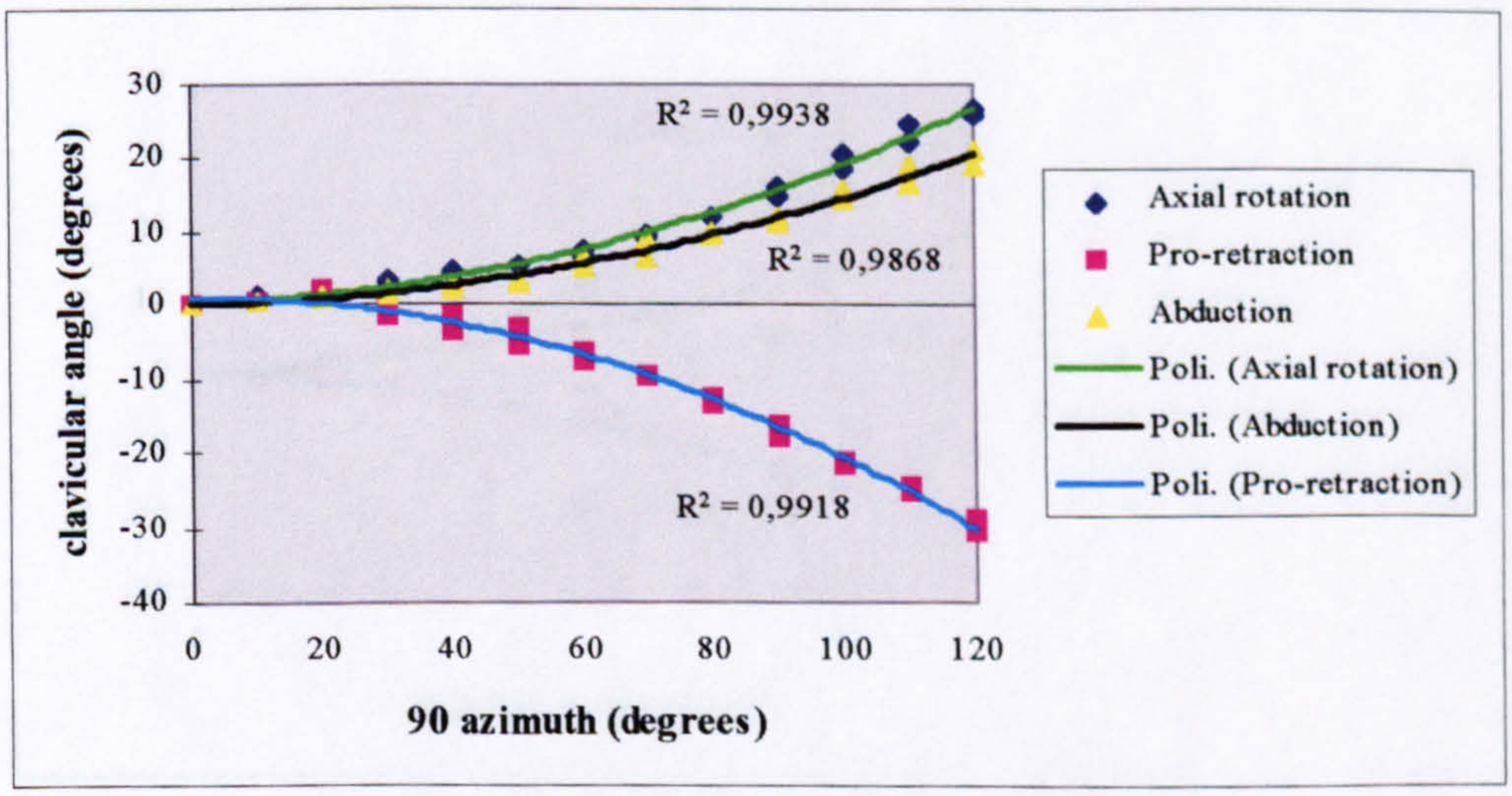

Figure 11.18 c: *Subject 9 (L/R=2,26) - inter observer*

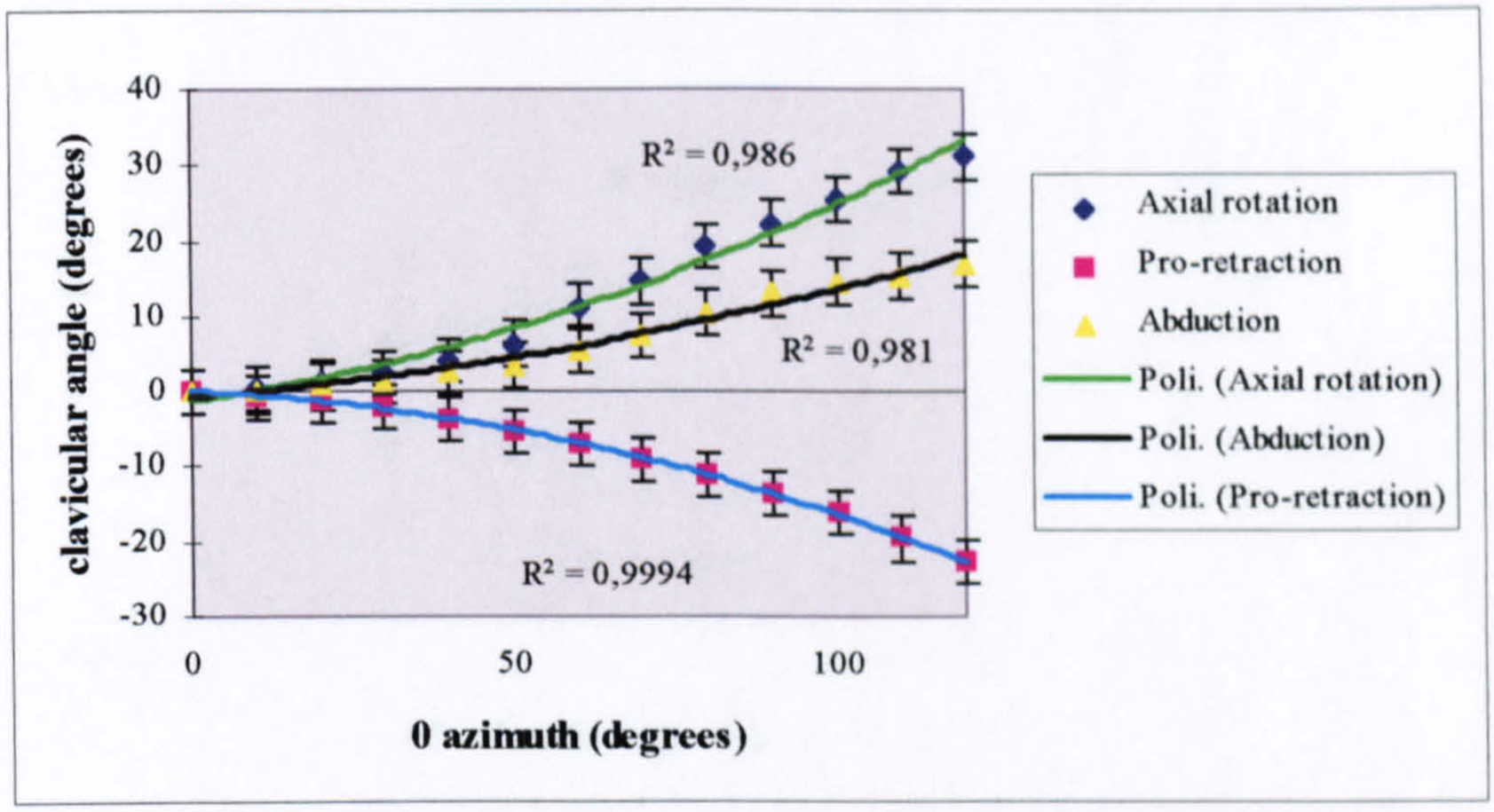

Figure 11.19 a: *Subject 10 (L/R=2,06) - observer 1*

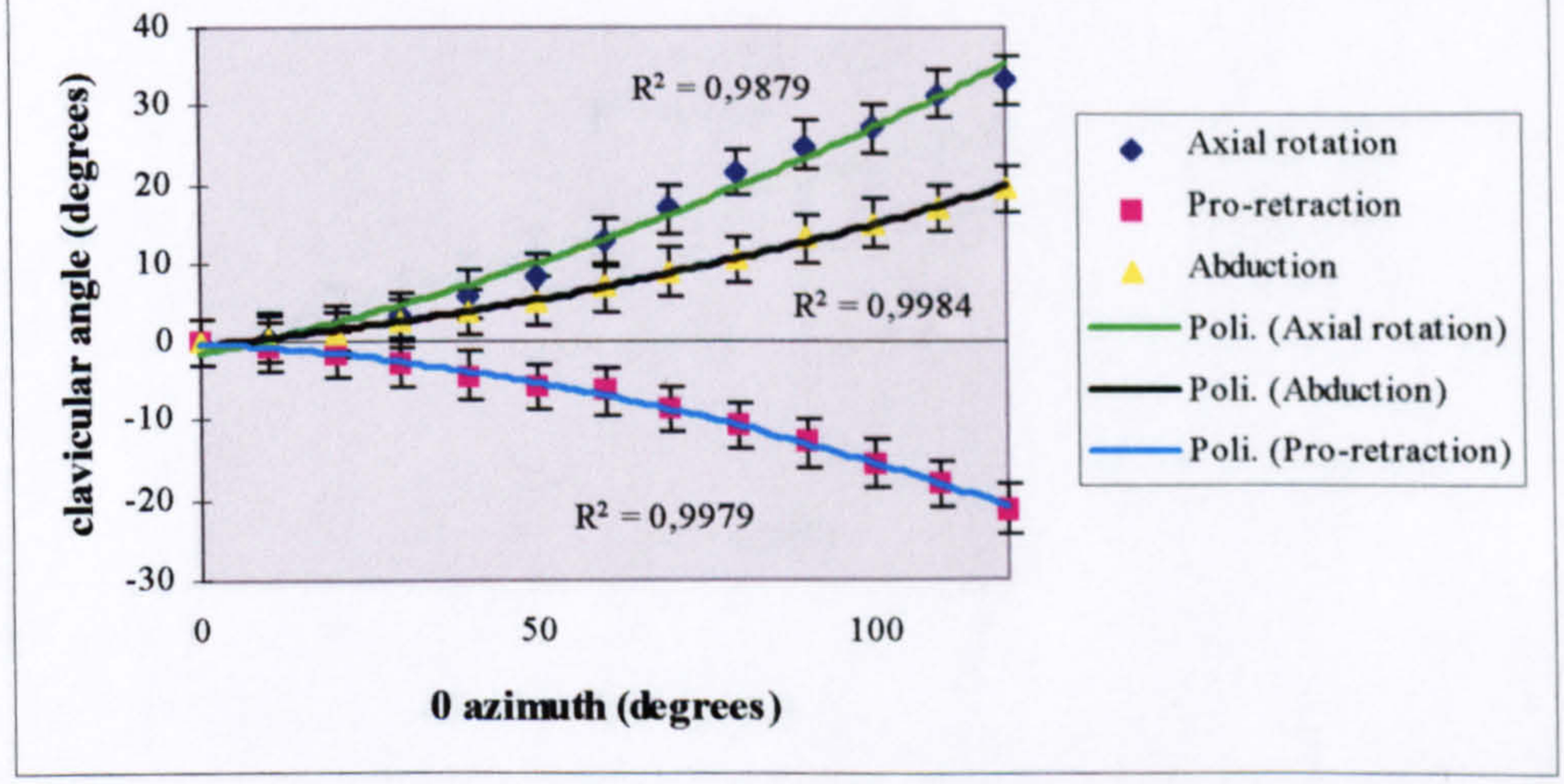

Figure 11.19 b: *Subject 10 (L/R=2,06) - observer 2*

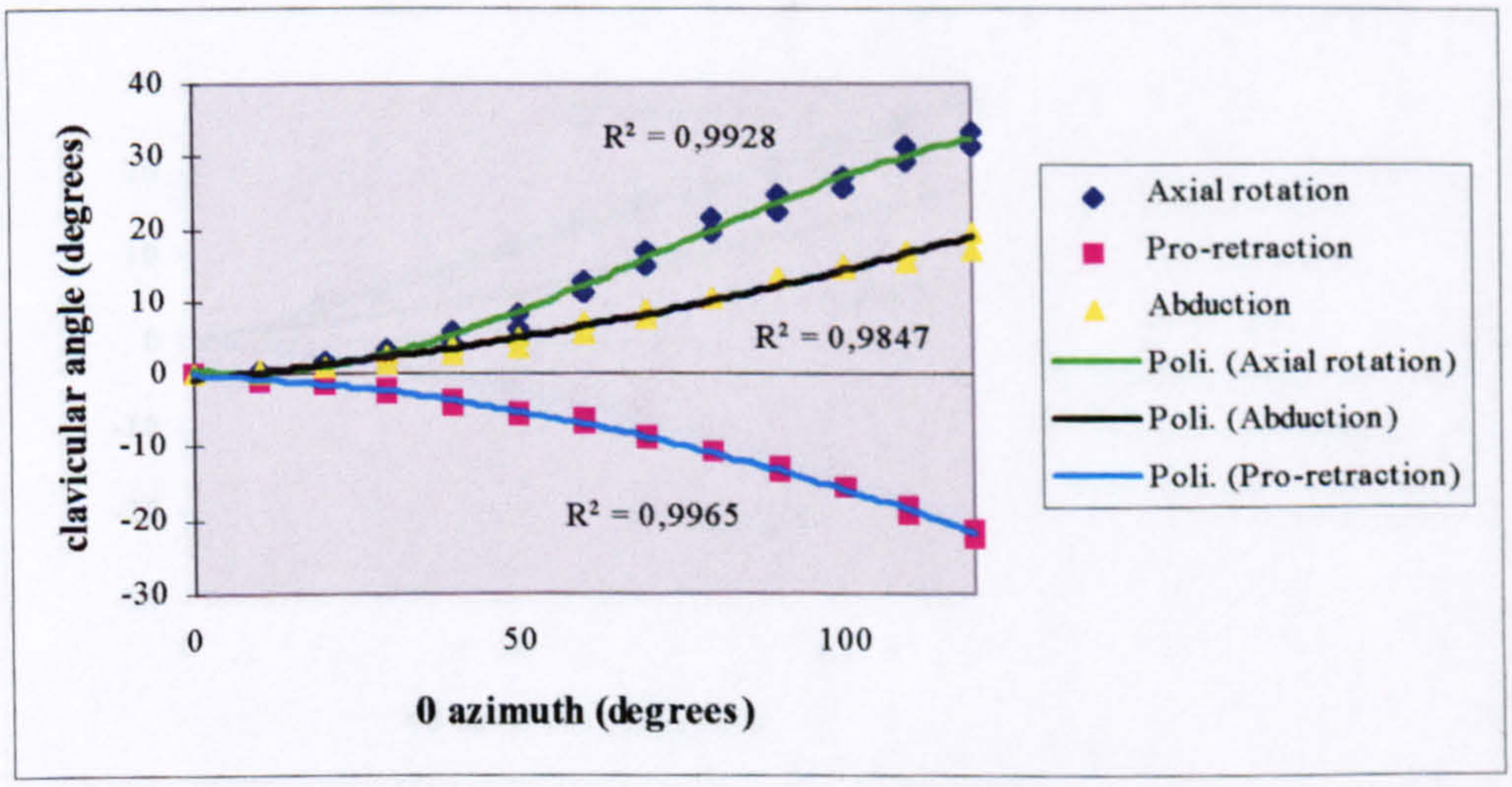

Figure 11.19 c: *Subject 10 (L/R=2,06) - inter observer*

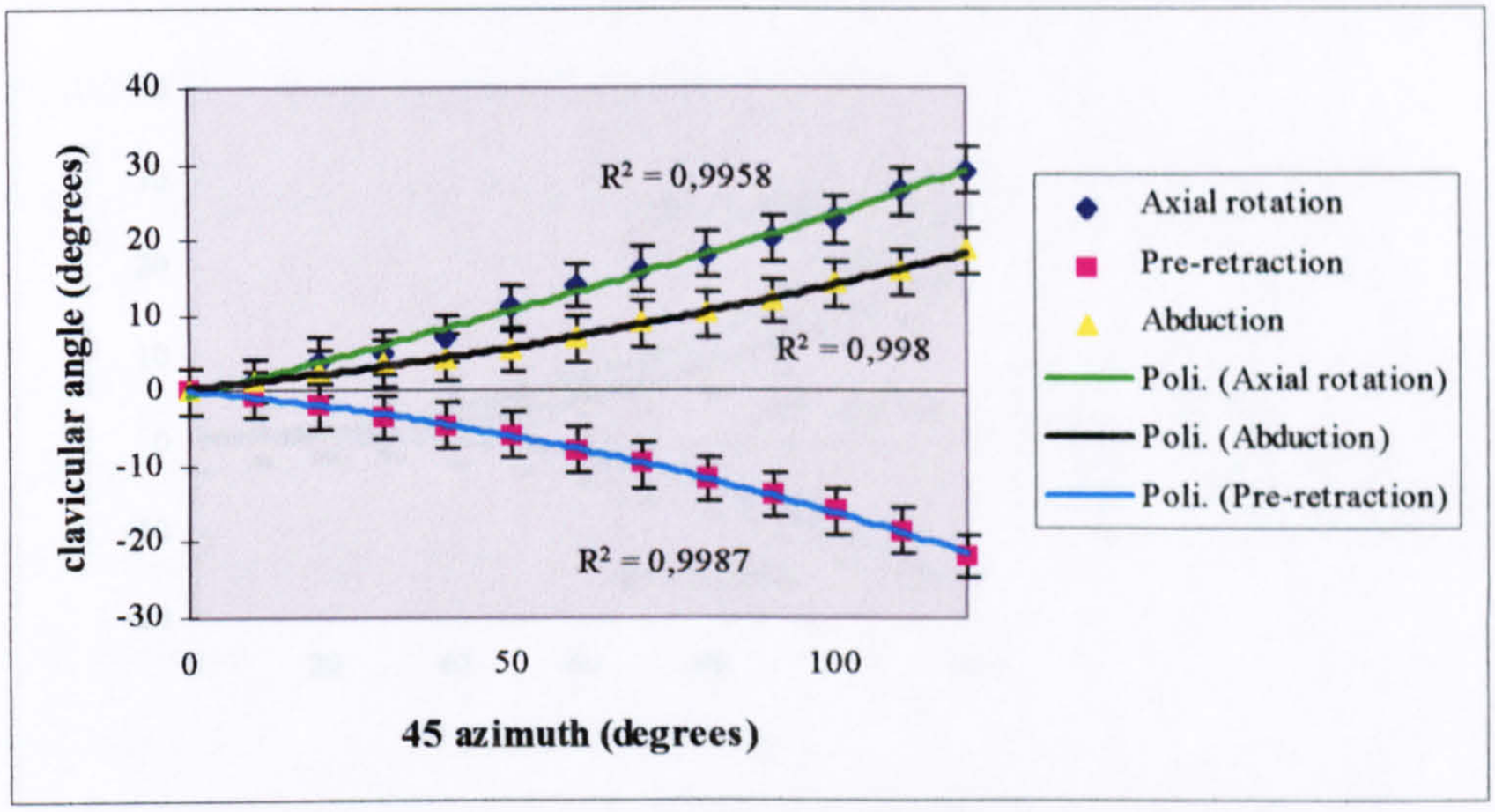

Figure 11.20 a: *Subject 10 (L/R=2,06) - observer 1*

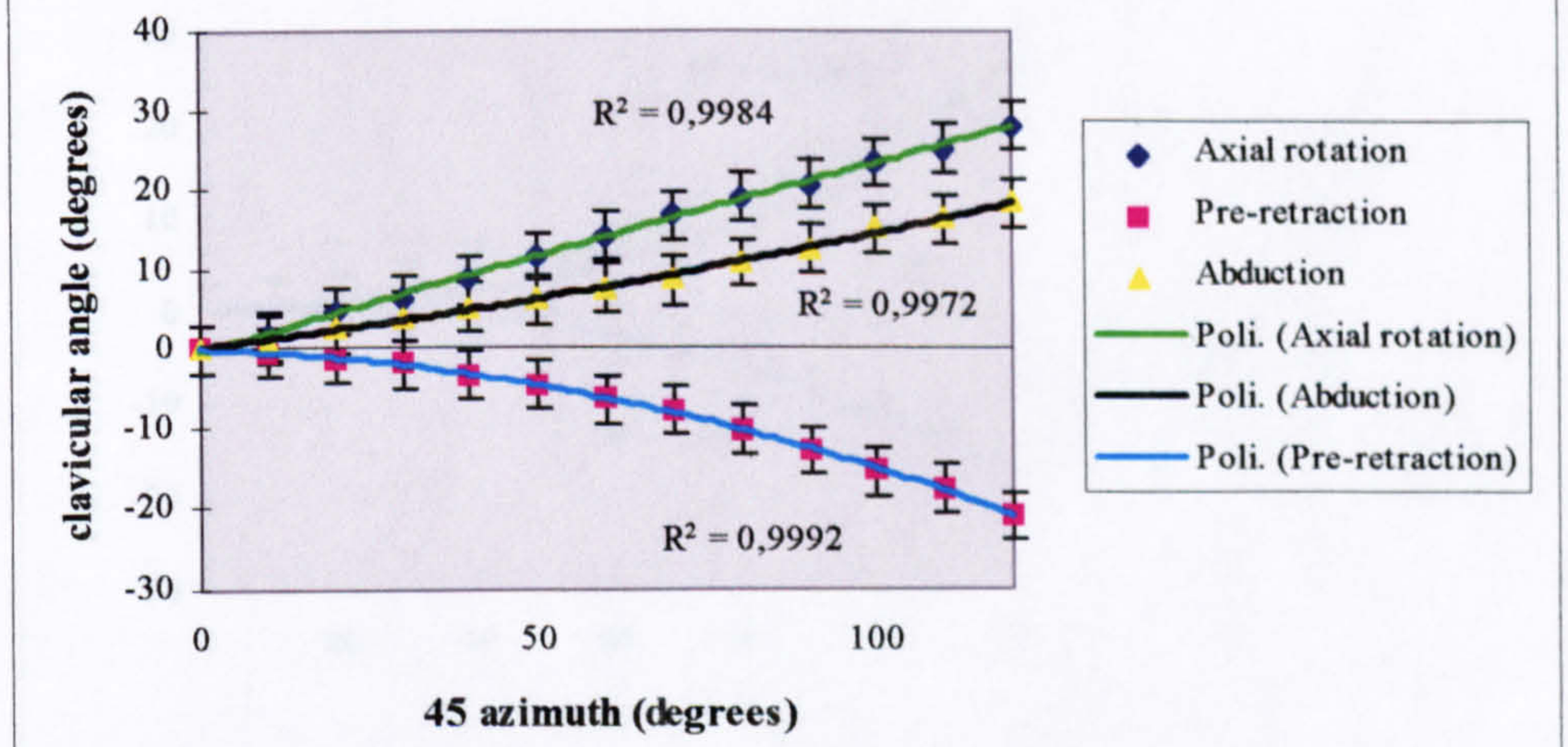

Figure 11.20 b: *Subject 10 (L/R=2,06) - observer 2*

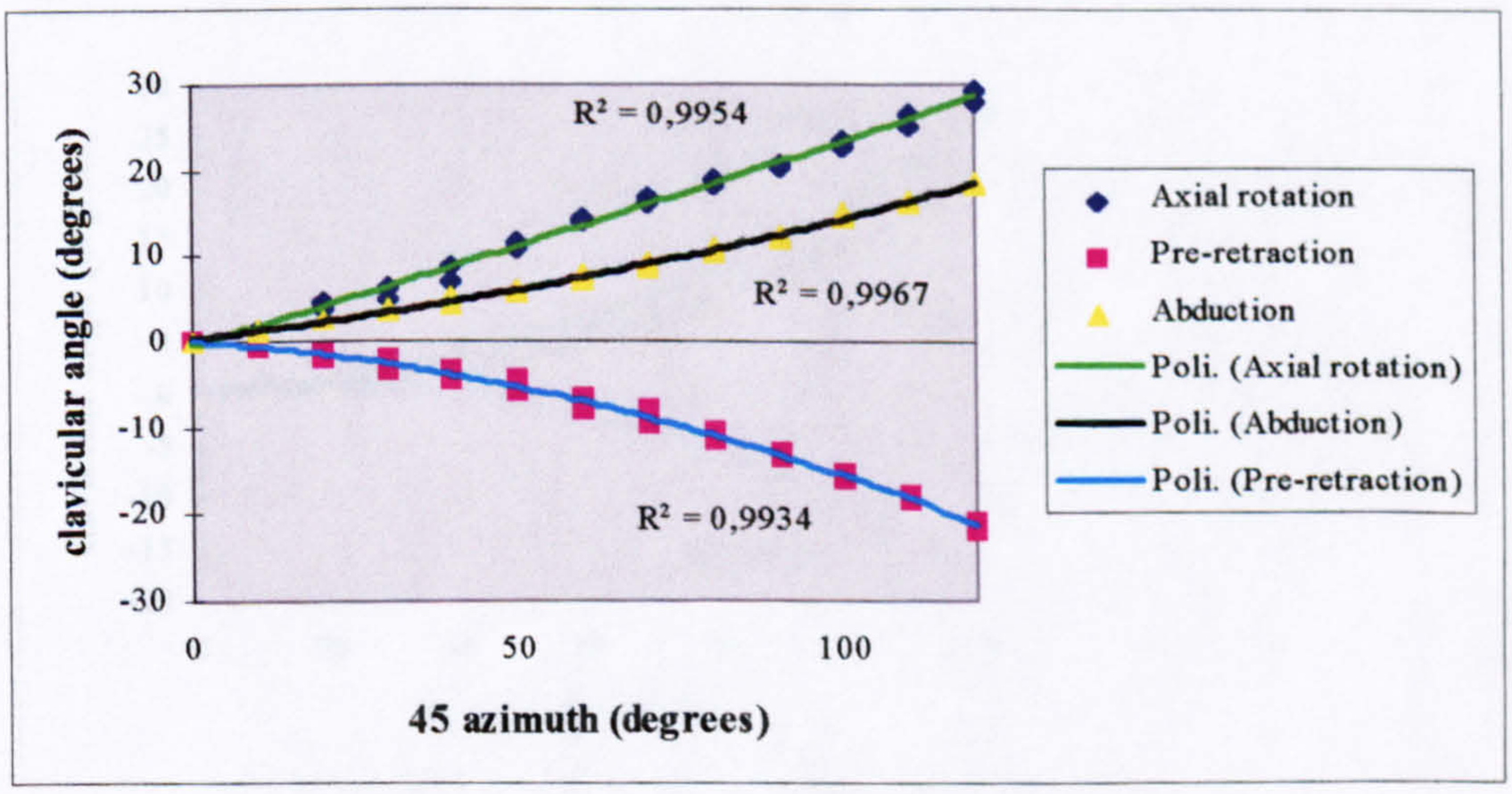

Figure 11.20 c: *Subject 10 (L/R=2,06) - inter observer*

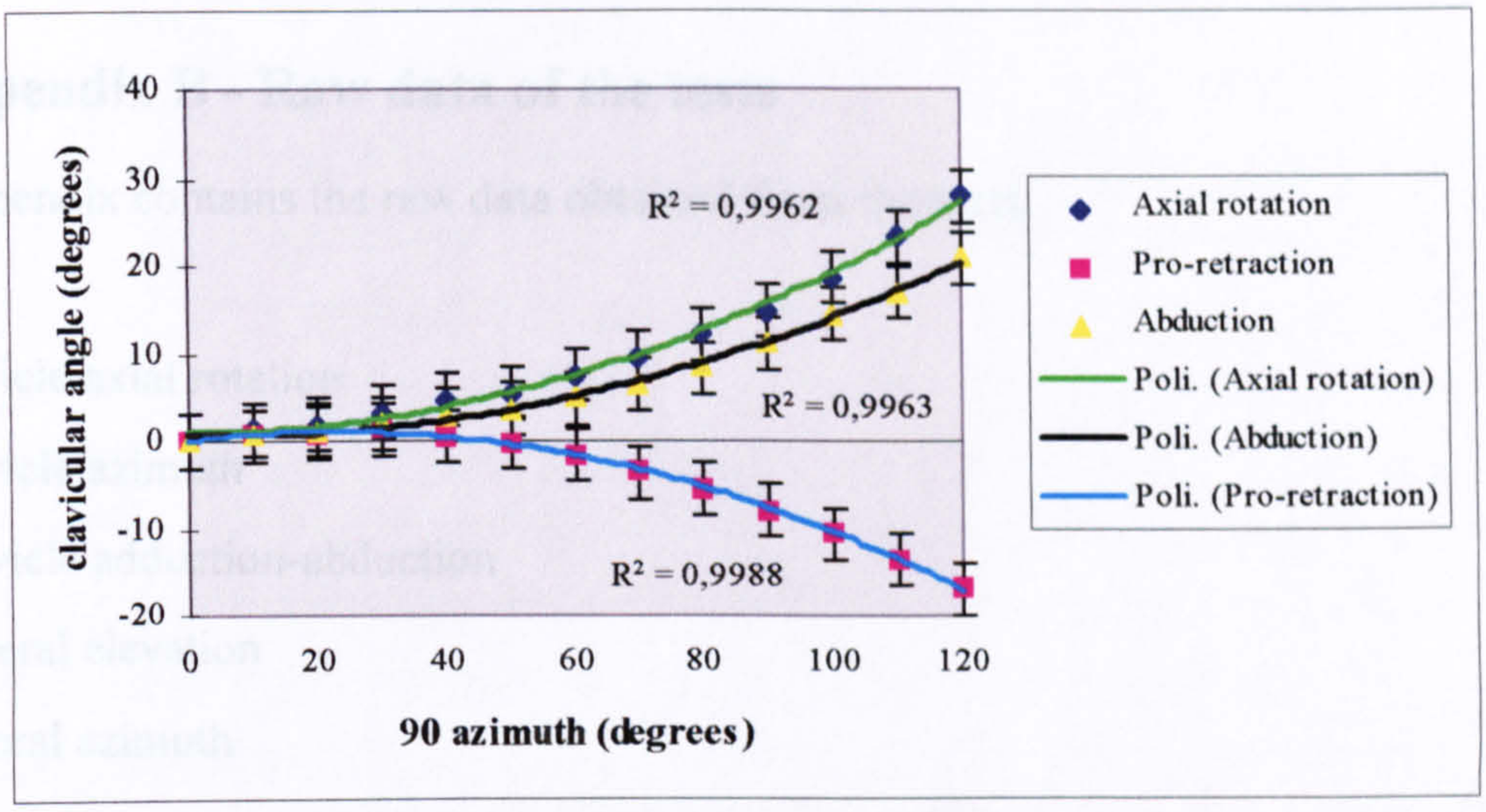

Figure 11.21 a: *Subject 10 (L/R=2,06) - observer 1*

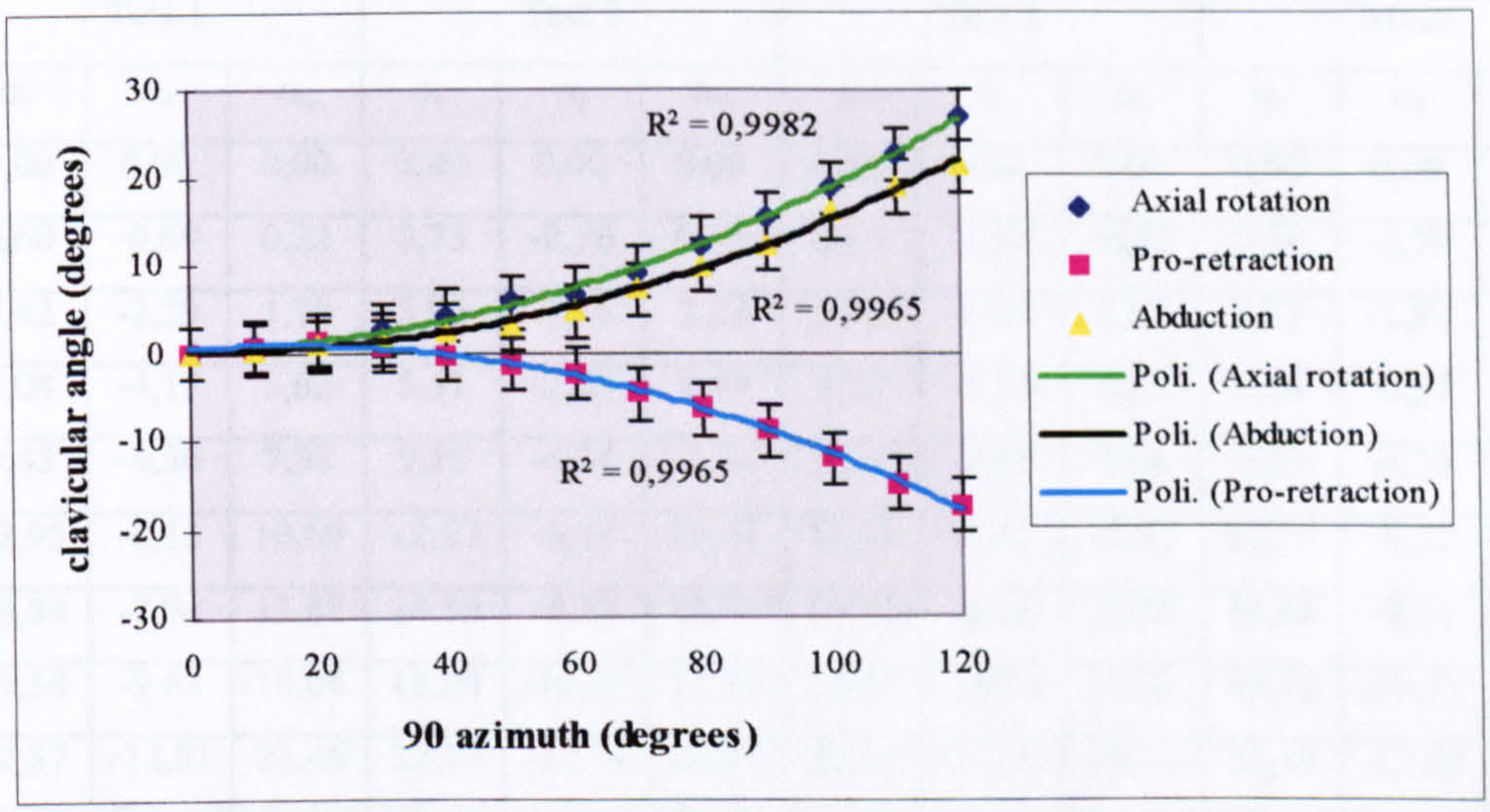

Figure 11.21 b: *Subject 10 (L/R=2,06) - observer 2*

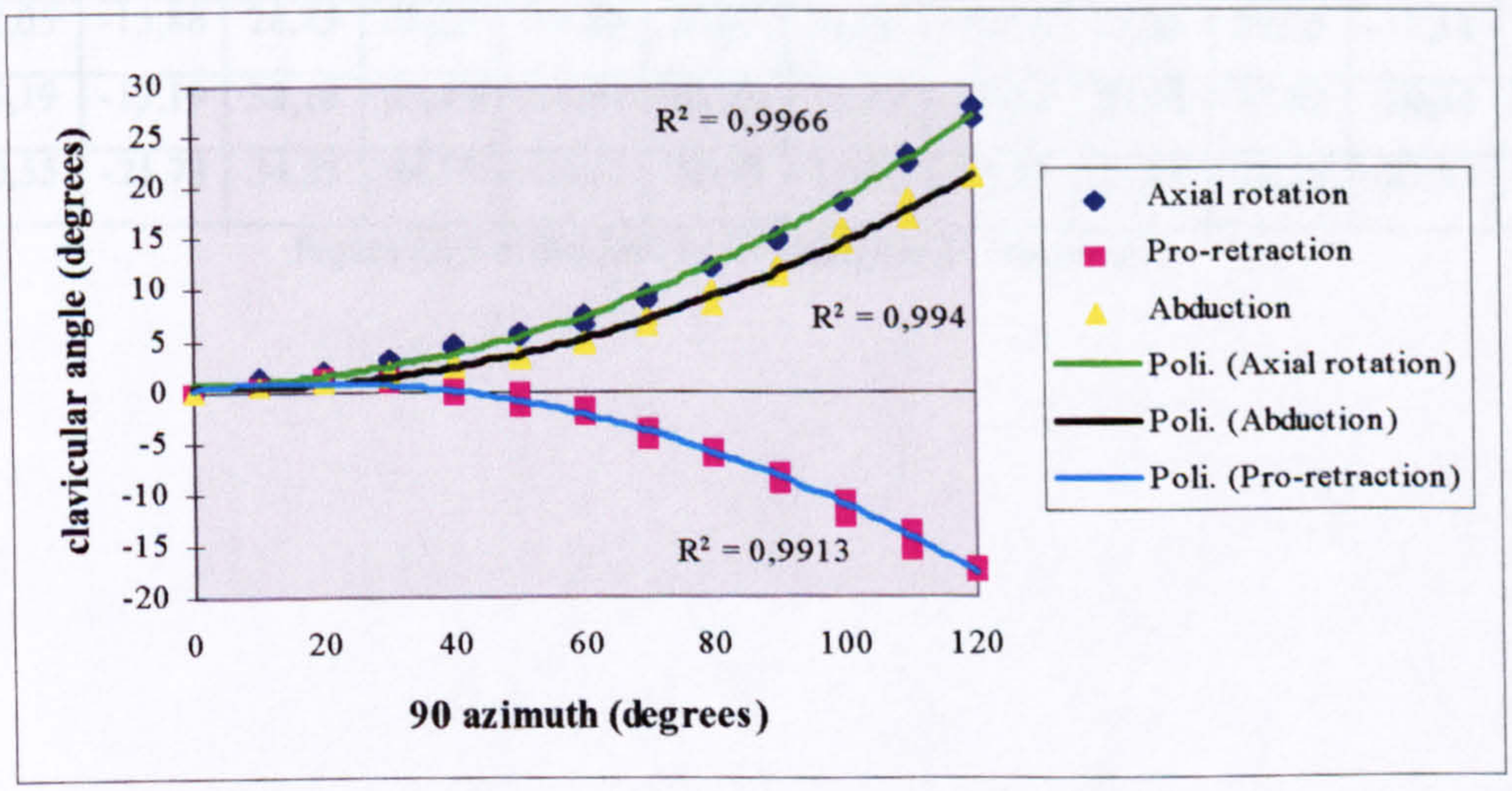

Figure 11.21 c: *Subject 10 (L/R=2,06) - inter observer*

12 Appendix B - Raw data of the tests

This Appendix contains the raw data obtained from the tests.

α_r = clavicle axial rotation

α_t = clavicle azimuth

α_a = clavicle adduction-abduction

β = humeral elevation

γ = humeral azimuth

β	Test 1			Test 2			Test 3			Mean		
	α_r	α_t	α_a	α_r	α_t	α_a	α_r	α_t	α_a	α_r	α_t	α_a
0	0,00	0,00	0,00	0,00	0,00	0,00	0,00	0,00	0,00	0,00	0,00	0,00
10	0,60	-0,69	0,22	0,73	-0,56	0,35	0,17	-1,12	-0,21	0,50	-0,79	0,12
20	3,42	-2,29	1,70	3,95	-1,76	2,23	3,79	-1,92	2,07	3,72	-1,99	2,00
30	7,04	-4,17	5,62	5,51	-2,84	4,49	5,57	-3,10	4,05	6,04	-3,37	4,72
40	9,43	-4,56	7,98	9,15	-4,84	7,70	9,11	-4,88	7,66	9,23	-4,76	7,78
50	12,95	-6,15	10,69	12,67	-6,43	10,41	12,63	-6,47	10,37	12,75	-6,35	10,49
60	14,84	-7,94	13,87	14,56	-8,22	13,59	14,52	-8,26	13,55	14,64	-8,14	13,67
70	19,58	-9,63	18,04	18,85	-10,36	17,31	18,87	-10,34	17,33	19,10	-10,11	17,56
80	22,87	-12,01	21,46	22,14	-12,74	20,73	22,16	-12,72	20,75	22,39	-12,49	20,98
90	25,91	-14,48	24,29	25,18	-15,21	23,56	25,20	-15,19	23,58	25,43	-14,96	23,81
100	32,05	-15,88	28,45	28,25	-18,68	24,65	28,95	-16,98	25,35	29,75	-17,18	26,15
110	36,19	-19,19	32,18	32,39	-21,99	28,38	33,09	-20,29	29,08	33,89	-20,49	29,88
120	40,55	-21,73	34,35	36,75	-24,53	30,55	37,45	-22,83	31,25	38,25	-23,03	32,05

Figure 12.1 a: Subject 1 (γ = 0 degrees) – observer 1

β	Test 1			Test 2			Test 3			Mean		
	α_r	α_t	α_a	α_r	α_t	α_a	α_r	α_t	α_a	α_r	α_t	α_a
0	0,00	0,00	0,00	0,00	0,00	0,00	0,00	0,00	0,00	0,00	0,00	0,00
10	1,15	-0,60	0,69	1,28	-0,47	0,82	0,72	-1,03	0,26	1,05	-0,70	0,59
20	3,79	-2,49	2,18	4,32	-1,96	2,71	4,16	-2,12	2,55	4,09	-2,19	2,48
30	8.86	-4,57	6,68	7,33	-3,24	5,55	7,39	-3,50	5,11	7,86	-3,77	5,78
40	11,35	-5,16	8,92	11,07	-5,44	8,64	11,03	-5,48	8,60	11,15	-5,36	8,72
50	13,18	-6,95	10,35	12,90	-7,23	10,07	12,86	-7,27	10,03	12,98	-7,15	10,15
60	15,49	-9,13	14,17	15,21	-9,41	13,89	15,17	-9,45	13,85	15,29	-9,33	13,97
70	21,13	-10,42	18,99	20,40	-11,15	18,26	20,42	-11,13	18,28	20,65	-10,90	18,51
80	24,55	-12,60	22,29	23,82	-13,33	21,56	23,84	-13,31	21,58	24,07	-13,08	21,81
90	27,60	-15,18	25,12	26,87	-15,91	24,39	26,89	-15,89	24,41	27,12	-15,66	24,64
100	32,56	-17,08	29,09	28,76	-19,88	25,29	29,46	-18,18	25,99	30,26	-18,38	26,79
110	36,87	-20,40	31,96	33,07	-23,20	28,16	33,77	-21,50	28,86	34,57	-21,70	29,66
120	41,46	-23,16	35,51	37,66	-25,96	31,71	38,36	-24,26	32,41	39,16	-24,46	33,21

Figure 12.1 b: Subject 1 (γ = 0 degrees) – observer 2

β	Test 1			Test 2			Test 3			Mean		
	α_r	α_t	α_a	α_r	α_t	α_a	α_r	α_t	α_a	α_r	α_t	α_a
0	0,00	0,00	0,00	0,00	0,00	0,00	0,00	0,00	0,00	0,00	0,00	0,00
10	0,14	-0,53	0,41	0,04	-0,63	0,31	0,06	-0,61	0,33	0,08	-0,59	0,35
20	2,55	-1,63	1,24	2,45	-1,73	1,14	2,47	-1,71	1,16	2,49	-1,69	1,18
30	4,86	-2,53	2,18	4,76	-2,63	2,08	4,78	-2,61	2,10	4,80	-2,59	2,12
40	5,15	-4,89	2,01	5.35	-4,69	2,21	7,05	-2,99	3,91	5,85	-4,19	2,71
50	7,47	-6,58	2,95	7,67	-6,38	3,15	9,37	-4,68	4,85	8,17	-5,88	3,65
60	12,35	-8,26	4,60	12,55	-8,06	4,80	14,25	-6,36	6,50	13,05	-7,56	5,30
70	16,81	-9,85	6,37	17,01	-9,65	6,57	18,71	-7,95	8,27	17,51	-9,15	7,07
80	19,37	-12,83	8,02	19,57	-12,63	8,22	21,27	-10,93	9,92	20,07	-12,13	8,72
90	25,53	-13,91	11,90	24,33	-15,11	10,70	24,63	-14,81	11,00	24,83	-14,61	11,20
100	27,90	-16,39	14,26	26,70	-17,59	13,06	27,00	-17,29	13,36	27,20	-17,09	13,56
110	33,88	-19,46	18,38	32,68	-20,66	17,18	32,98	-20,36	17,48	33,18	-20,16	17,68
120	38,55	-22,35	22,27	37,35	-23,55	21,07	37,65	-23,25	21,37	37,85	-23,05	21,57

Figure 12.2 a: Subject 1 (γ = 45 degrees) – observer 1

β	Test 1			Test 2			Test 3			Mean		
	α_r	α_t	α_a	α_r	α_t	α_a	α_r	α_t	α_a	α_r	α_t	α_a
0	0,00	0,00	0,00	0,00	0,00	0,00	0,00	0,00	0 00	0,00	0,00	0,00
10	0,24	-0,53	0,30	0,14	-0,63	0,20	0,16	-0,61	0,22	0,18	-0,59	0.24
20	2,55	-1,72	1,24	2.45	-1,82	1,14	2,47	-1,80	1,16	2,49	-1,78	1,18
30	5,15	-3,30	2,30	5,05	-3,40	2,20	5,07	-3,38	2,22	5,09	-3,36	2,24
40	6,60	-5,46	2,60	6,80	-5,26	2,80	8,50	-3,56	4,50	7,30	-4,76	3,30
50	9,90	-7,06	3,78	10,10	-6,86	3,98	11,80	-5,16	5.68	10,60	-6,36	4,48
60	13,13	-8,84	5,08	13,33	-8,64	5,28	15,03	-6,94	6,98	13,83	-8,14	5,78
70	16,10	-10,77	6,25	16,30	-10,57	6,45	18,00	-8,87	8,15	16,80	-10,07	6,95
80	18,99	-13,39	7,55	19,19	-13,19	7,75	20,89	-11,49	9,45	19,69	-12,69	8,25
90	23,10	-14,21	10,48	21,90	-15,41	9,28	22,20	-15,11	9,58	22,40	-14,91	9,78
100	28,09	-17,03	12,37	26,89	-18,23	11,17	27,19	-17,93	11,47	27,39	-17,73	11,67
110	32,14	-18,46	15,91	30,94	-19,66	14,71	31,24	-19,36	15,01	31,44	-19,16	15,21
120	37,27	-21,55	20,44	36,07	-22,75	19,24	36,37	-22,45	19,54	36,57	-22,25	19,74

Figure 12.2 b: Subject 1 ($\gamma = 45$ degrees) – observer 2

β	Test 1			Test 2			Test 3			Mean		
	α_r	α_t	α_a	α_r	α_t	α_a	α_r	α_t	α_a	α_r	α_t	α_a
0	0,00	0,00	0,00	0,00	0,00	0,00	0,00	0,00	0,00	0,00	0,00	0,00
10	1,01	0,43	0,41	0,80	0,22	0,20	0,77	0,19	0,17	0,86	0,28	0,26
20	1,20	1,14	0,60	0,99	0,93	0,39	0,96	0,90	0,36	1,05	0,99	0,45
30	1,32	0,53	0,74	1,11	0.32	0,53	1,08	0,29	0,50	1,17	0,38	0,59
40	1,60	-2,17	0,46	2,60	-1.17	1,46	2,40	-1,37	1,26	2,20	-1,57	1,06
50	2,57	-3,77	0,70	3,57	-2,77	1,70	3,37	-2,97	1,50	3,17	-3,17	1,30
60	6,04	-5,36	2,05	7,04	-4,36	3,05	6,84	-4,56	2,85	6,64	-4,76	2,65
70	11,53	-5,67	7,45	9,03	-8,17	4,95	9,53	-7,67	5,45	10,03	-7,17	5,95
80	15,43	-7,66	9,86	12,93	-10,16	7,36	13,43	-9,66	7,86	13,93	-9,16	8,36
90	19,61	-10,15	13,16	17,11	-12,65	10,66	17,61	-12,15	11,16	18,11	-11,65	11,66
100	24,32	-13,34	17,34	21,82	-15,84	14,84	22,32	-15,34	15,34	22,82	-14,84	15,84
110	25,23	-19,62	19,47	25,83	-19,02	20,07	29,13	-15,72	23,37	26,73	-18,12	20,97
120	31,16	-22,79	22,83	31,76	-22,19	23,43	35,06	-18,89	26,73	32,66	-21,29	24,33

Figure 12.3 a: Subject 1 ($\gamma = 90$ degrees) – observer 1

β	Test 1			Test 2			Test 3			Mean		
	α_r	α_t	α_a	α_r	α_t	α_a	α_r	α_t	α_a	α_r	α_t	α_a
0	0.00	0,00	0,00	0,00	0,00	0,00	0,00	0,00	0,00	0,00	0,00	0,00
10	0,44	0,93	0,27	0,23	0,72	0,06	0,20	0,69	0,03	0,29	0,78	0,12
20	1,59	1,72	0,74	1.38	1.51	0,53	1,35	1,48	0,50	1,44	1,57	0.59
30	2,35	0,70	1,21	2,14	0,49	1,00	2,11	0,46	0,97	2,20	0,55	1,06
40	3,62	-2,31	1,29	4,62	-1,31	2,29	4,42	-1,51	2,09	4,22	-1,71	1,89
50	4,49	-3,94	1,64	5,49	-2,94	2,64	5,29	-3,14	2,44	5,09	-3,34	2,24
60	7,30	-6,14	2,70	8,30	-5,14	3,70	8,10	-5,34	3,50	7,90	-5,54	3,30
70	12,83	-6,24	8,10	10,33	-8,74	5,60	10,83	-8,24	6,10	11,33	-7,74	6,60
80	15,97	-8,03	10,34	13,47	-10,53	7,84	13,97	-10,03	8,34	14,47	-9,53	8,84
90	20,83	-10,82	14,23	18,33	-13,32	11,73	18,83	-12,82	12,23	19,33	-12,32	12,73
100	25,77	-14,21	19,17	23,27	-16,71	16,67	23,77	-16,21	17,17	24,27	-15,71	17,67
110	27,79	-20,59	20,47	28,39	-19,99	21,07	31,69	-16,69	24,37	29,29	-19,09	21,97
120	32,60	-23,76	24,13	33,20	-23,16	24,73	36,50	-19,86	28,03	34,10	-22,26	25,63

Figure 12.3 b: Subject 1 (γ = 90 degrees) – observer 2

β	Test 1			Test 2			Test 3			Mean		
	α_r	α_t	α_a	α_r	α_t	α_a	α_r	α_t	α_a	α_r	α_t	α_a
0	0,00	0,00	0,00	0,00	0,00	0,00	0,00	0,00	0,00	0,00	0,00	0,00
10	1,10	-1,40	0,46	1,90	-0,60	1,26	2,10	-0,40	1,46	1,70	-0,80	1,06
20	3,24	-2,29	1,83	4,04	-1,49	2,63	4,24	-1,29	2,83	3,84	-1,69	2,43
30	7,45	-3,28	5,20	5,65	-3,48	3,40	5,95	-1,58	3,70	6,35	-2,78	4,10
40	6,94	-5,87	4,12	8,54	-4,27	5,72	8,94	-3,87	6,12	8,14	-4,67	5,32
50	9,35	-7,15	6,05	10,95	-5,55	7,65	11,35	-5,15	8,05	10,55	-5,95	7,25
60	11,66	-9,13	8,60	13,26	-7,53	10,20	13,66	-7,13	10,60	12,86	-7,93	9,80
70	12,56	-11,79	10,81	15,96	-8,39	14,21	15,46	-8,89	13,71	14,66	-9,69	12,91
80	15,15	-13,87	12,48	18,55	-10,47	15,88	18,05	-10,97	15,38	17,25	-11,77	14,58
90	18,15	-16,24	14,77	21,55	-12,84	18,17	21,05	-13,34	17,67	20,25	-14,14	16,87
100	20,01	-18,72	17,01	23,41	-15,32	20,41	22,91	-15,82	19,91	22,11	-16,62	19,11
110	23,57	-20,56	20,46	25,57	-18,56	22,46	25,47	-18,66	22,36	24,97	-19,16	21,86
120	25,77	-23,75	21,68	27,77	-21,75	23,68	27,67	-21,85	23,88	27,17	-22,35	23,08

Figure 12.4 a: Subject 2 (γ = 0 degrees) – observer 1

β	Test 1			Test 2			Test 3			Mean		
	α_r	α_t	α_a	α_r	α_t	α_a	α_r	α_t	α_a	α_r	α_t	α_a
0	0,00	0,00	0,00	0,00	0,00	0,00	0,00	0,00	0,00	0,00	0,00	0,00
10	0,52	-1,30	-0,12	1,32	-0,50	0,68	1,52	-0,30	0,88	1,12	-0,70	0,48
20	3,41	-2,30	2,17	4,21	-1,50	2,97	4,41	-1,30	3,17	4,01	-1,70	2,77
30	7,62	-3,78	5,34	5,82	-3,98	3,54	6,12	-2,08	3,84	6,52	-3,28	4,24
40	7,80	-5,97	5,17	9,40	-4,37	6,77	9,80	-3,97	7,17	9,00	-4,77	6,37
50	10,47	-7,15	7,47	12,07	-5,55	9,07	12,47	-5,15	9,47	11,67	-5,95	8,67
60	11,97	-8,32	10,66	13,57	-6,72	12,26	13,97	-6,32	12,66	13,17	-7,12	11,86
70	13,77	-11,21	11,52	17,17	-7,81	14,92	16,67	-8,31	14,42	15,87	-9,11	13,62
80	15,22	-13,70	12,41	18,62	-10,30	15,81	18,12	-10,80	15,31	17,32	-11,60	14,51
90	16,93	-16,38	13,20	20,33	-12,98	16,60	19,83	-13,48	16,10	19,03	-14,28	15,30
100	18,65	-18,76	15,24	22,05	-15,36	18,64	21,55	-15,86	18,14	20,75	-16,66	17,34
110	21,69	-21,08	17,84	23,69	-19,08	19,84	23,59	-19,18	19,74	23,09	-19,68	19,24
120	24,39	-23,47	19,46	26,39	-21,47	21,46	26,29	-21,57	21,36	25,79	-22,07	20,86

Figure 12.4 b: Subject 2 (γ = 0 degrees) – observer 2

β	Test 1			Test 2			Test 3			Mean		
	α_r	α_t	α_a	α_r	α_t	α_a	α_r	α_t	α_a	α_r	α_t	α_a
0	0,00	0,00	0,00	0,00	0,00	0,00	0,00	0,00	0,00	0,00	0,00	0,00
10	0,19	-0,39	0,05	0,49	-0,09	0,35	0,46	-0,12	0,32	0,38	-0,20	0,24
20	0,58	-1,05	0,40	0,88	-0,75	0,70	0,85	-0,78	0,67	0,77	-0,86	0,59
30	1,12	-1,58	1,11	1,42	-1,28	1,41	1,39	-1,31	1,38	1,31	-1,39	1,30
40	2,99	-1,99	2,05	2,04	-2,94	1,50	2,14	-2,84	1,40	2,39	-2,59	1,65
50	5,50	-2,98	3,19	4,55	-3,93	2,24	4,65	-3,83	2,34	4,90	-3,58	2,59
60	7,41	-4,27	5,08	6,46	-5,22	4,13	6,56	-5,12	4,23	6,81	-4,87	4,48
70	11,41	-4,60	8,32	8,71	-7,30	5,62	8,86	-7,15	5,77	9,66	-6,35	6.57
80	14,08	-6,19	10,53	11,38	-8,89	7,83	11,53	-8,74	7,98	12,33	-7,94	8,78
90	17,35	-7,98	13,01	14,65	-10,68	10,31	14,80	-10,53	10,46	15,60	-9,73	11,26
100	19,88	-10,56	15,31	17,18	-13,26	12,61	17,33	-13,11	12,76	18,13	-12,31	13,56
110	23,49	-13,26	19,51	19,39	-17,36	15,41	20,09	-16,66	16,11	20,99	-15,76	17,01
120	26,08	-16,75	23,25	21,98	-20,85	19,15	22,68	-20,15	19,85	23,58	-19,25	20,75

Figure 12.5 a: Subject 2 (γ = 45 degrees) – observer 1

β	Test 1			Test 2			Test 3			Mean		
	α_r	α_t	α_a	α_r	α_t	α_a	α_r	α_t	α_a	α_r	α_t	α_a
0	0,00	0,00	0,00	0,00	0,00	0,00	0,00	0,00	0,00	0,00	0,00	0,00
10	0,07	-0,39	-0,19	0,37	-0,09	0,11	0,34	-0,12	0,08	0,26	-0,20	0,00
20	1,13	-1,39	0,64	1,43	-1,09	0,94	1,40	-1,12	0,91	1,32	-1,20	0,83
30	1,37	-2,39	1,11	1,67	-2,09	1,41	1,64	-2,12	1,38	1,56	-2,20	1,30
40	3,74	-2,37	2,52	2,79	-3,32	1,97	2,89	-3,22	1,87	3,14	-2,97	2,12
50	5,70	-3,60	3,78	4,75	-4,55	2,83	4,85	-4,45	2,93	5,10	-4,20	3,18
60	6,70	-4,75	4,73	5,75	-5,70	3,78	5,85	-5,60	3,88	6,10	-5,35	4,13
70	11,63	-5,68	8,06	8,93	-8,38	5,36	9,08	-8,23	5,51	9,88	-7,43	6,31
80	14,04	-7,97	9,77	11,34	-10,67	7,07	11,49	-10,52	7,22	12,29	-9,72	8,02
90	17,07	-9,76	12,36	14,37	-12,46	9,66	14,52	-12,31	9,81	15,32	-11,51	10,61
100	20,29	-11,92	14,43	17,59	-14,62	11,73	17,74	-14,47	11,88	18,54	-13,67	12,68
110	24,27	-14,29	20,06	20,17	-18,39	15,96	20,87	-17,69	16,66	21,77	-16,79	17,56
120	26,51	-16,98	23,90	22,41	-21,08	19,80	23,11	-20,38	20,50	24,01	-19,48	21,40

Figure 12.5 b: Subject 2 ($\gamma = 45$ degrees) – observer 2

β	Test 1			Test 2			Test 3			Mean		
	α_r	α_t	α_a	α_r	α_t	α_a	α_r	α_t	α_a	α_r	α_t	α_a
0	0,00	0,00	0,00	0,00	0,00	0,00	0,00	0,00	0,00	0,00	0,00	0,00
10	0,19	0,20	0,04	0,54	0,55	0,39	0,44	0,45	0,29	0,39	0,40	0,24
20	0,92	0,80	0,24	1,27	1,15	0,59	1,17	1,05	0,49	1,12	1,00	0,44
30	1,92	0,90	0,94	2,04	1,02	1,06	0,90	-0,12	-0,08	1,62	0,60	0,64
40	2,88	0,30	1,42	3,00	0,42	1,54	1,86	-0,72	0,40	2,58	0,00	1,12
50	3,95	-0,29	2,54	4,07	-0,17	2,66	2,93	-1,31	1,52	3,65	-0,59	2,24
60	6,85	-0,39	5,54	4,30	-2,94	2,99	4,60	-2,64	3,29	5,25	-1,99	3,94
70	9,34	-1,80	6,90	6,79	-4,35	4,35	7,09	-4,05	4,65	7,74	-3,40	5,30
80	10,61	-3,48	9,26	8,06	-6,03	6,71	8,36	-5,73	7,01	9,01	-5,08	7,66
90	13,26	-5,28	10,63	10,71	-7,83	8,08	11,01	-7,53	8,38	11,66	-6,88	9,03
100	16,64	-7,93	13,03	13,68	-10,89	10,07	13,58	-10,99	9,97	14,60	-9,97	10,99
110	19,21	-10,52	15,12	16,25	-13,48	12,16	16,15	-13,58	12,06	17,17	-12,56	13,08
120	23,61	-13,61	18,90	20,65	-16,57	15,94	20,55	-16,67	15,84	21,57	-15,65	16,86

Figure 12.6 a: Subject 2 ($\gamma = 90$ degrees) – observer 1

β	Test 1			Test 2			Test 3			Mean		
	α_r	α_t	α_a	α_r	α_t	α_a	α_r	α_t	α_a	α_r	α_t	α_a
0	0,00	0,00	0,00	0,00	0,00	0,00	0,00	0,00	0,00	0,00	0,00	0,00
10	1,05	0,79	0,74	1,40	1,14	1,09	1,30	1,04	0,99	1,25	0,99	0,94
20	1,92	0,20	0,98	2,27	0,55	1,33	2,17	0,45	1,23	2,12	0,40	1,18
30	3,36	0,50	2,13	3,48	0,62	2,25	2,34	-0,52	1,11	3,06	0,20	1,83
40	4,49	-0,49	2,62	4,61	-0,37	2,74	3,47	-1,51	1,60	4,19	-0,79	2,32
50	5,92	-0,69	4,01	6,04	-0,57	4,13	4,90	-1,71	2,99	5,62	-0,99	3,71
60	8,43	0,01	6,37	5,88	-2,54	3,82	6,18	-2,24	4,12	6,83	-1,59	4,77
70	9,82	-0,60	8,02	7,27	-3,15	5,47	7,57	-2,85	5,77	8,22	-2,20	6,42
80	12,49	-3,90	9,97	9,94	-6,45	7,42	10,24	-6,15	7,72	10,89	-5,50	8,37
90	14,55	-5,69	11,56	12,00	-8,24	9,01	12,30	-7,94	9,31	12,95	-7,29	9,96
100	17,30	-8,44	13,59	14,34	-11,40	10,63	14,24	-11,50	10,53	15,26	-10,48	11,55
110	20,87	-11,55	16,19	17,91	-14,51	13,23	17,81	-14,61	13,13	18,83	-13,59	14,15
120	24,85	-14,63	19,37	21,89	-17,59	16,42	21,79	-17,69	16,32	22,81	-16,67	17,33

Figure 12.6 b: Subject 2 (γ = 90 degrees) – observer 2

β	Test 1			Test 2			Test 3			Mean		
	α_r	α_t	α_a	α_r	α_t	α_a	α_r	α_t	α_a	α_r	α_t	α_a
0	0,00	0,00	0,00	0,00	0,00	0,00	0,00	0,00	0,00	0,00	0,00	0,00
10	2,41	-1,69	0,60	3,57	-0,53	1,76	3,35	-0,75	1,54	3,11	-0,99	1,30
20	5,73	-2,49	2,13	6,89	-1,33	3,29	6,67	-1,55	3,07	6,43	-1,79	2,83
30	7,39	-3,68	4,02	8,55	-2,52	5,18	8,33	-2,74	4,96	8,09	-2,98	4,72
40	11,30	-4,89	7,20	12,46	-3,73	8,36	12,24	-3,95	8,14	12,00	-4,19	7,90
50	16,83	-4,94	10,96	14,61	-7,16	8,74	16,59	-5,18	10,72	16,01	-5,76	10,14
60	22,02	-6,56	13,43	19,80	-8,78	11,21	21,78	-6,80	13,19	21,20	-7,38	12,61
70	27,49	-9,15	15,79	25,27	-11,37	13,57	27,25	-9,39	15,55	26,67	-9,97	14,97
80	31,96	-10,55	17,92	27,94	-14,57	13,90	32,08	-10,43	18,04	30,66	-11,85	16,62
90	36,77	-12,63	20,28	32,75	-16,65	16,26	36,89	-12,51	20,40	35,47	-13,93	18,98
100	40,46	-14,85	22,40	36,44	-18,87	18,38	40,58	-14,73	22,52	39,16	-16,15	21,10
110	49,28	-16,62	26,47	44,16	-21,74	21,35	48,19	-17,71	25,38	47,21	-18,69	24,40
120	54,04	-19,22	28,71	48,92	-24,34	23,59	52,95	-20,31	27,62	51,97	-21,29	26,64

Figure 12.7 a: Subject 3 (γ = 0 degrees) – observer 1

β	Test 1			Test 2			Test 3			Mean		
	α_r	α_t	α_a	α_r	α_t	α_a	α_r	α_t	α_a	α_r	α_t	α_a
0	0,00	0,00	0,00	0,00	0,00	0,00	0,00	0,00	0,00	0,00	0,00	0,00
10	4,46	-1,29	1,19	5,62	-0,13	2,35	5,40	-0,35	2,13	5,16	-0,59	1,89
20	6,91	-2,29	2,72	8,07	-1,13	3,88	7,85	-1,35	3,66	7,61	-1,59	3,42
30	9,91	-3,40	4,60	11,07	-2,24	5,76	10,85	-2,46	5,54	10,61	-2,70	5,30
40	13,01	-4,69	6,84	14,17	-3,53	8,00	13,95	-3,75	7,78	13,71	-3,99	7,54
50	15,96	-3,97	10,49	13,74	-6,19	8,27	15,72	-4,21	10,25	15,14	-4,79	9,67
60	21,22	-5,37	13,32	19,00	-7,59	11,10	20,98	-5,61	13,08	20,40	-6,19	12,50
70	25,14	-7,36	15,32	22,92	-9,58	13,10	24,90	-7,60	15,08	24,32	-8,18	14,50
80	31,90	-9,06	18,39	27,88	-13,08	14,37	32,02	-8,94	18,51	30,60	-10,36	17,09
90	35,58	-11,44	20,40	31,56	-15,46	16,38	35,70	-11,32	20,52	34,28	-12,74	19,10
100	39,37	-13,67	22,40	35,35	-17,69	18,38	39,49	-13,55	22,52	38,07	-14,97	21,10
110	44,65	-15,63	25,17	39,53	-20,75	20,05	43,56	-16,72	24,08	42,58	-17,70	23,10
120	53,50	-18,43	29,42	48,38	-23,55	24,30	52,41	-19,52	28,33	51,43	-20,50	27,35

Figure 12.7 b: Subject 3 ($\gamma = 0$ degrees) – observer 2

β	Test 1			Test 2			Test 3			Mean		
	α_r	α_t	α_a	α_r	α_t	α_a	α_r	α_t	α_a	α_r	α_t	α_a
0	0,00	0,00	0,00	0,00	0,00	0,00	0,00	0,00	0,00	0,00	0,00	0,00
10	0,93	0,27	0,58	1,37	0,71	1,02	0,88	0,22	0,53	1,06	0,40	0,71
20	5,21	-0,92	2,46	5,65	-0,48	2,90	5,16	-0,97	2,41	5,34	-0,79	2,59
30	7,72	-1,21	4,94	7,34	-1,59	4,56	5,67	-3,26	2,89	6,91	-2,02	4.13
40	10,73	-2,59	6,35	10,35	-2,97	5,97	8,68	-4,64	4,30	9,92	-3,40	5,54
50	13,47	-3,98	8,94	13,09	-4,36	8,56	11,42	-6,03	6,89	12,66	-4,79	8,13
60	18,67	-4,80	12,45	17,96	-5,51	11,74	15,27	-8,20	9,05	17,30	-6,17	11,08
70	23,26	-6,57	15,52	22,55	-7,28	14,81	19,86	-9,97	12,12	21,89	-7,94	14,15
80	28,84	-8,17	19,05	28,13	-8,88	18,34	25,44	-11,57	15,65	27,47	-9,54	17,68
90	31,72	-10,12	21,65	31,01	-10,83	20,94	28,32	-13,52	18,25	30,35	-11,49	20,28
100	38,73	-11,89	25,30	38,32	-12,30	24,89	33,98	-16,64	20,55	37,01	-13,61	23,58
110	45,67	-14,37	28,71	45,26	-14,78	28,30	40,92	-19,12	23,96	43,95	-16,09	26,99
120	53,82	-17,74	29,07	53,41	-18,15	28,66	49,07	-22,49	24,32	52,10	-19,46	27,35

Figure 12.8 a: Subject 3 ($\gamma = 45$ degrees) – observer 1

β	Test 1			Test 2			Test 3			Mean		
	α_r	α_t	α_a	α_r	α_t	α_a	α_r	α_t	α_a	α_r	α_t	α_a
0	0,00	0,00	0,00	0,00	0,00	0,00	0,00	0.00	0,00	0,00	0,00	0,00
10	0,81	0,46	0,70	1,25	0,90	1,14	0,76	0,41	0,65	0,94	0,59	0,83
20	5,01	-0,33	2,23	5.45	0.11	2,67	4,96	-0,38	2,18	5,14	-0,20	2,36
30	7,84	-0,31	4,82	7,46	-0,69	4,44	5,79	-2,36	2,77	7,03	-1,12	4,01
40	8,31	-1,17	6,11	7,93	-1,55	5,73	6,26	-3,22	4,06	7,50	-1,98	5,30
50	13,50	-2,55	8,47	13,12	-2,93	8,09	11,45	-4,60	6,42	12,69	-3,36	7,66
60	17,92	-2,98	11,86	17,21	-3,69	11,15	14,52	-6,38	8,46	16,55	-4,35	10,49
70	24,02	-3,97	16,10	23,31	-4,68	15,39	20,62	-7,37	12,70	22,65	-5,34	14,73
80	30,11	-5,75	19,64	29,40	-6,46	18,93	26,71	-9,15	16,24	28,74	-7,12	18,27
90	35,18	-8,08	22,94	34,47	-8,79	22,23	31,78	-11,48	19,54	33,81	-9,45	21,57
100	41,25	-9,62	26,24	40,84	-10,03	25,83	36,50	-14,37	21,49	39,53	-11,34	24,52
110	46,08	-12,40	28,83	45,67	-12,81	28,42	41,33	-17,15	24,08	44,36	-14,12	27,11
120	52,77	-15,73	29,51	52,36	-16,14	29,10	48,02	-20,48	24,76	51,05	-17,45	27,79

Figure 12.8 b: Subject 3 ($\gamma = 45$ degrees) – observer 2

β	Test 1			Test 2			Test 3			Mean		
	α_r	α_t	α_a	α_r	α_t	α_a	α_r	α_t	α_a	α_r	α_t	α_a
0	0,00	0,00	0,00	0,00	0,00	0,00	0,00	0,00	0,00	0,00	0,00	0,00
10	0,42	1,40	0,45	0,08	1,06	0,11	0,13	1,11	0,16	0,21	1,19	0,24
20	1,24	2,20	1,39	0,90	1,86	1,05	0,95	1,91	1,10	1,03	1,99	1,18
30	4,88	1,59	3,04	4,54	1,25	2,70	4,59	1,30	2,75	4,67	1,38	2,83
40	5,50	1,01	5,44	4,56	0,07	4,50	4,61	0,12	4,55	4,89	0,40	4,83
50	8,03	-0,97	7,33	7,09	-1,91	6,39	7,14	-1,86	6,44	7,42	-1,58	6,72
60	12,44	-2,84	9,57	11,50	-3,78	8,63	11,55	-3,73	8,68	11,83	-3,45	8,96
70	14,20	-6,90	10,03	14,95	-6,15	10,78	16,96	-4,14	12,79	15,37	-5,73	11,20
80	18,37	-8,98	13,45	19,12	-8,23	14,20	21,13	-6,22	16,21	19,54	-7,81	14,62
90	26,25	-11,15	16,98	27,00	-10,40	17,73	29,01	-8,39	19,74	27,42	-9,98	18,15
100	32,96	-14,57	19,19	36,61	-10,92	22,84	37,17	-10,36	23,40	35,58	-11,95	21,81
110	39,36	-17,35	22,13	43,01	-13,70	25,78	43,57	-13,14	26,34	41,98	-14,73	24,75
120	43,62	-20,23	24,02	47,27	-16,58	27,67	47,83	-16,02	28,23	46,24	-17,61	26,64

Figure 12.9 a: Subject 3 ($\gamma = 90$ degrees) – observer 1

β	Test 1			Test 2			Test 3			Mean		
	α_r	α_t	α_a	α_r	α_t	α_a	α_r	α_t	α_a	α_r	α_t	α_a
C	0,00	0,00	0,00	0,00	0,00	0,00	0,00	0,00	0,00	0,00	0,00	0,00
10	1,27	1,99	0,92	0.93	1,65	0,58	0,98	1,70	0,63	1,06	1,78	0,71
20	3,82	2.58	2,33	3.48	2,24	1,99	3.53	2,29	2,04	3,61	2,37	2,12
30	3,98	1,38	3,51	3,64	1,04	3,17	3,69	1,09	3,22	3,77	1,17	3,30
40	5,73	0,61	5,21	4,79	-0,33	4,27	4,84	-0,28	4,32	5,12	0,00	4,60
50	7,53	-1,96	6,50	6,59	-2,90	5,56	6,64	-2,85	5,61	6,92	-2,57	5,89
60	9,54	-3,54	8,04	8,60	-4,48	7,10	8,65	-4,43	7,15	8,93	-4,15	7,43
70	10,83	-6,91	8,50	11,58	-6,16	9,25	13,59	-4,15	11,26	12,00	-5,74	9,67
80	19,50	-8,15	13,68	20,25	-7,40	14,43	22,26	-5,39	16,44	20,67	-6,98	14,85
90	24,90	-10,19	17,34	25,65	-9,44	18,09	27,66	-7,43	20,10	26,07	-9,02	18,51
100	30,84	-14,19	19,66	34,49	-10,54	23,31	35,05	-9,98	23,87	33,46	-11,57	22,28
110	34,40	-16,77	21,78	38,05	-13,12	25,43	38,61	-12,56	25,99	37,02	-14,15	24,40
120	43,40	-21,36	24,96	47,05	-17,71	28,61	47,61	-17,15	29,17	46,02	-18,74	27,58

Figure 12.9 b: Subject 3 ($\gamma = 90$ degrees) – observer 2

β	Test 1			Test 2			Test 3			Mean		
	α_r	α_t	α_a	α_r	α_t	α_a	α_r	α_t	α_a	α_r	α_t	α_a
0	0,00	0,00	0,00	0,00	0,00	0,00	0,00	0,00	0,00	0,00	0,00	0,00
10	0,94	-0,32	0,13	2,86	-2,24	2,05	2,53	-1,91	1,72	2,11	-1,49	1,30
20	3,26	-1,92	1,66	5,18	-3,84	3,58	4,85	-3,51	3,25	4,43	-3,09	2,83
30	5,92	-3,31	3,55	7,84	-5,23	5,47	7,51	-4,90	5,14	7,09	-4,48	4,72
40	8,83	-5,02	6,73	10,75	-6,94	8,65	10,42	-6,61	8,32	10,00	-6,19	7,90
50	12,84	-6,79	8,97	14,76	-8,71	10,89	14,43	-8,38	10,56	14,01	-7,96	10,14
60	18,61	-9,97	13,02	19,15	-9,43	13,56	16,84	-11,74	11,25	18,20	-10,38	12,61
70	23,08	-12,56	15,38	23,62	-12,02	15,92	21,31	-14,33	13,61	22,67	-12,97	14,97
80	27,07	-15,74	17,03	27,61	-15,20	17,57	25,30	-17,51	15,26	26,66	-16,15	16,62
90	31,88	-19,52	19,39	32,42	-18,98	19,93	30,11	-21,29	17,62	31,47	-19,93	18,98
100	33,54	-23,76	19,48	37,59	-21,52	23,53	37,35	-21,16	23,29	36,16	-22,15	22,10
110	39,99	-28,30	23,78	44,04	-26,06	27,83	43,80	-25,70	27,59	42,61	-26,69	26,40
120	46,35	-31,90	26,02	50,40	-29,66	30,07	50,16	-29,30	29,83	48,97	-30,29	28,64

Figure 12.10 a: Subject 4 ($\gamma = 0$ degrees) – observer 1

β	Test 1			Test 2			Test 3			Mean		
	α_r	α_t	α_a	α_r	α_t	α_a	α_r	α_t	α_a	α_r	α_t	α_a
0	0,00	0,00	0,00	0,00	0.00	0,00	0,00	0,00	0,00	0,00	0,00	0,00
10	1,99	-0,42	0,72	3,91	-2,34	2,64	3,58	-2,01	2,31	3,16	-1,59	1,89
20	4,44	-2,42	2,25	6,36	-4,34	4,17	6,03	-4,01	3.84	5,61	-3,59	3,42
30	7,44	-3,83	5,13	9,36	-5,75	7,05	9,03	-5,42	6,72	8,61	-5,00	6,30
40	11,54	-5,52	6,37	13,46	-7,44	8,29	13,13	-7,11	7,96	12,71	-6,69	7,54
50	13,97	-7,62	10,50	15,89	-9,54	12,42	15,56	-9,21	12,09	15,14	-8,79	11,67
60	20,81	-10,78	13,91	21,35	-10,24	14,45	19,04	-12,55	12,14	20,40	-11,19	13,50
70	24,73	-13,77	15,91	25,27	-13,23	16,45	22,96	-15,54	14,14	24,32	-14,18	15,50
80	29,01	-16,95	17,50	29,55	-16,41	18,04	27,24	-18,72	15,73	28,60	-17,36	17,09
90	32,69	-21,03	20,41	33,23	-20,49	20,95	30,92	-22,80	18,64	32,28	-21,44	20,00
100	34,45	-26,58	18,48	38,50	-24,34	22,53	38,26	-23,98	22,29	37,07	-24,97	21,10
110	38,96	-30,31	21,48	43,01	-28,07	25,53	42,77	-27,71	25,29	41,58	-28,70	24,10
120	44,81	-33,71	24,73	48,86	-31,47	28,78	48,62	-31,11	28,54	47,43	-32,10	27,35

Figure 12.10 b: Subject 4 ($\gamma = 0$ degrees) – observer 2

β	Test 1			Test 2			Test 3			Mean		
	α_r	α_t	α_a	α_r	α_t	α_a	α_r	α_t	α_a	α_r	α_t	α_a
0	0,00	0,00	0,00	0,00	0,00	0,00	0,00	0,00	0,00	0,00	0,00	0,00
10	0,72	-2,13	0,37	1,94	-0,91	1,59	0,52	-2,33	0,17	1,06	-1,79	0,71
20	3,00	-3,33	2,25	4,22	-2,11	3,47	2,80	-3,53	2,05	3,34	-2,99	2,59
30	6,18	-4,31	4,80	4,53	-5,96	3,15	5,82	-4,67	4,44	5,51	-4,98	4,13
40	8,59	-5,90	6,21	6,94	-7,55	4,56	8,23	-6,26	5,85	7,92	-6,57	5,54
50	11,33	-7,68	8,80	9,68	-9,33	7,15	10,97	-8,04	8,44	10,66	-8,35	8,13
60	12,88	-11,37	9,66	13,91	-10,34	10,69	16,11	-8,14	12,89	14,30	-9,95	11,08
70	18,47	-14,35	11,73	19,50	-13,32	12,76	21,70	-11,12	14,96	19,89	-12,93	13,15
80	24,05	-17,53	15,15	25,08	-16,50	16,18	27,28	-14,30	18,38	25,47	-16,11	16,57
90	27,93	-20,42	17,86	28,96	-19,39	18,89	31,16	-17,19	21,09	29,35	-19,00	19,28
100	32,67	-24,42	21,84	36,67	-20,42	25,84	35,69	-21,40	24,86	35,01	-22,08	24,18
110	38,61	-27,81	25,65	42,61	-23,81	29,65	41,63	-24,79	28,67	40,95	-25,47	27,99
120	44,76	-31,99	30,61	48,76	-27,99	34,61	47,78	-28,97	33,63	47,10	-29,65	32,95

Figure 12.11 a: Subject 4 ($\gamma = 45$ degrees) – observer 1

β	Test 1			Test 2			Test 3			Mean		
	α_r	α_t	α_a	α_r	α_t	α_a	α_r	α_t	α_a	α_r	α_t	α_a
0	0,00	0,00	0,00	0,00	0,00	0,00	0,00	0,00	0,00	0,00	0,00	0,00
10	1,60	-0.94	0,49	2,82	0,28	1,71	1.40	-1,14	0,29	1,94	-0,60	0,83
20	3,80	-1,94	2.02	5,02	-0,72	3.24	3,60	-2,14	1,82	4,14	-1,50	2,36
30	7,70	-2,12	4,68	6,05	-3,77	3,03	7,34	-2,48	4,32	7,03	-2,79	4,01
40	10,17	-3,70	6,97	8,52	-5,35	5,32	9,81	-4,06	6,61	9,50	-4,37	6,30
50	13,36	-6,10	9,33	11,71	-7,75	7,68	13,00	-6,46	8,97	12,69	-6,77	8,66
60	15,13	-10,67	9,07	16,16	-9,64	10,10	18,36	-7,44	12,30	16,55	-9,25	10,49
70	21,23	-13,25	13,31	22,26	-12,22	14,34	24,46	-10,02	16,54	22,65	-11,83	14,73
80	26,32	-16,14	16,85	27,35	-15,11	17,88	29,55	-12,91	20,08	27,74	-14,72	18,27
90	30,39	-20,32	20,15	31,42	-19,29	21,18	33,62	-17,09	23,38	31,81	-18,90	21,57
100	35,19	-24,73	24,18	39,19	-20,73	28,18	38,21	-21,71	27,20	37,53	-22,39	26,52
110	41,02	-28,41	27,77	45,02	-24,41	31,77	44,04	-25,39	30,79	43,36	-26,07	30,11
120	46,71	-33,19	32,14	50,71	-29,19	36,14	49,73	-30,17	35,16	49,05	-30,85	34,48

Figure 12.11 b: Subject 4 (γ = 45 degrees) – observer 2

β	Test 1			Test 2			Test 3			Mean		
	α_r	α_t	α_a	α_r	α_t	α_a	α_r	α_t	α_a	α_r	α_t	α_a
0	0,00	0,00	0,00	0,00	0,00	0,00	0,00	0,00	0,00	0,00	0,00	0,00
10	0,58	0,74	0,09	1,30	1,46	0,81	1,21	1,37	0,72	1,03	1,19	0,54
20	2,22	1,54	0,73	2,94	2,26	1,45	2,85	2,17	1,36	2,67	1,99	1,18
30	3,44	0,93	2,38	4,16	1,65	3,19	4.07	1,56	3,01	3,89	1,38	2,83
40	5,97	-0,05	3,58	6,69	0,67	4,30	6,60	0,58	4,21	6,42	0,40	4,03
50	8,01	-1,11	4,25	10,41	-3,51	6,65	10,02	-2,04	6,26	9,48	-2,58	5,72
60	11,58	-2,98	6,49	13,98	-5,38	8,89	13,59	-3,91	8,50	13,05	-4,45	7,96
70	15,07	-6,26	8,73	17,47	-8,66	11,13	17,08	-7,19	10,74	16,54	-7,73	10,20
80	18,95	-9,34	12,15	21,35	-11,74	14,55	20,96	-10,27	14,16	20,42	-10,81	13,62
90	24,35	-16,21	14,92	28,24	-12,32	18,81	27,35	-13,21	17,92	26,58	-13,98	17,15
100	29,56	-20,18	18,58	33,45	-16,29	22,47	32,56	-17,18	21,58	31,79	-17,95	20,81
110	37,75	-24,96	21,52	41,64	-21,07	25,41	40,75	-21,96	24,52	39,98	-22,73	23,75
120	42,01	-29,84	24,41	45,90	-25,95	28,30	45,01	-26,84	27,41	44,24	-27,61	26,64

Figure 12.12 a: Subject 4 (γ = 90 degrees) – observer 1

β	Test 1			Test 2			Test 3			Mean		
	α_r	α_t	α_a	α_r	α_t	α_a	α_r	α_t	α_a	α_r	α_t	α_a
0	0.00	0,00	0,00	0,00	0,00	0,00	0,00	0,00	0,00	0,00	0,00	0,00
10	0,91	1,33	0,26	1,63	2,05	0,98	1,54	1,96	0,89	1,36	1,78	0,71
20	3,16	1,92	1,67	3.88	2,64	2,39	3,79	2,55	2,30	3,61	2,37	2,12
30	4,32	0,72	2,85	5,04	1,44	3,57	4,95	1,35	3,48	4,77	1,17	3,30
40	5,67	-0,45	4,55	6,39	0,27	5,27	6,30	0,18	5,18	6,12	0,00	5,00
50	6,45	-1,41	5,42	8,85	-3,81	7,82	8,46	-2,34	7,43	7,92	-2,88	6,89
60	9,46	-4,48	6,96	11,86	-6,88	9,36	11,47	-5,41	8,97	10,93	-5,95	8,43
70	12,53	-7,27	9,80	14,93	-9,67	12,20	14,54	-8,20	11,81	14,00	-8,74	11,27
80	17,20	-9,51	13,38	19,60	-11,91	15,78	19,21	-10,44	15,39	18,67	-10,98	14,85
90	21,84	-16,25	16,28	25,73	-12,36	20,17	24,84	-13,25	19,28	24,07	-14,02	18,51
100	28,23	-20,80	20,05	32,12	-16,91	23,94	31,23	-17,80	23,05	30,46	-18,57	22,28
110	34,79	-25,38	22,17	38,68	-21,49	26,06	37,79	-22,38	25,17	37,02	-23,15	24,40
120	41,79	-30,97	24,65	45,68	-27,08	28,54	44,79	-27,97	27,65	44,02	-28,74	26,88

Figure 12.12 b: Subject 4 ($\gamma = 90$ degrees) – observer 2

β	Test 1			Test 2			Test 3			Mean		
	α_r	α_t	α_a	α_r	α_t	α_a	α_r	α_t	α_a	α_r	α_t	α_a
0	0,00	0,00	0,00	0,00	0,00	0,00	0,00	0,00	0,00	0,00	0,00	0,00
10	1,39	-0,60	0,75	1,88	-0,11	1,24	1,83	-0,16	1,19	1,70	-0,29	1,06
20	3,53	-1,10	2,12	4,02	-0.61	2,61	3,97	-0,66	2,56	3,84	-0,79	2,43
30	6,04	-1,69	3,79	6,53	-1,20	4,28	6,48	-1,25	4,23	6,35	-1,38	4,10
40	8,41	-1,73	5,59	8,06	-2,08	5,24	7,95	-2,19	5,13	8,14	-2,00	5,32
50	10,82	-2,31	7,52	10,47	-2,66	7,17	10,36	-2,77	7,06	10,55	-2,58	7,25
60	11,53	-4,78	7,47	13,60	-2,71	9,54	13,45	-2,86	9,39	12,86	-3,45	8,80
70	13,33	-7,06	9,18	15,40	-4,99	11,25	15,25	-5,14	11,10	14,66	-5,73	10,51
80	15,92	-9,14	10,25	17,99	-7,07	12,32	17,84	-7,22	12,17	17,25	-7,81	11,58
90	17,92	-11,31	12,54	19,99	-9,24	14,61	19,84	-9,39	14,46	19,25	-9,98	13,87
100	18,43	-14,63	13,43	22,62	-10,44	17,62	22,28	-10,78	17,28	21,11	-11,95	16,11
110	20,29	-17,41	16,18	24,48	-13,22	20,37	24,14	-13,56	20,03	22,97	-14,73	18,86
120	22,49	-18,29	18,40	26,68	-14,10	22,59	26,34	-14,44	22,25	25,17	-15,61	21,08

Figure 12.13 a: Subject 5 ($\gamma = 0$ degrees) – observer 1

β	Test 1			Test 2			Test 3			Mean		
	α_r	α_t	α_a	α_r	α_t	α_a	α_r	α_t	α_a	α_r	α_t	α_a
0	0,00	0,00	0,00	0,00	0,00	0,00	0,00	0,00	0,00	0,00	0,00	0,00
10	0,81	-0,79	0,17	1,30	-0,30	0,66	1,25	-0,35	0,61	1,12	-0,48	0,48
20	3,70	-1,28	2,46	4,19	-0,79	2,95	4,14	-0,84	2,90	4,01	-0,97	2,77
30	6,21	-1,48	3,93	6,70	-0,99	4,42	6,65	-1,04	4,37	6,52	-1,17	4,24
40	9,27	-1,72	6,64	8,92	-2,07	6,29	8,81	-2,18	6,18	9,00	-1,99	6,37
50	11,94	-2,61	8,94	11,59	-2,96	8,59	11,48	-3,07	8,48	11,67	-2,88	8,67
60	11,84	-5,28	9,53	13,91	-3,21	11,60	13,76	-3,36	11,45	13,17	-3,95	10,86
70	14,54	-8,07	11,29	16,61	-6,00	13,36	16,46	-6,15	13,21	15,87	-6,74	12,62
80	15,99	-8,31	13,18	18,06	-6,24	15,25	17,91	-6,39	15,10	17,32	-6,98	14,51
90	17,70	-10,35	13,97	19,77	-8,28	16,04	19,62	-8,43	15,89	19,03	-9,02	15,30
100	19,07	-14,25	14,16	23,26	-10,06	18,35	22,92	-10,40	18,01	21,75	-11,57	16,84
110	21,41	-16,83	15,56	25,60	-12,64	19,75	25,26	-12,98	19,41	24,09	-14,15	18,24
120	24,21	-19,42	17,48	28,40	-15,23	21,67	28,06	-15,57	21,33	26,89	-16,74	20,16

Figure 12.13 b: Subject 5 ($\gamma = 0$ degrees) – observer 2

β	Test 1			Test 2			Test 3			Mean		
	α_r	α_t	α_a	α_r	α_t	α_a	α_r	α_t	α_a	α_r	α_t	α_a
0	0,00	0,00	0,00	0,00	0,00	0,00	0,00	0,00	0,00	0,00	0,00	0,00
10	0,54	-0,04	0,40	0,33	-0,25	0,19	0,27	-0,31	0,13	0,38	-0,20	0,24
20	0,93	-0,70	0,75	0,72	-0,91	0,54	0,66	-0,97	0,48	0,77	-0,86	0,59
30	1,04	-1,66	1,03	1,70	-1,00	1,69	1,43	-1,27	1,42	1,31	-1,39	1,30
40	2,12	-2,86	1,38	2,78	-2,20	2,04	2,51	-2,47	1,77	2,39	-2,59	1,65
50	4,63	-3,85	2,32	5,29	-3,19	2,98	5,02	-3,46	2,71	4,90	-3,58	2,59
60	5,78	-6,90	3,45	7,50	-5,18	5,17	7,15	-5,53	4,82	6,81	-5,87	4,48
70	8,63	-7,38	5,54	10,35	-5,66	7,26	10,00	-6,01	6,91	9,66	-6,35	6,57
80	11,30	-9,97	7,75	13,02	-8,25	9,47	12,67	-8,60	9,12	12,33	-8,94	8,78
90	13,44	-12,89	9,10	16,93	-9,40	12,59	16,43	-9,90	12,09	15,60	-10,73	11,26
100	15,97	-13,97	10,40	19,46	-10,48	13,89	18,96	-10,98	13,39	18,13	-11,81	12,56
110	18,83	-15,41	12,85	22,32	-11,92	16,34	21,82	-12,42	15,84	20,99	-13,25	15,01
120	19,92	-17,92	15,59	23,41	-14,43	19,08	22,91	-14,93	18,58	22,08	-15,76	17,75

Figure 12.14 a: Subject 5 ($\gamma = 45$ degrees) – observer 1

β	Test 1			Test 2			Test 3			Mean		
	α_r	α_t	α_a	α_r	α_t	α_a	α_r	α_t	α_a	α_r	α_t	α_a
0	0,00	0,00	0,00	0,00	0,00	0,00	0,00	0,00	0,00	0,00	0,00	0 00
10	0,42	-0,04	0,29	0,21	-0,25	0,08	0,15	-0,31	0,02	0,26	-0,20	0.13
20	1,48	-1,04	0,99	1,27	-1,25	0,78	1,21	-1,31	0,72	1,32	-1,20	0,83
30	1,29	-2,47	1,03	1,95	-1,81	1,69	1,68	-2,08	1,42	1,56	-2,20	1,30
40	3,57	-4,24	1,85	4,23	-3,58	2,51	3,96	-3,85	2,24	3,84	-3,97	2,12
50	4,83	-5,47	2,91	5,49	-4,81	3,57	5,22	-5,08	3,30	5,10	-5,20	3,18
60	6,07	-7,38	3,10	7,79	-5,66	4,82	7,44	-6,01	4,47	7,10	-6,35	4,13
70	8,85	-8,46	4,28	10,57	-6,74	6,00	10,22	-7,09	5,65	9,88	-7,43	5,31
80	11,26	-10,75	5,99	12,98	-9,03	7,71	12,63	-9,38	7,36	12,29	-9,72	7,02
90	13,16	-13,67	7,45	16,65	-10,18	10,94	16,15	-10,68	10,44	15,32	-11,51	9,61
100	17,38	-15,83	9,52	20,87	-12,34	13,01	20,37	-12.84	12,51	19,54	-13,67	11,68
110	19,61	-17,18	12,40	23,10	-13,69	15,89	22,60	-14,19	15,39	21,77	-15,02	14.56
120	21,31	-18,95	16,24	24,80	-15,46	19,73	24,30	-15,96	19,23	23,47	-16,79	18,40

Figure 12.14 b: Subject 5 ($\gamma = 45$ degrees) – observer 2

β	Test 1			Test 2			Test 3			Mean		
	α_r	α_t	α_a	α_r	α_t	α_a	α_r	α_t	α_a	α_r	α_t	α_a
0	0,00	0,00	0,00	0,00	0,00	0,00	0,00	0,00	0,00	0,00	0,00	0,00
10	0,52	0,22	0,17	1,14	0,84	0,79	1,01	0,71	0,66	0,89	0,59	0,54
20	1,25	0,42	1,07	1,87	1,04	1,69	1,74	0,91	1,56	1,62	0,79	1,44
30	1,29	0,92	1,87	1,97	1,54	2,49	1,77	1,41	2,36	1.62	1,29	2,24
40	3,81	0,72	3,35	3,09	0,00	2,63	3,84	0,75	3,38	3,58	0,49	3,12
50	4,88	-0,37	4,47	4,16	-1,09	3,75	4,91	-0,34	4,50	4,65	-0,60	4,24
60	4,99	-2,35	4,18	6,17	-1,17	5,36	6,09	-1,25	5,28	5,75	-1,59	4,94
70	7,98	-3,84	5,64	9,16	-2,66	6,82	9,08	-2,74	6,74	8,74	-3,08	6,40
80	9,25	-5,32	6,90	10,43	-4,14	8,08	10,35	-4,22	8,00	10,01	-4,56	7,66
90	11,45	-7,15	7,82	13,48	-5,12	9,85	13,05	-5,55	9,42	12,66	-5,94	9,03
100	12,99	-8,79	9,78	15,02	-6,76	11,81	14,59	-7,19	11,38	14,20	-7,58	10,99
110	15,26	-10,77	11,87	17,29	-8,74	13,90	16,86	-9,17	13,47	16,47	-9,56	13,08
120	18,36	-13,15	13,65	20,39	-11,12	15,68	19,96	-11,55	15,25	19,57	-11,94	14,86

Figure 12.15 a: Subject 5 ($\gamma = 90$ degrees) – observer 1

β	Test 1			Test 2			Test 3			Mean		
	α_r	α_t	α_a	α_r	α_t	α_a	α_r	α_t	α_a	α_r	α_t	α_a
0	0,00	0,00	0,00	0.00	0,00	0,00	0,00	0,00	0,00	0,00	0,00	0,00
10	0,88	0,23	0,57	1,50	0.85	1.19	1,37	0,72	1,06	1,25	0,60	0,94
20	1,75	1,42	0,81	2,37	2,04	1,43	2,24	1.91	1,30	2,12	1,79	1,18
30	2,73	0,32	1,46	3,41	0,94	2,08	3,21	0,81	1,95	3,06	0,69	1,83
40	4,42	-0,17	3,55	3,70	-0,89	2,83	4,45	-0,14	3,58	4,19	-0,40	3,32
50	5,85	-1,22	3,94	5,13	-1,94	3,22	5,88	-1,19	3,97	5,62	-1,45	3,71
60	6,07	-3,36	4,01	7,25	-2,18	5,19	7,17	-2,26	5,11	6,83	-2,60	4,77
70	8,46	-5,65	6,66	9,64	-4,47	7,84	9,56	-4,55	7,76	9,22	-4,89	7,42
80	10,13	-7,32	7,61	11,31	-6,14	8,79	11,23	-6,22	8,71	10,89	-6,56	8,37
90	11,74	-9,26	8,75	13,77	-7,23	10,78	13,34	-7,66	10,35	12,95	-8,05	9,96
100	14,05	-10,41	11,34	16,08	-8,38	13,37	15,65	-8,81	12,94	15,26	-9,20	12,55
110	17,62	-11,80	12,94	19,65	-9,77	14,97	19,22	-10,20	14,54	18,83	-10,59	14,15
120	19,60	-13,77	15,12	21,63	-11,74	17,15	21,20	-12,17	16,72	20,81	-12,56	16,33

Figure 12.15 b: Subject 5 ($\gamma = 90$ degrees) – observer 2

β	Test 1			Test 2			Test 3			Mean		
	α_r	α_t	α_a	α_r	α_t	α_a	α_r	α_t	α_a	α_r	α_t	α_a
0	0,00	0,00	0,00	0,00	0,00	0,00	0,00	0,00	0,00	0,00	0,00	0,00
10	0,24	-0,66	-0,02	0,59	-0,31	0,33	0,67	-0,23	0,41	0,50	-0.40	0,24
20	1,09	-1,05	0,45	1,44	-0,70	0,80	1,52	-0,62	0,88	1,35	-0,79	0,71
30	2,22	-2,28	1,10	2,57	-1,93	1,45	2,55	-1,85	1,53	2,48	-2,02	1,36
40	5,07	-2,43	3,56	3,48	-4,02	1,97	3,75	-3,75	2,24	4,10	-3,40	2,59
50	7,40	-3,82	4,51	5,81	-5,41	2,92	6,08	-5,14	3,19	6,43	-4,79	3,54
60	10,30	-5,20	6,51	8,71	-6,79	4,92	8,98	-6,52	5,19	9,33	-6,17	5,54
70	11,13	-9,17	6,20	12,77	-7,53	7,84	13,18	-7,12	8,25	12,36	-7,94	7,43
80	14,15	-10,77	8,32	15,79	-9,13	9,96	16,20	-8,72	10,37	15,38	-9,54	9,55
90	17,23	-12,32	9,91	18,87	-10,68	11,55	19,28	-10,27	11,96	18,46	-11,09	11,14
100	19,57	-15,08	10,64	22,67	-11,98	13,74	22,38	-12,27	13,45	21,54	-13,11	12,61
110	22,24	-18,06	12,47	25,34	-14,96	15,57	25,05	-15,25	15,28	24,21	-16,09	14,44
120	24,18	-20,23	15,12	27,28	-17,13	18,22	26,99	-17,42	17,93	26,15	-18,26	17,09

Figure 12.16 a: Subject 6 ($\gamma = 0$ degrees) – observer 1

β	Test 1			Test 2			Test 3			Mean		
	α_r	α_t	α_a	α_r	α_t	α_a	α_r	α_t	α_a	α_r	α_t	α_a
0	0,00	0,00	0,00	0.00	0,00	0,00	0,00	0.00	0,00	0,00	0,00	0,00
10	0.39	-0.85	0.21	0,74	-0,50	0,56	0,82	-0,42	0,64	0,65	-0.59	0,47
20	!,38	-1,46	0,68	1,73	-1,11	1,03	1,81	-1,03	1,11	1,64	-1,20	0,94
30	3,02	-2,38	2,10	3,37	-2,03	2,45	3,45	-1,95	2,53	3,28	-2,12	2,36
40	6,91	-2,23	4,74	5,32	-3,82	3,15	5,59	-3,55	3,42	5,94	-3,20	3,77
50	9,23	-3,39	6,16	7,64	-4,98	4,57	7,91	-4,71	4,84	8,26	-4,36	5,19
60	12,70	-4,38	7,92	11,11	-5,97	6,33	11,38	-5,70	6,60	11,73	-5,35	6,95
70	13,54	-7,57	7,61	15,18	-5,93	9,25	15,59	-5,52	9,66	14,77	-6,34	8,84
80	16,26	-9,05	9,14	17,90	-7,41	10,78	18,31	-7,00	11,19	17,49	-7,82	10,37
90	19,64	-10,68	11,85	21,28	-9,04	13,49	21,69	-8,63	13,90	20,87	-9,45	13,08
100	21,13	-13,31	13,00	24,23	-10,21	16,10	23,94	-10,50	15,81	23,10	-11,34	14,97
110	24,52	-16,79	15,00	27,62	-13,69	18,10	27,33	-13,98	17,81	26,49	-14,82	16,97
120	26,30	-20,42	17,52	29,40	-17,32	20,62	29,11	-17,61	20,33	28,27	-18,45	19,49

Figure 12.16 b: Subject 6 (γ = 0 degrees) – observer 2

β	Test 1			Test 2			Test 3			Mean		
	α_r	α_t	α_a	α_r	α_t	α_a	α_r	α_t	α_a	α_r	α_t	α_a
0	0,00	0,00	0,00	0,00	0,00	0,00	0,00	0,00	0,00	0,00	0,00	0,00
10	0,91	-0,87	0,83	1,64	-0,14	1,56	1,59	-0,19	1,51	1,38	-0,40	1,30
20	3,45	-1,36	1,89	4.18	-0,63	2,62	4,13	-0,68	2,57	3,92	-0,89	2,36
30	4,51	-2,06	3,18	5,24	-1,33	3,91	5,19	-1,38	3,86	4,98	-1,59	3,65
40	6,03	-3,30	3,36	7,33	-2,00	4,66	7,55	-1,78	4,88	6,97	-2,36	4,30
50	8,05	-4,42	5,47	9,35	-3,12	6,77	9,57	-2,90	6,99	8,99	-3,48	6,41
60	10,45	-5,53	6,01	11,75	-4,23	7,31	11,97	-4,01	7,53	11,39	-4,59	6,95
70	12,57	-6,60	7,96	13,87	-5,30	9,26	14,09	-5,08	9,48	13,51	-5,66	8,90
80	15,15	-7,80	9,23	16,45	-6,50	10,53	16,67	-6,28	10,75	16,09	-6,86	10,17
90	21,13	-7,86	14,31	17,53	-10,16	10,71	19,88	-8,71	13,06	18,78	-8,91	11,96
100	23,18	-10,74	16,54	19,58	-13,04	12,94	21,93	-11,59	15,29	20,83	-11,79	14,19
110	25,42	-12,63	18,25	21,82	-14,93	14,65	24,17	-13,48	17,00	23,07	-13,68	15,90
120	27,51	-14,68	21,00	23,91	-16,98	17,40	26,26	-15,53	19,75	25,16	-15,73	18,65

Figure 12.17 a: Subject 6 (γ = 45 degrees) – observer 1

β	Test 1			Test 2			Test 3			Mean		
	α_r	α_t	α_a	α_r	α_t	α_a	α_r	α_t	α_a	α_r	α_t	α_a
0	0,00	0,00	0,00	0,00	0,00	0,00	0,00	0,00	0,00	0,00	0,00	0,00
10	1,08	-1,06	0,59	1,81	-0,33	1,32	1,76	-0,38	1,27	1,55	-0,59	1,06
20	4,15	-1,65	1,89	4,88	-0,92	2,62	4,83	-0,97	2,57	4,62	-1,18	2,36
30	5,72	-2,55	3,42	6,45	-1,82	4,15	6,40	-1,87	4,10	6,19	-2,08	3,89
40	7,66	-4,42	4,15	8,96	-3,12	5,45	9,18	-2,90	5,67	8,60	-3,48	5,09
50	10,52	-5,62	5,13	11,82	-4,32	6,43	12,04	-4,10	6,65	11,46	-4,68	6,07
60	12,20	-6,43	6,67	13,50	-5,13	7,97	13,72	-4,91	8,19	13,14	-5,49	7,61
70	13,71	-7,51	8,60	15,01	-6,21	9,90	15,23	-5,99	10,12	14,65	-6,57	9,54
80	15,96	-8,59	9,75	17,26	-7,29	11,05	17,48	-7,07	11,27	16,90	-7,65	10,69
90	22,00	-7,91	14,73	18,40	-10,21	11,13	20,75	-8,76	13,48	19,65	-8,96	12,38
100	23,67	-8,85	18,37	20,07	-11,15	14,77	22,42	-9,70	17,12	21,32	-9,90	16,02
110	26,49	-10,29	20,60	22,89	-12,59	17,00	25,24	-11,14	19,35	24,14	-11,34	18,25
120	28,27	-12,88	22,61	24,67	-15,18	19,01	27,02	-13,73	21,36	25,92	-13,93	20,26

Figure 12.17 b: Subject 6 (γ = 45 degrees) – observer 2

β	Test 1			Test 2			Test 3			Mean		
	α_r	α_t	α_a	α_r	α_t	α_a	α_r	α_t	α_a	α_r	α_t	α_a
0	0,00	0,00	0,00	0,00	0,00	0,00	0,00	0,00	0,00	0,00	0,00	0,00
10	0,97	0,13	0,32	1,39	0,55	0,74	1,36	0,52	0,71	1,24	0,40	0,59
20	1,53	0,73	0,91	1,95	1,15	1,33	1,92	1,12	1,30	1,80	1,00	1,18
30	2,93	0.33	1,73	3,35	0,75	2,15	3,32	0,72	2,12	3,20	0,60	2,00
40	3,68	-0,92	1,91	4,95	0,35	3,18	5,17	0,57	3,40	4,60	0.00	2,83
50	4,43	-1,51	2,62	5,70	-0,24	3,89	5,92	-0,02	4,11	5,35	-0,59	3,54
60	6,59	-3,41	3,97	7,86	-2,14	5,24	8,08	-1,92	5,46	7,51	-2,49	4,89
70	8,25	-5,33	5,04	10,32	-3,26	7,11	10,17	-3,41	6,96	9,58	-4,00	6,37
80	10,84	-6,41	7,03	12,91	-4,34	9,10	12,76	-4,49	8,95	12,17	-5,08	8,36
90	13,56	-8,21	8,86	15,63	-6,14	10,93	15,48	-6,29	10,78	14,89	-6,88	10,19
100	15,35	-12,05	10,34	18,09	-9,31	13,08	18,85	-8,55	13,84	17,43	-9,97	12,42
110	18,31	-13,64	13,81	21,05	-10,90	16,55	21,81	-10,14	17,31	20,39	-11,56	15,89
120	21,86	-16,53	16,87	24,60	-13,79	19,61	25,36	-13,03	20,37	23,94	-14,45	18,95

Figure 12.18 a: Subject 6 (γ = 90 degrees) – observer 1

β	Test 1			Test 2			Test 3			Mean		
	α_r	α_t	α_a	α_r	α_t	α_a	α_r	α_t	α_a	α_r	α_t	α_a
0	0,00	0,00	0,00	0,00	0,00	0,00	0,00	0,00	0,00	0,00	0,00	0,00
10	0,52	0,72	0,07	0,94	1,14	0,49	0.91	1,11	0,46	0,79	0,99	0,34
20	0,96	0.13	0,52	1,58	0,55	0,94	1,35	0,52	0,91	1,23	0,40	0,79
30	2,20	-0,07	1,21	2,62	0,35	1,63	2,59	0,32	1,60	2,47	0,20	1,48
40	3,29	-1,71	1,41	4,56	-0,44	2,68	4.78	-0,22	2,90	4,21	-0,79	2,33
50	4,71	-1,91	2,17	5,98	-0,64	3,44	6,20	-0,42	3,66	5,63	-0,99	3,09
60	5,68	-2,51	3,67	6,95	-1,24	4,94	7,17	-1,02	5,16	6,60	-1,59	4,59
70	8,71	-4,53	5,73	10,78	-2,46	7,80	10,63	-2,61	7,65	10,04	-3,20	7,06
80	11,84	-8,13	8,44	13,91	-6,06	10,51	13,76	-6,21	10,36	13,17	-6,80	9,77
90	14,78	-9,32	10,81	16.85	-7,25	12,88	16,70	-7,40	12,73	16,11	-7,99	12.14
100	16,65	-12,56	12,75	19,39	-9,82	15,49	20,15	-9,06	16,25	18,73	-10,48	14,83
110	19,40	-14,67	14,70	22,14	-11,93	17,44	22,90	-11,17	18,20	21,48	-12,59	16,78
120	22,82	-17,05	18,05	25,56	-14,31	20,79	26,32	-13,55	21,55	24,90	-14,97	20,13

Figure 12.18 b: Subject 6 ($\gamma = 90$ degrees) – observer 2

β	Test 1			Test 2			Test 3			Mean		
	α_r	α_t	α_a	α_r	α_t	α_a	α_r	α_t	α_a	α_r	α_t	α_a
0	0,00	0,00	0,00	0,00	0,00	0,00	0,00	0,00	0,00	0,00	0,00	0,00
10	1,29	-1,21	0,77	1,86	-0,64	1,34	1,95	-0,55	1,43	1,70	-0,80	1,18
20	6,87	-2,19	2,89	7,44	-1,62	3,46	7,53	-1,53	3,55	7,28	-1,78	3,30
30	12,58	-4,17	3,87	13,15	-3,60	4,44	13,24	-3,51	4,53	12,99	-3,76	4,28
40	15,61	-5,11	6,61	14,26	-6,46	5,26	14,47	-6,25	5,47	14,78	-5,94	5,78
50	22,78	-7,09	8,74	21,43	-8,44	7,39	21,64	-8,23	7,60	21,95	-7,92	7,91
60	27,55	-9,08	11,33	26,20	-10,43	9,98	26,41	-10,22	10,19	26,72	-9,91	10,50
70	33,89	-9,60	15,45	30,53	-12,96	12,09	30,30	-13,19	11,86	31,54	-11,95	13,10
80	40,07	-10,88	18,34	36,71	-14,24	14,98	36,48	-14,47	14,75	37,72	-13,23	15,99
90	41,98	-13,57	21,35	38,62	-16,93	17,99	38,39	-17,16	17,76	39,63	-15,92	19,00
100	43,33	-17,80	24,07	43,97	-17,16	24,71	40,02	-21,11	20,76	42,44	-18,69	23,18
110	47,04	-21,06	29,35	47,68	-20,42	29,99	43,73	-24,37	26,04	46,15	-21,95	28,46
120	52,27	-24,34	35,77	52,91	-23,70	36,41	48,96	-27,65	32,46	51,38	-25,23	34,88

Figure 12.19 a: Subject 7 ($\gamma = 0$ degrees) – observer 1

β	Test 1			Test 2			Test 3			Mean		
	α_r	α_t	α_a	α_r	α_t	α_a	α_r	α_t	α_a	α_r	α_t	α_a
0	0,00	0,00	0,00	0,00	0,00	0,00	0,00	0,00	0,00	0,00	0,00	0.00
10	3,80	-1,20	1,48	4,37	-0,63	2,05	4,46	-0,54	2,14	4,21	-0,79	1,89
20	6,43	-2,78	2,83	7,00	-2,21	3,40	7,09	-2,12	3,49	6,84	-2,37	3,24
30	11,35	-5,15	3,83	11,92	-4,58	4,40	12,01	-4,49	4,49	11,76	-4,74	4,24
40	18,12	-6,09	7,69	16,77	-7,44	6,34	16,98	-7,23	6,55	17,29	-6,92	6,86
50	25,23	-8,54	9,60	23,88	-9,89	8,25	24,09	-9,68	8,46	24,40	-9,37	8,77
60	27,45	-10,82	11,40	26,10	-12,17	10,05	26,31	-11,96	10,26	26,62	-11,65	10,57
70	30,63	-11,42	15,34	27,27	-14,78	11,98	27,04	-15,01	11,75	28,28	-13,77	12,99
80	36,06	-13,39	18,40	32,70	-16,75	15,04	32,47	-16,98	14,81	33,71	-15,74	16,05
90	39,63	-15,17	21,58	36,27	-18,53	18,22	36,04	-18,76	17,99	37,28	-17,52	19,23
100	42,76	-19,82	24,49	43,40	-19,18	25,13	39,45	-23,13	21,18	41,87	-20,71	23,60
110	46,22	-21,76	28,14	46,86	-21,12	28,78	42,91	-25,07	24,83	45,33	-22,65	27,25
120	50,77	-24,88	33,84	51,41	-24,24	34,48	47,46	-28,19	30,53	49,88	-25,77	32,95

Figure 12.19 b: Subject 7 (γ = 0 degrees) – observer 2

β	Test 1			Test 2			Test 3			Mean		
	α_r	α_t	α_a	α_r	α_t	α_a	α_r	α_t	α_a	α_r	α_t	α_a
0	0,00	0,00	0,00	0,00	0,00	0,00	0,00	0,00	0,00	0,00	0,00	0,00
10	1,40	-0,23	0,65	1,51	-0,12	0,76	0,78	-0,85	0,03	1,23	-0,40	0,48
20	5,92	-1,01	1,92	6,03	-0,90	2,03	5,30	-1,63	1,30	5,75	-1,18	1,75
30	8,03	-2,02	3,64	8,14	-1,91	3,75	7,41	-2,64	3,02	7,86	-2,19	3,47
40	10,08	-4,82	4,60	12,47	-2,43	6,99	11,47	-3,43	5,99	11,34	-3,56	5,86
50	16,77	-6,59	6,99	19,16	-4,20	9,38	18,16	-5,20	8,38	18,03	-5,33	8,25
60	20,96	-8,55	9,82	23,35	-6,16	12,21	22,35	-7,16	11,21	22,22	-7,29	11,08
70	25,09	-10,44	13,00	27,48	-8,05	15,39	26,48	-9,05	14,39	26,35	-9,18	14,26
80	26,82	-13,45	15,62	30,34	-9,93	19,14	29,45	-10,82	18,25	28,87	-11,40	17,67
90	33,32	-16,93	19,29	36,84	-13,41	22,81	35,95	-14,30	21,92	35,37	-14,88	21,34
100	38,77	-19,61	23,15	42,29	-16,09	26,67	41,40	-16,98	25,78	40,82	-17,56	25,20
110	42,60	-22,54	27,25	46,12	-19,02	30,77	45,23	-19,91	29,88	44,65	-20,49	29,30
120	45,82	-25,58	31,46	49,34	-22,06	34,98	48,45	-22,95	34,09	47,87	-23,53	33,51

Figure 12.20 a: Subject 7 (γ = 45 degrees) – observer 1

β	Test 1			Test 2			Test 3			Mean		
	α_r	α_t	α_a	α_r	α_t	α_a	α_r	α_t	α_a	α_r	α_t	α_a
0	0,00	0,00	0,00	0,00	0,00	0,00	0,00	0,00	0,00	0,00	0,00	0,00
10	1,03	-0,42	1,38	1,14	-0,31	1,49	0,41	-1,04	0,76	0,86	-0,59	1,21
20	2.26	-1,32	2,58	2,37	-1,21	2,69	1,64	-1,94	1,96	2,09	-1,49	2,41
30	3,70	-2,41	4.22	3,81	-2,30	4,33	3,08	-3,03	3,60	3,53	-2,58	4,05
40	4,10	-4,82	4,80	6,49	-2,43	7,19	5,49	-3,43	6,19	5.36	-3,56	6,06
50	7,81	-6,40	6,93	10,20	-4,01	9,32	9,20	-5,01	8,32	9,07	-5,14	8,19
60	13.53	-8,83	9,63	15,92	-6,44	12,02	14,92	-7,44	11,02	14,79	-7,57	10,89
70	21,12	-11,12	12,52	23,51	-8,73	14,91	22,51	-9,73	13,91	22,38	-9,86	13,78
80	27,45	-14,23	14,68	30,97	-10,71	18,20	30,08	-11,60	17,31	29,50	-12,18	16,73
90	32,06	-16,94	17,99	35,58	-13,42	21,51	34,69	-14,31	20,62	34,11	-14,89	20,04
100	40,02	-19,84	22,09	43,54	-16,32	25,61	42,65	-17,21	24,72	42,07	-17,79	24,14
110	46,53	-22,91	26,02	50,05	-19,39	29,54	49,16	-20,28	28,65	48,58	-20,86	28,07
120	48,26	-26,19	30,20	51,78	-22,67	33,72	50,89	-23,56	32,83	50,31	-24,14	32,25

Figure 12.20 b: Subject 7 (γ = 45 degrees) – observer 2

β	Test 1			Test 2			Test 3			Mean		
	α_r	α_t	α_a	α_r	α_t	α_a	α_r	α_t	α_a	α_r	α_t	α_a
0	0,00	0,00	0,00	0,00	0,00	0,00	0,00	0,00	0,00	0,00	0,00	0,00
10	1,29	1,31	0,95	1,34	1,36	1,00	0,88	0,90	0,54	1,17	1,19	0,83
20	1,98	2,69	2,48	2,03	2,74	2,53	1,57	2,28	2,07	1,86	2,57	2,36
30	4,43	1,50	3.66	4,48	1,55	3,71	4,02	1,09	3,25	4,31	1,38	3,54
40	5,83	-1,46	4,08	7,15	-0,14	5,40	7,12	-0,17	5,37	6,70	-0,59	4,95
50	10,50	-2,64	6,91	11,82	-1,32	8,23	11,79	-1,35	8,20	11,37	-1,77	7,78
60	13,52	-4,83	9,03	14,84	-3,51	10,35	14,81	-3,54	10,32	14,39	-3,96	9,90
70	14,87	-8,36	10,38	18,11	-5,12	13,62	18,32	-4,91	13,83	17,10	-6,13	12,61
80	21,05	-10,90	13,45	24,29	-7,66	16,69	24,50	-7,45	16,90	23,28	-8,67	15,68
90	27,73	-13,62	17,46	30,97	-10,38	20,70	31,18	-10,17	20,91	29,96	-11,39	19,69
100	32,59	-17,94	20,24	37,21	-13,32	24,86	36,91	-13,62	24,56	35,57	-14,96	23,22
110	38,82	-20,51	23,19	43,44	-15,89	27,81	43,14	-16,19	27,51	41,80	-17,53	26,17
120	43,31	-23,65	26,61	47,93	-19,03	31,23	47,63	-19,33	30,93	46,29	-20,67	29,59

Figure 12.21 a: Subject 7 (γ = 90 degrees) – observer 1

β	Test 1			Test 2			Test 3			Mean		
	α_r	α_t	α_a	α_r	α_t	α_a	α_r	α_t	α_a	α_r	α_t	α_a
0	0,00	0,00	0,00	0,00	0,00	0,00	0,00	0,00	0,00	0,00	0,00	0,00
10	2,79	1,31	0,47	2,84	1,36	0,52	2,38	0,90	0,06	2,67	1,19	0,35
20	3,57	2.89	1,30	3.62	2,94	1,35	3,16	2,48	0,89	3,45	2,77	1.18
30	4,40	1,50	1,89	4,45	1,55	1,94	3,99	1,09	1,48	4,28	1,38	1,77
40	4,10	-0,87	1,49	5,42	0,45	2,81	5,39	0,42	2,78	4,97	0,00	2,36
50	7,86	-2,55	3,15	9,18	-1,23	4,47	9,15	-1,26	4,44	8,73	-1,68	4,02
60	12,82	-4,04	5,14	14,14	-2,72	6,46	14,11	-2,75	6,43	13,69	-3,17	6,01
70	16,04	-7,79	7,08	19,28	-4,55	10,32	19,49	-4,34	10,53	18,27	-5,56	9,31
80	21,56	-10,00	10,74	24,80	-6,76	13,98	25,01	-6,55	14,19	23,79	-7,77	12,97
90	27,45	-12,61	14,04	30,69	-9,37	17,28	30,90	-9,16	17,49	29,68	-10,38	16,27
100	32,57	-15,66	17,65	37,19	-11,04	22,27	36,89	-11,34	21,97	35,55	-12,68	20,63
110	38,32	-19,15	21,19	42,94	-14,53	25,81	42,64	-14,83	25,51	41,30	-16,17	24,17
120	44,89	-22,90	23,90	49.51	-18,28	28,52	49,21	-18,58	28,22	47,87	-19,92	26,88

Figure 12.21 b: Subject 7 (γ = 90 degrees) – observer 2

β	Test 1			Test 2			Test 3			Mean		
	α_r	α_t	α_a	α_r	α_t	α_a	α_r	α_t	α_a	α_r	α_t	α_a
0	0,00	0,00	0,00	0,00	0,00	0,00	0,00	0,00	0,00	0,00	0,00	0,00
10	1,39	-1,90	0,01	1,42	-1,87	0,04	1,69	-1,60	0,31	1,50	-1,79	0,12
20	4,73	-2,18	2,81	3,40	-3,51	1,48	3,53	-3,38	1,61	3,92	-2,99	2,00
30	7,85	-3,56	4,53	6,52	-4,89	3,20	6,65	-4,76	3,33	7,04	-4,37	3,72
40	11,04	-4,95	6,59	9,71	-6,28	5,26	9,84	-6,15	5,39	10,23	-5,76	5,78
50	12,04	-10,46	6,78	14,72	-7,78	9,46	14,49	-8,01	9,23	13,75	-8,75	8,49
60	14,93	-11,85	8,96	17,61	-9,17	11,64	17,38	-9,40	11,41	16,64	-10,14	10,67
70	18,59	-13,82	11,85	21,27	-11,14	14,53	21,04	-11,37	14,30	20,30	-12,11	13,56
80	23,68	-16,20	15,27	26,36	-13,52	17,95	26,13	-13,75	17,72	25,39	-14,49	16,98
90	26,06	-19,33	18,44	29,08	-16,31	21,46	30,15	-15,24	22,53	28,43	-16,96	20,81
100	30,38	-21,55	22,78	33,40	-18,53	25,80	34,47	-17,46	26,87	32,75	-19,18	25,15
110	35,52	-24,86	25,51	38,54	-21,84	28,53	39,61	-20,77	29,60	37,89	-22,49	27,88
120	39,88	-27,40	27,68	42,90	-24,38	30,70	43,97	-23,31	31,77	42,25	-25,03	30,05

Figure 12.22 a: Subject 8 (γ = 0 degrees) – observer 1

β	Test 1			Test 2			Test 3			Mean		
	α_r	α_t	α_a	α_r	α_t	α_a	α_r	α_t	α_a	α_r	α_t	α_a
0	0,00	0,00	0,00	0,00	0,00	0,00	0,00	0,00	0,00	0,00	0,00	0,00
10	0.94	-0,81	0,48	0,97	-0,78	0,51	1,24	-0,51	0,78	1,05	-0,70	0,59
20	4,40	-1,38	3,29	3,07	-2,71	1,96	3,20	-2,58	2,09	3,59	-2,19	2,48
30	8,27	-2,96	5,59	6,94	-4,29	4,26	7,07	-4,16	4,39	7,46	-3,77	4.78
40	11,96	-4,55	8,53	10,63	-5,88	7,20	10,76	-5,75	7,33	11,15	-5,36	7,72
50	11,27	-8,86	8,44	13,95	-6,18	11,12	13,72	-6,41	10,89	12,98	-7,15	10,15
60	14,58	-11,04	11,26	17,26	-8,36	13,94	17,03	-8,59	13,71	16,29	-9,33	12,97
70	19,94	-12,61	14,80	22,62	-9,93	17,48	22,39	-10,16	17,25	21,65	-10,90	16,51
80	23,36	-14,79	18,10	26,04	-12,11	20,78	25,81	-12,34	20,55	25,07	-13,08	19,81
90	25,75	-18,03	20,27	28,77	-15,01	23,29	29,84	-13,94	24,36	28,12	-15,66	22,64
100	28,89	-19,75	22,42	31,91	-16,73	25,44	32,98	-15,66	26,51	31,26	-17,38	24,79
110	33,20	-23,07	25,29	36,22	-20,05	28,31	37,29	-18,98	29,38	35,57	-20,70	27,66
120	37,59	-26,43	29,24	40,61	-23,41	32,26	41,68	-22,34	33,33	39,96	-24,06	31,61

Figure 12.22 b: Subject 8 (γ = 0 degrees) – observer 2

β	Test 1			Test 2			Test 3			Mean		
	α_r	α_t	α_a	α_r	α_t	α_a	α_r	α_t	α_a	α_r	α_t	α_a
0	0,00	0,00	0,00	0,00	0,00	0,00	0,00	0,00	0,00	0,00	0,00	0,00
10	0,68	-0,82	0,12	0,99	-0,51	0,43	1,06	-0,44	0,50	0,91	-0,59	0,35
20	2,26	-1,62	0,95	2,57	-1,31	1,26	2,64	-1,24	1,33	2,49	-1,39	1,18
30	5,43	-1,96	2,75	4,65	-2,74	1,97	4,32	-3,07	1,64	4,80	-2,59	2,12
40	7,98	-3,46	4,34	7,20	-4,24	3,56	6,87	-4,57	3,23	7,35	-4,09	3,71
50	10,80	-5,05	5,28	10,02	-5,83	4,50	9,69	-6,16	4,17	10,17	-5,68	4,65
60	12,38	-8,93	5,63	15,16	-6,15	8,41	14,61	-6,70	7,86	14,05	-7,26	7,30
70	15,84	-10,52	7,40	18,62	-7,74	10,18	18,07	-8,29	9,63	17,51	-8,85	9,07
80	20,40	-13,30	11,05	23,18	-10,52	13,83	22,63	-11,07	13,28	22,07	-11,63	12,72
90	25,16	-15,68	12,53	27,94	-12,90	15,31	27,39	-13,45	14,76	26,83	-14,01	14,20
100	27,38	-18,91	14,74	28,97	-17,32	16,33	28,61	-17,68	15,97	30,20	-16,09	17,56
110	33,36	-20,88	17,86	34,95	-19,29	19,45	34,59	-19,65	19,09	36,18	-18,06	20,68
120	38,03	-23,87	22,75	39,62	-22,28	24,34	39,26	-22,64	23,98	40,85	-21,05	25,57

Figure 12.23 a: Subject 8 (γ = 45 degrees) – observer 1

β	Test 1			Test 2			Test 3			Mean		
	α_r	α_t	α_a	α_r	α_t	α_a	α_r	α_t	α_a	α_r	α_t	α_a
0	0,00	0,00	0,00	0,00	0,00	0,00	0,00	0,00	0,00	0,00	0,00	0,00
10	-0,05	-0,82	0,01	0,26	-0,51	0,32	0,33	-0,44	0,39	0,18	-0,59	0,24
20	3,26	-2,01	0,95	3,57	-1,70	1,26	3.64	-1.63	1.33	3,49	-1,78	1,18
30	6,72	-2,73	2,87	5,94	-3,51	2,09	5,61	-3,84	1,76	6,09	-3,36	2,24
40	8,93	-4,13	3,93	8,15	-4,91	3,15	7,82	-5,24	2,82	8,30	-4,76	3,30
50	12,23	-5,73	5,11	11,45	-6,51	4,33	11,12	-6,84	4,00	11,60	-6,36	4,48
60	13,16	-9,81	4,11	15,94	-7,03	6,89	15,39	-7,58	6,34	14,83	-8,14	5,78
70	16,13	-11,74	5,28	18,91	-8,96	8,06	18,36	-9,51	7,51	17,80	-10,07	6,95
80	18,02	-14,36	7,58	20,80	-11,58	10,36	20,25	-12,13	9,81	19,69	-12,69	9,25
90	21,73	-16,58	10,11	24,51	-13,80	12,89	23,96	-14,35	12,34	23,40	-14,91	11,78
100	24,57	-20,55	11,85	26,16	-18,96	13,44	25,80	-19,32	13,08	27,39	-17,73	14,67
110	28,62	-21,98	14,39	30,21	-20,39	15,98	29,85	-20,75	15,62	31,44	-19,16	17,21
120	35,75	-25,07	19,92	37,34	-23,48	21,51	36,98	-23,84	21,15	38,57	-22,25	22,74

Figure 12.23 b: Subject 8 (γ = 45 degrees) – observer 2

β	Test 1			Test 2			Test 3			Mean		
	α_r	α_t	α_a	α_r	α_t	α_a	α_r	α_t	α_a	α_r	α_t	α_a
0	0,00	0,00	0,00	0,00	0,00	0,00	0,00	0,00	0,00	0,00	0,00	0,00
10	0,70	0,12	0,10	0,75	0,17	0,15	1,13	0,55	0,53	0,86	0,28	0,26
20	1,89	0,83	0,89	1,94	0,88	0,94	2,32	1,26	1,32	2,05	0,99	1,05
30	3,30	-0,49	1,12	4,42	0,63	2,24	4,79	1,00	2,61	4,17	0.38	1,99
40	5,33	-2,44	2,19	6,45	-1,32	3,31	6,82	-0,95	3,68	6,20	-1,57	3,06
50	7,30	-4,04	3,43	8,42	-2,92	4,55	8,79	-2,55	4,92	8,17	-3,17	4,30
60	9,33	-6,27	4,34	11,39	-4,21	6,40	11,20	-4,40	6,21	10,64	-4,96	5,65
70	12,72	-8,48	5,64	14,78	-6,42	7,70	14,59	-6,61	7,51	14,03	-7,17	6,95
80	16,62	-10,47	8,05	18,68	-8,41	10,11	18,49	-8,60	9,92	17,93	-9,16	9,36
90	19,64	-14,12	11,19	23,27	-10,49	14,82	23,42	-10,34	14,97	22,11	-11,65	13,66
100	23,35	-16,51	15,37	26,98	-12,88	19,00	27,13	-12,73	19,15	25,82	-14,04	17,84
110	28,26	-19,29	19,50	31,89	-15,66	23,13	32,04	-15,51	23,28	30,73	-16,82	21,97
120	34,19	-22,06	23,86	37,82	-18,43	27,49	37,97	-18,28	27,64	36,66	-19,59	26,33

Figure 12.24 a: Subject 8 (γ = 90 degrees) – observer 1

β	Test 1			Test 2			Test 3			Mean		
	α_r	α_t	α_a	α_r	α_t	α_a	α_r	α_t	α_a	α_r	α_t	α_a
0	0,00	0,00	0,00	0,00	0,00	0,00	0,00	0,00	0,00	0,00	0,00	0,00
10	1,13	0,62	0,46	1,18	0,67	0,51	1,56	1,05	0,89	1,29	0,78	0,62
20	2,28	1,91	1,43	2,33	1,96	1,48	2,71	2,34	1,86	2,44	2,07	1,59
30	2,33	-0,32	1,19	3,45	0,80	2,31	3,82	1,17	2,68	3,20	0,55	2,06
40	4,35	-2,58	3,02	5,47	-1,46	4,14	5,84	-1,09	4,51	5,22	-1,71	3,89
50	6,22	-4,21	4,37	7,34	-3,09	5,49	7,71	-2,72	5,86	7,09	-3,34	5,24
60	7,59	-6,35	5,99	9,65	-4,79	8,05	9,46	-4,98	7,86	8,90	-5,54	7,30
70	11,42	-9,05	7,29	13,48	-6,99	9,35	13,29	-7,18	9,16	12,73	-7,74	8,60
80	13,16	-10,84	9,53	15,22	-8,78	11,59	15,03	-8,97	11,40	14,47	-9,53	10,84
90	16,86	-14,79	11,26	20,49	-11,16	14,89	20,64	-11,01	15,04	19,33	-12,32	13,73
100	21,80	-18,18	15,20	25,43	-14,55	18,83	25,58	-14,40	18,98	24,27	-15,71	17,67
110	26,82	-21,06	18,50	30,45	-17,43	22,13	30,60	-17,28	22,28	29,29	-18,59	20,97
120	31,63	-23,33	22,66	35,26	-19,70	26,29	35,41	-19,55	26,44	34,10	-20,86	25,13

Figure 12.24 b: Subject 8 ($\gamma = 90$ degrees) – observer 2

β	Test 1			Test 2			Test 3			Mean		
	α_r	α_t	α_a	α_r	α_t	α_a	α_r	α_t	α_a	α_r	α_t	α_a
0	0,00	0,00	0,00	0,00	0,00	0,00	0,00	0,00	0,00	0,00	0,00	0,00
10	0,37	-0,92	0,11	0,39	-0,90	0,13	0,74	-0,55	0,48	0,50	-0,79	0,24
20	1,22	-1,32	0,84	1,24	-1,30	0,86	1,59	-0,95	1,21	1,35	-1,19	0,97
30	3,45	-2,01	3,33	1,85	-3,61	1,73	2,14	-3,32	2,02	2,48	-2,98	2,36
40	5,07	-3,60	4,56	3,47	-5,20	2,96	3,76	-4,91	3,25	4,10	-4,57	3,59
50	7,40	-5,38	5,51	5,80	-6,98	3,91	6,09	-6,69	4,20	6,43	-6,35	4,54
60	11,14	-7,14	8,35	7,99	-10,29	5,20	8,86	-9,42	6,07	9,33	-8,95	6,54
70	14,17	-10,12	9,24	11,02	-13,27	6,09	11,89	-12,40	6,96	12,36	-11,93	7,43
80	18,19	-13,30	12,36	15,04	-16,45	9,21	15,91	-15,58	10,08	16,38	-15,11	10,55
90	21,27	-16,69	14,95	18,12	-19,84	11,80	18,99	-18,97	12,67	19,46	-18,50	13,14
100	25,27	-19,35	18,34	21,58	-23,04	14,65	20,77	-23,85	13,84	22,54	-22,08	15,61
110	28,94	-24,74	21,47	25,25	-28,43	17,78	24,44	-29,24	16,97	26,21	-27,47	18,74
120	32,88	-29,92	23,82	29,19	-33,61	20,13	28,38	-34,42	19,32	30,15	-32,65	21,09

Figure 12.25 a: Subject 9 ($\gamma = 0$ degrees) – observer 1

β	Test 1			Test 2			Test 3			Mean		
	α_r	α_t	α_a	α_r	α_t	α_a	α_r	α_t	α_a	α_r	α_t	α_a
0	0,00	0,00	0,00	0,00	0,00	0,00	0,00	0,00	0,00	0,00	0,00	0,00
10	0,52	-0,73	0,34	0,54	-0,71	0,36	0,89	-0,36	0,71	0,65	-0,60	0,47
20	1,51	-1,73	0,81	1,53	-1,71	0,83	1,88	-1,36	1,18	1,64	-1,60	0,94
30	4,25	-1,82	3,33	2,65	-3.42	1,73	2,94	-3,13	2,02	3,28	-2,79	2,36
40	6,91	-3,40	4,74	5,31	-5,00	3,14	5,60	-4,71	3,43	5,94	-4,37	3,77
50	9,23	-4,80	6,16	7,63	-6,40	4,56	7,92	-6,11	4,85	8,26	-5,77	5,19
60	13,54	-6,44	8,76	10,39	-9,59	5,61	11,26	-8,72	6,48	11,73	-8,25	6,95
70	16,58	-8,72	10,65	13,43	-11,87	7,50	14,30	-11,00	8,37	14,77	-10,53	8,84
80	21,30	-10,91	12,18	18,15	-14,06	9,03	19,02	-13,19	9,90	19,49	-12,72	10,37
90	23,68	-15.09	13,89	20,53	-18,24	10,74	21,40	-17,37	11,61	21,87	-16,90	12,08
100	28,83	-18,66	18,10	25,14	-22,35	14,41	24,33	-23,16	13,60	26,10	-21,39	15,37
110	31,22	-23,34	19,70	27,53	-27,03	16,01	26,72	-27,84	15,20	28,49	-26,07	16,97
120	34,70	-28,52	21,72	31,01	-32,21	18,03	30,20	-33,02	17,22	31,97	-31,25	18,99

Figure 12.25 b: Subject 9 ($\gamma = 0$ degrees) – observer 2

β	Test 1			Test 2			Test 3			Mean		
	α_r	α_t	α_a	α_r	α_t	α_a	α_r	α_t	α_a	α_r	α_t	α_a
0	0,00	0,00	0,00	0,00	0,00	0,00	0,00	0,00	0,00	0,00	0,00	0,00
10	0,93	-2,04	0,85	1,62	-1,35	1,54	1,59	-1,38	1,51	1,38	-1,59	1,30
20	3,47	-3,43	1,91	4,16	-2,74	2,60	4,13	-2,77	2,57	3,92	-2,98	2,36
30	5,96	-3,58	4,63	4,31	-5,23	2,98	4,67	-4,87	3,34	4,98	-4,56	3,65
40	7,95	-4,68	5,28	6,30	-6,33	3,63	6,66	-5,97	3,99	6,97	-5,66	4,30
50	11,97	-6,88	6,39	10,32	-8,53	4,74	10,68	-8,17	5,10	10,99	-7,86	5,41
60	15,59	-9,26	8,60	13,20	-11,65	6,21	13,03	-11,82	6,04	13,94	-10,91	6,95
70	17,72	-11,14	10,55	15,33	-13,53	8,16	15,16	-13,70	7,99	16,07	-12,79	8,90
80	19,74	-14,03	11,82	17,35	-16,42	9,43	17,18	-16,59	9,26	18,09	-15,68	10,17
90	22,03	-17,08	14,61	19,64	-19,47	12,22	19,47	-19,64	12,05	20,38	-18,73	12,96
100	25,85	-19,37	17,21	21,41	-23,81	12,77	21,22	-24,00	12,58	22,83	-22,39	14,19
110	29,39	-23,47	18,92	24,95	-27,91	14,48	24,76	-28,10	14,29	26,37	-26,49	15,90
120	32,18	-28,87	21,67	27,74	-33,31	17,23	27,55	-33,50	17,04	29,16	-31,89	18,65

Figure 12.26 a: Subject 9 ($\gamma = 45$ degrees) – observer 1

β	Test 1			Test 2			Test 3			Mean		
	α_r	α_t	α_a	α_r	α_t	α_a	α_r	α_t	α_a	α_r	α_t	α_a
0	0,00	0,00	0,00	0,00	0,00	0.00	0,00	0,00	0,00	0,00	0,00	0,00
10	1,10	-1,04	0,61	1,79	-0,35	1,30	1,76	-0,38	1,27	1,55	-0,59	1,06
20	4,17	-1,83	1,91	4,86	-1,14	2,60	4,83	-1,17	2,57	4,62	-1,38	2,36
30	7,17	-3,10	4,87	5,52	-4,75	3,22	5,88	-4,39	3,58	6,19	-4,08	3,89
40	9,58	-5,50	6,07	7,93	-7,15	4,42	8,29	-6,79	4,78	8,60	-6,48	5,09
50	12,44	-7,70	7,05	10,79	-9,35	5,40	11,15	-8,99	5,76	11,46	-8,68	6,07
60	14,79	-9,03	9,26	12,40	-11,42	6,87	12,23	-11,59	6,70	13,14	-10,68	7,61
70	17,30	-11,92	10,19	14,91	-14,31	7,80	14,74	-14,48	7,63	15,65	-13,57	8,54
80	20,55	-15,31	12,34	18,16	-17,70	9,95	17,99	-17,87	9,78	18,90	-16,96	10,69
90	22,30	-18,69	13,73	19,91	-21,08	11,34	19,74	-21,25	11,17	20,65	-20,34	12,08
100	24,34	-20,91	16,04	19,90	-25,35	11,60	19,71	-25,54	11,41	21,32	-23,93	13,02
110	27,16	-23,60	18,27	22,72	-28,04	13,83	22,53	-28,23	13,64	24,14	-26,62	15,25
120	30,94	-27,08	19,28	26,50	-31,52	14,84	26,31	-31,71	14,65	27,92	-30,10	16,26

Figure 12.26 b: Subject 9 (γ = 45 degrees) – observer 2

β	Test 1			Test 2			Test 3			Mean		
	α_r	α_t	α_a	α_r	α_t	α_{a_3}	α_r	α_t	α_a	α_r	α_t	α_a
0	0,00	0,00	0,00	0,00	0,00	0,00	0,00	0,00	0,00	0,00	0,00	0,00
10	1,61	0,85	0,96	0,98	0,45	0,33	1,13	0,47	0,48	1,24	0,59	0,59
20	2,17	2,05	1,55	1,54	1,65	0,92	1,69	1,67	1,07	1,80	1,79	1,18
30	2,88	0,17	1,68	2,58	-0,13	1,38	4,14	1,43	2,94	3,20	0,49	2,00
40	4,28	-1,78	2,51	3,98	-2,08	2,21	5,54	-0,52	3,77	4,60	-1,46	2,83
50	5,99	-2,56	4.18	4,42	-4,13	2,61	5,64	-2,91	3,83	5,35	-3,20	3,54
60	8,15	-5,95	5,53	6,58	-7,52	3,96	7,80	-6,30	5,18	7,51	-6,59	4,89
70	10,22	-8,94	7,01	8,65	-10,51	5,44	9,87	-9,29	6,66	9,58	-9,58	6,37
80	12,81	-12,92	10,00	11,24	-14,49	8,43	12,46	-13,27	9,65	12,17	-13,56	9,36
90	14,20	-17,25	10,50	15,34	-18,39	11,64	15,13	-18,18	11,43	14,89	-17,94	11,19
100	18,04	-20,89	13,73	19,18	-22,03	14,87	18,97	-21,82	14,66	18,73	-21,58	14,42
110	21,70	-23,87	15,70	22,84	-25,01	16,84	22,63	-24,80	16,63	22,39	-24,56	16,39
120	25,25	-28,25	18,26	26,39	-29,39	19,40	26,18	-29,18	19,19	25,94	-28,94	18,95

Figure 12.27 a: Subject 9 (γ = 90 degrees) – observer 1

β	Test 1			Test 2			Test 3			Mean		
	α_r	α_t	α_a	α_r	α_t	α_a	α_r	α_t	α_a	α_r	α_t	α_a
0	0,00	0,00	0,00	0,00	0,00	0,00	0,00	0,00	0,00	0,00	0,00	0,00
10	1,16	0,86	0,71	0,53	0,46	0,08	0,68	0.48	0,23	0,79	0,60	0,34
20	1.60	2,25	1,16	0,97	1,85	0,53	1,12	1,87	0.68	1,23	1.99	0,79
30	2,15	-2.01	1.16	1,85	-2,31	0,86	3,41	-0.75	2,42	2,47	-1,69	1,48
40	3,89	-3,72	2,01	3,59	-4,02	1,71	5,15	-2,46	3,27	4,21	-3,40	2,33
50	6,27	-4,81	3,73	4,70	-6,38	2,16	5,92	-5,16	3,38	5,63	-5,45	3,09
60	7,24	-6,96	7,23	5,67	-8,53	5,66	6,89	-7,31	6,88	6,60	-7,60	6,59
70	9,68	-9,25	9,70	8,11	-10,82	8,13	9,33	-9,60	9,35	9,04	-9,89	9,06
80	12,81	-11,92	10,41	11,24	-13,49	8,84	12,46	-12,27	10,06	12,17	-12,56	9,77
90	15,42	-15,36	11,45	16,56	-16,50	12,59	16,35	-16,29	12,38	16,11	-16,05	12,14
100	20,04	-20,51	15,14	21,18	-21,65	16,28	20,97	-21,44	16,07	20,73	-21,20	15,83
110	23,79	-24,50	18,09	24,93	-25,64	19,23	24,72	-25,43	19,02	24,48	-25,19	18,78
120	26,21	-29,87	20,44	27,35	-31,01	21,58	27,14	-30,80	21,37	26,90	-30,56	21,13

Figure 12.27 b: Subject 9 (γ = 90 degrees) – observer 2

β	Test 1			Test 2			Test 3			Mean		
	α_r	α_t	α_a	α_r	α_t	α_a	α_r	α_t	α_a	α_r	α_t	α_a
0	0,00	0,00	0,00	0,00	0,00	0,00	0,00	0,00	0,00	0,00	0,00	0,00
10	0,29	-1,00	0,03	0,58	-0,71	0,32	0,63	-0,66	0,37	0,50	-0,79	0,24
20	1,14	-1,40	0,50	1,43	-1,11	0,79	1,48	-1,06	0,84	1,35	-1,19	0,71
30	2,01	-2,45	0,89	2,80	-1,66	1,68	2,63	-1,83	1,51	2,48	-1,98	1,36
40	3,63	-4,04	2,12	4,42	-3,25	2,91	4,25	-3,42	2,74	4,10	-3,57	2,59
50	7,14	-4,64	4,25	6,09	-5,69	3,20	6,06	-5,72	3,17	6,43	-5,35	3,54
60	12,04	-6,24	6,25	10,99	-7,29	5,20	10,96	-7,32	5,17	11,33	-6,95	5,54
70	15,47	-8,22	8,14	14,42	-9,27	7,09	14,39	-9,30	7,06	14,76	-8,93	7,43
80	21,69	-8,80	12,86	17,79	-12,70	8,96	18,66	-11,83	9,83	19,38	-11,11	10,55
90	24,77	-11,19	15,45	20,87	-15,09	11,55	21,74	-14,22	12,42	22,46	-13,50	13,14
100	27,85	-13,77	16,92	23,95	-17,67	13,02	24,82	-16,80	13,89	25,54	-16,08	14,61
110	31,52	-17,16	17,75	27,62	-21,06	13,85	28,49	-20,19	14,72	29,21	-19,47	15,44
120	33,46	-20,34	19,40	29,56	-24,24	15,50	30,43	-23,37	16,37	31,15	-22,65	17,09

Figure 12.28 a: Subject 10 (γ = 0 degrees) – observer 1

β	Test 1			Test 2			Test 3			Mean		
	α_r	α_t	α_a	α_r	α_t	α_a	α_r	α_t	α_a	α_r	α_t	α_a
0	0,00	0,00	0,00	0,00	0,00	0,00	0,00	0,00	0,00	0,00	0,00	0,00
10	0,44	-0,81	0,26	0,73	-0,52	0,55	0,78	-0,47	0,60	0,65	-0,60	0,47
20	1,43	-1,81	0,73	1.72	-1,52	1,02	1,77	-1,47	1,07	1,64	-1.60	0.94
30	2,81	-3,26	1,89	3,60	-2,47	2,68	3,43	-2.64	2,51	3,28	-2,79	2,36
40	5,47	-4,84	3,30	6,26	-4,05	4,09	6,09	-4,22	3,92	5,94	-4,37	3,77
50	8,97	-5,06	5,90	7,92	-6,11	4,85	7,89	-6,14	4,82	8,26	-5,77	5,19
60	13,44	-5,54	7,66	12,39	-6,59	6,61	12,36	-6,62	6,58	12,73	-6,25	6,95
70	17,48	-7,82	9,55	16,43	-8,87	8,50	16,40	-8,90	8,47	16,77	-8,53	8,84
80	23,80	-8,41	12,68	19,90	-12,31	8,78	20,77	-11,44	9,65	21,49	-10,72	10,37
90	27,18	-10,59	15,39	23,28	-14,49	11,49	24,15	-13,62	12,36	24,87	-12,90	13,08
100	29,41	-13,08	17,28	25,51	-16,98	13,38	26,38	-16,11	14,25	27,10	-15,39	14,97
110	33,80	-15,76	19,28	29,90	-19,66	15,38	30,77	-18,79	16,25	31,49	-18,07	16,97
120	35,58	-18,94	21,80	31,68	-22,84	17,90	32,55	-21,97	18,77	33,27	-21,25	19,49

Figure 12.28 b: Subject 10 (γ = 0 degrees) – observer 2

β	Test 1			Test 2			Test 3			Mean		
	α_r	α_t	α_a	α_r	α_t	α_a	α_r	α_t	α_a	α_r	α_t	α_a
0	0,00	0,00	0,00	0,00	0,00	0,00	0,00	0,00	0,00	0,00	0,00	0,00
10	1,66	-0,31	1,58	1,59	-0,38	1,51	0,89	-1,08	0,81	1,38	-0,59	1,30
20	4,20	-1,70	2,64	4,13	-1,77	2,57	3,43	-2,47	1,87	3,92	-1,98	2,36
30	4,61	-3,93	3,28	5,83	-2,71	4,50	4,50	-4,04	3,17	4,98	-3,56	3,65
40	6,60	-5.03	3,93	7,82	-3,81	5,15	6,49	-5,14	3,82	6,97	-4,66	4,30
50	10,34	-6,51	4,76	12,36	-4,49	6,78	10,27	-6,58	4,69	10,99	-5,86	5,41
60	13,29	-8,56	6,30	15,31	-6,54	8,32	13,22	-8,63	6,23	13,94	-7,91	6,95
70	15,42	-10,44	8,25	17,44	-8,42	10,27	15,35	-10,51	8,18	16,07	-9,79	8,90
80	16,88	-12,89	8,96	18,88	-10,89	10,96	18,51	-11,26	10,59	18,09	-11,68	10,17
90	19,17	-14,94	10,75	21,17	-12,94	12,75	20,80	-13,31	12,38	20,38	-13,73	11,96
100	21,62	-17,12	12,98	23,62	-15,12	14,98	23,25	-15,49	14,61	22,83	-15,91	14,19
110	24,28	-20,58	13,81	27,60	-17,26	17,13	27,23	-17,63	16,76	26,37	-18,49	15,90
120	27,07	-23,98	16,56	30,39	-20,66	19,88	30,02	-21,03	19,51	29,16	-21,89	18,65

Figure 12.29 a: Subject 10 (γ = 45 degrees) – observer 1

β	Test 1			Test 2			Test 3			Mean		
	α_r	α_t	α_s	α_r	α_t	α_s	α_r	α_t	α_s	α_r	α_t	α_s
0	0,00	0,00	0,00	0,00	0,00	0,00	0,00	0,00	0,00	0,00	0,00	0,00
10	1,83	-0,31	1,34	1,76	-0,38	1,27	1,06	-1,08	0,57	1,55	-0,59	1,06
20	4,90	-1,10	2,64	4,83	-1,17	2,57	4,13	-1,37	1,87	4,62	-1,38	2 36
30	5,82	-2,45	3,52	7,04	-1,23	4,74	5,71	-2,56	3,41	6,19	-2,08	3,89
40	8,23	-3,85	4,72	9,45	-2,63	5,94	8,12	-3,96	4,61	8,60	-3,48	5,09
50	10,81	-5,33	5,42	12,83	-3,31	7,44	10,74	-5,40	5,35	11,46	-4,68	6,07
60	13,49	-7,22	6,96	15,51	-5,20	8,98	13,42	-7,29	6,89	14,14	-6,57	7,61
70	16,00	-8,61	7,89	18,02	-6,59	9,91	15,93	-8,68	7,82	16,65	-7,96	8,54
80	17,69	-11,55	9,48	19,69	-9,55	11,48	19,32	-9,92	11,11	18,90	-10,34	10,69
90	19,44	-14,14	11,17	21,44	-12,14	13,17	21,07	-12,51	12,80	20,65	-12,93	12,38
100	22,11	-16,73	13,81	24,11	-14,73	15,81	23,74	-15,10	15,44	23,32	-15,52	15,02
110	23,05	-19,71	14,16	26,37	-16,39	17,48	26,00	-16,76	17,11	25,14	-17,62	16,25
120	25,83	-23,19	16,17	29,15	-19,87	19,49	28,78	-20,24	19,12	27,92	-21,10	18,26

Figure 12.29 b: Subject 10 (γ = 45 degrees) – observer 2

β	Test 1			Test 2			Test 3			Mean		
	α_r	α_t	α_s	α_r	α_t	α_s	α_r	α_t	α_s	α_r	α_t	α_s
0	0,00	0,00	0,00	0,00	0,00	0.00	0,00	0,00	0,00	0,00	0,00	0,00
10	0,86	0,29	0,21	1,40	0,72	0,75	1,46	0,76	0,81	1,24	0,59	0,59
20	1,42	0,41	0,80	1,96	0,95	1,34	2,02	1,01	1,40	1,80	0,79	1,18
30	3,51	1,60	2,31	3,01	1,10	1,81	3,08	1,17	1,88	3,20	1,29	2,00
40	4,91	0,80	3,14	4,41	0,30	2,64	4,48	0,37	2,71	4,60	0,49	2,83
50	5,66	0,11	3,85	5,16	-0,39	3,35	5,23	-0,32	3,42	5,35	-0,20	3,54
60	7,10	-2,00	4,48	7,59	-1,51	4,97	7,84	-1,26	5,22	7,51	-1,59	4,89
70	9,17	-3,99	5,96	9,66	-3,50	6,45	9,91	-3,25	6,70	9,58	-3,58	6,37
80	12,96	-4,77	9,15	11,65	-6,08	7,84	11,90	-5,83	8,09	12,17	-5,56	8,36
90	15,68	-7,15	11,98	14,37	-8,46	10,67	14,62	-8,21	10,92	14,89	-7,94	11,19
100	16,62	-12,69	12,31	19,65	-9,66	15,34	19,92	-9,39	15,61	18,73	-10,58	14,42
110	21,28	-15,67	14,78	24,31	-12,64	17,81	24,58	-12,37	18,08	23,39	-13,56	16,89
120	25,83	-19,05	18,84	28,86	-16,02	21,87	29,13	-15,75	22,14	27,94	-16,94	20,95

Figure 12.30 a: Subject 10 (γ = 90 degrees) – observer 1

β	Test 1			Test 2			Test 3			Mean		
	α_r	α_t	α_a	α_r	α_t	α_a	α_r	α_t	α_a	α_r	α_t	α_a
0	0,00	0,00	0,00	0,00	0,00	0,00	0,00	0,00	0,00	0,00	0,00	0,00
10	0,41	0,30	-0,04	0,95	0,73	0,50	1,01	0,77	0,56	0,79	0,60	0,34
20	0,85	1,01	0,41	1,39	1,55	0,95	1,45	1,61	1,01	1,23	1,39	0.79
30	2,78	1,00	1,79	2,28	0,50	1,29	2,35	0,57	1,36	2,47	0,69	1,48
40	4,52	-0,09	2,64	4,02	-0,59	2,14	4,09	-0.52	2,21	4,21	-0,40	2,33
50	5,94	-1,14	3,40	5,44	-1,64	2,90	5,51	-1,57	2,97	5,63	-1,45	3,09
60	6,19	-3,01	4,18	6,68	-2,52	4,67	6,93	-2,27	4,92	6,60	-2,60	4,59
70	8,63	-5,30	6,65	9,12	-4,81	7,14	9,37	-4,56	7,39	9,04	-4,89	7,06
80	12,96	-5,77	10,56	11,65	-7,08	9,25	11,90	-6,83	9,50	12,17	-6,56	9,77
90	15,90	-8,26	12,93	14,59	-9,57	11,62	14,84	-9,32	11,87	15,11	-9,05	12,14
100	16,62	-14,31	13,72	19,65	-11,28	16,75	19,92	-11,01	17,02	18,73	-12,20	15,83
110	20,37	-17,30	16,67	23,40	-14,27	19,70	23,67	-14.00	19,97	22,48	-15,19	18,78
120	24,79	-19,67	19,02	27,82	-16,64	22,05	28,09	-16,37	22,32	26,90	-17,56	21,13

Figure 12.30 b: Subject 10 (γ = 90 degrees) – observer 2

13 Appendix C – Mathcad code

This Appendix contains the Mathcad code used to generate the sterno-clavicular model

Humeral elevation	Humeral azimuth	Clavicle axial rotation	Humeral elevation	Humeral azimuth	Clavicle adduction-abduction	Humeral elevation	Humeral azimuth	Clavicle azimuth

A=(Matrix of the mean values)

Matrix A

0	0	0	0	0	0	0	0	0
10	0	2	10	0	1	10	0	-1
20	0	4	20	0	2	20	0	-2
30	0	7	30	0	4	30	0	-3
40	0	9	40	0	6	40	0	-5
50	0	12	50	0	8	50	0	-6
60	0	16	60	0	10	60	0	-8
70	0	19	70	0	13	70	0	-10
80	0	23	80	0	15	80	0	-12
90	0	26	90	0	17	90	0	-15
100	0	30	100	0	20	100	0	-17
110	0	33	110	0	22	110	0	-21
120	0	37	120	0	25	120	0	-24
0	45	0	0	45	0	0	45	0
10	45	1	10	45	1	10	45	0
20	45	3	20	45	2	20	45	-1
30	45	5	30	45	3	30	45	-3
40	45	7	40	45	4	40	45	-4
50	45	10	50	45	6	50	45	-5
60	45	13	60	45	8	60	45	-7
70	45	17	70	45	10	70	45	-9
80	45	20	80	45	12	80	45	-11
90	45	24	90	45	14	90	45	-14
100	45	28	100	45	17	100	45	-16
110	45	32	110	45	20	110	45	-19
120	45	35	120	45	23	120	45	-22
0	90	0	0	90	0	0	90	0

10	90	1	10	90	1	10	90	1
20	90	2	20	90	1	20	90	2
30	90	3	30	90	2	30	90	1
40	90	5	40	90	3	40	90	-1
50	90	6	50	90	4	50	90	-2
60	90	9	60	90	6	60	90	-4
70	90	12	70	90	8	70	90	-6
80	90	15	80	90	11	80	90	-8
90	90	19	90	90	13	90	90	-11
100	90	24	100	90	17	100	90	-14
110	90	28	110	90	20	110	90	-17
120	90	33	120	90	23	120	90	-20

Where:

β=humeral elevation

γ= humeral azimuth

clavicle axial rotation

Mβγ := submatrix(A,0,38,0,1) Mβγ is an 39 x 2 matrix containing β and γ coordinates.

Mβγ is build by the column 0 and column 1 of matrix A

vz := $A^{<2>}$ vector obtained by column 2 of the matrix A (Original data)

clavicle adduction-abduction

Mβγ := submatrix(A,0,38,3,4) Mβγ is an 39 x 2 matrix containing β and γ coordinates.

Mβγ is build by the column 3 and column 4 of matrix A

vz := $A^{<5>}$ vector obtained by column 5 of the matrix A (Original data)

clavicle azimuth

Mβγ := submatrix(A,0,38,6,7) Mβγ is an 39 x 2 matrix containing β and γ coordinates.

Mβγ is build by the column 6 and column 7 of matrix A

vz := $A^{<8>}$ vector obtained by column 8 of the matrix A (Original data)

z := regress(Mβγ,vz,k) Returns a vector which interp uses to find the kth order polynomial that best fits the β (x) and γ (y) data values in Mβγ and vz.

k :=2 degree of polynomial fitting

i :=0...38 38=rows number submatrix Mβγ-1

fit(β) := interp(z,Mβγ,vz, β) polynomial fitting function

Returns interpolated γ (y) value corresponding to β (x). You get z from regress

β is the value of the independent variable at which you want to evaluate the regression curve.

predvzi :=fit[$(M\beta\gamma^{T})^{<i>}$] Predicted vz values

coeffs := submatrix(z,3,length(z)-1,0,0) coefficents for regression equation

corr(A,B) Returns the Pearson's r correlation coefficient of the elements in A and B.

R^2=corr(A,B)^2

$$R^2 := \frac{\overrightarrow{\sum(predvz - mean(vz))^2}}{\overrightarrow{\sum(vz - mean(vz))^2}}$$

14 Appendix D – Research Publication

This appendix contains a research publication written and published during the work undertaken within the thesis.

Reference:

Scattareggia Marchese, S., Johnson, G.R. (2000) Measuring the Kinematics of the Clavicle. Proceedings of the Sixth International Symposium on the 3D Analysis of Human Movement. Cape Town, South Africa, 37-40.

BEST COPY
AVAILABLE
Variable print
quality

TEXT BOUND INTO THE SPINE

MEASURING THE KINEMATICS OF THE CLAVICLE

S. Scattareggia Marchese[1] and G.R.Johnson[2]

[1]Signo Motus s.r.l.. Messina, Italy

[2]Centre for Rehabilitation and Engineering Studies (CREST), University of Newcastle, UK

Introduction

The shoulder complex may be considered as a spatial mechanism in which the scapula, clavicle and humerus all move in concert. However, reliable measurement of the spatial kinematics of these bones has not been possible until recently because of the difficulty of direct measurement and the absence of sufficiently accurate imaging techniques. With the development of instrumented palpation techniques (Pronk and van der Helm 1991, Barnett et al, 1999), it has been possible to make non-invasive measurements of the movements of the scapula. These studies have demonstrated the non-linear relationships between the spatial rotations of the scapula and the position of the humerus. Furthermore, the potential clinical uses of these measurements have been demonstrated in studies of patients after stroke (Johnson et al 1998). In order to achieve a full understanding of the kinematics of the shoulder complex, there is a need to measure reliably the movements of the clavicle. Inman and Saunders (1946) were the first to provide direct experimental measurement of the rotations of the clavicle on a single subject having a percutaneous steel pin attached directly to the clavicle. This demonstrated clearly the relatively large axial rotation which takes place during arm elevation. However, this work has been developed little since that time because of the difficulties of making non-invasive measurement of the axial rotation beneath the skin. The most recent approach has been to use mathematical modelling techniques. The Dutch Shoulder Group (Pronk et al 1993), after measuring the non axial rotations by direct palpation, used a procedure in which it is assumed that movements of the acromioclavicular joint are minimised. There still remains, therefore, a need for direct measurements which may validate the modelling studies and lead to more detailed clinical understanding.

This paper presents a palpation technique which, by relying on the particular geometry of the clavicle allows direct measurement of its spatial motion.

Method

The clavicle may be considered as a rigid body having spherical joints at each end (sterno-clavicular and acromio-clavicular). Therefore, apart from the ligamentous constraints, the axial rotation is not directly coupled to the other movements. This means that these rotations must be controlled in some way by a combination of muscle and ligamentous actions.

The challenge of using a palpation technique to measure all of the rotations of the clavicle is to find a way to exploit its natural geometry and make the simultaneous measurements of movements at more than one point. Furthermore, since the exact geometrical relationship between the AC joint and any chosen set of axes is not known, it is necessary to make measurements of the clavicle with respect to a co-ordinate system based in the trunk. In order to understand how this may be achieved by palpation, it is necessary to consider the geometry of the clavicle and the movements associated with the three angles of rotation. As a first approximation, the clavicle may be considered as a crankshaft as shown in figure 1, where:

L = *length of the clavicle*

R = *distance between the inner third and the outer third of the clavicle*

Having established this geometric model, it becomes clear that axial rotations can be deduced by palpation. In fact, it becomes possible to measure the rotations by the use of a palpation frame having three angular movement sensors as shown in Figure 1. These sensors are positioned on the structure in a serial-parallel chain, so that Sensor 1 measures a rotation in the transverse plane, while Sensors 2 and 3, connected to the inner and outer third of the clavicle respectively, both measure rotations in the coronal plane. The "connections" to the bone that, in reality, are not physically possible because of the presence of skin and muscles, are represented by single rotational degrees of freedom which permit the rotation of the clavicle. In order to allow motion within the assembly of the palpation frame and the clavicle it is necessary to add two more passive degrees of freedom:

(i) a translation between the link connecting Sensor 3 to the outer third of the clavicle for compensation of the distance between the outer third of the clavicle and this sensor during axial rotation of the clavicle around the inner third axis;

(ii) a rotation positioned before the connection of the outer third of the clavicle with the Sensor 3 linkage. The axis of rotation of this degree of freedom is coincident with the axis of the passive

linear one. Its rotation compensates the lack of parallelism between the Sensor 3 link and the outer third of the clavicle during axial rotation.

Analysis

Using spherical geometry, a theoretical solution has been established which expresses the rotations of the clavicle as functions of the rotations of the three sensors as follows:

If the rotations of the clavicle are defined as:

α_r = *clavicle axial rotation*

α_a = *clavicle abduction-adduction in the coronal plane*

α_t = *clavicle rotation in the transverse plane*

and

$\vartheta_1, \vartheta_2, \vartheta_3$ = *rotations of sensor 1, sensor 2 and sensor 3 respectively*

L = *clavicle length*

R = *Clavicle radius (distance between the inner third and the outer third)*

Then, by trigonometry, it can be shown that:

$$\alpha_r = arcsin\left(\frac{L}{R} \cdot \frac{sin\vartheta_3 - sin\vartheta_2}{\cos\vartheta_2}\right)$$

$$\alpha_a = \vartheta_2$$

$$\alpha_t = \vartheta_1$$

Validation and testing

The palpation fixture was constructed using specially designed rotation sensors based on the Hall effect. The outputs of the sensors were connected to an interface box to allow direct sampling by computer. The movement detector is shown in use in Figure 2 below.

Figure 2 The clavicular movement detector

In order to validate the algorithm (3) obtained above, a test rig was constructed having a wooden model of the clavicle attached to a further movement sensor to allow direct measurement of axial rotation. A typical output from the system is shown in Figure 4.

It will be noted, in the analysis, that the calibration of this system is dependent upon knowledge of the distances L and R, and a particularly important aspect of this work has been the need to develop a technique to measure the ratio L/R as defined in Figure 1. However, this ratio represents a simplified geometry of the clavicle and must be measured non-invasively as part of the experimental procedure. In order to achieve this, a special measurement fixture has been designed. The repeatability of this measuring procedure was studied by analysing the measurements made of 2 subjects on two occasions by 5 different observers. The greatest difference between any pair of measurements taken on the same subject was less than 10 per cent of the mean.

Following successful validation studies with the model and with the fixture for measuring clavicle geometry, the system has been used to measure clavicle movements associated with a range of positions of the humerus. Initially, repeatability studies have been performed, in order to further validate the technique.

This was performed by two observers making 3 replicate measurements on each of 5 subjects performing elevation movements. The angle of elevation was measured by a potentiometer attached to a sliding fixture to allow natural movements of the arm. Measurements were taken during elevation of the arm over a range of 120 degrees from the resting position at intervals of 10 degrees. These experiments were performed at azimuth angles of 0 degrees (movement in the coronal plane), 45 degrees and 90 degrees (movement in the sagittal plane). A total of 216 readings were taken for each subject. The mean values of each of the clavicular rotations were then calculated from all the observations of all the subjects at each azimuth.

Results

The studies of the repeatability of the clavicle measurement device showed that L/R ratio could be measured to within 10 per cent of the mean value.

The movements of the clavicle associated with coronal plane abduction and forward flexion are shown in Figure 3, where it can be seen that axial rotation and abduction increase almost linearly with arm elevation, over a range of approximately 50 degrees. A retraction of approximately 15 degrees is associated with 150 degrees of arm elevation. It was found that clavicle position was independent of shoulder internal/external rotation.

The sensitivity of predicted clavicle movements associated with the 10 per cent variation of the L/R ratio are shown in Figure 4.

Mathematical Model

Using all the data collected, a multiple regression model has been produced to predict clavicle position as a function of arm elevation (β) and azimuth (γ). The coefficients of this polynomial model were found to be as follows.

$$\alpha_r = 1.38 \cdot 10^{-3} \cdot \beta^2 - 2.849 \cdot 10^{-4} \cdot \gamma^2 - 4.762 \cdot 10^{-4} \cdot \beta \cdot \gamma + 0.153 \cdot \beta + 2.076 \cdot 10^{-3} \cdot \gamma + 0.685 \quad (R = 0.995)$$

$$\alpha_a = 1.077 \cdot 10^{-3} \cdot \beta^2 + 2.279 \cdot 10^{-4} \cdot \gamma^2 - 2.381 \cdot 10^{-4} \cdot \beta \cdot \gamma + 0.08 \cdot \beta - 0.035 \cdot \gamma + 0.804 \quad (R = 0.993)$$

$$\alpha_t = -1.299 \cdot 10^{-3} \cdot \beta^2 + 3.609 \cdot 10^{-4} \cdot \gamma^2 + 1.832 \cdot 10^{-4} \cdot \beta \cdot \gamma - 0.04 \cdot \beta - 5.006 \cdot 10^{-3} \cdot \gamma - 0.648 \quad (R = 0.995)$$

Discussion

While there have been several experimental studies of scapular movements, this is the first time that non-invasive measurement of complete clavicle movement has been achieved. Although other studies have reported measurements of abduction and protraction, direct measurement of axial rotation has not been achieved before. When comparing with the data of Pronk and van der Helm (1989) there is excellent agreement in measurements of protraction. However, while in this study the maximum reported abduction is 30 degrees, the earlier study reports only 10 degrees. This difference may be due to slight differences in the definitions of co-ordinate frames. The Pronk and van der Helm study use palpation of key bony landmarks using an instrumented palpator as opposed to the direct palpation technique used here. It is interesting to note, however, that in a later study (Pronk et al 1993), these authors report an elevation of 30 degrees agreeing well with these data.

When considering axial rotations, the only data with which these results can be usefully compared are probably those of Pronk et al (1993) which were achieved by mathematical optimisation rather than by direct measurement. In this study, they assumed that the axial rotations would be such as to minimise the rotations of the acromioclavicular joint. In fact, there is good agreement with this work that predicts a maximum value of 50 degrees.

Despite the development of palpation techniques for the measurement of movements of the shoulder girdle, it is important to point out the lack of validation that can be achieved. In the future is hoped that this can be done using imaging techniques. However, these are not yet sufficiently accurate or versatile to allow this to be done. In this situation, it is impossible to make direct comparisons. However, the final vindication will come only after a different technique is devised.

As far as the inter-subject variations are concerned, more work is required, since the data here have been derived from a small subject sample. Similarly, there is a need to study the movements at the acromioclavicular joint by making simultaneous measurement of the scapula and clavicle. Such studies will be of interest when studying the biomechanics of the complete shoulder girdle and in a number of clinical situations. when studying the possible effects of clavicle fracture or repair. In particular, they will be of great interest when studying further the variations of shoulder movement patterns in patients after stroke which have been presented earlier (Johnson et al 1998). In addition, it may be possible to study the effects on overall shoulder movements of fracture and repairs of the clavicle.

References

Barnett N.D., Duncan R.D.D. and Johnson G.R. (1999) The measurement of three dimensional scapulohumeral kinematics - a study of reliability. Clinical Biomechanics 14, 73-76.

Inman, V. T., Saunders M. and L. C. Abbott (1944) Observations on the Function of the Shoulder Joint Journal of Bone and Joint Surgery 26, 1-30.

Johnson G.R., Franklin P., Price C.I.M., Curless R. and Rodgers H. (1998) A study of the motion of the shoulder complex in patients with hemiplegia. Proceedings of Fifth International Symposium on the 3D Analysis of Human Movement, Chattanooga, Tennessee. July 2 –5 1998.

Pronk G.M. and van der Helm F.C.T. (1989) The role of the coracoclavicular mechanism in the motion between the scapula and the clavicle. Proc. 12th International Congress of Biomechanics. Los Angeles, USA. 654-655.

Pronk, G.M. and van der Helm, F.C.T. (1991) The palpator: an instrument for measuring the positions of bones in three dimensions J. of Med. Engng Technology 15 (1), 15-20.

Pronk, G.M., van der Helm, F.C.T. and Rozendaal, L.A. (1993) Interaction between the joints in the shoulder mechanism: the function of the costoclavicular, conoid and trapezoid ligaments. Proceedings of International Seminar on "Biomechanics and Joint Replacement in the Upper Limb". London.

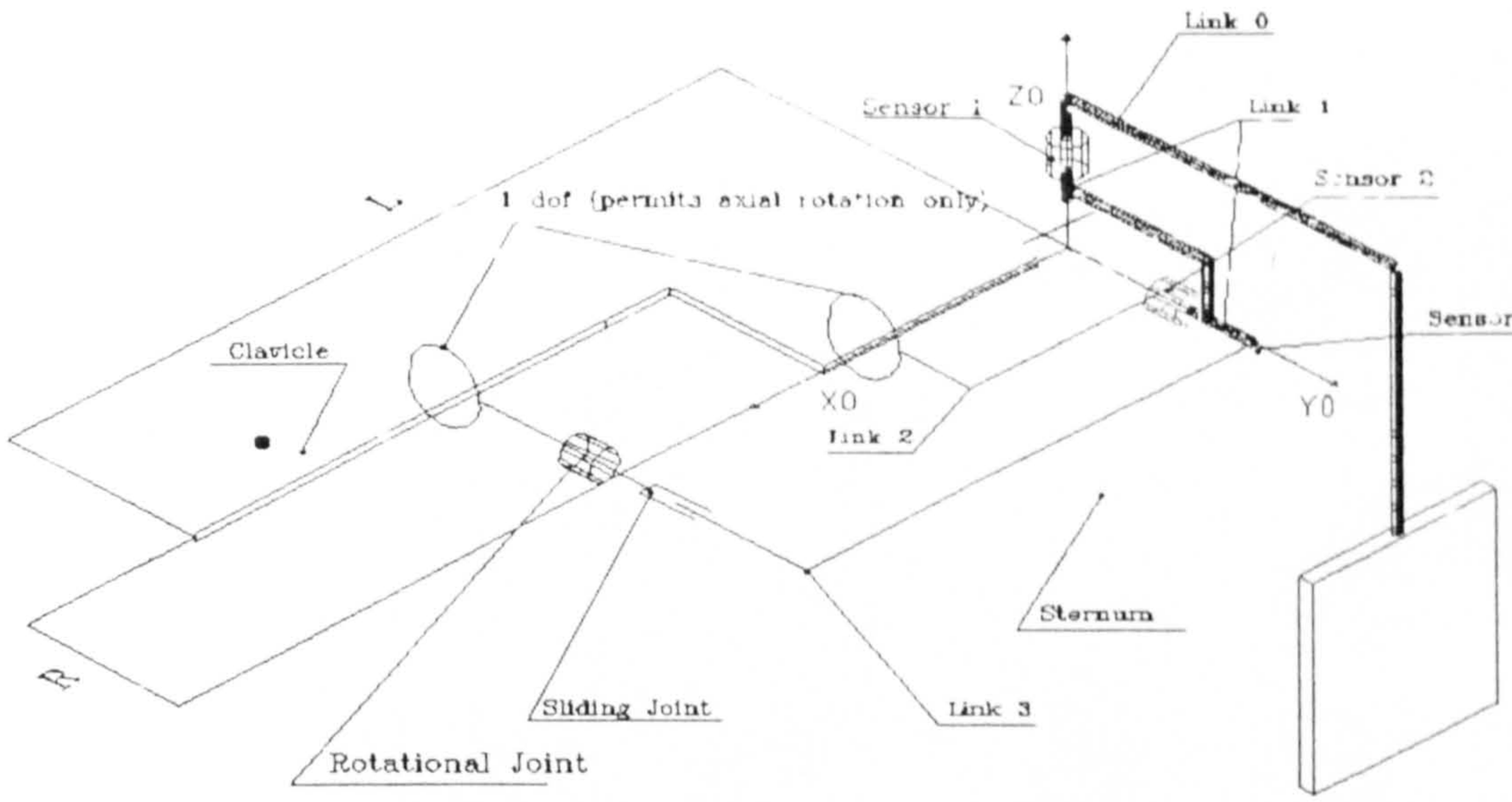

Figure 1. Diagrammatic arrangement of the measurement system

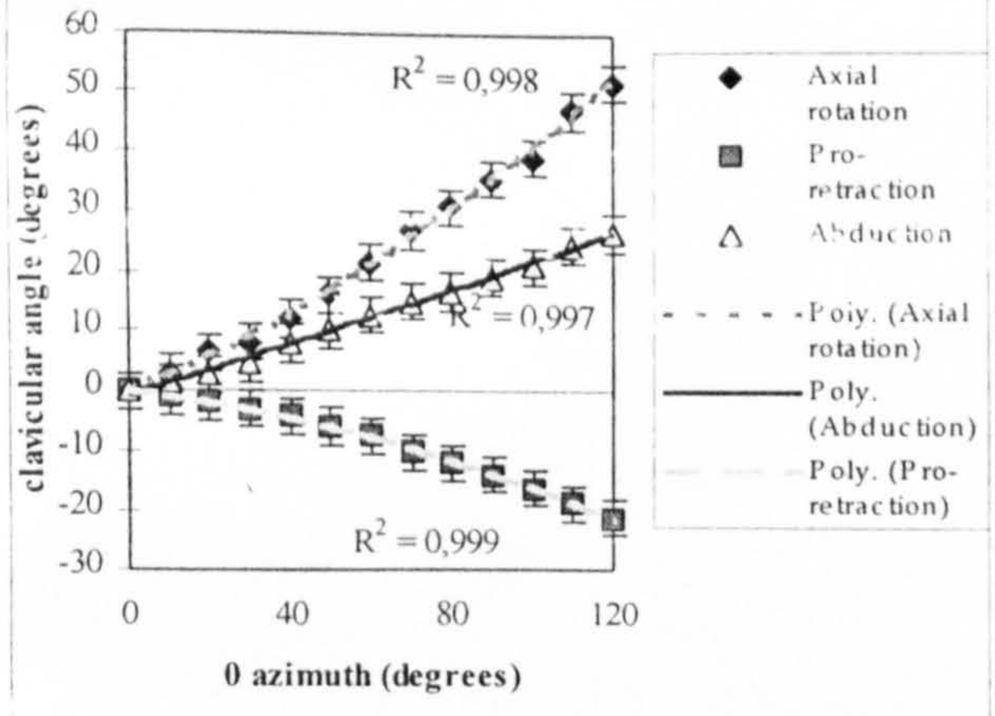

Figure 3. Graphs of axial rotation, pro/retraction and abduction of the clavicle versus angle of arm elevation (at zero azimuth)

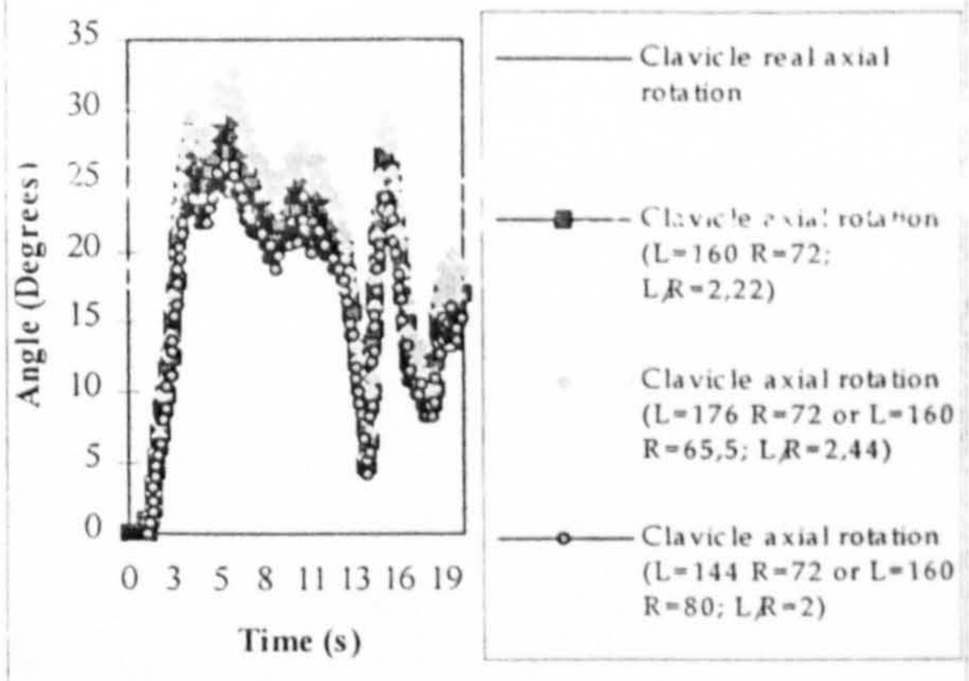

Figure 4. Graphs of computed axial rotation of model clavicle calculated for a range of values of L and R and compared with actual values